. 107 June 1, 1979
plete in one issue

ISSN 0003-2670

ANALYTICA CHIMICA ACTA

International journal devoted to all branches of analytical chemistry

ELSEVIER SCIENTIFIC PUBLISHING COMPANY

ANALYTICA CHIMICA ACTA

International journal devoted to all branches of analytical chemistry
Revue internationale consacrée à tous les domaines de la chimie analytique
Internationale Zeitschrift für alle Gebiete der analytischen Chemie

PUBLICATION SCHEDULE FOR 1979 (incorporating the section on Computer Techniques and Optimization).

	J	F	M	A	M	J	J	A	S	O	N	D
Analytica Chimica Acta	104/1	104/2	105	106/1	106/2	107	108	109/1	109/2	110/1	110/2	111
Section on Computer Techniques and Optimization			112/1			112/2			112/3			112

Scope. *Analytica Chimica Acta* publishes original papers, short communications, and reviews dealing with every aspect of modern chemical analysis, both fundamental and applied. The section on *Computer Techniques and Optimization* is devoted to new developments in chemical analysis by the application of computer techniques and by interdisciplinary approaches, including statistics, systems theory and operation research. The section deals with the following topics: Computerized acquisition, processing and evaluation of data. Computerized methods for the interpretation of analytical data including chemometrics, cluster analysis, and pattern recognition. Storage and retrieval systems. Optimization procedures and their application. Automated analysis for industrial processes and quality control. Organizational problems.

Submission of Papers. Manuscripts (three copies) should be submitted to:
for *Analytica Chimica Acta:* Dr. A. M. G. Macdonald, Department of Chemistry, The University, P.O. Box 363; Birmingham B15 2TT, England;
for the section on *Computer Techniques and Optimization:* Dr. J. T. Clerc, Universität Bern, Pharmazeutisches Institut, Sahlistrasse 10, CH-3012 Bern, Switzerland.

Information for Authors. Papers in English, French and German are published. There are no page charges. Manuscripts should conform in layout and style to the papers published in this Volume. Authors should consult Vol. 102, p. 253 for detailed information. Reprints of this information are available from the Editors or from: Elsevier Editorial Services Ltd., Mayfield House, 256 Banbury Road, Oxford OX2 7DE (Great Britain).

Reprints. Fifty reprints will be supplied free of charge. Additional reprints (minimum 100) can be ordered. An order form containing price quotations will be sent to the authors together with the proofs of their article.

Advertisements. Advertisement rates are available from the publisher.

Subscriptions. Subscriptions should be sent to: Elsevier Scientific Publishing Company, P.O. Box 211, 1000 AE Amsterdam, The Netherlands. The section on *Computer Techniques and Optimization* can be subscribed to separately.

Publication. *Analytica Chimica Acta* (including the section on *Computer Techniques and Optimization*) appears in 9 volumes in 1979. The subscription for 1979 (Vols. 104–112) is Dfl. 1179.00 plus Dfl. 135.00 (postage) (Total approx. U.S. $641.00). The subscription for the *Computer Techniques and Optimization* section only (Vol. 112) is Dfl. 131.00 plus Dfl. 15.00 (postage) (Total approx. U.S. $71.20). Journals are sent automatically by air mail to the U.S.A. and Canada at no extra cost and to Japan, Australia and New Zealand for a small additional postal charge. All earlier volumes (Vols. 1–95) except Vols. 23 and 28 are available at Dfl. 144.00 (U.S. $70.20), plus Dfl. 10.00 (U.S. $4.90) postage and handling, per volume.

Claims for issues not received should be made within three months of publication of the issue, otherwise they cannot be honoured free of charge.

Customers in the U.S.A. and Canada who wish to obtain additional bibliographic information on this and other Elsevier journals should contact Elsevier/North Holland Inc., Journal Information Center, 52, Vanderbilt Avenue, New York, NY 10017. Tel: (212) 867-9040.

ANALYTICA CHIMICA ACTA
VOL. 107 (1979)

ANALYTICA CHIMICA ACTA

International journal devoted to all branches of analytical chemistry

ELSEVIER SCIENTIFIC PUBLISHING COMPANY

Anal. Chim. Acta, Vol. 107 (1979)

Printed in The Netherlands

Analytica Chimica Acta, 107 (1979) 1—11

THE DETERMINATION OF PHYTOPLANKTON PIGMENTS BY HIGH-PERFORMANCE LIQUID CHROMATOGRAPHY

J. K. ABAYCHI and J. P. RILEY*

Department of Oceanography, University of Liverpool, P.O. Box 147, Liverpool L69 3BX (Gt. Britain)

(Received 8th November 1978)

SUMMARY

A simple high-performance liquid chromatographic method is described for the determination of chlorophylls, chlorophyll degradation products, and carotenoids in phytoplankton cultures and marine particulate matter. Pigment extraction is carried out with acetone and methanol. After evaporation of the combined extracts under reduced pressure, the pigments are separated on a Partisil-10 stationary phase with a mobile phase consisting of light petroleum (b.p. 60—80°C), acetone, dimethyl sulphoxide and diethylamine (75: 23.25: 1.5: 0.25 by volume). When chlorophyll *c* is present, a further development is performed with a similar, but more polar, solvent mixture. Detection is carried out spectrophotometrically at 440 nm. The method has a sensitivity for the chlorophylls of ca. 80 ng, and for carotene of ca. 5 ng. The coefficient of variation of the chromatographic stage of the procedure lies in the range 0.6—1.8%.

A knowledge of the plant biomass is, along with that of primary production, of crucial importance in any study of the fertility of the sea. The former parameter cannot, at present, be satisfactorily measured directly, but is usually estimated by determining some biochemical component of the plant cells (e.g. chlorophyll, ATP or DNA) and relating it to the amount of plant carbon by the application of an appropriate factor. Unfortunately, this factor varies considerably according to the species present and their metabolic and nutritional states, but even so such measurements can provide valuable information. The simplest and most widely adopted of these techniques is that developed for chlorophylls by Richards [1] and subsequently modified by others [2—4]. In this, spectrophotometric measurements are made at selected wavelengths on 90% acetone extracts of the separated phytoplankton. With simultaneous equations [2—5], it is possible to calculate the amounts of chlorophylls *a*, *b* and *c* and total carotenoids present in the sample. The method, which was the subject of an extensive investigation by a UNESCO working group [4], is subject to a number of drawbacks [6]: (i) there is serious overlap between the absorption bands of the chlorophylls, and the precision for chlorophylls *b* and *c* is therefore rather poor; (ii) there are considerable differences between the results obtained with the various sets of equations; (iii) chlorophyll degradation

products have absorption spectra similar to those of the chlorophylls and seriously interfere in the determination; (iv) the sensitivity is relatively low, necessitating the use of large water samples; (v) the values found for the total carotenoids are usually only very approximate. It is possible to overcome the majority of these difficulties by separating the pigments chromatographically before determining them. Such an approach may also provide useful informati about the state of the phytoplankton crop, via the chlorophyll degradation products (thus chlorophyllides are characteristic of moribund organisms and phaeophorbides occur when heavy zooplankton grazing has occurred), and about the classes of algae present via the characteristic xanthophylls.

Although column chromatography has been applied to the preparative separation of plant pigments for over a century, it is unsuitable for the estimation of marine biomass because of lack of sensitivity. Two-dimensional paper chromatography has been used in the separation and determination of the pigments of phytoplankton grown in culture [7, 8]. However, it too has insufficient sensitivity for the examination of natural phytoplankton populations and is only semiquantitative. Much greater success has been achieved with thin-layer chromatography, which gives much more efficient separations and possesses sufficient sensitivity for the quantitative determination of the pigments of algal blooms [9, 10]. Even so, the precision is, at best, ±5% and the separations of the chlorophyll degradation products and of certain xanthophylls are not very sharp.

It seemed likely that high-performance liquid chromatography (h.p.l.c.) with its much higher efficiency and continuity of monitoring might be more satisfactory. The first application of the technique to plant pigments was by Evans et al. [12] who separated phaeophytins *a* and *b* on Corasil II with a mobile phase consisting of a 1:5 (v/v) mixture of ethyl acetate and light petroleum. Eskins et al. [13] have employed two 0.62-m columns of C_{18}-Porasil B for preparative separation of plant pigments by means of programmed stepwise elution with methanol—water—ether. However, the method is of little value for routine application because of the time required (270 min) and also because the chlorophyll degradation products, other than phaeophytin, are not separated. Shoaf [14] has used h.p.l.c. to separate the chlorophylls *a* and *b* of a pigment extract from which the carotenoids had been previously removed. Good resolution of the two pigments and several of their unspecified degradation products was achieved on a 25-cm column of Partisil PXS 1025 by elution with aqueous 95% methanol; however, chlorophylls were not determined quantitatively. Thus, little attempt had been made to apply h.p.l.c. to the quantitative determination of plant pigments. A rapid method for the recognition and estimation of the array of pigments encountered in phytoplankton extracts — including chlorophyll degradation products — has therefore been devised. Since commercial h.p.l.c. equipment (particularly that with solvent programming) may be beyond the financial reach of many oceanograp laboratories, the work was carried out with a simple instrument constructed from readily available parts. For this reason, the technique developed involves stepwise elution with two solvent mixtures rather than gradient elution.

Development of the method

The procedure described by Garside and Riley [11] was adopted for the extraction of the pigments of algal cells because of its simplicity. Tests carried out with the h.p.l.c. technique endorsed the claim that it causes negligible degradation of both the chlorophylls and the xanthophylls. For convenience, an extract of grass was used in the early stages of the development of the method; however, later work showed that despite their higher content of lipids, extracts prepared from algae grown in culture behaved in an analogous fashion.

Preliminary studies showed that a more efficient separation of plant pigments could be achieved on a silica stationary phase than on a C_{18} reversed-phase medium. An empirical investigation was therefore made with a 30-cm column packed with Partisil 10 to find a solvent mixture which would give an efficient separation of the plant pigments. After over a hundred tests, a mixture was found which would satisfactorily resolve the individual carotenoids, chlorophylls *a* and *b*, and many of the degradation products of the latter pair (Fig. 1). This consists of light petroleum (b.p. 60—80°C), acetone, dimethyl sulphoxide and diethylamine in the ratio 75: 23.25: 1.5: 0.25 by volume. Unfortunately, this solvent is not sufficiently polar to elute phaeophorbide and chlorophyll *c*. With samples containing these pigments, it is necessary to carry out an additional, stepwise, elution with a more polar solvent. Further tests showed that excellent resolution of these compounds could be achieved (Fig. 2) by means of a mixture containing light petroleum (b.p. 60—80°C), acetone, methanol and dimethyl sulphoxide in the ratio 30:40:27:3 by volume, respectively. Some instrumental noise occurs at the change-over between the two solvents as a result of refractive index changes; this is not of any consequence, and could probably be eliminated by the use of solvent programming.

In order to identify the various peaks on the chromatograms, extracts of a range of algae from various classes were injected repeatedly onto the Partisil 10 column operated at a flow rate of 2 ml min^{-1}. The eluates corresponding with individual peaks of known retention times were collected and combined until a suitable quantity of pigment had been accumulated. The combined eluates were then taken rapidly to dryness in a rotary evaporator at <30°C and, after dissolution in appropriate solvents, were identified from their absorption spectra. Chlorophylls and their degradation products were characterized by their spectra in ether and in (1 + 9) water—acetone, based on data from Strickland [16]. Carotenoids were identified by comparison of their wavelengths of maximum absorption in hexane, ethanol and carbon disulphide with the tabulated values published by Davies [17]. Comparison of the absorption spectra with those of the pure pigments showed that the separated pigments were recovered in a satisfactorily pure state (see, e.g., Fig. 3). Identifications were confirmed by thin-layer chromatography on silica gel G [9]. The retention times of the various pigments are shown in Table 1 together with their standard deviations which indicate that the retention times are extremely reproducible.

Since the h.p.l.c. method provides pigments with a high degree of purity,

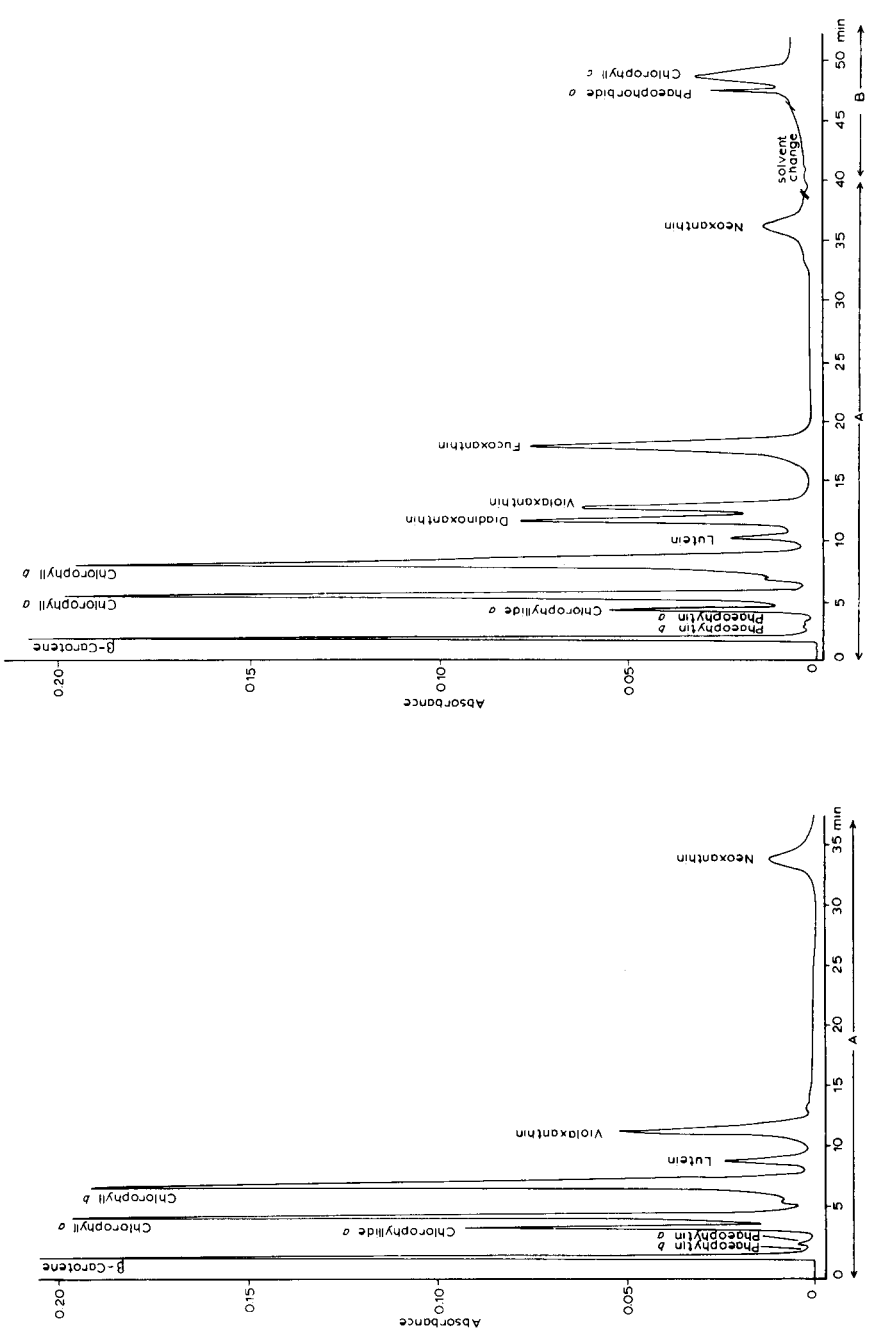

Fig. 1. Chromatogram of extract of pigments from *Dunaliella tertiolecta*.

Fig. 2. Chromatogram of extract of pigments from a mixed culture of *Phaeodactylum tricornutum* and *Dunaliella tertiolecta*.

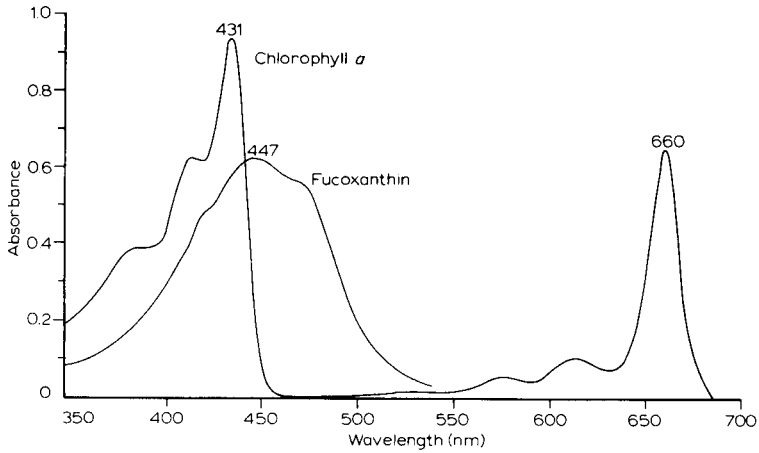

Fig. 3. Absorption spectra of chlorophyll *a* and fucoxanthin separated by h.p.l.c. from extract of *Phaeodactylum tricornutum* (4-cm cuvette).

TABLE 1

Retention times and corresponding coefficients of variation for various phytoplankton pigments on a 30-cm Partisil 10 column[a]

Pigment	Retention time (s)	Coefficient of variation (%)
	1st Mobile phase	
β-Carotene	107 ± 1	0.9
Echinenone	134 ± 1	0.7
Phaeophytin *b*	141 ± 1	0.7
Phaeophytin *a*	183 ± 1	0.5
Chlorophyllide *a*	237 ± 0.3	0.1
Chlorophyll *a*	293 ± 2	0.6
Chlorophyll *b*	424 ± 2	0.6
Diatoxanthin	478 ± 2	0.4
Myxoxanthophyll	488 ± 1	0.6
Lutein	533 ± 1	0.3
Diadinoxanthin	580 ± 3	0.5
Violaxanthin	664 ± 1	0.2
Fucoxanthin	809 ± 5	0.6
Neoxanthin	1773 ± 15	0.9
	2nd Mobile phase	
Phaeophorbide *a*	2395 ± 19 (622 in 2nd solvent)	0.8
Chlorophyll *c*	2497 ± 21 (724 in 2nd solvent)	0.8

[a]Solvent flow rate, 2 ml min^{-1}.

it is relatively easy to standardize the technique. For this purpose, an extract containing the desired pigment is injected into the instrument and the separated pigment is collected. After rotary evaporation at near ambient temperature (which has been shown not to lead to degradation), the pigment is immediately

dissolved in a known volume of an appropriate solvent and its concentration is determined photometrically. If the procedure is repeated with several different dilutions of the extract, a calibration curve can be constructed relating the chromatographic peak height to the photometrically determined amount of pigment. Figure 4 shows the calibration curves derived in this way for a number of pigments; the absorptivities shown in Table 2 are used for the evaluation of the pigment concentrations. From Fig. 4, it can be seen that the calibration is very closely linear (correlation coefficients ranging from 0.9966 for chlorophyll *c* to 0.9998 for β-carotene).

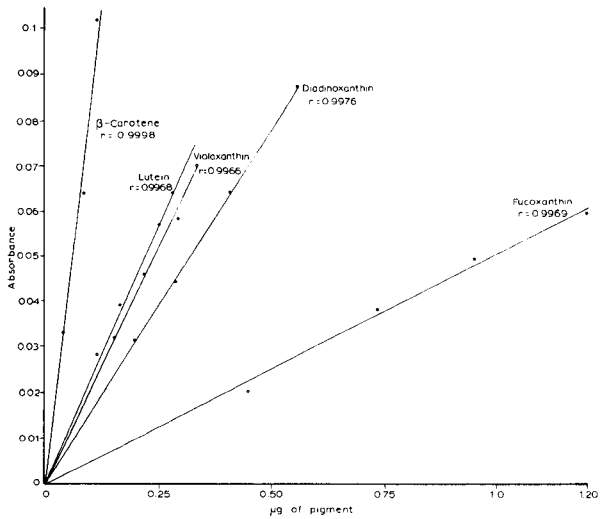

Fig. 4. Calibration curves for various pigments.

TABLE 2

Specific absorptivities used in calibration of the h.p.l.c. instrument

Pigment	$E_{1\,cm}^{1\%}$	Absorption maximum (nm)	Solvent	Reference
Chlorophyll *a*	911	663	90% Acetone	[18]
Chlorophyll *b*	525	645	90% Acetone	[18]
Chlorophyll *c*	1400	446	90% Acetone	[10]
β-Carotene	2592	453	Hexane	[19]
Echinenone	2153	458	Light petrol	[20]
Lutein	2550	445	Ethanol	[21]
Diadinoxanthin	2500	446	Ethanol	[17]
Violaxanthin	2550	443	Ethanol	[22]
Fucoxanthin	1060	449	90% Acetone	[23]
Neoxanthin	2243	439	Ethanol	[24]
Myxoxanthophyll	2160	478	Acetone	[25]

The sensitivity of the method varies considerably from one pigment to ai another. If a peak height of 5 mm is considered to be significant with a full scale deflection of 25 cm corresponding to 0.2 absorbance units, then the detection limit of the method varies from about 5 ng for β-carotene to about 80 ng for chlorophyll *a* (see Fig. 5). It should be noted, however, that this is not the maximum sensitivity which could be attained; the wavelength of 440 nm, at which the absorbance is measured, does not in general correspond with that of the absorbance maxima of the pigments, but is a compromise enabling reasonable sensitivity to be achieved for both chlorophylls and carotenoids. This probably reduces the attainable sensitivity by a factor of 2—3.

EXPERIMENTAL

Liquid chromatograph

Solvent was delivered at a rate of 2 ml min^{-1} and a pressure of about 14 kg cm^{-} by means of a Dosapro-Milton-Roy Minipump. Pulse damping was achieved by means of two sealed vertical stainless steel tubes (90 cm long, 4.5 mm bore) which were attached by 1-mm bore tubing to branches on the pump outlet. The column, constructed of 0.45-mm bore stainless steel tubing and packed with a 30-cm layer of Partisil 10 at a pressure of 350 kg cm^{-2}, had a plate count of 4600. For precision in sampling, the sample was introduced to the column by means of a Rheodyne syringe-loading sample injection unit fitted with a 20-μl sampling loop. The effluent from the column was fed to an 8-μl flow cell with a 1-cm lightpath in a Cecil CE 373 visible spectrophotometer operated at 440 nm and range expansion of 0.2A. The linear absorbance signal from the spectrophotometer was fed to a Honeywell chart recorder.

Reagents

Magnesium carbonate suspension. Suspend ca. 3 g of finely powdered basic magnesium carbonate in 100 ml of distilled water. Re-suspend immediately before use.

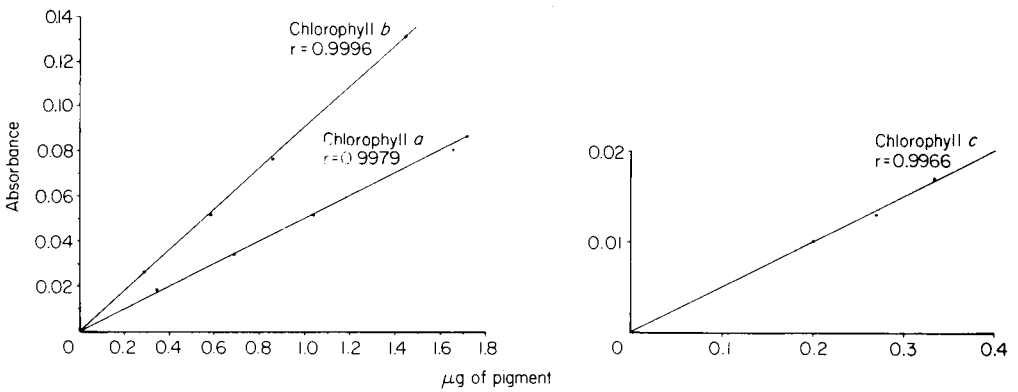

Fig. 5. Calibration curves for chlorophylls.

First mobile phase. Prepare, from glass-redistilled solvents, a mixture containing light petroleum (b.p. 60—80°C), acetone, dimethyl sulphoxide and diethylamine in the ratio 75:23.25:1.5:0.25 by volume. Before use, pass the mixture through a porosity 5 sintered glass filter under slight suction.

Second mobile phase. Prepare from glass-distilled solvents a mixture of light petroleum (b.p. 60—80°C), acetone, methanol and dimethyl sulphoxide in the volume ratio 30:40:27:3. Using a slight vacuum, filter the mixture through a sintered glass Buchner funnel (porosity 5) before use.

Procedure

To avoid degradation of the pigments, extraction of the sample and processing of the extract must be carried out as rapidly as possible in subdued light. Although it is possible to store the filtered organisms safely for up to a week at −20°C in closely stoppered nitrogen-filled tubes, the analysis should be completed without delay once the extraction has been commenced.

Extraction of pigments. Fit a glass filter holder with a 7-cm Whatman GF/C glass fibre filter and under slight suction coat it with a 1—2 mm layer of magnesium carbonate using the suspension. Filter a known volume of the sample, sufficient to provide ca. 5 μg of chlorophyll *a* (normally 2—10 l of sea water or 20—150 ml of cultures) under a vacuum not exceeding 0.3 bar. Wash the filter with a few ml of distilled water and then transfer it and its coating quantitatively to a test tube. Add 3—5 ml of acetone and gently disintegrate the filter with a glass rod. Place the test tube in an ultrasonic agitator for 5 min add 10 ml of methanol, mix and continue the ultrasonic treatment for a further 10 min. Decant the extract through a drawn-out glass tube containing a 2-cm layer of anhydrous sodium sulphate supported on a glass fibre plug. Collect the dry extract in a 25-ml pear-shaped flask. Wash the residue in the test tube and the drying column with about 2 ml of methanol and combine with the extract. If, exceptionally, the cell debris is not practically colourless, agitate it ultrasonically with 5-ml aliquots of methanol until no further pigment is extracted. Evaporate the combined extracts in vacuo in a rotary evaporator at a bath temperature not exceeding 40°C. Immediately after the last of the solvent has been removed, take up the residue in an exactly known volume (0.25—0.5 ml) of the first mobile phase.

Chromatographic separation of pigments. Equilibrate the h.p.l.c column with the first mobile phase. After equilibration has been achieved, inject a 20-μ aliquot of the pigment extract via the sampling valve. Develop the chromatogram with the first mobile phase at a flow rate of 2 ml min^{-1} until the last peak has appeared (ca. 30 min). Switch off the high pressure pump and rapidly transfer the solvent intake tube to the second mobile phase. Switch on the pump again immediately. Continue the development at a flow rate of 2 ml min until the elution of chlorophyll *c* is complete. Because of differences in refractive index between the two solvent systems some instrumental noise will be recorded when their interface enters the flow cell; however, a steady baseline should soon be re-established. Before carrying out the next injection the

apparatus should be allowed to re-equilibrate with the first mobile phase for a few minutes. If chlorophyll *c* and the phaeophorbides are not to be determined, the analysis can be terminated after the last carotenoid has been eluted, and the next sample can then be injected. However, there will be a tendency for strongly adsorbed materials, e.g. chlorophyll *c* and degradation products, to accumulate on the column. As this will cause its performance to deteriorate gradually, these compounds must be removed by eluting periodically with the second mobile phase. If used with care, the column should perform satisfactorily for several hundred injections.

Calibration

Extract the pigments from an aliquot of an appropriate species of phytoplankton which has been grown in culture to a reasonably high cell density. Inject 20 µl of the solution of the pigments in the first mobile phase into the liquid chromatograph. Develop the chromatogram and collect the fraction corresponding with each peak. Evaporate to dryness rapidly in a rotary evaporator at 30°C. Immediately dissolve the residue in 2.5 ml of an appropriate solvent (see Table 2) and measure the absorbance of the solution in a 4-cm microcuvette at the wavelength of maximum absorption of the particular pigment. Repeat the experiment with other dilutions of the extract. Plot a calibration curve of chromatographic peak height against the amount of pigment found photometrically.

RESULTS AND DISCUSSION

In order to assess the precision of the chromatographic step in the analysis, quintuplicate injections were made of an extract prepared from 200 ml of a mixed culture of *Phaeodactylum tricornutum* (Bacillariophyceae) and *Dunaliella tertiolecta* (Chlorophyceae). A typical chromatogram is shown in Fig. 2. The results of these injections are summarized in Table 3 which shows that the relative standard deviation is satisfactory, ranging from 0.6 to 1.7%. Tests were also carried out to assess the overall precision of the method by analyzing five separate 200-ml aliquots of another culture of the same organism. The results of these analyses (Table 3) indicate that the precision is considerably poorer, varying from 1.2 to 7.7%. It seems likely that much of this variation arises from the difficulty of ensuring that the phytoplankton cells are uniformly suspended in the rather dense culture at the time of sampling. This is borne out by the relative constancy of the coefficients of variation for the majority of the pigments.

Cultures of three species of phytoplankton from different classes were examined by the present method as well as by a reflectometric thin-layer chromatographic method [11] and the SCOR/UNESCO polychromatic procedure [4]. The results obtained from the latter were evaluated by the SCOR/UNESCO equations and also by the more recent ones of Jeffrey and Humphrey [5]. The carotenoids were determined collectively from the absorbance of

TABLE 3

Estimation of precision of h.p.l.c. method with a mixed algal culture

Pigment	H.p.l.c. stage only		Whole procedure	
	μg/100 ml	C.v. (%)	μg/100 ml	C.v. (%)
β-Carotene	0.74	1.1	0.24	3.7
Chlorophyll *a*	4.20	1.7	18.1	4.5
Chlorophyll *b*	2.79	0.6	17.1	4.4
Chlorophyll *c*	1.18	1.7	0.17	4.7
Lutein	0.12	1.6	0.61	4.8
Diadinoxanthin	2.91	0.6	0.14	6.7
Violaxanthin	0.25	1.5	0.91	4.5
Fucoxanthin	8.51	1.0	0.89	1.2
Neoxanthin	0.18	0.6	0.41	7.1

the 90% acetone extract at 480 nm by means of the equations of Strickland and Parsons [3]. The results of these comparative studies (Table 4) show that there is satisfactory agreement for all pigments between the two chromatographic methods. However, although the results for chlorophyll *a* by the

TABLE 4

Comparison between algal pigment analyses carried out by the present h.p.l.c. method, by re tometric t.l.c. and by the photometric method

Pigment	H.p.l.c.			T.l.c.			Polychromatic	
	μg/100 ml		% of total carotenoids	μg/100 ml		% of total carotenoids	SCOR/ UNESCO [4] μg/100 ml	Jeffrey an Humphre μg/100 m
Phaeodactylum tricornutum								
Chlorophyll *a*	2.68			2.80			2.9	3.0
Chlorophyll *b*	0.00			0.00			—0.005	—0.34
Chlorophyll *c*	0.44			0.47			0.59	0.43
β-Carotene	0.44		10.5	0.46		10.5		
Fucoxanthin	2.84	4.18	68.0	2.88	4.37	69.9	4.6	
Diadinoxanthin	0.90		21.5	1.03		23.6		
Chl. *a*: Chl. *c*	1:0.17			1:0.16			1:0.2	1:0.14
Dunaliella tertiolecta								
Chlorophyll *a*	4.53			4.40			4.3	4.5
Chlorophyll *b*	2.18			2.20			2.4	1.9
Chlorophyll *c*	0.00			0.00			0.04	0.17
β-Carotene	1.10		33.3	1.01		30.2		
Lutein	0.53	3.32	16.0	0.55	3.32	16.6	2.9	
Violaxanthin	1.27		38.5	1.33		40.2		
Neoxanthin	0.41		12.2	0.43		13.0		
Chl. *a*: Chl. *b*	1:0.48			1:0.50			1:0.52	1:0.42
Oscillatoria sp.								
Chlorophyll *a*	17.07			17.75			15.6	16.11
Chlorophyll *b*	0.00			0.00			—0.54	—2.27
Chlorophyll *c*	0.00			0.00			1.89	6.3
β-Carotene	1.97		45.3	2.08		46.8		
Echinenone	1.65	4.34	37.9	1.66	4.44	37.4	0.8	
Myxoxanthophyll	0.73		16.8	0.70		15.8		

polychromatic method were in reasonable accord with those derived chromatographically, many of those for the other chlorophylls were highly discrepant. Indeed, both versions of the polychromatic method indicated that considerable amounts of chlorophyll *c* and negative amounts of chlorophyll *b* were present in the blue-green algae *Oscillatoria* sp. which is free from both of these pigments Obviously, more work is required to reassess the polychromatic method, in particular with respect to the interference of chlorophyll degradation products, as these are nearly always present in environmental samples.

REFERENCES

1 F. A. Richards with T. G. Thompson, J. Mar. Res., 2 (1952) 150.
2 G. I. Creitz and F. A. Richards, J. Mar. Res., 14 (1955) 211.
3 J. D. H. Strickland and T. R. Parsons, A Practical Handbook of Seawater Analysis, Fisheries Research Board of Canada, 1968.
4 UNESCO Monographs on Oceanographic Methodology No. 1, 1966.
5 S. W. Jeffrey and G. H. Humphrey, Biochem. Physiol. Pflanz., 167 (1975) 191.
6 T. R. Parsons, J. Fish. Res. Bd. Can., 18 (1961) 1017.
7 S. W. Jeffrey, Biochem. J., 80 (1961) 336.
8 S. W. Jeffrey and E. B. Allen, J. Gen. Microbiol., 36 (1964) 277.
9 J. P. Riley and T. R. S. Wilson, J. Mar. Biol. Ass. U.K., 45 (1965) 583.
10 S. W. Jeffrey, Biochim. Biophys. Acta, 162 (1968) 271.
11 C. Garside and J. P. Riley, Anal. Chim. Acta, 46 (1969) 179.
12 N. Evans, D. E. Games, A. H. Jackson and S. A. Matlin, J. Chromatogr., 115 (1975) 325.
13 K. Eskins, C. R. Scholfield and H. J. Dutton, J. Chromatogr., 135 (1977) 217.
14 W. T. Shoaf, J. Chromatogr., 152 (1978) 247.
15 R. J. Hamilton and P. A. Sewell, Introduction to High Performance Liquid Chromatography, Chapman and Hall, London, 1977, 19.
16 J. D. H. Strickland, in J. P. Riley and G. Skirrow, Chemical Oceanography, Vol. I, Academic Press, London and New York, 1965, 494.
17 B. H. Davies, in T. W. Goodwin, Chemistry and Biochemistry of Plant Pigments, Vol. II, Academic Press, London and New York, 1976, 108.
18 L. P. Vernon, Anal. Chem., 32 (1960) 1144.
19 O. Isler, H. Lindlar, M. Montavon, R. Ruegg and P. Zeller, Helv. Chim. Acta, 39 (1956) 249
20 B. H. Davies, in T. W. Goodwin, Chemistry and Biochemistry of Plant Pigments, Academic Press, London and New York, 1965, 489.
21 H. H. Strain in Leaf Xanthophylls, Carnegie Institution, Washington D.C., 1938.
22 P. Karrer and E. Jacker, Helv. Chim. Acta, 26 (1943) 626.
23 C. Garside and J. P. Riley, Deep-Sea Res., 627 (1968) 15.
24 L. Cholnoky, K. Gyorgyfy, A. Ronai, J. Szablocs, Gy. To'th, G. Galasko, A. K. Mallams, E. S. Waight and B. C. L. Weedon, J. Chem. Soc. C, (1969) 1256.
25 S. Hertzberg and S. Liasen-Jensen, Phytochemistry, 8 (1969) 1259.

Analytica Chimica Acta, 107 (1979) 13—27

MINICOMPUTER-CONTROLLED, BACKGROUND-SUBTRACTED ANODIC STRIPPING VOLTAMMETRY: EVALUATION OF PARAMETERS AND PERFORMANCE[a]

STEVEN D. BROWN[b] and B. R. KOWALSKI*

Laboratory for Chemometrics, Department of Chemistry, BG-10, University of Washington, Seattle, Washington 98195 (U.S.A.)

(Received 15th January 1979)

SUMMARY

A new minicomputer-controlled anodic stripping voltammetry technique is described. The technique uses differential voltammetry at one electrode, and uses a rapid data-averaging algorithm to avoid the need for scan averaging; this allows excellent sensitivities and short analysis times, with adequate reproducibilities. Both linear-scan and staircase waveforms are discussed in conjunction with the technique, and the approximate Roe—Toni theory for linear-scan voltammetry is shown to apply. The system response is investigated for film thickness, scan rate, deposition time, electrode rotation rate, and metal concentration. Results were used to optimize the sensitivity of the technique. The metal ions Cd, Pb and Cu could be determined in solutions as dilute as 1—10 pg/ml^{-1} in 15 min. The viability of the technique in solutions showing a large background is also discussed, and a comparison is made with scan-averaged techniques.

Various approaches have been proposed with the aim of reducing the time of analysis for anodic stripping voltammetric (a.s.v.) techniques. These include the use of flow systems [1—3], thin-film electrodes [4], pulse and differential pulse techniques [5—11], rotating disk electrodes [12, 13], ring-disk electrodes [14, 15], and recently, computer-controlled instrumentation [16—22]. Most of the techniques mentioned above still utilize either long electrolysis times or long stripping times, and the actual time saving for environmentally realistic trace metal concentrations (i.e., in the parts-per-billion range and below) is small.

Both the sensitivity of the a.s.v. technique and the overall analysis time depend upon how the capacitive current contribution to the total current is removed or compensated. One approach to eliminating the capacitive contribution to the total current utilizes the concept of differential vol-

---

[a]Abstracted in part from the Dissertation of S. D. Brown, submitted in partial fulfilment of requirements for the Ph.D. degree, University of Washington.

[b]Present address: Department of Chemistry, University of California, Berkeley, CA 94720 (U.S.A.).

tammetry. Here, an attempt is made actually to measure the purely capacitive current, and to subtract it from the simultaneously measured total current, yielding only the faradaic current. This can be done by using two electrodes, one of which is placed in a solution having no depolarizer, so that no material deposits on the electrode, and essentially no faradaic current flows during a potential scan. The other electrode, placed in the analyte solution, passes both faradaic and capacitive currents during the potential scan, allowing either electronic or digital subtraction of the current generated by the first electrode from the second [23—26].

The above technique and the commoner pulse techniques are significantly better than simple linear-scan a.s.v., but both have serious disadvantages. Pulsed techniques require much slower scan rates than are feasible with linear scans, in order to allow the capacitive current to decay. By sampling after this delay, some of the faradaic current is lost, resulting in a somewhat lowered sensitivity. This has been observed for the staircase waveform in particular [21]. Differential voltammetric techniques do not involve losses of faradaic current, and are therefore quite sensitive. Both the capacitive and faradaic currents are particularly sensitive to the exact electrode surface area, however. Since no two electrode surfaces match exactly, the capacitive current is generally not well compensated.

Another method, which is a variant of differential voltammetry but uses only one electrode, has been described [16]. Here, one normal a.s.v. run with deposition step, rest period and stripping step is performed. Immediately after this a.s.v. run, the potential of the working electrode is switched to some potential where no depolarizer plates into the mercury, but where the mercury itself does not undergo dissolution. Stirring is begun, and after a set time the potential of the working electrode is switched to the rest potential, and the electrode is again scanned anodically, exactly as in the stripping step of the previous a.s.v. run. Since this scan produces essentially no faradaic current, primarily capacitive currents are observed. Thus, digital subtraction of this scan, called the background scan, from the first (analyte) scan, should remove the capacitive current contribution from the total current, leaving only faradaic current. This technique was first used for linear-scan a.s.v. by Kryger and Jagner [16—18], who combined it with a normalized averaging of multiple stripping steps. Turner et al. [22] have applied a similar approach to staircase and square-wave scan a.s.v.

Criticism has been directed toward this method of background compensation, however. Matson et al. [27] have claimed that the correction is not accurate because the activity of the film changes from analyte to background scan. For this reason, they claim that the method is poorly suited to trace analysis, particularly for metals near the mercury edge [27].

The intent of this paper is to demonstrate the accuracy and effectiveness of background subtraction methods like those first used by Kryger and Jagner [16]. Their method has, however, been improved by performing multipoint averaging in a single scan, obtaining enhanced signal-to-noise

ratios and eliminating the need for multiple scans, thus saving analysis time. To verify the efficacy of these techniques, it is demonstrated first that the approximate theory of Roe and Toni applies; then the parameters optimized from these studies are used in ultratrace analysis for some metals commonly determined by a.s.v.

THEORY

For thin-film mercury electrodes, the exact theory developed by DeVries and van Dalen [28—30] and a more approximate theory proposed by Roe and Toni [31] may be applied. Both are based on a linear scan. The theory for staircase-scan a.s.v. has been derived by Christie and Osteryoung [32].

The Roe and Toni relationships for the stripping peak current (i_p) and peak potential (E_p) are given by

$$i_p = nFAlC_R^0 \nu \cdot nF/RTe \tag{1}$$

$$E_p = E^{0\prime} + 2.3\, RT/nF^{-1} \log nF\delta l\nu/RTD_{ox} \tag{2}$$

where A is the electrode area, l the film thickness, ν the scan rate, C_R^0 the concentration of reduced species in the mercury at the start of the stripping step, D_{ox} the diffusion constant for the oxidized species, δ the thickness of the diffusion layer, e the base of Naperian logarithms, $E^{0\prime}$ the formal dissolution potential of the metal, and n, F, R and T have their usual meanings. These equations apply to a linear-scan a.s.v. experiment with a fixed diffusion layer thickness δ, generated by rotating the electrode during the scan.

Both the DeVries—van Dalen and the Roe-Toni theories have been experimentally verified for conventional a.s.v. [29, 30] with thin films and slow scans. In the limit of fast linear scans, they can be reduced to the Randles—Ševčik theory for rapid linear-scan voltammetry [33, 34]. Theoretical results obtained by DeVries [29] indicate that a thin film is needed when a fast scan rate is used, in order to maintain adequate resolution, which otherwise degrades substantially. Thus, a very fast scan rate, of the order of 1000—3000 mV s^{-1}, used in conjunction with an electrode of high surface area but low volume, should maximize the peak current and allow shorter deposition times.

During the deposition step, rotation of the electrode will substantially increase the amount of material plated onto a disk electrode, according to the Levich equation [35]:

$$i_d = 0.62nFA\, C_{ox}^0 D_{ox}^{2/3} \rho^{-1/6} \omega^{1/2} \tag{3}$$

where i_d is the deposition current, C_{ox}^0 the bulk concentration of oxidized species in solution, ρ the kinematic viscosity of the solution ($cm^2\ s^{-1}$) and $\omega = 2\pi f/60$, where f is the rotation speed in rpm.

Because high scan rates generate large capacitive currents in addition to large faradaic currents, and these currents must be compensated, background

subtraction is an obvious choice to accomplish this. A modification of the technique used by Kryger and Jagner [16—18] was chosen as the means of accomplishing background subtraction.

By combining eqns. (1) and (3) with Faraday's law:

$$C_R^0 = i_d t/nFAl \tag{4}$$

where t is the deposition time, the following equation is obtained:

$$i_p = 0.62\, n^2F^2(eRT)^{-1}\, D_{ox}^{2/3}\, \rho^{-1/6}\, \omega^{1/2}\, A\nu t C_{ox}^0 \tag{5}$$

This equation indicates linear relations between peak height and scan rate, deposition time, and bulk solution concentration. Equation (2) predicts a linear relation between the peak potential and the logarithm of the scan rate.

Verification of eqns. (2) and (5) will serve to establish the accuracy of background correction by the computer-controlled differential voltammetric technique, since one expects the most severe changes in the activities of the mercury film to be a function of the amount of reduced material contained in the film, and of the rate at which they are removed from the film. The amount contained in the film and the rate at which it is removed from the film are controlled by the deposition time and the scan rate, respectively. Further, one might expect the most stringent test of the method of background correction to be at very low analyte concentrations, as any systematic errors inherent in the background compensation will be magnified because of the very small analyte stripping peaks. For these reasons, each of the relations given by eqns. (2) and (5) were examined in turn.

EXPERIMENTAL

Cell and electrodes

The working electrode used was a commercial rotated disk electrode (RDE; Pine Instrument Company, Grove City, Pennsylvania). The body of the electrode was Teflon, and the disk was glassy carbon. Polishing, which is critical to electrode performance [12], was done as follows: after initial polishing with strips of no. 600 carborundum paper, careful polishing for 2—3 h with a suspension of 0.5-μm alumina on sebyl cloth was performed to generate a smooth surface. Subsequent gentle polishing with a suspension of 0.05-μm alumina on wet filter paper was used to obtain a mirrorlike finish. At the start of a series of runs, the electrode was briefly repolished with the 0.05-μm alumina suspension to insure a relatively constant electrode surface area. The nominal surface area of the disk was 0.45 cm^2.

The electrode was held in a Pine Instrument Company rotator, model ASR. The rotator had its lower electrode contact removed to avoid contamination of the solution with silver-loaded graphite particles [14]. The electrode was rotated at speeds ranging from 1,000 to 10,000 rpm via voltages applied to the external input by one of the digital-to-analog con-

verters provided on the computer interface. A check was made of the accuracy and precision of the speed of the rotation by monitoring the external output voltage of the rotation servomechanism circuit. Accuracy was within 1% and reproducibility was better than 0.2% when computer control was used.

The reference electrode was a Princeton Applied Research saturated calomel electrode. Electrical contact was made with the test solution by means of a bridge filled with saturated KCl, KNO_3, or NH_4NO_3 solution. The bridge tube was provided with a Vycor frit to contact the test solution; this frit was sealed into a length of heat-shrinkable Teflon tubing, so that only the frit and Teflon contacted the test solution.

The counter electrode was a length of heavy-gauge platinum wire bent into a small spiral and sealed into a glass ground joint. The purge tube contacted the test solution via a length of rigid 2-mm Teflon tubing.

The cell was a modified 200-ml clear fused silica beaker (Quartz Scientific). The top of the beaker was removed to make a container 65 mm in diameter by 70 mm in height with a capacity of 125 ml; normal analysis volumes were 65—80 ml. The reference and counter electrodes, as well as the purge tube, were held by a Teflon cover for the cell, which was also provided with a glass-stoppered port to allow easy access to the test solution for addition of reagents. The rotating disk working electrode fitted through a central opening in the cover; an annular space was provided to allow gas to escape from the otherwise airtight cell. The cell was not thermostated, but temperature fluctuations in the room were minimal (± 0.5°C).

Instrumentation

All measurements were made with a potentiostat designed to be controllable by the computer and computer-interface combination. A general-purpose interface [36] was built to allow a variety of instrumentation to be serviced by the laboratory computer. The interface was connected to a Digital Equipment Corporation (DEC) PDP-11/05 GT-40 minicomputer equipped with 24K core memory and hardware arithmetic capability, and with a Tektronix 4012 graphics terminal. Hardcopy was obtained from a Gould 5000 printer-plotter.

The potentiostat used for these studies was of conventional three-electrode design [37—40]. Input voltages were provided by two 12-bit digital-to-analog converters (DACs). DAC 1 was used to provide the electrolysis potential, which also acted as a baseline for the scan. The output scale used was ±2.5 V, allowing a resolution of 1.22 mV. DAC Ø was used to provide a voltage proportional to the desired scan rate, when linear-scan voltammetry is being performed. The output scale was +5 V, allowing a resolution of 1.22 mV s^{-1} in scan rates. For the staircase-scan technique, a single digital-to-analog converter generated the staircase directly. Output waveforms were monitored with a Tektronix T935 oscilloscope. Two logic level inputs selected the current-measuring feedback resistor by switching a CMOS

demultiplexer (an RCA CD4051 chip). Current ranges available varied from 50 to 200 μA. The output of the reference electrode amplifier was monitored with a digital voltohmmeter to obtain the potential applied to the working electrode. The potentiostat was housed in a 13 × 9 × 8-in. Vector Multi-Mod steel box for shielding, and the rotator, cell and potentiostat were placed in a Manostat glove box for protection from dust.

With this potentiostat, a variety of waveforms can be applied to the cell, including linear scan and a number of square wave-based functions. In this study, however, only linear-scan and staircase waveforms were used. The linear-scan waveform is shown in Fig. 1. Linear-scan rates of up to 5000 mV s^{-1} were possible, but all work reported here used rates of 100—3000 mV s^{-1}. Staircase step heights based on multiples of 1.22 mV/step were possible, but step heights of 4.88 mV were used to obtain reasonable sensitivity as well as good peak resolution [32]; large step heights degrade peak resolution, while small step heights are significantly less sensitive.

The band width of the potentiostat was measured by the method of Booman and Holbrook [37], and showed a —3db cutoff at 14 kHz.

Reagents

The hydrochloric and nitric acids, as well as the KCl, were Ultrex grade, (J. T. Baker Co.). Potassium nitrate, sodium acetate and acetic acid (all Baker Analyzed Reagents), perchloric acid and sodium hydrogencarbonate (both Mallinckrodt analytical grade) were also used. Airco pre-purified nitrogen, further purified by passage through a gas washing bottle containing vanadium(II) ions, and a second gas washing bottle containing supporting electrolyte, was used to remove oxygen from the test solution.

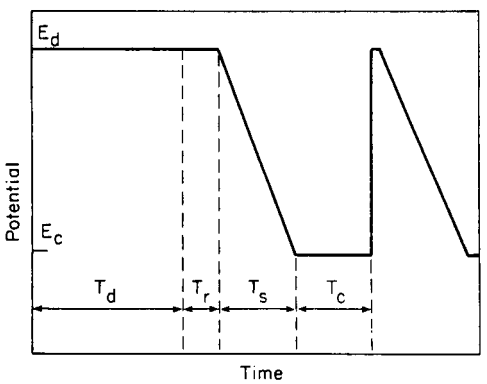

Fig. 1. Waveform used for linear-scan a.s.v. E_d is the deposition potential, E_c the film stripping potential, T_r is the rest period, T_s the scan time, and T_c the film stripping time.

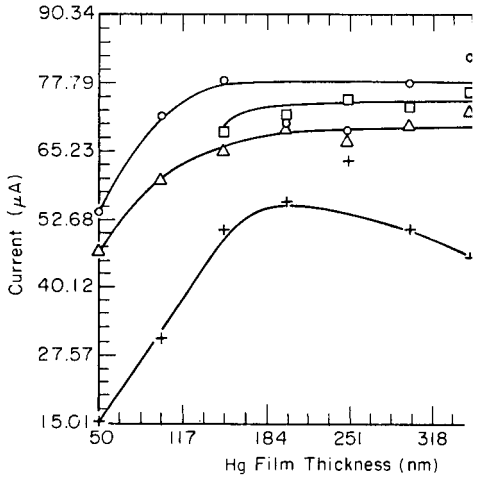

Fig. 2. Peak heights as a function of mercury film thickness. (□) Zn; (○) Cd; (△) Pb; (+) Cu.

The mercury(II) plating solution was prepared by dissolving mercury (Baker Instrumental Grade) in a minimum amount of Ultrex HNO_3, and diluting to give a 0.01 M $Hg(NO_3)_2$ solution.

Standard solutions were prepared by dissolving the appropriate salts (Alpha-Ventron ultrapure) in a minimum of Ultrex HNO_3, heating, and diluting to make 1000-ppm solutions. All solutions were prepared with water purified by passage through a high-efficiency, mixed-bed ion-exchanger (Corning 3508-B) and subsequently distilled in a Corning AG-2 still. Distilled water and all solutions were stored in thoroughly pre-leached linear polyethylene bottles to avoid severe contamination [41—44]. Analysis of water prepared in this way, by the a.s.v. technique reported here, showed metal concentrations well below ppb levels, with the primary contaminant being zinc, probably because of atmospheric fallout. The water was used within 72 h.

For studies on the sensitivity of the technique, specially purified water was prepared by repeatedly distilling the distilled water, and collecting it in a thoroughly pre-leached (with Ultrex HCl and HNO_3) Teflon FEP 1-l bottle. This water was used at once.

For all studies, the solutions of buffers used as supporting electrolytes were carefully purified by prolonged electrolysis over a mercury pool in a Princeton Applied Research electrolytic purification unit, with a PAR 174A as the means of controlling the potential. Electrolyses usually spanned 2 to 3 weeks at a potential of at least —1.6 V vs. SCE. These solutions were stored in pre-leached polyethylene bottles, or used at once for the ultratrace analysis studies. Blank levels for materials prepared in this manner were 1—10 pg ml^{-1} elements observable by a.s.v.

Solutions were transferred with an Eppendorf 100-μl pipette with disposable tips that had been pre-leached in an 8 M solution of Ultrex HNO_3 in distilled water. All glassware was leached with 5 M HNO_3 between uses, and the cell and electrodes were stored in ultrapure 5 M HNO_3 between analyses. A Beckman 4500 pH meter was used to measure the pH values of solutions.

Stripping voltammetry

To insure constant film thicknesses, a pre-plated thin-film electrode was used. Films were formed at —1000 mV vs. SCE, as it is claimed that such films are homogeneous [45]. Plating was done under computer control, and films were found to be reproducible to 1% by placing a silver coulometer in series with the cell. Film thicknesses were calculated assuming 100% efficiency [21] and homogeneous coverage. After plating, the electrode was maintained at —35 mV vs. SCE to remove impurities in the mercury film, but not to remove the film itself.

After preparation of the electrode, the cell was disconnected, rinsed with 3 M Ultrex HNO_3, and distilled water. The reference and counter electrodes were also rinsed with HNO_3 and water, and then the sample solution was introduced and purged for 5 min by bubbling nitrogen while rotating the working electrode at 1500 rpm. Before the deposition step, the nitrogen stream was diverted over the solution.

The a.s.v. experiment proceeded under complete program control, with parameters selected by the operator. The program monitored the deposition time and electrode rotation, performed the analyte scan, by using a variable point average, then performed the background scan, again by using point averaging, and any digital filtering [46] requested by the operator. The data were automatically checked for overflow, and displayed on the terminal. Data were stored on floppy disks for future reference.

The a.s.v. program consists of a FORTRAN driver with MACRO assembly-language subroutines to provide for linear-scan a.s.v., staircase-scan a.s.v., Fourier-domain digital filtering, data examination and storage. Although multiple normalized scans are possible [16], this capability was not used, for reasons discussed below. Details of this program will be furnished upon request.

Automatic multiple standard addition runs were used for the determination of metals.

RESULTS AND DISCUSSION

Effects of mercury film thickness on system response

In order to determine the optimal mercury film thickness for the determinations of Zn, Pb, Cd and Cu, a 75-ml solution of 0.1 M acetate buffer (pH 5.62), containing a spike of Cu, Zn, Pb, and Cd so that concentrations of the metals were 1 ng ml^{-1} in each case, was analyzed by linear-scan a.s.v. with the background correction. A single scan, based on a 16-point average, was used to analyze the solution. Mercury film thicknesses of 50 nm to 350 nm were used, and at least four runs were performed for each film thickness, with only the average results being reported here. Figure 2 summarizes the results found; it is clear that, for mercury films above 150 nm in thickness, the response is essentially constant, except in the case of copper, which shows an optimum response with mercury films having thicknesses between 200 and 250 nm. Zinc gave irreproducible values at very thin mercury films, and these are not plotted. These results agree with those of Pinchin and Newham [47] fairly well, although those authors found increased sensitivity for copper when very thin mercury films were employed.

Effects of deposition time and scan rate

The effects of varying deposition time on the peak heights of Pb, Cd and Zn were investigated. A 75-ml solution of 0.01 M acetate buffer, containing 1.66 ng Pb ml^{-1}, 4.33 ng Cd ml^{-1} and 0.80 ng Zn ml^{-1} (as determined by subsequent analysis of the solution) was examined. In all three cases, linear relations were observed for deposition times of 30—300 s. Least-squares slopes of 0.0297 $\mu A\ s^{-1}$ (Zn), 0.145 $\mu A\ s^{-1}$ (Pb) and 0.312 $\mu A\ s^{-1}$ (Cd) were observed, all with regression coefficients above 0.992. These results indicate from examination of slopes that the technique is more sensitive to Cd than

Pb or Zn, at least for the concentrations studied. Similar results have been obtained for conventional a.s.v. [47].

According to both the exact theory of linear-scan a.s.v. [30], and the approximate theory given by eqn. (5), peak heights should be linearly related to the scan rate. Peak widths should also increase with increasing scan rate, up to the limit of 101 mV predicted by Ševčik and Randles [33, 34]. The Ševčik—Randles theory shows a square-root relation between scan rate and peak height, however.

The same solution used for the deposition studies was used to study the effects of scan rate. Again, a linear relation was obtained in all cases. Least-squares slopes were observed to be 0.0117 μA s mV^{-1} for Pb, 0.0313 μA s mV^{-1} for Cd and 0.0087 μA s mV^{-1} for Zn; regression coefficients ranged from 0.972 for Pb to 0.997 for Cd. Peak width also increased, as can be seen from Table 1, where peak widths of the cadmium stripping peak are listed as a function of the scan rate; the maximum value observed, 100 mV, is in good agreement with the value predicted by theory. This agreement indicates the adequacy of eqn. (5) for rates up to 3500 mV s^{-1}, as system response is not noticeably degraded. It further indicates that the Ševčik—Randles limiting case is not reached for scan-rate effects on i_p, as there is no apparent tendency toward a square-root relation at high scan rates.

Effects of electrode rotation

Equation (5) predicts a linear relation between the square root of the electrode rotation rate and the peak height. Since the electrode rotation rate also affects the amount deposited by changing the diffusion layer, peak height was studied as a function of the square root of the electrode rotation rate. Again, linear response was found for rotation rates between 1000 and 6500 rpm. Least-squares slopes were 0.350 μA rpm$^{-1/2}$ for Pb and 0.738 μA rpm$^{-1/2}$ for Cd; regression coefficients were above 0.992. Above 6500 rpm, turbulence was observed in the solution, and bubbles were

TABLE 1

Effects of scan rate on cadmium peak halfwidth

Scan rate (mV s^{-1})	Peak height (μA)	Peak width[a] (mV)	Scan rate (mV s^{-1})	Peak height (μA)	Peak width[a] (mV)
3333	108	100	572	25	78
2850	95	100	500	23	77
2000	69	92	333	18	76
1330	50	88	250	13	75
1000	40	80	200	10.7	68
800	33	78	166	9.1	68
667	29	78	143	8.0	66

[a]Measured at half-height.

noticed at the electrode. Stripping currents were severely depressed as a result; rotations above 6500 rpm were thus not accessible with the cell design used here.

Peak position as a function of scan rate

Equation (2) predicts a logarithmic relation between scan rate and the shift in the peak potential for any given peak. The effects of varying scan rate on the peak potential for Pb, Cd, and Zn were investigated. Results were linear, with least-squares slopes of 63.3 mV for Pb, 68.5 mV for Cd and 71.3 mV for Zn. Regression coefficients ranged from 0.988 to 0.990. Since the three metals examined are capable of transferring two electrons, slopes of 29.5 mV should have resulted. In fact, the slopes are considerably higher, and potential shifts are more than predicted by theory, which could be the result of several factors. One possible cause is uncompensated resistance between reference and working electrodes, for potential shifts will result from any uncompensated resistance in the solution. Since larger currents result from rapid scan rates, the iR drop associated with any given scan rate also increases linearly with scan rate, having the effect of causing an additional potential shift to the peak in an anodic direction. Since the iR drop responds both to capacitive as well as faradaic current, even a small uncompensated resistance can lead to shifts of the order of those observed.

A second possible cause of the discrepancy is the assumption implicit in eqn. (2) of a constant diffusion layer δ, despite the fact that the scan rate is increased by a factor of about 250 through the runs. Since the peak potential depends linearly on δ as well as ν, the scan rate, changes in δ with ν will give anomalously high values for the slope of a plot of E_p versus log ν. This is exactly the situation observed here. A third factor in the discrepancy is the assumption of thin films and slow scan rates in the derivation of eqn. (2) [31]. Since the scan rates used in this study are by no means slow, there is no certainty that the theory should hold exactly.

It is likely that iR drop as well as changing thickness of the diffusion layer contribute to the error observed. No special effort was made in this work to optimize the cell geometry to minimize the iR drop, nor was positive feedback iR compensation employed [40] in these studies, and thus some small uncompensated resistance is likely in the 0.1 M supporting electrolyte used. If a 10 Ω resistance is assumed, a full-scale (150 μA) current gives rise to an error of 1.5 mV in the potential applied to the electrode; the shifts observed are of this order for slower scan rates. Since shifts of much greater magnitude are observed for the faster scan rates, changes in the diffusion layer must also be suspected. Errors here would be small at slow scan rates, but larger at the higher scan rates.

System response to metal concentration

Equation (5) predicts a linear response to changes in metal concentration and this response has been verified many times (see, e.g. [48]) in conventional

a.s.v. In background-subtracted a.s.v., work by Kryger and Jagner [17] has shown a linear response in the higher ng ml^{-1} range, but it is in the lower ng ml^{-1} and pg ml^{-1} ranges that this technique is most useful because of its speed and sensitivity, and it is in these ranges that any substantial systematic errors caused by major differences in film activity from analyte to background scan will become obvious.

For these reasons, the response of the system to pg ml^{-1} levels of trace metals was studied with the aims of verifying the Roe and Toni equation (eqn. 5) in these ranges, of establishing a detection limit for an optimized set of system parameters, and of observing the ability of the system to compensate background currents in very clean solutions.

A carefully purified 0.1 M acetate buffer was used for the simultaneous determination of ultra-trace levels of cadmium and lead. Plating at −800 mV (vs. SCE) for 300 s, followed by a single, rapid scan from −800 to −10 mV (vs. SCE) produced reasonable peaks. Figure 3 shows the determination of cadmium in one such solution, and Fig. 4 shows the plot for the simultaneous determination; there, increments of 7 pg ml^{-1} each of Pb and Cd were used to check the buffer purity. As can be seen from the two slopes, the system is slightly more sensitive to cadmium than to lead at pg ml^{-1} levels. Zinc was not examined, as clean buffers (pg ml^{-1}) could not be obtained with respect to this element.

For similar concentrations of copper, system response is also linear, but other factors also appear. A carefully purified 0.1 M KCl buffer was used to investigate the determination of copper at pg ml^{-1} levels. A 300-s deposi-

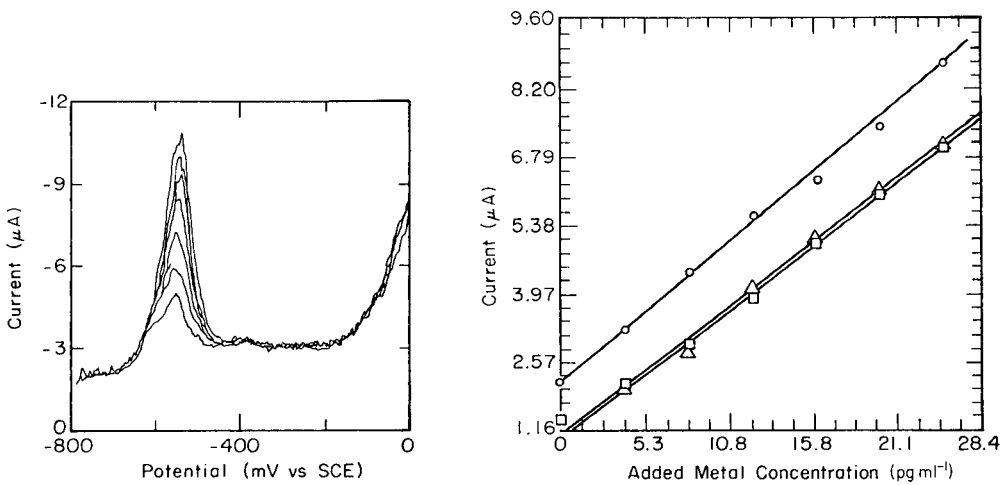

Fig. 3. Determination of cadmium at the pg ml^{-1} level corresponding to the concentrations shown in Fig. 4. The low background current and flat baseline indicate the accuracy of background correction.

Fig. 4. Standard addition plot for pg ml^{-1} levels of lead and cadmium. (□) Fourier-transformed Pb; (○) Cd; (△) Pb.

tion at —600 mV (vs. SCE), followed by a single, rapid scan to 0 mV was used, and reasonable peaks resulted. Peak quality and S/N ratio was not as good as for the Cd and Pb run, however. A least-squares slope of 0.29 μA ml pg^{-1} was obtained for solutions containing 18—49 pg Cu ml^{-1}. A blank Cu concentration of 18 pg ml^{-1} was determined by standard additions.

The constancy of the copper peak width and the symmetrical peak shape suggest that no unusual effects, such as those observed in conventional a.s.v. by Pinchin and Newham [47], occur in these concentration ranges. The peak widths (90 mV) were consistent with, but slightly larger than, widths observed at similar scan rates (900 mV s^{-1}). Some broadening of the peak for copper is indicated, as has been observed by Florence and Batley [49] in chloride solutions containing copper. Upon increasing the total copper concentration beyond about 50 pg ml^{-1}, deviations from linearity resulted; for much larger concentrations, of the order of ng ml^{-1}, peak shapes deteriorated substantially in chloride buffer, as observed by Pinchin and Newham [47]. In this case, determinations of copper in acetate buffer are superior. A comparison of the slopes of Fig. 4 with the slope observed for copper response indicates the lower sensitivity of a.s.v. for copper in chloride solution, as observed by Florence and Batley [49].

In no case was any distortion of peak shape observed that could be attributed to the background correction, in contrast to some claims [27].

System reproducibility and sensitivity

Various samples were analyzed to evaluate the reproducibility of background correction. Reproducibilities of 1—2% were readily obtainable for concentrations in the ng ml^{-1} range, while only slightly poorer reproducibilities (4—5%) were obtained at the pg ml^{-1} level. These results, run on the same film, are substantially better than the pg ml^{-1} reproducibilities previously reported [50], where values varied by 20—30%, primarily because of long (30 min) deposition times.

Another factor involved with reproducibility is the system signal-to-noise level. It was observed that the noise was largely constant for a given supporting electrolyte concentration and gain range. For a supporting electrolyte of 0.1 M KNO_3 and a full-scale range of 144 μA, the standard deviation of the noise was observed to be about 0.6 μA. With the 16-point average, the noise was reduced to 0.15 μA, a more acceptable level. With this noise level, noise-related fluctuations in the peak heights for all but the most dilute (pg ml^{-1}) solutions become relatively unimportant, in view of the variation of the value of the diffusion constant with temperature (about 1% deg^{-1}) [51]. Since the cell was not thermostated, this uncertainty became dominant in the determination of peak heights.

If the 0.15-μA value for noise is used, an approximate detection limit may be calculated, ignoring peak-height errors caused by temperature. The slopes of the calibration lines for Cd, Pb and Cu are given along with 4σ noise levels in Table 2. Detection limits on the order of 1 pg ml^{-1} are

TABLE 2

Sensitivity and approximate detection limits for cadmium, lead and copper

Element	Slope (μA ml pg^{-1})	4σ detection limit (pg ml^{-1})
Cd	1.11	0.54
Pb	0.85	0.71
Cu	0.29	2.1

readily achievable by the method. Inclusion of the 1% relative error of the diffusion constant will slightly increase these limits. Other contributions to the overall error are not as important.

Multiple scanning parameters

The use of multiple stripping scans [16—18] was avoided by using a multipoint averaging algorithm, which allowed very good *S/N* ratios in a single analyte scan followed by a single background scan, and resulted in considerable time savings.

Generally, 16—20 points were added to obtain a single data point; this requires a fast sampling rate, however. Although the system used [36] is capable of approximate sampling rates of 50—55 kHz, rates of 10—12 kHz were selected, to allow time for data checking and other overheads. A comparison of theoretical *S/N* ratios for multipoint averaging and multiscan averaging shows that the multiscan method will have a lower *S/N* than the multipoint method, because $\Sigma_{i=1}^{k}$ (fraction collected)$^{i-1} \leqslant k$, where k is the number of scans or points averaged, and the fraction collected is always less than 1 because of diffusion. In fact, with the fraction collected equal to 0.8 and k = 16, the multipoint method enjoys a *S/N* advantage of about 3, as well as the savings of time, scanning in a total of about 2 s as compared to 32 s for the multiscan method.

Staircase a.s.v. parameters

Background-corrected staircase-scan a.s.v. was also investigated and found to give linear relations for deposition time, but the sensitivity was considerably less than that observed for rapid linear-scan a.s.v. Baselines were only slightly better, while peak widths were much narrower.

Conclusions

The Roe and Toni equations hold well for background-subtracted, rapid-scan voltammetry. In all cases, the background subtraction does not appear to bias results by contributing systematic errors from the compensation process, even in very dilute solution. Peak widths are somewhat broadened by the fast scans, and peak shifts are more than those predicted by theory, however.

A multipoint-averaged single-scan background compensation technique

adds very little time to an analysis, requiring only a 5-min analysis time for solutions in the pg ml^{-1} range, and 1—2 min for more concentrated solutions. Somewhat longer analysis times with slightly lower sensitivities may be expected from multiple scanning techniques. Precision is excellent, with reproducibilities of less than 5% in very dilute solution.

From the evidence discussed above, the accuracy of background correction is clearly quite good, as is its reproducibility. Thus, the method must be regarded as an acceptable one for rapid-scan a.s.v., and particularly suited to ultra-trace determination because of its speed and sensitivity.

This work was partially supported by the Office of Naval Research. S.D.B. gratefully acknowledges the support during the 1977—78 year of an American Chemical Society Analytical Division Fellowship, sponsored by the Perkin-Elmer Corporation.

REFERENCES

1 S. H. Liberman and A. Zirino, Anal. Chem., 46 (1974) 20.
2 J. Wang and M. Ariel, J. Electroanal. Chem., 83 (1977) 217.
3 J. Wang and M. Ariel, J. Electroanal. Chem., 85 (1977) 289.
4 W. R. Matson, D. K. Roe and D. F. Carritt, Anal. Chem., 37 (1965) 1594.
5 E. P. Parry and R. A. Osteryoung, Anal. Chem., 37 (1965) 1634.
6 G. Barker and A. W. Gardner, Fresenius Z. Anal. Chem., 173 (1960) 79.
7 J. B. Flato, Anal. Chem., 44 (1972) 75A.
8 H. Sigerman and G. O'Dom, Am. Lab., 4 (6) (1972) 59.
9 G. D. Christian, J. Electroanal. Chem., 23 (1969) 1.
10 T. R. Copeland, J. H. Christie, R. A. Osteryoung and R. K. Skogerboe, Anal. Chem., 45 (1973) 2171.
11 P. Valenta, H. Rutzil, H. W. Nürnberg and M. Stoeppler, Fresenius Z. Anal. Chem., 285 (1977) 25.
12 T. M. Florence, J. Electroanal. Chem., 27 (1970) 273; 35 (1972) 237.
13 A. H. Miguel and C. M. Jankowski, Anal. Chem., 46 (1974) 1832.
14 R. E. Allen, Dissertation, Iowa State University, 1974.
15 R. E. Allen and D. C. Johnson, Talanta, 20 (1973) 305.
16 L. Kryger, D. Jagner and H. J. Skov, Anal. Chim. Acta, 78 (1975) 241.
17 L. Kryger and D. Jagner, Anal. Chim. Acta, 78 (1975) 251.
18 D. Jagner and L. Kryger, Anal. Chim. Acta, 80 (1975) 255.
19 M. Bos, Anal. Chim. Acta, 81 (1976) 21.
20 A. M. Bond and B. S. Grabarić, Anal. Chim. Acta, 88 (1977) 227.
21 U. Eisner, J. A. Turner and R. A. Osteryoung, Anal. Chem., 48 (1976) 1603.
22 J. A. Turner, U. Eisner and R. A. Osteryoung, Anal. Chim. Acta, 90 (1977) 25.
23 A. Zirino and M. Healy, Environ. Sci. Technol., 6 (1972) 243.
24 L. Sipos, P. Valenta, H. W. Nürnberg and M. Branica, J. Electroanal. Chem., 77 (1977) 263.
25 L. Sipos, S. Kozar, I. Kontusim and M. Branica, J. Electroanal. Chem., 87 (1978) 347.
26 E. Steeman, E. Temmerman and R. Verbennen, Anal. Chim. Acta, 96 (1978) 177.
27 W. R. Matson, E. Zink and R. Vitukevitch, Am. Lab., 9 (7) (1977) 59.
28 W. T. DeVries and E. van Dalen, J. Electroanal. Chem., 8 (1964) 366.
29 W. T. DeVries, J. Electroanal. Chem., 9 (1965) 448.
30 W. T. DeVries and E. van Dalen, J. Electroanal. Chem., 14 (1967) 315.

31 D. K. Roe and J. E. A. Toni, Anal. Chem., 37 (1965) 1503.
32 J. H. Christie and R. A. Osteryoung, Anal. Chem., 48 (1976) 869.
33 J. E. B. Randles, Trans. Faraday Soc., 44 (1948) 327.
34 A. Ševčik, Collect. Czech. Chem. Commun., 13 (1948) 349.
35 V. E. Levich, Physiochemical Hydrodynamics, Prentice-Hall, Englewood Cliffs, N.J., 1962.
36 J. D. S. Danielson, S. D. Brown, C. J. Appellof and B. R. Kowalski, ONR Technical Report, 1978.
37 G. L. Booman and W. B. Holbrook, Anal. Chem., 35 (1963) 1793.
38 W. W. Schwartz and I. Shain, Anal. Chem., 35 (1963) 1770.
39 G. L. Booman and W. B. Holbrook, Anal. Chem., 37 (1965) 795.
40 R. R. Schroeder and I. Shain, Chem. Instrum., 1 (1969) 233.
41 D. E. Robertson, in M. Zief and R. Speights (Eds.), Ultrapurity: Methods and Techniques, M. Dekker, New York, N.Y., 1972, p. 207.
42 M. Zief and J. W. Mitchell, Contamination Control in Trace Metal Analysis, J. Wiley, New York, 1976.
43 J. R. Moody and R. M. Lindstrom, Anal. Chem., 49 (1977) 2264.
44 R. W. Dabeka, A. Mykytiuk, S. S. Berman and D. S. Russell, Anal. Chem., 48 (1976) 1203.
45 M. Stulikova, J. Electroanal. Chem., 48 (1973) 33.
46 J. W. Hayes, D. E. Glover, D. E. Smither and M. W. Overton, Anal. Chem., 45 (1973) 277.
47 M. J. Pinchin and J. Newham, Anal. Chim. Acta, 90 (1977) 91.
48 W. Lund and M. Salberg, Anal. Chim. Acta, 76 (1975) 131.
49 T. M. Florence and G. E. Batley, J. Electroanal. Chem., 75 (1977) 791.
50 H. W. Nürnberg, P. Valenta, L. Mart, B. Raspor and L. Sipos, Fresenius Z. Anal. Chem., 282 (1976) 357.
51 E. Barendrecht, in A. J. Bard (Ed.), Electroanalytical Chemistry, Vol. 2, M. Dekker, New York, 1967, p. 53.

Analytica Chimica Acta, 107 (1979) 29—35

POTENTIOMETRIC STRIPPING ANALYSIS FOR ZINC, CADMIUM, LEAD AND COPPER IN SEA WATER

DANIEL JAGNER* and KERSTIN ÅRÉN

Department of Analytical Chemistry, University of Göteborg and Chalmers University of Technology, Fack, S-402 20 Göteborg (Sweden)

(Received 20th November 1978)

SUMMARY

Analytical procedures for the determination of zinc(II), cadmium (II), lead(II) and copper(II) in sea water by potentiometric stripping analysis are described. The results are compared with those obtained by a combined solvent extraction-atomic absorption method both in the laboratory and on-board ship. The detection limits for zinc, cadmium, lead and copper are 0.03, 0.03, 0,01 and 0.02 $\mu g\ l^{-1}$, respectively, for a total analysis time of about 75 min. A very thin mercury film is useful in the determination of lead and copper.

Potentiometric stripping analysis is based on the preconcentration of the trace metal analytes by means of potentiostatic reduction and amalgamation on a glassy carbon working electrode in a deaerated sample [1, 2]. After preconcentration, the potentiostatic circuitry is disconnected and the potential between the working electrode and a calomel reference electrode is recorded on a high-input impedance x-t recorder or on a pH meter [3]. Disconnection of the potentiostatic circuitry causes the amalgamated metals to be reoxidized consecutively. Mercury(II) ions, added to the sample prior to analysis, are normally used as oxidizing agent. The mercury(II) ions are also used for the formation of the thin mercury film which coats the glassy carbon electrode during potentiostatic reduction and amalgamation (plating) of the trace metal analytes.

Since potentiometric stripping analysis can be performed with very simple and easily automated instrumentation, it was considered of interest to investigate whether or not the technique could be used for the determination of some heavy metals in sea water.

EXPERIMENTAL

Chemicals

All chemicals used, except mercury(II) nitrate, were of Suprapur (Merck) grade. The 1000-ppm mercury(II) nitrate stock solution contained less than 0.2 $\mu g\ l^{-1}$ of zinc, cadmium, lead and copper.

Apparatus

The Potentiometric Stripping Analyzer (Radiometer, prototype) could be programmed to yield plating times of 1, 2, 4 to 64 min and plating potentials between 0 and −2 V vs. SCE. Two seconds before the end of the plating time, the recorder was started automatically and the paper feed was terminated after 1/16 of the plating time chosen. A new plating/stripping cycle was then initiated automatically. Polyethylene or glass beakers (65-ml capacity; Radiometer) were used as electrochemical cells. Stirring at a constant rate was achieved by a three-edged Teflon stirrer operated mechanically or by a magnetic stirrer bar.

The glassy carbon working electrode (Radiometer F 3500) had a total surface area of 8 mm^2 and was pressure-fitted into a Teflon rod with an outer diameter of 7 mm. No glue of any kind was used in the electrode. A saturated calomel electrode (Radiometer K 4040) was used as reference and a platinum foil (Radiometer P 10402) as counter electrode. All electrodes could be screwed tightly into the lid of the electrochemical cell. Inert gas could be bubbled through the cell by means of special inlets and outlets.

Atomic absorption measurements were done with a Perkin-Elmer 370 spectrometer equipped with an HGA 2100 graphite furnace atomizer.

Sampling

The sea water samples were acidified with hydrochloric acid to 0.1 M immediately after sampling and stored in polyethylene flasks.

Analytical procedures

Determination of cadmium, lead and copper. To 50 ml of the acidified sea water sample, mercury(II) ions are added to give a total concentration of 2—4 mg l^{-1}. The sample is placed in the analyzer, the stirrer is started, and a stream of nitrogen is passed through the sample at a rate of about 200 ml min^{-1}. The glassy carbon electrode is polished with 3-μm diamond paste for 10 s, rinsed carefully with acetone and then placed in position. The Analyzer is adjusted to a plating potential of −0.95 V vs. SCE and a plating time of 1 min. At least eight plating/stripping cycles, each cycle comprising 60 s of plating and 15 s of stripping, are then performed automatically. During this procedure, the sample is deaerated and the glassy carbon electrode is coated with a thin film of mercury. Immediately after completion of the last plating/stripping cycle, the plating potential and the plating time are adjusted to the value to be used during the subsequent analysis. Plating times are chosen as either 32 or 64 min, depending on the expected concentrations of trace metals. Immediately after the stripping curve has been recorded, a standard aliquot containing typically 0.5 μg Cd l^{-1}, 1.0 μg Pb l^{-1}, and 2.0 μg Cu l^{-1} is added to the sample. The standard solution should be sufficiently concentrated that the dilution effect can be neglected. After the addition of the standard aliquot, the Analyzer automatically starts the next plating/stripping cycle. If the mercury-coated glassy electrode is allowed to remain in contact with the

mercury(II)-containing sample for several minutes without an applied reducing potential, calomel may form on the surface [2, 3]. This will result in decreased sensitivity, especially for copper(II).

The analytical signal for each element is taken as the interval of time between two consecutive equivalence points on the time—potential curve [1—3]. The concentrations of the trace elements are evaluated by means of the normal equations for standard addition analysis.

Determination of zinc, cadmium and lead. To 50 ml of the acidified sea water, approximately 0.2 M sodium acetate is added to bring the pH value to about 4.7. After the addition of mercury(II) (2—4 mg l^{-1}), the buffered sample is transferred to the Analyzer and nitrogen (200 ml min^{-1}) is passed for deaeration. The glassy carbon electrode is polished, and coated with a thin mercury film exactly as described for the determination of cadmium, lead and copper. Immediately after completion of the last plating/stripping cycle, the plating potential is adjusted to —1.25 V vs. SCE and the plating time to the value to be used in the subsequent analysis, normally 32 or 64 min. After completion of the first plating/stripping cycle, standard aliquots containing typically 2.0 μg Zn l^{-1}, 0.5 μg Cd l^{-1} and 1.0 μg Pb l^{-1} are added and the next plating/stripping cycle is started automatically.

The lead and cadmium concentrations are evaluated from the normal standard addition procedure. Zinc and copper form a 1:1 intermetallic compound in the very thin mercury film on the glassy carbon electrode [4]. This compound is stripped at a potential very close to the stripping potential for copper. The zinc stripping plateau at approximately —1.0 V is consequently proportional to the difference between the zinc and copper concentrations in the sample. If the copper concentration is higher than the zinc concentration, which is seldom the case in sea water, no zinc plateau will be obtained. On addition of a standard aliquot of zinc a plateau will, however, appear, unless the sea water is heavily contaminated with copper. The zinc concentration can thus be determined only if the copper concentration is determined separately, e.g. by the procedure described above.

A.a.s. determination of trace metals. The combined solvent extraction—atomic absorption method used in the comparison between the two analytical methods has already been described elsewhere [5]. Briefly, it comprises solvent extraction with ammonium tetramethylenedithiocarbamate and *N*, *N*-diethylammonium diethyldithiocarbamate as mixed reagent and Freon as solvent. After back-extraction into nitric acid, the trace elements are determined by graphite-furnace analysis or, for zinc, by flame a.a.s.

RESULTS

Precision and detection limits

Curve (a) of Fig. 1 shows the potentiometric stripping curve recorded for 50.3 g of a Baltic sea-water sample buffered at pH 4.6 with acetate, after

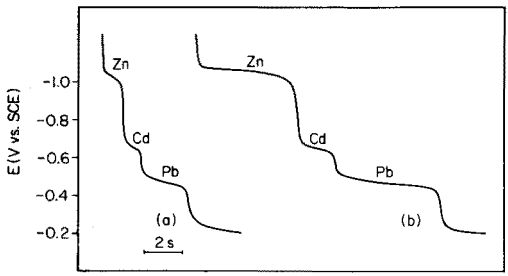

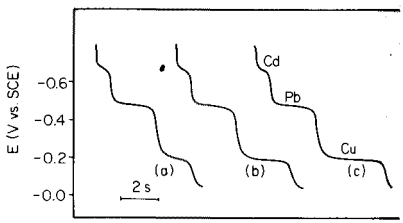

Fig. 1. Potentiometric stripping curve obtanied for a Baltic sea water sample before (curve a) and after (curve b) the addition of cadmium(II) (0.5 $\mu g\ l^{-1}$) zinc(II) (2.5 $\mu g\ l^{-1}$) and lead(II) (2.5 $\mu g\ l^{-1}$). Plating for 45 min at −1.25 V vs. SCE.

Fig. 2. Potentiometric stripping curve obtained for a Baltic sea water sample before (curve a) and after the addition of copper(II) to give concentrations of 2.5 $\mu g\ l^{-1}$ (curve b) and 5 $\mu g\ l^{-1}$ (curve c). Plating for 15 min at −80 V vs. SCE.

plating for 45 min at −1.25 V. Curve (b) shows the stripping curve recorded under the same experimental conditions after standard addition of cadium(II), lead(II) and zinc(II). Figure 2 shows the potentiometric stripping curves recorded during the subsequent determination of copper(II) in the same sample. The curves were recorded after plating for 15 min at −0.80 V; curves (b) and (c) correspond to standard additions of copper(II). The cadmium and lead signals in curves (a–c) of Fig. 2 correspond to the standard addition of cadmium(II) (1.0 $\mu g\ l^{-1}$ and lead(II) (5 $\mu g\ l^{-1}$) prior to the copper analysis, i.e. two standard aliquots of which only one (curve b) is shown in Fig. 1. From the results shown in Figs. 1 and 2, the concentrations of zinc(II), cadmium(II), lead(II) and copper(II) in the sea water were evaluated as 3.9, 0.24, 0.70 and 3.4 $\mu g\ l^{-1}$, respectively.

The reproducibility of potentiometric stripping analysis can be estimated from the cadmium and lead signals shown in Fig. 2. The relative standard deviation on consecutive plating/stripping in the same sample is typically 3–5% for cadmium and lead and 4–6% for zinc and copper.

The detection limits in potentiometric stripping analysis cannot be defined uniquely because they are inversely proportional to the plating time. If the maximum practical plating time is assumed to be 64 min, the detection limits for zinc(II) cadmium(II) and lead(II) in sea water can be estimated from Figs. 1 and 2 as 0.03 $\mu g\ l^{-1}$ and for copper(II) as 0.06 $\mu g\ l^{-1}$.

Accuracy

The accuracy of potentiometric stripping analysis in saline waters in the laboratory and during on-board analysis was estimated by comparison with the results obtained by the solvent extraction–a.a.s. method. Samples were taken during two different cruises on the Baltic. During the first cruise (BOSEX-77, Baltic Open Sea Experiment, September 1977), acidified samples were brought to the laboratory for subsequent analysis, whereas during the

second Baltic cruise (Soviet—Swedish expedition, April 1978) samples were analysed on-board. Extraction and back-extraction into nitric acid for the atomic absorption measurements was done on-board during both cruises.

Figure 3 shows the results from the analysis of eight different BOSEX samples by potentiometric stripping analysis and by atomic absorption spectrometry. While the results for zinc, cadmium and copper agree satisfactorily, the potentiometric stripping results for lead are significantly higher than the results obtained by a.a.s. The same tendency was shown in the on-board experiments. The mean cadmium value for 33 samples was 0.074 $\mu g\ l^{-1}$ by potentiometric stripping analysis and 0.056 $\mu g\ l^{-1}$ by atomic absorption. The corresponding values for copper(II) were 1.03 and 0.83 $\mu g\ l^{-1}$, respectively. The mean value for lead(II) — 0.51 $\mu g\ l^{-1}$ — obtained by potentiometric stripping was, however, more than twice as high as that obtained by atomic absorption spectrometry. This difference can be partly explained by contamination, because the on-board laboratory was not suitable for trace metal analysis. The difference is, however, so great that contamination can hardly be the only explanation. Furthermore, recent analysis of Baltic samples by anodic stripping voltammetry yielded similarly high lead values [6]. This seems to indicate that the amalgamated lead is affected by some constituent present in sea water. It is, however, difficult to explain why such constituents do not also affect the lead signal obtained from the standard aliquot added during standard addition analysis. Interference from Sn(IV) is, however, pos-

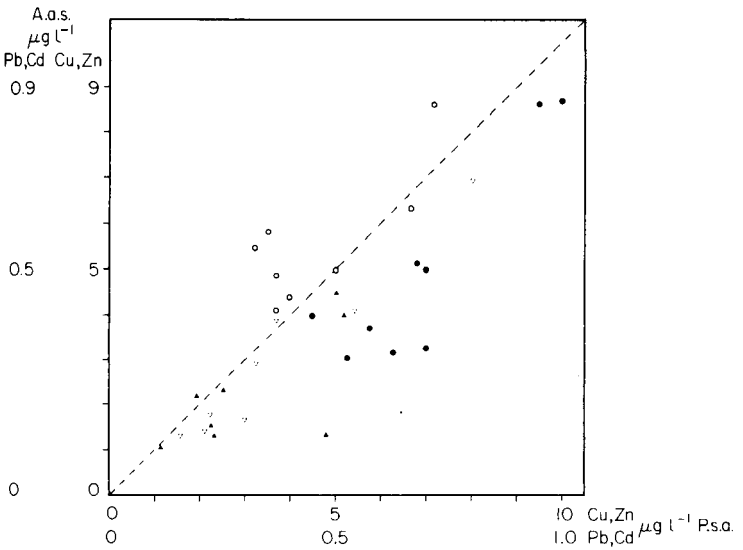

Fig. 3. Comparison between the results obtained by solvent extraction—atomic absorption and potentiometric stripping analysis on eight different Baltic sea water samples. (▲) Cd; (•) Pb; (▽) Cu; (○) Zn.

sible. Formation of an intermetallic compound seems to be the most likely explanation. Investigation of this possibility is in progress.

Calibration curve

All results given above were obtained by standard addition analysis. Potentiometric stripping is, however, also well suited to analysis by means of calibration curves, which decreases the time needed for analysis. Because no current is drawn through the sample during stripping, ohmic variations in the sample arising from variations in salinity, for example, do not affect the magnitude of the signal as in rapid-scanning anodic stripping voltammetry or differential pulse anodic stripping voltammetry. Furthermore, small variations in stirring rate from one sample to the next do not affect the magnitude of the signal because the same transport process is involved during the potentiostatic pre-concentration and the oxidative stripping. Possible effects of varying concentrations of surface-active agents can be excluded by the same argument That a calibration curve can in fact be used is shown in Fig. 4. Here the analytical signals obtained for seven different samples before the addition of a standard aliquot are plotted against the sample concentrations of cadmium(II), lead(II) and copper(II) as evaluated by subsequent standard additions.

Effect of stirring rate

Turbulent conditions in the electrochemical cell decrease the sensitivity of potentiometric stripping analysis [2]. For this reason, the rotation rate of the three-edged mechanical stirrer must be kept rather low. Stirring with a magnetic bar tends to create less turbulence and therefore often yields better sensitivity.

Analysis of lead and copper on a very thin mercury film

Unlike cadmium(II), both lead(II) and copper(II) can be plated directly onto a glassy carbon electrode. In analysis for these elements, it is thus possible to keep the mercury(II) concentration in the sample very low, which improves the sensitivity [7].

In order to determine the increase in sensitivity obtainable in potentiometri stripping analysis, 50 ml of a sea water sample was acidified with hydrochloric acid to a total concentration of 0.01 M, and mercury(II) (300 $\mu g\ l^{-1}$) was adde After deaeration and mercury pre-coating by the procedure described above, the sample was plated at −0.90 V vs. SCE for 16 min. The stripping curve obtained is shown in Fig. 5. Two standard aliquots, each containing 1 μg Pb l^{-1} and 2 μg Cu l^{-1} were then added, and the lead(II) and copper(II) concentrations of the sample were evaluated as 0.80 and 3.60 $\mu g\ l^{-1}$, respectively.

Comparison of the results shown in Fig. 5 with those shown in Figs. 1 and 2 indicates that the detection limit, for 64 min of plating, has decreased by a factor of approximately five for copper(II) and a factor of approximately three for lead(II). Obviously the very thin film procedure is more suitable if only lead(II) and copper(II) are to be determined. Zinc cannot be determined

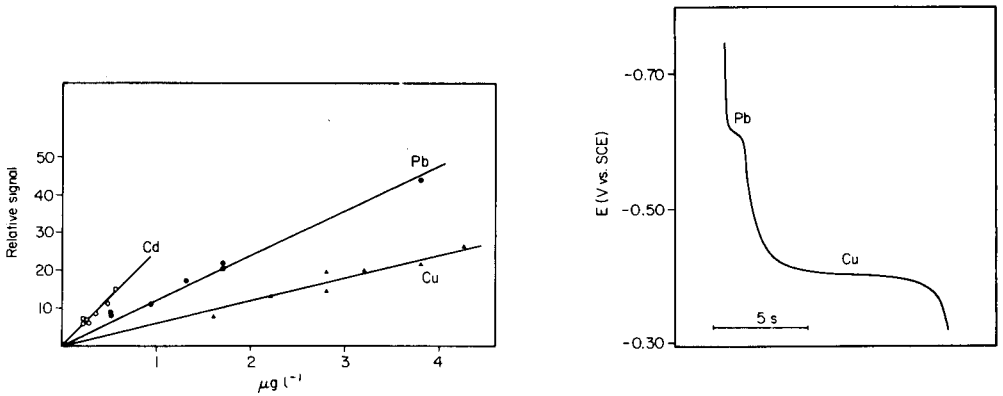

Fig. 4. Potentiometric stripping signals for cadmium(II), lead(II) and copper(II) recorded for seven different Baltic sea water samples plotted against the sample concentrations evaluated by subsequent standard addition analysis.

Fig. 5. Potentiometric stripping curves for lead and copper recorded after 16 min of plating at −0.90 V vs. SCE in a Baltic sea water sample containing 0.80 μg Pb l^{-1} and 3.60 μg Cu l^{-1}. The curve was obtained with a very thin mercury film.

when a very thin film is used because such a film is not sufficiently thick to prevent hydrogen evolution.

Conclusions

Potentiometric stripping analysis provides a simple instrumental approach to the accurate and precise determination of zinc, copper, lead and cadmium in sea water. The method involves very little sample pre-treatment. Because of the low concentrations of cadmium normally present in sea water, rather long plating times have to be exploited in the determination of this element. This is, however, compensated for by the fact that the analysis can be done almost unattended and that, in routine analysis of many samples, a calibration curve can be used.

REFERENCES

1 D. Jagner and A. Granéli, Anal. Chim. Acta, 83 (1976) 19.
2 D. Jagner and K. Årén, Anal. Chim. Acta, 100 (1978) 375.
3 D. Jagner, Anal. Chem., in press.
4 D. Jagner and L. Kryger, Anal. Chim. Acta, 80 (1975) 255.
5 L. -G. Danielsson, B. Magnusson and S. Westerlund, Anal. Chim. Acta, 98 (1978) 47.
6 L. Brügmann, Acta Hydrochim. Hydrobiol., 5 (1977) 3.
7 W. T. deVries and E. van Dalen, J. Electroanal. Chem., 14 (1967) 315.

Analytica Chimica Acta, 107 (1979) 37—46

THE DETERMINATION OF CADMIUM, LEAD AND COPPER IN URINE BY DIFFERENTIAL PULSE ANODIC STRIPPING VOLTAMMETRY

W. LUND* and R. ERIKSEN

Department of Chemistry, University of Oslo, Box 1033, Blindern, Oslo 3 (Norway)

(Received 2nd January 1979)

SUMMARY

Differential pulse anodic stripping voltammetry is used for the simultaneous determination of cadmium, lead and copper in different types of urine samples. Unlike most biological samples, urine can be analyzed directly for cadmium and lead without pretreatment of the sample; a significant increase in sensitivity is obtained if the analysis is carried out at an elevated temperature. The complete decomposition of urine with a mixture of nitric, perchloric and sulphuric acids is also described; this procedure makes it possible to determine copper simultaneously. Good agreement was obtained between the two procedures, and the recovery of metals from spiked samples was satisfactory for both methods. The relative merits of the two approaches are discussed.

The control of exposure to toxic metals has become an important part of most studies concerned with environmental pollution and occupational health hazards. Although there does not appear to be a simple relationship between exposure to toxic metals and their urinary excretion, the analysis of urine is often a convenient first step in an attempt to confirm such exposure.

Differential pulse anodic stripping voltammetry has proved a very useful method for the determination of low levels of some toxic metals in biological samples. Normally the organic material must be destroyed prior to the determination of the metals by anodic stripping voltammetry [1—7]. However, thallium [7—10], lead [10—14], copper [10] and cadmium [13] have been determined directly in urine without digestion of the sample. In this work the direct analysis of urine by anodic stripping voltammetry is compared with procedures involving a complete decomposition of the organic matrix. Three types of urine samples were studied; normal urine, spiked urine and urine from persons suspected to have been exposed to toxic metals.

EXPERIMENTAL

Apparatus

A Princeton Applied Research 174A Polarographic Analyzer and a Radiometer REC51/REA112 recorder were used. A home-made timer unit controlled the different steps in the stripping-voltammetric procedure. The

stirring rate was 500 rpm; a constant-rate magnetic stirrer and a Teflon-covered bar were used. A hanging mercury drop electrode (Metrohm E410) was used as the working electrode; the diameter of the capillary reservoir was 2.5—2.7 mm [15]. An Ag/AgCl electrode (Metrohm EA427) and a platinum coil served as reference and counter electrodes, respectively. The electrolytic cells (Metrohm EA880, 5 and 20 ml) were equipped with thermostatted jackets, through which water at 25.0 or 40.0°C circulated. Dissolved oxygen was removed from the samples by passing highly purified nitrogen through the cell for 20 min. During the experiments nitrogen was passed over the solution.

The urine samples were decomposed in 150-ml Erlenmeyer flasks, which were heated on a hot plate with thermostatic control; the hot plate was switched off automatically after a pre-set time. The flasks were equipped with glass ball condensers (Fig. 1) for reflux boiling during digestion. All glass equip-

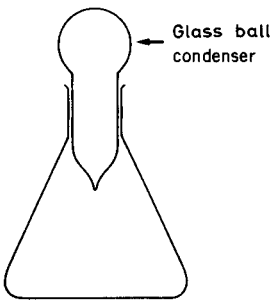

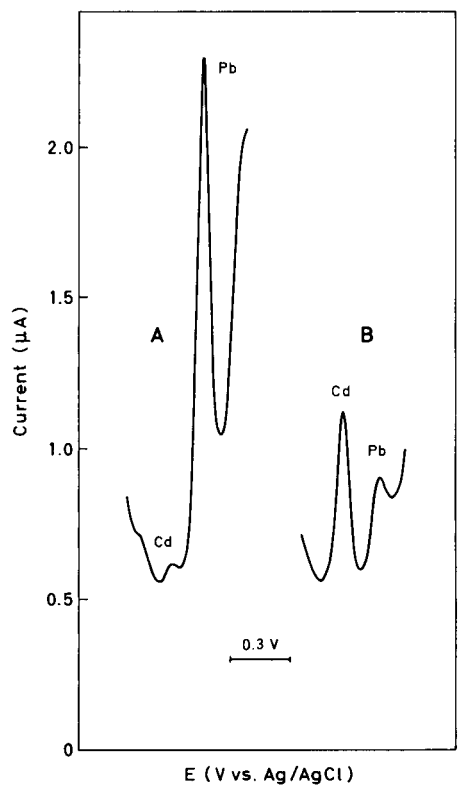

Fig. 1. Erlenmeyer flask with glass ball condenser for digestion of urine.

Fig. 2. Direct analysis of urine by anodic stripping voltammetry at 40°C. (A) Urine from smoker, 5 nM (0.6 ppb) Cd, 110 nM (23 ppb) Pb; (B) urine from person exposed to cadmium, 37 nM (4.2 ppb) Cd, 82 nM (17 ppb) Pb.

ment was cleaned thoroughly, normally with dichromate in nitric or sulphuric acid and then with diluted nitric acid before each new series of experiments. The cell and capillary were treated with dimethyldichlorosilane at regular intervals.

Samples and solutions

Standard metal solutions were prepared from the analytical-grade chloride salts, and acidified with perchloric acid. The different acids, sodium hydroxide and sodium acetate were all of Suprapur (Merck) quality.

Three types of urine samples were analyzed: (1) "normal" urine from persons not suspected of any particular exposure to metals, (2) normal urine spiked with 50 nM (5×10^{-8} mol l^{-1}) of cadmium, lead and copper, and (3) urine from persons suspected of exposure to cadmium. All samples were frozen rapidly and stored at −20°C in polyethylene bottles; the samples were found to be stable for months. Preliminary experiments proved the absence of significant adsorption of metals on the walls of the polyethylene containers. The urine samples were not stable at room temperature; in this case the concentration and voltammetric sensitivity for cadmium and lead changed with time. The decrease in sensitivity for lead was particularly marked, although the concentration of this metal remained nearly constant. Storage with acids instead of deep-freezing was not attempted because this would have rendered difficult the subsequent direct analysis of urine (see below).

Decomposition procedure

Transfer 50 ml of urine, 10 ml of nitric acid, 8 ml of perchloric acid and 1 ml of sulphuric acid to each Erlenmeyer flask (150 ml) and boil with reflux using the glass ball condenser (see Fig. 1) for 30 h on a hot plate. Remove the glass ball and heat the solution until fumes of sulphuric acid are observed. Dilute to 50 ml with water; the pH of the resulting solution should be 0.5—1.0.

Determine the blank values by taking 50-ml aliquots of water through the same digestion procedure.

Stripping-voltammetric procedure

Transfer a 10-ml aliquot of the sample to the electrolytic cell and deaerate for 20 min with nitrogen. If pure urine is analyzed (direct method), heat the sample to 40°C by circulating thermostatted water in the jacket surrounding the cell; when a mineralized sample is analyzed, circulate water at 25°C. Extrude a fresh mercury drop (diameter 0.9 mm), start the stirrer (500 rpm) and electrolyze for 5 min at −0.8 V vs. Ag/AgCl. Stop the stirrer and record the stripping voltammogram after a rest period of 30 s. Use the following instrument settings: scan rate 5 mV s^{-1}, pulse repetition time 0.5 s, and modulation amplitude 50 mV. If necessary, change the instrument sensitivity between the lead and copper peaks. Repeat the measurement at least once before adding small volumes (e.g. 50 μl) of the standard solutions and repeating the whole procedure, to determine the concentrations by the method of standard addition.

RESULTS AND DISCUSSION

Direct analysis

The direct analysis of urine by differential pulse anodic stripping voltammetry is illustrated in Fig. 2. Curve A refers to a normal urine, and curve B to urine from a person suspected of exposure to cadmium. The cadmium and lead peaks are observed at −0.55 V and −0.40 V vs. Ag/AgCl, respectively. The concentration of cadmium was found to be seven times higher for sample B than sample A, while the lead concentrations were of the same order of magnitude. Obviously the sensitivity for lead is very low for sample B, which may be explained by a prolonged storage of the sample at room temperature (see above). As shown in Fig. 2, the voltammetric background has a marked U-shape, with a minimum in the region of the cadmium peak; the background current is very high compared with the background of digested samples (see Fig. 4). Furthermore, the copper peak could not be distinguished from the background on these voltammograms.

These analyses were carried out directly on the urine samples, without any pH adjustments; the natural pH of urine is ca. 6. For some urine samples, a slight improvement in sensitivity and peak separation was achieved by decreasing the pH towards 5 (with perchloric acid). A similar procedure was used by Herbeuval et al. [12]. Kemula and Kublik [11] acidified the sample to ca. pH 1 with hydrochloric acid prior to the analysis, whereas Copeland et al. [13] preferred an acetic acid—acetate buffer; Franke and de Zeeuw [10] used a combination of these approaches with different reagents.

pH adjustments outside the range 5—6 resulted in a decrease in the cadmium peak and the appearance of interfering "organic" peaks at potentials close to that of the lead peak; the "organic" peaks were independent of metal concentration and deposition time. The background was higher in acidic than in alkaline solution. Sodium acetate was added to some samples (pH 6.5) without any significant effect being observed.

The voltammograms in Fig. 2 were obtained at 40°C; a significant increase in sensitivity was observed for both cadmium and lead at elevated temperature. The variation in peak height with temperature is shown in Fig. 3; a straight line relationship is obtained for lead, while the relationship for cadmium is curved. The temperature effect is much more pronounced than is normally found for simple inorganic samples. In the latter case the temperature coefficient is normally ca. 3% deg.$^{-1}$ at 25°C [16] (see also the results for digested samples below), whereas from Fig. 3 the temperature coefficient is 8% deg.$^{-1}$ for cadmium and 6% deg.$^{-1}$ for lead. The coefficient k was calculated from the equation

$$k = \mathrm{d}i/i\mathrm{d}T = \mathrm{d}(\ln i)/\mathrm{d}T \approx (\ln i_2 - \ln i_1)/(T_2 - T_1)$$

where i is the peak current and T the temperature; in these calculations T_1 and T_2 were 25 and 40°C, respectively. If the temperature interval 45—60°C is used, k becomes 8% deg.$^{-1}$ for cadmium and 4% deg.$^{-1}$ for lead. The high

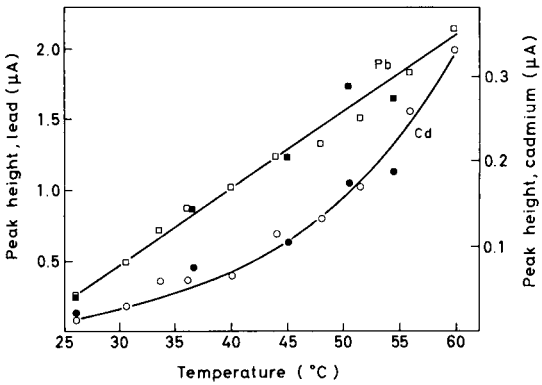

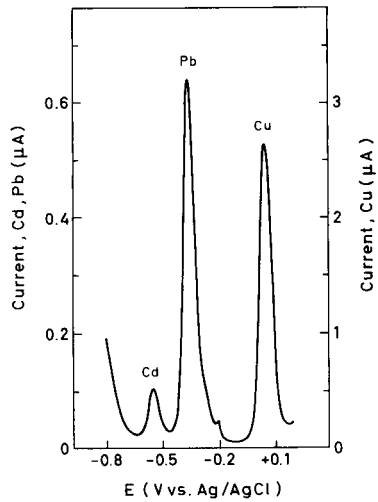

Fig. 3. Variation in peak height with temperature for pure urine (5 nM Cd and 110 nM Pb). The filled symbols indicate peak heights measured as the temperature was lowered from 60°C.

Fig. 4. Stripping voltammogram of a completely digested urine sample from an unexposed person. The peaks correspond to 3.3 nM Cd, 26 nM Pb and 164 nM Cu. After correction for blanks and sample dilution, the urine was found to contain 4.8 nM (0.5 ppb) Cd, 26 nM (5 ppb) Pb and 230 nM (15 ppb) Cu.

k values indicate that the electrode reaction is not fully diffusion-controlled, and probably depends on the rate of some chemical reaction. The peak potentials were not much influenced by the temperature.

The sensitivity of the method at 40—50°C was normally in the range 2—4 μA min^{-1} μM^{-1} for cadmium and 2—6 μA min^{-1} μM^{-1} for lead. However, for the latter metal a value as low as 1 μA min^{-1} μM^{-1} was occasionally observed in certain samples. The values are somewhat lower than those usually obtained for mineralized samples at 25°C (see below).

A deposition potential of −0.8 V was normally used. The lead and cadmium peaks were almost independent of the deposition potential in the region −0.8 to −1.1 V; the evolution of hydrogen prevented the use of potentials more negative than −1.1 V. The peak heights increased linearly with deposition time, provided that a 20-ml electrolytic cell was used; for a 5-ml cell a somewhat curved relationship was obtained, owing to the depletion of the sample solution.

When standard metal solutions were added to the urine samples, a linear increase in peak height with concentration was observed for all three metals. No time-effect (variation in peak height with time after the addition of standard) was noted.

Digested samples

The stripping voltammogram of a digested urine sample is shown in Fig. 4. The voltammogram has a low background and well defined peaks; the peak potentials are −0.55, −0.37 and +0.05 V vs. Ag/AgCl for cadmium, lead and copper, respectively. Because of the high concentration of copper, the instrumental current sensitivity must be lowered before the copper peak is recorded.

Different digestion procedures were investigated and a mixture of nitric, perchloric and sulphuric acids was finally preferred. Digestions without sulphuric acid also gave satisfactory results, but the presence of sulphuric acid was used to prevent the acid mixture being taken to dryness, as this would increase the explosion hazard. Treatment with nitric and perchloric acids, followed by heating to dryness and dissolution in hydrochloric acid, was also investigated, but the copper peak was less well defined in this case, owing to the presence of chloride. When urine was digested with only nitric acid, the resulting voltammogram indicated that the decomposition was far from complete. Even though a clear, colourless solution was obtained, the sensitivity was very low for all three metals, and a large peak at −0.13 V interfered with the lead and copper peaks. Possibly, the interfering peak was due to electroactive organic compounds (e.g. nitro compounds) which were formed during the incomplete digestion.

For completely digested samples, the sensitivity of the method was usually in the range 4—7 $\mu A\ min^{-1}\ \mu M^{-1}$ for cadmium and lead, and 3—7 $\mu A\ min^{-1}\ \mu M^{-1}$ for copper. These values agree well with those obtained in the analyses of teeth [1], whereas significantly lower values were found for digested wine samples [2].

The results of three independent digestions of a spiked urine sample are given in Table 1. The blanks refer to aliquots of water which were taken through the full acid digestion procedure. The blank values of cadmium (2—5 nM) are not significantly different from the concentration of this metal in the normal urine (Table 2). For lead and copper the mean blank values, 8 and 51 μM respectively, are significantly lower than the concentrations found in the normal urine (Table 2).

As indicated in Table 1, the precision of the method is 10—20% for cadmiur and lead, except for very low cadmium values, whereas the copper results are less precise (see also Table 2). The standard deviation calculated from parallel decompositions was often higher than that obtained from a single decomposition (see the results for lead); the variation in the results of different decompositions indicates that the conditions for this step should be controlled carefully. For lead, the results appear to be significantly different for the three decompositions.

Occasionally, it was found that the decomposition procedure did not result in complete digestion of the samples. The voltammograms of these samples showed a decreased sensitivity for cadmium, increased background currents and unusual pH effects; the cadmium peak increased significantly when the pH

TABLE 1

Analysis of a spiked urine sample and the corresponding blank values, after decomposition with a mixture of nitric, perchloric and sulphuric acids[a]

Sample	Decomposition No.	Cadmium		Lead		Copper	
		$\bar{x}$ (nM)	s_r (%)	$\bar{x}$ (nM)	s_r (%)	$\bar{x}$ (nM)	s_r (%)
Spiked urine[b]	1	56	4	117	8	360	19
	2	54	9	85	12	300	41
	3	51	7	91	9	250	18
	Av.	53	7	98	17	300	29
Blank	1	5	7	10	21	51	30
	2	2	44	6	18	51	20

[a] $\bar{x}$, Mean of triplicate analysis (nM = 10^{-9} mol l^{-1}); s_r, relative standard deviation; Av., mean and standard deviation of all results. [b] Blank values not subtracted.

was changed from 0.5 to 4. The samples also showed a marked u.v. absorption at 260 nm. However, additional heating of the solutions until the appearance of fumes of sulphuric acid was usually sufficient for obtaining satisfactory voltammograms.

In contrast to the results of Matson et al. [7], the copper peak was not much affected by incomplete digestion, probably because only traces of organic material are left in the solution after the prolonged reflux boiling used here. The results of Matson et al. referred to solutions with a brownish or yellowish colour.

The difficulties encountered in the decomposition of urine can possibly be ascribed to the presence of heterocyclic nitrogen compounds (e.g. purines) and amino acids (e.g. glycine) [17]. Such compounds are sometimes difficult to decompose with acids [18], but relatively stable nitrogen compounds may also be formed during the digestion step, through the action of nitric acid [19, 20].

The digested samples had a pH of ca. 1. No pH adjustment was made before the voltammetric analysis. It was found that the stripping peaks decreased when the pH was adjusted with either perchloric acid or sodium acetate; the peaks did not increase to their original value when the pH was readjusted back to 1, but remained almost constant. Above pH 5 the peaks decreased markedly.

The temperature effect was found to be less pronounced for the completely digested samples than for pure urine. A linear variation in the peak heights with temperature was observed, and the temperature coefficient was found to be 2.8% deg.$^{-1}$ for cadmium, 2.7 for lead and 3.2 for copper; these values agree well with the 3% deg.$^{-1}$ reported for inorganic samples [16].

The deposition potential was normally —0.8 V. The peak heights of copper and lead were found to be nearly independent of deposition potential in the

TABLE 2

Analysis of different urine samples; comparison of the direct method with the procedure involving decomposition with acids[a]

Urine	Method	Cadmium			Lead			Copper		
		n	$\bar{x}$ (nM)	s_r (%)	n	$\bar{x}$ (nM)	s_r (%)	n	$\bar{x}$ (nM)	s_r (%)
Normal	Direct	4	2	8	5	39	15	—	—	—
Spiked	Direct	4	48	7	4	89	7	—	—	—
	Decomposition	3	52	4	3	87	7	3	300	26
Smoker	Direct	4	5	36	4	113	14	—	—	—
	Decomposition	4	9	16	4	110	13	4	1220	16
Exposed	Direct	4	37	17	4	82	22	—	—	—
	Decomposition	4	42	3	4	73	7	4	390	10

[a] n, Number of aliquots; $\bar{x}$, mean (nM = 10^{-9} mol l^{-1}); s_r, relative standard deviation.

region —0.65 to —0.95 V, whereas the cadmium peak increased slightly with potential in this region. The variation in peak height with deposition time agreed well with the results for pure urine; a somewhat curved relationship was again obtained when the 5-ml cell was used. The respective calibration curves, constructed by means of several standard additions, were all linear.

Analysis of different samples; comparison of procedures

The results of the analysis of different urine samples are given in Table 2. The "normal" urine was taken from a young man (non-smoker). The spiked urine refers to the same sample, with 50 nM of each metal added. The smoker was a middle-aged woman who had smoked cigarettes for more than thirty years, whereas the exposed urine refers to a mixed urine sample from persons suspected of cadmium exposure. As shown in Table 2, the "normal" urine contained 0.2 ppb (2 nM) cadmium and 8 ppb (39 nM) lead. The amount of copper was not determined, but by subtracting 50 nM from the spiked sample a "normal" concentration of 16 ppb (250 nM) is obtained. These values agree well with those reported by other workers [6, 21—24]. The urine from the smoker contained significantly higher amounts of lead and copper (mean values 0.8 ppb Cd, 23 ppb Pb and 77 ppb Cu); the copper value is particularly high. The "exposed" urine seems to confirm the suspicion of occupational cadmium exposure, as a value of 4.5 ppb was found for cadmium (see also ref. 23), but this urine contained moderate amounts of the other metals (16 ppb Pb and 25 ppb Cu).

Satisfactory agreement between the direct analysis and the procedure involving decomposition is indicated in Table 2 for both cadmium and lead (copper could not be determined by the direct method used here). The cadmium results are slightly higher for the method involving decomposition.

However, as shown in Table 1, the blank values may vary significantly, and a better agreement would be obtained for cadmium if the blank value was higher than the 2 nM assumed in Table 2.

In Table 2 a somewhat better precision is indicated for the digested samples than for the pure urine. However, provided that parallel decompositions are carried out, the precision will usually be similar for the two methods. The relatively poor precision obtained for lead in the direct analysis of "exposed" urine is explained by the very low sensitivity found for lead for this particular sample (see Fig. 1, curve B). Furthermore, the standard addition curve was not fully satisfactory for this sample.

The recovery of cadmium and lead from spiked urine was calculated from the results given in Table 2. For both procedures the recovery was in the range 92—100%, which can be regarded as complete considering the precision of the two procedures.

Naturally the direct procedure is less time-consuming than the method involving wet decomposition. However, no attempt was made to minimize the time needed for a complete digestion. Possibly a shorter period of reflux boiling would give equally satisfactory voltammograms for most samples. But the 15-min digestion used by Golimowski et al. [4] is probably insufficient for complete decomposition of urine in all cases.

The sensitivity was normally lower, and the voltammetric background was higher, for pure urine samples than for fully digested samples; however, poor sensitivity was observed for cadmium in incompletely digested samples. As explained above, the sensitivity of the direct method is improved significantly as the temperature is increased; at 40°C it is not much lower than the sensitivity found for mineralized samples.

A disadvantage of the decomposition procedure is the contamination of the sample by the acids; for cadmium the blank value (2—5 nM) is of the same order of magnitude as the "normal" concentration in urine. Therefore, the determination of this metal is preferably carried out by the direct method at an elevated temperature. In contrast, copper cannot be determined with the direct procedure used here, but a well defined copper peak is obtained after decomposition, with a relatively low blank value. For lead, both methods give equally satisfactory results, but as already mentioned, the direct procedure is the faster.

In the voltammetric analyses discussed here, no interference from other toxic metals was noticed. If there is suspicion of thallium poisoning, this metal will interfere with the determination of cadmium, and the concentration of thallium must be determined separately. This can be done by masking the cadmium and lead peaks with EDTA [8—10]. However, lead can also be determined directly in urine in the presence of EDTA, provided that the solution is strongly acidified [14]. This fact is of particular interest when $Na_2CaEDTA$ is used as a detoxicant in clinical treatment of metal poisoning.

No attempt was made here to study the day-to-day variation in the urinary excretion of toxic metals from exposed persons. If this is to be done, the

results obtained for single samples should be given in terms of μg metal per gram creatinine, in order to take into account diurnal variations in the composition of the urine.

REFERENCES

1 M. Oehme, W. Lund and J. Jonsen, Anal. Chim. Acta, 100 (1978) 389.
2 M. Oehme and W. Lund, Fresenius Z. Anal. Chem, 294 (1979) 391.
3 S. Gomišček, V. Hudnik and M. Veber, in S. S. Brown (Ed.), Clinical Chemistry and Chemical Toxicology of Metals, Elsevier/North-Holland, Amsterdam, 1977, p.319.
4 J. Golimowski, P. Valenta, M. Stoeppler and H. W. Nürnberg, Fresenius Z. Anal. Chem., 290 (1978) 107.
5 W. Kisser, Arch. Toxicol., 34 (1975) 237.
6 B. Searle, W. Chan and B. Davidow, Clin. Chem., 19 (1973) 76.
7 W. R. Matson, R. M. Griffin and G. B. Schreiber in D. D. Hemphill (Ed.), Proceedings, University of Missouri's Fourth Annual Conference on Trace Substances in Environmental Health, Colombia, Missouri, 1971, p. 396.
8 A. R. Curtis, J. Assoc. Off. Anal. Chem., 57 (1974) 1366.
9 J. P. Franke, P. M. J. Coenegracht and R. A. de Zeeuw, Arch. Toxicol., 34 (1975) 137.
10 J. P. Franke and R. A. de Zeeuw, Arch. Toxicol., 37 (1976) 47.
11 W. Kemula and Z. Kublik, Nature, 189 (1961) 57.
12 X. Herbeuval, J.-L. Maso, P. Baudot, M.-F. Hutin and D. Burnel, Pathol. Biol., 23 (1975) 379.
13 T. R. Copeland, J. H. Christie, R. A. Osteryoung and R. K. Skogerboe, Anal. Chem., 45 (1973) 2171.
14 M. L. Girard, C. Dreux, F. Paolaggi and J. Delattre, Ann. Biol. Clin., 26 (1968) 401.
15 P. Sagberg and W. Lund, Anal. Chim. Acta, 94 (1977) 457.
16 R. Neeb, Inverse Polarographie und Voltammetrie, Verlag Chemie, Weinheim, 1969, p. 131.
17 H. A. Harper, Review of Physiological Chemistry, 13th edn., Lange Medical Publications, California, 1971, p. 385.
18 G. D. Martinie and A. A. Schilt, Anal. Chem., 48 (1976) 70.
19 T. T. Gorsuch, The Destruction of Organic Matter, Pergamon, Oxford, 1970, p. 21.
20 M. Roschig and H. Matschiner, Z. Med. Labortech., 12 (1971) 201.
21 K. Tsuchiya, M. Sugita, Y. Seki, Y. Kobayashi, M. Hori and Ch. B. Park, in T. B. Griffin and J. H. Knelson (Eds.), Lead, G. Thieme, Stuttgart, 1975, p. 95.
22 A. Azar, R. D. Snee and K. Habibi, in T. B. Griffin and J. H. Knelson (Eds.), Lead, G. Thieme, Stuttgart, 1975, p. 254.
23 W. Lund, B. V. Larsen and N. Gundersen, Anal. Chim. Acta, 81 (1976) 319.
24 L. Friberg, M. Piscator, G. F. Nordberg and T. Kjellstrøm, Cadmium in the Environment, CRC Press, Cleveland, Ohio, 2nd edn., 1974, p. 65.

Analytica Chimica Acta, 107 (1979) 47—58

ELECTROCHEMICAL STUDIES OF TECHNETIUM AT A MERCURY ELECTRODE

J. GRASSI

Laboratoire de Chimie Analytique, Institut National des Sciences et Techniques Nucléaires, Saclay (France)

J. DEVYNCK* and B. TRÉMILLON

Laboratoire d'Electrochimie Analytique et Appliquée, associé au C.N.R.S. (LA 216), Ecole Nationale Supérieure de Chimie de Paris, Université Pierre et Marie Curie, 11 rue Pierre et Marie Curie, 75231 Paris Cedex 05 (France)

(Received 18th September 1978)

SUMMARY

The electrochemistry of technetium was studied by polarography, cyclic voltammetry and coulometry in chloride and sulfate media as a function of pH in the range 1.5—13. Compounds of Tc(III) and Tc(IV) are produced by reduction of pertechnetate, and the system Tc(III)/Tc(IV) was investigated in acidic media. The potential—acidity diagram of technetium is described for two total pertechnetate concentrations. Evidence for the dismutation of Tc(III) below pH 4 is discussed.

The wide use of ^{99m}Tc in nuclear medicine has resulted in a great interest in the properties of this element. For almost all uses, it is necessary to reduce technetium from the heptavalent state (TcO_4^-) to a lower, more reactive one. This reduction step may be monitored by using electrochemical techniques. The electrochemical properties of technetium have been widely studied and have been the subject of several reviews [1—3].

Reduction of pertechnetate is possible in various media but most of the results have been obtained in chloride [4—6], sulphate [4, 5, 7] and perchlorate [8—10] media. However, interpretations of polarographic waves are contradictory with regard to the nature of the oxidation states involved during the reduction of TcO_4^- in acidic and alkaline media. Salaria et al. [4, 5] proposed a two-step polarographic reduction of TcO_4^- in acidic media involving respectively 4 electrons (Tc(VII)/Tc(III)) and 3 electrons (Tc(III)/Tc(0)). This scheme was contested by Zhdanov et al. [7] who suggested that the first step involves a reduction of Tc(VII) to Tc(IV) with formation of TcO_2.

The same discrepancies have been observed in alkaline medium. Salaria et al. [4] proposed a 3-electron step (Tc(VII)/Tc(IV)) followed by a 1-electron

step (Tc(IV)/Tc(III)) from results of coulometric measurements. Other authors [6—8, 10—14] have suggested an alternative scheme with Tc(V) as the intermediate and Tc(IV) as the final oxidation state.

Re-examining the whole problem of electrochemical reduction of pertechnetate in various buffered and unbuffered media by means of various polarographic techniques, Russel and Cash [15] were led to the same conclusions as Salaria et al. [4, 5], in good accord with the recent results of Grassi [16].

However, some interesting conclusions concerning intermediate trivalent and tetravalent oxidation states may be obtained from a systematic examination of polarographic and coulometric reduction in unbuffered media. Such a study is described in this paper, and a new potential —pH diagram more complete than the diagram proposed by Zoubov and Pourbaix in 1957 [17] is suggested. This diagram takes into account some of the numerous results gathered during recent years, and may be a valuable tool for further analytical studies of technetium.

EXPERIMENTAL

Reagents

Ammonium pertechnetate (NH_4^+ $^{99}TcO_4^-$; 17 mCi g^{-1}) was obtained from the Radiochemical Centre, Amersham (England). Solutions were standardized by controlled-potential coulometry at −500 mV vs. SCE in 0.5 M KCl − HCl solutions at pH 2, and by u.v. spectrometry. Tetraethylammonium perchlorate (for polarography) was supplied by Carlo Erba (Milan). All other reagents were of guaranteed purity (Prolabo, Paris).

Apparatus

Polarographic and voltammetric measurements were done with a Tacussel PRG 5 polarograph, equipped with a Tacussel GST P 3 function generator and a TRP Sefram x-y recorder. A PRT 20 potentiostat was used for controlled-potential coulometry. For cyclic voltammetric measurements, a Metrohm type 410 electrode was used. All electrode potentials were measured with an ISIS 4000 Tacussel millivoltmeter and are referred to the calomel (saturated KCl) electrode at 25°C.

Methods

Some properties of technetium may provide sources of errors in polarographic and coulometric measurements. Experiments were therefore carried out under the following conditions. All experiments were done in solutions of pH > 1.5, because it has been shown that pertechnetate may be rapidly reduced by mercury in strongly acidic medium [1, 4, 5, 9, 18]. This phenomenon may be observed as a lowering of the first reduction wave of pertechnetate, when this ion is placed in contact with mercury in strongly acidic solutions. The u.v. spectrum of pertechnetate is also modified under

these conditions. This side-reaction, which is slow above pH 1, may be an important factor during coulometry where the surface of the electrode is large. Experimental conditions were controlled so as to render the effect of this phenomenon negligible.

Technetium(III) solutions prepared by coulometry have strong reducing properties, so that care must be taken to avoid the presence of atmospheric oxygen in the solution. A leak-proof cell with argon bubbling in each compartment was used in these experiments [16].

Polarographic and voltammetric measurements. For each experiment, the supporting electrolyte was purged for 15 min before the addition of a known amount of concentrated TcO_4^- solution. The solution was then purged for a further 5 min. The dropping mercury electrode was put in position immediately before the run.

Coulometry. The same precautions were taken in coulometry. However, with the cell used in these experiments, it was impossible to avoid oxidation on removal of Tc(III) solution.

RESULTS

The electrochemical behaviour of pertechnetate was analyzed in acidic (pH 1—3.5), nearly neutral (pH 3.5—10) and alkaline media (pH > 10) with 0.5 M KCl—HCl and 0.5 M $NaHSO_4$—Na_2SO_4 as the supporting electrolyte.

The polarographic properties of pertechnetate in perchlorate medium are the same as those observed in the other two media but there is a re-oxidation of reduced technetium by the electrolyte.

Acidic media

Reduction of pertechnetate. In these solutions pertechnetate exhibited three reduction waves (Fig. 1). The first two (IA and IIA) were diffusion-controlled, while the third was related to a catalytic reduction of hydrogen [4, 16, 19]. The formation of technetium metal during the second step has been demonstrated by radiopolarographic measurements [20]. Salaria et al. [4, 5] and Zhdanov et al. [7] had previously shown that wave IA was irreversible. This result was confirmed by Russel and Cash [15]. Exchange of 4 electrons was confirmed by controlled-potential coulometry measurements (E = —0.5 V) which gave n = 3.98 ± 0.09 (P = 95%; 11 determinations) and n = 4.05 ± 0.14 (P = 95%; 7 determinations) in chloride and sulphate media, respectively, at pH 2. The polarogram obtained after coulometric reduction (E = —0.5 V) of pertechnetate in $NaHSO_4$—Na_2SO_4 medium (pH 2) also consists of three waves (Fig. 2), a reduction wave situated at the same potential as the second reduction step of Tc(VII) and two oxidation waves (IC and IIC). The reduction wave is clearly related to the formation of elemental technetium. It was followed closely by a large catalytic current which made accurate analysis impossible. The limiting current of the wave was, however, lower than expected for the reaction Tc(III) $\xrightarrow{+3e^-}$ Tc(0) (Fig. 2). It was established

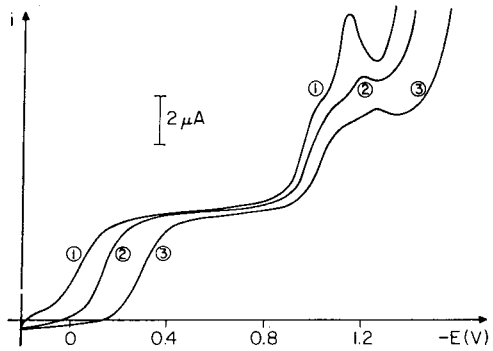

Fig. 1. Polarographic reduction of 0.59 mM TcO_4^- in 0.5 M Na_2SO_4—$NaHSO_4$: (1) pH 1.06; (2) pH 2.04; (3) pH 2.98.

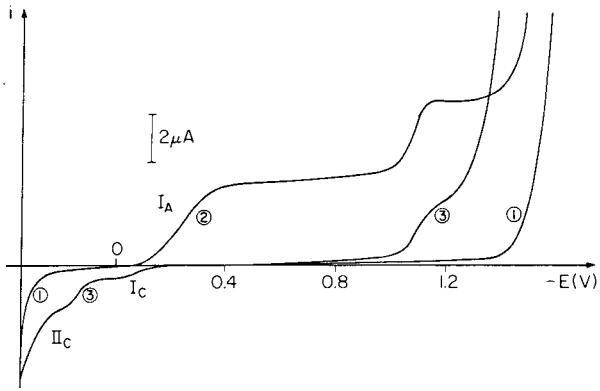

Fig. 2. Polarographic curves for Tc(III) in 0.5 M Na_2SO_4—$NaHSO_4$ at pH 2. (1) Residual current; (2) 0.29 mM TcO_4^- before electrolysis; (3) same solution after coulometry (E = —0.5 V).

experimentally [16] that this phenomenon did not result from either poor solubility or oxygen re-oxidation of Tc(III). The most likely explanation is that during the course of coulometry, part of the Tc(III) is transformed by an unknown reaction to non-electroactive species which could not be identified.

After a coulometric oxidation at the potential corresponding to the limiting current of wave IC (E = —0.05 V), the solution exhibited neither the reduction wave of Tc(III) nor waves IC and IIC. This clearly demonstrates that these three waves are correlated to Tc(III) reduction and oxidation, respectively. Re-oxidation of Tc(III) was also demonstrated by cyclic voltammetry. A voltammogram of TcO_4^- in 0.5 M $NaHSO_4$—Na_2SO_4 (pH 2) is shown in Fig. 3; only the oxidation current corresponding to wave IC is visible while that of wave IIC cannot be distinguished from the mercury

oxidation current. For the same reason re-oxidation of Tc(III) was not observed in chloride medium [20].

In 0.5 M HCl—KCl medium, it was also possible to observe a Tc(III) reduction wave after coulometric reduction of pertechnetate. As was the case in sulphate medium, Tc(III) appeared to be partially transformed during the course of coulometry.

It was impossible to assess the number of electrons involved during oxidation of Tc(III) by direct analysis of polarographic and coulometric measurements, because of the partial chemical transformation of Tc(III). However, this value can be obtained indirectly by comparing the diffusion currents of the three waves. By this method, a value $n = 1$ was calculated for wave IC. A value greater than 1 is not consistent with the current measured for the Tc(III) reduction wave or for wave IIC (even taking into account the partial conversion of Tc(III) during electrolysis). Formation of Tc(V) need not be considered.

Technetium(IV) formation during the first oxidation step was demonstrated after either coulometric or chemical oxidation (atmospheric oxygen) of Tc(III). In both cases it was possible to obtain a compound with the u.v. spectrum of the Tc(IV) complex, $[Tc(OH)_2(SO_4)_2]^{2-}$, described by Spitsyn et al. [21]. The number of electrons for wave IIC is much more difficult to determine, because of the proximity of the mercury oxidation current. It was possible to demonstrate formation of TcO_4^- after coulometry at $E = 0.2$ V in 0.5 M $NaHSO_4$—Na_2SO_4 at pH 2. This result is consistent with the relative importance of waves IC and IIC for pH values less than 2. The probable scheme for oxidation of Tc(III) is Tc(III) $\xrightarrow{-1e^-}$ Tc(IV) $\xrightarrow{-3e^-}$ Tc(VII).

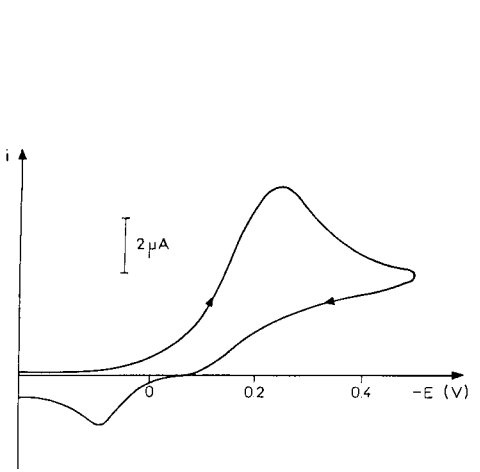

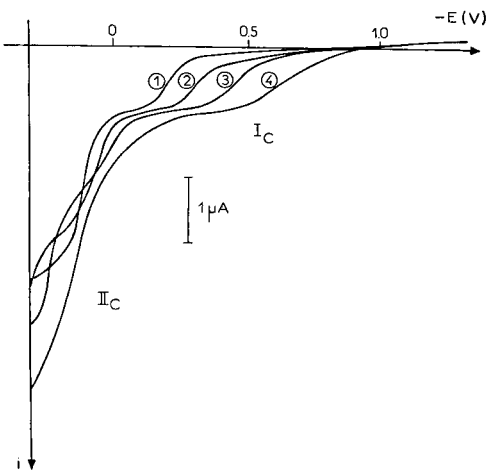

Fig. 3. Cyclic voltammogram of 0.93 mM TcO_4^- in 0.5 M Na_2SO_4—$NaHSO_4$ (pH 2), at a potential scan rate of 8.4 V min^{-1}.

Fig. 4. Dependence of polarographic curves of 0.3 mM Tc(III) on pH in 0.5 M Na_2SO_4—$NaHSO_4$. (1) pH 1.6; (2) pH 2; (3) pH 2.5; (4) pH 3.25.

Characteristics of Tc(III) obtained by coulometry. After coulometric reduction of 6×10^{-4} M pertechnetate ($E = -0.5$ V in 0.5 M $NaHSO_4$—Na_2SO_4 at pH 1.5) the solution was pale yellow. Addition of a carefully purged solution of sodium hydroxide induced a colour change. At pH 2.25, the solution was pale grey, and above pH 4.5 a black precipitate was visible. At the same time, a shift of wave IC towards more negative potentials was observed (Fig. 4). The corresponding half-wave potential changed linearly according to the equation: $E_{1/2}\,(V) = (0.286 \pm 0.033) - (0.123 \pm 0.013)$ pH. This variation was not linear above pH 3. This modification of the kinetic parameters of the electrochemical reaction may be illustrated by cyclic voltammetry [15, 16]. It appears that the electrochemical system involved is only quasi-reversible at pH values below 3.

After coulometric oxidation of Tc(III) ($E = -0.05$ V, wave IC) at pH 2, neither a reduction nor an oxidation current was observed, showing that the oxidation product of Tc(III) was unstable. This instability was confirmed by the cyclic voltammetric curves at various pH values, which showed that there was no reduction current for Tc(IV) below pH 1.5. This current appeared at about pH 2 and was as important as the oxidation current at pH 3.4. According to the criteria of Nicholson and Shain [22], this behaviour may be attributed to a chemical reaction of Tc(IV). It appears that the rate of this reaction increases with decreasing pH, indicating that protons are involved. This could be due to the formation of the electro-inactive complex $[Tc(OH)_2(SO_4)_2]^{2-}$ from TcO_2 as described by Spitsyn et al. [21]:

$$TcO_2 + 2H^+ + 2SO_4^{2-} \rightarrow [Tc(OH)_2(SO_4)_2]^{2-}$$

Neutral media

Above pH 3, in both chloride and sulphate media, the diffusion current of the first reduction wave of TcO_4^- (wave IA; see Fig. 2) decreased (Fig. 5). This diminution was accompanied by the appearance of a wave (IB; see Fig. 6) at a more negative potential ($E_{1/2} = -0.8$ V in 0.5 M KCl—HCl medium; $E_{1/2} = -0.78$ V in 0.5 M $NaHSO_4$—Na_2SO_4 medium) followed by a large catalytic current. For a given concentration of pertechnetate, wave IA began to decrease at a pH which depends on the medium (about pH 3 in the chloride medium and pH 4 in the sulphate medium). At a pH value two units higher than that at which wave IA began to decrease, only wave IB was observed. Waves IA and IB were both diffusion-controlled when this happened.

This evolution has previously been observed by Zhdanov and co-workers [15, 17], who suggested that it resulted from catalytic reduction of pertechnetic. acid. However, an alternative proposal is that the phenomenon is related to a system involving protons so that, in this pH range, the current can be limited by diffusion of H^+ ions in unbuffered medium. This scheme does not introduce pertechnetic acid, whose production at the electrode surface has not been established.

The latter hypothesis was confirmed by the study of complexing buffered

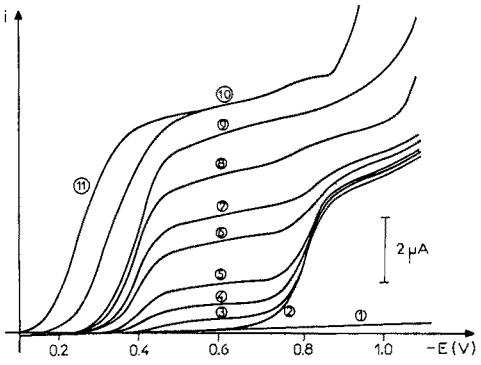

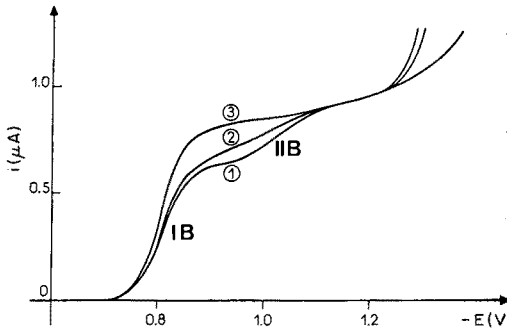

Fig. 5. Polarographic curves of 0.37 mM TcO_4^- in 0.5 M KCl at various pH values. (1) Residual current; (2) 7.74; (3) 4.72; (4) 4.21; (5) 3.91; (6) 3.59; (7) 3.47; (8) 3.30; (9) 3.17; (10) 2.62; (11) 2.09.

Fig. 6. Polarographic curves in 0.5 KCl—NaOH at pH 12 for TcO_4^- concentrations of (1) 0.44 mM; (2) 0.84 mM; (3) 4.1 mM.

media where this limitation occurred only at higher pH values. This was the case, for example, in the sulphate medium, buffered by the HSO_4^-/SO_4^{2-} couple up to pH 4. In the chloride medium, the diffusion current of wave IA was proportional to the concentration of free H^+ ions in the pH range where this limitation was observed. In sulphate medium, the variation was not linear because the HSO_4^- and H^+ ions could intervene in the reaction simultaneously. In neutral medium, the reduction of Tc(VII) results in formation of Tc(IV), probably in the form of TcO_2 according to the overall reaction

$$TcO_4^- + 2H_2O + 3e^- \rightarrow TcO_2\downarrow + 4OH^-$$

The presence of TcO_2 in neutral medium has already been proposed by several authors [7, 8, 10—14].

Alkaline media

In both chloride and sulphate media above pH 10, wave IB observed in neutral medium divided (Fig. 6, curve 1) and a new wave appeared at —1.1 V (wave IIB). Only the results obtained in KCl—NaOH medium are discussed here. Analysis of waves IB and IIB by Ilkovic's equation gave n values of 2 ($n = 2.15 \pm 0.3$) and 3 ($n = 3.15 \pm 0.4$), respectively. These results did not agree with those of the coulometric measurements: electrolysis at a potential corresponding to wave IB ($E = -0.9$ V) led to a result of 3 faraday per mole of pertechnetate. Electrolysis at lower potentials was made impossible by catalytic currents. The inconsistent results can be explained if adsorption phenomena are taken into account. Such phenomena can be demonstrated by examining the effects of pertechnetate concentration, the drop time of the electrode and surface-active compounds on polarographic curves.

When the concentration of pertechnetate was increased from 3×10^{-5} M to 6×10^{-3} M, the heights of waves IB and IIB varied as shown in Figs. 6 and 7. Below 5×10^{-4} M, the two waves increased in proportion to the concentration. For concentrations greater than 5×10^{-4} M, wave IIB remained stable while wave IB continued to increase in size. Such behaviour is characteristic of adsorption phenomena, the wave IIB being an adsorption post-wave varying in a manner conforming to theoretical calculation [23, 24], and in agreement with the description proposed by Sluyters-Rehbach et al. [25]. The adsorption of pertechnetate must be slight, for waves IB and IIB were observed simultaneously even at low concentration. Various workers [5, 6, 10, 11, 13] have not been able to demonstrate the phenomenon at the low concentrations ($TcO_4^- \leqslant 5 \times 10^{-4}$ M) used in their experiments. The existence of an adsorption effect was confirmed in the present work by the influence of drop time and by the presence in solution of compounds adsorbable at the electrode surface.

Results from polarograms obtained for different drop times agreed with those expected on the assumption that the electroactive compound is adsorbed [16]. Triton X-100, which is only slightly adsorbed in the potential range where waves IB and IIB appear, hardly affects the characteristics of the waves. In contrast, addition of tetraethylammonium perchlorate (TEAP) induced a change in the polarographic behaviour of pertechnetate: wave IIB was shifted towards more negative potentials with increasing TEAP concentration. In parallel, the limiting current of wave IB decreased while wave IIB increased. Clearly, the presence of TEAP, which is strongly adsorbed on the electrode in this potential range, enhances the adsorption of pertechnetate. The dependence of the limiting current of wave IIB on temperature and on head of mercury [4] agrees with the behaviour expected for an adsorption wave.

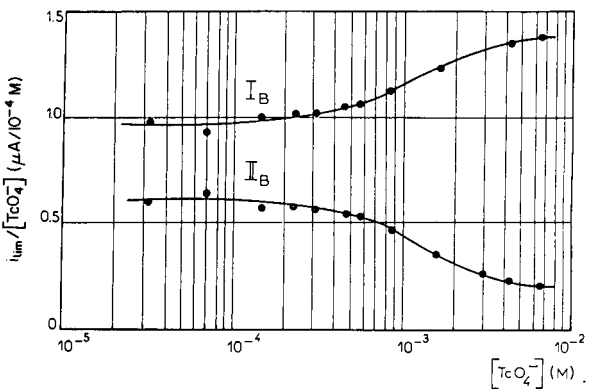

Fig. 7. Variation of the ratio $I_{lim}/[TcO_4^-]$ with TcO_4^- concentration for waves IB and IIB in 0.5 M KCl—NaOH at pH 12.

From these results it may be concluded that the two waves observed in the alkaline medium correspond to a single electrochemical system involving 3 electrons. This number cannot be determined by simple polarographic measurements because of the adsorption of pertechnetate, and this explains the contradictory results obtained by coulometry and polarography. The determination of 4 electrons by coulometry at −1.1 V was probably due to the proximity of catalytic reduction of water.

The polarographic reduction of pertechnetate in basic medium may be expressed as

$$TcO_4^- + 2H_2O + 3e^- \rightarrow TcO_2\downarrow + 4OH^-$$

DISCUSSION

In chloride and sulphate media, the reduction of pertechnetate at the mercury electrode resulted in different oxidation states depending on the pH of the solution.

In acidic medium (pH 1—3.5), polarographic and coulometric measurements clearly indicate the formation of Tc(III) during the first reduction step. The present results are in accord with those obtained by Salaria et al. and recently confirmed [15]. In sulphate medium, oxidation of Tc(III) to Tc(IV) occurs by a pH-dependent quasi-reversible process. This quasi-reversibility allows characterization of the species involved during the electrochemical process: on the basis of the data obtained, the potential—pH diagram proposed by Zoubov and Pourbaix [17] has been modified.

Oxidation of Tc(III) involves 1 electron and $2H^+$ ions; it can therefore correspond to one of the three following reactions:

$$Tc^{3+} + H_2O \rightleftarrows TcO^{2+} + 2H^+ + e^-$$

$$TcOH^{2+} + H_2O \rightleftarrows TcO(OH)^+ + 2H^+ + e^-$$

$$TcO^+ + H_2O \rightleftarrows TcO_2 + 2H^+ + e^-$$

In order to establish which of these reactions actually occurs, a formula for the Tc(IV) formed during oxidation must be proposed. The existence of TcO^{2+} and $TcO(OH)^+$ has been suggested by several authors [26—28]. Gorski and Koch [26] used electrophoretic mobility measurements to determine the equilibrium constants corresponding to the reactions:

$$TcO^{2+} + H_2O \rightleftarrows TcO(OH)^+ + H^+; \quad pK_2 = 1.36$$

$$TcO(OH)^+ + H_2O \rightleftarrows \underset{\downarrow}{TcO(OH)_2} + H^+; \quad pK_1 = 2.43$$
$$TcO_2 + H_2O$$

The methods of determination of these constants imply a soluble hydrated form of technetium dioxide, $TcO(OH)_2$. Gorski and Koch did not mention

the concentration of technetium used, thus it is difficult to be sure that their results were obtained under such conditions. A recent study of Noll et al. [29], who used the same technique, showed that TcO_2 at a concentration of 10^{-2} M exists in the colloidal state above pH 0.5. Thus the interpretation of Gorski and Koch is valid only if the concentration of Tc(IV) is less than the solubility of hydrated TcO_2. If their experiments were carried out under such conditions, the values proposed can be used to establish the potential—pH diagram at concentrations low enough for all Tc(IV) to be in a soluble form throughout the entire pH range. However, these values cannot be used to calculate the solubility product as proposed by Srivastava et al. [30]. The solubility of hydrated TcO_2 has been measured by Lefort [31] as close to 5×10^{-5} M at pH 14; this value may be rather high, because he did not take into consideration the existence of colloids.

The present experiments were done with a concentration of technetium such that the precipitation of TcO_2 must be considered. The linear variation of $E_{1/2}$ with pH between pH 1.6 and 3 suggests that only one species is involved. It is known that at pH 3, Tc(IV) exists as TcO_2; Tc(IV) precipitates in chloride medium above pH 2. It is, however, possible that in a highly acidic medium (pH < 1.5), other species such as TcO^{2+}, $TcO(OH)^+$ and Tc^{4+} occur. In the pH range studied, the oxidation of Tc(III) corresponds to the reaction: $TcO^+ + H_2O \overset{-e^-}{\rightleftarrows} TcO_2\downarrow + 2H^+$.

Potential—pH diagrams obtained for two technetium concentrations (10^{-4} M and 10^{-7} M) are shown in Fig. 8. In addition to the data provided by Pourbaix, these diagrams were established on the basis of the following

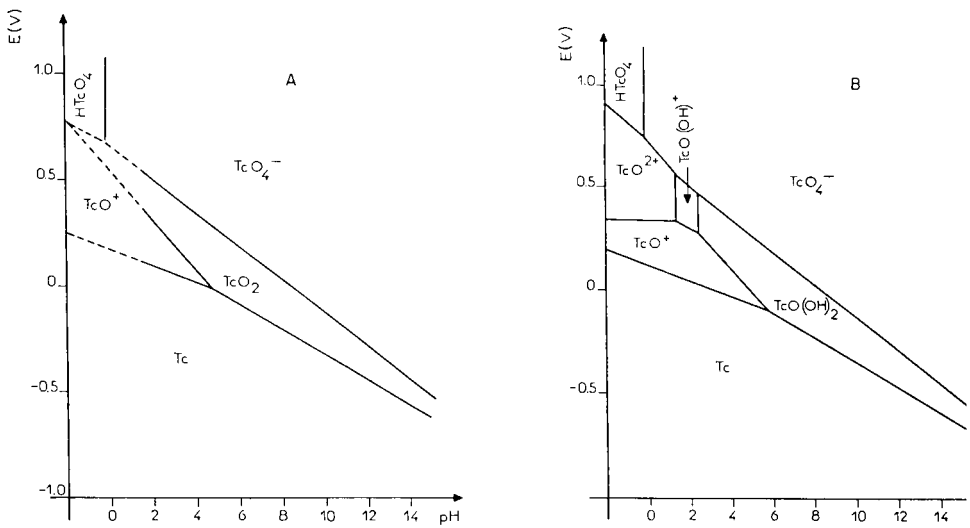

Fig. 8. Potential—pH diagrams for technetium at 25°C. (A) $[Tc]_{total} = 10^{-4}$ M; (B) $[Tc]_{total} = 10^{-7}$ M. Solubility of $TcO(OH)_2 = 5 \times 10^{-5}$ M [31]; potentials given vs. NHE.

reactions:

$TcO_2 + 2H^+ + e^- = TcO^+ + H_2O$;

$E = 0.319 - 0.1182\ pH - 0.0591 \log [TcO^+]$ (1)

based on the present experimental observations in the sulphate medium for 3×10^{-4} M Tc(III);

$TcO^+ + 2H^+ + e^- = Tc^{2+} + H_2O$;

$E = -0.031 - 0.1182\ pH + 0.059 \log [TcO^+]/[Tc^{2+}]$ (2)

$TcO^+ + 2H^+ + 3e^- = Tc(0) + H_2O$;

$E = 0.256 - 0.0394\ pH + 0.0197 \log [TcO^+]$ (3)

For a total technetium concentration of 10^{-7} M, the equilibria described by Gorski and Koch were included and the solubility of TcO_2 established by Lefort [31] was taken into account. The analysis of these diagrams (which are still incomplete) shows the important role which Tc(III) may play, as well as the complexity of the reactions in which the different oxidation states of technetium are involved.

For a total technetium concentration of 3×10^{-4} M, dismutation of Tc(III) can be predicted at pH 4.43. This agrees with the present experimental observations; in polarography the limitation of wave IA by diffusion of protons and the appearance of a wave corresponding to Tc(IV) formation were observed from pH 3.2 because of the difference between the pH measured in the bulk solution and the pH at the electrode surface in an unbuffered solution.

In this interpretation, the influence of possible sulphate complexes has not been considered, although their formation during the oxidation of Tc(III) is indicated. It has been assumed that these reactions are so slow as to exert no influence on the rate of the Tc(III) oxidation. This hypothesis is partly supported by the evolution of the voltammetric curves with pH [16], and by the fact that the slope of the curve $E_{1/2} = f(pH)$ was not modified.

The diagrams presented in Fig. 8 indicate a first reduction step of pertechnetate leading to the formation of Tc(IV). However, this step is not observed in polarography. The explanation of this apparent contradiction is based on kinetic considerations. From the oxidation of Tc(III) in sulphate medium, the following scheme may be proposed:

$$Tc(III) \xrightarrow[fast]{-e^-} Tc(IV) \xrightarrow[slow]{-3e^-} Tc(VII)$$

The quasi-reversibility of the system Tc(III)/Tc(IV), and the existence of at least one slow step between Tc(VII) and Tc(IV), explain the fact that the formation of Tc(III) by reduction of Tc(VII) is observed directly.

It has been demonstrated [16] that, even with the data available to date it is not possible to give a precise mathematical description of all the stages implicated during the reduction of pertechnetate in acidic media.

In neutral and alkaline media, the reduction of pertechnetate leads to formation of Tc(IV). Between pH 10 and pH 14, the corresponding polarographic wave divides because of adsorption of pertechnetate. Considering the

potential—pH diagrams, the following reduction can be suggested:

$$TcO_4^- + 4H_2O + 3e^- \rightleftarrows TcO_2\downarrow + 4OH^-$$

The fact that the wave is not pH-dependent may be linked to the total irreversibility of the system. Technetium dioxide is formed by a slow reaction following a charge transfer independent of pH.

We thank Professor J. A. Berger and Mr. A. Bardy for their helpful advice throughout this work.

REFERENCES

1 C. L. Rulfs and G. E. Boyd, Crit. Rev. Anal. Chem., 1 (1970) 335.
2 R. J. Magee and T. J. Cardwell in A. J. Bard (Ed.),: Encyclopedia of Electrochemistry of the Elements, Dekker, New York, 1974.
3 M. Iochev, H. Koch and H. Kupsch, Isotopenpraxis, 11 (1975) 369.
4 G. B. S. Salaria, C. L. Rulfs and P. J. Elving, J. Chem. Soc., (1963) 2479.
5 G. B. S. Salaria, C. L. Rulfs and P. J. Elving, Anal. Chem., 35 (1963) 979.
6 L. Astheimer and K. Schwochau, J. Electroanal. Chem., 8 (1964) 382.
7 S. I. Zhdanov, A. F. Kuzina and V. I. Spitsyn, Russ. J. Inorg. Chem., 15 (1970) 803.
8 A. F. Kuzina, S. I. Zhdanov and V. I. Spitsyn, Dokl. Akad. Nauk. SSSR, 144 (1962) 836.
9 C. L. Rulfs, R. Pacer and A. Anderson, J. Electroanal. Chem., 15 (1967) 61.
10 R. Munze, Z. Phys. Chem. (Leipzig), 238 (1968) 364.
11 R. Munze, Z. Phys. Chem. (Leipzig), 226 (1964) 415.
12 R. J. Magee, I. A. P. Scott and C. L. Wilson, Talanta, 2 (1959) 376.
13 H. H. Miller, M. T. Kelley and P. F. Thomason, Advances in Polarography, Vol. 2, Pergamon Press, 1959, p. 716.
14 R. Colton, J. Dalziel, W. P. Griffith and J. Wilkinson, J. Chem. Soc., (1960) 71.
15 C. D. Russel and A. G. Cash, J. Electroanal. Chem., 92 (1978) 85.
16 J. Grassi, Thesis, University Pierre et Marie Curie, Paris, (1977).
17 N. de Zoubov and M. Pourbaix, Centre Belge d'Etude de la Corrosion, report 50, 1957.
18 C. M. Nelson, G. E. Boyd and W. J. Smith, J. Am. Chem. Soc., 76 (1954) 348.
19 V. I. Spitsyn, A. F. Kuzina, S. I. Zhdanov and I. V. Kaimin, Russ. J. Inorg. Chem., 15 (1970) 662.
20 J. Grassi, P. Rogelet, J. Devynck and B. Trémillon, J. Electroanal. Chem., 88 (1978) 97.
21 V. I. Spitsyn, A. F. Kuzina, A. A. Oblova, M. I. Glinkina and L. I. Stepovaya, J. Radioanal. Chem., 30 (1976) 561.
22 R. S. Nicholson and I. Shain, Anal. Chem., 36 (1964) 706.
23 J. Heyrovsky and J. Kuta, Principles of Polarography, Academic Press, New York, 1966, 287.
24 S. G. Mairanovskii, Catalytic and Kinetic Waves in Polarography, Plenum Press, New York, 1968 p. 57.
25 M. Sluyters-Rehbach, C. A. Wijnhurst and J. H. Sluyters, J. Electroanal. Chem., 74 (1976) 3.
26 B. Gorski and H. Koch, J. Inorg. Nucl. Chem., 31 (1969) 3565.
27 J. Y. Guennec and R. Guillaumont, Radiochem. Radioanal. Lett., 13 (1973) 33.
28 A. Owunwanne, J. Marinsky and M. Blau, J. Labelled Compd., 13 (1976) 159.
29 B. Noll, S. Seifert and R. Munze, Zentralinst. Kernforsch. Rossendorf. Dresden (Ber.), (1975) 145.
30 S. C. Srivastava, G. Meinken and P. Richards, Int. J. Appl. Radiat. Isotopes, 28 (1977) 8
31 M. Lefort, Bull. Soc. Chim. Fr. (1969) 882.

Analytica Chimica Acta, 107 (1979) 59—66

DIFFERENTIAL PULSE POLAROGRAPHIC DETERMINATION OF THE *N*-NITROSO DERIVATIVE OF A TRIPEPTIDE IN PHARMACEUTICAL DOSAGE FORMS

D. G. PRUE*, F. Q. GEMMILL JR., and R. N. JOHNSON

Ayerst Laboratories Inc., 64 Maple St., Rouses Point, NY 12979 (U.S.A.)

(Received 18th September 1978)

SUMMARY

A method is described for determining a tripeptide (pareptide) in tablets and capsules, which is based on the pulse polarographic measurement of its *N*-nitroso derivative. The electrochemical behavior of the derivative was found to be similar to that of other *N*-nitrosamines with regard to the effects of temperature, pH, and mercury pressure. The reduction process is irreversible and complicated by adsorption. Optimum conditions for preparation of the *N*-nitroso derivative, which appear to be atypical, are presented. Spectroscopic data from i.r., m.s., n.m.r. and u.v. analyses suggest that the derivative differs from the parent compound only in that it has a single *N*-nitroso group on the proline segment of the tripeptide chain. Replicate assays on tablets containing 2 mg of pareptide gave excellent precision with a coefficient of variation of 0.37%. Comparison of results obtained on capsules containing 2 mg of pareptide and stored at high temperatures showed good correlation between the polarographic and an h.p.l.c. method. Results obtained with a number of possible decomposition products indicate that the polarographic method is specific for pareptide.

Pareptide, L-prolyl-*N*-methyl-D-leucyl glycinamide sulfate, has been synthesized by a four-component condensation procedure [1], and has been shown to have potential clinical applicability with regard to the treatment of Parkinson's disease and depression [2, 3]. Pareptide itself does not possess electrochemical activity, but it can be converted by reaction with nitrite to a polarographically reducible *N*-nitroso derivative. The reduction of *N*-nitrosamines at the dropping mercury electrode has been investigated and is generally well understood. In acidic solution, *N*-nitrosamines undergo an irreversible 4-electron reduction to the corresponding hydrazine, and in basic solutions undergo an irreversible 2-electron reduction to nitrous oxide and the precursor amine [4, 5].

The object of this work was to develop an analytical method which was sensitive and specific for pareptide in the presence of possible decomposition products, and suitable for its determination in tablets and capsules. The method presented here is based on a nitrosation reaction carried out under mild conditions, and subsequent detection of the derivative by polarography. This approach has been used in successful analyses for other pharmaceutically

important compounds which have a secondary amine functional group, e.g., ephedrine [6] and adrenaline, methylamphetamine and clorprenaline [7]. The electrochemical behavior of *N*-nitrosopareptide, conditions for its formation, and characterization of the derivative are also discussed.

EXPERIMENTAL

Instrumentation

All polarograms were obtained with a Princeton Applied Research polarographic analyzer and recorder (Model 171) equipped with a mechanical drop knocker (Model 172). A Beckman fiber-junction saturated calomel electrode (SCE) was used as the reference electrode and a platinum wire was employed as the auxiliary electrode. The dropping mercury electrode (DME) had the following characteristics (open circuit) in acetate buffer, pH 4.75, $m = 5.08 \times 10^{-4}$ g s^{-1}.

The following instrumentation was used for characterization of *N*-nitrosopareptide: Cary u.v. spectrophotometer model 14, Beckman i.r. spectrophotometer model 12, Varian n.m.r. spectrometer model EM-360, and LKB mass spectrometer model 9000.

Chemicals

Pareptide was synthesized [1] at Ayerst Research Laboratories, Montreal, Quebec, Canada. For characterization studies, *N*-nitrosopareptide solutions were prepared by dissolving 2 g of pareptide in acetic acid 1 + 1), then adding 10 ml of 10% sodium nitrite solution and allowing the mixture to stand overnight at room temperature. The reaction mixture was evaporated to dryness and extracted with acetone. The acetone was removed under vacuum and the resulting oil dissolved in 10 ml of distilled water. The solution was lyophilized to give an amorphous solid.

N-nitroso-L-(—)-proline was prepared by the method of Lijinsky et al. [8]. Colorless crystals were obtained (m.p. 104–105°C; $[\alpha]_D^{25} = -187.4°$; C = 0.29 in water).

All other chemicals were of laboratory-reagent grade.

Analytical procedure for tablets and capsules

Calibration. Weigh out 5, 10 and 15 mg of pareptide reference standard and quantitatively transfer to separate 100-ml volumetric flasks. Dissolve and dilute to volume with acetic acid (1 + 19). Pipet 20.0 ml of each standard into separate 25-ml volumetric flasks, add 2.0 ml of aqueous sodium nitrite solution (70 mg ml^{-1}) and dilute to volume with water. Mix and leave to stand for 60 min. Pipet 5.0 ml of each reaction mixture into separate 50-ml volumetric flasks containing 5.0 ml of 2 M ammonium sulfamate solution. Swirl, leave for 5 min, and dilute each solution to volume with pH 4.75 acetate buffer (0.5 M sodium acetate and 0.5 M acetic acid). Transfer a quantity of standard solution to the polarographic cell and deaerate for 5 min

with nitrogen. Insert the electrodes and scan from —0.5 V to —1.2 V at 5 mV s^{-1}, with a drop time of 1 s, a current range of 20 μA and a pulse amplitude of 100 mV. Measure the peak current at —0.83 V for each standard and construct a calibration curve in the conventional manner.

Sample preparation. Weigh out the equivalent of 10 mg of pareptide from a tablet or capsule powder pool and quantitatively transfer to a 250-ml extraction bottle. Add 100.0 ml of acetic acid (1 + 19) and shake on a mechanical shaker for 60 min. Centrifuge the mixture and pipet 20.0 ml of the clear supernatant liquid into a 25-ml volumetric flask. Proceed with the nitrosation reaction as described above. Calculate the sample strength from the equation: mg/tablet (or capsule) = $U \times (W_a/W_s)$, where U = mg of pareptide corresponding to the measured peak current, W_a = average tablet or capsule weight (mg), and W_s = sample weight (mg).

It should be noted that *N*-nitrosamines may have carcinogenic properties, so that due precautions should be taken.

RESULTS AND DISCUSSION

Polarographic study

The *N*-nitroso derivative of pareptide gives a single well-defined polarographic wave in pH 4.75 acetate buffer with a peak potential of —0.83 V vs. SCE. The differential pulse current increases linearly with concentration in the range 0.1—40 μg ml^{-1} (Table 1). At concentrations above 40 μg ml^{-1}, there is a change in the slope of the curve and a second linear range is observed. The $E_{1/2}$ values remain essentially unchanged in the lower concentration range, but tend to become more negative with increasing concentration in the upper portion of the curve. Similar trends have been reported and

TABLE 1

Polarographic data for the reduction of various amounts of *N*-nitrosopareptide in 0.5 M acetate buffer, pH 4.75

Conc. (μg ml^{-1})	i_d (μA)	—E 1/2 (mV)	Slope (μA/μg ml^{-1})
300	149.0	0.92	0.50
200	105.9	0.90	0.50
100	62.0	0.88	0.62
40	30.0	0.85	0.75
20	15.9	0.84	0.80
10	8.03	0.83	0.80
5	4.00	0.83	0.80
1	0.788	0.83	0.79
0.5	0.390	0.83	0.78
0.3	0.225	0.83	0.75
0.1	0.078	0.83	0.78

generally, in a well-buffered medium, are ascribed to specific adsorption of the reactant and/or electrode product [9].

The effects of temperature and pH on the reduction of *N*-nitrosopareptide were studied. The dependence of the differential pulse current on the temperature in the range 20—40°C was 0.6% per degree with the greatest change being 1.0% per degree between 20 and 25°C. The $E_{1/2}$ values were shifted to more negative potentials with increasing pH between 1.4 and 5.2, which is in general accord with results on other *N*-nitrosamines and supports the mechanism of reduction of the protonated species in acidic solution.

The reversibility of the reduction was assessed by the scan reversal technique [10]. Accordingly, in the pulse mode reversible electroreductions produce an anodic wave equal in height to the cathodic wave, whereas totally irreversible electroreductions yield an anodic wave only about one-seventh the height of the cathodic wave. The value of the cathodic to anodic wave height ratio for *N*-nitrosopareptide was 5.2:1 suggesting an irreversible electrode process. Classical logarithmic analysis, where values of $\log (\bar{i}_d - \bar{i})/\bar{i}$ are plotted vs. values of E, gave $n = 1.06$, which is in good agreement with values of n obtained for the irreversible reduction of *N*-nitrosoproline [11].

Dependence of the limiting current on the mercury head pressure was studied in the d.c. mode with a drop time of 2 s. For diffusion-controlled wave the height of the wave is approximately proportional to $h^{2/3}$ when a mechanically-controlled drop time is used [11]. A bivariate curve-fitting program was used to calculate the power of h, and values of 0.72 and 0.68 were found for concentrations of 20 and 300 $\mu g\ ml^{-1}$, respectively. These results suggest that the limiting currents are diffusion-controlled.

Figure 1 shows typical differential pulse polarograms of *N*-nitrosopareptide at concentrations between 0.1 and 1.0 $\mu g\ ml^{-1}$. For a drop time of 1 s, a currer range of 1 μA, and a modulation amplitude of —100 mV, the detection limit was 0.05—0.1 $\mu g\ ml^{-1}$ or $1.5—3.0 \times 10^{-7}$ M.

Derivative formation and characterization

Secondary amines react with nitrous acid, which can be generated in the presence of the amine by the action of mineral acids on sodium nitrite. The product is the polarographically reducible nitrosamine. Pareptide reacted with nitrous acid by virtue of the secondary amine in the proline segment of the tripeptide chain. Nitrosation was complete in 1 h at room temperature in an acetic acid medium, but failed to give a measurable product when the reaction was conducted in dilute mineral acids, e.g., H_2SO_4, HCl and $HClO_4$. Figure 2 illustrates the dependence of the rate of nitrosation on the concentration of sodium nitrite and on the reaction time. The concentration of acetic acid played a less important role in the nitrosation reaction, the same rate being obtained at concentrations of 5, 10 and 25%.

Nitrite is reduced at nearly the same potential as *N*-nitrosopareptide and must be completely removed before the polarographic measurement. The addition of ammonium sulfamate efficiently destroys the excess of nitrite from the reaction.

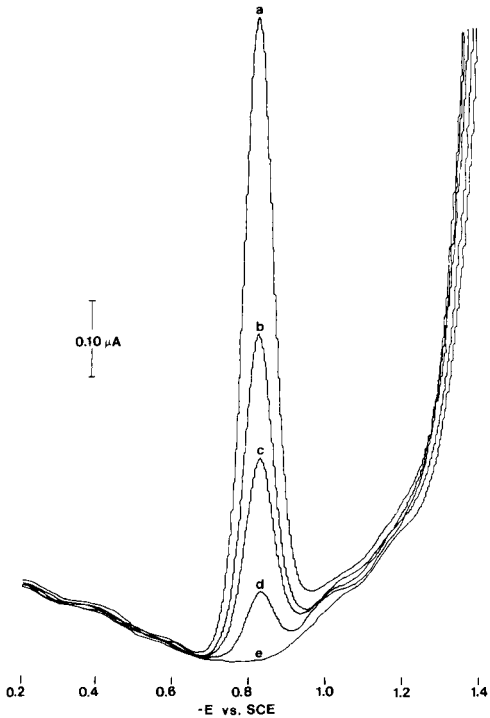

Fig. 1. Differential pulse polarograms of *N*-nitrosopareptide in acetate buffer pH 4.75; (a) 1.0 μg ml^{-1}, (b) 0.5 μg ml^{-1}, (c) 0.3 μg ml^{-1}, (d) 0.1 μg ml^{-1}, and (e) supporting electrolyte.

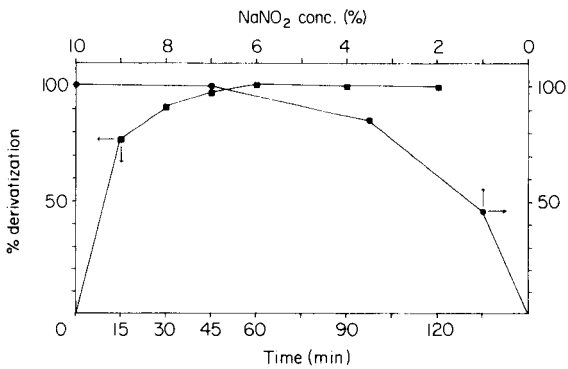

Fig. 2. Influence of the concentration of sodium nitrite and the reaction time on the nitrosation of pareptide at room temperature.

The i.r. spectra of *N*-nitrosoproline and other *N*-nitroso amino acids contain a medium band at 1430—1450 cm^{-1} which is attributed to the *N*-nitroso group [8]. This region of the i.r. spectrum of *N*-nitrosopareptide was

obscured by other strong absorptions; the spectrum does, however, rule out the occurrence of three other possible reactions. Reaction of the primary amide with nitrous acid can give the corresponding carboxylic acid while the secondary amide could nitrosate. No bands for carboxylic acid or secondary nitrosamide were present, consequently the primary and secondary amide groups were left intact. Formation of an *N*-nitro derivative was also ruled out, because i.r. bands for *N*-nitro were absent.

The n.m.r. spectrum of *N*-nitrosopareptide showed the disappearance of the resonance from the amine proton on the proline moiety and the appearance of a resonance attributable to the methylene protons adjacent to the proline nitrogen. Comparison of the mass spectra of *N*-nitrosopareptide and pareptide showed ions at *m/e* 328 and *m/e* 299, respectively. The origins of these ions and additional mass spectral data are listed in Table 2.

Analysis of *N*-nitrosopareptide by u.v. spectrophotometry showed absorption maxima at 343 and 227 nm. Similar absorptions were observed for *N*-nitrosoproline. The parent amines in both cases have only single maxima at 262 nm (see Table 3). Other nitroso compounds have similar absorption characteristics [8, 12, 13] while *N*-nitro compounds do not have the absorption maximum at 340—345 nm [14].

The combination of spectroscopic and polarographic data strongly suggests a derivative containing a single nitroso group bonded to the secondary amine in proline. The nitrosation reaction is indicated by

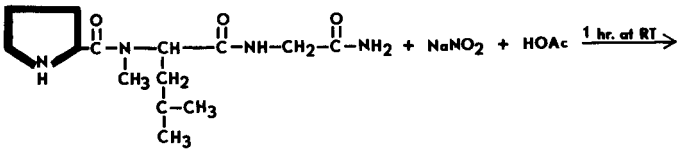

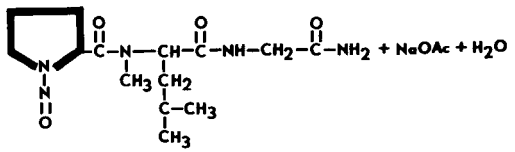

Analytical application

Analysis of pharmaceutical dosage forms can often be complicated by the presence of surfactants that distort, suppress, or completely inhibit a polarographic wave. When the technique of standard addition does not successfully circumvent this problem, a preliminary clean-up step can be employed to remove the surfactant or isolate the compound of interest before the polarographic measurement. Another approach which has proven successful is dilution of the sample solution to concentrations at or below the low $\mu g\ ml^{-1}$ range. This approach simplifies sample preparation and minimizes analysis

TABLE 2

Mass spectroscopic data for *N*-nitrosopareptide and pareptide

m/e	Relative abundance (%)	Origin	*m/e*	Relative abundance (%)	Origin
N-nitrosopareptide			*Pareptide*		
328	1	$[M + H]^+$	299	1	$[M + H]^+$
310	8	$[M - NH_3]^+$	298	2	M^+
297	25	$[M - NO]^+$	241	6	$[M - C_2H_3NO]^+$
254	2	$[M -$ glycinamide$]^+$	100	40	$[$methylisoamylamine $- H]^+$
100	100	$[$methylisoamylamine $- H]^+$	70	100	$[$proline $- H]^+$
70	30	$[$proline $- H]^+$			

TABLE 3

U.v. absorption data for *N*-nitroso compounds and their parent amines

Compound	λ_{max} (nm)	ϵ_{max} (l mol^{-1} cm^{-1})	λ_{min} (nm)
N-Nitrosopareptide	343, 227	76, 6580	292, shoulder
N-Nitroso-L-proline	343, 236	91, 6720	295, 202
Pareptide	262	46	251
L-Proline	262	6.9	235

time, but demands that the measurement technique have excellent sensitivity. It is evident from the data in Table 1 that differential pulse polarography has sufficient sensitivity for determining *N*-nitrosopareptide at very low concentrations and is therefore a suitable technique, provided that acceptable precision, accuracy and selectivity can be achieved.

The excellent precision of the method was illustrated by ten analyses of tablets containing, nominally, 2 mg of pareptide: a mean result of 1.96 mg/tablet was obtained, with a coefficient of variation of 0.37%. Accuracy and selectivity were assessed by determining the pareptide content of capsules that had been subjected to thermal stress. Comparison of the polarographic results with results obtained by an inherently-selective h.p.l.c. procedure [15] indicates that the polarographic method is accurate even when pareptide has undergone decomposition (Table 4). Additional information on selectivity

TABLE 4

Polarographic and h.p.l.c. results on pareptide capsules subjected to thermal stress

Sample	Storage	Found (% Claim)	
		H.p.l.c.	Polar.
1	4 wks. at 4°C	101.7	99.0
2	4 wks. at 62°C	73.6	71.8
3	34 wks. at 40°C	91.0	93.8

was obtained from an examination of the $E_{1/2}$ values for pareptide and some of its possible decomposition products after nitrosation by the recommended procedure. Thus prolylleucine showed a wave at a half-wave potential of —0.90 V and proline a wave at —1.08 V, but no responses were obtained for leucylglycine, leucine, methylleucine, glycine or glycinamide at concentrations of 10 μg ml^{-1}. These results also support the conclusion that *N*-nitroso-pareptide contains a single nitroso group.

The authors express their appreciation to C. Orzech and R. Daley for valuable discussions, to G. Schilling for providing mass spectroscopic data, and to R. Pickering for providing h.p.l.c. data.

REFERENCES

1 A. Failli, K. Sestanj, H. U. Immer and M. Götz, Arzneim.-Forsch. Drug Res., 27 (1977) 2286.
2 K. Voith, Arzneim.-Forsch. Drug Res., 27 (1977) 2290.
3 T. A. Pugsley and W. Lippman, Arzneim.-Forsch. Drug Res., 27 (1977) 2293.
4 H. Lund, Acta. Chem. Scand., 11 (1957) 990.
5 W. F. Smyth, P. Watkiss, J. S. Burmicz and H. O. Hanley, Anal. Chim. Acta, 78 (1975) 81.
6 H. Burghardt, H. Jäger and M. von Stackelberg, J. Electroanal. Chem., 17 (1968) 191.
7 R. Vilvala and J. Halmekoski, Farm. Aikak, 84 (1975) 171.
8 W. Lijinsky, L. Keefer and J. Loo, Tetrahedron, 26 (1970) 5137.
9 G. Pezzatini and R. Guidelli, J. Chem. Soc. Faraday Trans. 1, 69 (1973) 794.
10 K. B. Oldham and E. P. Parry, Anal. Chem., 42 (1970) 229.
11 K. Hasebe and J. Osteryoung, Anal. Chem., 47 (1975) 2412.
12 R. Zahradnik, E. Svatek and M. Chvapil, Collect. Czech. Chem. Commun., 24 (1959) 347.
13 R. N. Hesgeldine and J. Jandev, J. Chem. Soc., (1954) 961.
14 R. N. Jones and G. D. Thorn, Can. J. Res., 276 (1949) 828.
15 Unpublished in-house procedure.

Analytica Chimica Acta, 107 (1979) 67—73

ORIGIN AND ELIMINATION OF INTERFERENCES FROM SILICONIZATION PROCEDURES IN ANODIC STRIPPING VOLTAMMETRY

M. OEHME

Department of Chemistry, University of Oslo, Box 1033, Blindern, Oslo 3 (Norway)

(Received 9th November 1978)

SUMMARY

Interferences caused by organic impurities can be a serious problem in trace analysis for heavy metals by differential pulse anodic stripping voltammetry. Organic impurities, which originate from siliconization treatment of the capillary of the hanging mercury drop electrode, can cause high background currents, interfering signals and peak broadening, especially in the concentration range below 5 ppb. A new method of siliconization for glass capillaries which avoids these problems is reported. A reference electrode with a polyacrylamide gel-stiffened internal electrolyte is recommended, to avoid difficulties such as adsorption of organic material on low-leakage diaphragms of the Vycor type, which are often used in trace analysis.

The main advantage of the hanging mercury drop electrode (h.m.d.e.), which is normally used in anodic stripping voltammetry (a.s.v.), is the easy replacement of the old mercury drop by a new one of the same size. Penetration of water into the glass capillary is normally prevented by treatment with a siliconizing agent. The electrolytic cell is often also siliconized in trace analysis, to prevent losses of metals by adsorption. Normally a solution of dimethyldichlorosilane (DMCS) is used for this treatment [1, 2]. In this paper, it is shown that organic impurities in DMCS can cause severe interferences in trace analysis by differential pulse anodic stripping voltammetry. Especially in the concentration range of 1—5 ppb or lower, interpretation of the lead and copper signals is often complicated and prone to error. Although these interferences can be more serious than many other types of positive or negative contamination of the sample, there are few references to such effects in the literature [3, 4]. The new method of siliconization proposed eliminates the problem of interfering organic peaks. Other advantages are lower background currents and improved stability of the siliconized surface in alkaline solutions.

EXPERIMENTAL

Apparatus

A Princeton Applied Research 174A Polarographic Analyzer and a Radiometer REC 51/REA 112 recorder were used. A home-made timer unit

controlled the different steps in the stripping voltammetric procedure. A magnetic stirrer (Internationale Laboratoriumsapparate, M 10) and a Teflon-covered bar were used to stir the sample solution. A hanging mercury drop electrode (Metrohm E 410) was used as working electrode with a platinum coil counter electrode. The reference electrode was an Ag/AgCl electrode, which was filled with 3 M KCl and had a Vycor tip diaphragm (Princeton Applied Research K 65), or a gel-stiffened type (see below). The electrolytic cell (Metrohm EA 876) had a volume of 20 ml. Dissolved oxygen was removed from the solution by passing highly purified nitrogen for 10 min; during experiments nitrogen was passed over the solution.

All glass equipment was cleaned thoroughly with chromic acid and diluted nitric acid before each new series of experiments.

Reagents and solutions

Standard metal solutions were prepared from analytical-grade chloride salts. Dimethyldichlorosilane was obtained in analytical-grade quality from different companies (Fluka, E. Merck-Schuchard, Aldrich Chemical Company, Pierce Chemical Company). Except for one sample, which was stored under inert gas (Fluka), no differences were observed in quality concerning electroactive impurities. Hexamethyldisilazane (HMDS, puriss., Fluka) was delivered under argon.

The 0.1 M acetate buffer used consisted of a 1:1 mixture of Suprapur acetic acid and sodium acetate (both E. Merck). The water was deionized and purified by a Millipore Milli-Q water system.

For siliconization, 5% (v/v) solutions of the reagent were prepared in analytical-grade carbon tetrachloride or benzene.

Preparation of the reference electrode

To prepare the internal reference solution, add 10 g of polyacrylamide (BDH Chemicals Ltd., M.W. $> 5 \times 10^6$) to 90 ml of 3 M KCl (Suprapur, E. Merck) in a plastic bottle. Wait for one day or longer until the electrolyte has become highly viscous. Then press the gel from the plastic bottle through a small tube into the electrode body (Fig. 1), which is fitted with a ceramic diaphragm of 1.5-mm diameter. Fill the Ag/AgCl cartridge (Metrohm EA 420) with 3 M KCl under vacuum and place it into the reference electrode body (see also ref. 5).

Preparation of the capillaries

Remove old silicone films by passing ethanolic 3% (w/v) sodium hydroxide solution through the capillary for about 10 min by means of a water jet pump. Repeat this procedure with chromic acid and 10% (v/v) nitric acid (Suprapur) to remove organic and inorganic impurities. Rinse the capillary between treatments with distilled water for about 10 min. Then dry the capillary for an hour at 180°C.

Suck one of the siliconization solutions or the pure siliconization agent

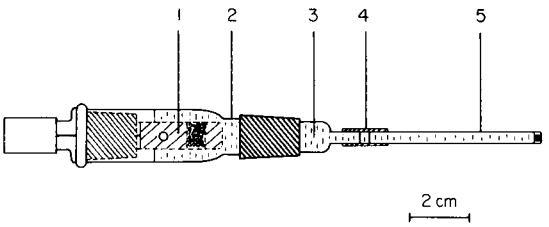

Fig. 1. Reference electrode with gel-stiffened electrolyte. (1) Ag/AgCl cartridge; (2) electrode body; (3) internal electrolyte consisting of 3 M KCl stiffened with polyacrylamide; (4) Teflon connecting tube; (5) glass tube with ceramic diaphragm.

through the capillary for a few seconds. Then dry the capillary at 180°C for several hours. Best results were obtained with pure HMDS or with 5% (v/v) solutions of HMDS in benzene and a drying period of 18 h (see below).

Measuring procedure

Transfer 20 ml of 0.1 M acetate buffer to the electrolytic cell and deaerate for 15 min. Extrude a fresh mercury drop (diameter 0.84 mm) and record the background current in the range −0.8 to +0.2 V vs. Ag/AgCl, without any waiting time or stirring. Use the following instrument settings: scan rate 10 mV s^{-1}, pulse repetition time 0.195 s (obtained after modification of the instrument) and modulation amplitude 50 mV. After the extrusion of a new drop, start the stirrer and electrolyse for 5 min at −0.8 V. Stop the stirrer and record the stripping voltammogram of the blank solution. Add 50 μl of the standard metal solution, repeat the procedure and determine the concentrations of Cd, Pb and Cu by the method of standard addition.

RESULTS AND DISCUSSION

Siliconization procedure

The fact that stripping voltammograms occasionally show signals which interfere with the determination of lead and copper below the 5 ppb level, led to a closer analysis of these phenomena. Especially at short electrolysis times (1—5 min) and high instrumental sensitivities, these interferences were considerable. In these cases, increased background current and diminished sensitivity were also observed.

Both the interference on the lead signal and the signal in the copper region were independent of the electrolysis time. This and the shape of the signals (see Fig. 2, curve a) led to the assumption that they were caused by organic impurities. These substances originated from the siliconization solution consisting of 5% (v/v) DMCS in carbon tetrachloride. Solutions made from older batches showed an increased content of such impurities, which are probably hydrolysis products of DMCS on contact with air. Because of the two reactive chlorine atoms, many different polymerization products can be obtained,

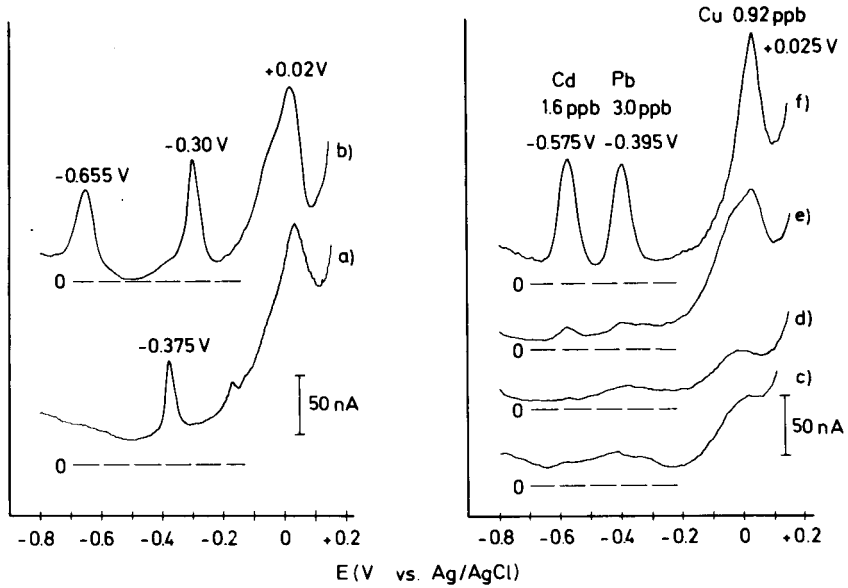

Fig. 2. Stripping voltammograms of capillaries treated with DMCS by different methods. Electrolyte solution: 0.1 M acetate buffer pH 4.6. Curves (a—d) show the voltammograms obtained for the capillary background without pre-electrolysis: (a) 5% (v/v) DMCS in CCl_4, heated for 2 h at 180°C; (b) pure DMCS, heated for 18 h at 180°C; (c) 5% (v/v) DMCS stored under inert gas in CCl_4, heated for 2 h at 180°C; (d) as c, but heated for 18 h. Curve (e) is the same as (d) but after electrolysis for 5 min. Curve (f) is the same as (e) after adding 1.6 ppb Cd, 3.0 ppb Pb and 0.9 ppb Cu.

and non-volatile products can be formed by cross-linking reactions. After siliconization with solutions of DMCS which were more than 3—4 months old, small droplets of an oily substance were observed on the glass surface even though the capillaries were heated at 300°C for 10 h. These capillaries were completely unfit for use.

The quality of commercially available DMCS was very variable. Figure 2 (curve b) shows interference signals for a capillary, siliconized with pure DMCS from a newly opened bottle. Capillaries treated with DMCS which had been distilled and stored under an inert gas and diluted with CCl_4 just before use showed a relatively acceptable background current (Fig. 2, curves c and d). Prolonged heating of these capillaries at 180°C gave no essential reduction of the background current.

However, handling DMCS under inert gas is time-consuming and the siliconization solutions must be prepared immediately before use. The penetration of even small traces of water into the siliconization solution leads to increased background signals within a short time. As can be seen in Fig. 2 (curves e and f), the copper signal is deformed by organic impurities from DMCS, which are partly adsorbed on the mercury surface [3].

Other methods and reagents for the siliconization of the glass surface were therefore investigated. Less suitable for siliconization are silicone oils (e.g. Rhodorsil SI 1107, Dow Chemical); they do not react directly with the polar hydroxyl groups of the glass, impurities in the oil are mostly non-volatile and the mercury drop detaches more easily. In addition, after heating the silicone film, capillaries were often clogged by glassy residues. Trimethylchlorosilane, which has only one chlorine atom and thus precludes the problem of cross-linking, is not reactive enough and the silicone film becomes damaged after only a few hours.

Finally hexamethyldisilazane (HMDS) was used as siliconization agent. The product was very clean and capillaries treated with the pure reagent showed a very low background current (Fig. 3, curve d). An equally useful background could be obtained with a solution of 5% (v/v) HMDS in carbon tetrachloride (Fig. 3, curves a and b) or benzene (Fig. 3, curve c). The stability of the silicone layer against dilute alkaline solutions was tested by placing mercury-filled capillaries in a 0.1 M sodium acetate solution adjusted to pH 10 with sodium hydroxide. After 6 h in this solution, the capillaries treated with pure HMDS or HMDS in benzene were still usable. For all other capillaries, siliconized with DMCS or with solutions of DMCS or HMDS in CCl_4,

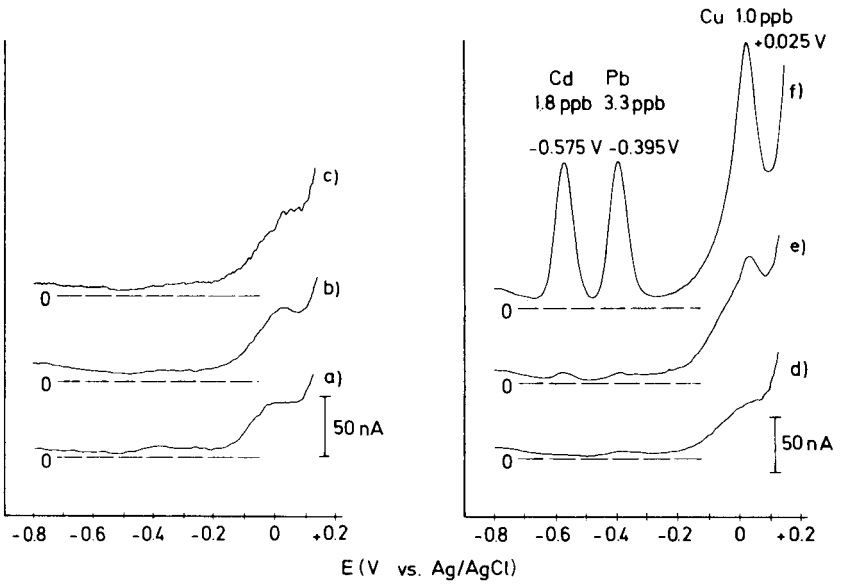

Fig. 3. Stripping voltammograms of capillaries treated with HMDS by different methods. Electrolyte solution: 0.1 M acetate buffer pH 4.6. Curves (a—d) show the voltammograms obtained for the capillary background without pre-electrolysis: (a) 5% (v/v) HMDS in CCl_4, heated for 2 h at 180°C; (b) as (a) but heated for 18 h; (c) 5% (v/v) HMDS in benzene, heated for 18 h at 180°C; (d) pure HMDS, heated for 18 h at 180°C. Curve (e) is the same as (d) but with electrolysis for 5 min. Curve (f) is the same as (e) after adding 1.8 ppb Cd, 3.3 ppb Pb and 1.0 ppb Cu.

the mercury drop did not adhere sufficiently after this period. One explanation is that both the reaction product of DMCS, hydrogen chloride, and the solvent CCl_4 are partly adsorbed on the glass surface, producing polar groups which facilitate penetration of water into the capillary. In comparison, the reaction product of HMDS, ammonia, shows less tendency to be adsorbed. In addition, HMDS is less sensitive to atmospheric moisture and is therefore easier to handle.

For most purposes, treatment of the capillary with pure HMDS or a solution of HMDS in benzene, followed by heating for 2 h at 180°C is sufficient. At pH 10, this silicone film is stable for several hours. Better stability against alkaline solutions can be obtained by heating the capillary for 18 h at 180°C. No improvement was obtained at higher temperatures or longer heating times. Figure 3 (curve e) shows the background of a capillary treated with pure HMDS at 180°C for 18 h after an electrolysis time of 5 min in 0.1 M acetate buffer; curve f was obtained after a standard addition of Cd, Pb and Cu to the solution. Even at this low concentration perfectly shaped signals were obtained.

Effects on reference electrode

Another effect observed in these experiments was the adsorption of surface-active substances and organic impurities on the surface of the low-leakage diaphragm of the reference electrode, which consists of an unglazed Vycor tip of low resistance. When this is exposed to solutions containing large quantities of organic material, e.g. in biological samples, some organic matter is adsorbed on the surface. Desorption is strongly pH-dependent and other solutions can be contaminated by a polluted diaphragm (see Fig. 4). In addition, such diaphragms are damaged at low pH-values and when exposed to different environments compared with the internal filling solution [6]; effective cleaning is therefore difficult. To overcome these problems, a low-leakage reference electrode with a ceramic diaphragm and an internal reference solution stiffened with polyacrylamide was designed [5]. No contamination of the sample solution by leakage of the reference electrode was then observed.

In contrast to reference electrodes in which polyvinyl alcohol or agar gels are used as stiffening agent, the electrode with polyacrylamide is serviceable even with large differences in salt concentration over the diaphragm and with concentrated internal reference solutions such as 3 M KCl. Neither precipitate nor turbidity was observed. The diaphragm was easy to clean with dilute nitric acid.

Figure 4 shows the background current of a solution measured first with a reference electrode with a ceramic diaphragm and an internal gel electrolyte (Fig. 4, curve a) and afterwards with a reference electrode with a contaminated low-leakage diaphragm (Fig. 4, curve b).

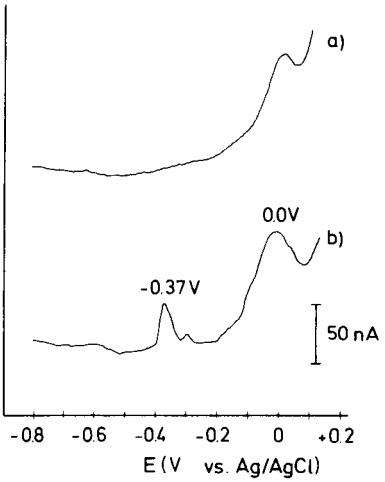

Fig. 4. Stripping voltammograms obtained for blank solutions of 0.1 M acetate buffer pH 4.6 after electrolysis for 2 min, with different reference electrodes. The capillary was treated with pure HMDS. (a) Reference electrode with a ceramic diaphragm and a gel-stiffened internal electrolyte; (b) Reference electrode with a contaminated, low-leakage, Vycor-type diaphragm.

This work was supported by a postdoctoral fellowship from the Royal Norwegian Council for Scientific and Industrial Research. The author thanks Dr. W. Lund for helpful discussions.

REFERENCES

1 R. Neeb, Inverse Polarographie und Voltammetrie, Verlag Chemie, Weinheim, 1969, p. 90.
2 F. Vydra, K. Štulík and E. Juláková, Electrochemical Stripping Analysis, Ellis Horwood, Coll House, Westergate, Chichester, 1976, p. 138.
3 E. Eriksrud, J. Electroanal. Chem., 49 (1974) 77.
4 M. Oehme, W. Lund and J. Jonsen, Anal. Chim. Acta, 100 (1978) 389.
5 S. Ertl, Application report AF-UB-76.03.17, Polymetron AG, Hombrechtikon, Switzerland.
6 Princeton Applied Research Corp., Instruction Sheet 9050-A-MD.

Analytica Chimica Acta, 107 (1979) 75—82

DIFFERENTIAL PULSE POLAROGRAPHIC DETERMINATION OF SULFURIC ACID

KENNETH W. HANCK* and J. F. McGAUGHEY**

Department of Chemistry, North Carolina State University, Raleigh, North Carolina 27650 (U.S.A.)

(Received 18th October 1978)

SUMMARY

Acetonitrile is used as a solvent for the determination of micromolar amounts of sulfuric acid by differential pulse polarography. Contaminants in the supporting electrolyte and solvent present the biggest problems to the accurate determination of sulfuric acid. The detection limit is 2×10^{-7} M. Nitric acid, bromide, soluble sulfates, and ammonium hydrogensulfate interfere under certain conditions.

Sulfuric acid is usually determined indirectly by measuring either total acidity or total sulfate [1, 2]. Interference from other acids, sulfates or hydrogensulfates is eliminated either by the apparatus used for sample collection or by chemical separation techniques. Early d.c. polarographic studies of the reduction of Brønsted acids in acetonitrile by Coetzee and Kolthoff [3] indicated that sulfuric acid was reducible at a potential well removed from other common acids; sulfate and hydrogensulfate were found to be electro-inactive.

The polarographic reduction of sulfuric acid in acetonitrile appeared to offer a method for the direct determination of sulfuric acid. This paper describes the use of differential pulse polarography (d.p.p.) for the determination of sulfuric acid at levels likely to be encountered in the determination of sulfuric acid aerosol.

EXPERIMENTAL

Reagents

Spectrophotometric grade acetonitrile was obtained from Aldrich Chemical Company (Gold Label) or from Burdick and Jackson Labs. For the determination of H_2SO_4 in the absence of HNO_3, acetonitrile purchased from either vendor could be used as received.

The quaternary ammonium perchlorates (Eastman Chemical, Inc.) tetra-

**Present address: Research Triangle Institute, Research Triangle Park, NC 27709, U.S.A.

butyl (TBAP) and tetraethyl (TEAP) were used as supporting electrolytes at a concentration of 0.1 M. TBAP was purified by dissolving it in as little acetone as possible (without heating) and then precipitating it by the addition of deionized water [4]. This procedure was repeated four times. The recovered TBAP was dried at 75°C under vacuum for 24 h.

The TEAP was purified as follows: dissolve approximately 100 g of TEAP in 1.5 l of deionized water and add 0.01 M $AgClO_4$ until precipitation of bromide is complete (approximately 50 ml). Boil the solution for 15 min to coagulate the colloidal suspension of silver bromide and then filter. Reclaim the TEAP, dissolve in 300 ml of acetonitrile, add 20 ml of 18 M H_2SO_4 and allow to stand with stirring for 5 h. Vacuum-distil the acetonitrile while periodically adding water to maintain a volume of 300—400 ml until about 300 ml of water has been added. Recrystallize the TEAP four times from water or until the residual H_2SO_4 concentration is below 10^{-6} M as determined by d.p.p. Finally dry at 60°C under vacuum for 48 h.

Sulfuric and nitric acids (Fisher Scientific) were reagent grade and required no further purification. Stock solutions (0.3 M) of the acids were prepared in acetonitrile. Working solutions (10^{-3} M) were prepared from the stock solution Stock solutions were standardized by titration with a standard aqueous sodium hydroxide solution: 10 ml of the stock solution was diluted to ca. 60 ml with deionized water and titrated to the end-point with bromophenol blue indicator. (It was shown that the presence of acetonitrile does not affect the end-point.)

Nitrogen gas (Air Products) used for deaerating the acetonitrile was passed through a Ridox (Fisher Scientific Co.) column to remove traces of oxygen; the Ridox was entirely adequate for this purpose.

Electrodes and cell

The working electrode was a dropping mercury electrode (DME; Sargent-Welch, S-29487 capillary) which was used in conjunction with a PAR 172 drop timer (Princeton Applied Research Corp.). The DME and drop timer assembly were enclosed in a Faraday cage. A silver—silver ion reference electrode was prepared by immersing a silver wire into acetonitrile that contained 0.1 M TBAP and 0.1 M silver nitrate. The filling solution for the salt bridge was 0.1 M TBAP in acetonitrile. This electrode and salt bridge differed only slightly from a more sophisticated model that was used as a guide [5]. All potentials reported are expressed against the SCE, which is 300 mV more negative than the operational Ag^+/Ag electrode in acetonitrile. The salt bridge, in both cases, was made of Pyrex, the lower openings of the H-tube being fitted with medium porosity glass frits. A platinum wire was used as the auxiliary electrode (10 cm of 26-gauge platinum wire).

The cell, designed and constructed in-house, consisted of three chambers—sample, isolation, and reference—separated by two glass frits [6]. The sample chamber typically holds 40 ml of solvent. A rubber serum cap was used to provide a flexible air-tight seal between the DME and the Teflon cell top.

Electronic equipment

The measurements were made with a PAR 174 Polarographic Analyzer and plotted on a Hewlett—Packard Moseley 7001A X-Y recorder. Determinations of sulfuric acid were usually made with a 1-s drop time (1.54 mg Hg s^{-1}), 50-mV modulation amplitude and a scan rate of 5 mV s^{-1}.

RESULTS AND DISCUSSION

Sulfuric acid is irreversibly reduced at the DME, exhibiting a half-wave potential of —1.20. The original work involving the polarographic reduction of sulfuric acid was done at concentrations greater than 10^{-3} M [3]. However, when micromolar concentrations were examined, three major problems emerged: (1) a calibration curve that intersected the concentration axis rather than the orgin; (2) non-reproducible peak currents; and (3) the inability to distinguish between sulfuric acid and nitric acid. The first two problems became apparent only at low concentrations of sulfuric acid (10^{-4}—10^{-5} M) and were later attributed to problems with the supporting electrolyte and dissolved oxygen. The third problem was attributed to the solvent.

Solvent

The polarographic reduction of sulfuric acid in two brands of spectrophotometric-grade acetonitrile was examined before and after the acetonitrile was purified according to a procedure used successfully by several workers [7—9]. Aldrich acetonitrile required purification in order to distinguish nitric acid from sulfuric acid. The reduction of sulfuric acid in the absence of nitric acid was unaffected by purification of the solvent. Consequently, except for experiments using H_2SO_4/HNO_3 mixtures, Aldrich acetonitrile was used as received. Burdick and Jackson acetonitrile was sufficiently pure as received to allow nitric and sulfuric acids to be distinguished.

Supporting electrolyte

Tetraethylammonium perchlorate was used in the original work on the reduction of Brønsted acids and was therefore the initial choice here. A scan of the blank solvent (0.1 M TEAP, recrystallized four times) over the entire potential range available revealed a peak at approximately—0.2 V (Fig. 1, peak A). On addition of sulfuric acid, a second peak (designated B) formed at approximately +0.15 V with a corresponding decrease in peak A. The height of this second peak and that of the sulfuric acid peak at about —1.3 V decreased simultaneously with each rescan of the polarogram. A time lapse of 10 min or more between rescans resulted in greater decreases in peak height for both peaks than was observed for immediate rescans. The peak heights corresponding to B and sulfuric acid as a function of time were then studied with the results illustrated in Fig. 2. With sufficient sulfuric acid added to the cell to eliminate peak A, a plot of peak height versus time for sulfuric acid parallels that of peak B. The difference between the initial and final peak

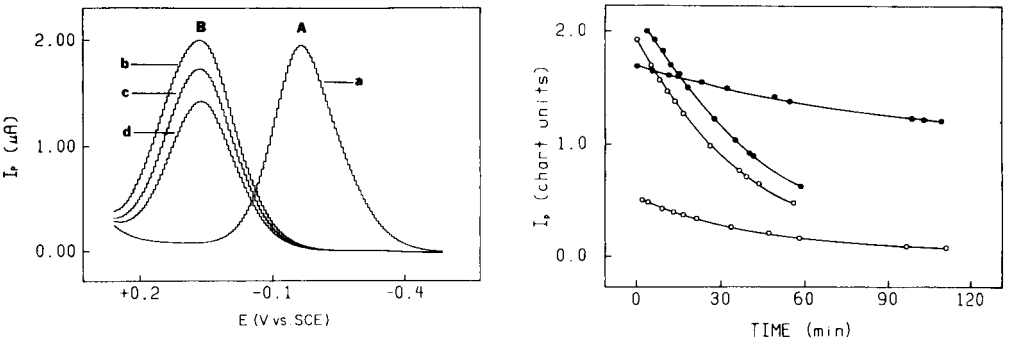

Fig. 1. Differential pulse polarograms of impurities A and B. (a) 0.1 M TEAP; (b) 0.1 M TEAP after addition of H_2SO_4; (c) rescan of (b) after a 10 min delay; (d) rescan of (c) after a 10 min delay.

Fig. 2. Comparison of the peak heights of impurity B (○) and H_2SO_4 (●) as a function of time at different concentrations of sulfuric acid. The sharply descending curves pertain to a higher concentration of sulfuric acid than the more horizontal curves.

heights for sulfuric acid was compared to that of peak B over the same time span. With the cell volume remaining constant, the peak height is directly proportional to the number of moles present. The above comparison consistently indicated a mole ratio of 1:1.

Purification of the acetonitrile did not reduce the height of peaks A or B. Decreasing the concentration of TEAP did reduce peaks A and B, which indicated that the supporting electrolyte was the source of the problem. Tetraethylammonium bromide is a common impurity in TEAP. The addition of tetraethylammonium bromide to the cell resulted in an increase in the peak height at −0.25 V. After addition of sulfuric acid, the second peak at +0.15 V did not appear. The source of peaks A and B is clearly not bromide. The peaks were also observed with a platinum working electrode, indicating that they were not the result of adsorption on, or chemical interaction with, mercury.

In an effort to overcome these problems, tetrabutylammonium perchlorate (TBAP) was substituted for TEAP as the supporting electrolyte. Differential pulse polarograms of a 0.1 M TBAP solution in acetonitrile showed a small wave at approximately −0.2 V, as found in the TEAP. After addition of sulfuric acid to the solution, the behavior observed was the same as described for TEAP (Fig. 1). No wave was observed for hydrobromic acid indicating that the bromide had been removed.

A single impurity could be responsible for both peaks A and B. The impurity is initially electroactive at −0.2 V and reacts rapidly with sulfuric acid, producing a species which is electroactive at +0.15 V. This species reacts slowly with sulfuric acid and becomes electroinactive. The purification procedures given in the experimental section for TEAP and TBAP successfully remove the impurity. If used within a week of purification, either electrolyte

produces blank polarograms free of peaks A and B, and sulfuric acid peaks which are invariant with time. Since TBAP was easier to purify, it was adopted as the supporting electrolyte.

Dissolved oxygen

Oxygen is more difficult to remove from acetonitrile than from aqueous solutions. Deaeration times of 30 min were required to reduce the dissolved oxygen level to acceptable levels. To prevent rapid re-absorption of oxygen from air, the cell top must fit tightly around the DME. A rubber septum was used for this purpose. Enclosing the cell in a glove bag filled with nitrogen is also satisfactory.

Determination of sulfuric acid

The irreversibility of the reduction of sulfuric acid at the DME is characterized by a very broad peak with a peak width at half the maximum height of about 150 mV. Typical d.p. polarograms of 10^{-6}—10^{-5} M H_2SO_4 in acetonitrile are given in Fig. 3.

The slope of the calibration curve was calculated by the least-squares method to be 0.0038 ± 0.00005 $\mu A\ \mu g^{-1}$ of sulfuric acid with a y-intercept of −0.0027 ± 0.0059 (95% confidence level, two-tailed test, based on each addition being measured five times). The null hypothesis that the y-intercept is zero (i.e. the calibration curve intersects the origin) is accepted as true, because the computed statistic t does not exceed the tabulated t value 2.201 (95% confidence level, two-tailed test, 11 degrees of freedom).

The detection limit for sulfuric acid was found to be 0.7 μg (2.0×10^{-7} M). This was determined by application of the t test (95% confidence level, one-tailed test, 8 degrees of freedom). From a plot of experimentally determined t values versus concentration, the useful lower concentration limit, found from a preselected value of t [10], was about 10 μg of sulfuric acid (2.0×10^{-6} M). The upper limit of the linear range was 200 μg of sulfuric acid. The analytical sensitivity, defined [10] as the slope of the calibration curve divided by the standard deviation at the midpoint of the calibration curve (105 μg), was 1.59 μg^{-1} of sulfuric acid.

Nitric acid is the only mineral acid which appears to interfere with the determination of sulfuric acid. The halfwave potential for nitric acid is not available in the literature [3]. Differential pulse polarograms run to determine the position of the nitric acid peak relative to that of sulfuric acid showed that the halfwave potential of nitric acid was approximately 0.2 V more negative than that of sulfuric acid. As shown in Fig. 4, the two peaks are so broad that they overlap but are still distinguishable as two individual waves. This peak separation appears to be a function of the water content of the solvent and is observed only when the acetonitrile (Aldrich Gold Label) has been purified. Without the purification step, the two acids are polarographically indistinguishable. Therefore, the moisture content of the sample would alter the selectivity of the method for sulfuric acid and could be considered as an interferent.

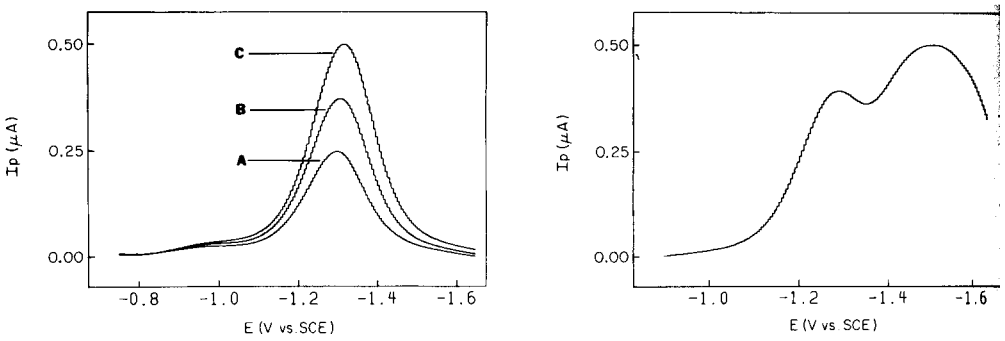

Fig. 3. Differential pulse polarograms of sulfuric acid in acetonitrile containing 0.1 M TBAP. Curves A, B and C represent the addition of 50, 100 and 150 μl of 7.2×10^{-3} M H_2SO_4 to 40 ml of solution.

Fig. 4. Differential pulse polarogram of 10^{-5} M HNO_3 and 10^{-5} M H_2SO_4 in acetonitrile containing 0.1 M TBAP.

The sulfate and hydrogensulfate anions are reported to be electrochemically inactive [3]. This fact was substantiated by the following experiments. Approximately 1 g of solid ammonium sulfate was added to 40 ml of acetonitrile in the polarographic cell. A subsequent d.p.p. showed no peaks. When the same procedure was followed with ammonium hydrogensulfate, a peak appeared at the same potential as that of sulfuric acid. This peak was thought to be due to a residual acidic impurity. In an attempt to remove this impurity, a few crystals of ammonium hydrogensulfate were repeatedly washed with fresh portions of acetonitrile for several days; these crystals were then dried, weighed, and placed in a known volume of acetonitrile, and the mixture was stirred for several days. The concentration of the ammonium hydrogensulfate in the acetonitrile was found to be 5×10^{-4} M by recovering the undissolved salt. A d.p. polarogram of a 5-ml aliquot of the solution showed a peak at -1.3 V vs. SCE with a peak height equivalent to 88 μg of sulfuric acid. This implies that the ammonium hydrogensulfate contained a 12% impurity of sulfuric acid even after extensive washing of the crystals, whereas an aqueous titration of the hydrogensulfate with sodium hydroxide indicated only a 1% acidic impurity. Two possible explanations for the polarographic wave can be given: (1) hydrogensulfate is electroactive or (2) sulfuric acid is in some way formed in solution.

Hydrogensulfate was shown to be electrochemically inactive by the following experiments. Tetramethylammonium hydrogensulfate ($TMAHSO_4$; actual analysis of the salt was 63% as the hydrogensulfate and 37% as the sulfate), which is insoluble in acetonitrile, was dissolved in methanol. An aliquot of this solution was then added to acetonitrile which was 10^{-5} M in sulfuric acid. The sulfuric acid peak decreased following the addition of the

$TMAHSO_4$—$(TMA)_2SO_4$ solution and no other peak appeared. The number of moles of sulfuric acid removed was approximately equal to the number of moles of $(TMA)_2SO_4$ added via the methanol solution. As sulfate is a stronger base than the hydrogensulfate, there is a decrease in sulfuric acid concentration and an increase in the hydrogensulfate concentration. Several aliquots of a known concentration of tetraethylammonium hydrogensulfate ($TEAHSO_4$), which is soluble in acetonitrile, were added to a cell containing only supporting electrolyte in acetonitrile. No peaks were observed.

Since hydrogensulfate gave no response, it can be assumed that sulfuric acid is formed in solution. It is therefore postulated that a proton from the ammonium ion associates with the hydrogensulfate to form sulfuric acid, the latter being the stronger base in acetonitrile: $NH_4^+ + HSO_4^- \rightarrow NH_3 + H_2SO_4$. A few milligrams of $NaHSO_4$ were subjected to the same washing and dissolution procedure as the $(NH_4)HSO_4$. No peak was observed for 5 ml of the $NaHSO_4$ solution. Here, the cation is not a source of protons and therefore sulfuric acid would not be formed.

Based on the above experiments, soluble sulfates would be negative interferents and ammonium hydrogensulfate would be a positive interferent. However, because of the very limited solubility of most sulfates and ammonium hydrogensulfate in acetonitrile, the possible errors introduced would be very small.

Even though bromide has been discounted as the impurity in the supporting electrolyte, its presence is a problem in that it indirectly reduces the sulfuric acid concentration. Sulfuric acid, being a weak acid in acetonitrile, ionizes to a small extent producing solvated protons. These protons then associate with bromide to form hydrobromic acid, which is a weaker acid than sulfuric acid in acetonitrile and exhibits a wave at —0.9 V. The formation of hydrobromic acid thus reduces the sulfuric acid concentration. Therefore, bromide is a negative interference in the determination.

Conclusions

Determinations of micromolar amounts of sulfuric acid are possible by differential pulse polarography in acetonitrile. The most crucial factor is the purification of the supporting electrolyte. Halides, soluble in acetonitrile, are negative interferents. Soluble sulfates and ammonium hydrogensulfate. are electrochemically inactive but are shown to interfere, negatively in the case of sulfates and positively in the case of ammonium hydrogensulfate. However, because of the limited solubility of these compounds in acetronitrile, the potential error is negligible. The ability to distinguish sulfuric and nitric acids appears to be a function of the water content of the acetonitrile. The moisture content of a sample would therefore reduce the selectivity of the method for sulfuric acid.

REFERENCES

1 V. Dharmarijan, R. L. Thomas, R. F. Maddalone and P. W. West, Sci. Total Environ., 4 (1975) 279.
2 J. Forrest and L. Newman, J. Air Pollut. Control Assoc., 23 (1973) 761.
3 J. F. Coetzee and I. M. Kolthoff, J. Am. Chem. Soc., 79 (1957) 6110.
4 J. F. Coetzee, D. K. McGuire and J. L. Hedrick, J. Phys. Chem., 67 (1963) 1814.
5 D. T. Sawyer and J. L. Roberts, Jr., Experimental Electrochemistry for Chemists, J. Wiley, New York, 1974.
6 J. F. McGaughey, M. S. Thesis, North Carolina State University, Raleigh, N. C., 1976.
7 J. F. Coetzee, Pure Appl. Chem., 13 (1966) 429.
8 G. Kew, M. K. DeArmond and K. W. Hanck, J. Phys. Chem., 78 (1974) 727.
9 C. K. Mann, in A. J. Bard (Ed.), Electroananlytical Chemistry, Vol. 3, M. Dekker, New York, 1969, p. 57.
10 J. D. Ingle, Jr., J. Chem. Educ., 51 (1974) 100.

Analytica Chimica Acta, 107 (1979) 83—89

ELECTROGENERATION OF GOLD(III) IN HALIDE MEDIA

GARY D. CHRISTIAN**, MARIANNE CHATEAU-GOSSELIN and GASTON J. PATRIARCHE

Institut de Pharmacie, Université Libre de Bruxelles, Campus Plaine, B.P. 205/1, 1050 Bruxelles (Belgium)

(Received 30th October 1978)

SUMMARY

Gold(III) was electrogenerated with high efficiency at constant current in halide media by oxidation of freshly electrodeposited gold on a platinum electrode. The electrolytes tested were 0.0005—1 M HCl, NaCl, HBr, and NaBr. Potentiometric studies indicated that the tetrahaloaurate(III) complex was generated in each case with oxidation potentials ranging from 0.83 to 1.15 V. Arsenic(III) (20 μeq) was titrated potentiometrically in 0.1 M NaBr by using a gold indicating electrode; the efficiency was 99.90 ± 0.05%. Iron(II) was titrated in 0.01 M HCl to a biamperometric end-point with gold-plated platinum wire indicating electrodes polarized at 100 mV. Recoveries were 100.7 ± 1.8% (0.7 mg) and 100.4 ± 2.3% (0.4 mg). This new system allows titrations over a wide range of acidities and oxidation potentials.

Numerous oxidizing agents have been generated coulometrically. The oxidation potentials of these range from weak to strong. A few titrants include iodine [1], hexacyanoferrate(III) [2], bromine [3], chlorine [4], hypobromite [5], manganese(III) [6], cerium(IV) [7], and silver(II) [8]. Many of these, especially the stronger oxidizing agents, must be generated under strict conditions of acidity and/or temperature and the oxidation potential is constant or limited in range.

If haloaurate(III) complexes could be generated efficiently, this would afford a versatile titrating system. In principle, the potential of the titrant could be varied at will by changing the concentration and/or nature of the complexing agent. In addition, it should be possible to titrate over a wide range of acidities. The present paper reports on a study of the constant-current oxidation of gold metal in halide media. The effects of the halide concentration and acidity on the species generated have been determined. Titrations of arsenic(III) and iron(II) with different methods of end-point detection are described.

EXPERIMENTAL

Reagent-grade chemicals were used throughout. Bromide and chloride (acid and neutral) supporting electrolytes were standardized by titrating with

**Permanent address: Department of Chemistry, University of Washington, Seattle, WA 98195 (U.S.A.).

silver nitrate by the Volhard method. Gold(III) solutions were standardized iodimetrically [9] with electrogenerated iodine. An iron(II) solution prepared from iron(II) ammonium sulfate was standardized by titrating with coulometrically generated cerium(IV) [7]. Iodide solutions were standardized with electrogenerated bromide [4]. Standard arsenic(III) solutions were prepared from primary-standard arsenic trioxide [10].

Coulometric titrations were done with the apparatus previously described [11, 12]. The generating current was 9.65 mA unless otherwise stated. Amperometric measurements were made by recording the current on a polarograph [13], and potentiometric measurements with a Leeds-Northrup potentiometer (Model 8687). Potentials were measured against a saturated calomel electrode, but all values are reported vs. the normal hydrogen electrode. Current—voltage curves were recorded on the polarograph. The titration cell was a 100-ml beaker and solution volumes were 50.0 ml unless otherwise stated. The cathode (platinum foil) was isolated by placing it in a glass tube fitted with a sintered glass end. The supporting electrolyte served as catholyte. Spectrophotometric measurements were made with a Bausch and Lomb Spectronic 20 or a Cary Model 14 recording spectrophotometer.

Gold-plated electrodes were prepared by cathodically polarizing a 2-cm^2 platinum foil electrode in a stirred solution (25 ml) containing 500 mg of gold(III) chloride at a current of ca. 20 mA for 500—1000 s. For the amperometric titrations, slightly different conditions were employed: a 1-cm^2 electrode was plated in 25 ml of 0.1 M hydrochloric acid containing 500 mg of gold(III) chloride at a current of 8 mA for 30 min. The electrode was replated after every five titrations.

RESULTS AND DISCUSSION

In non-complexing media, water is oxidized before gold (E° = 1.23 V for $H_2O = 1/2\ O_2 + 2\ H^+ + 2e^-$; E° = 1.50 V for $Au = Au^{3+} + 3e^-$). Electrolytic oxidation of gold in non-complexing media is reported to produce gold(III) oxides which can be reduced [14, 15]. However, in complexing media, the oxidation potential for the Au/Au(III) is shifted to values less positive than that for water. The standard potential for the $Au/AuCl_4^-$ couple is 1.00 V [16] and that for the $Au/AuBr_4^-$ couple is 0.87 V [17]. The standard potential for $Cl^- = 1/2Cl_2 + e^-$ is 1.36 V, and that for $Br^- = 1/2\ Br_2 + e^-$ is 1.09 V [10]. Hence, it should be possible to produce the respective haloaurate(III) complexes by oxidation of gold in aqueous solution without oxidation of water or of the halide.

The standard potential for the Au/AuI_4^- couple is estimated at 0.56 V [18], which is probably too close to the potential of 0.54 V for the I^-/I_3^- couple for successful generation of tetraiodoaurate, unless the iodide concentration were sufficiently low that the I^-/I_2 (aq.) couple (E° = 0.62 V) would dominate over the former. Urosov et al. [19] have reportedly prepared $HAuCl_4$ by anodic dissolution of gold in hydrochloric acid solution. A study was undertaken

to determine the gold(III) species generated from gold metal and to determine the formal potentials under varying conditions of halide concentration and acidity.

Studies of the potentials

Two approaches were taken to estimate the formal potential of the generated species and hence to ascertain the composition or oxidation state of the species. First, the gold electrode was polarized anodically for 500.0 s in 50.0 ml of halide supporting electrolyte at a constant current of 9.65 mA. The potential of this solution was then measured with a gold indicating electrode. If the assumed reaction is $Au + 4Cl^- = AuCl_4^- + 3e^-$, then the concentration of gold(III) generated in the solution would be 3.33×10^{-4} M. The corresponding Nernst equation at 25°C is

$$E = E^\circ - (0.0591 \times 4/3) \log[Cl^-] + (0.0591/3) \log[AuCl_4^-] \quad (1)$$

where $E^\circ = 1.00$ V, and the formal potential is given by

$$E^{\circ\prime} = E^\circ - (0.0591 \times 4/3) \log[Cl^-] \quad (2)$$

From the measured potential (E) and the gold(III) concentration, a formal potential ($E^{\circ\prime}_{gen.}$ in Table 1) was calculated by using eqn. (1). This was compared with the predicted formal potential calculated by using eqn. (2) and the chloride concentration and standard potential. ($E^{\circ\prime}_{calc.}$ in Table 1). A second comparison was made with an experimentally determined formal potential which was obtained as follows. A solution identical in composition to the one assumed from anodically oxidizing gold was prepared by adding gold(III) chloride solution to the supporting electrolyte to give a concentration

TABLE 1

Formal potentials of generated gold species in chloride and bromide solutions. Potentials are given in V vs. NHE.

Electrolyte	Concentration (M)[a]	$E^{\circ\prime}_{gen.}$	$E^{\circ\prime}_{meas.}$	$E^{\circ\prime}_{calc.}$
HCl	0.0200	1.149	1.134	1.13
HCl	0.09607	1.09	1.036	1.08
HCl	0.9659	1.011	0.964	1.01
NaCl	0.1000	1.131		1.08
NaCl	1.000	1.027		1.00
HBr	0.000515	1.133		1.16
HBr	0.00854	1.015		1.03
HBr	0.0881	0.924		0.95
HBr	0.9006	0.828		0.87
NaBr	0.01000	1.072	1.002	1.03
NaBr	0.1000	1.034	0.913	0.95
NaBr	1.000	0.851	0.848	0.87

[a]For potential calculations, the listed halide concentrations were corrected for the amount of halide consumed in reacting with the 3.33×10^{-4} M gold(III), i.e. $[X^-]$ decreased by 1.33×10^{-3} M.

of 3.33×10^{-4} M. The measured potential of this solution was used to calculate an experimental formal potential from eqn. (1) ($E^{\circ\prime}_{meas.}$ in Table 1). Activity coefficients were neglected in these calculations. [Activity coefficients are actually included in the measured formal potentials, $E^{\circ\prime}_{gen.}$ and $E^{\circ\prime}_{meas.}$. Under these conditions, $E^{\circ\prime}_{gen.}$ and $E^{\circ\prime}_{meas.}$ would be equal but $E^{\circ\prime}_{calc.}$ would be expected to differ by $-(0.0591/3) \log (\gamma^4_{Cl^-}/\gamma_{AuCl_4^-})$ V; the difference would be +0.007 V with activity coefficients of 0.75, the approximate situation for the 0.1 M electrolytes.]

Table 1 summarizes the data obtained in chloride solutions as well as bromide solutions. There is good agreement between the potential of the generated species in hydrochloric acid and the calculated or measured potential of the tetrachloroaurate ion for all concentrations of hydrochloric acid studied. If the generated species is assumed to be chlorine, the concentration of generated chlorine would be about 5×10^{-4} M and a corresponding formal potential ($E^{\circ\prime}_{gen.}$) for the couple in 0.001 M HCl would be 1.219 V, compared to a predicted value ($E^{\circ\prime}_{calc.}$) of 1.53 V. Likewise, if AuCl were generated, the $E^{\circ\prime}_{gen.}$ would be 1.124 V and the $E^{\circ\prime}_{calc.}$ would be 1.35 V (from E° = 1.17 V [20]). For the generation of gold(I), $E^{\circ\prime}_{gen.}$ would be 1.311 V compared to an $E^{\circ\prime}_{calc.}$ value of 1.68 V (the standard potential [20]); Erenbrug and Peshchevitski [18] have reported the standard potential of the Au/Au(I) (aq.) couple to be 1.85 V, which would simply change both $E^{\circ\prime}_{gen.}$ and $E^{\circ\prime}_{calc.}$ by 0.17 V.

Chemically, it is unlikely that a gold(I) species would be generated. Gold(I) chloride is insoluble but is decomposed in cold water to gold(III) trichloride and gold [21]. Gold(I) also disproportionates. The data in Table 1 offer strong evidence that $AuCl_4^-$ was generated in chloride media and $AuBr_4^-$ in bromide media. It was noted that at high halide concentrations (> 0.1 M), the plated gold would tend to come off the electrode surface at a rate faster than predicted by the rate of current flow. It is likely that the freshly plated gold tended to be oxidized by atmospheric oxygen in these high concentrations of halide to form the haloaurate(III) complex. Churchill and Laxen [22], for example, studied the dissolution of gold in cyanide solutions and found that it depended on the rate of stirring and on the cyanide and oxygen concentration at the gold surface.

Efficiency of generation

In principle, end-points should be detected potentiometrically with a gold indicating electrode. A platinum electrode should be suitable for many redox titrations; in this case, the potential of the couple titrated would be followed. The titration of arsenic(III) was chosen to study the titration efficiency. This couple is electrochemically irreversible and the arsenic should not react directly at the electrode. Therefore, the overall titration efficiency should give an estimate of the generating efficiency for the production of the gold(III) species. A series of titrations was performed at 9.65 mA by using a gold wire indicating electrode in 0.1 M sodium bromide buffered at pH 8 with orthophosphate [23] or with sodium hydrogencarbonate. The amount

of arsenic taken was 19.83 μeq, and the amount found was 19.81 ± 0.01 μeq for four titrations; these titrations were done on two separate days. This indicates a high current efficiency in this medium (99.90 ± 0.05%). Reproducible potentiometric titration curves with arsenic were not always achieved, and the problem appeared to lie in the proper pretreatment and/or plating of the indicating electrode. It should be pointed out also that the generating efficiencies were poor if the generating electrode was plated from a gold cyanide bath or if a gold wire electrode was used. Apparently the gold must be loosely plated and freshly prepared; the plating from cyanide solutions adhered too tightly.

Potentiometric titrations of iron(II) were sucessfully performed in 0.01 M hydrochloric acid when either a platinum or a gold indicating electrode was used. For 10 μeq of iron, the results were in the range 98—103% of theory.

Amperometric titrations

It was possible to use amperometric end-point detection in the titrations because gold(III) is electrochemically reducible. Biamperometric titrations were examined with a pair of platinum wire electrodes polarized with 100 mV. During initial titrations, a small amount of gold metal plated on the cathode; after this had occurred, the polarity of the two electrodes was reversed for each titration. Hence, the indicating anode was effectively a gold electrode which was oxidized in the halide medium at the same potential as the gold(III) was reduced (electrochemically reversible couple); this was a necessary condition to obtain a biamperometric current from the excess of gold(III) generated titrant beyond the equivalence point.

Figure 1 shows the titration curve obtained for iron(II) in 0.01 M hydro-

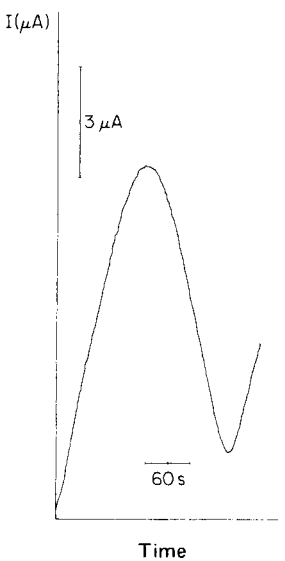

Fig. 1. Biamperometric titration curve for the titration of iron(II) in 0.01 M HCl. Generating current, 3 mA.

chloric acid; the shape is typical for a titration in which both the titrand and titrant have reversible couples, with the rise beyond the end-point being due to the excess of gold(III), as predicted. A series of eight 698.1-μg iron(II) samples was titrated successively in the same solution after a pretitration had been done, with a generating current of 4.5 mA. The recovery was 100.7% with a coefficient of variation of ± 1.8%. A second series of four 407.6-μg iron(II) samples titrated at 3 mA gave a mean recovery of 100.4 ± 2.3%. In these titrations, the rise of the amperometric current beyond the end-point diminished for successive titrations, and this affected the precision. The precision could probably be improved by doing the titrations singly. This phenomenon was not observed in the titration of organic pharmaceutical compounds.

It should be possible also to utilize spectrophotometric end-point detection in these titrations, because the gold(III) species absorb in the visible region.

The present study suggests that electrogeneration of gold(III) species should offer a versatile redox titration system in which the complexing species, the acidity, and the oxidation potential can be varied at will. In addition to the species studied here, it may be possible under some conditions to generate gold(I) species. Gold(I) forms a stable thiosulfate complex [$Au(S_2O_3)_2^{-3}$; $K = 10^{26}$] that is electrochemically reducible at a gold electrode; the standard potential of the thiosulfatoaurate/gold couple is 0.153 V [24]. Electrochemical oxidation of gold in acetonitrile gives gold(I) species [25]. Gold(III) species have been used in potentiometric or amperometric titrations of a variety of substances, including nitron [26], cysteine [27], sodium dithionate [28], rubeanic acid [29], mercury(I) [30], iron(II) ammonium sulfate [31, 32], hydrazine sulfate and hydroquinone [32], hexacyanoferrate(II) [33], and iodide [34]. In addition, it has been utilized in coulometric titrations with iodine and bromine [35].

G. D. C. acknowledges support from the Commission for Educational Exchange between the United States of America and Belgium and G. J. P. acknowledges support from the National Science Belgium Foundation (F.N.R.S.).

REFERENCES

1 W. J. Ramsey, P. S. Farrington and E. H. Swift, Anal. Chem., 22 (1950) 332.
2 A. M. Hartley and J. J. Lingane, Anal. Chim. Acta, 11 (1954) 475.
3 R. J. Meyers and E. H. Swift, J. Am. Chem. Soc., 70 (1948) 1047.
4 W. S. Wooster, P. S. Farrington and E. H. Swift, Anal. Chem., 21 (1949) 1457.
5 G. M. Arcand and E. H. Swift, Anal. Chem., 28 (1956) 440.
6 P. S. Tutundzic and S. Mladenovic, Anal. Chim. Acta, 12 (1955) 382, 390.
7 N. H. Furman, W. D. Cooke and C. N. Reilley, Anal. Chem., 23 (1951) 945.
8 J. J. Lingane and D. G. Davis, Anal. Chim. Acta, 15 (1956) 201.
9 V. E. Herschlag, Ind. Eng. Chem., Anal. Ed., 13 (1941) 561.
10 G. D. Christian, Analytical Chemistry, 2nd. edn., J. Wiley, New York, 1977, pp. 315, 329.

11 G. J. Patriarche and J. J. Lingane, Anal. Chem., 39 (1967) 168.
12 G. J. Patriarche and J. J. Lingane, Anal. Chim. Acta, 49 (1970) 25.
13 G. D. Christian, J. Electroanal. Chem., 11 (1966) 94.
14 K. Ogura, S. Haruyama and K. Nagasaki, J. Electrochem. Soc., 118 (1971) 531.
15 J. W. Schultze and K. J. Vetter, Ber. Bunsenges. Phys. Chem., 75 (1971) 470.
16 N. Bjerrum and A. Kirshner, Kgl. Danske Videnskab. Selskab. Math-fys., V, No. 1 (1918).
17 G. Grube and T. Morita, Z. Electrochem., 38 (1932) 117.
18 A. M. Erenbrug and B. I. Peshchevitskii, Zh. Neorg. Khim., 14 (1969) 2714.
19 K. Kh. Urosov, T. M. Sosipatrov, D. N. Abakumov and V. I. Shilenko, in K. M. Saldadze (ed.), Ionoobmen Membrany Electrodialize, Izdatel'stvo Khimia, Leningradsboe Otdelenie, Leningrad, 1970, p. 246.
20 W. M. Latimer, The Oxidation States of the Elements and Their Potentials in Aqueous Solutions, 2nd edn., Prentice-Hall, New York, 1952, p. 195.
21 J. R. Partington, General and Inorganic Chemistry, 3rd edn., Macmillan, London, 1958, p. 356.
22 M. Churchill and P. A. Laxen, Gov. Met. Lab., No. C 25-64 (1966) 15 pp.
23 G. D. Christian and W. C. Purdy, J. Electroanal. Chem., 3 (1962) 363.
24 J. Pouradler and M. C. Gadet, J. Chim. Phys. Physicochim. Biol., 66 (1969) 109.
25 A. D. Goolsby and D. T. Sawyer, Anal. Chem., 40 (1968) 1978.
26 N. Ganchev, A. Dimitrova and L. Futekov, Natura (Plovdiv, Bulg.), 3 (1970) 59.
27 G. N. Shaposhnikova and N. G. Galfayan, Dokl. Akad. Nauk Arm. SSR, 58 (1974) 165.
28 P. N. Pandey, M. M. Singh and Y. D. Upadhya, Indian J. Chem., Sect. A, 14 A (1976) 288.
29 N. G. Galfayan, G. N. Shaposhnikova and V. M. Tarayan, Arm. Khim. Zh., 28 (1975) 94.
30 V. M. Tarayan, G. N. Shaposhnikova and G. S. Acharyan, Arm. Khim. Zh., 27 (1974) 350.
31 O. C. Saxena, Chim. Anal. (Paris), 52 (1970) 647.
32 V. A. Maslov, P. I. Chaikin and M. N. Ermolaeva, Sb. Tr., Vses. Nauch.-Issled. Proekt.-Konstr. Inst. Yuvelirnoi, Promsti., No. 1 (1971), 22.
33 P. F. Ol'Khovich and A. T. Pilipenko, Ukr. Khim. Zh., 36 (1970) 388.
34 V. M. Tarayan and G. N. Shaposhnikova, Uch. Zap., Erevan. Gos. Univ., (3) (1968) 123.
35 M. Becka and P. Tischer, Metalloberflaeche, 25 (1971) 261.

Analytica Chimica Acta, 107 (1979) 91—100

KINETIC DETERMINATION OF FORMALDEHYDE AND HEXAMETHYLENETETRAMINE WITH A CYANIDE-SELECTIVE ELECTRODE

M. A. KOUPPARIS, C. E. EFSTATHIOU and T. P. HADJIIOANNOU*

Laboratory of Analytical Chemistry, University of Athens, Athens (Greece)

(Received 18th September 1978)

SUMMARY

An automatic potentiometric reaction-rate method is described for the determination of formaldehyde and hexamethylenetetramine. The formaldehyde reacts with cyanide, and the reaction rate is followed with a cyanide-selective electrode. The time required for the reaction to consume a fixed amount of cyanide, and therefore for the potential to increase by a preselected amount (8.0 mV), is measured automatically and related directly to the formaldehyde concentration. The average error for the determination of 60—300 μg of formaldehyde in a sample volume of 1.00 ml was about 1.3%. Amounts of hexamethylenetetramine in the range 50—250 μg in a sample volume of 0.050 ml were determined after acid hydrolysis to formaldehyde with an average error of about 1.6%. Measurement times were in the range 18—80 s for both determinations. The method has been applied to the determination of hexamethylenetetramine in pharmaceutical preparations.

The selectivity and the sensitivity of kinetic methods of analysis combined with the selectivity and sensitivity of ion-selective electrodes provides an excellent and versatile combination, which may lead to totally new analytical schemes. This has been one of the primary objectives in this laboratory.

The cyanide-selective electrode has been used for the direct potentiometric determination of cyanide in a variety of matrices [1, 2], as well as for the indirect determination of aromatic *m*-dinitro compounds [3] and for monitoring reactions involving cyanide [4—6]. In this paper, a new kinetic method is described for the determination of formaldehyde and its derivative, hexamethylenetetramine methenamine, hexamine, urotropine), a condensation product with ammonia; the rate of the cyanide—formaldehyde reaction is followed with a cyanide-selective electrode.

The method is based on the well-known addition reaction of hydrogen cyanide to carbonyl compounds, which is extensively used in organic synthesis but rarely in analytical applications, because of its incompleteness and the high toxicity of cyanide solutions. In the proposed method, a very dilute cyanide solution (ca. 1.6×10^{-5} M) is treated with a large excess of unknown or standard formaldehyde solution, and the reaction is monitored with the cyanide-selective electrode. The time required for the potential to change by

a preselected amount (8.0 mV) is measured automatically and related directly to the formaldehyde concentration. Commercial equipment and an auxiliary double-switching network are easily combined and provide automatic results shortly after the start of the reaction.

Behavior of the cyanide-selective electrode in weakly alkaline and neutral solutions

The Orion 94-06 cyanide-activity electrode used is supposed to have Nernstian response toward cyanide ion in accordance with the equation $E = E' - (RT/F) \ln a_{CN^-}$, where all the terms have their conventional meanings. The cyanide-selective electrode is actually an iodide-selective electrode based on an AgI/Ag_2S membrane. The response of the electrode is due [7] to a replacement reaction which liberates iodide at the membrane surface: $AgI_{(s)} + 2CN^- \rightleftharpoons Ag(CN)_2^- + I^-$. The iodide and cyanide ions exchange between the eroding electrode surface and the sample solution. A steady state is quickly established between the cyanide activity in the bulk solution and the iodide activity in this very thin erosion layer, so that variations in the cyanide activity are readily followed.

The cyanide activity for a given concentration of cyanide salt depends on pH because of the equilibrium $HCN \rightleftharpoons H^+ + CN^-$ ($pK_{HCN} = 9.14$). Consequently the electrode should be used for direct potentiometric determinations of cyanide in strongly alkaline solutions with a minimum pH 12 to ensure complete dissociation of the hydrogen cyanide [6—9]. Under these conditions, Nernstian response is obtained over the range 10^{-2}—10^{-6} M. Although cyanide solutions more concentrated than 10^{-2} M may be measured equally well, such measurements are not recommended because the membrane is rapidly dissolved

It has been pointed out that the influence of pH on the electrode potential can be predicted from a logarithmic diagram of the HCN/CN^- system [6]. The potential response of the cyanide-selective electrode as a function of pH would then follow the equation [10]

$$E = E' + 2.303\,(RT/F)\,[pK_{HCN} - \log C_T + \log (10^{-pH} + K_{HCN})] \qquad (1)$$

where C_T is the total cyanide concentration in the solution, i.e. $[CN^-] + [HCN]$ and K_{HCN} is the dissociation constant of HCN.

It has been shown that the iodide-selective electrode measures only the cyanide activity in the pH range 7—11 [9]. Calibration curves may be obtained for the Orion cyanide electrode in the pH range 6.4–12.5 [4], but the experimental shifts of these curves along the potential axis differ significantly from the theoretical shifts calculated from eqn. (1). These curves did not show any decreased electrode sensitivity at the lower pH values, though such losses would be expected because of the very small percentage of free cyanide ions at such pH values.

In the present work, the cyanide-selective electrode had to be used in weakly alkaline or neutral cyanide solutions. Therefore, it was deemed advisable to study again its controversial behavior in the pH range 7—10. The dependence

of potential on pH was found to differ from that predicted by eqn. (1); the increase in potential with decreasing pH was much smaller than predicted, and the sensitivity was not affected unfavorably by pH. For example, the linearity of the working curve extended to 2×10^{-6} M KCN at pH 7.8, whereas at pH 12 the lowest linearity limit that could be obtained was about 10^{-5} M KCN.

The only problem associated with the use of the electrode in the pH range 7—10 was a noticeable potential drift toward higher values (lower cyanide activities). The rate of this drift increased with decreasing pH and increasing stirring rate and temperature of the solution. Bubbling moist pure nitrogen through the solution at a flow rate of about 1.2 l min^{-1} increased the drift considerably (Fig. 1). Covering the cell with a PVC film stopped the drift, which started again after removal of the film. Therefore, the drift must be attributed to the volatility of hydrogen cyanide (b.p. 25.7°C), and perhaps this is the only justification for recommending a high pH for the cyanide solutions to be measured. Therefore, it is possible but not practical to employ the cyanide-selective electrode for potentiometric measurements in weakly alkaline or neutral cyanide solutions. Nevertheless, the electrode may be used in kinetic measurements in this pH range, provided that constant conditions of pH, stirring, temperature and solution surface will ensure a constant drift rate which will be included in all blanks.

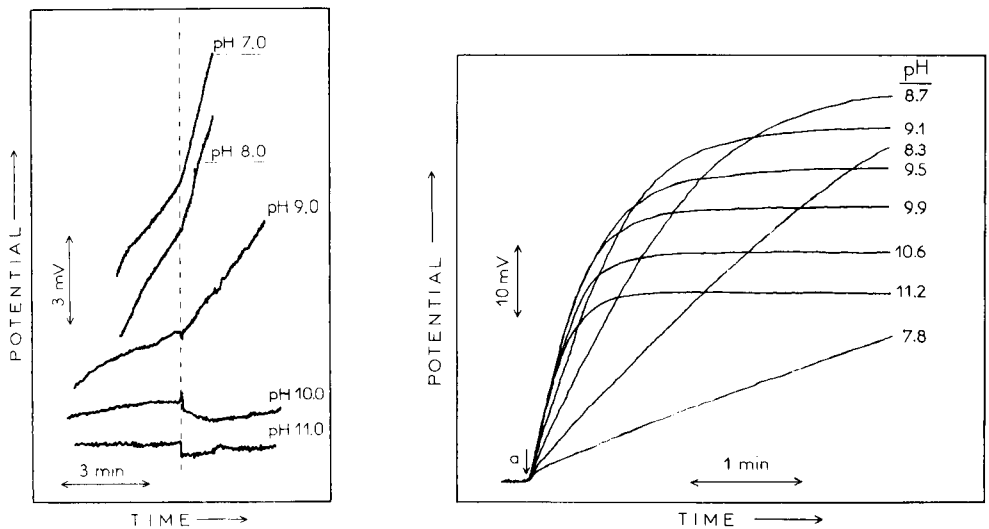

Fig. 1. Effect of pH, stirring and degassing on the drift of the cyanide responsive electrode. Effects of stirring are shown to the left of the vertical dashed line, and effects of stirring plus N_2 bubbling are shown to the right of the line.

Fig. 2. Recorded curves of cell voltage vs. time for the formaldehyde—cyanide reaction at various pH values. Initial concentrations: 1.5×10^{-5} M KCN, 2.5×10^{-4} M formaldehyde; a ↓: formaldehyde injection.

Since this electrode possesses a pseudo-Nernstian response toward cyanide [7], it is very probable that there is, to a lesser extent, a response toward the dicyanoargentate ion which is formed by the dissolution of the silver iodide in the membrane.

Reaction of hydrogen cyanide with formaldehyde

Formaldehyde reacts with hydrogen cyanide to form glycolonitrile. This reaction has been used for the determination of formaldehyde by adding a slight excess of potassium cyanide and determining the excess by the Volhard method [11]. Generally, hydrogen cyanide is added to carbonyl compounds by nucleophilic attack of the positively polarized carbon atom; the reaction product is a cyanohydrin [12]:

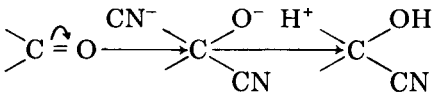

The response of the cell for a dilute solution of potassium cyanide with an excess of formaldehyde at various pH values is shown in Fig. 2. The reaction rate varies greatly with the pH of the reaction mixture. An initial equilibrium is quickly established between the reactants at the higher pH values. As the pH decreases the equilibrium constant increases but the equilibrium is more slowly established. Probably the mechanism involves the reversible formation of an intermediate which finally is rearranged irreversibly to $HOCH_2CN$.

If formaldehyde is present in large excess over total cyanide (at least six-fold excess), and the pH remains constant in the range 7—8, the reaction rate is expressed by $d[HCN]/dt = -k[HCN][HCHO]$ or $d[CN^-]/dt = -k[CN^-][HCHO]$. Rearrangement of the latter equation gives $d \ln [CN^-]/dt = -k[HCH$ Then if a_{CN^-} is replaced by $f[CN^-]$, where f is the activity coefficient, in the Nernst equation, differentiation gives $dE/dt = -(RT/F)(d \ln [CN^-]/dt)$. Combination of these last two equations gives

$$dE/dt = k\,(RT/F)\,[HCHO] \qquad (2)$$

Since all terms except [HCHO] in eqn. (2) are constant and [HCHO] remains practically constant during the reaction because the formaldehyde is in large excess over cyanide (the ratio of formaldehyde to total cyanide is in the range 7—35), the rate of change of potential is essentially constant. Therefore, dE/dt may be replaced by $\Delta E/\Delta t$, which is the measurable parameter:

$$\Delta E/\Delta t = k\,(RT/F)\,[HCHO] \qquad (3)$$

Acid hydrolysis of hexamethylenetetramine

Hexamethylenetetramine (hexamine) is hydrolyzed on heating with acid:

$$(CH_2)_6N_4 + 6H_2O + 4H^+ \rightarrow 4NH_4^+ + 6HCHO$$

This reaction has been used for the titrimetric determination of hexamine [13]. The kinetics of the reaction at constant acidity can be expressed by

$d[HCHO]/dt = 6k_{obs}[hex]$, and from the stoichiometry of the reaction

$$d[HCHO]/dt = 6k_{obs}([hex]_0 - [HCHO]/6) \quad (4)$$

where $[hex]_0$ is the initial hexamine concentration. Integration of eqn. (4) gives

$$[HCHO] = 6[hex]_0(1 - e^{-k_{obs}t}) \quad (5)$$

Combination of eqns. (3) and (5) gives

$$(\Delta E/\Delta t)_t = 6k\,(RT/F)[hex]_0(1 - e^{-k_{obs}t}) \quad (6)$$

Therefore, the kinetics of the hydrolytic reaction can be studied by measuring, at various time intervals, the quantity $(\Delta E/\Delta t)_t$ which is proportional to concentration of the formaldehyde formed.

For $t = \infty$, $(\Delta E/\Delta t)_t$ becomes $(\Delta E/\Delta_t)_\infty$ which is equal to $6k\,(RT/F)[hex]_0$. Combination of this equality with eqn. (6) gives

$$(\Delta E/\Delta t)_t = (\Delta E/\Delta t)_\infty(1 - e^{-k_{obs}t}) \quad (7)$$

or

$$\ln[1 - (\Delta E/\Delta t)_t/(\Delta E/\Delta t)_\infty] = -k_{obs}t \quad (8)$$

Thus, if the left-hand term of eqn. (8) vs. time is plotted, the observed rate constant, k_{obs}, of the hydrolytic reaction may be calculated from the slope of the curve. $\Delta E/\Delta t$ values should be corrected for the blank.

EXPERIMENTAL

Instrumentation

An Orion cyanide-selective electrode (Model 94-06) was used as the indicator electrode. When not in use, the electrode was kept in air. Before measurements were started, the electrode was conditioned for about 20 min in a stirred dilute KCN solution (ca. 2×10^{-5} M) buffered to pH 7.8, to avoid later irregular potential drifts. A double-junction silver—silver chloride electrode (Orion Model 90-02) was used as the reference electrode; its outer chamber was filled weekly with a 10% (w/v) KNO_3 solution.

A thermostated double-walled 50-ml beaker was used as reaction cell. The reaction mixtures were stirred magnetically.

A Heath-Schlumberger Model EU-205 B recorder system was used to record the response curves. An EU-200-30 pH/pIon electrometer was inserted between the electrodes and the recorder for impedance matching.

A solid-state double switching network was used in conjunction with the recording system for automatic time measurements [14]. For the present work, this system was adjusted so that it was activated after a premeasurement period, equivalent to a potential change of about 4 mV, and then the time required for the cell voltage to change by 8.0 mV was measured accurately (±0.01 s).

Reagents

All solutions were prepared with deionized distilled water from reagent-grade materials.

Potassium cyanide. A 0.100 M stock solution was prepared by dissolving 6.51 g of KCN in water and diluting to 1 l. Mixed working solution (2×10^{-5} M KCN—1.25×10^{-3} M EDTA) was prepared fresh daily from this stock solution and a 0.050 M EDTA solution by appropriate dilution.

Formaldehyde. For the standard 1.000 M stock solution, 85 ml of commercial solution (Merck, p.a., 35% w/w) was diluted to 1 l. The solution was standardized iodimetrically. Standard working solutions in the range 0.002—0.010 M were prepared daily by appropriate dilution.

Hexamethylenetetramine. For the 0.100 M standard stock solution, 14.02 g of hexamethylenetetramine (p.a.) was dissolved in water and diluted to 1 l. Working solutions were prepared daily by appropriate dilution.

Composite phosphate—triethanolamine buffer pH 7.8. This was prepared daily by mixing 25.0 ml of 2.0 M NaH_2PO_4 solution, 25.0 ml of 2.0 M triethanolamine solution and about 40.0 ml of water, adjusting with 2 M NaOH to pH 7.8 and diluting to 100 ml.

Procedures

(A) Kinetic determination of formaldehyde. Into the thermostated (30.0°C) reaction cell, pipet 15.00 ml of composite KCN—EDTA solution and 4.00 ml of buffer solution. Start the stirrer and after the potential has stabilized at a value of E_0 (after about 20 s) adjust the recorder pen to one side (lower potential) of the chart. Adjust the voltage reference sources (VRS) of the control system so that the time measurement starts at E_1 and stops at E_2 ($\Delta E = E_2 - E_1 = (E_0 + 12.0) - (E_0 + 4.0) = 8.0$ mV). Reset the "Start" button on the timer and inject quickly 1.00 ml of formaldehyde standard or sample solution into the reaction cell with a 1.00-ml syringe. The analysis is completed automatically and the number on the timer is recorded. Empty the cell with suction, rinse with water and repeat the procedure for each analysis without changing the potential levels on the control system. For each series of unknown include four standards.

(B) Kinetic determination of hexamethylenetetramine. Into 25-ml vials with well-fitting stoppers, pipet 10.00 ml of standard or sample solution containing 20—100 mg of hexamethylenetetramine and 10.00 ml of 4.0 M sulfuric acid. If solid samples are used, transfer an accurately weighed amount of hexamethylenetetramine standard reagent or sample to the vials and pipet in 20.00 ml of 2.0 M sulfuric acid. Stopper the vials tightly, shake and immerse them in a water bath thermostated at 60°C for 30 min. Shake while cooling. Pipet 0.050 ml of the hydrolyzed hexamethylenetetramine solution with a micropipet and analyze by procedure A.

(C) Determination of hexamethylenetetramine mandelate in pharmaceutical tablets. Weigh at least 20 tablets of the sample and pulverize well in a mortar. Weigh an appropriate amount of the pulverized sample containing 20—100 mg of hexamethylenetetramine and analyze by procedure B.

(D) Determination of acid hydrolysis rate constant of hexamethylenetetramine. Into a vial containing 20 ml of 2 M sulfuric acid, thermostated at various temperatures, add the necessary amount of hexamethylenetetramine to give a concentration of about 0.060 M. At various time intervals, analyze 0.050-ml portions of the solution by procedure A. From the slopes of the recorded reaction curves, calculate the rate constant k_{obs} of the acid hydrolysis of hexamethylenetetramine according to eqn. (8).

RESULTS AND DISCUSSION

Kinetic determination of formaldehyde

Figure 3 shows typical recorded curves of the formaldehyde—cyanide reaction. The calibration graph obtained from these curves was a straight line. As the automatic measurement of time intervals is easier than measurement of slopes, the former approach was used for construction of the calibration curves.

Analysis of aqueous formaldehyde solutions gave the results shown in Table 1. The average error was about 1.3% and measurement times were about 18—80 s. The calibration curve was valid for at least 5 h. Ten replicate determinations were made with 0.008 M and 0.003 M formaldehyde samples. The average measurement times were 25.00 s (range, 0.41 s) and 56.04 s (range, 2.10 s) and the relative standard deviations were 0.54% and 1.5%, respectively. The effect of temperature on the reaction rate is shown in Fig. 4. A difference of 1°C can cause an error of about 7%.

Any substance which reacts with cyanide or formaldehyde would interfere and should be eliminated prior to the measurements. Sulfide and iodide ions interfere seriously with the cyanide electrode, and must be absent. The interference of those metal ions which form cyanide complexes is avoided by

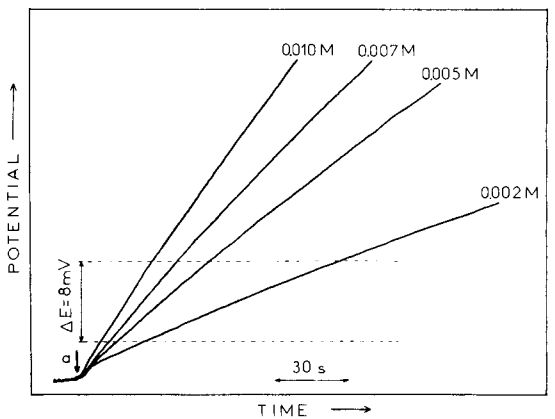

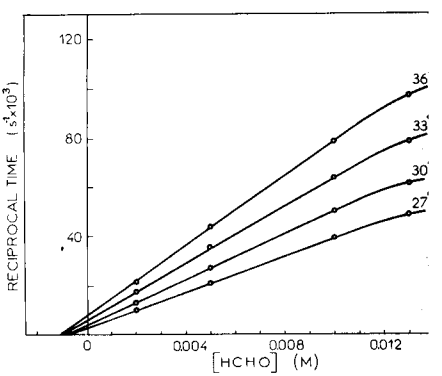

Fig. 3. Recorded curves of cell voltage vs. time for the formaldehyde—cyanide reaction.

Fig. 4. Effect of temperature on reaction rate in formaldehyde determination.

TABLE 1

Automatic results for aqueous formaldehyde solutions

$s^{-1} \times 10^{3a}$	HCHO (μg ml^{-1})		Error (%)	$s^{-1} \times 10^{3a}$	HCHO (μg ml^{-1})		Error (%)
	Taken	Found[b]			Taken	Found[b]	
12.84	60.1	59.0	−1.8	36.64	210.2	213.0	+1.3
17.55	90.1	89.5	−0.7	45.45	270.3	269.9	−0.1
22.85	120.1	123.8	+3.1	49.87	300.3	298.6	−0.6

[a]Average of two values. [b]Calculated from $1000/\Delta t = 3.72 + 0.15457$ (μg HCHO); correlati coefficient, 0.9998.

adding EDTA to the cyanide working solution. Several substances were tested for their effect on the formaldehyde determination. Methanol, ethanol, urea, glycerol, hexamethylenetetramine, ethyleneglycol, ascorbic acid, glucose, fructose, galactose, lactose, mannitol and sorbitol did not interfere even in high concentrations (ca. 0.1 M). Table 2 shows the effect of various aldehydes and ketones on the formaldehyde determination when present in equal amour ($5\ \mu$mol).

Kinetic determination of hexamethylenetetramine

The proposed kinetic method for the determination of formaldehyde was applied to the determination of hexamethylenetetramine, the well-known drug for urinary tract infections. Hexamethylenetetramine was hydrolyzed to formaldehyde by acid solution and determined as formaldehyde. Table 3 shows the results obtained for aqueous solutions; 50—250 μg of hexamethylenetetramine in 0.050 ml could be determined with an average error of about 1.6% and measurement times of 18—80 s. Ten hexamethylenetetramine samples (43.3 mg) were analyzed by procedure B; the average measurement time was 36.30 s (range, 0.97 s) and the relative standard deviation was 0.96%

The accuracy of the method was checked by recovery experiments, in which hexamethylenetetramine was added to tablet samples. The average recovery was 98.8% (Table 4). None of the substances used as diluents in the tablet preparation interfered. The accuracy was further tested by comparing

TABLE 2

Effect of various aldehydes and ketones on formaldehyde determination[a]

Interferent	Error (%)	Interferent	Error (%)
Acetaldehyde	+9.0	Salicylaldehyde	+5.8
Chloral	+14.7	Acetone	+4.8
Benzaldehyde	+11.6	Methyl n-propyl ketone	+1.0

[a]Formaldehyde and interferent were present in equal amounts ($5\ \mu$mol).

TABLE 3

Results for determination of hexamethylenetetramine in aqueous solutions

$s^{-1} \times 10^{3a}$	Hexamine (μg/0.050 ml)		Error (%)	$s^{-1} \times 10^{3a}$	Hexamine (μg/0.050 ml)		Error (%)
	Taken	Found[b]			Taken	Found[b]	
13.64	46.7	46.8	+0.2	29.59	116.8	118.5	+1.5
19.42	70.1	72.8	+3.8	38.93	163.6	160.6	−1.8
23.59	93.5	91.6	−2.0	54.85	233.6	232.1	−0.6

[a]Average of two values.
[b]Calculated from $1000/\Delta t = 3.23 + 0.22236$ (μg hex); correlation coefficient, 0.99997.

TABLE 4

Recovery of hexamethylenetetramine added to tablet samples (Mandelamine)

Hexamine (mg)				Recovery (%)
Initially present[a]	Added	Total	Found[b]	
31.2	16.2	47.4	47.6	101.2
33.8	21.6	55.4	54.8	97.2
24.3	25.4	49.7	49.0	97.2
48.5	20.9	69.4	70.0	102.9
53.4	23.9	77.3	76.2	95.4

[a]Calculated from the percentage hexamethylenetetramine content of Mandelamine.
[b]Average of two measurements.

values for pharmaceutical tablets containing hexamethylenetetramine mandelate with those obtained by the USP titrimetric method [15] (based on a modified Nessler reagent). There was satisfactory agreement between the results obtained by the two methods (Table 5).

For the determination of the rate constant of the acid hydrolysis of hexamethylenetetramine, experiments were carried out at three different temperatures. From plots of the left-hand term of eqn. (8) vs. time, the values obtained for the observed rate constant, k_{obs}, were 0.040 ± 0.003 min^{-1}, 0.082 ± 0.001 min^{-1} and 0.202 ± 0.007 min^{-1} for 33, 38 and 49°C respectively, in 2 M sulfuric acid. From the above data a value of 19.8 ± 1.3 kcal mol^{-1} was obtained for the activation energy of the acid hydrolysis reaction.

Conclusion

The proposed potentiometric kinetic method for the determination of formaldehyde is faster than titrimetric or spectrophotometric methods, simple, sensitive, accurate, selective, and has all the now-conventional advantages of ion-selective electrodes. The method can be employed in analyses for hexamethylenetetramine, reducing substantially the analysis time.

TABLE 5

Comparison of potentiometric kinetic and USP titrimetric methods for the determination of hexamethylenetetramine mandelate in pharmaceutical tablets (0.5 g)

Preparation	Methenamine mandelate (mg/tablet)	
	Kinetic method[a]	USP method[a]
Amigdalin tablets (Athen-pharm)	538 ± 5	528 ± 3
Mandelamine tablets (Warner-Chilcott)	490 ± 11	484 ± 6
Mandurin tablets (ASL Lab.)	481 ± 8	504 ± 5

[a]Average of three determinations.

This research was supported in part by a grant from the Greek National Institute of Research.

REFERENCES

1 D. G. Vickroy and G. L. Caunt, Tobacco, 174 (1972) 50.
2 J. H. Riseman, Am. Lab., 4 (1972) 63.
3 S. S. M. Hassan, Anal. Chem., 49 (1977) 45.
4 R. A. Llenado and G. A. Rechnitz, Anal. Chem., 44 (1972) 468.
5 W. R. Hussein, L. H. von Storp and G. G. Guilbault, Anal. Chim. Acta, 61 (1972) 89.
6 B. Fleet and H. von Storp, Anal. Chem., 43 (1971) 1575.
7 J. W. Ross, in R. A. Durst (Ed.), Proceedings of Symposium on Ion Selective Electrodes, N.B.S. Spec. Publ. 314, 1969, p. 84.
8 Orion Research Inc., Instruction Manual 94-06, 11 Blackstone Street, Cambridge, Mass., U.S.A.
9 K. Tóth and E. Pungor, Anal. Chim. Acta, 51 (1970) 221.
10 B. Gyorgy, L. L. Andre, L. Stehli and E. Pungor, in Proceedings of the International Measurement Confederation on Electrochemical Sensors, Veszprem, Hungary, 1968, p. 111.
11 G. Romijn, Fresenius Z. Anal. Chem., 36 (1897) 18.
12 L. F. Fieser and M. Fieser, Advanced Organic Chemistry, 5th edn., Reinhold, New York, 1965, p. 418.
13 L. G. Chatten, Pharmaceutical Chemistry, Vol. 1, 1966, p. 222.
14 C. E. Efstathiou and T. P. Hadjiioannou, Anal. Chim. Acta, 89 (1977) 55.
15 US Pharmacopeia, XVII, p. 384.

Analytica Chimica Acta, 107 (1979)101—104

SINGLE-POINT POTENTIOMETRIC TITRATIONS WITH ION-SELECTIVE ELECTRODES

G. HORVAI, K. TÓTH and E. PUNGOR*

Institute for General and Analytical Chemistry, Technical University, Budapest (Hungary)

(Received 27th November 1978)

SUMMARY

A single-point potentiometric titration method is described for the determination of silver(I), chloride and sulphate with ion-selective electrodes. Relative standard deviations in the range 0.1—1.25% can be obtained, depending on the quality of the electrodes used.

Single-point potentiometric titration [1—5] is a general term for a class of simplified titrations in which a certain amount of reagent is added to the sample and the potential of an appropriate electrode in the resulting solution is measured. The precision and accuracy of the result are similar to those obtainable by the usual titration methods. The advantages of such methods are obvious with regard to time-saving and to applications in automated analytical systems.

Johansson and Backén [1] and Åström [2] perfected the single-point acid—base titration described earlier by Leithe [3], while Damokos and Havas [4] developed independently a similar approach. In these methods, the analyte — a strong base or acid — is added to a mixture of weak acids or bases; if the weak components are chosen carefully, the pH of the final solution becomes a strictly linear function of the concentration of analyte. The change of pH per unit change of the analyte concentration is so high that a single pH measurement is enough to obtain a result similar in accuracy and precision to the conventional titration with a strong acid or base.

Ivaska [5] used a different approach to the single-point potentiometric acid—base titration. Thus, a weak acid is titrated with a strong base to a preset potential, which corresponds to a titration degree of about 50%, and the equivalence point is calculated from the volume of titrant required to attain the preset potential. Frost [6] applied a known subtraction method — which can also be regarded as a single-point procedure — for the measurement of low concentrations of chloride, and noticed that if a nearly equivalent amount of silver ion was added to the sample, the precision was significantly higher than otherwise.

In this paper, a novel approach to single-point potentiometric titrations is discussed. The method is based, like other titrations, on a stoichiometric re-

action between the analyte and some reagent. The potentiometric sensor may detect the analyte or the reagent or both. The case when only the analyte is sensed is considered first. An approximately 90—95% fraction of the equivalent volume of the reagent is added to the sample solution; this is easily and quickly accomplished as will be shown. Then the remaining 5—10% of the analyte is measured by direct potentiometry. Direct potentiometry is of limited precision, but in this method only a small fraction of the analyte is measured with this low precision, whereas the bulk (90—95%) is measured with the usual volumetric precision. Accordingly, the overall precision will be only slightly less than the volumetric precision. Since this is achieved by a single addition of reagent, the method remains a single-point potentiometric titration. If the reagent rather than the analyte is sensed by the electrode, the situation is very similar, the only difference being that a 5—10% excess of the reagent is added.

The procedure suggested here is similar to the known subtraction technique and to the technique developed by Ivaska [5], but it makes fewer demands on the electrode performance than the other two methods in obtaining the same degree of precision. This single-point titration method is a realization of the general idea of combining a less precise but rapid and simple analytical method with a precise but time-consuming technique. The same principle has been applied to spectrophotometric titrations by Nishimura and Noriki [7], and has been discussed in general terms by Ingman and Still [8] in a theoretical treatment of the subject.

EXPERIMENTAL

Reagents and equipment

Analytical-grade reagents were used without further purification, except for dioxane which was treated with potassium hydroxide overnight, refluxed for 6 h over sodium and finally distilled. Silver nitrate and sodium chloride were pretreated as described by Schulek and Szabó [9].

A Radiometer PHM 64 pH meter was used in combination with a Radelkis OP-CN-7112D cyanide-selective electrode and an OP-820 silver chloride double-junction reference electrode; a very old Orion 94-82A lead electrode was also used.

Procedure

To 20.00 ml of 10^{-2} M silver nitrate solution which was 10^{-1} M in KNO_3, 10^{-1} M sodium chloride solution was added from a 3-ml all-plastic syringe until the potential of the cyanide-selective electrode — applied here as a silver-ion sensor — changed by about 80 mV. The degree of titration is thus about 95%. After stabilization (about 1 min), the potential was read. The amount of reagent added was measured by reweighing the syringe.

Ten parallel single-point titrations were made. After each of them, the electrode was standardized in 5×10^{-4} M silver nitrate solution containing

10^{-1} M KNO_3. Before and after the whole series of measurements, two-point calibration of the electrode was done in 10^{-3} M and 10^{-4} M silver nitrate solutions, both of which were 10^{-1} M in KNO_3.

For comparison, 20.00-ml aliquots of the 10^{-2} M silver nitrate solution were titrated potentiometrically with the 10^{-1} M sodium chloride solution.

Determinations of approximately 5×10^{-4} M sulphate in 50% dioxane solution [10] were done in a similar way: 10^{-2} M lead nitrate solution was added in excess, until the potential of the lead electrode reached approximately the potential measured in the standardizing solution, which was 2×10^{-5} M lead nitrate in 50% dioxane. Here again, conventional potentiometric titration was used for control.

RESULTS AND DISCUSSION

The average of ten determinations of silver ion was 1.0046×10^{-2} M with a relative standard deviation of 0.09%. This result agreed well with the 1.004×10^{-2} M value obtained by conventional potentiometric titration.

The average of eleven determinations of sulphate was 1.261×10^{-3} M with a relative standard deviation of 1.24%. The potentiometric titrations of sulphate gave similar results, but the standard deviation was much greater and therefore could not be used for control.

It should be noted that the electrodes used drifted somewhat: the cyanide-selective electrode used for silver drifted 1.1 mV during the course of the ten determinations, while the lead-selective electrode drifted 7.8 mV. The results are, however, only slightly affected by electrode drift because (a) the speed of the single-point titration makes frequent restandardization of the electrode possible, (b) standardization can be done near the measured concentration, and (c) only a fraction of the potentiometric error appears in the total error.

Chloride in tap water can also be determined by the single-point method: one result was 4.82×10^{-4} M with a relative standard deviation of 0.7% from nine measurements. In this case, a chloride-selective electrode was used near its lower detection limit, thus rendering the results somewhat less precise.

The above results show, and it follows from the principle of the single-point titration method discussed here, that the method can be used successfully even with electrodes which are of less than satisfactory performance for conventional purposes. This is in contrast to the other single-point titrations mentioned earlier. Moreover, relatively slow reactions and electrodes with slow response can be used in single-point titrations of this type because only one potential reading is required.

The limitations of the method can easily be seen but they are not very serious. The reaction between sample and reagent must be of exactly known stoichiometry. The concentration of the residual analyte (or of the excess of reagent), which is much less than the original sample concentration, must not be lower than the detection limit of the electrode. The ionic strength and the concentration of possible interfering ions should be approximately the same in the sample and in the standardizing solution; these requirements are,

however, less strict than in the case of conventional direct methods because the error in the potential reading influences the total error of the determinatic to a much smaller extent.

If for some reason reliable standardizing solutions cannot be prepared, i.e. if the standardization cannot be done as described in Experimental, then the standard addition method should be used to determine the concentration of the unreacted analyte or the excess of reagent.

In the experiments described, the equivalence point was approached to 5—10%. This seems to be a good compromise in many cases between the highe precision obtainable by coming closer to the equivalence point and the increasing problems which are encountered with unstable potentials or uncertainties in electrode behaviour at the low concentrations of measured ion near the equivalence point. In certain cases, the solubility or the equilibrium dissociation of the reaction product cannot be neglected. In such cases, corrections can be made by using the appropriate solubility product or equilibrium constant.

It is also possible to obtain sensitive and almost proportional voltage signals in the continuous control of a sample stream by using an automated version of the single-point titration discussed here. To this end, the sample stream is mixed in a given constant ratio of flow rates with a reagent stream containing the reagent in about 90—95% (or 105—110%) of the equivalent of the nomina sample concentration and the potential is measured in the mixed stream. This will be discussed in a subsequent paper.

The authors acknowledge valuable discussions with Dr. Ari Ivaska.

REFERENCES

1 G. Johansson and W. Backén, Anal. Chim. Acta, 69 (1974) 415.
2 O. Åström, Anal. Chim. Acta, 88 (1977) 17; 97 (1978) 259.
3 W. Leithe, Chem. - Ing.-Tech. Z., 36 (1964) 112.
4 T. Damokos and J. Havas, Hung. Sci. Instrum., 36 (1976) 7.
5 A. Ivaska, Talanta, 21 (1974) 377, 387.
6 J. G. Frost, Anal. Chim. Acta, 48 (1969) 321.
7 M. Nishimura and S. Noriki, Anal. Chim. Acta, 66 (1973) 351.
8 F. Ingman and E. Still in E. Wänninen (Ed.), Analytical Chemistry — Essays in Memory of Anders Ringbom, Pergamon Press, Oxford, 1977, p. 183.
9 E. Schulek and Z. L. Szabó, A kvantitativ analitikai kémia elvi alapjai és módszerei, Tankönyvkiadó, Budapest, 1973.
10 J. W. Ross, Jr. and M. S. Frant, Anal. Chem., 41 (1969) 967.

Analytica Chimica Acta, 107 (1979) 105—112

STABILITY OF TERNARY COPPER—NITRILOTRIACETIC ACID COMPLEXES

EBBE STILL*

Laboratory of Inorganic and Analytical Chemistry, Helsinki University of Technology, Otaniemi (Finland)

(Received 30th October 1978)

SUMMARY

A copper-selective electrode was used to investigate ternary copper—nitrilotriacetic acid complexes by means of combined pH and pM measurements. The theory presented for the evaluation of the stability of mixed-ligand complexes is based on the conditional constants. The emphasis is on the formation of 1:1:1 complexes of the type copper(II)—NTA—(hydroxide, amino acid, ammonia, triphosphate).

In chelate complexes a multidentate ligand reacts with a metal ion. With a sufficiently high number of donor atoms in the ligand, these ions will combine in only one, or, at the very most, two different stoichiometric ratios, so that a simple stoichiometry of the chelate complexes will usually be obtained. In systems where the ligand has a large number of coordination centres, the chelates formed are frequently protonated and acid complexes are formed. For metal ions forming stable hydrolysis products, the chelates formed may also bind hydroxide ions. In some cases, the ligand can be deprotonated by coordination of a weakly acidic group to the metal ion and the complex will then exhibit basic properties.

When the metal ion in the 1:1 chelate is coordinatively unsaturated, a second ligand can be accepted and a biligand or a mixed-ligand (also called ternary) complex will be formed. Mixed-ligand complexes are frequently formed in solutions containing two or more different ligands. A knowledge of the stability of these species is essential for the understanding of many problems in analytical chemistry and biochemistry.

Combined pH and pM measurements have to some extent been used for equilibrium studies [1]. The concept of conditional constants was introduced in analytical chemistry to master the complicated equilibria which one has to deal with in complexiметry. The concept has been used for the evaluation of stability constants of chelate complexes [2] from combined pH and pM measurements. A plot of a conditional constant versus pH will immediately give the protonated and deprotonated (or mixed hydroxide) species present

*Present address: Department of Chemistry, Åbo Akademi, SF-20500 Åbo 50, Finland.

in solution and a graphical method will provide good estimates of the unknow stability constants. These can then be refined by algebraic calculations.

This paper discusses the use of combined pH and pM measurements for equilibrium studies of chelate complexes. The theory is presented for 1:1 chelates under the influence of various side-reactions. The formation of mixed ligand chelates is included. The theory is applied to the evaluation of stability constants of ternary chelates formed in the copper—nitrilotriacetic acid (NTA system. A copper-selective electrode was used as pM sensor in the experimenta work. The publication of this investigation was prompted by two recent articl [3, 4] which suggest that a copper-selective electrode could not be used for evaluation of the stability of Cu—NTA and Cu—EDTA complexes.

1:1 Chelates

The cation M and the anion L (all charges are omitted) are assumed to react in a 1:1 ratio forming a number of acidic and basic complexes. In analogy to neutralization reactions where pH measurements of a well-buffered solution should be used for the calculation of the stability of the acid, it is necessary to use a metal buffer solution for the measurements. The concentration of free metal ion in a solution containing 1:1 chelates will be determined by the conditional constant [2]

$$K^{M,L'}_{(ML)'} = [(ML)']/[M]\,[L'] = K^{M,L}_{ML}\,\alpha_{ML(H,\,OH)}/\alpha_{L(H)} \qquad (1)$$

where $[(ML)'] = \Sigma[MH_iL] = \cdots + [MH_2L] + [MHL] + [ML] + [MOHL] + \cdots$, and $[L'] = \Sigma[H_iL] = [L] + [HL] + [H_2L] + \cdots$. $\alpha_{L(H)}$ and $\alpha_{ML(H,\,OH)}$ denote the side-reaction coefficients or α-coefficients (distribution coefficients) of the species shown in the subscripts [2].

The mass-balance equations give

$$C_M = [M'] + [(ML)']\,;\ [(ML)'] = C_M - [M'] \qquad (2)$$

$$C_L = [L'] + [(ML)']\,;\ [L'] = C_L - C_M + [M'] \qquad (3)$$

$[M']$ is the total concentration of uncomplexed metal ion. If $[M']$ differs from $[M]$, it is mostly a question of the hydrolysis of the metal ion.

Equations (1—3) give

$$\log K^{M,L}_{ML} + \log \alpha_{ML} = pM + \log \alpha_L + \log (C_M - [M'])/(C_L - C_M + [M']) \qquad (4)$$

The left-hand side of eqn. (4), $\log K^{M,L}_{(ML)'}$, will contain the unknown constants of the chelates. Through a gradual change of the pH of the solution, a series of combined pH and pM measurements will be obtained, and a plot of log $K^{M,L}_{(ML)'}$ versus pH will give a figure resembling a logarithmic diagram. From this plot the unknown stability constants can be evaluated by graphical methods [2] and refined by algebraic calculations.

The ratio C_M:C_L in the solution can be varied. The calculated conditional constant will not alter unless some other reactions occur in the solution. Another possibility is that systematic errors in the readings or in the standard ization of the solutions are present in a significant amount.

A simplification can be obtained [2] by preparing a solution with a $C_M : C_L$ ratio of 0.5:1. If in addition strong complex formation prevails in the solution ($[M'] \ll C_M$) eqn. (4) will take the simple form

$$\log K_{ML}^{M,L} + \log \alpha_{ML} = pM_{0.5} + \log \alpha_L \quad (5)$$

1:1 and 1:2 chelates

If the metal ion also takes up a second ligand, the mass-balance equations will become

$$[(ML)'] = C_M - [M'] - [(ML_2)'] \quad (6)$$

$$[L'] = C_L - C_M + [M'] - [(ML_2)'] \quad (7)$$

$[(ML_2)']$ denotes the sum of the concentrations of the different mononuclear biligand complexes, acidic as well as basic.

The constants of the monoligand chelates can be determined by inserting eqns. (6) and (7) into eqn. (4). The expressions contain the concentration of $(ML_2)'$, which is unknown. A convenient way to solve the problem is to prepare a solution mixed in the same $C_M : C_L$ ratio as mentioned before, i.e., 0.5:1. The quotient $[(ML)'] : [L']$ will then be equal to unity as long as $[M']$ is negligible, thus if $[M'] \ll C_M$

$$[(ML)']/[L'] = \{C_M - [M'] - [(ML_2)']\}/\{C_M + [M'] - [(ML_2)']\} = 1 \quad (8)$$

Under the given conditions the formation of biligand chelates will not affect the calculations and eqn. (4) can be used for evaluation of the stability constants of the 1:1 chelates. The reason is that the pM measurements are done at the second equivalence point for the titration of M with L; at this point, $[L'] = [(ML)'] + 2[M']$.

It is generally not favourable to perform measurements in a solution assumed to have reached an equivalence point, because small analytical errors may affect the calculated constants. The influence of analytical errors will be the more severe, the higher the stability constant of the biligand chelate, $L + ML = ML_2$. For experiments with $C_M : C_L \neq 0.5:1$, the stability of ML_2 must be known. The constants of the 1:2 chelates can be determined if a large excess of the ligand is added to the solution.

Mixed-ligand chelates

If mixed-ligand chelates of the composition MLA, MLA_2, ... are formed, $[(ML)']$ denotes the sum of the concentrations of all species with a 1:1 stoichiometry for M:L, i.e.

$$\alpha_{ML} = \alpha_{ML(H,OH,A)} = \alpha_{ML(H,OH)} + \alpha_{ML(A)} - 1 \quad (9)$$

$$\text{where } \alpha_{ML(A)} = 1 + [A]\, K_{MLA}^{ML,A} + [A]^2\, K_{MLA_2}^{ML,2A} + \cdots \quad (10)$$

Mixed-ligand complexes of the type MLA_i can be treated in an analogous way as the preceding group of mononuclear monoligand complexes. A series of pH and pM measurements under appropriate conditions may suffice.

The experiments can be performed as potentiometric titrations at fixed pH values, or by varying the pH value of a solution with a fixed $C_M : C_L : C_A$ ratio with A preferably in a large excess so that the approximation $[A] \cong C_A/\alpha_{A(H)}$ is valid [5].

The influence of biligand complexes $(ML_2)'$ can again be avoided by preparing the solution with $C_M : C_L = 0.5:1$. The ratio $[(ML)']:[L']$ remains equal to unity as long as a considerable amount of free M′ ions is not present ($[M'] = \alpha_{M(OH,A)}[M]$).

In a system with known stability constants for acidic and basic ML and ML_2 chelates, it is possible to determine the pL by pM measurements, and the constants of mixed-ligand complexes can be calculated from measured pM and pH values. An example illustrating the method is presented below.

EXPERIMENTAL

All chemicals were of reagent grade, and were used as received. The NTA solution was standardized against the copper(II) sulfate solution [6]. The protonation constants of the ligands were taken from the literature [7]. The following logarithmic protonation constants (mixed) [8] for NTA were used in the calculations: 9.81, 2.57, 1.97. For conversion of concentration constant a modified form of Kielland's table was used [8].

The potential readings were taken at 25°C in solutions of ionic strength 0.1 mol l^{-1} ($NaNO_3$) with a Radiometer PHM 28 for the pH measurements and a Radiometer PHM4b equipped with a copper-selective Selectrode [9] for the pM measurements. For the calculation of $\alpha_{NTA(Na)}$, the value $\log K_{NaNTA} = 1.2$ was used [7].

RESULTS

The stability of Cu—NTA—OH complexes

It was of interest to check the performance of the Selectrode against a known system. The Cu—NTA system was chosen as the model. In the following paragraphs, L denotes the fully dissociated anion of NTA. The calculated values of the conditional constant $\log K^{Cu,L}_{(CuL)'}$ according to eqn. (4) are plotted as a function of pH in Figs. 1 and 2. The plots immediately give a survey of the equilibria and the species present in solution. The plot is nearly horizontal between about pH 3 and pH 7 showing that acidic complexes are not formed significantly in this region. The curvature of the plot on the basic side shows that Cu—NTA complexes with one and two hydroxide groups are formed. The $C_{Cu}:C_L$ ratio in the solution is 0.59:1 and the influence of the CuL_2 complex cannot be disregarded in the pH region 7—11.

The constant $\log K^{Cu,L}_{(CuL)'}$ is corrected for the formation of the biligand complex according to eqns. (6) and (7). The concentration of CuL_2 can be calculated in the following way. The mass-balance equations give

$$C_L - C_{Cu} + [Cu'] = [L'] + [CuL_2] = [L'] + K^{Cu,2L}_{CuL_2}[Cu][L']^2/\alpha_L^2 \qquad (11)$$

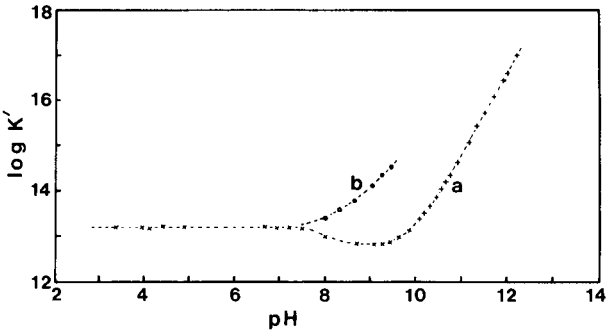

Fig. 1. The conditional constant log $K^{Cu,L}_{(CuL)'}$ calculated from eqn. (4) as a function of pH. (a) C_{Cu} = 0.0050 mol l^{-1}, C_L = 0.0085 mol l^{-1}; (b) the influence of ammonia in a total concentration of 0.10 mol l^{-1} for C_{Cu} = 0.0050 mol l^{-1} and C_L = 0.0100 mol l^{-1}.

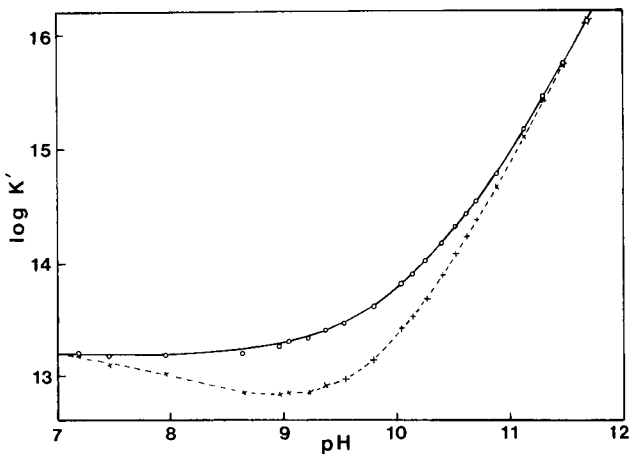

Fig. 2. The experimental points (×) from Fig. 1(a) and the data points corrected for the formation of the 1:2 complex (○). The solid curve denotes the theoretical curve calculated with the stability constants given in the text.

This equation allows [L'] to be determined from measured [Cu] values and gives the concentration of CuL_2. The constant log $K^{CuL,L}_{CuL_2}$ = 4.47 is taken from the literature [7]. In the acidic region the concentration of biligand complex is negligible, and eqn. (4) and the plot give the value log $K^{Cu,L}_{CuL}$ = 13.2. The corrected experimental points are shown in Fig. 2. The plot gives the following approximate values of the constants: log $K^{CuL,OH}_{CuOHL}$ = 4.2, log $K^{CuOHL,OH}_{Cu(OH)_2L}$ = 2.9. The algebraic calculations were performed as an optimization of the conditional constant log $K^{Cu,L}_{(CuL)'}$ [10]. The results are: log $K^{Cu,L}_{CuL}$ = 13.19 ± 0.02, log $K^{CuL,OH}_{CuOHL}$ = 4.40 ± 0.02, log $K^{CuOHL,OH}_{Cu(OH)_2L}$ = 3.08 ± 0.03.

The stability of Cu—NTA—amino acid complexes

Recently, the importance of mixed-ligand complex formation has been

recognized, and a book reviewing different aspects of mixed-ligand chelate formation has been published [11]. The Cu—NTA—amino acid system has been quite well investigated and is therefore suitable as a model system. The mixed-ligand complexes formed in the system have a 1:1:1 stoichiometry. The mass-balance equations (A = amino acid, negligible amounts of CuA, CuA_2, ... are assumed)

$$C_{Cu} = [Cu'] + [CuL] + [CuOHL] + [Cu(OH)_2L] + [CuL_2] + [CuLA] \quad (12)$$

$$C_L = [L'] + [CuL] + [CuOHL] + [Cu(OH)_2L] + 2[CuL_2] + [CuLA] \quad (13)$$

$$C_A = [A'] + [CuLA] + ([CuA] + 2[CuA_2] + \cdots \quad (14)$$

yield the equation from which [L'] can be determined:

$$C_L - C_{Cu} + [Cu'] = [L'] + [CuL_2] \quad (15)$$

Consequently, the concentrations of CuL, CuOHL, $Cu(OH)_2L$, and CuL_2 can be calculated from measurements of pH and pM. Since [CuLA] is determined by eqn. (12), and [A'] by eqn. (14), $\log K_{CuLA}^{CuL,A}$ can be calculated. The formation of acidic and basic complexes of CuLA can be investigated by varying the pH of the solution.

The formation of mixed-ligand complexes between CuNTA and various amino acids was investigated as a potentiometric titration at about pH 9. In Fig. 3 the increase in measured pCu value of the solution is plotted as a function of total concentration of the ligands α-alanine, β-alanine and proline. The following values were obtained: $\log K_{CuLA}^{CuL,A} = 5.63$ for α-alanine, 4.48 for β-alanine, 6.14 for proline, and 5.40 for arginine. Reported literature values [11] are 5.42, 4.56, 6.24, and 5.22, respectively (25°C, $\mu = 0.073$). The calculations were based on the following logarithmic protonation constants (mixed) of the amino acids [7]: 9.92, 10.39, 10.71, and 9.14.

The stability of the Cu—NTA—NH_3 and Cu—NTA—P_3O_{10} complexes

The stability of the mixed-ligand chelate between CuNTA and NH_3 was determined in a similar way to the Cu—NTA—OH system. An excess of ammonia was added to the solution, the pH of the solution was varied by the addition of base, and the stability of the 1:1:1 chelate was calculated from eqn. (10). Figure 1 (curve b) shows the conditional constant as a function of pH. The value of the stability constant obtained is $\log K_{CuLA}^{CuL,A} = 2.55$, when $\log K_{HA} = 9.37$.

The formation of the ternary Cu—NTA—P_3O_{10} complex was investigated as a potentiometric titration at pH 9.15. Weak complex formation was observ with $\log K_{CuLA}^{CuL,A} = 2.5$.

DISCUSSION

The aim of the present investigation was to show that a copper-ion selectiv electrode of the type recommended by Hansen et al. can be used as a pM

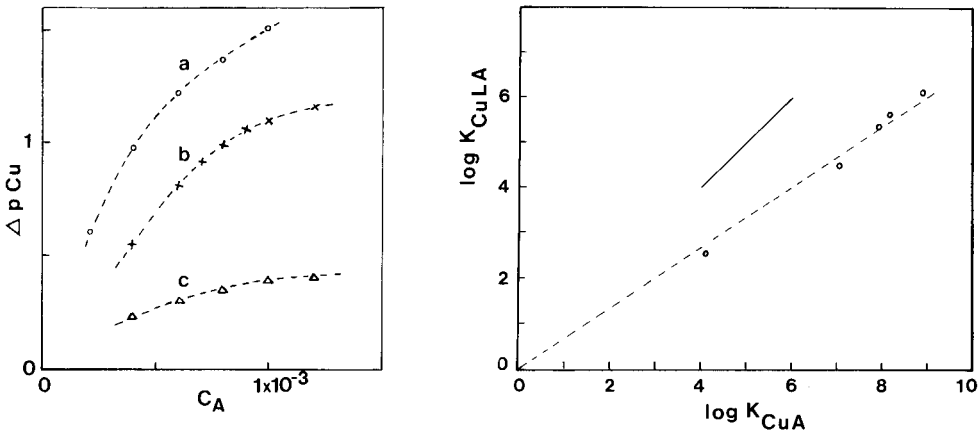

Fig. 3. The increase in measured pCu values in a potentiometric titration as a function of added amino acid. (a) α-Alanine at pH 9.07; (b) proline at pH 9.00; (c) β-alanine at pH 8.87.

Fig. 4. Log $K_{CuLA}^{CuL,A}$ as a function of log $K_{CuA}^{Cu,A}$ for the ligands with nitrogen as donor atom. The solid line has a slope of one.

sensor for evaluation of the stability of CuNTA and ternary Cu—NTA—(hydroxide, amino acid, ammonia, triphosphate) complexes. The performance of the electrode was satisfactory. It should be noted, however, that the earlier workers [3, 4] used solid-state electrodes made from pellets of mixed sulfides obtained by precipitation with an excess of sulfide; this procedure leads to the formation of some copper(I) in the membrane. The different types of electrode may not behave in exactly the same way.

The crystal structure of the sodium salt of CuNTA has been reported [12]. The structure shows a distorted octahedral coordination for copper with four Cu—NTA bonds and two additional contacts to neighbouring NTA molecules. In aqueous solution the latter bonds are probably replaced by water molecules, and the formation of the ternary complexes indicated above becomes comprehensible.

The tendency to form mixed-ligand complexes can be characterized by the difference in stability between the MLA and MA complexes [11]

$$\Delta \log K = \log K_{MLA}^{ML,A} - \log K_{MA}^{M,A} \text{ for } MA + ML = MLA + M \qquad (16)$$

In Fig. 4 log $K_{CuLA}^{CuL,A}$ is plotted as a function of log $K_{CuA}^{Cu,A}$ for the ligands with nitrogen as donor atom. A linear relationship is observed. The slope is less than one, which means that $\Delta \log K$ is negative, and the equilibrium of reaction (16) is more to its left-hand side. The very high pCu values recorded during the titrations justify, however, the assumption of negligible amounts of CuA, CuA_2,..., complexes made in eqn. (14).

The examples given above show that mixed-ligand complex formation can be used for the preparation of metal buffer solutions.

The author thanks Professor J. Růžička, The Technical University of Denmark, for the Selectrode, and Marianna Nurminen, M.Sc., for much of the experimental work. The paper was presented at the Analysdagarna Conference Lund, Sweden, in June 1976.

REFERENCES

1 F. J. C. Rossotti and H. Rossotti, The Determination of Stability Constants, McGraw-Hill, New York, 1961.
2 A. Ringbom and L. Harju, Anal. Chim. Acta, 59 (1972) 33, 49.
3 G. Nakagawa, H. Wada and T. Hayakawa, Bull. Chem. Soc. Jpn., 48 (1975) 424.
4 G. J. M. Heijne and W. E. van der Linden, Anal. Chim. Acta, 96 (1978) 13.
5 L. Harju, Anal. Chim. Acta, 63 (1973) 95.
6 E. Still, Anal. Chim. Acta, 107 (1979) 377.
7 L. G. Sillén and A. E. Martell, Stability Constants of Metal Ion Complexes, Special Publication Nos. 17 and 25, The Chemical Society, London, 1964 and 1972.
8 A. Ringbom, Complexation in Analytical Chemistry, Wiley—Interscience, New York, 1963.
9 E. H. Hansen, C. G. Lamm and J. Růžička, Anal. Chim. Acta, 59 (1972) 403.
10 E. Still, to be published.
11 H. Sigel (Ed.), Metal Ions in Biological Systems, Vol. 2, M. Dekker, New York, 1973.
12 E. Whitlow, Inorg. Chem., 12 (1973) 2286.

Analytica Chimica Acta, 107 (1979) 113—119

A NEW COATED-WIRE COBALT(II)-SELECTIVE ELECTRODE BASED ON THE BENZALKONIUM TETRATHIOCYANATOCOBALTATE(II) ION PAIR

K. BURGER* and G. PETHÖ

Department of Inorganic and Analytical Chemistry of the L. Eötvös University, Budapest (Hungary)

(Received 17th October 1978)

SUMMARY

A cobalt-selective electrode based on the benzalkonium tetrathiocyanatocobaltate(II) ion pair is described. The response is Nernstian (slope 29.3 mV/pCo) in the cobalt concentration range 10^{-1}—10^{-4} M in solutions with a constant ionic strength of 3.0 M made up with KSCN at 25°C. The electrode is suitable for end-point detection in titrations of cobalt(II) with EDTA as well as for direct potentiometric determinations of cobalt(II), even in the presence of large amounts of several metal ions (Ni^{2+}, Fe^{2+}, Mn^{2+}, Mg^{2+}, Ca^{2+}, Ba^{2+}) and anions (HCO_3^-, Br^-, I^-, NO_3^-, SO_4^{2-}).

Coated-wire electrodes containing, as electroactive materials, negatively charged halide complexes of the metal ions to be determined have often been recommended for analytical purposes. Mercury(II) [1], copper [2], zinc [3] and iron(III) [4, 5] ions have been measured as their tetrachloro complexes. The ion-pair complexes formed by these complex anions with long-chain quaternary ammonium ions were incorporated into a polyvinyl chloride (PVC) matrix used for coating the platinum wire electrode, the ion-exchange process of the complex anion governing the electrode potential. The metal ion activity (concentration) in the solution could then be calculated from the e.m.f. measurements after appropriate calibration.

Several unsuccessful [6—8] attempts have been made to produce cobalt-selective electrodes with a reversible Nernstian response over a reasonable concentration range. The measurement of cobalt(II) with an ion-selective electrode has been possible only in an indirect way, with a copper-selective electrode, on the basis of the interaction between the cobalt ion and the EDTA complex of copper [9]. In the present paper, development of an electrode based on complex ion exchange which is suitable for direct determination of cobalt(II), is reported.

EXPERIMENTAL

Apparatus

Changes in e.m.f. were measured with an Orion Model 701 digital millivoltmeter; pH was measured with a Radelkis OP-205 precision pH meter and a Radiometer G200B glass electrode. Titrations were done with an automatic burette (Radiometer ABU 12). The temperature was precisely adjusted with an ultrathermostat (VEB MLW TB 25). Solutions were mixed with a magnetic stirrer (Radelkis OP-912/3). A calomel electrode (Radiometer K100) served as the reference electrode.

Preparation of the electroactive material

Wherever possible, analytical-reagent grade chemicals were used.

The electroactive material was a quaternary ammonium tetrathiocyanato cobaltate(II) complex. Benzalkonium chloride (a mixture of alkyldimethylbenzylammonium chlorides of general formula $C_6H_5CH_2N(CH_3)_2RCl$ where $R = C_8H_{17}$—$C_{18}H_{37}$; Ph. HgVI) [10] served as the quaternary ammonium compound. Of the possible cobalt(II) complexes, the thiocyanate complex was chosen, because its stability, reflected by the stepwise formation constant [11], is sufficiently high to ensure the formation of the tetrathiocyanato complex which serves as parent substance for the electrode, in 3.0 M potassiur thiocyanate solutions. The low protonation constant of the thiocyanate ion [12] ensures a favourable pH dependence for the electrode.

The electroactive material was prepared as follows. Aqueous phase (150 ml) containing 0.1 M $CoCl_2$ and 2.7 M KSCN was shaken with 30 ml of benzene containing 0.05 M benzalkonium chloride. After the mixture had been shaker for about 15 min, a dark blue oily layer appeared between the aqueous and organic phases. This oil was separated, washed twice with benzene and placed on a water bath to ensure complete evaporation of the benzene. The viscous dark blue oily material obtained was the ion-pair compound, (benzalkonium)$_2$ $Co(SCN)_4$.

Preparation and calibration of the electrode

Among the substances which may be considered [13] for the electrode matrix, polyvinyl chloride was selected because of its well-defined structure and simplicity in preparation. The oil obtained by the extraction procedure was mixed with a 10% (w/v) PVC solution in tetrahydrofuran (THF), so that the ratio of oil to PVC was 7:2. Before use, THF was distilled from sodium borohydride to remove its peroxide and water impurities. A platinum wire (about 1.5 cm long and 2 mm diameter) sealed into the end of a glass tube was immersed in this mixture, and then dried in air for 12 h. After drying, th electrode was dipped in a solution containing 0.1 M $CoCl_2$ and 2.7 M KSCN for 3 h, and then in a solution containing 0.3 M NaCl and 2.7 M KSCN for 20 min. The electrode was then suitable for measuring cobalt(II). A mercury drop placed into the glass tube served as electrical contact.

The response of the electrode to cobalt(II) was determined in the concentration range 10^{-1}—10^{-5} M in solutions containing 3.0, 2.0, and 1.0 M KSCN. Special care was taken to ensure that the concentration of thiocyanate ions in each of the three series was exactly the same. Some typical calibration curves are shown in Fig. 1.

All of the results reported were obtained with coated wire electrodes. A membrane prepared as described could, however, be fixed to a PVC tube containing 0.1 M $CoCl_2$ with a silver—silver chloride electrode as internal reference. The results for calibration of this type of electrode were very similar to those reported, with an identical slope of 29.3 mV/pCo, but different E_0.

RESULTS AND DISCUSSION

Characteristics of the electrode

The electrode gives a fully linear response in the cobalt concentration range 10^{-1}—10^{-4} M in solutions of 3.0 M KSCN (Fig. 1). The slope of the curves approaches the value calculated from the Nernst equation (see Table 1). Decrease in the thiocyanate concentration results in decrease of the linear range of the curve. It must be noted that to produce an appropriate reversible electrode function in the broadest possible concentration range, the thiocyanate concentration must be high enough to ensure that tetrathiocyanatocobaltate(II), i.e. the potential-determining ion, is the predominant cobalt(II) species in the system.

Table 1 shows the temperature-dependence of the slope of the calibration curves compared with the theoretical values calculated from the Nernst equation. For the determination of the experimental slopes, the linear section of the calibration curves was fitted with a least-squares fitting computer program to the experimental points; the correlation coefficients of this fit are

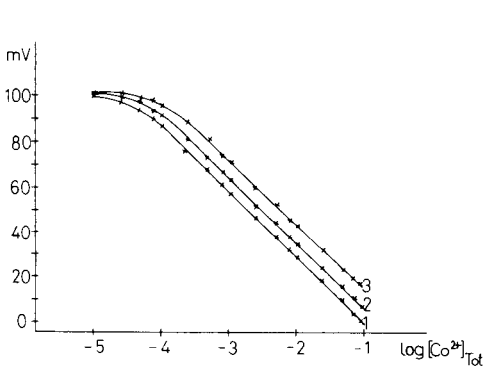

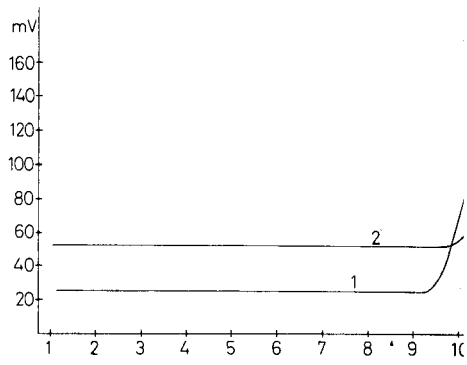

Fig. 1. Calibration curves in solutions containing different amounts of thiocyanate: (1) 3.0 M; (2) 2.0 M; (3) 1.0 M.

Fig. 2. The pH dependence of the electrode at cobalt concentrations of (1) 10^{-2} M; (2) 10^{-3} M.

TABLE 1

Calculated and measured slopes of the calibration curve obtained in 3.0 M KSCN at different temperatures

Temperature (°C)	Slope (mV)		R^a
	Calculated	Measured	
5	27.57	28.50	0.9999
10	28.07	28.62	0.9998
20	29.06	29.46	0.9999
25	29.55	29.30	0.9999
30	30.05	29.17	0.9999
40	31.04	30.68	0.9999
50	32.03	31.94	0.9999

[a]Correlation coefficient $R = m\sigma_x/\sigma_y$ where m is the slope.

also given in Table 1. The slight differences between calculated and measured values are caused by the effect of temperature on the dissociation equilibria of the complexes, i.e. on the $Co(SCN)_4^{2-}$ concentration. Precise measurements should therefore be performed in thermostated systems. If temperature differences occur during measurements, the errors caused must be considered. For example, the experimental errors arising from a change of 1°C in temperature are ±3.2%, ±2.6%, ±1.9% and ±1.2% for 10^{-1}, 10^{-2}, 10^{-3}, and 10^{-4} M solutions, respectively.

The curves in Fig. 2 show the pH-dependence of the electrode response; clearly, the electrode function is pH-independent from pH 1 up to about pH 9—10. At higher pH values, hydrolysis of the cobalt(II) complex starts.

The response time of the electrode is short; constant potentials are achieved within about 15 s and efficient stirring reduces the time further.

The electrode can be stored in air. Prior to measurements, dipping in the two solutions described above is then necessary. The absolute value of the electrode potential may decrease during storage of the electrode, but its concentration dependence remains unchanged for several months. The reproducibility of the potential measurements was found to be ±0.1 mV. This means, for example, a difference of ±0.78% in the case of 10^{-3} M cobalt(II) concentration.

Titration curves of cobalt(II) with EDTA obtained with the new electrode as indicating electrode are shown in Fig. 3. It can be seen that the electrode gives a sharp potential jump even in 5×10^{-3} M cobalt(II) solutions. These test solutions were buffered at pH 5—6 with hexamethylenetetramine and contained 3 M KSCN. Figure 4 shows the experimental points for the EDTA titration of a 5×10^{-2} M cobalt(II) solution compared with the calculated titration curve. The good fit obtained clearly indicates that the new electrode besides its applicability in analyses for cobalt — is also suitable for studies of coordination chemical equilibria in cobalt complex systems.

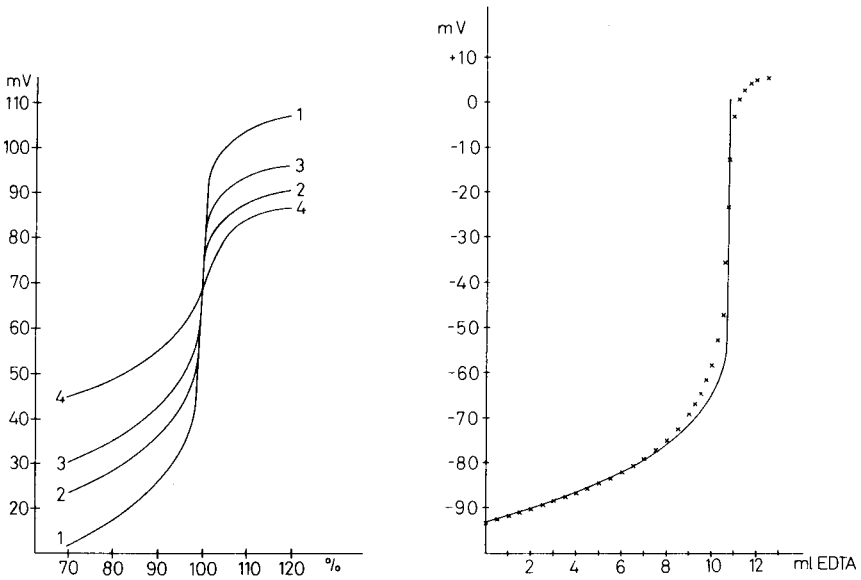

Fig. 3. Titration curves of cobalt(II) with 0.1 M EDTA in solutions of different cobalt concentration: (1) 10^{-1} M; (2) 10^{-2} M; (3) 5×10^{-3} M; (4) 10^{-3} M.

Fig. 4. Experimental and calculated titration curves for 5×10^{-2} M cobalt(II) with 5×10^{-2} M EDTA. Crosses indicate the experimental points; the full line is the calculated curve.

Effect of interfering ions

It could be predicted that cations which do not form very stable complexes or precipitates with thiocyanate, and anions which do not produce complexes or precipitates with cobalt(II), would not interfere in the measurements. On this basis, the effects of nine cations and five anions on the selectivity of the electrode was examined. The method suggested by I.U.P.A.C. [14] was used: the calibration curves shown in Fig. 5 were constructed from measurements of the potential in series of solutions containing a constant concentration of the interfering ion and increasing concentrations of cobalt(II). The following empirically modified Nikolsky equation [15] served as the basis for calculation of the selectivity coefficients (K) from these curves: $E = E_0 + 0.029 \log ([\mathrm{Co}] + K [\mathrm{I}])$ where [Co] and [I] indicate the concentration of cobalt and the interfering ion, respectively, in the solution of constant ionic strength. The value of K was calculated by dividing the cobalt concentration at the intersection of the two linear parts of the calibration curve by the concentration of the interfering ion in the solution. The results are shown in Table 2; the Table does not contain cations which form precipitates with thiocyanate or anions which precipitate cobalt(II), where prior treatment would obviously be required.

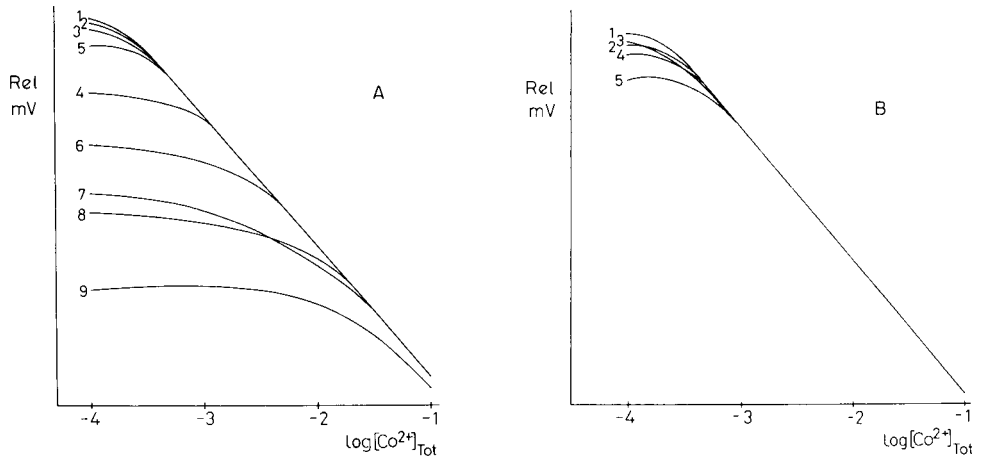

Fig. 5. Calibration curves for the determination of the selectivity coefficients. (A) Cations: (1) 10^{-1} M Ba^{2+}; (2) 10^{-1} M Mg^{2+}; (3) 10^{-1} M Ni^{2+}; (4) 10^{-1} M Ca^{2+}; (5) 10^{-1} M Fe^{2+}; (6) 10^{-2} M Mn^{2+}; (7) 10^{-2} M Cr^{3+}; (8) 10^{-2} M Fe^{3+}; (9) 10^{-2} M Zn^{2+}. (B) Anions: (1) 10^{-1} M NO_3^-; (2) 10^{-1} M HCO_3^-; (3) 10^{-1} M Br^-; (4) 10^{-1} M SO_4^{2-}; (5) 10^{-1} M I^-.

TABLE 2

Selectivity coefficients, K, for different ions

Interfering cation	K	Interfering anion	K
Ba^{2+} [a]	1.1×10^{-3}	NO_3^- [a]	1.1×10^{-3}
Mg^{2+} [a]	1.6×10^{-3}	HCO_3^- [a]	1.4×10^{-3}
Ni^{2+} [a]	1.9×10^{-3}	Br^- [a]	1.8×10^{-3}
Ca^{2+} [a]	6.6×10^{-3}	SO_4^{2-} [a]	1.8×10^{-3}
Fe^{2+} [a]	1.1×10^{-2}	I^- [a]	2.4×10^{-3}
Mn^{2+} [b]	1.2×10^{-2}		
Cr^{3+} [b]	9.77×10^{-1}		
Fe^{3+} [b]	1.51		
Zn^{2+} [b]	14.79		

[a]Measured in 10^{-1} M solutions of the interfering ion.
[b]Measured in 10^{-2} M solutions of the interfering ion.

Conclusions

The new electrode proved to be suitable for end-point indication in cobalt(II) titrations with EDTA, as well as for the direct potentiometric determination of cobalt(II) even in the presence of a number of heavy and transition metals and also some anions.

Considering the great significance of cobalt(II) complexes in biological and coordination chemistry, one of the most important domains of practical application of this electrode should be in the examination of cobalt(II) complex equilibria. Results achieved so far in this field will be published elsewhere [16].

REFERENCES

1 R. W. Cattrall and Chin-Poh Pui, Anal. Chem., 48 (1976) 552.
2 R. W. Cattrall and Chin-Poh Pui, Anal. Chim. Acta, 83 (1976) 355.
3 R. W. Cattrall and Chin-Poh Pui, Anal. Chim. Acta, 87 (1976) 419.
4 R. W. Cattrall and Chin-Poh Pui, Anal. Chem., 47 (1975) 93.
5 R. W. Cattrall and Chin-Poh Pui, Anal. Chim. Acta, 78 (1975) 463.
6 E. B. Buchanan, Jr., and J. L. Seago, Anal. Chem., 40 (1968) 517.
7 H. Hirata and K. Higashiyama, Talanta 19 (1972) 391.
8 D. E. Ryan, and M. T. Cheung, Anal. Chim. Acta, 82 (1976) 409.
9 Orion: Analytical Methods Guide No. 5 (1972).
10 Pharmacopoeia Hungarica VI, Medicina, Budapest, 1967. p. 504.
11 Stability Constants of Metal Complexes, Spec. Publ. No. 17, The Chemical Society, London, 1964.
12 Stability Constants of Metal Complexes, Suppl. No. 1, Spec. Publ. No. 25, The Chemical Society, London, 1971.
13 R. W. Cattrall and H. Freiser, Anal. Chem., 43 (1971) 1905.
14 K. Cammann, Das Arbeiten mit ionselektiven Elektroden, 2 Aufl. Springer-Verlag, Berlin, 1977, p. 163.
15 B. P. Nikolsky, M. M. Schulz and A. A. Belyustin, in G. Eiseman (Ed.), Glass Electrodes for Hydrogen and other Cations, M. Dekker, New York, 1967.
16 K. Burger and G. Pethö, Inorg. Chim. Acta, (in preparation).

Analytica Chimica Acta, 107 (1979) 121—128

BEHAVIOUR OF IODIDE-SELECTIVE ELECTRODES AT LOW CONCENTRATIONS OF IODIDE

ADAM HULANICKI*, ANDRZEJ LEWENSTAM and MAGDALENA MAJ-ŻURAWSKA
Institute of Fundamental Problems in Chemistry, University of Warsaw, Warsaw (Poland)
(Received 3rd October 1978)

SUMMARY

The influence of adsorption of iodide ions and redox processes on the response mechanism of solid-state iodide-selectives electrode is discussed. Such effects can cause non-Nernstian calibration curves for iodide concentrations below 10^{-5} M. A semi-empirical equation is given which explains the electrode response under the conditions normally applied.

The solid-state iodide-selective electrode is based on a polycrystalline membrane containing silver iodide, usually mixed with silver sulphide in various proportions. The potential response of such electrodes, in the absence of interfering ions, was described by Buck [1] by the equation

$$E = E^0_{AgI/Ag} - RT/F \ln 0.5 \{[I]_A + ([I]^2_A + 4K_{so})^{\frac{1}{2}}\} \quad (1)$$

where K_{so} represents the solubility product of silver iodide, $E^0_{AgI/Ag} = E^0_{Ag^+/Ag} + (RT/F) \ln K_{so}$, and $[I]_A$ is the analytical concentration of iodide ions in solution. In the concentration range where the membrane solubility can be neglected, i.e. $[I]_A \geqslant 10^{-7}$ M, the potential response should vary linearly with iodide activity, the slope being close to that theoretically expected, i.e 58—60 mV per decade. For lower concentrations, the E vs. $[I]_A$ plot bends because of the significant contribution of the iodide ions arising from the solubility of silver iodide, and finally becomes parallel to the concentration axis at a potential which should correspond to $(K_{so})^{\frac{1}{2}}$ at a given ionic strength and temperature.

This relatively simple picture is, however, not valid in most experiments [2—4], and below $[I]_A = 10^{-5}$ M the calibration curve is rarely linear. The observed deviations may be negative or positive, depending on whether the observed potential is more negative or positive than that predicted by eqn. (1). Positive deviations correspond to a decrease of the iodide concentration and have been explained by the oxidation of iodide by dissolved oxygen [2], by the influence of interstitial silver ions [4], and by leakage of soluble silver salts from the membrane [5]. Oxidation reactions can be eliminated by flushing the sample solution with an inert gas or by addition of ascorbic acid

as a reducing agent [2]. The two remaining processes should be affected by various modes of electrode storage and conditioning. For negative deviations, which correspond to an increase in the surface concentration of iodide, no satisfactory explanation has been given although such phenomena have been observed [2, 3] and it has been noted that when the electrode is calibrated by the spiking technique it is less susceptible to negative deviations than in the serial dilution method [2]. Vesely [6] mentioned that the existence of positive or negative deviations may be connected with the presence of β-AgI or γ-AgI which may exhibit different solubilities and adsorptive properties. These phenomena have also been discussed by Pungor [7]. To eliminate adsorption phenomena, Vesely polished the electrode surface before each measurement. Vesely also indicated that the presence of Ag_3SI may be responsible for changes in the membrane properties.

Recently, van de Leest and Geven [8] showed that non-Nernstian behaviour of this type is connected with adsorption of ions at the electrode.

This paper describes an attempt to give a comprehensive explanation of the mechanisms which influence the electrode response in the low concentration ranges, including adsorption and redox processes at the electrode surface.

EXPERIMENTAL

Apparatus and reagents

Iodide-selective electrodes were made from membranes pressed at 14 ton cm and mounted in an epoxy resin body. The internal surface of the membrane was covered with a silver layer to provide electric contact, and the outer surface was polished with abrasive papers (nos. 600 and 800) until a shiny surface was obtained. The composition of the membranes containing AgI and Ag_2S is shown in Table 1. The salts were precipitated simultaneously from appropriate amounts of 0.6 M solutions of silver nitrate, 0.2 M potassium iodide and sodium sulphide with an excess of either iodide or silver ions. All the steps of membrane preparation were carried out in the dark to preclude decomposition of silver iodide by light.

Iodide-selective electrodes manufactured by Radelkis (OP-I-7111-C) and Radiometer (F-10321) were used for comparison.

TABLE 1

Composition of membranes

Membrane no.	Mole fraction of AgI	Excess of ion during precipitation	Membrane no.	Mole fraction of AgI	Excess of ion during precipitation
1	1.00	3% Ag^+	5	0.80	3% I^-
2	0.95	6% Ag^+	6	0.75	3% Ag^+
3	0.90	6% Ag^+	7	0.67	3% I^-
4	0.80	3% Ag^+	8	0.50	10% Ag^+

A pH-meter (PHM-64), autoburette (ABU-13) and recorder (REC 61; Radiometer) were used in all measurements. The reference electrode was a silver chloride electrode with a salt bridge (Orion 90-02) but all the potential values shown were recalculated versus the saturated calomel electrode.

The stock solution of iodide (1 M KI) was kept in a dark bottle and diluted before measurements with twice-distilled water.

All reagents were of analytical grade.

All solutions in which the electrodes were tested were 0.1 M in sodium nitrate. Unless otherside mentioned, the solutions contained 4 g of ascorbic acid per 100 cm^3 [5] to prevent oxidation of iodide and to keep the redox potential constant. Solutions containing 10^{-8}—10^{-4} M iodide were prepared by suitable additions of 10^{-4}—10^{-2} M KI solutions. Experiments in higher concentration ranges were carried out in separately prepared solutions containing $NaNO_3$, ascorbic acid and 10^{-3}—10^{-1} M KI. All measurements were done in a thermostated vessel at 20 ± 0.5°C, unless otherwise stated.

RESULTS AND DISCUSSION

The slopes of the E vs. $[I]_A$ plots for all the electrodes tested were 58—60 mV/pI in the linear part. The upper limit of the linear range was 0.1 M; the value of $E^0_{AgI/Ag}$ was about —380 mV vs. SCE, which is in good agreement with the standard potential of the corresponding second-order electrode.

Calibration curves for the lower concentration range (Fig. 1) were linear down to 10^{-5} M iodide, in the case of electrodes for which the membrane material had been precipitated in the presence of excess of iodide. Such electrodes usually showed positive deviations (curve A). Other electrodes tested had linear ranges extending to 2×10^{-7} M KI, but the potential readings at this extreme dilution were not stable with time. The positive deviations observed initially became negative after more than 15 min. Transiently, good linearity was obtained and eqn. (1) seemed to be obeyed. Such a potential drift corresponds to an increase in the iodide concentration at the electrode surface, which can be explained by adsorption of iodide ions at the electrode surface, as confirmed by other experiments.

When the electrode was immersed in 100 cm^3 of a solution containing 0.1 M $NaNO_3$ and 4% ascorbic acid, to which iodide soluton was then added, the first response was observed for a bulk concentration of 6×10^{-8} M KI. Further stepwise increases of concentration up to 4×10^{-6} M iodide caused large potential drifts before stable readings were attained. A more detailed study of this process (Fig. 2) showed that in 10^{-7} M KI a well stabilized potential was attained after 40 min. When the electrode was transferred to another solution of the same composition without rinsing, the same stable potential reading was readily reproduced without initial potential drift. Such experiments were carried out several times, and it was found that the reproducibility of the potentials increased for longer "saturation" times and for larger concentrations (Table 2).

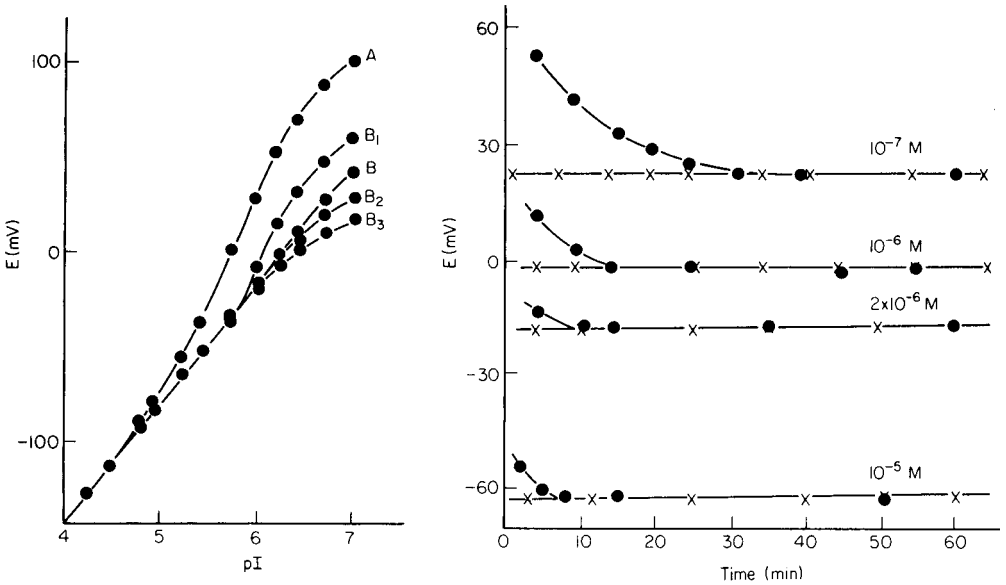

Fig. 1. Calibration curves in 0.1 M $NaNO_3$—1% ascorbic acid. (A) Electrodes 5 and 7; (B) other electrodes (including Radelkis OP-I-7111C); (B_1) potential readings after 5 min; (A and B) after 10 min; (B_2) after 20 min; (B_3) after 60 min. pI corresponds to the analytical concentration of iodide.

Fig. 2. Potential changes in potassium iodide solutions of different concentrations as a function of time. Points (•) correspond to measurements when the electrode (no. 8) was placed in the solution for the first time; points (×) indicate readings when the electrode was transferred to another solution of the same concentration.

TABLE 2

Reproducibility of potential readings after transference of the electrode to a new solution

[I] (M)	Time of measurement (min)	Potential reproducibility (mV)		
		Electrode 1	Electrode 8	Radelkis electrode
1×10^{-7}	15	±4	±5	±4
1×10^{-7}	60	±1	±1	±1
1×10^{-6}	60	±1	±1	±1
2×10^{-6}	10	±0.5	±0.5	±0.5
1×10^{-5}	5	±0.5	±0.5	±0.5

To confirm the adsorption mechanism of these processes, the temperature relationships were investigated. Calibration curves were obtained over the whole concentration range at 0°, 5°, 20° and 25°C with a waiting time of 1 h to ensure steady readings, and the linear range was extrapolated to 10^{-7} M

iodide. From the actual potential measurements for 10^{-7} M iodide, the iodide concentrations were read from the extrapolated plots for the different temperatures. The results (Table 3) indicate that the lower the temperature, the larger is the positive error of determination. However, such changes are not regular, and are different for different electrodes. This may explain why in some studies such processes were not noted as interfering [2]; with some electrodes, the errors are scarcely significant at the higher temperatures.

In the range 10^{-7}—10^{-8} M, the effect of the iodide concentration added was studied in detail at 20°C, at which all the electrodes exhibited some adsorption effects. The electrode was initially equilibrated in 10^{-8}—10^{-7} M KI solutions. Immediately afterwards, the calibration curves were checked for the concentration range 10^{-4}—10^{-6} M and extrapolated to 10^{-8} M iodide. From this graph, the concentrations were read from the potentials measured previously, and compared with the known concentrations of the diluted solutions. The difference between these values corresponds to the excess of iodide at the electrode surface (ΔC) over the analytical concentration in the bulk solution and is due to the contribution of the membrane solubility and of the adsorbed species. When the adsorption term (AT) given by $\Delta C - K_{so}/[I]_T$, where $[I]_T$ is the total iodide concentration read from the extrapolated linear calibration graph, was plotted against the analytical concentration in the solution, a typical adsorption isotherm was obtained (Fig. 3). The saturation level corresponds to about 1.5×10^{-7} M at 20°C.

Those experiments seem to indicate that adsorption phenomena play a significant role in the behaviour of the electrode at low concentrations. Nevertheless, it must be kept in mind that the state of the electrode surface is important. Freshly polished smooth membranes are less liable to adsorption so that the adsorption term becomes smaller. Adsorption is most significantly reduced by dispersing the active substance in a plastic material; therefore, with the Radiometer electrode negative deviations were never observed. Comparison of the results obtained for an electrode made of pure silver iodide (no. 1) with those for one containing 50% silver sulphide (no. 8) shows that increase in the mole fraction of silver iodide gives larger adsorption effects (Table 3). When experiments similar to those indicated in Fig. 3 were done with electrode no. 8, no deviations were observed at 25°C.

TABLE 3

Iodide concentrations read from extrapolated linear calibration curve for 10^{-7} M KI at different temperatures

Temperature (°C)	Iodide concentration ($\times 10^{-7}$ M)		
	Electrode 1	Electrode 8	Radelkis electrode
25	2.5	1.0	1.5
20	3.0	4.0	2.5
5	6.0	4.5	5.5
0	12.0	6.0	6.0

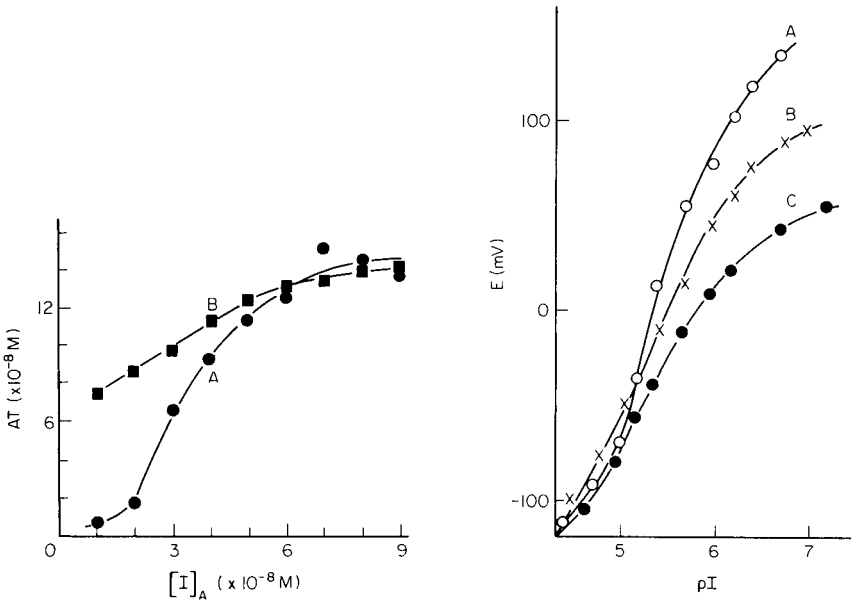

Fig. 3. The excess of iodide concentration as indicated by the electrode (AT, see text) as a function of iodide concentration added: (A) electrode 1; (B) Radelkis electrode.

Fig. 4. The effect of ascorbic acid on the calibration curve: (A) 0.1%; (B) 1.0%; (C) 4% ascorbic acid. Electrode 5.

The positive deviations from linearity of the potential response, i.e., the potential values which are more positive than those which correspond to the solubility model, are obviously due to an excess of silver ions at the electrode surface. This may be related to the influence of the silver(I) concentration arising from crystal defects or to oxidation of iodide which leaves more than equivalent concentrations of silver ions in the vicinity of the sensing surface. Therefore, for electrodes showing such behaviour, measurements were done with varying amounts of ascorbic acid which decreases the redox potential of the solution. A change from 0.1% to 4% of ascorbic acid decreased the positive deviations (Fig. 4), because of the process $Ag^+ + e = Ag$.

It may seem strange that positive deviations, connected with an excess of silver ions at the electrode surface, should be observed for electrode membranes obtained by precipitation with an excess of iodide. This however can be explained by the fact that the precipitates formed under such conditions are of different physical form and need much longer washing to remove adsorbed ions. Because washing is carried out with air-saturated water, oxidation of iodide is favoured, leaving an excess of silver ions. This is in agreement with the general tendency that more oxidizing conditions promote positive deviations, whereas reducing conditions give negative deviations. The long-term reversibility of these processes can be clearly seen when the electro potential is recorded in an air-saturated solution, then after the addition of

ascorbic acid, and again in the absence of a reducing agent (Fig. 5). Because of the slowness of such changes in rapid measurements, accidental readings may be observed and the nature of the deviations becomes obscure. This complex behaviour depends on the preparation of the electrode and its conditioning, on the temperature and on the composition of the solution; these effects can produce a series of differently shaped curves (Fig. 6). The shorter range of linearity obtained in calibration by the serial dilution method can obviously be explained by the fact that the transferred electrode has already a complete layer of adsorbed iodide ions.

Generalized treatment of electrode response

The formal description of the behaviour of iodide-selective electrode is based on the assumption that the potential of the electrode depends on the total iodide concentration, $[I]_T$, in the solution in the vicinity of the sensing membrane. This total concentration results from various contributions: the analytical concentration, $[I]_A$; the solubility of the membrane, $[I]_s$; exchange processes with interfering ions, $[I]_E$; reduction reactions which liberate iodide, β; and adsorption of iodide at the electrode surface, γ. Adsorption depends on the analytical iodide concentration and for $[I]_A = 0$, $\gamma = 0$. To take into

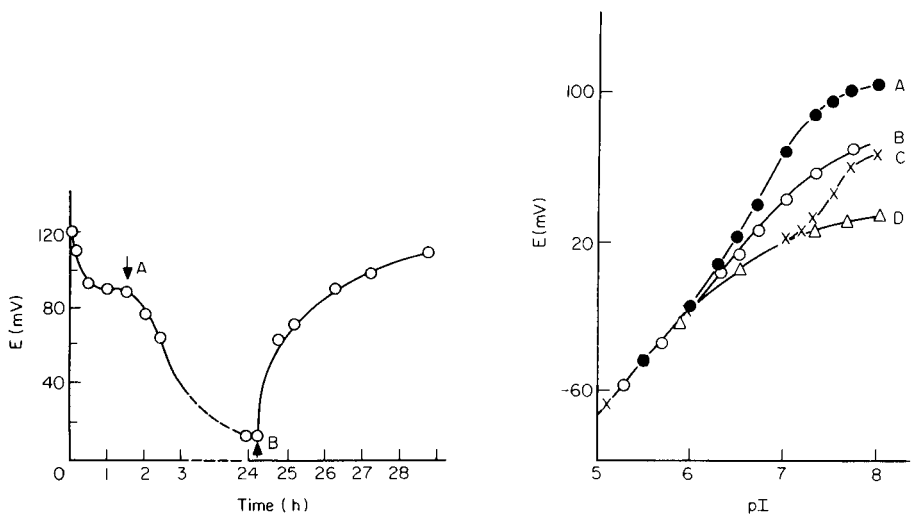

Fig. 5. Potential changes of electrode 1 in presence of ascorbic acid. Initial solution 0.1 M $NaNO_3$; point A marks the addition of ascorbic acid to give a concentration of 4%; point B indicates the transference of the electrode to 0.1 M $NaNO_3$.

Fig. 6. Calibration curves at low concentrations for electrode 1. The points correspond to experimental values recorded in 0.1 M $NaNO_3$ media. (A) Potential reading after 30 min at 25°C; (B) after 15 min with 4% ascorbic acid added at 20°C; (C) after 30 min with 4% ascorbic acid added at 20°C; (D) after 24 h with 4% ascorbic acid. The lines shown are calculated for the following parameters: $K_{so} = 9 \times 10^{-16}$; (A) $\beta - \alpha = -8 \times 10^{-8}$, $\gamma = 0$; (B) $\beta - \alpha = 0$, $\gamma = 0$; (C) $\beta - \alpha = 0$, $\gamma > 0$, read from Fig. 3; (D) $\beta - \alpha = 0$, $\gamma = 1.5 \times 10^{-7}$.

account all those effects

$$[I]_T = [I]_A + [I]_s + [I]_E + \beta + \gamma \quad (2)$$

The electrode response is connected with the equilibrium between silver and iodide ions at the electrode surface, which can be expressed by the solubility product $K_{so} = [Ag]_T [I]_T$. The total concentration of silver ions, $[Ag]_T$, in the vicinity of the membrane may be considered as the sum of the solubility of the membrane material, $[Ag]_s$, and the contribution α arising from leaching of soluble silver salts from the membrane and oxidation reactions of the iodide dissolved from the membrane. This may also be interpreted as the influence of interstitial silver ions: $[Ag]_T = [Ag]_s + \alpha$. If it is assumed that, at the membrane surface, $[Ag]_s = [I]_s$, that the amount of iodide added gives the same iodide concentration at the electrode surface as in the bulk solution, and that $[I]_E = 0$ in the absence of interfering ions, then the following semi-empirical equation can be derived for the potential of the iodide-selective electrode.

$$E = E^0_{AgI/Ag} - (RT/F) \ln 0.5 \{([I]_A + \beta - \alpha + \gamma) + [([I]_A + \beta - \alpha + \gamma)^2 + 4 K_{so}]^{\frac{1}{2}}\} \quad (3)$$

The value $\beta - \alpha$ can be obtained from a graph such as that presented in Fig. 3 in the absence of added iodide.

When $\beta - \alpha + \gamma = 0$, eqn. (3) reduces to eqn. (1). This occurs not only for the simplified approximate situation in the absence of the additional effects usually observed in practical measurements, but also when such effects compensate each other, which can happen for strictly defined conditions depending on the electrode membrane, solution, temperature and time of measurement.

For better confirmation of the validity of this formal description of the electrode response, theoretical calibration curves were calculated, assuming $K_{so}(AgI) = 9 \times 10^{-16}$. This value is close to that mentioned by Kontoyannakos et al. [2], but it may differ for various electrodes because of the different forms of AgI present in the membrane, quite apart from the possible presence of Ag_3SI. The values $\beta - \alpha + \gamma$ were chosen in such a manner as to obtain curves which correspond as closely as possible to experimental points. The experimental points and the calculated curves shown in Fig. 6 support the view that the suggested phenomena allow a reasonable explanation of at least most of the irregularities observed on calibration curves for the iodide-selective electrodes at low iodide concentrations.

REFERENCES

1 R. P. Buck, Anal. Chem., 40 (1968) 1432.
2 J. Kontoyannakos, G. J. Moody and J. D. R. Thomas, Anal. Chim. Acta, 85 (1976) 47.
3 I. Sekerka and J. F. Lechner, Anal. Chim. Acta, 93 (1977) 139.
4 W. E. Morf, G. Kahr and W. Simon, Anal. Chem., 46 (1974) 1538.
5 R. P. Buck, Anal. Chem., 48 (1976) 23R.
6 J. Vesely, Collect. Czech. Chem. Commun., 39 (1974) 710.
7 E. Pungor, Ion-selective Electrodes, Akademiai Kiado, Budapest, 1978, p. 161.
8 R. E. van de Leest and A. Geven, J. Electroanal. Chem., 90 (1978) 97.

Analytica Chimica Acta, 107 (1979) 129—138

EVALUATION AND APPLICATION OF INTERNAL STANDARDIZATION IN ATOMIC ABSORPTION SPECTROMETRY WITH ELECTROTHERMAL ATOMIZATION

TAKEO TAKADA* and KUNIO NAKANO

Department of Chemistry, College of Science, Rikkyo (St. Paul's) University, Nishi-Ikebukuro, Toshima-ku, Tokyo 171 (Japan)

(Received 19th September 1978)

SUMMARY

A new dual-channel system developed for use in atomic absorption spectrometry is used to assess the internal standard technique for electrothermal atomization. Cobalt was found to be a suitable internal standard for iron determinations, and is used for determination of 7—330 ng Fe ml^{-1} in water samples. With use of the internal standard technique, fluctuations caused by atomizer variables are reduced and interferences from many cations are also decreased.

Compared with conventional flame methods, electrothermal atomization makes the determination of trace metals more rapid and much more sensitive. However, the absorbance from electrothermal atomizers is variable, because of factors such as atomizer temperature, heating rate, sample amount, etc. This is considered to be the cause of the decreased accuracy and precision of the analytical results obtained when such atomizers are used.

In order to minimize the variations in signals arising from atomizer conditions, a definite amount of an element can be added to each sample as an internal standard. As the absorbances of the analyte and standard elements are considered to be similarly influenced by the various factors, the ratio of the absorbances may be free from the influence of variable conditions. The use of an internal standard to increase the precision of emission spectroscopic methods was introduced by Gerlach and Schweitzer [1]. The application of an internal standard to atomic absorption spectrometry has been difficult because the instruments are monochromatic, and few examples are known [2—4]. Rules for selecting internal standard elements have not yet been completely discussed, nor has any practical application to electrothermal atomic absorption been published.

In the present paper the utilization of an internal standard method is described, whereby most of the errors associated with the atomizer and atomization process are compensated. Samples of water were selected for investigation because total iron in water can be measured rapidly by elec-

trothermal atomic absorption spectrometry. The optimum conditions for the analysis, including the choice of the proper internal standard, are described.

EXPERIMENTAL

Apparatus

A dual-channel atomic absorption spectrometer was designed in this laboratory and assembled by Nippon Jarrell-Ash Co. The burner assembly was replaced by a carbon-tube atomizer (Varian-Techtron model 63). The instrument has two separate channels, one of which is used for the analyte element and the other for the element added; the ratio of the absorbances at the two wavelengths is measured.

A block diagram of photometric system is shown in Fig. 1. Two hollow-cathode lamps are placed at right angles to each other, one for the analyte element, one for the standard element. The hollow-cathode lamps are alternately pulsed by a square-wave current. The light from the hollow-cathode lamps is combined by a half-mirror and after, passing through the small carbon tube, it is split again into two beams by a second half-mirror. Each beam falls in the slit of a monochromator and each is detected with a photo-detector. The sample and internal standard signals are amplified synchronously with each lamp current by each lock-in amplifier. The intensities are converted into absorbances by two operational amplifiers. The sum, difference and ratio of the two absorbance signals are computed by analog computer. Each absorbance signal and the ratio of the signals are recorded on a three-pen recorder (Model B 361, Rika Denki Co.). Absorbances were obtained by measurement of peak heights.

The atomizer consists of a pair of carbon rods which hold a carbon tube,

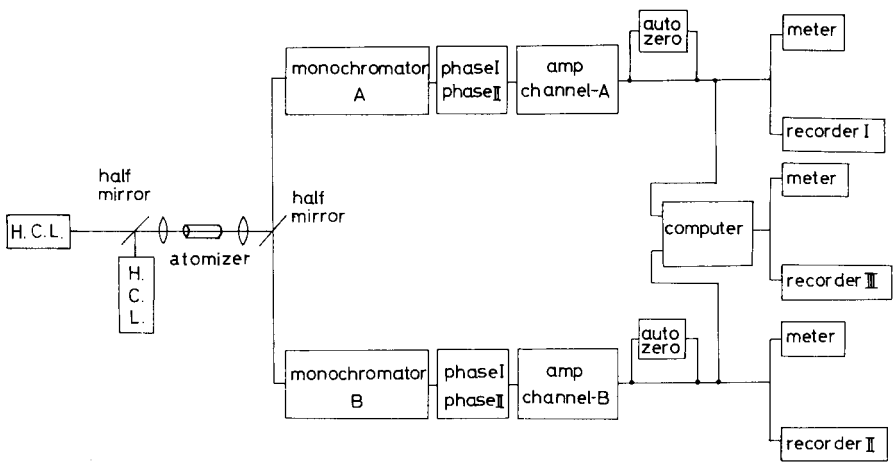

Fig. 1. Block diagram of dual wavelength system. H.C.L. = hollow-cathode lamp; AMP = amplifier.

and a power supply unit. The carbon rod holder is cooled by water. Nitrogen gas (4.0 l min^{-1}) was employed for sheathing. The power unit provides the necessary current for the carbon tube in a preselected sequence of drying, ashing and atomizing. The atomizing cycle can be operated in two modes, a "step" mode when a constant selected voltage is applied for a preset period of time, or a "ramp" mode when the voltage is linearly increased to a chosen voltage at a preselected rate.

The temperature of the carbon tube was measured with a Chino IR-PH Radiamatic pyrometer, which has a temperature range of 1000—3500°C.

Reagents and procedure

Standard solutions. In all cases, stock solutions of copper, cobalt, and nickel were prepared from their analytical reagent-grade chlorides in doubly distilled, deionized water. The final stock solutions (100 $\mu g\ ml^{-1}$ of each element) were adjusted to 0.1 M in hydrochloric acid and various other concentrations were made by dilution with 0.1 M hydrochloric acid. A standard solution of iron (100 μg Fe ml^{-1}) was prepared by dissolving analytical-reagent grade ammonium iron(II) sulphate in doubly distilled water acidified to 0.1 M in hydrochloric acid. The working standard solutions were prepared daily.

Water sample preparation. Iron-free 6 M hydrochloric acid (10 ml) was added to 100 ml of sample solution, which was then evaporated to 20 ml. After cooling, the solution was transferred to a 50-ml volumetric flask and a known amount of an internal standard added.

Operation

The carbon tube was adjusted for maximum signal, taking care that the only radiation from both lamps reaching the detector was that passing through the carbon tube. Before use, the tube was purified by heating to a very high temperature. The sample was injected from a 5-μl pipette. The wavelengths and lamp currents used were: Fe, 248.3 nm, 16 mA; Co, 240.7 nm, 15 mA; Ni, 232.0 nm, 15 mA; Cu, 324.7 nm, 8 mA. The drying, ashing, atomization cycle was done automatically.

RESULTS AND DISCUSSION

The internal standard for a particular element must have the same relative properties with respect to the matrix and atomizer. These can be determined experimentally by making absorbance measurements on the elements as a function of the atomization conditions.

Drying and ashing conditions

Before use, the carbon tube was purified at a high temperature. The sample was then applied, dried, ashed and finally atomized. The optimum drying and ashing conditions were established as follows.

For each measurement, 5 μl of an 0.05 μg ml^{-1} iron solution was injected. No significant change in the intensity was oberved when the drying time was varied from 10 to 20 s at a drying voltage of 2.0 V with an atomizing temperature of 2630°C. Therefore, the voltage for the drying cycle was chosen as 2.0 V for 14 s so as to remove solvent by gentle boiling, thus preventing losses by sputtering. Ashing was accomplished in 5—10 s at a voltage of 2.0 V. Consequently, all of the following experiments were carried out with ashing at 2.0 V for 10 s.

Furnace temperature and atomization behavior of elements

To obtain the rate of atomization and thus the number of free atoms in an atomization cell, the behavior of various metals was studied with respect to their volatility. Figure 2 shows the change in temperature of carbon tube with step atomization voltage. The measurements pertain to the temperature of a spot on the outside of the carbon tube. Although the temperature difference between the outside and inside of the tube was not estimated, it can be considered that there is little difference of temperature because the tube has a small cross-section and high electric resistance at this position,

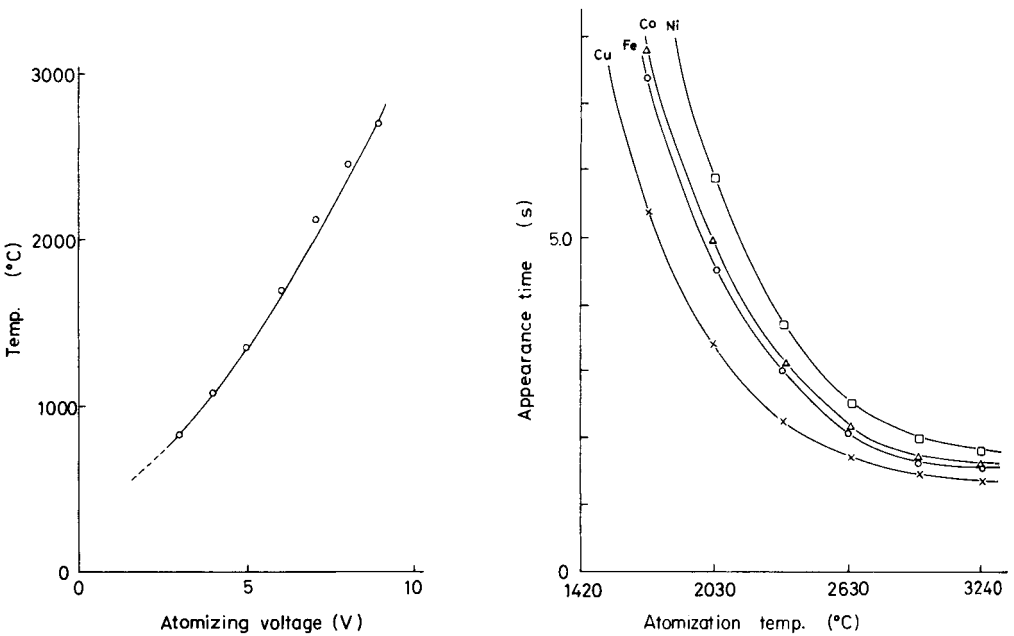

Fig. 2. Variation of carbon tube temperature with atomization voltage during preset time of 3 s. Drying, 2.0 V, 14 s; ashing, 2.0 V, 10 s.

Fig. 3. Variation of the appearance time of the absorption signal with carbon tube temperature. Drying and ashing as for Fig. 2; 5-μl sample; concentrations (μg ml^{-1}) Fe 0.02, Co 0.05, Ni 0.20, Cu 0.05.

and the temperature of the whole tube rises rapidly and homogeneously as power is supplied. The precision of the temperature values was ± 5%.

Figure 3 shows that the appearance time (i.e. the time between starting the atomization phase and the appearance of the absorption signal) of the absorption signal of various elements depends on the atomization temperature. The elements were atomized by employing identical heating procedures (step mode, 4~10 V; 10 s). It is clear from the results that increasing atomization temperatures are accompanied by marked decreases in the appearance time, though considerably less so in the higher temperature range. Iron and cobalt have almost identical thermal behavior, unlike the other elements investigated. Thus it should be possible to use cobalt as an internal standard for iron.

Choice of internal standard

Effect of atomization temperature. The effect of atomization temperature on the absorbance of cobalt, nickel and copper alone, and when used as internal standards for iron absorbance measurements, is illustrated in Fig. 4. When the atomization temperature was raised from about 1800 to 2900°C, a gradual increase in the peak absorbance of iron was shown in the absence of an internal standard. However, as demonstrated in Fig. 4, the absorbance of iron and cobalt varied similarly when the temperature was changed and the ratio of iron to cobalt absorbances remained almost constant from 2100 to 2900°C. In contrast, Fig. 4 shows that copper would be a poor internal standard for iron.

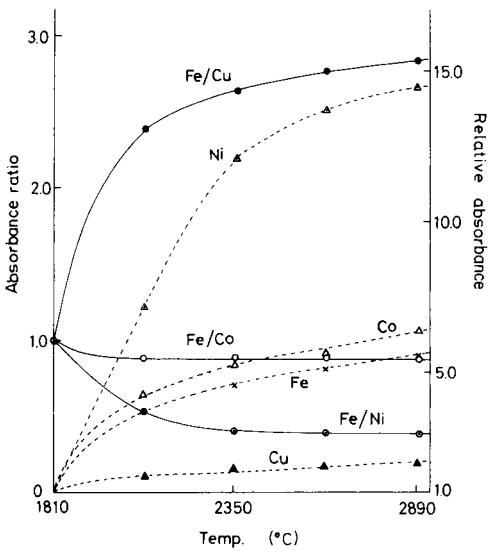

Fig. 4. Effect of the atomization temperature on absorbance and absorbance ratio. Drying and ashing as for Fig. 2; 3-s atomization. Concentrations ($\mu g\ ml^{-1}$): Fe 0.02, Co 0.05, Ni 0.20, Cu 0.05; 5-μl sample.

Effect of atomization time. In the step-mode operation, a constant selected voltage is applied for a preset time; when this time is changed from 1 to 10 s the furnace temperature increases rapidly. Therefore, the effect of atomization time on absorption intensity was studied. Figure 5 shows the change in absorbance of each element and absorbance ratio of iron to each element with a preset atomization time, holding all other conditions constant, and with an atomization voltage of 9 V. Atomization temperature increases with increasing atomization time, as would be expected, increasing by 900°C during the 9 s. As can be seen from Fig. 5, metal atom production is also affected by the atomization time used; atomization is achieved in 3—4 s, but the temperature of the furnace is increased until all the element to be measured is atomized. The recommended instrumental conditions are summarized in Table 1.

Effect of amount of sample. Aliquots of 5, 10, 15 and 20 μl of 0.02 μg Fe ml^{-1} standard solutions were used to examine the effect of amount of sample introduced into the carbon tube on the absorbance. The atomization temperature was 2630°C and the atomization time 3 s. Figure 6 shows that the absorbance of iron increases proportionally with the amount of sample introduced, but that the absorbance ratios remain relatively constant, again demonstrating the value of the internal standard method. The ratio of iron to cobalt absorbanced showed little change for 5—20 μl of sample.

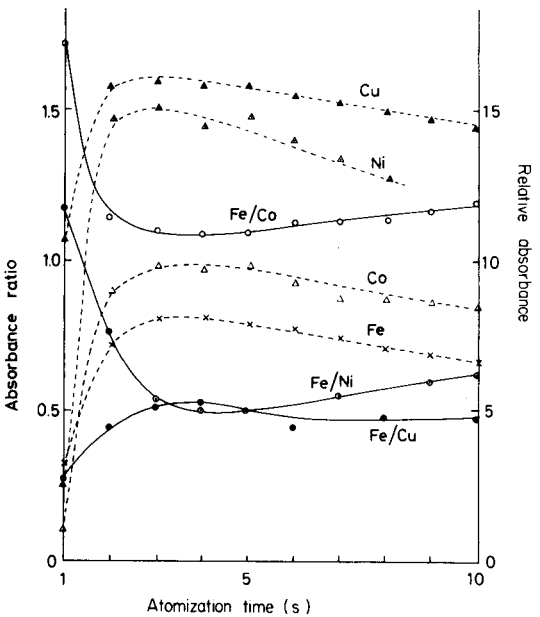

Fig. 5. Effect of the atomization time on absorbance and absorbance ratio. Concentrations (μg ml^{-1}): Fe 0.02, Co 0.05, Ni 0.20, Cu 0.05; 5-μl sample.

TABLE 1

Operating conditions for measurement of iron

Fe wavelength 248.3 nm, lamp current 18 mA (A channel)	
Co wavelength 240.7 nm, lamp current 16 mA (B channel)	
Drying	2.0 V for 14 s
Ashing	2.0 V for 10 s
Atomizing	9.0 V for 3 s
Nitrogen sheathing gas	4 l min^{-1}

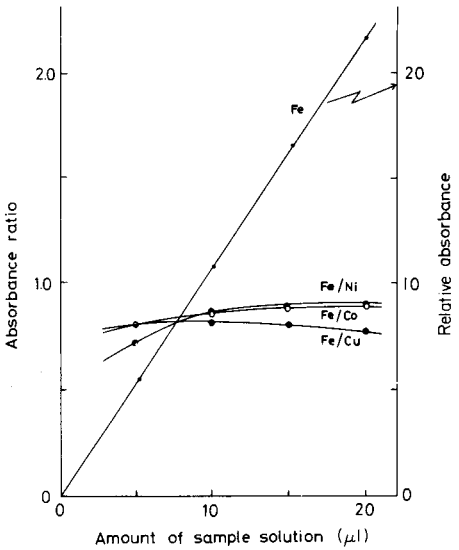

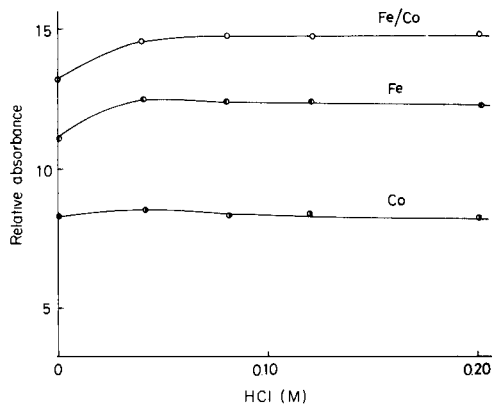

Fig. 6. Effect of the sample volume on absorbance and absorbance ratio. Conditions as Fig. 4.

Fig. 7. Effect of hydrochloric acid concentration on absorbance and absorbance ratio. Concentrations (μg ml^{-1}): Fe 0.04, Co 0.04; 5-μl sample.

Interference studies

Several possible interferences were examined. Chemical and physical interferences are assumed to occur, such as the influence of anions, cations, pH and refractory matrices, and the formation of stable oxides or other molecules.

Acid interferences. The absorbances of aqueous 0.04 μg Fe ml^{-1} and 0.04 μg Co ml^{-1} solutions containing various concentrations of hydrochloric acid were measured under the standard conditions in Table 1. As seen in Fig. 7, the absorbance of iron is slightly increased by addition of hydrochloric acid, but the absorbance change of cobalt is small. Thus the absorbance ratio increases at relatively low acidities, so that the internal

standard is without effect. It is thought that this results from the iron being hydrolysed at low acid concentrations. Consequently, hydrochloric acid should be used to keep the pH below 1, to suppress interference by hydrolysis.

Cation interferences. Interference by cations is common in electrothermal atomic absorption spectrometry. In this study, the effect of nine cations on the iron: cobalt absorbance ratio was measured. The solutions used contained Fe (0.05 μg ml^{-1}) and Co (0.05 μg ml^{-1}) in 0.1 M hydrochloric acid. Other cations were added mostly as chlorides; silicon was added as sodium silicate.

Figure 8 shows that copper, cadmium and chromium cause little enhancement of absorbance ratio except at high (500 ppm) concentrations. When the sample contains sodium, potassium or lead at 500 μg ml^{-1}, noticeable reduction of the absorbance ratio occurs. The presence of more than 50 μg ml^{-1} magnesium greatly increases the absorbance ratio because magnesium causes considerable depression of cobalt absorbance. On the contrary, it was found that the presence of about 5 μg ml^{-1} calcium decreased the absorbance ratio. This may result from a change in the vaporization rate of either iron or cobalt from the carbon tube. It was thought that one of the principal advantages of the internal standard method would be a correction of such matrix effects. Indeed, in flame atomic absorption spectrometry, an internal standard largely overcomes these interference problems [5].

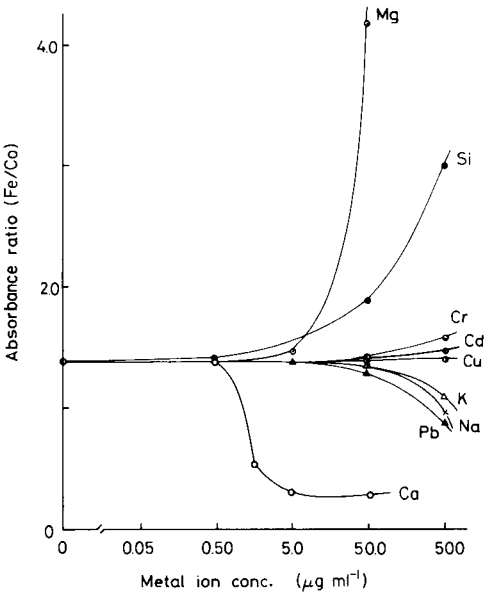

Fig. 8. Effect of cations on the iron: cobalt absorbance ratio. Conditions as in Table 1. Concentrations (μg ml^{-1}): Fe 0.05, Co 0.05.

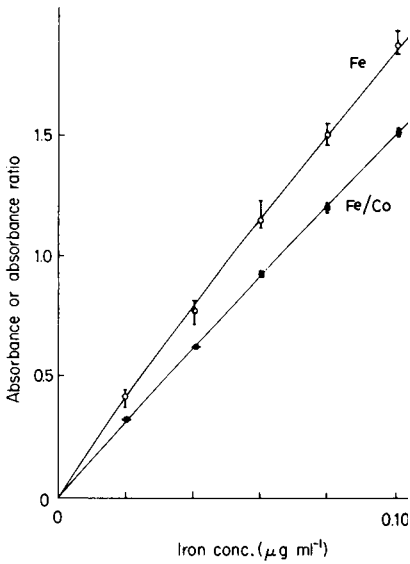

Fig. 9. Calibration graph, for the direct and internal standard methods for iron. Conditions as in Table 1.

TABLE 2

Comparison of measurements of iron in waters by the direct and internal standard methods. Five analyses were done in each case.

Sample		TPTZ method[a] (ng ml^{-1})	Direct method			Internal standard method		
			Range (ng ml^{-1})	Mean	R.s.d. (%)	Range (ng ml^{-1})	Mean	R.s.d. (%)
Boiler water	1	98	101—113	107	4.3	100—105	103	2.5
	2	35	32—36	34	4.7	33—35	34	2.6
	15	110	104—115	107	4.6	110—114	112	1.6
	32	23	24—28	26	6.0	26—27	27	1.7
Glacier water	1	7	8—9	8	6.5	8—9	8	1.7
	2	28	25—30	27	8.4	27—28	27	2.0
	3	331	305—331	321	4.7	319—326	322	1.0
Mean					5.6			1.9

[a]Spectrophotometric determination (see text).

Obviously, however, in electrothermal work, internal standard and analyte elements must have the same physical and chemical properties with respect to the matrices, as well as similar general atomization characteristics.

For all elements except calcium, the absorbance ratio of iron to cobalt is independent of the type or amount of matrix until the amount of matrix is 100 times that of iron. Hence cobalt is considered to be the most suitable internal standard for the determination of iron in water.

Precision and accuracy

For the determination of iron in water, the step mode atomization procedure was employed and the time and voltage settings in Table 1 were used. The calibration curves for the direct and internal standard methods are given in Fig. 9 for comparison. The calibration lines are based on replicate (5) measurements of five standards of different concentrations. With cobalt as an internal standard, the iron values are more reproducible than those obtained by the single-channel method.

Table 2 summarizes the precision and accuracy data obtained with the internal standard and direct methods, under the recommended conditions. A series of iron determinations on different water samples utilizing a cobalt internal standard gave relative standard deviations of 1.0—2.4%. The direct method under the same conditions had relative standard deviations of 4.3—8.4%. The median deviation for the direct method was 5.6%, and for the internal standard method was 1.9%. Again the internal standard method improves the precision of the measurements. The accuracy of the method was ascertained by comparison with a spectrophotometric procedure based on the iron(II)—2, 4, 6-tris(2′-pyridyl)-s-triazine complex [6, 7] in 100-mm cells at 595 nm.

Conclusions

For internal standardization in electrothermal atomic absorption spectrometry, the choice of the internal standard element is extremely important. The first requirement is that the analyte and standard element are quite similarly influenced by changes in experimental variables. Therefore, the physical and chemical properties of both elements must be very similar.

By using cobalt as an internal standard, the determination of iron is made more accurate and precise by reducing the influence of atomizer temperature variations, minimizing the effect of changing the amount of sample injected and, sometimes, decreasing the interferences from cations. Another advantage is that the internal standard will also correct for sample dilution errors because both the internal standard element and the sample element will be subject to the same dilution effect.

REFERENCES

1 W. Gerlach and E. Schweitzer, Foundations and Methods of Chemical Analysis by the Emission Spectrum, Vol. 2, Voss Adam Hilger, London, 1929, p. 2.
2 L. R. P. Butler and A. Strasheim, Spectrochim. Acta, 7 (1965) 1207.
3 F. J. Feldman, Anal. Chem., 42 (1970) 719.
4 K. Nakano, T. Takada and T. Satho, Nippon Kagaku Zasshi, 91 (1970) 293.
5 T. Takada, unpublished data.
6 F. H. Case and E. Koft, J. Am. Chem. Soc., 81 (1959) 905.
7 P. F. Collins, H. Diehl and G. F. Smith, Anal. Chem., 31 (1959) 1862.

Analytica Chimica Acta, 107 (1979) 139—158

OPTIMIZATION OF TEMPERATURE IN CARBON-FURNACE ATOMIC EMISSION SPECTROMETRY WITH COMMERCIALLY AVAILABLE ELECTROTHERMAL ATOMIZERS

D. LITTLEJOHN** and J. M. OTTAWAY*

Department of Pure and Applied Chemistry, University of Strathclyde, Cathedral Street, Glasgow G1 1XL (Great Britain)

(Received 3rd November 1978)

SUMMARY

For instruments without automatic background emission correction, optimization of the applied temperature may be necessary to achieve the lowest analyte detection limits. Optimum temperatures of less than the maximum available are reported for most elements with commercially available instruments in which the heating rate and the final temperature are subject to independent control. Temperature optimization, however, has little effect on furnaces in which the final temperature and the rate of heating are controlled solely by the same applied voltage. Improved emission detection limits are reported for many elements as a result of temperature optimization.

The carbon furnace differs in many respects from established emission sources. Unlike the arc, spark or plasma, spectra are produced without the complicating influence of the electrical conduction of highly ionized vapours and are comparatively free from the chemical action of hydrocarbon flames [1]. Excitation occurs through a purely thermal process depending only on the temperature attained by the furnace during atomization of discrete micro-samples [2], which in general is less than 3200 K. The carbon furnace is therefore a comparatively cool emission source and although relatively free of ionization interferences [3, 4], atomic energy levels above the ground state are significantly less populated than with arc, spark or plasma excitation. The low temperature is partially compensated by the greater mean residence time of the atoms in the carbon tube, which is $\geqslant$ 1 s for most elements atomized in a Perkin-Elmer HGA 2100 furnace operated with interrupted gas flow [5]. In contrast, atom transit times of 0.23—0.48 ms have been reported for a plasma jet, 0.7—5.0 ms for a d.c. arc and 3.2—9.7 ms for an air—acetylene flame [6]. As a result, detection limits for carbon-furnace atomic emission spectrometry (c.f.a.e.s.) compare well with these systems for many elements [7—10], but are limited in some cases by an inability to atomize refractory species or

**Present address: I.C.I. Ltd., Petrochemicals Division, P.O. Box 90, Wilton, Middlesbrough, Cleveland TS6 8JE (Gt. Britain).

to sufficiently populate the higher energy levels of volatile elements with high excitation potentials.

To overcome both these problems, Ottaway and Shaw [7] proposed a modification to increase the tube temperature of a Perkin-Elmer HGA 72 tube by reducing the thickness of the carbon wall at the centre of the tube. Improvements in detection limits obtained with this modified tube appear to be associated with the exponential increase in the emission intensity with temperature. However, the rate of atomization and the maximum instantaneous concentration of atoms are probably also improved by the increase in heating rate encountered with this tube design. Kinetic models of atomization [11—13] have considered in detail the relationship between tube temperature, heating rate and atomic absorption sensitivity. However, with the exception of the initial study by Ottaway and Shaw [7] and a recent application of rapid furnace heating to the determination of involatile elements [8], there has been little investigation of the effects of tube temperature and heating rate on c.f.a.e.s. detection limits.

The magnitude of the atomic emission signal depends on the atom concentration and vapour-phase temperature, and the peak atomic emission intensity represents a balance between the rates of change of both parameters. Since the production and removal of atoms in most atomizers occurs while the tube temperature is still increasing, the peak signal usually occurs after the maximum concentration of atoms has been reached [7, 14]. To determine the effects of different combinations of heating rate and tube temperature on c.f.a.e.s. detection limits, the thermal parameters of a number of commercially available furnace atomizers have been investigated. The systems considered involve furnaces where either the heating rate and final equilibrium tube temperature are subject to independent control or the heating rate is a function of the final temperature set.

Experiments have indicated that the balance between heating rate, tube temperature and change in atom concentration, and the variation of these parameters at different atomization settings is significant in determining detection limits for many elements. When the equilibrium temperature can be altered without changing the heating rate, optimum detection limits for some elements are achieved at temperature settings lower than the maximum available. The magnitude of the optimum temperature depends on the volatility of the species and varies with the dimensions of the atomizer tube, being lowest for the smaller furnaces. If the rate of heating changes with the temperature setting, similar peak atomic emission to background emission ratios are observed over a range of temperature settings of sufficient magnitude to give efficient atomization, indicating that the tube temperature does not exert a direct spectroscopic influence on the detection limit.

The HGA 72 atomizer interfaced with a Perkin-Elmer 306 spectrometer or the HGA 2200 with a PE 272 spectrometer [8] proved the most useful for the measurement of sensitive atomic emission signals. Improved detection limits for systems without wavelength-modulation background correction are

presented for a number of elements, with standard graphite tubes at the optimum temperature settings.

EXPERIMENTAL

Instrumentation

Four instrumental systems were used: a Perkin-Elmer (PE) HGA 72 atomizer with a PE 306 spectrometer, a PE HGA 2200 atomizer with a PE 272 spectrometer, a PE HGA 74 atomizer with a PE 360 spectrometer, and a Varian CRA 90 minifurnace with a Varian AA 375 spectrometer. Each system was coupled to a Servoscribe RE 541.20 potentiometric strip-chart recorder operated at a speed of 2 cm s^{-1} during the atomization sequence. The spectral bandwidth of the Perkin-Elmer spectrometers was set at 0.2 nm, unless otherwise indicated; the alternative slits of reduced height were employed with the PE 272 and 360. The AA 375 was set at the slit position designed for use with the CRA 90 minifurnace which corresponds to a spectral bandwidth of 0.5 nm. The instruments were operated according to the manufacturers' instructions for the measurement of atomic absorption signals. For emission measurements, the monochromator was adjusted to the required wavelength by means of the appropriate hollow-cathode lamp, which was then disconnected. If suitable lamps were not available, the monochromator was adjusted to the approximate wavelength and then peaked on the line by using the atomic emission signal obtained during the atomization of a suitable standard solution. Atomic absorption measurements were made at the wavelengths of the emission lines indicated in the text.

Experiments were done with the normal graphite tubes of each atomizer but modified "high-temperature" HGA 72 tubes, prepared by removing approximately 1 mm from the outside of the tube up to 0.5 cm either side of the injection hole [7] were also used. The design and application of the HGA 72 [7, 9, 14], HGA 2200 [8] and CRA 90 [15] atomizers for c.f.a.e.s. have been described previously. The design and operation of the HGA 74 are similar to those of the HGA 2200; important differences in application will be noted in the text where appropriate. To reduce the reflection of tube wall radiation into the monochromator, the quartz window at the right side of the HGA 2200 and 74 atomizers was removed and replaced with an opaque, non-reflecting material [8]. Otherwise, the furnace heads were unmodified.

Samples were transferred to the centre of the tubes with 5-, 20- and 50-μl Oxford micropipettes, and atomized in an atmosphere of research-grade argon (99.996%) with the furnace programmes given in Table 1. During atomization the gas flow through the PE tubes was interrupted (gas-stop operation) to enhance atom residence times and allow a higher vapour temperature to be achieved during the lifetime of the atom population. The background emission signal from the tube was measured under the same conditions and the intensity at the time of the peak atomic emission subtracted from the combined signal to give the net maximum atomic emission intensity.

TABLE 1

Atomizer programmes

Atomizer	Sample volume[a] (μl)	Drying				Atomization[a]	
		Time (s)	Temp. (K)	Time (s)	Temp. (K)	Time (s)	Temp. (K)
HGA 72[b]	20 or 50	40	373	15	673	10	2000—3000
HGA 2200	20	45	373			5—7	1500—3000
HGA 74	20 or 50	40	373	10	873—1273	10	2100—2800
CRA 90	5	60	333	10	423	5	1400—3000

[a]As indicated in text where necessary. [b]Standard and modified tubes.

Tube wall temperatures were measured with an Ircon series 1100 optical pyrometer as described previously [16]. The pyrometer was focused on the inside of the tube through the injection hole and the temperature during atomization recorded on the Servoscribe RE 541.20 at a speed of 2 cm s^{-1}. Detection limits were calculated from 7 to 10 injections of a standard solution giving an emission-to-background ratio of between 1.0 and 2.0, and are defined as that concentration giving a signal above the background equal to twice the standard deviation of the peak emission signals obtained from these standard solutions.

Chemicals

Stock solutions of the required elements were prepared from reagents of the highest available purity by dissolving the appropriate amount of a suitable salt in distilled water and nitric or sulphuric acid to give a final acid concentration of 10^{-2} M. Working standards were prepared from these stock solutions when required.

TEMPERATURE DEPENDENCE OF THE SIGNAL-TO-BACKGROUND RATIO IN CARBON-FURNACE ATOMIC EMISSION SPECTROMETRY

Ottaway and Shaw [7] modified a standard HGA 72 carbon-furnace tube by reducing the wall thickness at the centre to increase the maximum temperature available from 2510 K to 2880 K. The observed improvements in detection limits for a number of elements were thought to be associated mainly with the exponential increase of emission intensity with temperature. This conclusion implied that sensitivity could be further enhanced at even higher tube temperatures. Subsequently, the output power of the HGA 72 furnace control unit was adjusted so that a maximum temperature of 2823 K was obtained for standard tubes and 3073 K for the modified version. When the furnace was operated at these temperatures, a decrease in the ratio of the atomic emission to the tube background emission was observed for many

elements and consequently poorer detection limits were encountered. This was most severe for elements of lower atom appearance temperatures.

The influence of temperature on the signal-to-background ratio can be assessed by considering the individual temperature dependences of the atomic emission intensity and the tube wall continuum. When self-absorption is negligible and there is a Boltzmann distribution of energy, the intensity of atomic emission (I_a) is related to temperature (T) by [2, 17]

$$I_a = [K\ L\ hc\ A_{xy}\ g_x\ N_t/4\pi\ B(T)\ \lambda_{xy}]\ \exp\ [-E_x/kT] \quad (1)$$

where all the terms are as previously defined. The intensity of the tube wall continuum (I_b), the background signal, is also related exponentially to temperature through Wien's approximation of Planck's law [16]

$$I_b = [K\ 2hc^2/\lambda^5]\ \exp\ [-hc/\lambda kT] \quad (2)$$

where K in eqns. (1) and (2) is a spectrometer constant. The detection limit depends on the ratio, I_a/I_b, which can therefore be expressed as,

$$I_a/I_b = XN_t \exp\ [-E_x/kT]/Y \exp\ [-hc/\lambda kT] \quad (3)$$

where X and Y are constants covering the unchanging parameters in eqns. (1) and (2), E_x is the energy of the upper state of the transition, λ is the spectral line wavelength, and h, c and k have their usual meanings and values. For a resonance line, when $E_x = hc/\lambda$, the ratio I_a/I_b will not vary with temperature provided that N_t, the concentration of analyte atoms at the time of measurement, is the same for each temperature setting. Although the atomic emission intensity and hence sensitivity increase exponentially with temperature [7], so also does the background signal. Consequently, temperature does not exert a direct spectroscopic influence on the detection limit, if the contribution of the shot-noise component to signal irreproducibility is insignificant. Equation (3) will apply to all conventional carbon-furnace atomic absorption/emission spectrometer systems.

Since c.f.a.e.s. signals generally peak after the atomic absorption maximum has been attained [7, 14], N_t in eqn. (3) will always be less than N_{max}, the maximum concentration of atoms generated in the tube. If, however, by changing the tube temperature and/or heating rate, the peak atomic emission can be made to occur closer to the time of the maximum atom concentration, the signal-to-background ratio and detection limit will be improved for all elements, since the value of N_t in eqn. (3) will be increased. The effects of temperature and heating rate on the time of the peak atomic emission signal and the magnitude of the I_a/I_b ratio have been considered for a number of commercial carbon-furnace atomizers.

MEASUREMENT OF ATOMIC EMISSION FROM CARBON-FURNACE ATOMIZERS OPERATED AT HEATING RATES INDEPENDENT OF THE TEMPERATURE SETTING

HGA 72

Like most furnace atomizers, the HGA 72 is voltage-controlled and a change

of voltage setting should therefore alter both the final equilibrium temperature of the tube and the heating rate. Although this occurs at lower temperature settings, it was noticed that for voltages near the maximum of 10 V, the heating rates become similar, as indicated in Fig. 1(a) for a standard HGA 72 tube. The atomic and background emission intensities measured at the settings used in Fig. 1(a) increased rapidly with temperature, as expected. To allow comparison of the signal-to-background ratios over the temperature interval of interest, the intensity scale was contracted by decreasing the photomultiplier tube voltage on the PE 306 spectrometer as the temperature was increased. Background emission signals were adjusted to a similar magnitude on the recorder chart at each temperature. This is illustrated in Fig. 2 for atomic emission signals obtained at 403.08 nm for atomization of manganese at various atomization settings. Comparison of the atomic emission-to-background emission ratios indicates a 3.4-fold improvement when the tube wall temperature is reduced from 2813 K, measured at the time of the peak-height atomic emission signal at 999 units, to 2523 K, the equivalent wall temperature at 600 units. Since the shot-noise component of the recorded signals is not altered significantly by this temperature reduction, a similar improvement in detection limit is also achieved, from 7 to 2 ng ml^{-1}. The variation of the I_a/I_b ratio for manganese with tube wall temperature is illustrated in greater detail in Table 2. The ratio is a maximum at a setting of 600 units. As suggested by eqn. (3), maximization of the ratio implies that at the time of measurement, N_t, the concentration of atoms in the tube is greater than at other temperature settings. This is indicated by the atomic absorption values given in Table 2, each of which is recorded at the time of the corresponding maximum atomic

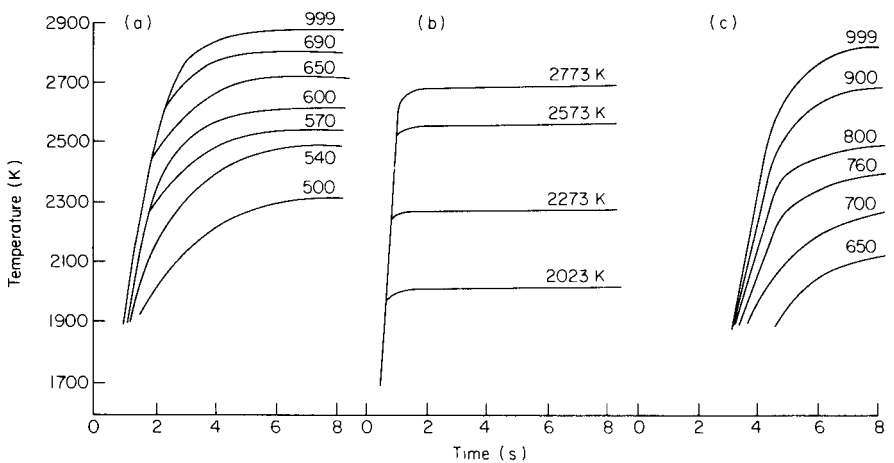

Fig. 1. Variation of tube temperature with time for (a) HGA 72 at atomization settings of 999, 690, 650, 600, 570, 540 and 500 units; (b) HGA 2200 at preset temperatures of 2023, 2273, 2573 and 2773 K; and (c) HGA 74 at atomization settings 999, 900, 800, 760, 700 and 650 units. All temperatures measured with an optical pyrometer.

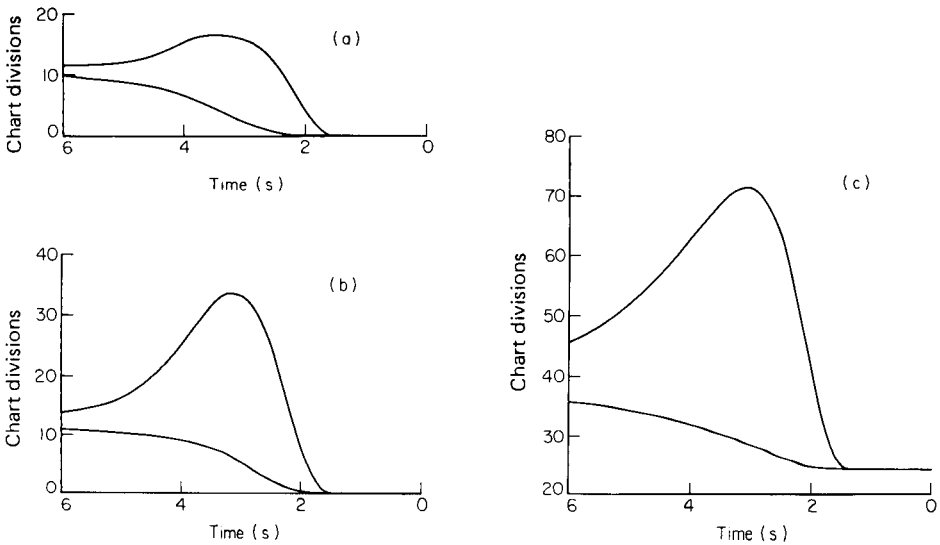

Fig. 2. Carbon-furnace atomic emission and background emission signals for manganese measured with the HGA 72/PE 306 system at 403.08 nm for atomization settings of (a) 999 units, (b) 700 units and (c) 600 units, corresponding to wall temperatures at the centre of the tube of (a) 2813 K, (b) 2673 K and (c) 2523 K, at the time of maximum atomic emission; (c) gives the optimum I_a/I_b ratio and lowest detection limit. Conditions: 50 μl of 0.2 μg Mn ml^{-1} solution, atomization in argon under gas-stop conditions, spectral bandpass 0.2 nm. The photomultiplier tube voltage is increased with decreasing temperature to maintain similar signal magnitudes on the recorder chart. The lower curve in each instance is the background signal.

emission signal and measured under the same experimental conditions given above which also show a maximum at a setting of 600 units. It is also observed that the difference between the time of the peak atomic absorption (Table 3) and atomic emission signals (Table 2) is least at the optimum temperature setting.

The shift of the atomic emission peak time and the optimization of the I_a/I_b ratio can be explained by considering the influence of temperature and heating rate on the rates of supply and removal of analyte atoms during atomization. The shape of a time-resolved carbon-furnace atomic absorption signal has been described in terms of the supply and removal functions [13]. If the time constant of the supply function is shorter than the time constant of the removal function, atomization may be complete by the time of the peak absorption signal. This is more likely to occur when fast heating rates are employed and the gas flow is interrupted during atomization, as in this investigation. Under these conditions, the rising slope of the transient signal, although controlled by both the supply and removal functions, will be dominated by the former, and the decay of the absorbance pulse will represent only the removal function [17].

TABLE 2

Variation with temperature of the manganese I_a/I_b ratio, time of the peak atomic emission signal and relative atom concentration at that time, measured by a.a.s. for an HGA 72 atomizer

Atomization setting (arbitrary units)	Tube wall temp. at peak a.e. signal (K)	I_a/I_b[a]	Time to peak a.e. signal (s)	Atomic absorbance at time of peak a.e. signal
999	2813	1.91	3.5	0.10
650	2663	3.23	3.2	0.13
600	2523	5.00	3.0	0.17
570	2403	4.29	3.5	0.13
540	2213	4.00	4.0	0.11
500	2023	3.92	4.5	0.11

[a]Measured at 403.08 nm for 20 μl of 0.2 μg Mn ml^{-1} solution; PE 306 spectrometer.

TABLE 3

Effect of HGA 72 tube heating rate and temperature on manganese atomic absorption signals

Atomization setting (arbitrary units)	Equilibrium tube wall temp. (K)	Heating rate (K s^{-1})	Rel. rate of atom production (abs. s^{-1})	Peak[a] absorbance	Time to peak absorbance (s)	$1/\tau_R$ (s^{-1})
999	2873	800	0.38	0.31	2.25	1.15
690	2803	800	0.38	0.30	2.25	1.16
650	2713	800	0.36	0.29	2.25	1.11
600	2623	800	0.38	0.29	2.25	1.06
570	2573	750	0.36	0.28	2.25	1.03
540	2503	600	0.30	0.24	2.30	0.82
500	2323	400	0.20	0.20	2.70	0.73

[a]Measured at 403.08 nm for 20 μl of 0.2 μg Mn ml^{-1} solution.

When the same rapid heating rate is applied to raise the tube temperature to different equilibrium values, both the slope of the rising absorption signal and the peak absorbance will be independent of the temperature setting, provided that it is sufficiently above the analyte appearance temperature. The decay of the signal however, will be greater at higher temperatures owing to the increased rate of loss of atoms by diffusion and expansion. The results presented in Table 3 suggest that a situation in approximate agreement with this model exists during the atomization of manganese in the HGA 72. As the atomization setting is decreased from maximum power (999 units) to 600 units, the equilibrium tube temperature is reduced from 2873 to 2623 K. However, the heating rate remains apparently unaltered at 800 K s^{-1}, as measured from the section of the pyrometer tracings (Fig. 1a) corresponding to the period just

before the appearance of atoms to the time of maximum atom concentration. When manganese atomic absorption signals were measured at these atomization settings, the relative rate of production of atoms, based on the slope of the rising absorption signal, was observed to be constant. The relative rate of removal of atoms ($1/\tau_R$) was calculated from the exponential decay of the absorbance pulse, and defined as the slope of the graph of $\ln A_t/A_{max}$ against time, where A_{max} is the maximum absorbance and A_t the absorbance t seconds later [17]. The rate of removal of atoms was observed to increase with increasing temperature setting, as would be expected from the temperature dependence of the expansion and diffusion removal time constants [13].

Contrary to the model presented above, a small but definite decrease of the peak absorbance value was recorded as the atomization setting was reduced from 999 to 600 units. This discrepancy may be related to a slight decrease of the heating rate from 800 K s^{-1} that cannot be observed from the optical pyrometer tracings used to construct Fig. 1(a). The variation of the peak absorbance value over this range is however much smaller than that found at settings below 570 units, and overall only small changes are observed in the time-resolved atomic concentration profile for manganese between 600 to 999 units.

Since the maximum atomic emission intensity at any setting represents a balance between the change in atom concentration and the magnitude of the tube temperature, the peak emission occurs progressively later in the atomization sequence as the temperature setting is increased from 570 to 999 units. Consequently, N_t, the concentration of atoms left in the tube, is smaller at the peak time and the I_a/I_b ratio is impaired as shown in Fig. 2 and Table 2.

At atomization settings lower than 570 to 600 units (Table 3), the HGA 72 exhibits the characteristics of a conventional voltage-controlled atomizer, where reduction of the equilibrium temperature is accompanied by a slower heating rate. Under these conditions the change of atomic concentration with time is different at each setting. As indicated in Table 3, heating rates lower than the maximum available give lower peak absorbance values that occur later in the atomization sequence. This occurs because the rate of atom production is reduced and the influence of the removal function on the rising slope of the signal is greater than at higher heating and atomization rates. Consequently, the concentration of atoms at the time of peak atomic emission, N_t, becomes progressively lower and the I_a/I_b ratio is again impaired and reduced from the maximum value.

It is interesting that the variation of this ratio with temperature is less for settings lower than the optimum than for those above it. Although the concentration of atoms in the HGA 72 furnace at the time of peak atomic emission is approximately the same as, e.g., at 500 and 999 units (as indicated by the atomic absorption values given in Table 2), the I_a/I_b ratio is greater at the lower temperature. The reason for this may be related to the greater distribution of atoms along the tube temperature gradient at higher temperatures owing to increased vapour expansion as the tube is heated more rapidly, giving

a smaller total emission intensity compared to the total tube background emission. At the lower temperature setting, the atom population is more likely to be localized in the central, hotter section of the furnace at the time of the peak emission signal. Thus it appears that, for many elements, the optimum signal-to-background ratio is obtained at the atomization setting that gives the maximum possible heating rate and the minimum equilibrium tube temperature above the atom appearance temperature of the species of interest.

Optimum atomization settings and temperatures for the measurement of atomic emission of a number of elements are given in Tables 4 and 5 for the HGA 72 atomizer operated with standard and modified tubes [7]. For each

TABLE 4

Temperature-optimized c.f.a.e.s. detection limits for an HGA 72 atomizer operated with standard carbon tubes

Element	Wavelength (nm)	Optimum atomization setting (arbitrary units)	Optimum a.e. peak temp. (K)	Detection limits (ng ml^{-1})		
				Temp. optimized	Standard tube (max. power)[a]	Modified (max. po
Ba	553.55	650	3003	0.8	4.3	4.1
Eu	459.40	690	2823	1.4[b]	53	23
Li	670.78	670	2773	0.054	0.07	0.09
Yb	398.80	600	2733	0.28	0.58	0.36
Cr	425.43	600	2653	0.77	3.7	2.1
Cu	324.75	600	2613	1.4	3.6	2.6
Sn	286.33	600	2573	8.8	—	—
In	410.18	540	2293	50	—	—

[a]Values from [7]. [b]Pyrolytically coated tube used.

TABLE 5

Temperature-optimized c.f.a.e.s. detection limits for an HGA 72 atomizer operated with standard and modified "high temperature" carbon tubes

Element[a]	Standard tube		Modified tube		Earlier work [7][b] Detection limit (ng ml^{-1})	
	Optimum temp./ (K)/ (units)	Detection limit (ng ml^{-1})	Optimum temp./ (K)/ (units)	Detection limit (ng ml^{-1})	Standard tube	Modified tube
Sc	2773/690	27	2873/520	15	140	14
Co	2613/620	15	2703/440	14	52	10
Ni	2593/600	20	2573/380	40	112[c]	23[c]
Mg	2553/650	3	2513/300	6	94	1.1
Mn	2523/560	2	2513/320	4	7.4	4.4
Fe	2523/650	6	2593/380	6.8	16	10

[a]Wavelengths given in Table 9; Sc, 402.04 nm; Mg, 285.21 nm. [b]Maximum power, 999 units [7]. [c]341.48 nm.

of the elements considered, there is a setting at which the I_a/I_b ratio is maximized. However, variations in the calibration of applied voltage may give different optimum settings for other HGA 72 units. It is likely, though, that the optimum temperature at these settings, defined as the wall temperature at the centre of the tube measured at the time of the peak-height atomic emission intensity, will be similar in all HGA 72 units, if the heating rates are the same. Since local thermal equilibrium exists in the tube during atomization under the conditions described [2], the value of the optimum wall temperature will be very similar to that of the vapour temperature that determines the intensity of the peak-height atomic emission.

Detection limits obtained at the optimum settings are compared in Tables 4 and 5 to previously reported values measured at maximum power (999 units) when that setting gave an equilibrium temperature of 2510 K for the standard tube and 2880 K for the modified version. It is important to note that these temperatures are the final maximum temperatures attained by the tubes and not the values at the time of the peak atomic emission signal, which were not recorded by Ottaway and Shaw [7] in their initial study. As might be expected, maximum I_a/I_b ratios for volatile elements are obtained at lower temperature settings than for elements with high atom appearance temperatures.

The optimum detection limits for the HGA 72 described here are, in general, considerably better than previously reported values for the standard tube design. However, the improvement compared to previous results for the modified tube is marginal for most of the elements considered. It appears that the detection limits for certain elements, calculated by Ottaway and Shaw [7] using the modified tube, were obtained when atomization at 999 units (maximum power) gave temperatures at the time of peak atomic emission that were close to the optimum temperatures determined here. This is supported by the observation that close to the optimum value (±50 to 100 K), the I_a/I_b ratio and hence the detection limit do not vary greatly. The greatest improvements in detection limits are observed for elements that have optimum atomization settings and temperatures furthest from the temperature previously employed, such as barium, europium, chromium, indium and tin. The comparative results given in Table 5 for optimization with standard and modified tubes indicates that although the maximum temperatures for these tubes differ by 300 K, the optimum temperatures and detection limits are similar. The settings at which the optimum I_a/I_b ratios are achieved with the modified tube are lower than for the standard design because of the smaller mass of carbon at the centre of this tube.

Clearly, for many of the elements considered in this work, c.f.a.e.s. detection limits for the HGA 72 furnace are enhanced when the atomization setting used is less than maximum. For some involatile elements, the optimum temperature has not yet been obtained because of the restrictions imposed by the maximum temperature and heating rate available with this atomizer. The optimization of the atomization temperatures of an HGA 2200 furnace for the measurement of atomic emisson from involatile elements, however, has

been discussed in detail elsewhere [8]. The general application of this furnace in the emission mode is considered briefly in the following section.

HGA 2200

The HGA 2200 atomizer incorporates maximum power heating with temperature control as an alternative mode of operation to conventional voltage heating. This allows the graphite tube to be heated with maximum power at the same very rapid rate to any preset atomization temperature (Fig. 1(b)). The temperature is monitored optically by a silicon photodiode in a similar manner to that proposed by Lundgren et al. [18]. At the atom appearance temperatures of most elements, the heating rate is about 2000 K s^{-1}, which is 2.5 times the maximum rate obtainable with the standard HGA 72 atomizer and 3—4 times the maximum rate achieved when the HGA 2200 is operated (like the HGA 74) with voltage controlled heating [8].

Like the HGA 72, the HGA 2200 atomization temperature setting can be adjusted to maximize the atomic emission detection limits for most elements. This can be achieved, however, only when maximum power heating is applied. Under conventional heating, the HGA 2200 performs like the HGA 74 (see below). Detection limits obtained with maximum power heating at the apparent optimum temperatures for a number of elements have been presented previously [8], but are included in Table 9 (see below) for comparison of the HGA 2200 and HGA 74 atomizers.

Maximum atomic emission-to-background emission ratios were achieved at settings lower than the maximum temperature available for all the elements investigated. This is illustrated for molybdenum, iron and cadmium in Fig. 3, where at temperature settings very much higher than the atom appearance

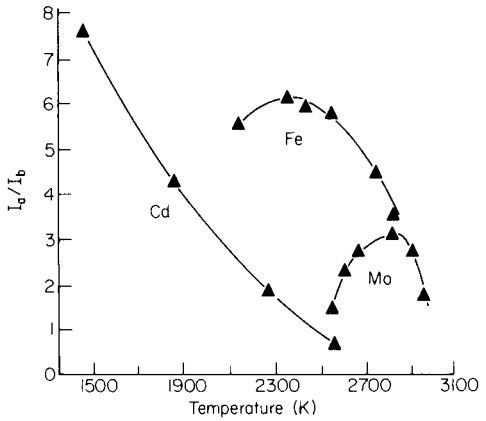

Fig. 3. The variation with temperature of I_a/I_b ratios for molybdenum, iron and cadmium in the HGA 2200 atomizer operated under maximum power heating with temperature control in the PE 272 spectrometer. Molybdenum, 20 μl of 0.5 μg ml^{-1} solution at 379.83 n with pyrolytically coated tubes; iron, 20 μl of 5.0 μg ml^{-1} solution at 371.99 nm; cadmium, 20 μl of 10.0 μg ml^{-1} solution at 326.11 nm. Atomization in argon under gas-stop condition, 0.2 nm bandwidth.

temperature, the I_a/I_b ratio is greatly decreased. With maximum power heating the final equilibrium tube temperature is reached before the peak atomic emission signal is attained and hence the optimum temperatures given in Table 9 are the actual temperatures set on the control console. In general, these optimum temperatures are lower than those obtained with the HGA 72 (Tables 4 and 5); this may be related to the faster heating rate and smaller furnace dimensions of the HGA 2200. Detection limits obtained with the HGA 2200/PE 272 system, however, are of similar magnitude to those obtained with the HGA 72/PE 306 system.

Optimum temperatures for the measurement of atomic emission from volatile elements such as cadmium were difficult to determine with both the HGA 72 and 2200 atomizers. The I_a/I_b ratio for these elements increased continuously with decreasing temperature (Fig. 3). A maximum was not obtained since the level of radiation at the temperature corresponding to the largest I_a/I_b ratio measured was very low, and a further decrease in temperature produced a radiation level lower than could be detected at maximum photomultiplier tube voltage and scale expansion. When the emission intensity is so low, shot noise tends to be excessive compared to the magnitude of the signal and so the best detection limits for volatile elements will not be achieved at the temperature of the maximum I_a/I_b ratio.

A similar explanation to that described previously for the HGA 72 furnace can be proposed to explain temperature optimization with the HGA 2200, when this atomizer is operated with maximum power heating. As the temperature is reduced from the maximum of 3200 K towards the optimum value, the rate of atomization remains the same since the heating rate is constant, and the time-resolved atomic concentration profile will be approximately similar at each setting. Consequently, as the equilibrium tube temperature is reduced, the maximum atomic emission signal occurs progressively closer to the start of the atomization sequence and to the time of the maximum atom concentration, and the I_a/I_b ratio is enhanced. At temperatures lower than the optimum, reduction in the rate of atomization will cause the ratio to be decreased.

CRA 90 Minifurnace

Optimization of the atomization temperature for the measurement of atomic emission with conventional furnace–spectrometer systems can be achieved with atomizers that can be operated at the same heating rate irrespective of the final equilibrium temperature required. The Varian CRA 90 minifurnace is operated in this way, and it is therefore to be expected that the CRA 90 will show a variation of the I_a/I_b ratio with the atomization temperature setting. Atomic emission signals for lithium, manganese, chromium and molybdenum were measured at a number of furnace settings. The temperature settings at which the maximum I_a/I_b ratios were observed are shown in Table 6, together with the detection limits. In each case, the maximum I_a/I_b value was achieved at the fastest heating rate, 800 K s^{-1}. The optimum temperatures are

TABLE 6

Temperature-optimized c.f.a.e.s. detection limits for lithium, manganese, chromium and molybdenum obtained with a Varian CRA 90 atomizer

Element	Wavelength (nm)	Optimum temp. setting (K)[a]	Detection limit (ng ml^{-1})
Li	670.78	2323	0.24
Mn	403.08	2023	2000
Cr	425.43	2323	300
Mo	379.83	2473	200

[a]The optimum heating rate was 800 K s^{-1} in all cases.

much lower than the corresponding values for the HGA 72 and HGA 2200 atomizers. These results suggest that the optimum temperature for any element decreases with the length and diameter of the atomizer tube.

Matousek and Smythe [15] have recently discussed the use of a Varian CRA 63 minifurnace for the c.f.a.e.s. determination of lithium; the detection limit given in Table 6 is comparable with their value. The detection limits for the other elements, however, are considerably worse than those measured with the HGA 72 and 2200 atomizers. This is probably related to the furnace size and the very much shorter residence time of the atoms in the minifurnace tube compared with the larger furnaces. Linear ranges were also found to be impaired with the minifurnace, extending less than two orders of magnitude for the elements investigated. The use of the peak integration facility of the Varian AA 375 spectrometer did not improve the linear range significantly.

With Perkin-Elmer furnaces, the inert purge gas flows through the graphite tube and for the measurement of sensitive atomic emission signals, it is usually necessary to interrupt this flow. With the CRA 90, the gas does not flow direct through the minifurnace but provides an inert envelope to protect the graphite from atmospheric oxygen. The detection limits presented here were measured with the standard CRA 90 gas flow rate which may have disturbed the atomic vapour and impaired atomic emission sensitivity. Matousek and Smythe [15] reported a tripled lithium emission intensity on modifying the gas flow rate during atomization. Similar improvements may be attained for the other elements discussed above, but even so it is unlikely that the CRA 90 will prove as sensitive for the measurement of atomic emission signals as atomizers with larger tubes.

MEASUREMENT OF ATOMIC EMISSION FROM A CARBON FURNACE ATOMIZER OPERATED AT HEATING RATES DEPENDENT ON THE TEMPERATURE SETTING

HGA 74

The change of the HGA 74 tube temperature with time during atomization at a number of power settings is shown in Fig. 1(c). As with most conventiona

voltage-controlled furnaces, the heating rate depends on the temperature setting chosen and becomes slower as the final equilibrium temperature attained by the furnace is decreased. The influence of this relationship on the I_a/I_b ratio for manganese at 403.08 nm is illustrated in Fig. 4. The photomultiplier tube voltage and scale expansion controls were adjusted to give similar background signal intensities on the recorder chart. It appears that changing the atomization setting does not greatly affect the I_a/I_b ratio. This suggests that at the time of maximum atomic emission the concentration of atoms in the furnace must be approximately the same for each setting, and this is confirmed by the manganese atomic absorption signals (Table 7) which were measured at the time of maximum atomic emission. Unlike the HGA 72, the time of the maximum atomic absorption and emission signals are unchanged as the temperature decreases (Tables 7 and 8). As the heating rate is reduced from a maximum of 570 K s^{-1} at 999 units, the rate of production of atoms becomes slower, as measured from the slope of the rising absorbance pulse. Although the removal of atoms, based on the exponential decay of the absorption signal [17], is decreased at lower temperatures the overall balance of the supply and removal functions causes a decrease in the peak absorbance as the temperature setting is decreased (Table 8). Hence both the time-resolved atomic concentration

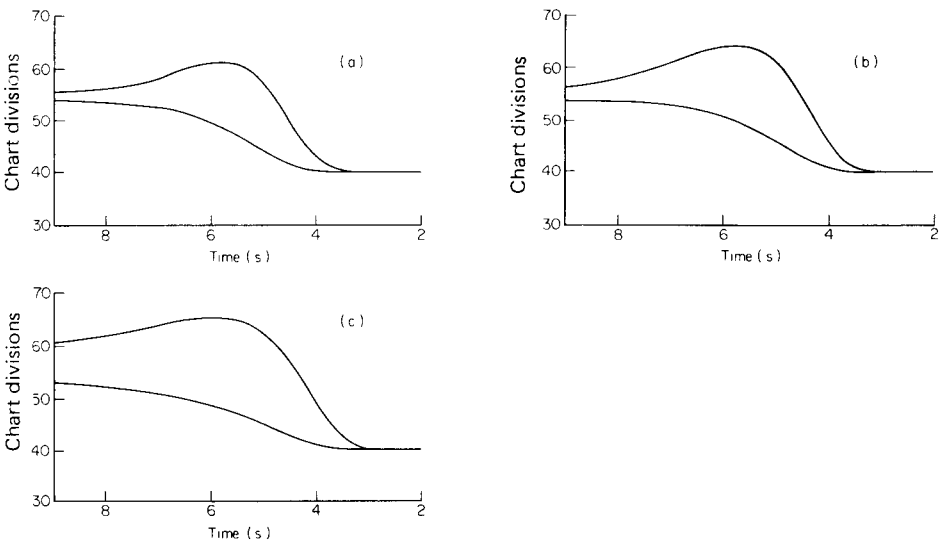

Fig. 4. Carbon-furnace atomic emission and background signals for manganese measured with the HGA 74/PE 360 system at 403.08 nm, for atomization settings of (a) 999 units, (b) 900 units and (c) 760 units corresponding to wall temperatures at the tube centre of (a) 2743 K, (b) 2603 K and (c) 2373 K at the time of maximum atomic emission. Conditions: 20 μl of 1.0 μg Mn ml^{-1} solution; atomization in argon under gas-stop conditions; spectral bandwidth 0.2 nm; photomultiplier tube voltage increased with decreasing temperature to maintain similar signal magnitude on each recorder chart. The lower curve in each instance is the background signal.

TABLE 7

Variation with temperature of manganese atomic emission measurements[a] for an HGA 74 atomizer

Atomization setting (arbitrary units)	Tube wall temp. at peak signal (K)	I_a/I_b	Atomic absorbance at time of peak emission[b]
999	2743	2.0	0.28
900	2603	1.9	0.27
800	2423	2.1	0.25
760	2323	2.2	0.27
700	2203	2.4	0.26
650	2123	2.1	0.25

[a]For 20 μl of 1.0 μg Mn ml^{-1} solution at 403.08 nm. [b]The time to the peak atomic emission signal was 5.5 s in all cases.

TABLE 8

Effect of HGA 74 tube heating rate and temperature on manganese atomic absorption signals[a]

Atomization setting (arbitrary units)	Equilibrium tube wall temp. (K)	Heating rate (K s^{-1})	Rel. rate of atom production (abs. s^{-1})	Peak absorbance	Time to peak absorbance (s)	$1/\tau_R$ (s^{-1})
999	2813	570	0.96	0.80	3.75	0.83
900	2673	550	0.90	0.78	3.75	0.83
800	2483	500	0.90	0.73	3.70	0.65
760	2403	390	0.80	0.64	3.75	0.54
700	2273	250	0.68	0.50	3.75	0.48
650	2093	200	0.56	0.37	3.90	0.36

[a]Measured at 403.08 nm for 20 μl of 1.0 μg Mn ml^{-1} solution.

profile and tube temperature are altered, unlike the atomizers in the previous section, where the atomic concentration profile was similar for a range of temperature settings. The combined effect of these changing parameters for the HGA 74, gives similar I_a/I_b ratios at each atomization setting at least down to 650 units and so temperature optimization does not apply over the interval 650—999 units. Provided that the shot-noise contribution to signal irreproducibility can be ignored, it appears that similar detection limits will be obtained at all temperatures sufficiently great to ensure efficient atomization

Typical c.f.a.e.s. detection limits for the HGA 74/PE 360 system are listed in Table 9 and compared with those for the HGA 2200 operated with maximum power heating and temperature control [8]. Since the HGA 74 and HGA 2200 furnace heads are of similar design, and the PE 360 and PE 272 spectrometers interfaced with the atomizers have similar optics, the poorer

TABLE 9

Carbon-furnace atomic emission detection limits for the HGA 74/PE 360 and HGA 2200/PE 272 systems

Element	Wavelength (nm)	HGA 74/PE 360[a] Detection limit (ng ml^{-1})	HGA 2200/PE 272 [8]	
			Detection limit (ng ml^{-1})	Optimum temp. setting (K)
Li	670.78	0.2	—	—
Ba	553.55	4.5	—	—
Cr	425.43	8	4	2573
Mn	403.08	45	6	2423
Co	345.35	88	32	2573
Ni	352.45	120	15	2573
Fe	371.99	500	17	2373

[a]Maximum power (999 units).

detection limits encountered with the HGA 74 are probably related to the slower heating rate of this atomizer. It appears, however, that atomic emission temperature optimization does not apply when both the heating rate and tube temperature are changed simultaneously, as observed for the HGA 74 furnace.

CONCLUSIONS

It has been shown that the c.f.a.e.s. detection limits for a number of elements are increased when temperatures lower than the maximum available are chosen to atomize and excite the analyte species. Although the reduction of tube temperature from the maximum setting decreases the absolute intensities of both atomic and background emission, there is a setting for most elements at which the I_a/I_b ratio is a maximum. Detection limits at this optimum setting are lower than at other temperatures. A comparison of atomic absorption and emission signals indicates that temperature optimization of this type is encountered with atomizers where the heating rate and temperature setting are subject to independent control. Under these conditions the same heating rate can be used to atomize samples and raise the tube temperature to different equilibrium values. Consequently, the magnitude and rate of change of atom concentration with time during atomization is approximately the same. As the temperature is reduced from the maximum atomization setting, the peak atomic emission occurs closer to the time of maximum atom concentration, and the I_a/I_b value is increased. The extent to which temperature can be reduced to improve the signal-to-background ratio in this way is limited by the ability of the spectrometer to measure the emission intensities produced at or near the optimum temperature. At this temperature, the detection limit will be improved compared with higher temperature settings if the contribution of shot noise to signal irreproducibility is negligible. This was shown

to apply to the atomic emission from an HGA 2200 atomizer operated at maximum power heating and with temperature control, a CRA 90 minifurnace and an HGA 72 atomizer over a limited temperature range near maximum power. Other atomizers such as the HGA 74 and the HGA 2200 operated with conventional voltage-controlled heating, do not exhibit the characteristics which allow c.f.a.e.s. temperature optimization as the heating rate depends on the temperature setting. The atomization rate is therefore different at each setting and similar signal-to-background ratios and detection limits are encountered over a range of temperatures.

When temperature optimization can be achieved, decreasing the atomization temperature from the maximum value also has the advantage of allowing the maximum atomic emission signal to be measured when the background signal is almost constant. If atomization temperatures higher than the optimum value are used, the combined background and atomic emission signal reaches a maximum while the temperature and hence background signal are still rapidly increasing. Considerable errors in signal measurement may therefore be introduced when this background signal is subtracted from the combined signal.

The magnitude of the optimum temperature setting appears to be related to the volatility of the element and varies with the atomizer dimensions, being lower for smaller furnaces like the CRA 90. As with atomic absorption analysis, increasing the heating rate improves the c.f.a.e.s. detection limits at all temperature settings. In general, lowest detection limits were encountered with the longer HGA 72 furnace operated with the PE 306 spectrometer. Similar values were obtained with the HGA 2200 atomizer operated under maximum power heating and with optimization of the equilibrium temperature. This latter system has been shown [8] to be particularly useful for the determination of involatile and carbide-forming elements. The detection limits for volatile species, however, are poor in comparison to those for other elements. Thus modifications to the design of the atomizer tube are necessary to allow the measurement of sensitive atomic emission signals from lead, bismuth, indium, etc. [9]. This will be considered elsewhere in a general discussion of the effect of tube design and temperature gradient on the intensity of atomic emission signals.

A quantitative expression describing the time-dependence and shape of transient c.f.a.e.s. signals generated with different combinations of tube temperature and heating rate has not been considered. Such an expression would require factors to account for the production and removal of atoms, and the effect of temperature on atomic emission intensity. When a combined signal of the atomic and background emissions is measured, a term accounting for the rapidly changing tube wall continuum radiation that constitutes, directly or indirectly [16], the background signal, would also be necessary.

If automatic background correction such as that provided by wavelength modulation [10, 19] is used, it is likely to alter the atomization setting at which optimum atomic emission signals are achieved with the furnaces

considered here. In this case, detection limits are controlled by the signal-to-noise ratio (S/N) rather than the signal-to-background ratio. When signal reproducibility is dominated by shot noise, increasing the temperature will improve S/N, and hence the detection limit at the time of maximum emission intensity will be the same for each temperature setting. This happens because the shot noise increases as the square root of the signal intensity, which has an exponential dependence on temperature. If the concentration of atoms at the peak emission decreases with an increase in the temperature setting, S/N may still be improved if the influence of temperature on the atomic emission intensity is greater than that of the reduction in the concentration of emitting atoms. It is likely that optimum temperature settings with wavelength modulation background correction will be higher than those obtained with conventional spectrometer systems.

The results presented here demonstrate that for those commercially available instruments giving the best c.f.a.e.s. detection limits (i.e. those with fast heating rates), significant improvement in performance is achieved for nearly all elements by the correct choice of atomization temperature or setting. Parts per billion detection limits have been achieved for a wide range of elements by c.f.a.e.s. which consequently provides an alternative emission source suitable for simultaneous multi-element analysis. Unfortunately, the best detection limits for different elements are achieved at different temperatures, which for simultaneous multi-element analysis, will entail either selection of compromise working conditions or a completely different design of furnace and sample introduction system.

The authors are indebted to the Perkin-Elmer Corporation and Varian Instrument Co. Ltd., for the short-term loans of the HGA 2200-PE 272 and the CRA 90-AA 375 systems, respectively. The gift of the HGA 74 and PE 360 by the British Steel Corporation, Ravenscraig Works and the award of a research grant to J. M. O. by the Royal Society for the purchase of the HGA 72 are also gratefully acknowledged. The Salters' Company are thanked for the award of a research scholarship to D. L.

REFERENCES

1 A. S. King, Astrophys. J., 27 (1908) 353.
2 D. Littlejohn and J. M. Ottaway, Analyst, 104 (1979) 208.
3 J. M. Ottaway and F. Shaw, Analyst, 101 (1976) 582.
4 R. C. Hutton, Ph.D. Thesis, University of Strathclyde, Glasgow, 1977.
5 R. E. Sturgeon, C. L. Chakrabarti and P. C. Bertels, Anal. Chem., 47 (1975) 1250.
6 V. D. Malykh and M. A. Serd, Opt. Spectrosc. (U.S.S.R.), 16 (1964) 203.
7 J. M. Ottaway and F. Shaw, Appl. Spectrosc., 31 (1977) 12.
8 D. Littlejohn and J. M. Ottaway, Anal. Chim. Acta, 98 (1978) 279.
9 D. Littlejohn and J. M. Ottaway, Analyst, 103 (1978) 662.
10 M. S. Epstein, J. R. Moody, T. J. Brady, T. C. Rains and I. L. Barnes, Anal. Chem., 50 (1978) 874.
11 B. V. L'vov, Atomic Absorption Spectrochemical Analysis, Hilger, London, 1970.

12 R. E. Sturgeon, C. L. Chakrabarti and C. H. Langford, Anal. Chem., 48 (1976) 1792.
13 W. M. G. T. van den Broek and L. de Galan, Anal. Chem., 49 (1977) 2176.
14 J. M. Ottaway and F. Shaw, Analyst, 100 (1975) 438.
15 J. P. Matousek and L. E. Smythe, Appl. Spectrosc., 32 (1978) 54.
16 D. Littlejohn and J. M. Ottaway, Analyst, 102 (1977) 553.
17 D. Littlejohn and J. M. Ottaway, Analyst, 103 (1978) 595.
18 G. Lundgren, L. Lundmark and G. Johansson, Anal. Chem., 46 (1974) 1028.
19 M. S. Epstein, T. C. Rains and T. C. O'Haver, Appl. Spectrosc., 30 (1976) 324.

Analytica Chimica Acta, 107 (1979) 159—167

DETERMINATION OF VOLATILE MERCURY COMPOUNDS IN AIR WITH THE COLEMAN MERCURY ANALYZER SYSTEM

R. DUMAREY, R. HEINDRYCKX, R. DAMS and J. HOSTE*

Institute for Nuclear Sciences, Rijksuniversiteit Gent, Proeftuinstraat 86, B-9000 Gent (Belgium)

(Received 23rd November 1978)

SUMMARY

A simple but very selective cold-vapour atomic absorption system is described for the determination of volatile mercury compounds at very low levels in ambient air. Three different absorbers are compared: activated charcoal, silver-coated sea sand and gold-coated sea sand. To eliminate interferences, a two-step desorption unit is used. After thermal desorption, the mercury is measured by using a modified MAS-50 spectrophotometer. The effects of flow rate and desorption temperature are discussed. The detection limit is 0.1 ng. Above 1 ng, the reproducibility is about 1%. Calibration is done by injection of elemental mercury vapour. The method with gold-coated sand absorbers is most satisfactory and is suitable for the analysis of ambient outdoor and indoor air. All likely volatile mercury compounds are absorbed, and a wide range of mercury concentrations can be determined. In routine application, one analysis takes about 3 min.

In recent decades the mercury levels in the environment have risen considerably because of human activities such as industrial development, increased power consumption and the use of mercurials in agriculture and medicine, etc. [1, 2]. Elemental mercury is known to be the major environmental form. It can be determined directly in air at concentrations as low as 15 ng m^{-3} with cold-vapour atomic absorption devices [3, 4]. This technique is not suitable for detection in ambient air in rural and in remote areas. Moreover, it does not detect the more toxic methylmercury(II) and dimethylmercury compounds or mercury(II) chloride compounds in air, unless these are converted to elemental mercury prior to analysis. Therefore, many indirect methods have been developed in which an enrichment step on efficient adsorbers is used. A large volume of air can be sampled and the mercury is determined by resonance absorption of the 253.7-nm wavelength line after desorption. The adsorber can be a liquid such as an acidified solution of potassium permanganate [5] or a solid such as activated charcoal [6], silver [7] or gold [8]. These adsorbers collect not only elemental mercury but also the inorganic mercury(II) and organic RHgX and R_2Hg compounds.

This paper describes an atomic absorption spectrometric method for the determination of volatile mercury compounds in air; the apparatus used is

simple and relatively cheap. Mercury is collected from ambient air by amalgamation with gold which is employed as a very thin film on grains of sea sand. It has been reported that absorbers composed of sheets or grains of silver or gold show considerable memory effects and poor reproducibility [9]. The absorber applied here has no detectable memory effect and allows an accurate determination of nanogram quantities of mercury. After collection, the mercury is thermally desorbed and measured in the optical cell of the spectrometer.

EXPERIMENTAL

Preparation of the absorption tubes

Three different absorbers were tested for collection of volatile mercury compounds in air: activated charcoal, and silver- and gold-coated sea sand. The absorption tubes were constructed of quartz tubing (8 mm o.d., 6 mm i.d. and 140 mm long) (Fig. 1). At a point 60 mm from the outlet, two indentations were made to keep the packing in place together with two quartz wool plugs.

Activated charcoal (Merck No. 9624, 20-35 mesh) was purified by heating for 1 h in a quartz tube placed in a tube furnace at 800—900°C, with a stream of mercury-free nitrogen gas passing through. The mercury content of this purified charcoal was lower than the limit of detection of the analytical system. The activated charcoal packing in the absorption tube was 40 mm long.

A very thin film of silver on sea sand was obtained as follows. Water was added to a mixture of equal amounts of acid-washed sea sand (Merck No. 7712, 50—140 mesh) and Ag_2O to give a homogeneous slurry. After drying at 90°C, the mixture was transferred to a quartz tube and heated for 1 h in a furnace at 800°C while nitrogen gas was passed. Viewed under a microscope, the resulting sand seemed to be 80—100% coated. The coating was 35% silver by weight. The silver-coated sand packings were 20 mm long.

Gold-coated sea sand was prepared by an analogous procedure with $HAuCl_4$ [8, 10]. The resulting sand was 40—70% coated. The coating was 15—20% gold by weight. The gold-coated sand packings were 15 mm long.

Sea sand was used instead of glass beads to prevent melting of the carrier during desorption at 800°C.

Prior to sampling, all tubes must be treated to reduce the blanks. The activated charcoal tubes were heated at 600°C for 5 min while nitrogen gas was passed through. For new absorption tubes, several heat treatments were required to obtain a mercury content lower than the limit of detection. After several analyses, this treatment must be repeated because of a gradual build up of residual mercury.

The gold and silver absorption tubes were heated to 800°C for 2 min while carrier gas was passed through. Freshly prepared tubes showed a slight increase in response and reproducibility after they had been preconditioned several times with some mercury. After these pretreatments, no mercury

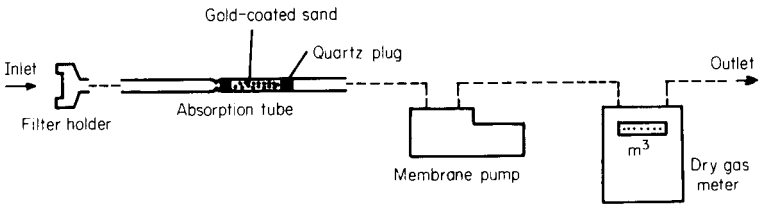

Fig. 1. Air sampling apparatus.

remained on the absorbers. The tubes were capped with Teflon stoppers until required for sampling.

Air sampling

Field samples were collected by drawing air through the absorber with a small pump (KNF, No 5 ANE membrane pump) at flow rates of 2.5—3.5 l min^{-1}. The air sampling set-up is shown in Fig. 1. A prefilter (Whatman GF/A, 13-mm diameter) is used to retain particulates and solid mercury compounds. The volume of air is measured by a calibrated dry gas meter. The volume sampled depends on the expected mercury concentrations. The loaded samplers can be stored for several days without change in mercury content [10].

Apparatus for mercury determination

The set-up is shown in Fig. 2. The nitrogen carrier gas is purified from mercury by passing through an activated charcoal scrubber(I) and dried with a silica gel scrubber(II). The flow is adjusted by means of a pressure regulator followed by a suitable restricting coil or valve. The necessary desorption temperature is obtained by using a coil of about 1 m of nichrome wire (6 Ω m^{-1}) round the absorption tube; the wire is connected to a 14 A, 220 V a.c. input variable transformer (Rheotor, No 21/22 P).

The mercury desorbed from the sampler (tube A) is carried to a second fixed gold absorber (tube B) to eliminate possible interferences collected

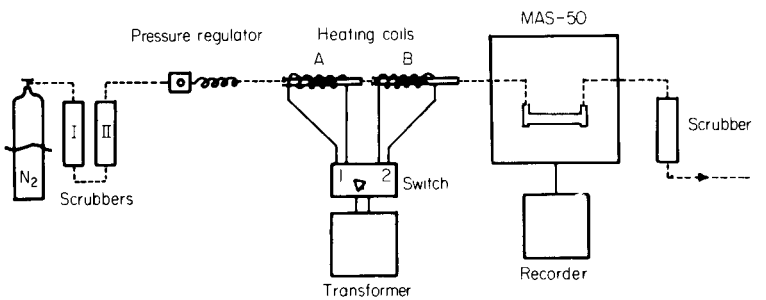

Fig. 2. Apparatus for determination of mercury. For details, see text.

during the sampling. This second absorber also helps to avoid small variations in flow rate caused by differences in absorber packing. The heating coil provided is identical to that for the first absorber.

After desorption from the second tube, the elemental mercury is swept into a Coleman MAS-50 Mercury Analyzer System. The MAS-50 was modified by replacing the original 155-mm plastic optical cell with a 190-mm quartz cell with quartz windows (Fig. 3); this results in sharper response peaks with very little tailing. Inlet and outlet (I) are made of Teflon. The outlet is fitted with eight circular openings (2-mm diameter) to allow even removal of the mercury vapour. The openings are surrounded by a hollow Teflon ring (III), the outlet of which is connected to a scrubber filled with activated charcoal. The whole cell is sealed tightly with rubber O-rings. The absorption tube is connected to the MAS-50 with Tygon tubing; this connection is kept as short as possible to reduce the dead volume and possible losses of mercury by absorption on, or diffusion through, the tubing wall [11].

Output signals from the MAS-50 spectrophotometer are fed to a recorder with variable input (Kipp & Zonen BD 8).

Calibration

Calibration is done by injection of known amounts of air saturated with mercury vapour. A calibrated, gas tight 0—5 ml syringe is used to trap mercury vapour above a metal pool in a closed flask fitted with a three-layer rubber septum. The flask is maintained at 20.0 ± 0.5°C in a constant temperature bath. The amount of mercury vapour contained in 1 ml of air at 20°C and 1 atmosphere pressure at equilibrium over the pool is 13.19 ng [7]. For calibration, several different amounts of mercury vapour are injected through an injection port with septum and are collected on the second gold absorber.

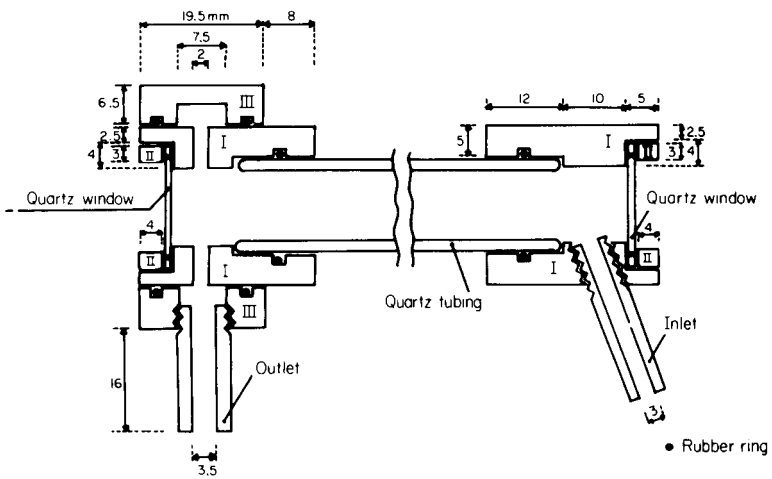

Fig. 3. Modified optical cell. All dimensions are given in mm.

To obtain reproducible injection results, the pressure in the standardization flask has to be kept at 1 atmosphere. Accordingly, the system used consists of two flasks, one of which is open to the air via a capillary. For large volumes, a few minutes are allowed to elapse to re-establish equilibrium between liquid and gaseous mercury. This equilibration is facilitated if the mercury surface is kept clean.

A complete calibration curve is recorded at the beginning of each series of analyses. Standards are run intermittently to check the stability of the system.

Procedure

After calibration of the system, the sampling tube to be analysed is connected to the permanent absorber with a short length of Tygon tubing. The nitrogen gas flow is adjusted to 0.100 l min^{-1} and the sampler is heated for 1 min at about 800°C. After cooling, the sampling tube is removed from the system and capped for further use. The carrier gas is reconnected, the fixed absorber is then heated at 800°C and the percentage transmittance (% T) is recorded. The absorber is allowed to cool and the system is then ready for the next determination. One determination takes about 3 min.

RESULTS AND DISCUSSION

Absorber characteristics

Activated charcoal was found to be unsuitable as the absorber. Table 1 shows the influence of different desorption times (on the fixed gold absorber) on the mercury recovery after desorption from a 0.5-g packing of activated charcoal. Desorption was done at 600°C at a nitrogen flow rate of 0.100 l min^{-1}. Desorption is incomplete, even after heating for 3 min. Activated charcoal has also a high capacity for collecting interfering compounds. Gradual increase of the temperature during desorption results in a multiple instead of a single mercury peak. Because a single-beam spectrophotometer was used, so that simple background correction was impossible, the use of charcoal as collector was rejected.

When the silver-coated absorber is used, the desorption is fast and complete. The ratio between the absorption signal obtained by desorption from the silver absorber and the signal obtained by direct injection is 0.24 ± 0.01 for 20 ng of mercury. Dimethylmercury is not absorbed at all and methylmer-

TABLE 1

Recovery of mercury from activated charcoal after different desorption times

Time(s)	15	30	60	90	180
Recovery (%)[a]	30.2 ± 2.4	88.0 ± 0.7	95.0 ± 0.3	96.8 ± 0.3	97.7 ± 0.3

[a]Based on absorbance measurements for five determinations.

cury(II) chloride only partially [10]. On prolonged use, the silver coating is slowly converted to the sulfide by hydrogen sulfide and sulfur dioxide resulting in a slight decrease of response.

Gold-coated sand is the only one of the three collectors tested which is capable of collecting the total content of volatile mercury compounds in ambient air. The ratio of the absorption signal for 20 ng of mercury with respect to the direct injection signal is 0.720 ± 0.002, i.e. the response with gold is three time greater than with silver. Gold is not affected by sulfur compounds and so can be used almost indefinitely. The gold absorber retains 1—3 μg of mercury per gram before breakthrough occurs. The capacity of the collector depends on the rate of mercury collection and the size of the carrier granules; the value cited is a lower limit because the injections used contained mercury at higher concentrations than are found in ambient air.

Desorption temperature and flow rate

The effect of desorption temperature on peak height (%*T*) was examined at a constant flow rate of the carrier gas (0.100 l min^{-1}). Heating at temperatures lower than 450°C resulted in incomplete desorption and very long desorption times. Increasing the desorption temperature to 600°C caused a rapid increase in peak-height signals, but further increases to 800°C improved the signals only by about 20%. Changes in temperature above 600°C had little effect on the relative standard deviation. Obviously, sharper signals are obtained at higher temperatures.

The rate at which the nitrogen gas and the elemental mercury vapour flow through the optical cell is important (Fig. 4). At low flow rates, the temperature in the absorption tube and the average mercury concentration in the cell were higher, resulting in larger signals. This implies a longer time of analysis. The relative standard deviation increased with increasing flow rate.

To obtain sharp but reproducible responses, a compromise must be found between flow rate and desorption temperature. A flow rate of 0.100 l min^{-1} and a temperature of ca. 800°C were selected as the optimal conditions for analysis.

Calibration curves and detection limits

The calibration curve based on peak height shows a deflection above 20 ng. The curve based on the corresponding absorbance values is linear up to 65 ng (see Fig. 5). The slope of both curves is greatly affected by the mercury desorption rate. For better precision, the linear part of the calibration curve should be used; this can be done by changing the volume of air sampled as required, depending on the expected mercury content (Table 2). Because of the better linearity and the higher sensitivity, absorbance values were used for all further tests. The output of the MAS-50 apparatus (0—200 mV) is proportional to the percentage transmittance (100—0% *T*). Conversion to absorbance values can be done with a logarithmic converter [12].

Whenever the variables affecting the shape of the transmittance peaks

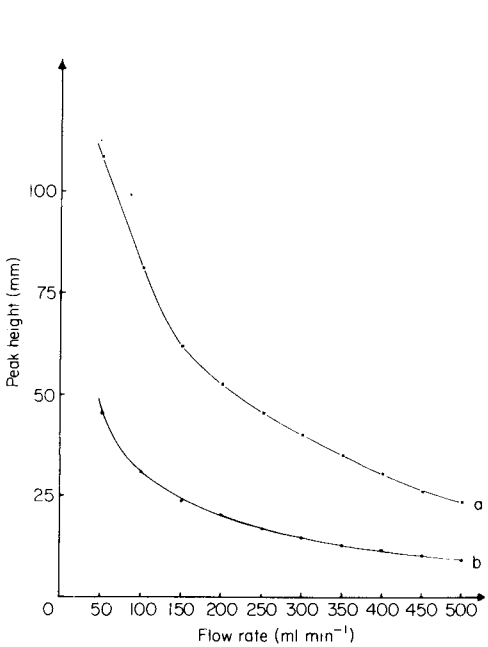

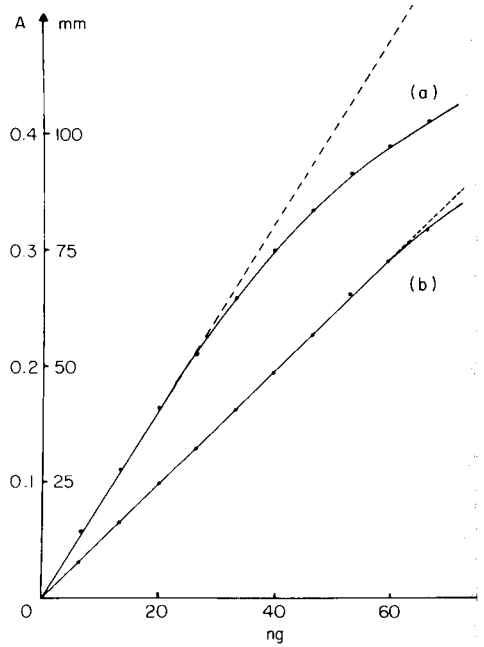

Fig. 4. Effect of flow rate on peak height for (a) 45 ng Hg and (b) 20 ng Hg.

Fig. 5. Calibration curves based on (a) peak height and (b) absorbance.

cannot be controlled carefully, integrated peak areas should be measured. Integrated peak areas can be obtained by cutting and weighing the recorded signals or more precisely by use of a digital integrator [13, 14].

The detection limit, defined as the concentration corresponding to the signal three times higher than the average noise level, was determined by the absorbance method. At 0.100 l min^{-1} and 800°C and with 10 × expansion of the recorder scale, the detection limit is 0.1 ng (standard deviation, 10%). This amount corresponds approximately to 50 l of ambient air or to a sampling period of 15—20 min at the flow rate used. The reproducibility increases with increasing mercury levels. Above 1 ng a relative standard deviation of ca. 1% can be obtained. For lower mercury levels, the response can be doubled by using a gas-stop technique: during the thermal desorption step, carrier gas is not passed through the apparatus; then after total release of mercury (30s), the gas flow is re-started and the absorbance is measured.

Interferences

Because of the collection technique used, and the two-step desorption procedure, no interfering effects were found. Water did not interfere but it can condense on the quartz windows of the optical cell. Wet absorption tubes can be dried before analysis by heating at 50°C without detectable loss of mercury.

TABLE 2

Results of field sample analysis

	Sample size (m^3)	Mercury content (ng m^{-3})
Location A (university laboratories)		
Polarography lab	0.005	2616
Purification room	0.005	1610
(ventilated)	0.005	1448
	0.005	1498
office	0.020	205
Location B ("uncontaminated" building)		
Lab	0.300	158
	0.250	151
Office	0.250	99
Room (recent mercury spillage)	0.175	789
Computer room	0.250	54
Reactor hall	0.250	56
Location C (outdoor urban environment)		
Day 1	3000	7.3
2	3000	7.4
3	3000	7.0
4	3000	7.4
5	3000	6.7

Analysis of field samples

Several air samples were taken from areas with different degrees of contamination. The results of the analyses summarized in Table 2 include only the volatile mercury content in ambient air. Particulate mercury compounds were not measured; the determination of mercury as aerosol implies collection on filters. Two possibilities for analysis have been described, i.e. wet digestion and pyrolysis [10, 15]. Digestion with nitric acid in a Teflon bomb is unsuitable because of the long decomposition time, possible mercury losses and large reagent blanks, and the necessity for a second apparatus based on reduction-aeration [16]. Pyrolysis of the filter at 600°C was found to be more efficient but serious interfering effects occurred because of compounds also collected on the filter. A procedure for sampling and determination of particulate mercury compounds is presently being developed.

The authors thank M. Nagels for technical assistance. One of the authors (R. D.) is indebted to the "Instituut voor Wetenschappelijk Onderzoek in Nijverheid en Landbouw-IWONL" for financial support.

REFERENCES

1 J. M. Wood, Environmental Pollution bv Mercury in J. N. Pitts Jr. and R. L. Metcalf, Advances in Environmental Science and Technology, Wiley-Interscience, Vol. 2, 1979, p. 39.
2 Mercury in the Environment, Environ. Sci. Technol, 4 (1970) 890.
3 A. F. Jepsen, Measurements of Mercury Vapor in the Atmosphere in E. L. Kothny, Trace Elements in the Environment, American Chemical Society, (1973), 81.
4 C. H. James and J. S. Webb, Bull. Inst. Mining Met., 691 (1964) 633.
5 Y. Kimura and V. L. Miller, Anal. Chim. Acta, 27 (1962) 325.
6 Y. Matsumura, Atmos. Environ., 8 (1974) 1321.
7 S. J. Long, D. R. Scott and R. J. Thompson, Anal. Chem., 45 (1973) 2227.
8 J. D. Aubort, H. Rollier and A. Ramuz. Trav. Chim. Aliment. Hyg., 68 (1977) 155.
9 J. Scullman and G. Widmark, Int. J. Environ. Anal. Chem., 2 (1972) 29.
10 R. S. Braman and D. L. Johnson, Environ. Sci. Technol., 8 (1974) 996.
11 P. Kivalo, A. Visapää and R. Bäckman, Anal. Chem., 46 (1974) 1814.
12 J. D. Aubort and R. Ramuz, Trav. Chim. Aliment. Hyg., 68 (1977) 151.
13 G. W. Kalb, At. Absorpt. Newsl., 9 (1970) 84.
14 R. J. Thomas, R. A. Hangstrom and E. J. Kuchar, Anal. Chem., 44 (1972) 512.
15 P. E. Trujillo and E. E. Campbell, Anal. Chem., 47 (1975) 1629.
16 W. R. Hatch and W. L. Ott, Anal. Chem., 40 (1968) 2085.

Analytica Chimica Acta, 107 (1979) 169—175

DETERMINATION OF ALKYLMERCURY COMPOUNDS IN FISH TISSUE WITH AN ATOMIC ABSORPTION SPECTROMETER USED AS A SPECIFIC GAS CHROMATOGRAPHIC DETECTOR

RAGNAR BYE* and PER E. PAUS

Central Institute for Industrial Research, Oslo 3 (Norway)

(Received 12th October 1978)

SUMMARY

Atomic absorption spectrometry is used as a specific gas chromatography detector in the determination of alkylmercury compounds in fish. An electrical furnace "cracks" the organic mercury molecules in the chromatographic effluent. An extraction procedure has been developed which improves the precision of the method. The detection limit is 0.3 ppm of mercury for 0.5-g samples.

The determination of organic mercury compounds in biological material has been described by a number of authors [1]. West$\phi\phi$'s methods [2] have formed the basis of the gas chromatographic techniques, and several variations have been described, all involving extraction of alkylmercury halides. A cleanup procedure is necessary to remove fatty acids and amino acids, which could otherwise poison the column. The cleanup is achieved by adding to the organic phase a reagent, such as sodium sulphide [3], cysteine [2], sodium thiosulphate [4] or glutathione [5], which forms a strong water-soluble alkylmercury complex to extract the mercury complex into the aqueous phase. A halide is added to the aqueous phase, and the alkylmercury halides formed are re-extracted into an organic phase. Aliquots of this phase are finally injected into the gas chromatograph.

When direct gas chromatographic methods are used in the determination of alkylmercury compounds, interferences are often a problem, especially with the electron capture detector, which is very sensitive to other halogen compounds. Some workers have solved this problem by utilizing atomic absorption as a specific mercury detector. Gonzales and Ross [6] burned the effluent in an oxygen atmosphere and led the gases through a MAS 50 mercury analyzer (an atomic absorption instrument). Longbottom [7] cooled the gases from the flame ionization detector and led the gases through such a mercury analyzer, but reported that it was less sensitive than the electron capture detector for dialkyl mercury compounds.

---

*Current address: University of Oslo, Department of Chemistry, Oslo 3 (Norway).

In this paper a method is described in which the effluent from the column is led through a steel tube in a furnace at a temperature at which the organic mercury molecules are cracked. The products are then led through a 10-cm quartz cuvette placed in the beam from a hollow-cathode lamp in an atomic absorption spectrometer.

For many of the methods described, the calibration curves have been obtained from measurements of peaks from pure standard solutions of organic mercury compounds. There are doubts about the correctness of such a procedure, because it does not take into account the fact that appreciable amounts of mercury may be lost during the many extraction steps used in the analysis, especially in work with small samples and small volumes. A standard addition procedure should be used for calibration, and the standard organic mercury solution should be added as early as possible in the procedure. The method (described below) is a modification of that of Longbottom et al. [4]. The precision achieved is greater than that obtained by previous workers because of improvements in the extraction sequence.

EXPERIMENTAL

Apparatus and operating conditions

A schematic diagram of the apparatus is shown in Fig. 1. A Perkin-Elmer model 800 gas chromatograph was used for all experiments. The following operating conditions were found to be satisfactory: column, 10% SP 2300 on Chromosorb W 80—100 mesh; oven temperature 145°C; inlet temperature 200°C; carrier gas, nitrogen at a pressure of 3.5 k Pa cm^{-2} measured at the g.c. inlet; flow-rate, 90 ml min^{-1}.

The furnace was made by winding a nichrome resistance wire around a quartz tube 6 cm long, 4 mm o.d., 2 mm i.d. This unit was placed inside another quartz tube (7 cm long, 8 mm o.d., 6 mm i.d.). The nichrome wire coil was connected to a 0—230-V Variac transformer. The circuit was equipped with a voltmeter and ammeter. The furnace was operated at about 10 V and

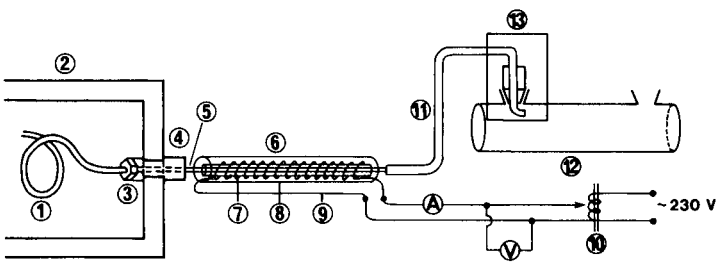

Fig. 1. The complete apparatus for measuring organic mercury compounds in gas chromatographic effluents. (1) Column, stainless steel; (2) gas chromatograph; (3) g.c. oven; (4) Teflon joint; (5) stainless steel tube; (6) electrical furnace; (7) inner quartz tube; (8) outer quartz tube; (9) resistance wire; (10) Variac transformer; (11) PVC tube; (12) 10-cm quartz cuvette; (13) inlet device for the cuvette (see Fig. 2).

2.3 A; the temperature was then about 620°C (see also Fig. 4). From the end of the stainless steel tube, a PVC tube led to the inlet device (Fig. 2) for the cuvette.

To homogenize the sample, a Bellco No. 1977 12-ml graduated tissue grinder was used (Fig. 3).

The Perkin-Elmer model 303 atomic absorption spectrometer was run at the 254-nm mercury line. Deuterium background correction was essential. The signals were recorded on a Perkin-Elmer 159 chart recorder.

Reagents and standard solution

All reagents were of analytical-reagent grade. The water was freshly distilled.

Bromine reagent. Potassium bromide (360 g) was dissolved in 700 ml of water. Concentrated sulfuric acid (110 ml) was added to 100 ml of water. After cooling to room temperature, the solutions were mixed and made up to 1 l with water.

Potassium iodide, 3 M. The solution must be kept dark and cooled.

Standard organic mercury solution (20 ppm Hg per compound). The following salts were weighed on a microbalance: 25.03 mg of methylmercury chloride (CH_3HgCl), 26.43 mg of ethylmercury chloride (C_2H_5HgCl) and 31.22 mg of phenylmercury chloride (C_6H_5HgCl). The salts were transferred to a 1-l volumetric flask, dissolved in benzene and made up to volume with the same solvent.

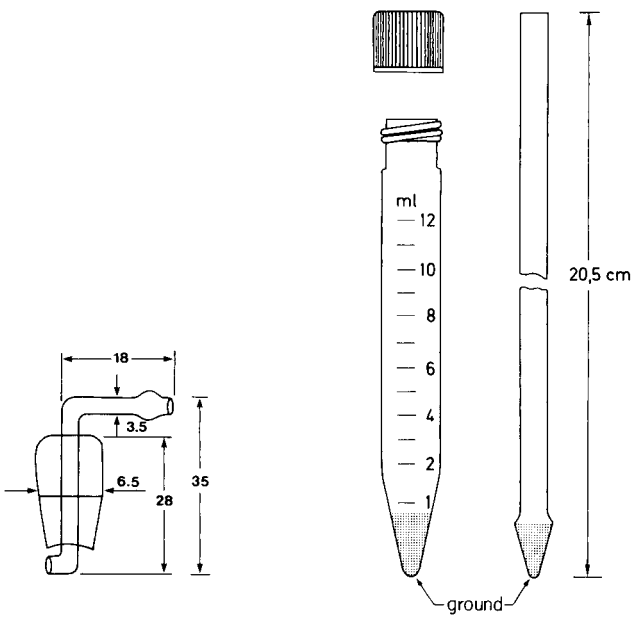

Fig. 2. Inlet device for the cuvette. Measurements in mm.

Fig. 3. Graduated tissue grinder, "Bellco" No. 1977, 12-ml.

Procedure for determination of organic mercury compounds in fish

Three weighed 0.5-g portions of frozen fish were transferred to three tissue grinders, 0.5 g of 1 M copper sulphate solution was added to each, and 50-and 100-μl of the standard mercury solution were added to two of the samples. To each sample 2 ml of bromine reagent were added, and the samples were homogenized well. After homogenization, the rod was lifted carefully from the solution and rinsed with water until the total volume of sample, reagents and water was exactly 7 ml. Toluene (3.5 ml) was pipetted into each solution, the grinders were shaken for 2 min, and the mixture was centrifuged for 10 min at 2000 rpm.

A 3-ml portion of each toluene phase was pipetted into one of three centrifuge tubes, with a separate pipette for each sample. To the residue in each grinder, 3.5 ml of toluene was added and the operation repeated, the 3.0-ml portion of each toluene phase being transferred, with the same pipettes as before, to the appropriate centrifuge tube. To each tube, 2.0 ml of 5×10^{-3} M sodium thiosulphate solution was added. These were shaken for 2 min and centrifuged for 15 min.

Graduated pipettes (2 ml), equipped with Peleus balloons, were inserted through the organic phases into the lower aqueous phases, and as much aqueou phase as possible (but equal volumes of 1.6—1.9 ml) was taken from each tube, starting with the tube in which the cloudy layer between the phases was thickest. These volumes were transferred to three centrifuge tubes, and the same volumes of potassium iodide solution were added to each. From that moment the solutions had to be kept in the dark. Benzene (1.0 ml) was added to each tube; the tubes were shaken vigorously for 2 min and centrifuged for 10 min. Each benzene phase was transferred to a 3-ml "Microflex" tube with screw cap and septum, containing a few crystals of anhydrous sodium sulphate. Suitable aliquots (5—25 μl) of the solutions were injected into the gas chromatograph and measured on the atomic absorption instrument optimized at 254 nm with deuterium background correction and suitable scale expansion.

RESULTS AND DISCUSSION

Effect of the furnace temperature

To establish the optimal furnace temperature, aliquots of a benzene solution containing a constant amount of methylmercury and ethylmercury chlorides were injected into the gas chromatograph at different Variac outputs. The temperatures of the injection port and column were not varied. The results (Fig. 4) show that the signals were almost independent of the furnace power consumption above 13 W. To ensure complete cracking, 23 W was chosen as the working power, giving a furnace temperature of about 620°C

Extraction procedure

Benzene was used as solvent in the final extraction. Although benzene has a molecular absorption maximum at 254 nm, which is also the mercury

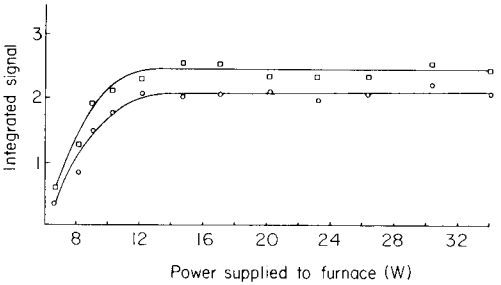

Fig. 4. Effect of power to the furnace on signals for aliquots with a constant amount of methylmercury (○) and ethylmercury chloride (□).

absorption line, spectral interference from benzene was easily avoided by selecting a column that separated benzene and alkylmercury compounds almost completely. Complete separation is important, because the deuterium background corrector cannot compensate for the large absorption from benzene. One reason for using benzene was that its polarity allowed easy dissolution of the alkylmercury halides for preparing the standard solution. Benzene can be obtained very pure; this is important because the solvent must be free from alcohols which can cause alkyl—alkoxy exchange in the organomercury compounds.

In the procedure described, 3.5 ml of toluene was added but only 3.0 ml was transferred to the next tube. Some mercury is therefore lost at this stage. This procedure was chosen because it increased the reproducibility of the method considerably, although the detection limit was poorer; in these determinations improvement of the precision was considered to be more important. The same argument is also valid for the other extraction volumes recommended. The stability constants given by Schwarzenbach and Schellenberg [8] were used to calculate the yield of the several complexing reactions in the procedure; these yields indicated that every reaction is almost quantitative.

Determination of alkylmercury compounds in a fish sample

Alkylmercury compounds in a fish were determined as described. Only methylmercury (not ethyl- or phenyl-mercury) was detected; typical examples of the peaks obtained are shown in Fig. 5. The peaks were measured in three ways: by measuring the peak heights, by peak triangulation, and by cutting and weighing the chart paper. These methods gave almost identical results, so that measuring the peak height is recommended.

The calibration curves showed linear ranges up to 10 ppm Hg for methylmercury and ethylmercury chlorides in mixtures. From these graphs, the fish samples was found to contain 2.2 ppm of mercury as methylmercury.

In order to assess the reproducibility of the method, four samples were taken from one fish (from the same tissue area). To each sample, 50 μl of

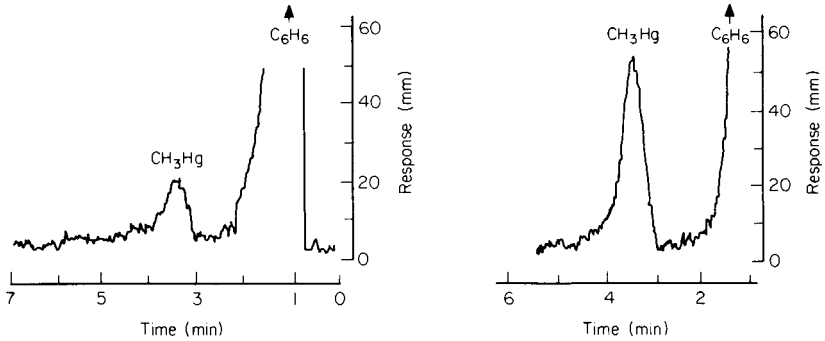

Fig. 5. Peaks obtained from (a) the fish sample, and (b) the sample with 2.32 ng Hg added as CH_3HgCl. Ethylmercury and phenylmercury peaks did not appear in the sample chromatogram, therefore peaks for these compounds after standard addition are not shown

standard organic mercury solution was added, and the whole procedure was applied to each sample. Four aliquots of the benzene phase from each sample were injected into the gas chromatograph, hence 16 measurements were made. The peak heights, mean values and standard deviations for each sample are given in Table 1. These data were used in calculating the overall precision of the method. The standard deviation of the pooled data was 2.1 mm. The weighted mean for the pooled data was 98.8 mm, hence the relative standard deviation for the whole method was 2.15%. The absolute detection limit of the method was about 3.5×10^{-9} g mercury. If 25 μl of solution is injected into the chromatograph and the size of the sample is 0.5 g, this is equivalent to 0.3 ppm of mercury in the sample.

TABLE 1

Measurements of peak heights (mm) for four samples, [a]with four injections for each sample

Injection No.	Sample			
	1	2	3	4
1	95.5	99.5	98.5	96.5
2	95.0	96.5	97.5	101.0
3	99.5	98.0	99.0	100.5
4	98.0	102.0	101.5	101.5
x	97.0	99.0	99.1	99.9
s	2.1	2.3	1.7	2.3
s_r(%)	2.2	2.3	1.7	2.3

[a]The sample contained only methylmercury. The total amount of mercury injected into the chromatograph was 5.5×10^{-8} g Hg (in 25 μl).

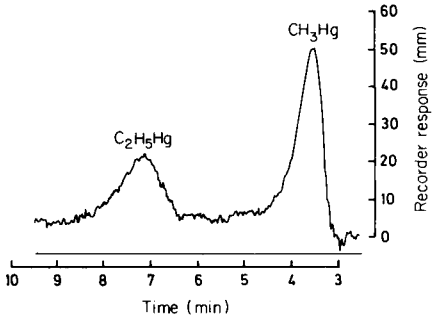

Fig. 6. Peaks from a sample containing both methylmercury and ethylmercury. The ethyl peak is the smaller.

Applications

The method described can be used not only for determinations of methylmercury, but also for other alkylmercury compounds. An example of responses for methylmercury and ethylmercury in a sample is shown in Fig. 6. The method is not restricted to fish samples, but should be useful for all kinds of biological materials. However, it is important that the fat content is low, otherwise the cloudy layer between the toluene and the aqueous thiosulphate phase will be too thick.

REFERENCES

1 J. A. Rodriguez-Vazquez, Talanta, 25 (1978) 299.
2 G. Westøø. Acta Chem. Scand., 20 (1966) 2131; 21 (1967) 1790; 22 (1968) 2277.
3 J. C. Gage, Analyst, 86 (1961) 457.
4 J. E. Longbottom, R. C. Dressman and J. C. Lichtenberg, J. Assoc. Off. Anal. Chem., 56 (1973) 1297.
5 K. Sumino, Kobe J. Med. Sci., 14 (1968) 115.
6 J. G. Gonzales and R. T. Ross, Anal. Lett., 5 (1972) 683.
7 J. E. Longbottom, Anal. Chem., 44 (1972) 1111.
8 G. Schwarzenbach and M. Schellenberg, Helv. Chim. Acta, 48 (1965) 28.

Analytica Chimica Acta, 107 (1979) 177—190

HOCHDISPERSE KIESELSÄURE ALS SPURENFÄNGER ZUR MULTI-ELEMENTANREICHERUNG

E. JACKWERTH* und J. MESSERSCHMIDT

Institut für Spektrochemie und angewandte Spektroskopie, D-4600 Dortmund (Bundesrepublik Deutschland)

(Eingegangen den 4. Dezember, 1978)

SUMMARY

Highly dispersed silicic acid as a trace collector for multi-element preconcentration

The purity and sorption properties of commercially available, highly dispersed silicic acid are investigated and compared with those of pure activated carbon for use as trace collectors. For a series of elements, the blanks and their fluctuations caused by silicic acid are significantly smaller, so that detection limits are improved. Activated carbon, however, is the better adsorbent for preconcentration of chelate complexes; in general, recoveries are much higher than are obtainable under similar conditions with the silicic acid. As examples of the applicability of hydrophobic silicic acid as a trace collector, about ten trace elements are preconcentrated from the pure aluminium, gallium and magnesium metals.

ZUSAMMENFASSUNG

Für die Anwendung als Spurenfänger wurden Reinheit und Sorptionseigenschaften handelsüblicher hochdisperser Kieselsäuren im Vergleich zu reiner Aktivkohle untersucht. Es zeigte sich, daß die durch Kieselsäure verursachten Blindwerte und Blindwertschwankungen für eine Reihe von Elementen wesentlich geringer sind als bei Aktivkohle, wodurch das Nachweisvermögen gegenüber der heute im Handel befindlichen Aktivkohlen verbessert wird. Aktivkohle ist jedoch für die Anreicherung von Chelatkomplexen das bessere Sorptionsmittel; die damit erzielbaren Anreicherungsausbeuten liegen im allgemeinen deutlich höher als in vergleichbaren Versuchen mit hochdisperser Kieselsäure. Am Beispiel der Anreicherung von etwa 10 Elementspuren aus den reinen Metallen Aluminium, Gallium und Magnesium wird die Andwendbarkeit hydrophobierter Kieselsäure als Spurenfänger nachgewiesen.

"Spurenfänger-Reaktionen" haben wegen ihrer hohen Leistungsfähigkeit seit langem ihren festen Platz in der Spurenanalyse. Prinzip ist die Fällung der Spuren in Gegenwart eines zu einigen Milligramm mit ausgefällten Niederschlags, des Spurenfängers; dieser wird im allgemeinen so ausgewählt, daß viele der interessierenden Elemente möglichst vollständig mitgerissen werden, um sie anschließend durch Filtrieren oder Zentrifugieren aus der Probenlösung abtrennen zu können [1, 2]. Die gewollt geringe Selektivität der Methode beruht vor allem darauf, daß für den Mitreißprozess oft gleichzeitig mehrere Mechanismen verantwortlich sind: Adsorption oder Chemisorption an der

geladenen oder ungeladenen Oberfläche des Spurenfängers, Spureneinbau ins Kristallgitter sowie "mechanisches" Mitreißen schwerlöslicher Spurenverbindungen sind die hier bekanntesten Vorgänge. Zur Leistungsfähigkeit tragen auch die verhältnismäßig einfache Handhabung der Methode sowie die selbst bei extrem geringen Spurenkonzentrationen zu erzielenden hohen Anreicherungsausbeuten bei: Schon die klassischen Regeln von Fajans und Erdey-Grúz [3] und Hahn und Imre [4] z.B. sagen, daß die Vollständigkeit von Mitreißvorgängen von der Konzentration der Spurenlösung unabhängig sein können.

Trotz ihrer zahlreichen Vorteile besitzt diese Anreicherungstechnik jedoch einen in manchen Fällen entscheidenden Nachteil: Die Elemente des eingesetzten Niederschlags gelangen im weiteren Verlauf der Analyse als neue Matrix mit ins Spurenkonzentrat und können hier Störungen bei der Spurenbestimmung verursachen. Zu bedenken ist auch, daß mit dem Spurenfänger eingeschleppte Verunreinigungen zu einer merklichen Belastung der Blindwerte führen können. Vom Prinzip her günstiger ist es deshalb, solche Stoffe als "Mitreiß-Reagenzien" zu verwenden, die unter den Arbeitsbedingungen als inert angesehen werden können. Hierzu gehören etwa die in Säure praktisch unlöslichen Silberhalogenide, von deren geladener Oberfläche adsorbierte Spurenverbindungen vollständig wieder abgelöst werden können [5—7]. Ähnlich wirken Ionenaustauscher [2] oder die zur Spurenanreicherung ebenfalls vielseitig verwendbare Aktivkohle [8]. Ein besonderer Vorteil bei der Verwendung von Aktivkohle mit ihrem guten Adsorptionsvermögen liegt darin, daß eine saubere Trennung von Spuren und Matrix meist schon dann erzielt wird, wenn man die mit einem geeigneten Gruppenreagenz versetzte Probenlösung lediglich durch eine dünne Kohleschicht filtriert. Gegenüber den "klassischen" Techniken, bei denen der Spurenfänger in der Probenlösung ausgefällt und nachfolgend abgetrennt wird, ergibt diese Arbeitsweise eine wesentliche Vereinfachung und Beschleunigung des Anreicherungsprozesses. Vielfach lassen sich dabei auch in Wasser leicht lösliche Spurenverbindungen adsorptiv anreichern, was die Palette der nutzbaren Reagenzien erweitert und den Selektivitäts-Spielraum für den Analytiker beträchtlich vergrößert. Insgesamt wird die Spurensorption damit häufig zu einer vorteilhaften Alternative zur Extraktion.

Eingeschränkt wird die Anwendung von Aktivkohle als Spurenfänger jedoch in der Reinststoffanalyse, und zwar durch den oft störenden Eigengehalt der Kohle an Verunreinigungen. Auch bei den reinsten heute im Handel erhältlichen Sorten findet man für einige Elemente (z.B. Fe, Mn, Mg) noch Gehalte von 100 ppm und darüber. Zum Glück sind zahlreiche andere Metallionen in weit geringerer Konzentration enthalten, so daß die Blindwertbelastungen hier vielfach in noch tragbaren Grenzen bleiben. Versuche, Aktivkohle aufzureinigen, erbrachten bisher noch wenig befriedigende Ergebnisse. Dies zeigten eigene Untersuchungen mit HCl und HNO_3 als Extraktionsmittel [8] sowie neuere Arbeiten von Vanderborght und Van Grieken, in denen die Kohle mit 48 %iger HF und nachfolgend mit 12 M HCl mehrere Tage geschüttelt wurde

[9]: Der Aschegehalt als Maß für die Gesamtverunreinigungen geht zwar merklich zurück, die Gehalte der großen Zahl analytisch interessanter Schwermetallionen verringern sich aber durch diese Behandlung meist nur auf etwa ein Fünftel. Offensichtlich befindet sich ein Teil der Spuren nicht-auswaschbar im Innern der Kohlepartikel verteilt. Ihre weitgehende Entfernung gelingt allenfalls unter Zerstörung der aktiven Oberfläche. Wir sind deshalb der Meinung, daß ein auch für die extreme Spurenanalyse geeignetes Material am ehesten durch Aktivieren einer aus einer hochreinen organischen Verbindung hergestellten Ausgangskohle erhalten werden kann. Weiterhin bleibt die Möglichkeit, nach anderen Spurenfänger-Materialien Ausschau zu halten, die in ihren Sorptions-Eigenschaften der Aktivkohle vergleichbar, in Bezug auf ihre Reinheit jedoch wesentlich besser sind. Als Ansatz in Dieser Richtung kann die Verwendung spezieller Kieselgele [10] oder mit geeigneten chelatbildenden funktionellen Gruppen behafteter Gläser [11, 12] bzw. Kieselgele [13—15] angesehen werden.

In der vorliegenden Arbeit wurden die Reinheit und Sorptionseigenschaften verschiedener hochdisperser Kieselsäuren im Vergleich zu handelsüblicher Aktivkohle untersucht. Am Beispiel der Multi-Elementanreicherung aus einigen Reinstmetallen wurde die Anwendbarkeit für die praktische Analyse getestet.

PHYSIKALISCHE EIGENSCHAFTEN UND REINHEIT DER VERWENDETEN SORPTIONSMITTEL

Die folgend referierten Daten über physikalische Eigenschaften der in dieser Arbeit verwendeten Sorptionsmittel entstammen im wesentlichen einer Arbeit von Wagner und Brünner [16] sowie Schriften der Hersteller bzw. Lieferfirmen [17, 18], die zum Teil umfangreiche Übersichten über die zugehörige Originalliteratur enthalten.

Aktivkohle. (Merck, Darmstadt; Art.-Nr. 2186) Spezifische Oberfläche, etwa 800 $m^2 g^{-1}$; Methylenblautiter nach DAB 6, 14; Korngröße, 97% < 90 μm [19].

Hochdisperse Kieselsäure. (Aerosil, Degussa, Frankfurt/M): Aerosil ist ein Siliciumdioxid mit kugelförmigen Partikeln, das aus $SiCl_4$ durch Hydrolyse in der Wasserstoff—Luft-Flamme gewonnen wird. Aus einer größeren Zahl unterschiedlicher Typen wurden folgende zwei für unsere Versuche ausgewählt.

Aerosil 380. Spezifische Oberfläche (nach BET), 380 ± 30 $m^2 g^{-1}$; mittlere Korngröße, 7 μm. Das Material ist hydrophil und reagiert in wäßriger Suspension schwach sauer. Es besitzt in geringem Umfang Mikroporen. Die an der Partikeloberfläche befindlichen SiOH-Gruppen sind zu chemischen Umsetzungen befähigt. Weiterhin wurden Ionenaustausch-Reaktionen mit organischen und anorganischen Kationen sowie Sorptionsvorgänge für zahlreiche Verbindungen, u.a. für eine Reihe von Farbstoffen, beobachtet. Je nach Reaktivität der sorbierten Stoffe können dafür unspezifische (physikalische) oder spezifische Sorptionsmechanismen (Chemisorption) diskutiert werden. Wasserstoffbrücken scheinen für die Bindung von Molekülen eine wichtige Rolle zu spielen. Interessant ist ferner, daß in Wasser dispergierte Aerosil-Teilchen zur Anode wandern, also negativ geladen sind.

Aerosil R 972. Spezifische Oberfläche (nach BET), 120 ± 30 $m^2 g^{-1}$; mittlere Korngröße, 16 μm; durch Umsetzung der —OH-Gruppen mit Dimethyldichlorsilan hergestellte hydrophobe Kieselsäure, bei der etwa 75% der oberflächenständigen Silanolgruppen durch Dimethylsilylgruppen ersetzt sind. Chemisorptions-Vorgänge wie an hydrophilem Aerosil werden dadurch ausgeschaltet. Das Material wird von Wasser praktisch nicht mehr benetzt, sehr gut dagegen von organischen Verbindungen. Durch ihre unterschiedliche Verteilung im Zweiphasensystem Wasser/Tetrachlorkohlenstoff kann man leicht prüfen, ob hydrophiles oder hydrophobes Aerosil vorliegt.

Untersuchungen zur Reinheit der Sorptionsmittel

Zur Bestimmung des Eigengehalts an den für unsere Arbeiten interessanten Elementspuren wurden die Sorbentien mit Säure vollständig aufgeschlossen. Nachfolgend wurden die Spuren unter Berücksichtigung der Reagenzienblindwerte durch Flammen-AAS ("Injektionsmethode") [20, 21] bestimmt.

Aktivkohle. 0,5 g wurden mit 2 ml 96 %iger H_2SO_4 und 1 ml 65 %iger HNO_3 im Quarzbecher zum Sieden erhitzt, wobei weitere Salpetersäure bis zum vollständigen Aufschluß der Kohle tropfenweise zugesetzt wurde. Die klare und farblose Lösung wurde mit Wasser in einen 5-ml Meßkolben übergespült und mit Wasser zur Marke ergänzt.

Aerosil 380 bzw. R 972. 0,25 g wurden mit 1 ml 40 %iger HF und 1 ml 65 %iger HNO_3 im Teflonbecher abgeraucht. Die Lösung wurde bis zur Trockne eingeengt; der Rückstand wurde in 2,0 ml 20 %iger HNO_3 gelöst.

Die Ergebnisse der Analysen sind in Tab. 1 zusammengestellt. Analysendaten

TABELLE 1

Eigengehalte der Sorbentien an Elementspuren. Die mit "<" bezeichneten Werte sind die Garantiegrenzen für Reinheit [23]

Element	Spurengehalt ($\mu g\ g^{-1}$)		
	Aktivkohle	Aerosil R 972	Aerosil 380
Ag	<0,2	<0,2	<0,2
Bi	<2	<3	<2
Cd	<0,1	<0,1	<0,08
Co	<0,6	<0,4	<0,3
Cr	1,3	<2	<1
Cu	18	<0,2	<0,1
Fe	156	1,6	1,1
Ga	<4	<4	<3
In	<2	<2	<2
Mg	90	0,7	<0,08
Mn	150	<0,2	<0,2
Ni	1,9	<0,5	<0,4
Pb	2,3	<1	<0,9
Tl	<1	<1	<0,8
Zn	3,4	0,3	0,4

für weitere Elemente sowie für Aktivkohle anderer Hersteller siehe [9, 22]. Die tabellierten Werte zeigen, daß Aktivkohle durch Spuren wie Cu, Fe, Mg, Mn, Ni, Pb und Zn zum Teil wesentlich stärker verunreinigt ist, als die vergleichend untersuchten Kieselsäuren. Mit Ausnahme der Werte für Fe und Zn lagen die Spurengehalte hier unterhalb der Nachweisgrenzen, so daß lediglich die Garantiegrenzen für Reinheit $c_G = 6 \cdot \sigma_B$ als höchstmögliche Elementgehalte aus den Meßwertschwankungen der Spurenbestimmung errechnet werden konnten [23]. Das Nachweisvermögen der Flammen-AAS reicht für die Mehrzahl der untersuchten Elemente nicht aus, um "echte" Analysenwerte zu erhalten. Zu beachten ist, daß bei Einsatz von jeweils 50 mg Sorptionsmittel zur Spurenanreicherung entsprechend den Arbeitsvorschriften, allenfalls mit einem Zwanzigstel der in Tab. 1 angegebenen Spurenmengen als Blindwerte zu rechnen ist.

Die bei Verwenden von Aerosil R 972 anstelle von Aktivkohle erzielbare Verbesserung im Nachweisvermögen vergleichbarer Verbundverfahren zeigen die Werte der Tab. 2. Hier wurden in jeweils 25 Parallelversuchen unter Anlehnung an die Anreicherungsvorschrift (siehe weiter unten) je 50 mg Sorptionsmittel aus einer Suspension auf ein kleines Papierfilter gesaugt, nach dem Trocknen bei 120°C vom Filter geschabt und einer Säurebehandlung unterworfen: für Aktivkohle, mit 1 ml 65 %iger HNO_3 bis zur Trockne abgeraucht und Rückstand mit 2,0 ml 20 %iger HNO_3 aufgenommen und zentrifugiert (Meßlösung); für Aerosil, mit 600 µl 36 %iger HCl und 200 µl 65 %iger HNO_3 bis zur Trockne abgeraucht und Rückstand mit 1,0 ml 65 %iger HNO_3 und 1,0 ml Methanol/Wasser (1 + 1) aufgenommen und zentrifugiert (Meßlösung). Aus den Streuungen der durch Flammen-AAS (Injektionsmethode) gemessenen Elementsignale wurden die 3σ-Grenzen berechnet. Da Probenmaterial bei diesen Versuchen nicht eingesetzt wurde, können die tabellierten Daten allerdings nur als Schätzwerte für Nachweisgrenzen angesehen werden, sie lassen aber einen Vergleich der Sorptionsmittel in Bezug auf die Blindwertbelastung von Anreicherungsprozessen zu.

TABELLE 2

Aus den Streuungen der Sorptionsmittel-Blindwerte errechnete 3σ-Grenzen als Schätzwerte für die Nachweisgrenzen der Anreicherung und Spurenbestimmung durch Flammen-AAS (Die tabellierten Werte beziehen sich auf die Meßlösung)

Element	Nachweisgrenze (µg ml^{-1})		Element	Nachweisgrenze (µg ml^{-1})	
	Aktivkohle	Aerosil R 972		Aktivkohle	Aerosil R 972
Bi	0,5	0,5	Mg	0,7	0,03
Cd	0,01	0,01	Mn	0,4	0,03
Co	0,08	0,08	Ni	0,08	0,08
Cu	0,06	0,02	Pb	0,2	0,2
Fe	0,9	0,05	Pd	—	0,2
In	0,6	0,5	Zn	0,08	0,06

UNTERSUCHUNGEN ZUM SORPTIONSVERMÖGEN HOCHDISPERSER KIESELSÄUREN

Verglichen mit Aktivkohle ist die spezifische Oberfläche der bei unseren Untersuchungen verwendeten Kieselsäuren deutlich geringer. Dementsprechend kann man erwarten, daß der durch Oberflächenaktivität bedingte Anteil an der Sorption von Spurenverbindungen beim Übergang von Aktivkohle zu Aerosil zurückgeht. Insbesondere das weitgehende Fehlen von Mikroporen dürfte hier eine Rolle spielen.

Auf der anderen Seite zeichnen sich die eingesetzten Kieselsäuren durch einen sehr geringen Teilchendurchmesser aus. Man kann deshalb annehmen, daß die dichtere Packung dieser Teilchen beim Durchsaugen von Probenlösungen wie ein Mikrofilter wirkt, welches auch sehr kleine Partikel schwerlöslicher Spurenverbindungen zurückhält. Dieser Mechanismus für die Anreicherung von Elementspuren ist etwa bei den Chelaten mit Ammoniumpyrrolidindithiocarbamidat als Komplexbildner anzunehmen: Solange die Gesamtmenge der mit diesem Reagenz ausgefällten Elemente noch im Bereich oberhalb von etwa 100 μg liegt, findet man unter geeigneten Arbeitsbedingungen eine zumeist quantitative Anreicherung der Elemente Bi, Cd, Co, Cu, Fe, In, Ni, Pb, Pd, Tl und Zn, auch wenn die vorhandene Menge einzelner dieser Elemente sehr viel geringer ist. Unterhalb von 100 μg Gesamt-Spurenmenge gehen die Ausbeuten vor allem von Zn und Cd jedoch rasch zurück, und auch In und Tl werden schließlich nicht mehr vollständig angereichert. Sollen diese problematischen Spuren aus sehr reinen Materialien durch Sorption an Aerosil abgetrennt werden, so empfiehlt es sich, ein analytisch weniger interessantes Element in Mengen von etwa 100 μg als "primären Spurenfänger" zuzugeben, es gemeinsam mit der zu bestimmenden Elementgruppe auszufällen und abzufiltrieren. Störungen der nachfolgenden Spurenbestimmung durch das Zusatzelement können wegen der geringen Menge des Zusatzes im allgemeinen vernachlässigt werden. Ähnliche Abhängigkeiten der Anreicherungsausbeuten von der vorhandenen Gesamt-Spurenmenge beobachtet man auch beim Filtrieren von mit Fällungsmitteln versetzten Probenlösungen durch Membranfilter unterschiedlicher Porenweiten [24].

Wie aus zahlreichen Untersuchungen an in Wasser leicht löslichen Chelaten hervorgeht, geht die Sorptionsleistung der hochdispersen Kieselsäuren jedoch über eine bloße Mikrofiltration hinaus. Dies zeigen auch die Ergebnisse der Tab. 3. Dazu wurden wäßrige Lösungen (75 ml) mit je 10 μg der Elemente Cd, Co, Cu, Ni und Zn mit Natriumacetat auf pH 8—9 eingestellt und mit einem Komplexbildner versetzt (1 mg 1,10-Phenanthroliniumchlorid bzw. Xylenolorange in wenig Wasser gelöst oder 0,5 ml Hexylamin bzw. Benzylamin) Im Falle der Verwendung von Aktivkohle wurden die so behandelten Spurenlösungen durch mit 50 mg Kohle gleichmäßig beschichtete Filter gesaugt; die Kieselsäure wurde in gleichen Mengen den Lösungen zugesetzt; die Suspensionen wurden anschließend 15 min gerührt und dann zentrifugiert. Die sorbierten Spurenanteile wurden nach Säurebehandlung der Sorptionsmittel durch Flammen-AAS bestimmt.

TABELLE 3

Sorbierte Anteile löslicher Spurenverbindungen
(Arbeitsvolumen: 75 ml; pH-Wert: 8—9; Sorptionsmittel-Menge: 50 mg; Spuren-Mengen: je 10 μg)

Reagenz	Sorptionsmittel	Ausbeute der Anreicherung (%)				
		Cd	Co	Cu	Ni	Zn
1 mg 1,10-Phenanthrolin	Aktivkohle	91	57	31	12	84
	Aerosil R 972	91	74	>95	19	92
	Aerosil 380	77	39	80	39	79
1 mg Xylenolorange	Aktivkohle	81	>95	>95	75	82
	Aerosil R 972	3	7	7	4	3
	Aerosil 380	<0,5	<1	<1	4	13
0,5 ml Hexylamin	Aktivkohle	92	93	87	86	83
	Aerosil R 972	84	88	89	85	88
	Aerosil 380	72	63	69	81	35
0,5 ml Benzylamin	Aktivkohle	92	89	90	93	73
	Aerosil R 972	82	93	80	95	90
	Aerosil 380	61	77	60	85	36

Die Zahlenwerte für die Sorptionsraten der Tab. 3 lassen einige Schlüsse zu, die durch weitere, hier im Einzelnen nicht aufgeführte Untersuchungen mit anderen Elementen und Komplexbildnern gestützt sind, und die für die Anwendung der verschiedenen Sorptionsmittel als Spurenfänger von Interesse sein können.

(1) Aktivkohle ist für lösliche Chelatkomplexe in der Regel das bessere Sorptionsmittel. Wie frühere Arbeiten gezeigt haben, gilt dies vor allem dann, wenn die Chelatbildnermoleküle Atomgruppen mit π-Orbitalen enthalten, die mit dem Elektronensystem der Kohlemoleküle in Wechselwirkung treten können. Das abweichende Verhalten der Phenanthrolinchelate beruht auf den besonderen Bindungsverhältnissen des konjugierten Elektronensystems im Molekül des Chelatbildners, wodurch — wie wir meinen — Kohle und Metallion in Konkurrenz zueinander treten. Näheres hierzu siehe [25].

(2) Unter den zwei verwendeten Aerosilen liefert das hydrophobe Material meist die höheren Sorptionswerte. Wir führen dies auf die für organische Verbindungen bessere Benetzbarkeit der hydrophobierten Teilchenoberfläche zurück.

(3) Eine gewisse Bedeutung für die Sorption von Chelaten an Kieselsäure könnte auch die für das hydrophile Aerosil beschriebene negative Oberflächenladung haben. Mit Ausnahme der ungeladenen Xylenolorange—Chelate handelt es sich bei den hier untersuchten löslichen Metallverbindungen um kationische Komplexe. Diese liefern dementsprechend einen zum Teil recht hohen Sorptionsgrad, während die Xylenolorange—Chelate von beiden Aerosilen praktisch nicht sorbiert werden.

Multi-Elementanreicherung aus den Metallen Aluminium, Magnesium und Gallium mit hydrophobem Aerosil als Spurenfänger

Um die praktische Anwendbarkeit hochdisperser Kieselsäure als Spurenfänger zu demonstrieren, wurden Arbeitsvorschriften für die Analyse der Metalle Aluminium, Magnesium und Gallium ausgearbeitet. Aufgrund der in den Vorversuchen erwiesenen besseren Sorptionsfähigkeit wurde dazu das hydrophobierte Aerosil R 972 eingesetzt. Als Gruppenreagenz wurde Ammoniumpyrrolidindithiocarbamidat (APDTC) verwendet. Es wurden Arbeitsbedingungen gewählt, unter denen die Analyse dieser Probenmaterialien — vom unterschiedlichen Löseprozess einmal abgesehen — nach einer einheitlichen Anreicherungsvorschrift gelingt.

Reagenz—Aerosil-Suspension. APDTC (1,000 g) wird in 50,0 ml Methanol gelöst. Anschließend werden 1,000 g Aerosil R 972 sowie 50,0 ml Wasser zugesetzt. Durch intensives Rühren wird ein Absetzen der Suspension verhindert. Die Suspension muß täglich frisch angesetzt werden.

Arbeitsvorschrift zu Spurenanreicherung. Die je nach Probenmaterial unterschiedlich herzustellende Probenlösung (siehe weiter unten) wird mit 5,0 ml Reagenz—Aerosil-Suspension versetzt, 15 min intensiv gerührt und anschließend zentrifugiert. Die überstehende Lösung wird durch ein mittelhartes Papierfilter (ϕ 23 mm) gesaugt (zerlegbare Filternutsche nach Mattaei; Schleicher & Schüll, Dassel/Einbeck); das abzentrifugierte, mit den Spurenverbindungen beladene Aerosil wird mit wenig Wasser auf das Filter gespült. Durch dieses Vorzentrifugieren der Suspension wird der nachfolgende Filtriervorgang wesentlich beschleunigt. Filter und Niederschlag werden in einem 10-ml Becherglas etwa 30 min bei 120°C getrocknet. Der Niederschlag wird vom Filter geschabt und mit 200 μl 65 %iger HNO_3 und 600 μl 36 %iger HCl bis zur Trockne abgeraucht. Der erkaltete Rückstand wird mit 1,0 ml 65 %iger HNO_3 und 1,0 ml Methanol/Wasser-Gemisch (1 + 1) aufgenommen. Der Methanolzusatz hat dabei die Aufgabe, die Benetzung des Aerosils zu verbessern. Nach kurzem Zentrifugieren werden die angereicherten Elemente in aliquoten Teilen von je 50 μl durch Flammen-AAS (Injektionsmethode [20, 21]; Acetylen—Luft-Flamme) bestimmt. Parallel zur Spurenanreicherung werden unter analogen Bedingungen die Reagenzienblindwerte ermittelt und berücksichtigt.

Zur Herstellung von Eichlösungen werden 5,0-ml Anteile der Reagenz—Aerosil-Suspension entsprechend der Arbeitsvorschrift durch Papierfilter gesaugt. Nach Trocknen und Abschaben des Aerosils werden die Eichzusätze in Form verdünnter Spurenlösungen mit Mikroliter-Pipetten dosiert. Die Proben werden — wie beschrieben — mit Königswasser abgeraucht und entsprechend weiterbehandelt.

Anreicherung von Bi, Cd, Co, Cu, Fe, In, Ni, Pb, Pd und Zn aus Aluminium

In Vorversuchen wurden zunächst die zur vollständigen Anreicherung der Elementspuren erforderlichen Mengen an APDTC und an Aerosil ermittelt. Dazu wurden jeweils mehrere Einwaagen von 5 g reinem Aluminiummetall

nach Spurenzusatz entsprechend der nachfolgenden Arbeitsvorschrift gelöst und analysiert. Abbildung 1 zeigt die Abhängigkeit der Spurenausbeute vom APDTC-Zusatz bei Einsatz von je 100 mg Aerosil R 972, Abb. 2 den Einfluß der Aerosil-Menge bei Verwenden von je 50 mg APDTC. Bei allen nachfolgenden Untersuchungen wurden Aerosil bzw. APDTC in Mengen von je 50 mg eingesetzt.

In Tab. 4 sind die für diese Bedingungen erhaltenen Ausbeuten der Spurenanreicherung zusammengestellt. Für die Untersuchungen in den unteren Spurenbereichen war es erforderlich, aus dem zur Verfügung stehenden Aluminium die Verunreinigungen vor allem durch Cu, Fe, Ni, Pb und Zn zu entfernen, bevor definierte Spurenmengen erneut zudotiert wurden. Hierzu wurden die entsprechend der Vorschrift hergestellten Probenlösungen mit je 50 mg APDTC versetzt und durch mit 50 mg Aktivkohle beschichtete Filter gesaugt. Die so aufgereinigten Filtrate wurden anschließend als Probenmaterial verwendet.

Wie bereits erwähnt, werden Spuren Zn und Cd nur dann quantitativ angereichert, wenn die Gesamtmenge aller mit APDTC ausgefällten Elemente größer als etwa 100 µg ist. Andernfalls muß der Spurengehalt durch Zusatz eines bei der Analysenaufgabe nicht gefragten Elements aufgestockt werden. Cu und Co sind dazu besonders gut, In ist weniger gut geeignet. Abbildung 3 zeigt den Verlauf der Anreicherung von je 0,5 µg Cd bzw. Zn aus 5 g aufgereinigtem Aluminium in Gegenwart ansteigender Cu—Gehalte.

Bei der Bestimmung von Pd können Schwierigkeiten auftreten, wenn der Aerosil-Rückstand nach Abrauchen mit Königswasser bei hoher Temperatur auf der Heizplatte verbleibt. Offensichtlich bewirken Zersetzungsprodukte des APDTC die Reduktion des Palladiums; es verbleibt bei der nachfolgenden

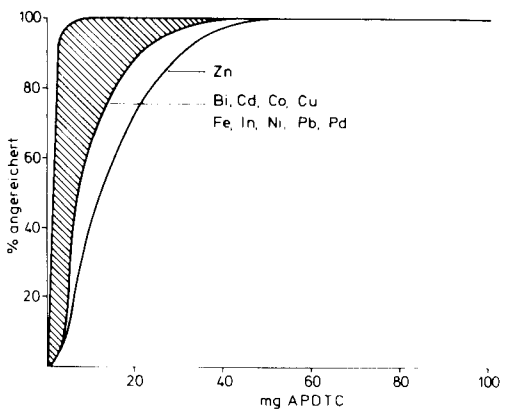

Abb. 1. Abhängigkeit der Anreicherung von 50 µg der angegebenen Elemente aus Lösungen von 5 g Reinst-Aluminium vom Reagenz-Zusatz (Sorptionsmittel: 100 mg Aerosil R 972).

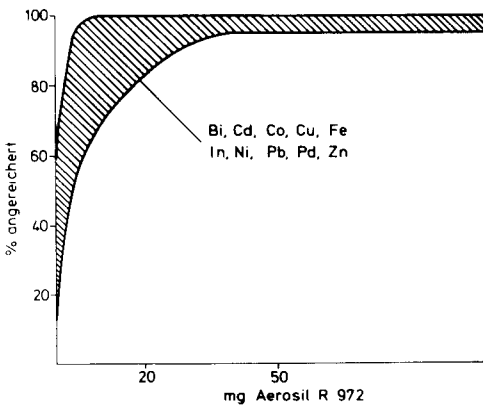

Abb. 2. Abhängigkeit der Anreicherung von 2,5 µg der angegebenen Elemente aus Lösungen von 5 g Reinst-Aluminium von der Sorptionsmittel-Menge (Reagenz: 50 mg APDTC).

TABELLE 4

Analyse von Aluminium

Element	Eichumfang ($\mu g\ g^{-1}$)	Ausbeute der Anreicherung (%)	Spurengehalt ($\mu g\ g^{-1}$)	rel. Standard-abweichung (N = 10) (%)
Bi	0,2—10	95	1,2	2,8
Cd	0,2—10	95	0,21	3,4
Co	0,05—10	>95	0,22	5,9
Cu	0,06—10	>95	2,5	2,4
Fe	0,2—10	95	2,0	5,1
In	0,2—10	>95	1,0	2,3
Ni	0,05—10	95	0,20	3,5
Pb	0,2—10	>95	0,90	2.2
Pd	0,1—10	>95	0,20	8,9
Zn	0,2—10	>95	0,40	6,3

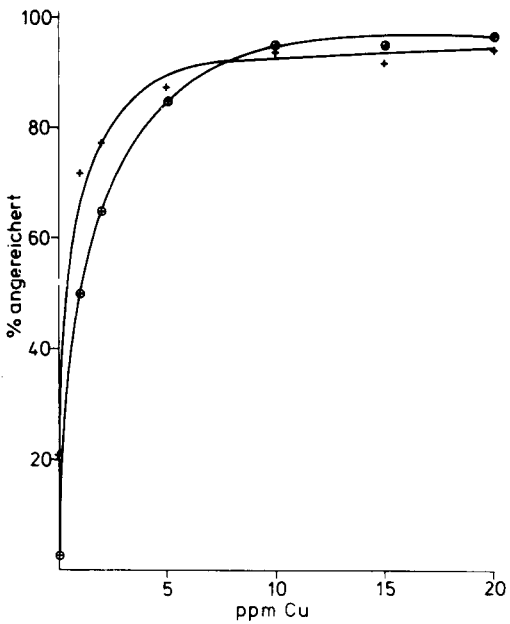

Abb. 3. Abhängigkeit der Anreicherung von je 0,5 μg Cd^{2+} (+) und Zn^{2+} (⊕) aus Lösungen von 5 g Reinst-Aluminium vom Kupfergehalt des Probenmaterials.

Säurebehandlung des Aerosils weitgehend ungelöst im Rückstand. Diese Schwierigkeiten deuten sich auch in der für die Pd-Anreicherung und -Bestimmung erhöhten Standardabweichung an (Tab. 4). Um Pd-Verluste zu vermeiden sollte das zugesetzte Königswasser deshalb nur bis gerade zur Trockne abgeraucht werden.

Arbeitsvorschrift. Zur Erhöhung der Lösegeschwindigkeit wird auf dem zerspanten Aluminium zuvor eine geringe Menge Silber zementiert. Dazu wird die Einwaage von 5 g Al mit 0,5 ml einer 0,01 M $AgNO_3$-Lösung und 25 ml 0.5 M H_2SO_4 versetzt. Anschließend wird bis zur beginnenden Wasserstoff-Entwicklung erwärmt. Die Säure wird dekantiert, das Metall wird mehrfach mit Wasser gewaschen.

Unter Kühlung in Wasser wird das Aluminium in 100 ml 20 %iger HCl gelöst; nach vollständigem Lösen werden 5 ml 65 %iger HNO_3 zugesetzt. Die Lösung wird so weit auf der Heizplatte eingeengt, bis das Aluminiumsalz auszukristallisieren beginnt. Dann wird mit Wasser auf 100 ml verdünnt und auf Raumtemperatur abgekühlt. Unter starkem Rühren werden tropfenweise 20 ml 25 %iger Ammoniaklösung zugegeben. Beim anschließenden Erwären auf 60—70°C geht das dabei ausgefällte Hydroxid wieder klar in Lösung. Nach Abkühlen auf Raumtemperatur werden 20 ml 2,5 M Natriumacetatlösung zugesetzt, wobei sich ein pH-Wert von etwa 3,0 einstellt. Die mit Wasser auf etwa 150 ml verdünnte Lösung wird nach der Arbeitsvorschrift zur Spurenanreicherung weiter behandelt. Angaben zur Aufreinigung der Natriumacetatlösung sind in der Arbeitsvorschrift für Gallium enthalten.

Anreicherung von Bi, Cd, Co, Cu, Fe, In, Ni, Pb und Zn aus Magnesium

Für die Analyse des Magnesiums wurden die beim Aluminium als optimal ermittelten Reagenz- und Sorptionsmittel-Mengen übernommen. Weiterhin war es auch hier erforderlich, in analogen Versuchen das als Probenmaterial eingesetzte Magnesium aufzureinigen sowie Cu als zusätzlichen Spurenfänger für Cd, In und Zn zuzusetzen, falls die Gesamt-Spurenmenge im Probenmaterial wesentlich unterhalb von 100 μg liegt. Werte für die Anreicherung und Bestimmung der Elementspuren sowie die statistischen Daten des Analysenverfahrens sind in Tab. 5 zusammengestellt.

Arbeitsvorschrift. Einwaagen von 5 g zerspantem Magnesium werden im

TABELLE 5

Analyse von Magnesium

Element	Eichumfang ($\mu g\ g^{-1}$)	Ausbeute der Anreicherung (%)	Spurengehalt ($\mu g\ g^{-1}$)	rel. Standard-abweichung ($N = 10$) (%)
Bi	0.1—10	>95	0,39	3,3
Cd	0,04—10	95	0,38	3,0
Co	0,04—10	95	0,13	8,1
Cu	0,04—10	>95	0,40	1,5
Fe	0,04—10	95	0,58	3,5
In	0,2—10	95	0,40	3,3
Ni	0,04—10	95	0,40	1,8
Pb	0,1—10	>95	0,39	3,3
Zn	0,04—10	95	0,38	5,6

250-ml Becherglas mit 35 ml Wasser sowie portionsweise unter Kühlen mit insgesamt 35 ml 37 %iger HCl versetzt. Gegen Ende des Löseprozesses wird 1 ml 65 %iger HNO_3 zugesetzt. Zur Entfernung überschüssiger HCl wird die Lösung auf etwa 30 ml eingedampft, dann mit Wasser auf etwa 100 ml verdünnt und auf Raumtemperatur abgekühlt. Es werden 20 ml 2,5 M Natriumacetatlösung zugesetzt, wobei sich ein pH-Wert von 5—5,5 einstellt. Die mit Wasser auf etwa 150 ml verdünnte Lösung wird nach der Arbeitsvorschrift zur Spurenanreicherung weiter behandelt. Angaben zur Aufreinigung sind in der Arbeitsvorschrift für Gallium enthalten.

Anreicherung von Bi, Cd, Co, Cu, In, Ni, Pb und Pd aus Gallium

Auch für die Analyse des Galliums wurden die beim Aluminium als optimal ermittelten Reagenz- und Sorptionsmittel-Mengen übernommen. Wegen der Hydrolyseempfindlichkeit des Galliums ist eine Spurenanreicherung in nur schwach saurer bis neutraler Probenlösung nicht möglich. Andererseits reicht die Komplexstabilität der meisten APDTC-Chelate nicht aus, um in stark sauren Lösungen brauchbare Anreicherungsausbeuten erzielen zu können. Auch die Überführung des Galliums in Hydroxokomplexe mit einer Spurenanreicherung in alkalischer Lösung verbietet sich, da die dazu erforderlichen Alkalihydroxide nicht in genügender Reinheit zur Verfügung stehen bzw. nur schwierig aufgereinigt werden können. Übrig bleibt die Maskierung der Matrix mit einem vorgereinigten preiswerten Komplexbildner, etwa mit Hilfe von Tartrat in ammoniakalischer Lösung. Tartrat kann auch in höher konzentrierter Lösung nach Zusatz von APDTC durch Filtration durch Aktivkohle leicht genügend weit aufgereinigt werden. Dasselbe gilt für das in den Arbeitsvorschriften für die Analyse von Aluminium bzw. Magnesium eingesetzte Natriumacetat.

Für die Anreicherung von Cadmiumspuren bei Gesamtspurenmengen unter etwa 100 μg ist auch beim Gallium der Zusatz eines Hilfsspurenfängers, z.B. von 100 μg Cu^{2+} oder Co^{2+} erforderlich; dies wurde bereits im Zusammenhang mit der Analyse von Aluminium ausführlich diskutiert. Für Spuren Fe und Zn bleiben die Anreicherungsausbeuten jedoch so gering, daß auf eine Bestimmung verzichtet wurde. Wie ebenfalls beim Aluminium beschrieben, wurde das für unsere Untersuchungen vorhandene Gallium zur Spurenanreicherung in den in Tab. 6 angegebenen unteren Elementbereichen vor der Dosierung kleiner definierter Spurenmengen aufgereinigt. Analysenwerte sowie die statistischen Daten des Analysenverfahrens sind in Tab. 6 zusammengestellt.

Arbeitsvorschrift. Galliummetall (5 g) werden in 50 ml 20 %iger HCl unter portionsweisem Zusatz von insgesamt 7,5 ml 65 %iger HNO_3 in der Wärme gelöst. Die Lösung wird auf etwa 10—15 ml eingeengt, wobei die Galliumsalze auskristallisieren. Mit Wasser wird bis auf etwa 50 ml verdünnt; dann werden 75 ml 1 M Natriumtartratlösung zugegeben. Die Lösung wird auf etwa 70°C erwärmt, wobei der ausgefällte Niederschlag wieder klar in Lösung geht. Nach Abkühlen auf Raumtemperatur gibt man unter Rühren 10 ml 25 %iger Ammoniaklösung zu, wobei das zunächst ausfallende Galliumhydroxid wieder aufgelöst wird. Die Lösung wird auf Raumtemperatur abgekühlt, mit Wasser

TABELLE 6

Analyse von Gallium

Element	Eichumfang ($\mu g\ g^{-1}$)	Ausbeute der Anreicherung (%)	Spurengehalt ($\mu g\ g^{-1}$)	rel. Standardabweichung ($N = 10$) (%)
Bi	0,1—10	>95	0,36	6,8
Cd	0,1—10	94	—	—
Co	0,08—10	>95	0,39	3,3
Cu	0,08—14	>95	0,37	6,0
In	0,2—60	>95	0,49	7,8
Ni	0,08—12	94	0,38	3,7
Pb	0,1—20	94	0,37	6,7
Pd	0,1—10	>95	0,38	4,4

auf etwa 150 ml verdünnt und nach der Arbeitsvorschrift zur Spurenanreicherung weiter behandelt.

Zur Aufreinigung der Puffer- und Komplexbildner-Lösungen. Für Natriumtartrat (1 M Lösung), 230 g Natriumtartrat werden zu 1 l in Wasser gelöst. Es werden 10 ml einer wäßrigen 2 %igen Lösung von Ammoniumpyrrolidindithiocarbamidat zugegeben und durch ein mit 50 mg feinpulvriger reinster Aktivkohle beschichtetes Filter gesaugt.

Für Natriumacetat (2,5 M Lösung), 205 g Natriumacetat (wasserfrei) werden zu 1 l in Wasser gelöst. Es werden 10 ml einer wäßrigen 2 %igen Lösung von Ammoniumpyrrolidindithiocarbamidat zugegeben und durch ein mit 50 mg feinpulvriger reinster Aktivkohle beschichtetes Filter gesaugt.

LITERATUR

1 R. Bock, Methoden der Analytischen Chemie, Bd.1, Trennungsmethoden, Verlag Chemie, Weinheim/Bergstr., 1974.
2 O. G. Koch und G. A. Koch-Dedic, Handbuch der Spurenanalyse, Springer-Verlag, Berlin, Heidelberg, New York, 1974.
3 K. Fajans und T. Erdey-Grúz, Z. Phys. Chem., 158 (1932) 97.
4 O. Hahn und L. Imre, Z. Phys. Chem., 144 (1929) 161.
5 G. Graffman, Doktorarbeit, Bochum 1969.
6 H. Berndt, Doktorarbeit, Bochum 1975.
7 E. Jackwerth und G. Graffman, Fresenius Z. Anal. Chem., 251 (1970) 81.
8 E. Jackwerth, J. Lohmar und G. Wittler, Fresenius Z. Anal. Chem., 266 (1973) 1.
9 B. Vanderborght und R. Van Grieken, Anal. Chim. Acta, 89 (1977) 399.
10 G. Knapp, B. Schreiber und R. W. Frei, Anal. Chim. Acta, 77 (1975) 293.
11 K. F. Sugawara, H. H. Weetall und D. G. Schucker, Anal. Chem., 46 (1974) 489.
12 D. M. Hercules, L. E. Cox, S. Onisick, G. D. Nichols und J. C. Carver, Anal. Chem., 45 (1973) 1973.
13 D. E. Leyden und G. H. Luttrell, Anal. Chem., 47 (1975) 1612.
14 D. E. Leyden, G. H. Luttrell, W. K. Nonidez und D. B. Werho, Anal. Chem., 48 (1976) 67.
15 D. E. Leyden, G. H. Luttrell, A. E. Sloan und N. J. DeAngelis, Anal. Chim. Acta, 84 (1976) 97.

16 E. Wagner und H. Brünner, Angew. Chem., 72 (1960) 744.
17 Aerosil, Herstellung, Eigenschaften und Anwendung, Firmenschrift Degussa, Frankfurt/M.
18 Hydrophobes Aerosil, Herstellung, Eigenschaften und Anwendung, Firmenschrift Degussa, Frankfurt/M.
19 Merck, Darmstadt, persönliche Mitteilung.
20 E. Sebastiani, K. Ohls und G. Riemer, Fresenius Z. Anal. Chem., 264 (1973) 105.
21 H. Berndt und E. Jackwerth, Spectrochim. Acta, Part B, 30 (1975) 169.
22 H. A. van der Sloot, Netherlands Energy Research Foundation Report ECN-1 (1976).
23 H. Kaiser, Fresenius Z. Anal. Chem., 216 (1966) 80.
24 H. Berndt, unveröffentlicht.
25 E. Piperaki, H. Berndt und E. Jackwerth, Anal. Chim. Acta, 100 (1978) 589.

Analytica Chimica Acta, 107 (1979) 191—200

AN INVESTIGATION OF ATOM COLLECTION PHENOMENA IN THE ATOMIC ABSORPTION SPECTROMETRY OF COPPER

J. KHALIGHIE, A. M. URE and T. S. WEST*

The Macaulay Institute for Soil Research, Craigiebuckler, Aberdeen, AB9 2QJ (Gt. Britain)

(Received 30th November 1978)

SUMMARY

Analyte collection within a premixed air—acetylene flame for atomic absorption spectometric measurements is described. Copper species of the aspirated solution are collected for fixed periods of time on a water-cooled silica tube positioned within the flame, with the flame burning normally. At the end of a specified time, collection is stopped, the coolant water is quickly flushed out of the silica tube, and the copper species that evaporate into the analyzing radiation beam in the flame, and are atomized, are measured by atomic absorption at 324.8 nm. Aqueous and hydrochloric acid solutions were examined, and the effects of varying flame conditions, positions of the collector and signal measurement, etc., are discussed. A characteristic concentration of 0.0008 ppm was obtained for 0.01 ppm Cu^{2+} solution. With the same equipment in the absence of a collector tube, the value was 0.04 ppm. The presence of a 10,000-fold amount of Al^{3+} enhanced the sensitivity of the collection technique slightly.

In normal atomic absorption measurements in flames, the atoms pass rapidly through the analyzing beam of radiation in a uniform flow pattern. This is satisfactory where there is a sufficient number of atoms at any instant within the rapidly expanding flame gases. But, the residence time of atoms in the flame is very limited, ca. 10^{-3} s, and when the atomization process is slow or the population otherwise becomes sufficiently dilute, the absorption signals become correspondingly small. Any device that could increase the residence time of the atoms or temporarily accumulate species in the flame and then release them quickly for measurement should increase the signal. Ideally, one would like to use the flame as a medium for generating and preconcentrating atoms before the usual measurement stage.

The idea of an atom trap was realised by Stephens et al. [1] who placed a water-cooled silica tube in the flame, thus causing metal atoms or their precursor species in the flame to condense on the surface of the tube. When a sufficient number of atoms or their compounds had been collected, the coolant was ejected thus allowing the tube to warm up rapidly, so that it released its collected species to the flame. The transient signal from the generated atoms would be greater than that observed in the normal technique for the same analyte concentration, provided that the collection is reasonably efficient and

that the species can subsequently be released and atomized rapidly enough to produce measurable atomic absorption (or fluorescence) signals.

In the experiments described below, copper was used as the analyte because of its agricultural importance and its physical and spectroscopic properties. A water-cooled silica tube was used as the collector because its very low coefficient of thermal expansion (5×10^{-7} °C^{-1}) ensures that it can resist the repeated thermal shocks brought about by rapid alternation of the trapping and releasing cycles. Subsequent papers will deal with the behaviour of other species and will investigate different trap materials and other phenomena associated with in situ collection of species for atomic absorption/emission spectrometry.

EXPERIMENTAL

Apparatus

The absorption measurements were done with a Varian-Techtron AA6 atomic absorption spectrometer with a 0.5-nm spectral band-pass, and a Varian copper hollow-cathode lamp. The air pressure was set at 38 kg cm^{-2} throughout the measurements, and absorption was measured at 324.8 nm.

An air—acetylene burner head (20 cm slot) was adapted by fitting clamps to it by which the silica tube could both be held in the flame at various heights and adjusted laterally for centering in the flame. The normal adjustment facility on the instrument permitted the assembly to be moved vertically. A silica tube (4 mm o.d.) was positioned ca. 0.5 cm above the primary reaction zone of the flame and cold tap water was passed through the tube during collection (Fig. 1). After completion of the collection cycle, air was blown through the tube via the control tap system.

Procedure

In order to collect the analyte, each sample solution was aspirated normally into the flame for some time while cooling water passed through the silica tube at a rate of ca. 2.5 l min^{-1} so that an appreciable proportion of the analyte species condensed on the cool surface of the tube in the flame. The tem-

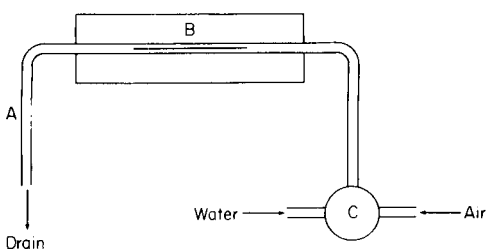

Fig. 1. Block diagram of silica tube atom trap (A), burner (B) and water/air control system (C).

perature of the inlet water was ca. 14°C; it rose to 15—16°C after passage through the tube in the flame. At lower flow rates, inefficient collection was observed particularly for metallic species more volatile than copper. After a preset interval, the sample solution was replaced by the blank solution and the water was flushed out of the tube rapidly by a blast of air via the control tap system. The air blast was shut off as soon as the water had been expelled. The surface of the tube heated up rapidly (ca. 10—12 s), the trapped species vaporized and the absorbance of the copper atoms was measured in the flame with the analyzing beam of the hollow-cathode lamp at grazing incidence on the upper surface of the silica tube. After complete release of the trapped species as shown by a zero absorbance signal, the next cycle of collection may be initiated without extinguishing the flame, by passing water through the tube again. Figure 2 shows the absorption signal obtained during the collection, A → B, of 0.1 ppm Cu^{2+} solution for 60 s followed by the insertion of the blank, B → C, and the release C → D.

RESULTS AND DISCUSSION

The silica tube was located ca. 0.5 cm above the primary reaction zone of the flame (i.e. ca. 1.0 cm above the burner head) since this appeared to allow good collection with minimal upset of the flame-flow characteristics. This setting of the burner-tube assembly, referred to as the 'burner', was used subsequently. Figure 3 shows the results of initial experiments involving collection

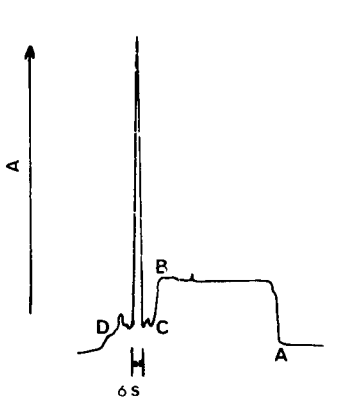

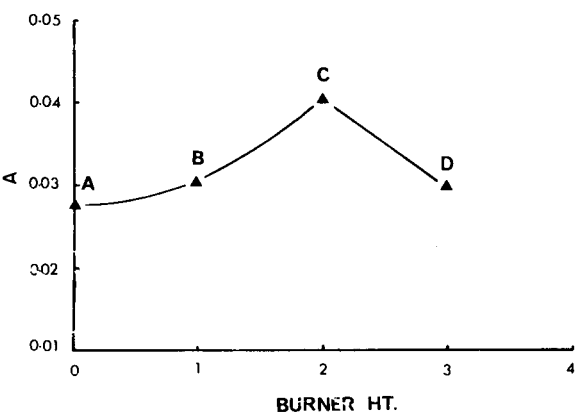

Fig. 2 (left). Peak release signal obtained following collection of 0.1 ppm Cu^{2+} in 0.1 M HCl for 1 min. The aspiration of the Cu solution begins at A. Collection ceases at B and the blank (water) is aspirated thereafter. The coolant water is switched off at C and back on again at D.

Fig. 3 (right). Collection of 0.1 ppm Cu^{2+} in 0.1 M HCl at various heights in the flame, *A*, *B*, *C* and *D* represents 2, 8, 25 and 37% obscuration of the beam by the upper parts of the collector tube. (The approximate height in mm above the lowest burner setting may be obtained by adding 3 to the numbers on the abscissa.)

from 0.1 ppm Cu^{2+} solution in 0.1 M HCl for 60 s. at increasing burner (3—7) heights i.e. at decreasing heights of measurement in the flame. The best peak signal from released atoms was obtained when the burner was raised into the beam so that there was about 25% obscuration of the light beam by the upper surface of the silica tube. This differs from the 10% figure recommended by Stephens et al. [1].

To clean the tube after each experiment, Stephens et al. sprayed 1 M HCl for 30 s into the flame immediately after the release of trapped analyte. To observe its effects, hydrochloric acid was incorporated in the Cu^{2+} solution in the present experiments and in the blank solution during the release. This was compared with the performance of aqueous solutions of Cu^{2+}, and the use of distilled water as a blank. The results (Table 1) show that the best characteristic concentration (sensitivity), standard deviation and percentage relative standard deviation were obtained for 0.1 ppm Cu^{2+} in 1 M HCl with HCl as the blank. The data suggest that the most efficient collection occurs from HCl media (B) and (C), and that the most reproducible conditions are obtained when the same medium is used for collection and blank solutions, (C) and (D).

The best characteristic concentration that could be obtained with this apparatus in the normal mode, i.e. without the silica tube in the flame, was 0.04 ppm. The collection technique for 60 s with 0.1 ppm Cu^{2+} solution was about three times more sensitive under the same conditions. As will be seen subsequently, the sensitivity is considerably greater for more dilute copper(II) solutions. A reason for the better sensitivity obtained with hydrochloric acid in the solutions is probably that it minimizes the formation of oxide on the tube by maximizing the copper-chloride ion-pairing in the clotlet particles in the flame. In the case of copper, it is virtually certain that the trapped species is predominantly copper metal. A bright film of metallic copper was seen on the tube when strong solutions were aspirated. Because of the desirability of limiting the aspiration of strong acids into the instrument, with the concomitant risk of contamination, the concentration of hydrochloric acid was reduced to 0.1 M; this gave almost the same sensitivity as 1 M HCl.

TABLE 1

Comparison of hydrochloric acid and water as collection and blank media during the collection/release of copper from 0.1 ppm solutions over a period of 60 s (Each result is the average of 6 readings.)

Media		Characteristic concentration[a] (ppm)	s	s_r (%)
Solvent	Blank			
(A) H_2O	1 M HCl	0.015	0.0036	12.4
(B) 1 M HCl	H_2O	0.014	0.0034	10.6
(C) 1 M HCl	1 M HCl	0.013	0.0019	5.7
(D) H_2O	H_2O	0.018	0.0018	7.0

[a]For 1% absorption (absorbance 0.0044).

To test the efficiency of collection from different dilutions, various concentrations of copper(II) in water and in 0.1 M HCl were collected for different lengths of time. The results (Fig. 4) show the enhancement in sensitivity that is obtained when 0.1 M HCl rather than water is used as the solvent and as the blank. Figure 4 also shows that the absorbance is almost linearly dependent on collection time for the more dilute copper(II) solutions (up to 10 min for 0.01 ppm Cu^{2+} in 0.1 M HCl). This differs somewhat from the findings of Stephens et al. [1], but there are sufficient differences between the thermal performances of the two apparatuses used to account for the divergence (see below). Figure 5 shows the effect of collection time (2—8 min) on the analytical growth curves for various concentrations of copper(II) in 0.1 M HCl.

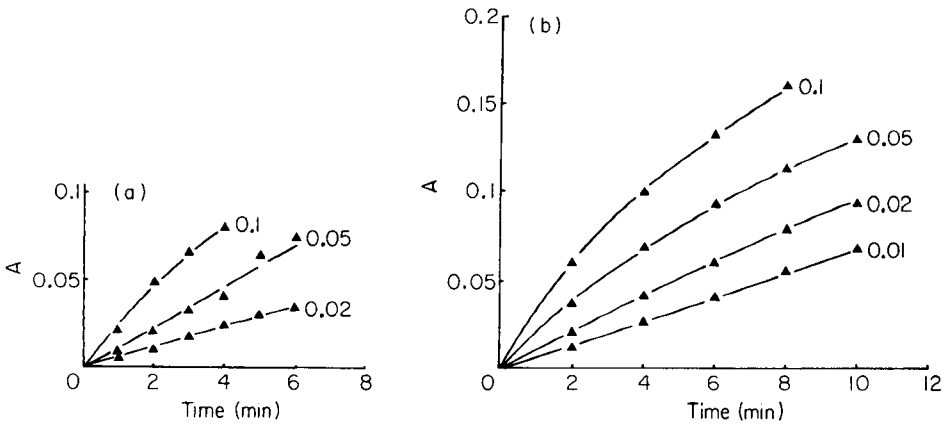

Fig. 4. Collection of 0.1—0.01 ppm Cu^{2+} as a function of time from (a) aqueous solutions (b) 0.1 M HCl solutions.

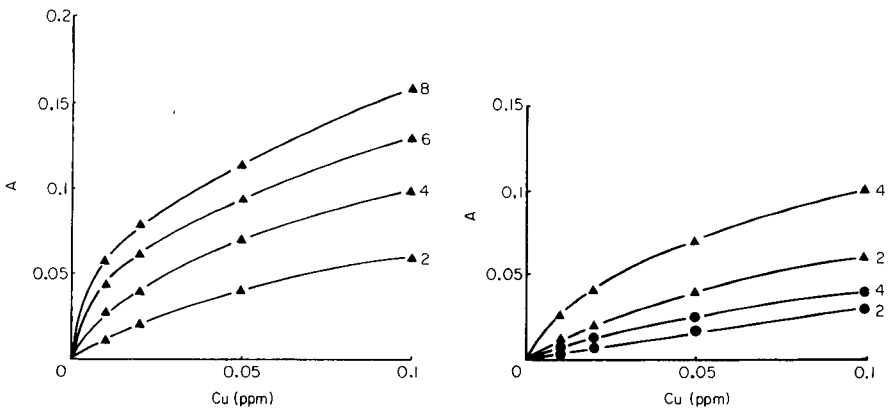

Fig. 5 (left). Collection of copper(II) from 0.1 M HCl as a function of concentration and collection time (2, 4, 6, 8 min).

Fig. 6 (right). Comparison of the collection of copper(II) on 4-mm (▲) and 7-mm (●) o.d. silica tubes with collection times of 2 and 4 min as indicated.

The effects of flame conditions

The effects of flame conditions on the trapping and release of copper were investigated by aspirating 0.1 ppm Cu^{2+} solutions and releasing in fuel-rich and lean flames for both aqueous and 0.1 M HCl media. In these experiments, the richness of the flame was restricted to a level such that no carbon deposited on the tube. In the lean flame, the fuel supply was reduced until the primary reaction zone became quite small and was bright blue as opposed to green in the fuel-rich experiments. The same air pressure was maintained in both series of experiments.

The best sensitivity was obtained when a fuel-rich flame was used for collection and release (Table 2). This could be due to the lower concentration of oxygen in such flames, where the degree of dissociation of oxide would be larger so that less copper oxide and more copper atoms would be collected on the surface of the tube. The slightly lower temperature of the fuel-rich flame could also have some slight influence, as could differences in flame size and burning velocities. The use of a fuel-rich flame when analyte species are being released is apparently not very important. The results for collection in a lean flame and release in a rich flame were not very different from those observed when both collection and release were done in a lean flame.

In the conventional atomic absorption technique, i.e. without the silica tube, no significant difference in absorbance was observed for 0.1 ppm Cu^{2+} in 0.1 M HCl between the lean and rich flames.

The relationship between sensitivity and copper(II) concentration for different collection times

Figure 5 shows the effect of collection time on the analytical growth curve for various concentrations of copper(II). The decreasing slopes of the growth curves, reflect the decreasing efficiency of collection as the concentration increases. For a 2-min collection time, the characteristic concentration was

TABLE 2

Effect of flame conditions on the trapping and release of 0.1 ppm Cu^{2+} from aqueous and 0.1 M HCl media with collection for 1 min

Flame condition		Peak absorbance	
Collection	Release	Aqueous	0.1 M HCl
Rich	Rich	0.024	0.030
Lean	Lean	0.018	0.020
Lean	Rich	0.018	0.023
Rich	Lean	0.022	0.029

ca. 0.004 ppm compared with 0.04 by the normal technique without collection. For an 8-min collection time, the value was about 0.0008 ppm. Thus gains of 10—50-fold in sensitivity can be obtained for dilute solutions with quite modest collection times. At higher concentrations, the improvement in sensitivity with collection is less than at these low concentrations, but the gains are still appreciable. The detection limit for collection from 0.1 M HCl was 0.0015 ppm, which again compares favourably with ca. 0.02 ppm for the normal technique.

Diameter of collecting tube

To test the effects of using silica tubes of wider diameter on collection efficiency, different copper(II) concentrations were collected for 2 and 4 min on a tube of 7-mm outer diameter, and the absorbance signals were measured in the usual way. The sensitivity of the technique was more than halved for the larger tube (Fig. 6).

It was certainly the case that the larger tube upset the normal flow pattern of the premixed air—acetylene flame to a much greater extent, and with some burner heads and with still larger tubes (10 mm), the flame was split so much that it did not re-unite immediately above the tube. Thus, even though the flame was not split by the 7-mm tube, it is possible that many of the released atoms bypassed the analyzing beam of radiation centred above the tube, thus yielding poorer sensitivities. In addition, there is little doubt that the larger tube takes appreciably longer to warm up during the release cycle so that the pulse of released atoms is broader and, therefore, shows lower peak absorption signals. On this basis, there is a case for examining narrower tubes with thinner walls.

Efficiency of trapping and location of free atoms in trapping flames

To establish what fraction of the atomic species in the flame was being collected, a measure (Y) of the number of atoms passing the cold collecting tube, i.e. not being collected, is needed, together with a measure (X) of the total number of atoms passing the tube while it is hot and assumed not to be collecting any atomic species. A reasonable measurement of Y and X was obtained as follows.

A blank solution and a 1 ppm Cu^{2+} solution in 0.1 M HCl were successively nebulized with the collector tube cooled continuously, and the respective absorbances (A and B, Table 3) were measured at different burner heights. The difference ($B - A$) is a measure of the free analyte not collected on the cold silica tube (Y). This experiment was repeated with a hot silica tube, i.e. with the cooling water flushed out and the tube allowed to heat up for over 30 s. The difference between the blank and sample solution absorbances (D — C, Table 3) gave a measure of X, the total number of atoms available for collection. Figure 7 shows how the tube obstructed the light beam as the burner was raised from the zero position, about 5 mm below the height normally used (setting 2, see Fig. 3), to a height of 17 mm. Between 9 and 10 mm the light

TABLE 3

Apparent percentage of free analyte around the collector tube at various height settings

Increasing burner height[a] (mm)	Cold tube				Hot tube		
	0.1 M HCl	Y	1 ppm Cu in 0.1 M HCl		0.1 M HCl	X	1 ppm Cu in 0.1 M HC
	A	$(B-A)$	B	% Free analyte	C	$(D-C)$	D
0	0.00	0.03	0.03	60	0.00	0.05	0.05
5	0.11	0.04	0.15	57	0.08	0.07	0.15
6	0.19	0.04	0.23	57	0.20	0.07	0.27
8	0.47	0.09	0.56	75	0.55	0.12	0.67
9	0.88		0.90	—[b]	1.14		1.15
10	1.22		1.23	—[b]	1.23		1.25
11	0.71	0.13	0.84	—[b]	0.76	0.03	0.79
12	0.68	0.14	0.82	—[b]	0.74	0.06	0.80
13	0.84	0.16	1.00	—[b]	0.80	0.10	0.90
14	0.83	0.05	0.88	50	0.63	0.10	0.73
15	0.57	0.06	0.63	100	0.43	0.06	0.49
16	0.38	0.07	0.45	100	0.33	0.07	0.40
17	0.08	0.36	0.44	100	0.31	0.08	0.39

[a]An assessment of the meaning of these height settings in terms of obscuration of the light beam by the silica tube may be seen in Fig. 7. [b]Obstruction of the light beam by the collecting tube.

beam was almost completely obscured by the tube, while at 12 mm (point X, Fig. 7) it was partially transmitted through the tube. At heights of 14—17 mm, the beam passed below the tube.

The percentage of free analyte may reasonably be calculated from the data in Table 3 as follows: % free analyte = $(B - A) \times 100/(D - C)$. Table 3 shows that at burner settings up to 6 mm above the zero position, almost 60% of the analyte from the 1-ppm Cu^{2+} solution bypassed the tube as free analyte, i.e. the trapping efficiency was ca. 40%. The sensitivities obtained with much more dilute solutions showed that the collection efficiency was considerably greater with 0.01 ppm solutions than with 0.1 ppm solutions.

At a setting corresponding to 8 mm, at which point the centre of the light beam passed immediately above the upper surface of the tube, the apparent percentage of free analyte increased sharply to 75%. This may be due to partial release of copper species, initially trapped on the lower surface of the tube, and a local build-up of high concentration as these are swept up closely around the periphery of the tube before being diluted by the flame gases. The figures obtained at settings of 9—13 mm were of no significance since the beam was then physically obstructed by the collector tube. As the beam began to pass below the tube (at 14 mm) a value of 50% free analyte was recorded; this

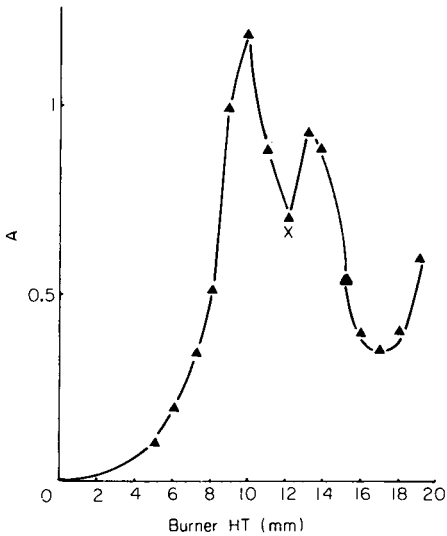

Fig. 7 (left). Obstruction of the light beam by the water-cooled collector tube in the flame at various height settings.

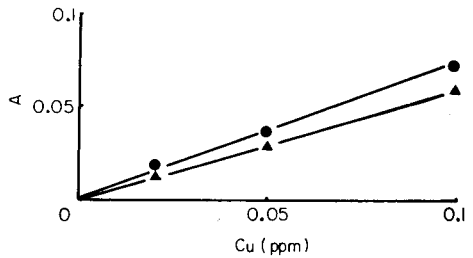

Fig. 8 (right). Analytical curves obtained by collection for 1 min for aqueous solutions in absence (▲) and presence (●) of 1000 ppm Al^{3+}.

rose sharply to 100% at settings in the area below the tube, and would be expected where no trapping can take place and where the flame flow dynamics are virtually normal.

The effect of aluminium on the collection technique

The effect of aluminium(III) was investigated for aqueous and 0.1 M HCl solutions of copper(II). First, 0.1 ppm Cu^{2+} was collected on the tube for 1 min and the signal from the released analyte was measured (Table 4, step 1). Then a 0.1 ppm Cu^{2+}—1000 ppm Al^{3+} solution was passed for 1 min and the resulting signal was measured upon release (step 2). At this point the tube had become coated with a white deposit of aluminium oxide. Copper (0.1 ppm) was then collected for 1 min on the coated tube and the signal again was measured on release (step 3). Finally, a 0.1 ppm Cu^{2+}—1000 ppm Al^{3+} solution was passed for 1 min and the absorbance was again measured (step 4) as before. The reason for the equal absorbance readings in step 1 is that these results were taken with two different silica tubes. It is reasonable to suppose that no two tubes will behave in exactly the same way because of differences in surface characteristics, wall thickness, etc. Normally the more sensitive result is obtained from 0.1 M HCl solutions.

In the normal atomic absorption technique, 100 ppm Al^{3+} depresses the signal for 0.1 ppm Cu^{2+} by ca. 10%, but Table 4 shows that in both water and in 0.1 M HCl the absorbance signal for copper increased when aluminium was present in the solution, although the enhancement was larger for aqueous solution. When the tube was previously coated with Al_2O_3, the signal increased

TABLE 4

The effect of 1000 ppm aluminium on the collection of 0.1 ppm Cu^{2+} from HCl and aqueous solutions on different tubes

Tube 1		Tube 2	
0.1 M HCl	Peak absorbance	Aqueous	Peak absorbance
(1) Cu^{2+}	0.030	Cu^{2+}	0.030
(2) Cu^{2+} + Al^{3+}	0.034	Cu^{2+} + Al^{3+}	0.036
Tube is coated ↓		Tube is coated ↓	
(3) Cu^{2+}	0.024	Cu^{2+}	0.044
(4) Cu^{2+} + Al^{3+}	0.032	Cu^{2+} + Al^{3+}	0.038

again for aqueous solutions, but decreased for 0.1 M HCl solutions. In step 4, the slight enhancement obtained (relative to step 1) was significant only for the aqueous solution.

Figure 8 shows a comparison of the analytical growth curves for Cu^{2+} alone and Cu^{2+} solutions containing 1000 ppm Al^{3+}. When the collector tube was previously coated with alumina before the copper solution was sprayed, the growth curve was almost identical to that for the copper—aluminium mixtures. It was also observed that the alumina-coated tubes released copper more rapidly than uncoated tubes, i.e. 6 opposed to 10 s. There did not, however, seem to be a significant narrowing of the contour of the signal peak that might account for the better signal. It seems highly probable that the alumina acts by providing a larger more active surface area for atom trapping.

Conclusions

The use of a water-cooled silica tube as a collector for copper atoms in an air—acetylene flame permits useful analyses to be performed by atomic absorption measurements on 0.01 ppm Cu^{2+} solutions, i.e. at and below the lowest level possible by the conventional technique. The characteristic concentration obtained with 0.01 ppm Cu^{2+} solution is more than 50 times better than that of the conventional technique. Copper is not particularly susceptible to interferences in atomic absorption spectrometry, but the presence of a 10,000-fold (concentration) amount of Al^{3+}, which interferes suppressively in the conventional technique, actually enhanced the sensitivity because of the effect of the alumina deposit on the surface of the collector tu

The thermal characteristics of the collector system used here are different from those reported by Stephens et al. [1]. Signal release for copper took 10—20 s, opposed to the 2—3 s reported by the earlier workers. This may be due partly to the use of thicker walled tubing in the present work, but it coul also be explained by the relative positions of the tube in the flame, both with respect to the analyzing beam of radiation and the height of the atom trap above the burner head.

REFERENCES

1 C. Lau, A. Held and R. Stephens, Can. J. Spectrosc., 21 (1976) 100.

Analytica Chimica Acta, 107 (1979) 201—209

ALGORITHM FOR DETERMINATIONS OF SODIUM, POTASSIUM, CALCIUM AND LITHIUM OVER WIDE CONCENTRATION RANGES BY FLAME EMISSION SPECTROMETRY

J. E. PATTERSON

Chemistry Division, DSIR, Lower Hutt (New Zealand)

(Received 6th December 1978)

SUMMARY

The application of atomic absorption spectrometers for flame emission determinations over wide concentration ranges, with the burner slot aligned parallel to the optical axis, is discussed. A large spectral bandwidth and an aperture reducing mask are necessary at high concentrations. A simple algorithm, conveniently used with programmable calculators, accurately relates concentration to intensity up to 1000 $\mu g\ cm^{-3}$ for Na and K, 200 $\mu g\ cm^{-3}$ for Ca and, less accurately, 500 $\mu g\ cm^{-3}$ for Li. Only two standards are required for determinations within the stated concentration ranges.

Modern atomic absorption spectrometers usually provide facilities for measuring flame emission signals. The merit of using such spectrometers for this purpose and the role of flame shape and burner configuration have been discussed by Koirtyohann and Pickett [1]. The use of a laminar-flow burner with its slot parallel to the optical axis was found to confer the same advantages in emission as in absorption, namely a greater signal, and for barium, an improvement in line-to-background emission intensity ratio. This is because less of the cooler outer zone of the flame is observed than when the burner slot is perpendicular to the optical axis. At higher analyte concentrations the burner slot is usually set perpendicular to the optical axis to preserve calibration linearity. The nebulizer uptake rate is sometimes reduced also.

This paper examines the application of an atomic absorption burner set with its slot parallel to the optical axis for the flame emission determinations of some alkali and alkaline earth metals at concentrations up to nearly 1 $mg\ cm^{-3}$. A simple algorithm is used to obtain concentrations from the measured intensities. This approach allows wide concentration ranges to be covered with only two standards, e.g. 0.5 and 100 $\mu g\ cm^{-3}$ for sodium determinations. Results obtained are usually within ± 3% of the actual concentration. Large numbers of samples can be analysed rapidly without dilution (especially if a programmable calculator or computer is interfaced directly) for major and minor components.

THEORY

If resonance lines are used, a plot of emission intensity against concentration will be linear at low concentrations but at higher concentrations the plot will curve towards the concentration axis and become parabolic [2—6]. At high concentrations the emission intensity is proportional to (concentration)$^{N-1}$ where N is about 2 for Na, Ca and K and 2.4 for Li [2]. For burner slot lengths of 50 or 100 mm, the transition region between the linear and parabolic regions occurs within an order of magnitude of 10 μg cm^{-3}.

Emission intensity may be plotted against concentration on log—log graph paper. The resulting plot usually has two linear segments, one with unit slope at low concentrations and the other with a slope of about 0.5 at high concentrations. A curved transition region links the two linear segments. In general, N^{-1} is the slope of the tangent to this plot. With experimental data the slope of the chord between successive standards is $(Nc)^{-1}$ and best approximates to the tangent at high and very low concentrations. As measurements for increasingly concentrated standards are plotted, Nc should reach a constant value Ns (Fig. 1). Several factors influence the experimental values obtained for Ns as indicated in the following paragraphs.

(a) Spectral bandwidth. The peak intensity of a resonance line has a maximum value, being no more than the intensity of a black body at the same wavelength and flame temperature [5]. Further increases in concentration result in more broadening which becomes the means by which more energy reaches the monochromator. The spectral bandwidth of the monochromator must be sufficiently wide to receive this energy, including the extremities

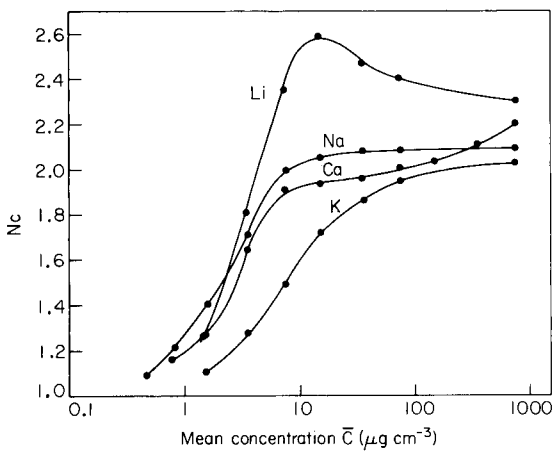

Fig. 1. The exponent Nc plotted against mean concentration $\bar{C}$. $\bar{C} = (C_1 + C_2)/2$ and $Nc = \ln(C_1/C_2)/\ln(I_1/I_2)$ where C_1 and C_2 are successive standards and I_1 and I_2 are the respective intensities. Table 1 gives the experimental conditions.

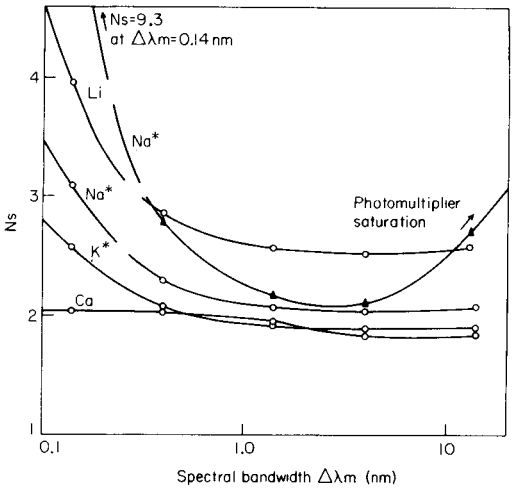

Fig. 2. The exponent *Ns* (limiting value of *Nc* at high concentrations) as a function of spectral bandwidth for Na, K, Ca and Li. The effect of increased concentration is also shown. Two standards, each showing full self-absorption are used in the calculation of *Ns*: (○) 100 and 50 μg cm^{-3}; (▲) 1000 and 500 μg cm^{-3}. Flames and wavelengths as in Table 1. Asterisks indicate that the doublet is transmitted at wider spectral bandwidth.

of the line (line wings), otherwise the calibration curve of intensity plotted against concentration flattens out, and approaches the concentration axis as self-reversal becomes dominant. Two specified standards have been used to determine the exponent *Ns* for various values of spectral bandwidth (Fig. 2). By using a more concentrated pair of standards the effect of concentration on *Ns* is shown for sodium.

(b) Photomultiplier saturation. In general the spectral bandwidth should increase as concentration increases to accommodate the increasing line width, but at large light intensities the output current of a photomultiplier may no longer be proportional to the incident light intensity as the last dynode potential may be changed by the high current flowing. In this case curvature increases and *Ns* exceeds 2 (Fig. 2). An aperture-reducing mask placed over the flame compartment entrance window can be used to reduce the light input and can also discriminate against the cooler outer zones of the flame where self-reversal occurs.

(c) Self-reversal. Self-absorption in a flame should lead to a value of 2 for *Ns* at high concentrations [3]. However, self-reversal causes more curvature and $Ns > 2$, because this process removes radiation at the centre of the line.

(d) Minor contributions. Mask aperture, flame composition and observation height all affect *Ns* to a minor degree. Delayed vaporization of the analyte in the flame may also have an effect. Flame inhomogeneities can modify *Ns* as observation of diluted zones will give an added linear response reducing *Ns* towards unity. An extended transition region is the result. This occurs in air—hydrogen flames in particular (Fig. 3), the flame being very narrow. Under an appropriate set of instrumental conditions, *Ns* is

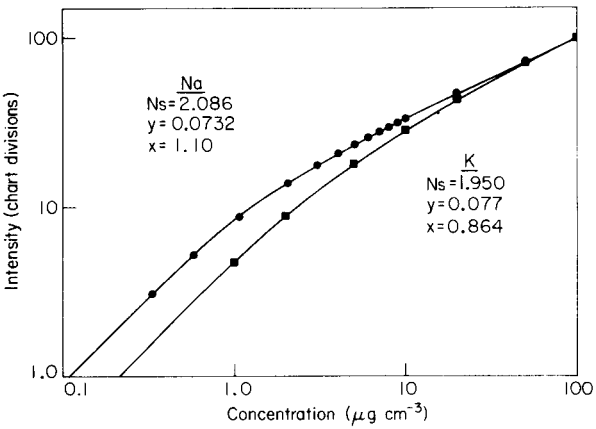

Fig. 3. Intensities for (•) Na and (▪) K plotted against concentration from experimental points and calculated lines from eqn. (3). Conditions as in Table 1.

constant from day to day and may be used with confidence in the calculation of concentrations.

Calculation of concentrations

Two relationships exist depending on the concentration range. At low concentrations $C \propto I$ or:

$$C = (C_b/I_b)I \tag{1}$$

where C_b is the concentration of a linear standard (e.g. 0.5 μg cm^{-3} Ca) and I_b its intensity. At high concentrations $C \propto I^{Ns}$ or:

$$C = C_s I^{Ns}/I_s^{Ns} \tag{2}$$

where C_s is the concentration of a fully self-absorbed standard (e.g. 100 μg cm^{-3} Ca) and I_s its intensity.

Equations (1) and (2) may be combined provided that the influence of eqn. (1) is diminished at higher concentrations. This is analogous to the peak intensity nearing the maximum value allowed for a black body at the flame temperature, line broadening thus becoming dominant. A suitable combination of eqns. (1) and (2) is:

$$C = C_s\,(I/I_s)^{Ns} + C_b\,(I/I_b)\,\exp\,(-yI^x) \tag{3}$$

The factor $\exp(-yI^x)$, where x is a constant with a value close to unity which allows transition region behaviour to be more closely matched and y is a normalizing variable, is justified by the boundary conditions: $\exp(-yI^x) \to 0$ for large I, and $\exp(-yI^x) \to 1$ for small I.

Calculation of Ns, x *and* y

$$Ns = \ln(C_1/C_2)/\ln(I_1/I_2) \tag{4}$$

TABLE 1

Operating conditions for flame emission measurements

Conditions	Na	K	Ca	Li
Spectrometer	PE403	PE305BG	PE403	PE305BG
Wavelength (nm)	589.0 589.6	769.9	422.6	670.8
Spectral bandwidth (nm)	4	1.4	0.4	1.4
Filter	Order sorting	UG5	none	none
Mask hole diameter (mm)[a]	6	5	6	5
Observation height (mm)	8	8	12	8
Gain (arbitrary 0—1000)	280	570	400	315
Photomultiplier (Hamamatsu)	R292	R446	R292	R446
Flame	Air—C_2H_2	Air—H_2	N_2O—C_2H_2—Ar[b]	N_2O—C_2H_2—Ar[b]
Flame adjustment	Lean[c]	Richer[c]	Lean	Lean
Flow rate per cm burner slot length ($cm^2\ s^{-1}$)	28	62	55	55
Standards[d]	NaCl	KCl	$CaCl_2 \cdot 2H_2O$	Li_2CO_3
Standardization	—	F.e.s. ($COOHC_6H_4COOK$)	Gravimetric	A.a.s. (LiF)
Buffer (1 mg cm^{-3} as metal)	KCl[e]	NaCl[f] or CsCl[g]	KCl[e]	KCl[e]
Concentration range ($\mu g\ cm^{-3}$)	0—100	0—100	0—500	0—100

[a]The mask was located at the entrance window of the PE403 and at the burner end on the PE305BG.
[b]1 l min^{-1} argon to reduce ionization and flame noise.
[c]A richer flame reduces ionization in poorly buffered samples, and reduces, for sodium, background emission bands of calcium.
[d]Acidified with 0.1 M HCl.
[e]The KCl buffer contained 0.08 μg Na cm^{-3} and 0.03 μg Ca cm^{-3}.
[f]The NaCl buffer contained less than 0.01 μg K cm^{-3}.
[g]The CsCl buffer contained less than 0.01 μg K cm^{-3}.

where C_1 and C_2 are the concentrations of two fully self-absorbed standards (e.g. 50 and 100 $\mu g\ cm^{-3}$ Ca) and I_1 and I_2 are the respective intensities.

To calculate x, the intensity I_t of a standard C_t (e.g. 2 $\mu g\ cm^{-3}$ Ca) in the transition region must be known. Equation (3) can be solved for x by successive substitution of C_t, C_b for C and I_t, I_b for I. Thus

$$x = \gamma^{-1} \ln(\alpha/\beta) \tag{5}$$

where $\alpha = \ln[C_t - C_s(I_t/I_s)^{Ns}] - \ln(I_t C_b) + \ln I_b$, $\beta = \ln[1 - (C_s/C_b)(I_b/I_s)^{Ns}]$, and $\gamma = \ln(I_t/I_b)$. x varies inversely with the length of the transition region

(Figs. 2 and 3) and may relate directly to the homogeneity of the atom population in the observed flame zone.

Ns and x are constant for standard operating conditions (Table 1), recalculation being unnecessary before each analysis. Deviations from standard conditions do not have an undue influence on *Ns* or x.

The parameter y is calculated by substitution of C_b for C and I_b for I in eqn. (3). Thus $y = -\beta I_b^{-x}$. β is a measure of sensitivity since it contains the ratio I_b/I_s; y also varies with scale expansion because of the factor I_b^{-x}. A digital readout or 10-fold scale expansion allows a precise determination of I_b. The parameter y is determined each time standards are aspirated, thus avoiding the need to adjust the instrument to give the same readings each day.

Generalization

Equation (3) may be generalized so that C_s may have any value above C_b, e.g. C_m. Thus for $C_m = K(I_m)^{Ns} + C_b\ (I_m/I_b)\ \exp\ (-yI_m^x)$,

$$K = [C_m - C_b\ (I_m/I_b)\ \exp\ (-yI_m^x)]/I_m^{Ns} \quad (6)$$

For $C_b = KI_b^{Ns} + C_b\ \exp\ (-yI_b^x)$,

$$y = -\ln[1 - (K/C_b)I_b^{Ns}]/I_b^x \quad (7)$$

Equations (6) and (7) are evaluated alternately to approach a fixed value for y and K. For an initial value of $y = 0.1$, only four or five iterations are necessary. Equation (3) becomes

$$C = KI^{Ns} + C_b\ (I/I_b)\ \exp\ (-yI^x) \quad (8)$$

Equations (6—8) can readily be programmed, given values for *Ns* and x, to provide an extremely flexible means of obtaining concentrations over a wide range.

EXPERIMENTAL

Operating conditions are summarized in Table 1. Determinations of standard solutions of sodium, potassium, calcium and lithium were carried out on Perkin Elmer models 403 and 305BG spectrometers. Both instruments were fitted with 73-mm tapered-slot water-cooled burners [7] which allowed improved performance and short warm-up times. The use of a nitrous oxide burner head may be preferable for use with the air—acetylene flame because of lower heat transfer from the flame. Calibrated 10-turn potentiometers were fitted in place of the regular gain controls on both instruments to allow easier and more reproducible setting of the photomultiplier voltage. Some noise reduction was also noted.

The unregulated heater voltage supplying the power supply vacuum tubes in the PE403 caused slight changes in the photomultiplier voltage as mains voltage variations occurred. Signal changes of 2—3% were normally observed in the emission mode (double-beam atomic absorption measure-

TABLE 2

Standard and maximum errors within a given concentration range

Element	Range (μg cm^{-3})	Standard error[a] (μg cm^{-3})	Maximum error (μg cm^{-3})	Maximum % error at	Concn. (μg cm^{-3})
Na	0.33—100	±0.04	+0.10	+3.3	0.33
K	1—100	±0.25	+0.7	+2.0	10.0
Ca	0.53—500	±7.66	−24.0	−4.9	500
Ca	0.53—100	±0.16	−0.43	−2.15	20.0
Li	1—100	±0.34	+0.51	+5.7	4.9

[a]Standard deviation of the differences between actual and calculated concentrations.

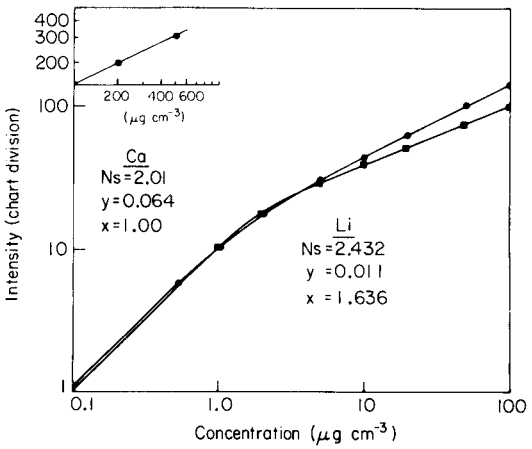

Fig. 4. Intensities for (•) Ca and (▪) Li plotted against concentration from experimental points and calculated lines from eqn. (3). Conditions as in Table 1.

ments were unaffected). A simple regulator, based on a cheap operational amplifier and a temperature-compensated zener diode, was added to the photomultiplier power supply; this reduced the dependence of emission signals on mains voltage variations by a factor of at least 20.

RESULTS AND DISCUSSION

The satisfactory results obtained by using the suggested procedure are summarized in Table 2. The log—log calibration graphs are given in Figs. 3 and 4. The larger error for calcium in the 0—500 μg cm^{-3} range is almost entirely due to the error in the determination of the 500 μg cm^{-3} standard. Calcium standards of 1000 and 500 μg cm^{-3} gave values for *Ns* of 3.1 at a spectral bandwidth of 0.14 nm, 2.2 at 0.4 nm and 2.0 at 1.4 nm. A wider spectral bandwidth is required at these high concentrations and a smaller mask aperture may also be needed.

The lithium results are more difficult to fit to the algorithm as self-reversal probably plays a dominant part in determining the unusual nature of its calibration curve. The transition region is short (Fig. 4) and consequently x should exceed 1 but values of x above 1 produce an indented transition region which worsens the fit elsewhere. Changing Ns to 2.48 and x to 1.547 reduces the maximum error to −3.0%.

The sodium and potassium results fit closely for the concentrations given. The sodium and potassium results are satisfactory up to 1000 $\mu g\ cm^{-3}$ while lithium and calcium determinations are more restricted in range because Ns (Fig. 1) does not reach a completely constant value under the present operating conditions. A small mask size (hole diameter 2 mm) can be used to extend the upper concentration limits.

The close agreement between the experimental and calculated results (Figs. 3 and 4, Table 2) allows the use of eqn. (3) or eqn. (8) in practical situations. Determinations of Na, K, Ca, and Li in natural waters, including geothermal fluids and brines, dissolved solids from rock and foods and other miscellaneous samples have been carried out in this laboratory by the method outlined. Close agreement was obtained with determinations by atomic absorption spectrometry on diluted solutions.

The principal advantages of the method are as follows.

(a) Fewer dilutions are necessary and often the same solution can be used for the determination of major and minor constituents by flame emission or absorption as necessary.

(b) A wide range of concentrations may be covered with only two standards; the parameters Ns and x need to be determined only once as Ns depends mainly on spectral bandwidth and x on flame type and geometry, which leaves the parameter y to be determined each time from C_s, I_s, C_b and I_b.

(c) The algorithms presented allow concentrations to be obtained readily from measured intensities with a programmable calculator. (Direct interfacing with an HP 9815A calculator in this laboratory results in a direct printout of concentration; Ns and x are constants in the program.)

(d) Reversion to atomic absorption spectrometry is easy as the burner slot is always parallel to the optical axis.

(e) Background interferences in flame emission measurements of the elements cited are low; atomic absorption can still be used to determine small concentrations in high solid content solutions.

(f) The compression of results, because of the non-linear response, allows a chart recorder to be used for reasonably accurate determinations over at least two decades of concentration, but for better accuracy a digital display is to be preferred.

(g) The generalized eqns. (6—8) give greater flexibility in the choice of the higher standard, which can have any value above C_b suitably close to the sample concentration. The equations can also be used successfully for curvature correction in atomic absorption spectrometry. $Ns = 2$, $x = 1$ are suggested starting values. More than five iterations may be required for cases of slight curvature.

Possible disadvantages of the method include:
(a) some spectrometers have limited maximum bandwidths, e.g. 1 nm, thus preventing wide-range sodium determinations by this method;
(b) the range of sample types may be restricted, as in other flame methods, e.g. where the total dissolved solids or organic content is high;
(c) the choice of flames is limited by the needs for maximum atomization and excitation on the one hand and minimum ionization on the other. The flame types have been chosen (Table 1) so that, in suitably buffered samples, curvature is not influenced by these factors.

The method described will prove to be of value in laboratories where large numbers of aqueous samples of variable composition have to be analysed, since major components (e.g. sodium and calcium) can be determined at the same dilution used for the minor components. Programs have been written for various Reverse Polish notation calculators.

R. L. Goguel, H. P. Rothbaum, and W. C. Tennant are thanked for constructive criticism and encouragement, especially during the initial stages of the preparation of the text.

REFERENCES

1 S. R. Koirtyohann and E. E. Pickett, Appl. Spectrosc., 23 (1969) 597.
2 N. S. Poluektov, Techniques in Flame Photometric Analysis, Consultants Bureau, New York, 1961.
3 J. D. Winefordner, W. W. McGee, J. M. Mansfield, M. L. Parsons and K. E. Zacha, Anal. Chim. Acta, 36 (1966) 25.
4 P. J. T. Zeegers, R. Smith and J. D. Winefordner, Anal. Chem., 40 (1968) 26A.
5 R. Herrmann and C. T. J. Alkemade, Chemical Analysis, Vol. XIV, Chemical Analysis by Flame Photometry, 2nd revised edn., (translated by Paul T. Gilbert, Jr.), Interscience, New York, 1963, pp. 45, 46.
6 J. A. Dean, Flame Photometry, McGraw-Hill, New York, 1960.
7 R. Goguel, Spectrochim. Acta, Part B, 26 (1971) 313; N. Z. J. Sci., 13 (1970) 603.

Analytica Chimica Acta, 107 (1979) 211—218

DETERMINATION OF THE TOTAL CONTENT AND DISTRIBUTION OF CADMIUM, COPPER AND ZINC IN HUMAN PAROTID SALIVA

F. J. LANGMYHR* and B. EYDE

Department of Chemistry, University of Oslo, Oslo 3 (Norway)

J. JONSEN

Department of Microbiology, University of Oslo, Oslo 3 (Norway)

(Received 15th November 1978)

SUMMARY

The contents of cadmium, copper and zinc, and the distribution of these metals among the protein fractions of human parotid saliva were determined by atomic absorption spectrometry. The proteins were separated by gel filtration. The contents of metal were found to be 3.5 ppb Cd, 88 ppb Cu and 49 ppb Zn. In the protein fractions, zinc was distributed over a wide range, the highest contents being found in proteins of high molecular weight. Cadmium was found in the fractions which contained the largest amounts of zinc. Copper was present in a relatively narrow range of proteins of intermediate molecular weight.

During the past 20 years, interest in the biological role of metals has increased remarkably. Atomic absorption spectrometry (a.a.s.) has greatly facilitated studies of the concentration and distribution of trace metals in biological materials, and a large number of papers has been published on the application of this technique to the determination of metals in samples of human, animal and plant origin. During recent years more emphasis has been laid on quantifying the distribution of species of the elements.

A survey of the literature showed that — in addition to the main constituents — eighteen trace elements have been determined in saliva or parotid saliva. The methods employed in these analyses were emission spectroscopy, spectrophotometry, fluorimetry, neutron activation analysis and a.a.s. Some of the data reported for the trace elements vary considerably (up to more than two orders of magnitude), and there are reasons to believe that some of the methods are subject to systematic errors. The only previous speciation study of human saliva described the isolation and characterization of a zinc protein [1].

The present investigation was started with the purpose of developing a.a.s. methods for the determination of the total content of cadmium, copper and zinc in human parotid saliva, and of establishing the distribution of the three metals among the protein fractions. Analysis of saliva has potentialities as a simple technique for establishing exposure to toxic metals; in addition, the method has the advantage that sampling is easy and painless.

EXPERIMENTAL

Atomic absorption equipment and measurements

The a.a.s. measurements were made with the Pye Unicam model SP 2900 and the Perkin-Elmer models 360 and 400S instruments, all equipped with background correctors and graphite furnaces; the P-E 360 instrument also had a P-E AS-1 autosampler. The graphite furnaces were purged with argon of 99.9% purity (by volume).

The spectrometers and furnaces were set up, adjusted and run as recommende by the manufacturers. The hollow-cathode and background corrector lamps were heated for about 15 min, and the electrodeless discharge lamp for cadmium for 30 min, before the start of the measurements, which were made at the following wavelengths: cadmium, 228.8 nm; copper, 324.7 nm; and zinc, 213.9 nm.

Solutions were introduced into the graphite furnaces with 2-μl pipettes (Oxford, U.S.A.), or a 5—50-μl adjustable Finn pipette (Kemistien, Finland).

Reagents and standard solutions

Primary 1000-ppm standard solutions of the three metals were prepared by dissolving 1 g of high-purity metal in 15 ml of (1 + 1) nitric acid and diluting the solution to 1 l with water. Secondary metal standard solutions were prepared by dilution with water; only freshly prepared solutions were employed in the analysis.

The secondary standard solutions employed in the analysis of the protein fractions covered the concentration ranges up to 20 ppb of cadmium, 500 ppb of copper and 100 ppb of zinc; all these solutions were 0.01 M with regard to the buffer solution mentioned below. Another series of standard solutions was prepared without the buffer.

A primary 0.1 M buffer solution was prepared by dissolving 13.80 g of $NaH_2PO_4 \cdot H_2O$ and 17.80 g of $Na_2HPO_4 \cdot 2H_2O$ in water and diluting the soluti to 1 l; the pH of this buffer is 6.88. Before use for elution, the buffer was diluted 10 times with water. The effect of phosphate on the a.a.s. measurements was compensated for by maintaining the same buffer concentration in the metal standard solutions and in the eluates.

The acids were of Suprapur quality (Merck). Water was purified by ion exchange; however, it still contained appreciable amounts of the metals to be determined.

Preliminary work

All glass and plastic equipment (except for the 5-ml polystyrene tubes) was cleaned by soaking for 24 h in a 5% detergent solution (Deconex), and then fo 24 h in 3% nitric acid; it was finally rinsed thoroughly with deionized water.

To ensure that metals were not lost by adsorption on the walls of the polystyrene tubes, some of the tubes used for collecting the fractions were filled with 5% nitric acid, stoppered and left for 24 h or 2 weeks. No increase of the metal content in the acid could be detected by a.a.s.

Samples, sampling and sample preparation

From a female, aged 28, and a smoker with normal taste acuity, samples of parotid saliva were collected by placing a plastic-covered Lashley cup over one of the Stenson's ducts. Secretion was stimulated with lemon candies. The first 5—10 ml of saliva were discarded. A portion of about 120 ml was first collected, and 6 months later the same volume was taken from the same subject. Both samples were collected at a rate of 1—2 ml min^{-1}; from the two samples, volumes of 100 and 50 ml, respectively, were transferred to plastic bottles, and the saliva was freeze-dried with phosphorus pentoxide as the drying agent. The lyophilized samples were stored at about —20°C.

Preparation of the protein fractions

Gel filtration was done with Sephadex G-150 (fine-grade; Pharmacia Fine Chemicals, Sweden) contained in a polyethylene tube. The column was prepared as specified by the manufacturer; the packing was checked and the void volume determined with dextran blue 2000. The column was operated at a pressure of 30 cm of water and connected to an automatic fraction collector equipped with 5-ml polystyrene (thrombotest) tubes. The whole equipment was placed in a cold room at 4°C.

The lyophilized sample was dissolved in 5 ml of water, the solution was transferred to the top of the column, and elution was done with the 0.01 M buffer solution at a rate of about 0.46 ml min^{-1}. In each fraction tube, 75 drops (about 5 ml) of eluate were collected; the total number of fractions was 120. The tubes were sealed with plastic stoppers, and stored at about —20°C.

Analysis of parotid saliva

Preliminary work demonstrated that a concentration of chloride (added as the sodium salt) corresponding to the amounts found in the present samples (about 1400 mg l^{-1}) reduced the peak heights for all metals by about 30%. For this reason, the analyses were based on the standard addition technique. The solutions were prepared as follows. Into four 10-ml sample bottles, 1 ml of whole saliva was pipetted, to one of the bottles 1 ml of water was added, and to the remaining bottles 1 ml was added from a series of three standard solutions of the metal to be determined, covering the range up to 20 ppb Cd, 400 ppb Cu, and 60 ppb Zn.

Zinc and copper were determined by transferring 2 and 20 μl, respectively, to the graphite furnace, the further procedure being as described below for the analysis of the protein fractions, except that a 30-s ashing time was used.

The analysis for cadmium was complicated by the presence of large amounts of sodium chloride which absorbs strongly at 228.8 nm. Preliminary measurements indicated that this non-specific absorption exceeded the compensating capacity of the background corrector. The chlorides were therefore removed before the atomization of cadmium by evaporation with either

nitric or sulfuric acid. Two series of solutions were prepared as described above; in one series the metal standard solutions added were 0.42 M with regard to nitric acid, and in the other 0.11 M with regard to sulfuric acid (an increase in the concentration of sulfuric acid gave precipitates, probably of calcium sulfate, with the samples). Cadmium was determined as described below for the analysis in the protein fractions, except that a 30-s ashing time was used.

Three standard addition curves were plotted for the determination of copper and zinc; for cadmium, two sets of three curves were recorded, one set for each of the two evaporation procedures. The data were corrected for the contents of metal in the water and reagents added.

Analysis of the protein fractions

The content of zinc in the fractions was determined as follows. The calibration data were obtained with 2-μl portions of the zinc standard solutions which had the same buffer concentration as the eluates. The calibration curve for zinc (and for the two other metals) was not corrected for the content of zinc in the buffer, and consequently did not pass through the origin.

From each of the fractions 1—30 (in which zinc is not likely to be present), two 2-μl portions were analyzed by the following program: drying at about 100°C for 20 s, ashing at 600°C for 20 s, atomizing at 2100°C for 8 s, and cleaning at about 2500°C for 2 s.

The zinc-bearing proteins were expected in the fraction range 31—70. The same program was used to analyze three 2-μl portions of each fraction. To ensure that the sensitivity was constant, a zinc standard solution was atomized after every 10 fractions. Fractions 71—120 were analyzed as described above for the range 1—30. The analysis was completed by replotting a calibration curve.

Cadmium was determined as described above for zinc, except that 20-μl portions were taken of each fraction, and that the sample was dried at 100°C for 30 s, ashed at 300°C for 20 s, and atomized at 1450°C for 5 s, the tube being cleaned by heating for 5 s at 2100°C.

Copper was determined with the autosampling device. The scheme for fraction analysis was the same as for zinc, except that 20-μl aliquots were taken of all fractions and that three portions were atomized from each of fractions 57—75. The a.a.s. program consisted of drying at 100°C for 30 s, ashing at 850°C for 20 s, and atomizing (at miniflow) at 2550°C for 11 s, with cleaning of the tube at 2750°C for 3 s.

The total content of zinc and the distribution of zinc among the proteins were established by analyzing the 100-ml portion of saliva. The 50-ml sample was employed in the determination and distribution of cadmium and copper.

Some randomly selected fractions representing low, intermediate and high metal contents, were also analyzed by the standard addition technique; the results for the three metals in these samples were in good agreement with the data obtained by measurements against the standard curves.

Blank analysis

The contents of cadmium, copper and zinc in the water and in the buffer were determined by the standard addition technique. As the contents in water were found to vary during the investigation, it was necessary to run blanks with all series of analysis. Typical data from the analysis of water purified by ion exchange were 0.2 ppb Cd, 1.8 ppb Cu and 3.8 ppb Zn; the values for the 0.01 M buffer were 1.1, 2.8 and 7.4 ppb, respectively. The purity of the water was not improved by double distillation in a silica still.

Recovery from the column

By summing the metal content in the fractions and comparing the sum with the amounts added (calculated from a content of 3.5 ppb Cd, 88 ppb Cu and 49 ppb Zn in parotid saliva, see Table 1), the recoveries were 96% for Cd, 105% for Cu, and 87% for Zn.

Calculation of the recovery was complicated by the impurities of cadmium, copper and zinc in the phosphate buffer used for elution; the distribution of the impurities among the fractions and the adsorption of the metals on the column are not known.

Precision

The precision of the methods was established as follows. Separate standard solutions of cadmium (10 ppb), copper (70 ppb) and zinc (20 ppb) were prepared, all solutions being 0.01 M with regard to the phosphate buffer. From 7 atomizations of the cadmium and zinc solutions (sample volumes of 20 and 2 μl, respectively), and 8 measurements of the copper solution (with the autosampler and sample volumes of 20 μl), the relative standard deviations were calculated to be 4.1% for Cd, 3.0% for Cu and 6.1% for Zn.

A second series of measurements was based on mixing equal volumes of saliva and standard solutions of cadmium (20 ppb, 0.42 M in nitric acid or 0.11 M sulfuric acid), copper (50 ppb) and zinc (20 ppb), transferring 2 μl

TABLE 1

Analytical results (in ppb) for the contents of cadmium, copper and zinc in parotid saliva, calculated form the standard addition curves

Metal[a]	Concentration ($\bar{x}$) and relative standard deviations (s_r)						Previous data
	1		2		3		
	$\bar{x}$	s_r	$\bar{x}$	s_r	$\bar{x}$	s_r	
Cadmium (a)	4.5	15	4.0	22	3.8	18	
Cadmium (b)	2.0	10	3.3	9.1	3.2	9.4	
Copper	91	7.7	82	11	90	10	
Zinc	51	7.8	50	8.0	47	17	27—82

[a](a) Evaporated with nitric acid; (b) evaporated with sulfuric acid.

of the saliva/zinc mixture and 20 μl of the other mixtures to the furnace, and atomizing the three metals by the programs given above. Before the atomization of cadmium, the chlorides were removed as described above by evaporation with either nitric or sulfuric acid. The relative standard deviations were found to be 3.4% for Cd (10 atomizations, evaporation with nitric acid), 2.7% for Cd (10 atomizations, evaporation with sulfuric acid), 5.5% for Cu (7 atomizations) and 5.4% for Zn (7 atomizations).

RESULTS AND DISCUSSION

Table 1 lists the data obtained for the content of cadmium, copper and zinc in parotid saliva. For comparison, the data from a previous determination [2] of zinc in parotid saliva are also given. The present results for zinc lie within the very wide range of previous data. For cadmium, the differences between the averages and relative standard deviations obtained by evaporation with nitric or sulfuric acid were shown to be insignificant by statistical methods.

The contents of copper and zinc in the present samples of parotid saliva are considerably lower than in human blood, while the content of cadmium is about the same.

Table 2 lists the analytical data for the fractions of human parotid saliva; Fig. 1 shows the distribution of the three metals among the proteins. As can be seen, zinc is distributed over a wider fraction range than cadmium and copper. Cadmium is found mainly in the fractions containing the largest amounts of zinc.

A cadmium- and zinc-containing protein (metallothionein) with a molecular weight of about 10^4 has been described [3]. The Sephadex G-150

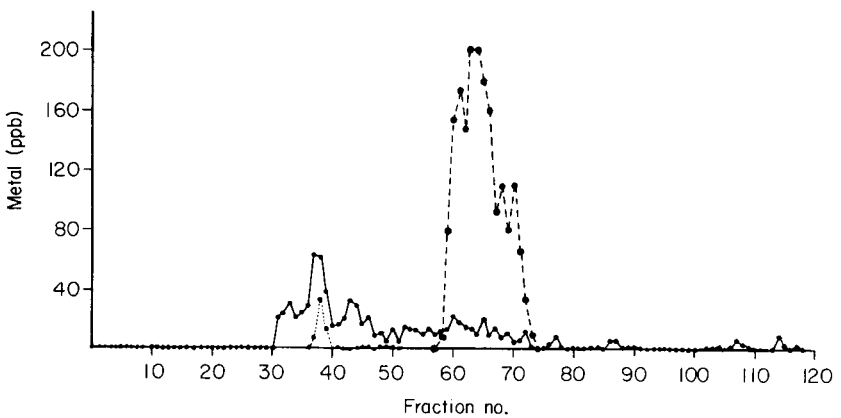

Fig. 1. The distribution of cadmium (...), copper (---) and zinc (—) among the protein fractions of human parotid saliva. The data from Table 2 for cadmium and copper were multiplied by 2 in order to obtain the results for 100 ml of saliva.

TABLE 2

The distribution of cadmium, copper and zinc among the protein fractions of human parotid saliva. The contents are given in ppb.

Fraction[a]	Cd	Zn	Fraction	Cu	Zn	Fraction	Zn
1—30	—[b]	—	57	—	10	84	2
31	—	21	58	5	12	85	—
32	—	24	59	40	13	86	6
33	—	31	60	77	22	87	6
34	—	21	61	87	18	88	1
35	—	24	62	74	17	89	2
36	—	29	63	110	16	90	2
37	4.5	63	64	110	11	91	1
38	17	61	65	89	20	92—101	—
39	7	38	66	80	9	102	1
40	—	15	67	46	14	103	1
41	0.5	17	68	55	8	104	2
42	—	21	69	40	11	105	—
43	—	32	70	55	5	106	2
44	0.5	29	71	33	6	107	7
45	0.5	17	72	18	12	108	4
46	0.5	21	73	5	2	109	2
47	—	9	74	—	—	110	1
48	1	10	75	—	—	111—113	—
49	1	5	76	—	4	114	9
50	1	13	77	—	9	115	3
51	—	5	78	—	2	116	—
52	—	15	79	—	—	117	3
53	—	14	80	—	1	118—120	—
54	—	14	81	—	1		
55	—	10	82	—	1		
56	—	14	83	—	1		

[a]Cadmium was not found in fractions 51—120. Copper was not found in fractions 1—57 and fractions 74—120. [b]A dash indicates that the signal could not be distinguished from that of the blank.

employed in the present work separates globular proteins in the molecular weight range 5×10^3—4×10^5; even without special calibration, it could be concluded that the present cadmium- and zinc-containing proteins had a molecular weight above 10^4.

Henkin et al. [1] used the same separation technique as in the present work to isolate a zinc protein from human parotid saliva, the molecular weight being approximately 3.7×10^4. From a comparison of their distribution curves and other data with those from the present study it seems possible that the fractions having the highest concentrations of zinc contain the same zinc protein.

Copper was found only in a relatively narrow fraction range containing proteins of intermediate molecular weight.

REFERENCES

1 R. I. Henkin, R. E. Lippoldt, J. Bilstad and H. Edelhoch, Proc. Nat. Acad. Sci. U.S.A., 72 (1975) 488.
2 R. I. Henkin, C. W.. Mueller and R. O. Wolf, J. Lab. Clin. Med., July (1975) 175.
3 J. H. R. Kägi, B. L. Vallee and J. M. Carlson, J. Biol. Chem., 235 (1960) 3460; 236 (1961) 2435.

Analytica Chimica Acta, 107 (1979) 219—229

SOLVENT EXTRACTION WITH AMMONIUM PYRROLIDINEDITHIOCARBAMATE AND 2,6-DIMETHYL-4-HEPTANONE FOR THE DETERMINATION OF TRACE METALS IN EFFLUENTS AND NATURAL WATERS

K. M. BONE* and W. D. HIBBERT

Herman Research Laboratory, State Electricity Commission of Victoria, 14 Howard Street, Richmond, Victoria 3121 (Australia)

(Received 4th September 1978)

SUMMARY

A method is described for the determination of ten trace metals (V, Cr, Fe, Co, Ni, Cu, Zn, Mo, Cd, Pb) in aqueous samples by simultaneous solvent extraction followed by flame atomic absorption spectrometry. 2,6-Dimethyl-4-heptanone is preferred to 4-methyl-2-pentanone as the solvent, and ammonium pyrrolidinedithiocarbamate to sodium diethyldithiocarbamate as the extractant except when relatively large amounts of iron are present. Calibration graphs are linear, usually over the range 0—50 $\mu g\ l^{-1}$. The effects of interfering substances, in particular iron, are shown, and the need for calibration by standard additions is demonstrated. The general need for preoxidation of samples is discussed.

Solvent extraction followed by flame atomic absorption spectrometry (a.a.s.) is widely used for the determination of trace metals in aqueous systems. However, when such methods are used, many factors may affect both the accuracy and the precision of the results, as well as the applicability of the method. This paper describes a solvent extraction method, developed as part of an environmental study, which has been routinely applied for four years to the analysis of natural waters and aqueous effluents. Ten elements (vanadium, chromium, iron, cobalt, nickel, copper, zinc, molybdenum, cadmium and lead) can be simultaneously extracted and determined. The method is discussed in terms of choice of reagents, extraction pH, and the species of the elements extracted. Discussion centres around the choice of 2,6-dimethyl-4-heptanone (diisobutyl ketone; DIBK) as the organic solvent and the final choice of ammonium pyrrolidinedithiocarbamate (APDC) as the chelating agent after a detailed comparison of the two chelating agents commonly used — APDC and sodium diethyldithiocarbamate (NaDDC).

EXPERIMENTAL

Apparatus

A Varian-Techtron AA5 and a Perkin-Elmer Model 460 spectrometer were

used for atomic absorption measurements. Other equipment included a Philips PW 9408 Digital pH meter and a Varian Model 635 spectrophotometer.

All glassware for all operations was soaked in 6% (v/v) nitric acid for one week before initial use, and was subsequently stored under 6% (v/v) nitric acid.

Sampling

Samples were pressure-filtered at the collection site through 0.45-μm filters (142-mm diameter) into polyethylene bottles containing sufficient 50% (v/v) nitric acid to give a final acid concentration of 1% (v/v). The filters, bottles and pressure filtration equipment were soaked in 6% v/v nitric acid for at least one week prior to use and then thoroughly rinsed with deionized water. The pressure filtration equipment consisted of a plastic pressure vessel and a Millipore YY4014200 filter holder, which was plastic-coated to avoid contamination of samples. (Used filters were stored in acid-cleaned petri dishes and after dissolution in nitric acid, were analysed by flame atomic absorption spectroscopy, as in the method used by Chen et al. [1].)

Standards

Stock standard solutions (1000 mg l^{-1}) of Fe, Ni, Cu, Zn, Cd, Pb and Cr(III) were prepared by dissolving the metal (minimum 99% purity) in the minimum volume of an appropriate mineral acid. Stock solutions (1000 mg l^{-1}) of Cr(VI) and V(V) were prepared from potassium dichromate and ammonium vanadate, respectively. Mo, Co and V(IV) (as $VOSO_4$) standards, each 1000 mg l^{-1}, were purchased as prepared solutions. The Mn standard (1000 mg l^{-1}) was prepared from potassium permanganate after reduction to Mn(II) with hydrogen peroxide.

A working standard was prepared by appropriate dilutions of stock standards so that the final metal concentrations were: Mn and Fe, 10 mg l^{-1}; V(V), Mo and Pb, 5 ml l^{-1}; Cr(III), Co, Ni, Cu, Zn and Cd, 2 mg l^{-1}. The standard was preserved by adding 10 ml of nitric acid per litre.

Reagents

A buffer solution was prepared by dissolving 500 g of AR ammonium acetat in 1 l of deionized water. The solution was purified by the addition of 25 ml of 5% (w/v) APDC, followed by three successive extractions with 10-ml portions of DIBK. It was found that only V, Cr(III) and Mo could not be successfully removed from the buffer in this manner.

An aqueous 5% (w/v) solution of APDC was prepared each day. Since a fraction of the APDC is often water-insoluble [2], the solution was filtered through a Whatman No 41 filter paper. Portions (500 ml) of the solution were purified by a single extraction with 10 ml of DIBK. All eleven elements, including Cr(III), were at least partially removed from the APDC by this extraction. A 5% (w/v) solution of NaDDC was prepared, filtered and purified in the same way as APDC.

Deionized water (conductivity <50 μS m^{-1}) for the reagent blank was

further purified by solvent extraction with dithizone. This involved adding 2 ml of buffer (not containing APDC) to 400 ml of deionized water, shaking for 1 min with 20 ml of a freshly prepared, saturated solution of dithizone in DIBK, and removing any dithizone which dissolved in the aqueous phase by extractions with DIBK. Dithizone was used in preference to APDC because on acidification of the water, the unreacted APDC decomposes forming products which tend to hamper subsequent solvent extraction and also the oxidation of Cr(III) to Cr(VI).

The cerium(IV) sulphate solution (1% w/v) was prepared daily by dissolving 1 g of cerium(IV) sulphate in 100 ml of 2% (w/v) sulphuric acid.

Procedures

Oxidation of samples. Duplicate 300-ml volumes of each sample were transferred to 500-ml conical flasks. Further 300-ml volumes of each sample, together with appropriate additions of the working standard (usually 1 or 2 ml), were also transferred to conical flasks. A watch glass was placed over each flask. A 5-ml aliquot of the cerium(IV) solution was added to each solution, and the flasks were heated on a steam bath for 20 min. If, during heating, the yellow colour of cerium(IV) was discharged, more oxidant was added. After digestion, samples were allowed to cool and were transferred to 500-ml separating funnels.

Extraction procedure. Sufficient buffer was added to adjust the pH to the required value in the range 3—6. To avoid contamination, the amount of buffer needed to achieve the desired pH was predetermined on a separate aliquot of the sample. After the addition of 20 ml of the chelate solution and 8 ml of DIBK, the separating funnels were shaken by hand for 2 min if APDC was used, or 1.5 min for NaDDC. After at least 5 min for phase separation, the aqueous phase was either discarded, or collected for pH measurement. The organic phase was collected in dry, stoppered flasks and subsequently analysed by flame a.a.s. The aspiration of organic solvents into the hotter nitrous oxide—acetylene flame was done cautiously. Instrumental conditions were generally as recommended by the manufacturers (Table 1). The reagent blanks were determined by using deionized water purified with dithizone, and the same batch of 50% (v/v) nitric acid that was used during sampling. Calibration of the blank was achieved by adding working standard to the purified water. The zero setting was established by aspirating pure ketone into the flame. Deionized water and 6% (v/v) nitric acid were aspirated periodically to prevent nebulizer clogging. The variable nebulizer on the Perkin-Elmer Model 460 was set at such a position that the uptake rate was about 3 ml min^{-1}, and the sensitivity loss, determined for copper, was not greater than 20% of the maximum sensitivity. This enabled determination of 11 elements with a minimum of 8 ml of ketone. Before the determination of copper, the burner was immersed in nitric acid to eliminate memory effects by removing copper from the burner surface [3].

Extraction efficiencies. To determine extraction efficiencies, the organic

TABLE 1

Instrumental conditions

Element	Wavelength (nm)	Flame[a]	Burner length (cm)	Other conditions
V	318.5	NA	5	Fuel-rich flame
Cr	357.9	AA	10	Fuel-rich flame. Burner lowered 4 mm.[b]
Mn	279.5	AA	10	Acid back-extract used.
Fe	248.3	AA	10	
Co	240.7	AA	10	
Ni	232.0	AA	10	
Cu	324.7	AA	10	Burner immersed in 2% (v/v) HNO_3 for 2 min prior to use.
Zn	213.9	AA	5	
Mo	313.3	NA	5	Fuel-rich flame
Cd	228.8	AA	10	
Pb	283.3	AA	10	Scale expansion x 2 used

[a]AA, air-acetylene; NA, nitrous oxide—acetylene. [b]Burner heights for other elements were set to the point at which the flame began to attenuate the light path.

phase after the above extraction procedure was shaken for 1 min with 10 ml of 25% (v/v) nitric acid, and the two phases were than left in contact overnight to ensure complete back-extraction of the metals. The acid phases were then compared with standards made up in DIBK-saturated 25% (v/v) nitric acid, and the extraction efficiencies were calculated. For V and Mo, potassium chloride was added to both standards and the acidic back-extracts to suppress ionization. This acid extraction procedure was also used for the determination of manganese, in which case it was done within 15 min of the completion of the organic extraction.

Relative sensitivities. The sensitivities for the metal—pyrrolidinedithiocarbamate (metal—PDC) chelates in DIBK and methyl isobutyl ketone (MIBK) were determined by extracting aliquots of a standard solution with APDC and DIBK or MIBK as the solvent. The absorbances of several elements in each ketone phase were then compared. Results were corrected for the differing water solubilities, and the slightly differing extraction efficiencies, of the two ketones.

RESULTS AND DISCUSSION

The ranges of trace metals found in filtered samples at selected sites on the Latrobe Valley river system over a period of 4 years are given in Table 2. The extraction method was found to be suitable for natural waters including sea water, and for effluents from power station operation which are low in total organic carbon. Precision values at two concentrations of each element are

TABLE 2

Concentration ranges ($\mu g\ l^{-1}$) of filterable trace metals in Latrobe Valley rivers at selected sites (1974—1977)

V	Cr	Fe	Co	Ni	Cu	Zn	Mo	Cd	Pb
<10	<0.3—3.5	50—480	<0.5—2.5	0.5—7	1.0—7	<0.1—30	<2—13	<0.2—4.0	<1—1

TABLE 3

Characteristics of the recommended procedures

Element	Linear range ($\mu g\ l^{-1}$)	Precision[a] (%)	Blank ($\mu g\ l^{-1}$)	Characteristic concentration ($\mu g\ l^{-1}$)	Working pH ranges[b]	
					For APDC	For NaDDC
V	0—50	4.3 (50)	<3	10	3.4—5.1 (92)	3.9—5.7 (86)
Cr	0—40	6.9 (5) 2.2 (20)	0.3	0.9	4.1—5.6 (88)	4.3—5.7 (90)
Mn[c]	0—300	4.2 (25)	1.0	4	3.4—4.6 (53)	4.8—5.7 (85)
Fe	0—40	3.6 (25)	2.0	1.4	3.4—5.1 (93)	3.9—5.7 (99)
Co	0—40	4.8 (5) 2.9 (20)	0.3	1.3	3.4—5.1 (96)	3.9—5.7 (98)
Ni	0—40	3.6 (5) 2.6 (20)	0.3	1.3	3.4—5.1 (91)	3.9—5.7 (92)
Cu	0—40	1.9 (5) 1.4 (20)	1.0	0.7	3.4—5.1 (95)	3.9—5.7 (94)
Zn	0—40	1.7 (5) 1.7 (20)	1.0	0.4[d]	3.4—5.6 (93)	3.9—5.7 (92)
Mo	0—50	2.4 (50)	<1	4.4	3.4—5.1 (95)	4.3—5.2 (87)
Cd	0—50	6.6 (5) 1.5 (20)	0.3	0.5	3.4—5.1 (71)	3.9—5.7 (93)
Pb	0—70	4.5 (13) 3.3 (50)	0.7	5	3.4—5.6 (88)	3.9—5.7 (95)

[a]Expressed as percentage coefficient of variation. Value in parentheses is the corresponding concentration in $\mu g\ l^{-1}$ for the quoted precision.
[b]Range within which extraction efficiency is high and does not change greatly with pH. Values in parentheses are the average extraction efficiency over the quoted range, expressed as percentage.
[c]Measured in the acid back-extract.
[d]5-cm burner.

given in Table 3. These were each determined by replicate analysis of six 300-ml aliquots of a standard solution. Table 3 also indicates the minimum blank values and characteristic concentrations achieved. The recommended purification of reagents reduced most blank values to less than 1 $\mu g\ l^{-1}$.

Table 4 gives results from an interlaboratory study for six trace metals. The samples were 1% (v/v) nitric acid spiked with the metals. The reliability of the samples was checked in this laboratory by the extraction method and in another laboratory by anodic stripping voltammetry (a.s.v.) before they were sent to

TABLE 4

Validity of method

Element	Expected value ($\mu g\ l^{-1}$)	This method ($\mu g\ l^{-1}$)	A.s.v. ($\mu g\ l^{-1}$)	Interlaboratory mean[a] ($\mu g\ l^{-1}$)
Cd	2.0	2.0 ± 0.1	1.7 ± 0.2	2.1 ± 0.7
	25	26 ± 1	22 ± 3	23 ± 4
Pb	11	12 ± 1	10.2 ± 1.0	9.0 ± 4.9
	95	95 ± 1	99 ± 4	96 ± 19
Zn	7.5	7.6 ± 0.1	7.3 ± 1.1	10.1 ± 6.7
	75	70 ± 5	74 ± 1	83 ± 26
Cr[b]	8.5	6.7 ± 2.0	—	6.6 ± 2.5
	110	103 ± 7	—	70 ± 45
Cu	6.0	7.4 ± 1.4	5.5 ± 2.4	6.0 ± 3.5
	125	117 ± 8	119 ± 6	110 ± 24
Ni	12.0	11.7 ± 0.3	—	9.6 ± 1.5
	105	104 ± 1	—	95 ± 16

[a]Eight laboratories. Means do not include values in columns 3 and 4.
[b]Total chromium. Chromium added to samples as Cr(III).

other laboratories for analysis. Results by a.a.s. and a.s.v. are in good agreemei with each other and with the expected values. Despite the large deviations, the agreement of the means of the interlaboratory test with the expected values is also good for most elements.

Choice of organic solvent and chelating agent

DIBK was preferred to the more commonly used MIBK. It possesses good combustion properties, a high boiling point and low miscibility with water: 0.06 ± 0.02 ml/100 ml of water at 20°C. The miscibility of DIBK with water was measured spectrophotometrically by using the $\pi \rightarrow \pi^*$ peak at 290 nm. MIBK is partially miscible with water (2.15 ml/100 ml of water at 25°C [4]) and this has two major disadvantages: the miscibility varies significantly both with temperature and with the ionic strength of the aqueous phase. Brooks et al. [5] found that the miscibility of sea water with MIBK increased by 15% when the temperature was increased from 20°C to 30°C. Heated samples must therefore be returned to within 2°C of the same temperature to prevent the introduction of significant errors during extraction. Jones and Eddy [6] observed that when brines were extracted the recovery of MIBK was nearly complete, whereas the miscibility loss of MIBK to 100 ml of aqueous solution was 2.5 ml. Assuming the same extraction efficiency for both cases, this volun difference will cause errors when brine solutions are compared with aqueous blanks and standards. Crump-Wiesner and Purdy [7] observed a similar effect.

The main property which has encouraged the wide use of MIBK is the greater sensitivity provided in a.a.s. compared with other solvents [8]. However, measurements in this laboratory have shown that the loss of sensitivity

incurred by the use of DIBK is only about 20% on average. Everson and Parker [4] have suggested the use of 3-heptanone, but it is more soluble in water than DIBK, and their data for nebulization efficiencies indicate that the sensitivity in 3-heptanone is greatly reduced relative to MIBK.

Kinrade and Van Loon [9] considered the suitability of many chelating agents, using the criterion that a satisfactory chelating agent should efficiently extract all the desired elements over a reasonably wide range of pH. They concluded that a mixed reagent containing APDC and diethylammonium diethyldithiocarbamate (DDDC) was the most satisfactory choice. (DDDC and NaDDC have essentially the same chelating properties [10].)

In this work, the extraction properties of APDC and NaDDC were studied in the pH range 3—6, which is indicated [5, 9—11] as being the best range for quantitative extraction of all the elements of interest. Ammonium acetate solution added to 1% (v/v) nitric acid solutions was used to achieve strongly buffered solutions in this pH range. It has been suggested [9] that acetate may interfere with extraction of lead, but no interference was observed.

Overall, APDC was found to have the better properties, mainly because aspiration of the DIBK phase after extraction with NaDDC (or DDDC) in the pH range 3—6, revealed a major drawback: a large component of the absorption signals from standards, samples and blanks was non-atomic in nature. Furthermore, this non-atomic blank varied from blank to sample, and from sample to sample, and thus was a potential source of error. While simultanous background correction would largely overcome this problem, it would result in a loss of precision and an increase in detection limit. The half-life of decomposition of diethyldithiocarbamate at pH 9 is three orders of magnitude greater than that at pH 5 [10], thus decomposition products are a possible cause of the problem; extraction at pH 9, although unsatisfactory for many elements, gave no non-atomic signal. The non-atomic effect also occurred when MIBK was used, although this may not be so when the extraction conditions are different. If the reduction in signal-to-noise ratio can be tolerated, then the use of NaDDC with simultaneous background correction is satisfactory and for high concentrations of iron is preferable to the use of APDC (see below). Because of this, extraction efficiencies for the NaDDC—DIBK system are given in Table 3. Although the extraction efficiency was low for cadmium with APDC, it was constant over the working range of the method.

Stability

Stability tests were done by comparing freshly extracted solutions with those which had been extracted at varying time intervals beforehand. All elements, except molybdenum, vanadium and manganese, were found to be stable (within 5%) for 24 h. Vanadium and molybdenum can be satisfactorily determined within 1.5 and 2 h, respectively. Measurements outside these time limits may result in error.

Repeated tests showed the stability behaviour of the manganese chelate in DIBK to be erratic. The manganese in some DIBK solutions immediately

started to decompose, whereas in others it remained stable for up to 2 h. These results are consistent with those of Jenne and Ball [12] for Mn—PDC in MIBK. This behaviour made the determination of manganese in DIBK phases unsatisfactory. However, acid back-extractions, after using NaDDC as the chelating agent, afforded reliable manganese determinations. NaDDC was used because it gave better extraction efficiencies for manganese (see Table 3) and back-extraction eliminated the background problem.

Extraction pH and shaking times

The pH values given in Table 3 are those measured after extraction. In some early work [see, e.g., 5, 11], the pH values quoted were determined after the addition of buffer but before the addition of the chelating agent. However many chelating agents have acid—base properties, and it is therefore more relevant to measure the pH immediately before or after extraction [see, e.g., 9, 10, 12, 13].

To examine the effects of shaking time, aliquots of a standard solution were extracted. The results indicated minimum shaking times of 2 min for APDC and 1.5 min for NaDDC, for a concentration factor of 300 to 8. These shaking times were determined for concentrations at the top of the linear working range, and it is probable that the times required for equilibration would be less for lower concentrations or lower concentration factors.

Oxidation states of chromium and vanadium

Both vanadium and chromium can exist in natural samples in more than one stable oxidation state. Chromium can occur as Cr(III) and Cr(VI) [14, 15] and vanadium as V(IV) and V(V) [16]. Crump-Wiesner and Purdy [7] found that V(IV) and V(V) could be quantitatively extracted with cupferron in MIBK, and postulated that the V(V) complex was formed in both cases. These authors found the APDC complex of vanadium too unstable in MIBK for satisfactory analysis. In the present work on extraction of vanadium with APDC and DIBK, extraction of both V(IV) and V(V) was quantitative and instability problems did not hamper the analyses. For chromium, it has been noted [13, 17] that only Cr(VI) is extracted with APDC—MIBK; for the conditions used here, this finding was confirmed for extraction into DIBK. Strong APDC solutions extract Cr(III), but it seemed preferable to oxidize Cr(III) to Cr(VI), and then to extract the Cr(VI) into DIBK, thus obtaining a total chromium value.

Some initial experimentation with the oxidation of Cr(III) showed that potassium permanganate, hydrogen peroxide and potassium persulphate were unsatisfactory; they interfered with the extraction and oxidation was incomplete at the pH of the acidified samples. In contrast, cerium(IV) yielded rapid and complete oxidation of Cr(III) to Cr(VI) in pure solutions at room temperature, below pH 1. In the quantities used, it did not interfere with the extraction. However, oxidation of Cr(III) with Ce(IV) in natural samples, which was tested by the addition of known amounts of Cr(III), was sometim

not quantitative. The exceptions were probably caused by the existence of other oxidizable material in solution, and necessitated calibration of samples by the addition of known amounts of Cr(III).

Calibration and the effects of interfering agents

Interference effects with APDC extractions have been observed by many workers. A common interfering element in natural samples is iron, and so the interference of iron in the APDC—DIBK method was studied in detail. Table 5 shows, for both APDC and NaDDC, the absorbances obtained for several elements after extraction in the presence of iron (10 mg l^{-1}; 3 mg) expressed as a percentage of the absorbance obtained after extraction in the absence of iron. Results for NaDDC were measured with simultaneous background correction. It can be seen that NaDDC is generally less affected by the presence of high levels of iron, hence extraction with NaDDC is preferable for samples high in iron. Scrutiny of Table 5 indicates that the reduction of sensitivity caused by iron is generally not due to a reduction in extraction efficiency; in fact, for some elements, extraction efficiencies are improved (this was verified several times). The reason why iron interferes is therefore unclear, but could involve a reduction in the percentage of other elements reaching the flame. It is worth noting that Jenne et al. [18] found that the Fe—APDC precipitate formed from 5 mg of iron did not readily dissolve in MIBK, whereas the APDC—DIBK method gives no such problem.

The recovery of trace elements by extraction was not constant with matrix for the samples under consideration. For example, the coefficients of variation for the addition of standard to several trade effluents varied, depending on the element, from 16% to 35%; these numbers relate to a single batch of extractions, hence variations in reagents and instrumental conditions can be discounted. The variations are far greater than the measured precisions (Table 3) and indicate marked interferences. Because of this, calibration by the standard additions method was adopted. Of course, the use of this technique restricts measurements to the linear ranges of the calibration graphs, as listed in Table 3.

TABLE 5

Effect of iron on sensitivity and extraction efficiency for the APDC and NaDDC systems

Element	Relative sensitivity (%)[a]		Relative extraction efficiency (%)[a]	
	APDC	NaDDC	APDC	NaDDC
V	86	100	100	100
Cr	56	71	78	86
Co	78	79	100	100
Ni	98	86	100	100
Cu	91	100	108	95
Zn	108	98	103	97
Pb	43	100	100	100
Cd	53	96	118	98

[a]Extraction in the presence of Fe expressed relative to extraction with no added Fe.

For the given concentration factor of 300:8, the calibration plots behaved erratically outside these regions. The reasons for this are probably related to inadequate equilibration times with manual shaking. A reduction of the concentration factor to 100:8 extended the linear range by a factor of about three, and was therefore used for the measurement of higher concentrations.

Pre-oxidation of samples

The pre-oxidation of samples with cerium(IV) sulphate helped to convert the trace metals to extractable forms and to minimize interferences from organic compounds, as well as oxidizing Cr(III) to Cr(VI).

Trace elements can occur in aqueous solutions in many different forms. The chemical speciation of trace elements in natural waters has been discussed [19, 20]. Certain species may escape analysis unless samples are acidified and/or oxidized before analysis [21, 22]. For example, Segar and Cantillo [23] measured iron and copper in filtered (0.4-μm) sea water by APDC—MIBK extraction, and compared the results with those obtained by graphite-furnace a.a.s. techniques. The comparison showed that a significant proportion of the iron and copper was not extractable, even though samples were adjusted to pH <1 for storage, and recovery of added standards was quantitative. Oxidation was therefore considered to be necessary to obtain total metal contents. Cerium(IV) sulphate was chosen as the oxidant mainly becaus of its ability to oxidize Cr(III) to Cr(VI) without interfering in the subsequent extraction. Leoni et al. [24] have demonstrated that although it is not as efficient as dichromate or permanganate, cerium(IV) is effective for use with natural waters. To increase its efficacy, oxidation was carried out with heating in the work reported here.

Conclusions

The APDC—DIBK extraction system can be recommended for samples containing less than 3 mg of iron. DIBK behaves similarly to MIBK in extracti with the advantage that its negligible miscibility with water eliminates potenti sources of error. APDC is preferred to NaDDC because it does not cause a large non-atomic signal from the ketone phase. However, if the sample to be extracted contains more than 3 mg of iron, then the NaDDC—DIBK system with simultaneous background correction is recommended, because NaDDC lessens the interference of iron.

The instability of the manganese chelates of APDC and NaDDC in DIBK made measurement in the organic phase unsatisfactory. However, manganese could be successfully determined in the acid extract of the organic phase.

Cerium(IV) sulphate is effective for the oxidation of Cr(III) to Cr(VI), and does not interfere with the extraction. Because of the existence of non-labile species of trace elements, it is advisable to acidify and oxidize samples prior to extraction, and cerium(IV) can also be used for this purpose.

Particularly in the analysis of effluents, calibration by the method of standard additions is essential for accurate results.

The authors thank the State Electricity Commission of Victoria for permission to publish this paper, the Victorian EPA, particularly Dr. B. Robinson and Dr. H. Blutstein, for the interlaboratory study results, and Mr. G. Fabris for the a.s.v. measurements.

REFERENCES

1 K. Y. Chen, C. S. Young, T. K. Jan and N. Rohatgi. J. Am. Water Pollut. Control Fed., 46 (1974) 2663.
2 R. E. Mansell, At. Absorpt. Newsl., 4 (1965) 276.
3 S. R. Koirtyohann and J. W. Wen, Anal. Chem., 45 (1973) 1986.
4 R. J. Everson and H. E. Parker, Anal. Chem., 46 (1974) 2040.
5 R. R. Brooks, B. J. Presley and I. R. Kaplan, Talanta, 14 (1967) 809.
6 J. L. Jones and R. D. Eddy, Anal. Chim. Acta, 43 (1968) 165.
7 H. J. Crump-Wiesner and W. C. Purdy, Talanta, 16 (1969) 124.
8 J. E. Allan, Spectrochim. Acta, 17 (1961) 459.
9 J. D. Kinrade and J. C. Van Loon, Anal. Chem., 46 (1974) 1894.
10 J. Stary, The Solvent Extraction of Metal Chelates, Pergamon Pess, London, 1964, p. 164.
11 S. Sprague and W. Slavin, At. Absorpt. Newsl., 3 (1964) 11, 160.
12 E. A. Jenne and J. W. Ball, At. Absorpt. Newsl., 11 (1972) 90.
13 M. R. Midgett and M. J. Fishman, At. Absorpt. Newsl., 6 (1967) 128.
14 R. Fukai, Nature, 213 (1967) 901.
15 J. F. Pankow, D. P. Leta, J. W. Lin, S. E. Ohl, W. P. Shun and G. E. Janauer, Sci. Total Environ., 7 (1977) 17.
16 M. Kalk, Nature, 198 (1963) 1010.
17 T. R. Gilbert and A. M. Clay, Anal. Chim. Acta, 67 (1973) 289.
18 E. A. Jenne, J. W. Ball and C. Simpson, J. Environ. Qual., 3 (1974) 281.
19 W. Stumm and P. A. Brauner in J. P. Riley and G. Skirrow (Eds.), Chemical Oceanography, Vol. 1, 2nd edn., Academic Press, London, 1975.
20 A. Y. Cantillo and D. A. Segar in Symposium Proceedings of the International Conference on Heavy Metals in the Environment, Vol. 1, Toronto, October 1975, p. 183.
21 R. A. A. Muzzarelli and R. Rocchetti. Anal. Chim. Acta, 69 (1974) 35.
22 G. E. Batley and T. M. Florence, Anal. Lett , 9 (1976) 379.
23 D. A. Segar and A. Y. Cantillo in Proceedings of the International Conference on Environmental Sensing and Assessment, Vol. 1, Las Vegas, September 1975, p. 6—5.
24 C. Leoni, O. G. Lovato and G. Bellucci, Industria Conserve, 48 (1973) 19.

Analytica Chimica Acta, 107 (1979) 231—243

THE ACCURATE DETERMINATION OF TOTAL SULPHUR AND DISULPHIDE AND POLYSULPHIDE COMPOUNDS IN PETROLEUM PRODUCTS BY METAL REDUCTION AND FLAME EMISSION SPECTROMETRY

J. F. ALDER* and K. KARGOSHA

Chemistry Department, Imperial College of Science and Technology, London, SW7 2AY (Gt. Britain)

(Received 3rd October 1978)

SUMMARY

Conditions for the determination of total sulphur and disulphide/polysulphide in petroleum products are described. The sulphur is reduced by heating with sodium or Devarda's alloy under reflux with subsequent liberation of H_2S and measurement of the chemiluminescent S_2 emission intensity in a hydrogen—argon diffusion flame. The precision and accuracy are good. Applications to light distillates and waxy residues are discussed.

Sulphur is present in petroleum products in many forms including sulphur, mercaptans, sulphides, polysulphides, thiophenes and related compounds. These may impart both desirable and undesirable properties. The oxides of sulphur formed on combustion are corrosive and unpleasant; many sulphur compounds are catalyst poisons and thus present problems in the refining processes, whereas polysulphides may influence the viscosity characteristics of heavy residues. Certain natural sulphur compounds or sulphur-containing additives act as oxidation or corrosion inhibitors in lubricating oils or impart extreme pressure properties to cutting oils. Because of its many roles, sulphur is an important element in industrial processes involving petroleum products and its determination and speciation are of great significance.

Several metal reduction methods are available for the determination of total sulphur in petroleum products. Acid reduction with zinc under reflux has been used for the determination of disulphides [1]; Raney nickel [2], potassium [3] and magnesium [4] have been used in the analysis of various materials for total sulphur.

In previous work [5], it was shown that a modified Lassaigne fusion could be employed for the rapid determination of sulphur in oils and fuels. The product was fused with sodium and the hydrogen sulphide, liberated in the subsequent hydrolysis of the sodium sulphide formed, was passed into a cool argon—hydrogen diffusion flame. The emission from the S_2 species was monitored by using a simple filter photometer. This provided a rapid but rather

imprecise method for the determination of sulphur. The reasons for the imprecision probably lay mainly in the loss of volatile sulphur species — the recovery of sulphur from the samples was later estimated to be 50—60% — and inadequate control of the heating and fusion procedures. The present study was concerned in part with estimating the recovery of sulphur species by this method, and with optimization of the pretreatment conditions in order to maximize recovery and improve both precision and accuracy.

Disulphides and polysulphides play many very important roles in the wool, synthetic polymer, rubber, petroleum and protein industries. Most of these roles are connected with the S—S bond and the presence of cross-linking sites. The analytical difficulties which arise in the determination of disulphides and polysulphides arise more from the type of samples encountered than from the measurement techniques available. Many different quantitative methods have been reported for the determination of disulphide and polysulphide in the presence of other sulphur compounds [6]. These can be largely divided into chromatographic (t.l.c. and g.c.) methods [7] and metal reduction followed by chemical separation and determination [8].

The method of Wronski [9], which is probably the most recent chemical separation—metal reduction method, is based on conversion of disulphides by sodium aluminium bis(2-methoxyethoxy)dihydride in benzene solution to hydrogen sulphide and thiols which can be either directly titrated, after dilution with alcohol, or separated by extraction and determined in the presence of each other by selective masking with acrylonitrile. This is a simple and sensitive method: sulphur at the 0.1-ppm level in hydrocarbons can be determined with a relative standard deviation of 0.5—1.5%, but the recovery for di-t-butyl disulphide is only 75%. Metals such as zinc and sodium, and hydrides such as sodium borohydride and lithium aluminium hydride, which have been used for the reduction of disulphides and polysulphides to mercapt[10], suffer from poor reduction efficiency for tertiary disulphides, except fo the zinc reduction method under reflux conditions which is expected to yield 85—90% recovery for di-t-butyldisulphide. This recovery is, however, achieved only by heating the sample for 1.5 h and purging for 3 h.

In the present study the metal reduction method worked out previously was modified in order to differentiate between some of the various species of sulphur found in petroleum products and to permit their determination by chemiluminescent flame photometry.

EXPERIMENTAL

Apparatus and reagents

The hydrogen—argon diffusion flame and burner assembly and generating cell [5] are outlined in Fig. 1. The emitted radiation is passed through a circular variable wavelength filter (Barr and Stroud, Glasgow) with a band pass of about 20 nm at 348 nm. The filtered light is focused onto an E.M.I. 9781A photomultiplier and the signal is passed via an amplifier and backing-o

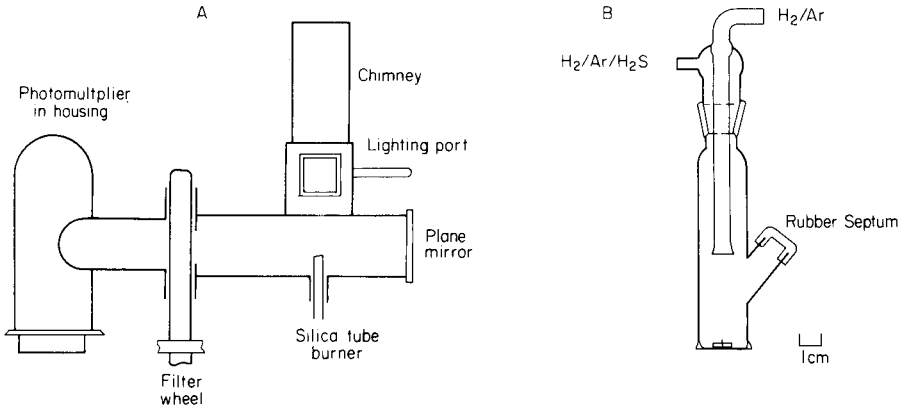

Fig. 1. (A) Burner assembly and (B) generating cell.

unit to a strip-chart recorder. Samples are introduced by a variable-volume (50—250 μl) ejection pipette (Finpipette, Jencons Ltd.). Figure 2 is a schematic diagram of the sample introduction system.

Aqueous standards were prepared from analytical-reagent grade sodium sulphide nonahydrate (B.D.H.). Organic standards were prepared from di-t-butyl disulphide (Aldrich Chemical Co.), diphenyl sulphide, ethanethiol, benzene potassium sulphonate, dimethyl sulphoxide, diphenyl disulphide, diphenyl trisulphide and 1,3-dithiane, all of which were of the highest purity available, made up in white spirit or liquid paraffin.

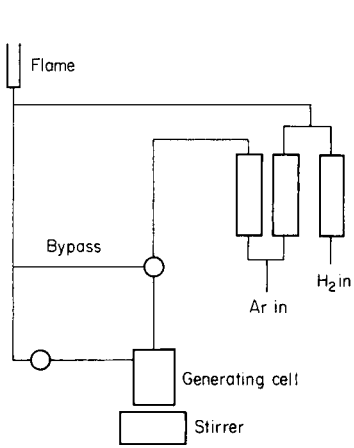

Fig. 2. Schematic diagram of sample introduction system.

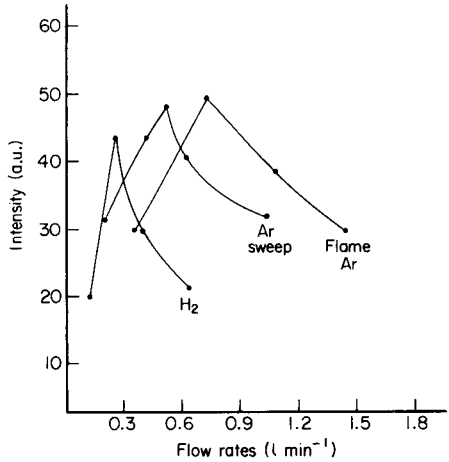

Fig. 3. Optimization of flow rates. H_2 pressure, 1 p.s.i.; Ar pressure, 1.5 p.s.i. When one curve was being obtained the other flow rates were at their optimum setttings.

The sodium sulphide solution was stabilized initially with a pH 11 borate—NaOH buffer but a better method was to use aqueous 20% (w/v) NaOH. The stock 1000-ppm solutions thus prepared were stable for up to one week (Table 1) but were standardized by iodimetric titration [11] before use.

Organic solutions were prepared fresh daily (Table 1). Refrigeration of the organic solutions was unnecessary when solutions were prepared daily.

Improvement of the sodium fusion method for total sulphur determination

In the previous method for the estimation of total sulphur by sodium fusion [5], the initial reduction of the sample was carried out in an open tube over a flame. Although this permitted rapid analyses, results were not reproducible and recoveries were poor. Attempts were therefore made to improve this open-tube method and the subsequent liberation of H_2S from the sodium sulphide formed. Although recoveries of about 80% were obtainable, this did not give good reproducible analyses. The poor recovery of sulphur in the reduction process is due to the conflicting processes of sample vaporization on heating the sample and of the reduction of the sulphur species which needs elevated temperatures for reasonably rapid reaction.

To improve recovery, precison and duration of the reduction process, a reflux method was devised. The apparatus comprised a 10-ml three-neck flask fitted with a nitrogen purge; the Liebig condenser was of single-surface type (10 cm long) with a delivery tube which passed the purge gas into a 10-ml round-bottom flask containing the absorbing solution.

A 1-ml aliquot of a standard solution of di-t-butyl disulphide in liquid paraffin or white spirit was placed in the reflux flask with a freshly chopped-up 2-mm cube of sodium. The flask was fitted to the condenser and the delivery

TABLE 1

Stability of standard solutions

Aqueous solutions (initial concentration, 100 ppm S as Na_2S)

In aqueous solution	S found (ppm) ± s.d.[a]	In 20% (w/v) NaOH solution	S found (ppm) ± s.d.
after 8 h	89 ± 1	after 3 days	99.5 ± 1
after 24 h	75 ± 1	after 7 days	99.0 ± 1

Organic standard solutions (S added as di-t-butyl disulphide)

In liquid paraffin S added (ppm)	S found (ppm) ± s.d.[a]		In white spirit S added (ppm)	S found (ppm) ± s.d.	
	Fresh	After 24 h		Fresh	After 24 h
260	262 ± 3	202 ± 2	260	257 ± 2	202 ± 2
195	194 ± 2	160 ± 1	195	192 ± 2	152 ± 2
130	129 ± 2	107 ± 2	130	129 ± 2	104 ± 1

[a]Calculated for 4—6 analyses.

tube immersed in 8 ml of 5% (w/v) sodium hydroxide in the collector flask. The whole system was purged with nitrogen at a rate of 4 ml min^{-1}. The contents of the flask were refluxed under pre-determined conditions of temperature and time. The reflux was stopped, the flask was allowed to cool and then removed, and the contents were transferred to a 25-ml beaker (to remove the possibility of explosion). The contents of the absorber flask were diluted to 10 ml with 5% sodium hydroxide solution and used to rinse the reflux flask; the washings were then transferred to the beaker. The mixture was carefully stirred and transferred to a separating funnel, shaken for 1 min and allowed to stand until the lower (aqueous) phase cleared. The lower layer was transferred to a 10-ml graduated flask. The sulphide concentration was then determined after acidification of a sample of the solution in the generation vessel (Fig. 1B), by liberation of the H_2S into the diffusion flame and measurement of the S_2 emission intensity [5].

Purging the reflux system ensures complete removal of any H_2S formed, or present in the sample, from the condenser and it is then trapped in the sodium hydroxide. The amount of sulphur trapped in the sodium hydroxide is small; two samples of light distillates containing 300 and 260 ppm sulphur were refluxed in this manner. The contents of the absorber flask were analysed by standard addition and found to contain only 2 and 1 ppm sulphur, respectively.

Optimization of reflux conditions

Duplicate 1-ml aliquots of di-t-butyl disulphide were refluxed as described above at 272, 345, and 380°C for liquid paraffin solvent, and at 157, 173 and 190°C for white spirit solvent, for 20-, 30- and 40-min periods. After subtraction of the solvent blank signal, the recorded S_2 emission signal intensity was compared with aqueous samples containing the same original sulphide concentration and the recoveries were calculated (Table 2). As can be seen, there is little difference between 345 and 380°C or 173 and 190°C for the recoveries

TABLE 2

Optimization of temperature and duration of refluxing

Temperature (°C)	Heating time (min)	S recovery (%)	Temperature (°C)	Heating time (min)	S recovery (%)
Liquid paraffin			*White spirit*		
380	20	63	190	20	67
	30	95		30	89
	40	70		40	73
345	20	61	173	20	66
	30	94		30	90
	40	70		40	74
272	20	15	157	20	30
	30	50		30	60
	40	47		40	40

from liquid paraffin and white spirit, respectively. In both cases, therefore, the lower temperatures were chosen for the analyses, so as to minimize loss of volatile sulphur-containing species. The reason for the decrease in yield after about 30 min is the formation of an emulsion on mixing of the reduced sample with aqueous sodium hydroxide and subsequent difficulty in separating the aqueous layer.

Optimization of gas flows and stirring

The argon flows through the cell and into the flame, and the hydrogen flow to the flame were optimized (Fig. 2). Hydrogen sulphide was generated continuously by hydrolysis of a crystal of sodium sulphide with dilute hydrochloric acid. The results are illustrated in Fig. 3, which shows that the flow rates are quite critical for maximum emission intensity from the flame.

The rate of stirring of the mixture in the gas generating cell was found to be important. The stirring affects the rate of mixing of the analyte solution and the hydrochloric acid in the vessel and the subsequent generation and release of hydrogen sulphide. The recovery reaches a maximum just before the onset of splashing in the cell and for optimum recovery the stirring speed should be maintained just below this critical value.

Calibration curves

Calibration solutions were made up from di-t-butyl disulphide in white spirit and liquid paraffin to represent low and high boiling petroleum products, respectively, and from sodium sulphide in 20% NaOH. The solvent blanks were 1.5 and 0.5 ppm S for the white spirit and liquid paraffin, respectively; these were subtracted before plotting.

The calibration curves are shown in Fig. 4. The linear portion of the curves lie in the range 5—70 ppm S in the original sample, corresponding to 0.5—7.0 μ of sulphide in the 100-μl aliquot taken. The shape of the curves is similar to those obtained by other workers [12]; the curves do not coincide because of the different recoveries of sulphur. As the origin of the emission is chemiluminescent, it is not easy to say what causes the non-linearity. It may be due to quenching effects in the higher concentration and kinetic effects in the lower region where the S + S recombination may be incomplete; these points have been discussed elsewhere [12, 13] but warrant further investigation. The recovery (and relative standard deviation) of the method compared to aqueous solutions on 10 replicate analyses of samples containing 150 ppm sulphur was 95% (±7%) for liquid paraffin solvent, and 90% (±8%) for white spirit solvent.

Analysis of petroleum products

Samples provided by B. P. Research Ltd. and previously analyzed by x-ray fluorescence (x.r.f.) were analyzed by the reflux method. The samples had to be diluted with white spirit for the light distillates and liquid paraffin for the waxy residues, to bring the final solution into the correct concentration range (Table 3). The results, obtained from calibration curves established

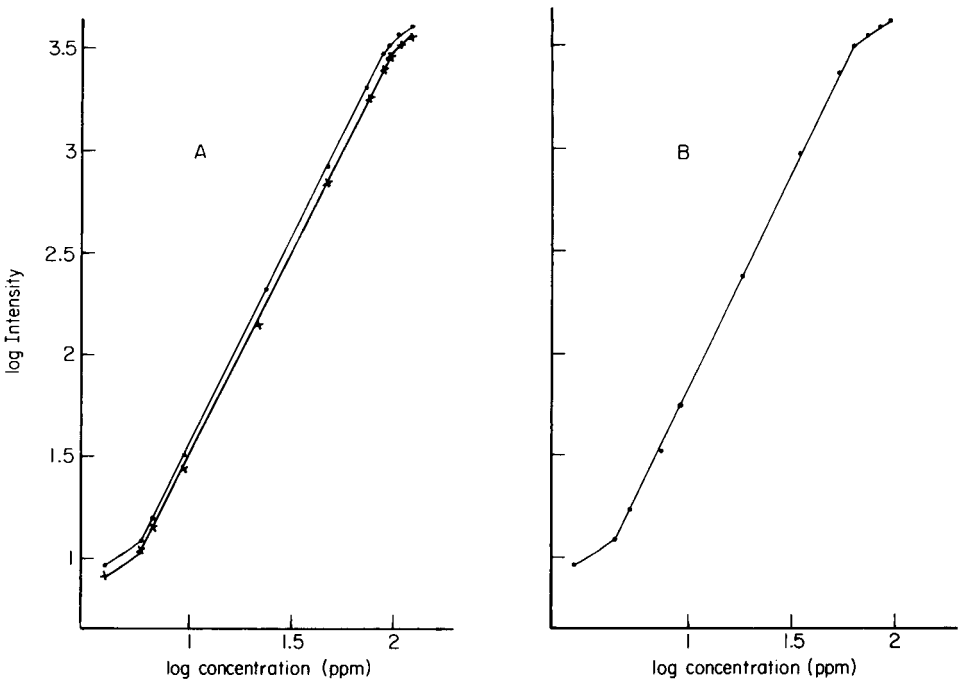

Fig. 4. Calibration curves for organic (A) and aqueous (B) solutions. Curve (a) is for liquid paraffin solutions and curve (b) for white spirit.

TABLE 3

Analysis of petroleum products

Sample	% S found (± s.d.)	% S present[a]	Sample	% S found (± s.d.)	% S present[a]
Light distillates			*Waxy residues*		
8014	0.01 ± 0.002	0.01	9246	0.63 ± 0.02	0.62
7935	0.20 ± 0.015	0.24	9245	0.79 ± 0.065	0.75
8136	0.025 ± 0.002	0.03	8630	3.65 ± 0.3	3.73
7914	0.18 ± 0.01	0.2	8634	1.5 ± 0.1	1.39
7956	0.2 ± 0.025	0.26	7990	2.29 ± 0.15	2.24
9143	1.05 ± 0.06	0.95	7927	2.2 ± 0.18	2.11
9142	0.14 ± 0.01	0.11	8635	3.3 ± 0.2	3.33

[a]Data supplied by B. P. Research.

with organic solutions taken through the procedure, compare most favourably with those obtained by x.r.f.

Determination of disulphide and polysulphide

The reduction conditions with sodium are so drastic that all organic sulphur-containing compounds appear to be converted to sulphides. Whereas total

sulphur is a very useful quantity in many applications, particularly where the petroleum product is to be used as a fuel, there are many cases where more discerning methods for sulphur determination are required. One of these is the determination of disulphide and polysulphide, which play an important role in lubricant and polymer technology.

Several reducing agents were therefore studied for their suitability as specific reductants for the disulphide and polysulphide linkages. After preliminary experiments, described later, to obtain the best conditions for each reducing agent, a series of comparative tests were carried out; the results are summarized in Table 4. The apparatus described above was used; 100 mg of the metal was placed in the reflux flask and 1 ml of a solution of di-t-butyl disulphide, (0.032% w/v) in liquid paraffin was added. The flask was purged with nitrogen (4 ml min^{-1}) and the contents heated to 320°C on a calibrated isomantle for 40 min. The flask was cooled and to the contents were added 2 ml of concentrated hydrochloric acid. The contents were heated again under reflux for 20 min at 120°C. The liberated H_2S was collected in 10 ml of cooled 5% (w/v) sodium hydroxide solution. A 0.1-ml aliquot of this sample was treated as described above to liberate H_2S in the generating cell and pass it into the cool hydrogen diffusion flame. The signal due to the S_2 chemiluminescent emission was recorded and compared to that from standardized aqueous sodium sulphid solutions to obtain the amount of sulphide (as S) in the sample.

RESULTS

Reducing agents

Magnesium. Commercially available magnesium powder was employed (B.D.H. Ltd.). The addition of concentrated hydrochloric acid to the flask after the initial reduction step resulted in an uncontrollably vigorous reaction. The use of (1 + 9) HCl gave a more moderate reduction, but the recoveries obtained were very low.

TABLE 4

Results from different reducing agents
(The sample contained 0.032% S as di-t-butyl disulphide in liquid paraffin; 1-ml aliquots were used. The normalized data for 0.032% S are intercomparable for Tables 4—8.)

Reductant	Signal intensity (a.u.)	Reductant	Signal intensity (a.u.)
Mg (fine powder)	Unsuccessful	Zn amalgam	81
Zn (powder)	19	50% Zn—50% $SnCl_2$	10
Zn (granular)	79	Cu (foil clippings)	23
Zn (foil clippings)	81	Devarda's alloy (50% Cu, 45% Al, 5% Zn)	100[a]

[a]Normalized to 100.

Zinc. Powdered zinc gave low recoveries (Table 4) and was not studied further. Granular zinc was much better and gave similar results to the zinc amalgam and zinc foil. (The amalgam was made by grinding granular zinc in liquid nitrogen, washing with water and treating with 2% (w/v) $HgCl_2$ solution; it was stored under water.) The Zn–$SnCl_2$ mixture, which is a powerful reducing agent, gave poor results.

Copper and Devarda's alloy. Copper clippings (<40 mesh) gave low results but Devarda's alloy (50% Cu, 45% Al, 5% Zn) was most efficient and was therefore used in subsequent work. Different weights of the alloy were employed in the reduction of 1 ml of the sample solutions, and 100 mg proved to be the optimum.

Temperature and duration of heating

The conditions of reduction particularly in the first part with the alloy alone and then in the presence of hydrochloric acid are quite critical. In the first step the reduction is thought to proceed via partial reduction of the S—S bond and formation of metal sulphides. Extending the duration of the heating at 320°C during the first part of the reduction results in increased recovery up to about 40 min (Fig. 5); to obtain this curve, the heating time during the second stage was kept constant at 20 min.

The second stage of reduction which involves the alloy and hydrochloric acid is thought to occur through two processes: decomposition of metal sulphides and also reduction of some S—S and S—H bonds to hydrogen sulphide by hydrogen [10]:

$$(\text{t-Bu})\text{—S—S—(t-Bu)} \xrightarrow{(H)} 2(\text{t-Bu})\text{—SH} \xrightarrow{(H)} 2(\text{t-Bu})\text{H} + H_2S$$

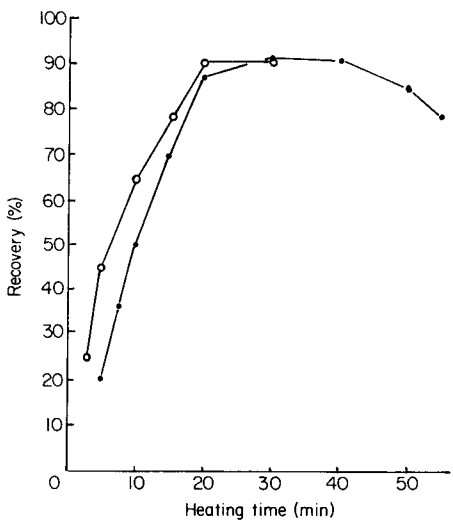

Fig. 5. Effect of duration of heating on the sulphur recovery: (•) first stage; (○) second stage.

The optimum period of heating the solution during the second stage was determined in the usual way and found to be 20 min at 120°C. The amount of concentrated hydrochloric acid employed in this step was varied in order to obtain the optimum recovery of S. The concentration of the sodium hydroxide solution in the absorber was also varied in order to optimize the conditions; this concentration should not be so high that the solution must be rendered acid in the subsequent step, and the minimum concentration compatible with good recovery is best. These experiments indicated the use of 2 ml of concentrated hydrochloric acid and 10 ml of 5% (w/v) sodium hydroxide in the absorbing flask (Table 5).

During the heating process, the sodium hydroxide solution becomes warm as the purge nitrogen passes through. This leads to loss of H_2S (about 5—7%) and must be minimized. The flask was therefore kept cool in an ice bath thoughout the experiment.

Optimization of other parameters

When nitrogen was bubbled through the solution in the flask, lower recoveries (about 5%) were found, possibly because of more rapid removal of the hydrogen from the solution. Passing the purge gas over the surface of the liquid improved the recoveries; this use of purge gas is not always essential, but is advisable in many cases to avoid atmospheric oxidation.

The order of addition of reagents in the reduction process was also investigated as well as the effect of omitting the Devarda's alloy. The results obtained (Table 6) show that the last method is by far the most efficient; this underlines the role that the reducing alloy plays in the initial reduction of the S—S bond.

To check whether any H_2S passed through the absorbing flask a second flask was put in series containing the same 5% sodium hydroxide solution; no sulphide was detected in this flask.

TABLE 5

Effect of amount of acid and concentration of sodium hydroxide in absorbing solution (Sample as for Table 4)

Amount of HCl (ml)	Intensity (a.u.)		
	H_2O absorber	Aq. 2% NaOH absorber	Aq. 5% NaOH absorber
0.5	24	24	24
1.0	29	56	24
1.5	16	86	87
2.0	6	95	100
2.5	3	85	100[a]

[a]Normalized to 100, all other signals referred to this.

TABLE 6

The effect of order of addition of reagents on signal intensity
(Sample as for Table 4)

Method	Intensity (a.u.)
Add 2 ml 11 M HCl; heat 60 min	$< 2^a$
Add 100 mg Devarda's alloy + 2 ml 11 M HCl: heat 60 min	8
Add 2 ml 11 M HCl; heat 20 min; add 100 mg alloy; heat 40 min	19
Add 100 mg alloy; heat 40 min; add 2 ml 11 M HCl; heat 20 min	100^b

[a]NaOH absorbing solution became acid.
[b]Signal normalized to 100 and others referred to it.

Interference studies

Several other sulphur-containing organic compounds were tested by this method. The compounds were dissolved in liquid paraffin, where possible, to give solutions containing 0.032% S. The results, summarized in Table 7, show that thiols and, of course, dissolved hydrogen sulphide interfere, as does elemental sulphur (Table 8). In view of the proposed mechanism of the reduction of the S—S bonds it is not surprising about the effect of thiols. The interference can, however, be easily removed by previously shaking 5 ml of the analyte solution with 5 ml of aqueous 1 M silver nitrate. The silver mercaptide precipitates, is centrifuged out and can be determined separately if required. The sulphur can be removed by then shaking the solution with mercury (2 g for 10 ml of sample) which forms mercury sulphide; this too can be readily centrifuged out and determined separately. Recovery tests of the disulphide from solutions containing other sulphur compounds are shown in Table 8.

The determination of disulphide in the presence of monosulphide

In order to test the applicability of the method for the determination of the disulphide species in the presence of monosulphide, solutions containing 32 ppm S as di-t-butyl disulphide were made up in liquid paraffin in the presence of 300—400 ppm S as dimethyl sulphide and diphenyl sulphide. The effect on the recovery is illustrated in Fig. 6. It can be seen that there is only a modest interference by these other species.

Recovery from light distillates

Recovery tests were carried out on di-t-butyl disulphide and diphenyl trisulphide light distillate fractions diluted with white spirit to bring their sulphur levels down to between 300 and 1000 ppm. These samples had previously been analysed for total sulphur by x.r.f. and some also by the proposed method (Table 3). The samples were first shaken with 1 M silver nitrate and then mercury to remove any mercaptans or sulphur. As can be seen from Table 9, the recovery is good for both the disulphide and trisulphide species.

TABLE 7

Potential interference of sulphur containing compounds on disulphide determination (All species sulphur-containing compounds were present at a level of 0.032% sulphur by weight calculated on their molecular formula, and made up in liquid paraffin. The signal for di-t-butyl disulphide was normalized to 100 and all other signals referred to that.)

Compound	Intensity (a.u.)	Compound	Intensity (a.u.)
Liquid paraffin	<1	Dimethyl sulphide	2
Di-t-butyl disulphide	100	Dimethyl sulphoxide	0.03
Ethylmercaptan	110	Benzene potassium sulphonate[a]	2
Diphenyl trisulphide[a]	95	1,3-Dithiane[a]	1
Diphenyl sulphide	<1		

[a]Dissolved first in a little benzene and then diluted with liquid paraffin.

TABLE 8

Recovery of disulphide sulphur (0.032% S) in presence of 100-fold amounts of interfering compounds

Interferent	Intensity (a.u.)	Interferent	Intensity (a.u.)
[Di-t-butyl disulphide]	100[a]	Dimethyl sulphoxide	96
Ethyl mercaptan	>350	Benzene potassium sulphonate	96
Ethyl mercaptan[b]	110	1,3-Dithiane	100
Diphenyl sulphide	130	Elemental sulphur[c]	>350
Dimethyl sulphide	145	Elemental sulphur[c, d]	98

[a]The signal is normalized to 100.
[b]5 ml of sample washed with 5 ml of 1 M $AgNO_3$ prior to analysis.
[c]Dissolved first in a little aniline and then in liquid paraffin.
[d]10 ml of sample shaken with 2 g of mercury prior to analysis.

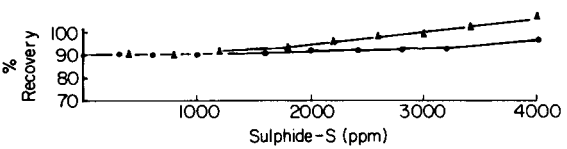

Fig. 6. Interference of monosulphides on disulphide determination. (▲) Dimethyl sulphide; (●) diphenyl sulphide.

Conclusions

This work has shown that the combination of metal reduction of sulphur compounds to sulphides in petroleum products coupled with release of hydrogen sulphide into a cool flame and measurement of the S_2 emission provides a useful method for the determination of total sulphur and for the separate determination of sulphur species. The method is capable of good

TABLE 9

Recovery tests from light distillates diluted with white spirit

Original sample	S in diluted sample (ppm)	Di-t-butyl disulphide		Diphenyl trisulphide	
		Added (ppm)	Recovery (%)	Added (ppm)	Recovery (%)
7866	400	320	90	320	89
7914	800	420	92	410	90
7956	520	250	91	240	92
7957	330	200	93	200	92
8110	450	180	90	180	91
9142	300	150	90	150	91
9143	950	120	91	120	90

precision and accuracy as well as versatility. With selective separation of the species, mercaptans with acrylonitrile [14], hydrogen sulphide with silver nitrate and sulphur with mercury, these species could all be analysed separately and thus provide S, -SH, H_2S, (S_2 and S_n) in the same sample.

The authors are grateful to B. P. Research, Sunbury, for the provision of the analyzed samples and to the Reza Pahlavi Cultural Foundation for support of K. K.

REFERENCES

1 J. H. Karchmer and M. T. Walker, Anal. Chem., 30 (1958) 85.
2 I. Honarkhah, Bull. Iran. Petrol. Inst., 50 (1973) 21.
3 A. D. Campbell, M. J. Brown and D. J. Hannah, Anal. Chim. Acta, 78 (1975) 234.
4 S. Shiffman and C. W. Frank, Anal. Chem., 46 (1974) 1804.
5 J. F. Alder, M. A. Pinches, T. S. West and R. W. Williams, Lab. Pract., 25 (1976) 455.
6 G. R. Umbreit, P. C. Barbat and J. V. Wisniewski, Facts Methods, 7 (1966) 1.
7 H. Norkamura and Z. Tamura., J. Chromatogr., 96 (1974) 195, 211.
8 T. L. C. de Souza and S. P. Bhatia, Anal. Chem., 48 (1976) 2234.
9 M. Wronski, Talanta, 21 (1974) 776.
10 J. H. Karchmer (Ed.), The Analytical Chemistry of Sulfur and its Compounds, Vols. 1 and 2, Interscience-Wiley, New York, 1970, 1972.
11 I. M. Kolthoff, R. Belcher, V. A. Stenger and G. Matsuyama, Volumetric Analysis, Vol. 3, Interscience, New York, 1957, p. 291.
12 G. L. Everett, T. S. West and R. W. Williams, Anal. Chim. Acta, 68 (1974) 387.
13 D. G. Greer and T. J. Bydalek, Environ. Sci. Technol., 7 (1970) 153.
14 M. Wronski, Analyst, 85 (1960) 526.

Analytica Chimica Acta, 107 (1979) 245—251

ATOMIC ABSORPTION SPECTROMETRY OF TIN WITH ELECTROTHERMAL ATOMIZATION IN A MOLYBDENUM MICROTUBE

KIYOHISA OHTA and MASAMI SUZUKI*

Department of Chemistry, Faculty of Engineering, Mie University, Kamihama-cho, Tsushi, Mie-ken 514 (Japan)

(Received 9th October 1978)

SUMMARY

The atomic absorption spectrometry of tin with atomization in a molybdenum microtube is described. The addition of hydrogen to the argon purge gas improves the efficiency of atomization of tin; measurements are best done at 224.61 nm. Phosphoric acid lowers the atomization temperature of tin, and depresses the interferences from diverse elements. Tin in canned foods (fruit juices and drinks) can be determined by direct atomization after dilution with phosphoric acid. Prior extraction is necessary for analysis of geological materials.

The recent growing demand for the determination of low concentrations of tin has involved several studies of flame atomic absorption spectrometry, but this technique lacks adequate sensitivity. Flameless atomic absorption spectrometry allows the determination of traces of tin in small samples, but little work on tin in food and geological materials has been described. Meranger [1] determined tin stabilizers in alcoholic beverages with a graphite furnace. Trachman et al. [2] investigated the graphite-furnace method for sub-ppm levels of tin in solvent extracts from plastic barrier films stabilized with organotin compounds and in biological tissues.

Several authors have used tantalum-lined graphite furnaces to improve the sensitivity for some elements. Metal atomizers have some important advantages: background emission in the 200—300-nm region is lower than that for graphite atomizers at the same temperature, and electrical requirements for heating are less demanding. This paper describes the electrothermal atomic absorption spectrometry of tin with a molybdenum micro-tube atomizer and a fast-response amplifier system, and its application to the determination of tin in food and geological materials.

EXPERIMENTAL

Apparatus and solutions

The monochromator, photomultiplier, signal control unit and Memoriscope were the same as used previously [3]. The light source was a tin

hollow-cathode lamp (Hamamatsu TV Co.). A deuterium lamp (Original Hanau D200F) was used for correction of background from molecular species.

The molybdenum micro-tube atomizer (0.5-mm diameter, 17-mm long) and absorption chamber (300 ml) have been described [4], as has the method of measuring the tube temperature [5]. The argon used as purge gas in the absorption chamber was mixed with hydrogen. All sample solutions were injected with glass micro-pipettes.

Tin stock solution was prepared by dissolving pure tin metal in hydrochloric acid, all reagents were of analytical-reagent grade, and deionized-distilled water was used in all dilutions.

General procedure

The sample solution (1 μl) was placed in the micro-tube atomizer. The absorption chamber was flushed with a mixture of argon (480 ml min^{-1}) and hydrogen (20 ml min^{-1}). The sample was dried at 100°C for 7 s, ashed at 200—300°C for 5 s, and atomized by heating to a final temperature of 2100°C. All atomic absorption signals were traced on the Memoriscope and peak heights were measured. Measurements were made at the 224.61-nm line.

Recommended procedure for geological materials

Decompose 0.1—0.3 g of sample with 2 ml of nitric acid (14 M) and 2 ml of hydrofluoric acid (40%) in a Uni-Seal decomposition vessel by heating at 120°C for 2 h. After decomposition, transfer the solution to a Teflon beaker and evaporate by heating on a water bath. Take up the residue in 11 M hydrochloric acid and repeat the evaporation. Dissolve the residue in hydrochloric acid to give a solution of acidity 9.6 M in a volume of 10 ml. Transfer 2.5 ml of this solution to a separatory funnel, add 0.5 ml of 5% (w/v) potassium chlorate solution, and extract tin with 3 ml of methyl isobutyl ketone. Then shake the organic phase vigorously with 3 ml of water to strip tin. Mix suitable aliquots of the aqueous phase with equal volumes of phosphoric acid and proceed as above. Take aliquots of standard tin(II) chloride solutions through the entire procedure to prepare calibration curve.

RESULTS AND DISCUSSION

Atomic absorption characteristics of tin

Tin was atomized from various compounds and complexes to establish its atomization characteristics in the molybdenum micro-tube atomizer. Tin(II) chloride and tin(IV) sulphate were used as the aqueous solutions. Chloride, thiocyanate, *N*-benzoyl-*N*-phenylhydroxylamine (BPHA), 8-hydroxyquinolinate and diethyldithiocarbamate (DDTC) complexes of tin(IV) were extracted as described in the literature [6—10]. Figure 1 shows the Memoriscope traces of tin absorption for the various compounds and complexes; all samples contained the same tin concentration. As can be seen, the absorption

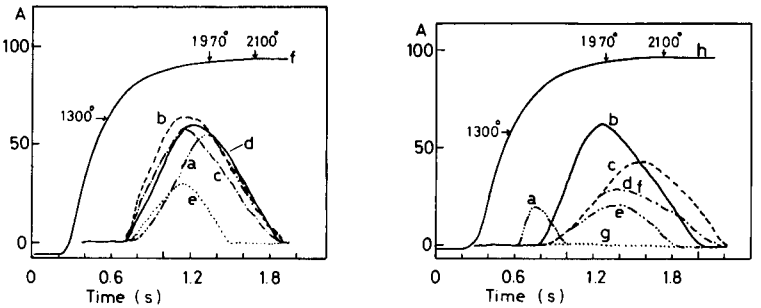

Fig. 1. Memoriscope traces for tin (0.5 ng), in the molybdenum micro-tube atomizer. (a) Aqueous tin(II) chloride solution; (b) aqueous tin(IV) sulphate solution; (c) tin(IV) chloride in MIBK; (d) tin(IV)—BPHA complex in chloroform; (e) tin(IV) thiocyanate complex in MIBK; (f) temperature increase. Gas flow rates, 480 ml Ar min^{-1} and 20 ml H_2 min^{-1}.

Fig. 2. Effect of hydrogen flow rate on atomization of 0.5 ng of tin: (a) 500 ml Ar min^{-1}; (b) 480 ml Ar min^{-1} and 20 ml H_2 min^{-1}; (c) 400 ml Ar min^{-1} and 100 ml H_2 min^{-1}; (d) 300 ml Ar min^{-1} and 200 ml H_2 min^{-1}; (e) 200 ml Ar min^{-1} and 300 ml H_2 min^{-1}; (f) 100 ml Ar min^{-1} and 400 ml H_2 min^{-1}; (g) 500 ml H_2 min^{-1}; (h) temperature increase.

profiles varied for atomization of different compounds. The profiles for the sulphate and 8-hydroxyquinolinate were very similar. The tin absorption was significantly lower for atomization from the DDTC and thiocyanate complexes; thiourea also affected the tin atomization. The absorption profiles for tin in the presence of DDTC and thiourea are not shown because they were very similar to those obtained for the thiocyanate complexes. DDTC, thiocyanate and thiourea probably formed sulphides with tin during the ashing step, thus affecting tin atomization. The variations in the absorption profiles may result from the different thermal stabilities of the tin compounds.

Some hydrogen was essential for effective atomization, but the tin absorption decreased with increasing flow rate of hydrogen. Figure 2 shows the Memoriscope traces obtained for the atomization of tin(II) chloride at different flow rates of hydrogen with a total gas flow of 500 ml min^{-1}. The absorption for tin was lower in the absence of hydrogen, although the appearance temperature was also lower; there was no absorption in pure hydrogen. The cooling effect of the high flow rates of hydrogen may be responsible for decreasing the tin absorption. Clearly the optimum flow rate of hydrogen is 20 ml min^{-1}. The reason for higher appearance temperatures in the presence of hydrogen is not clear. The effect of hydrogen on tin atomization is probably due to the formation of easily dissociated SnH species. The effectiveness of hydrogen for atomization of tin in carbon rod and carbon filament atomizers has already been reported [11, 12]. Rubeška [13] explained the effect of hydrogen by assuming that free tin atoms are formed through reactions of tin oxide with hydrogen. Aggett and Sprott

[14] measured appearance temperatures of 1140°C and 1400°C for carbon rod and tantalum strip atomizers, respectively; they concluded that free tin atoms are formed by thermal dissociation of the oxide in tantalum strip atomizers, but by reduction of the oxide with graphite in graphite atomizers. Sturgeon et al. [15] reported an appearance temperature of 1287°C (1560 K) for atomization of tin in a graphite furnace, and suggested carbon reduction of the oxide as the atomization mechanism. The appearance temperature was 1550°C for atomization of tin in the molybdenum micro-tube atomizer; this higher temperature is probably due to thermal dissociation playing the major role in tin atom production. However, a convincing description of the atomization mechanism in the molybdenum micro-tube atomizer does not appear possible, because the picture is complicated by the presence of hydrogen around the atomizer.

Tin absorption was measured at 224.61 and 235.48 nm by atomizing 0.5 ng of tin. The temperatures showing maximum absorption were 1970°C at 224.61 nm and 2020°C at 235.48 nm (Fig. 3). The tin absorption was lower at 235.48 nm than that at 224.61 nm, which indicates that the population of tin atoms in the $^3P_1$ energy level corresponding to the 235.48-nm line is less than that in the $^3P_0$ ground state corresponding to the 224.61-nm line at the temperature in the micro-tube atomizer. Parsons et al. [16] reported that the zero level is the more densely populated at 1727°C (2000 K) whereas at 2027°C (2300 K) and above the $^3P_1$ level is the more densely populated. Measurement at 224.61 nm is clearly preferable.

The absolute sensitivity under the optimized conditions was 8.6×10^{-12} g (for 1% absorption). The coefficient of variation evaluated from seven measurements of 0.2 ng of tin was 2.8%.

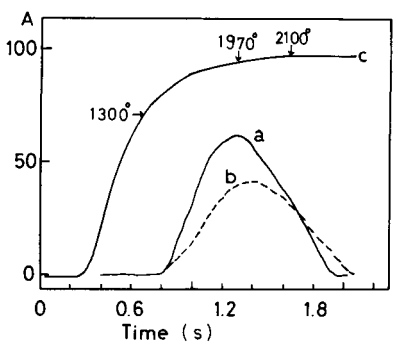

Fig. 3. Effect of analytical lines on tin absorption (0.5 ng Sn): (a) 224.61 nm; (b) 235.48 nm; (c) temperature increase. Gas flow rates, 480 ml Ar min^{-1} and 20 ml H_2 min^{-1}.

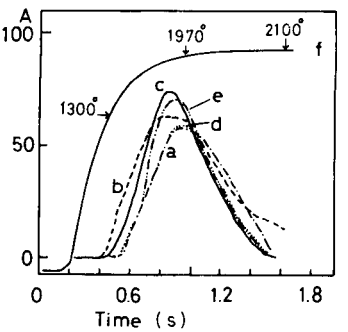

Fig. 4. Effect of acids on atomization of 0.5 ng of tin: (a) 0.05 M HCl; (b) 0.05 M H_2SO_4; (c) 0.05 M H_3PO_4; (d) 0.05 M $HClO_4$; (e) 4 μg tartaric acid; (f) temperature increase. Gas flow rates, 480 ml Ar min^{-1} and 20 ml H_2 min^{-1}.

Interferences

The effects of phosphoric, perchloric, nitric, sulphuric, oxalic, citric and tartaric acids on tin atomization were tested; the mineral acids were used at the 0.05 M level and organic acids were added at concentrations of 4 $\mu g\ \mu l^{-1}$. Neither perchloric nor nitric acid had any significant effect, whereas the other acids enhanced the tin absorption (Fig. 4). The most striking effect was observed with phosphoric acid, which lowered the temperature showing maximum absorption, gave a narrower absorption profile, and improved the sensitivity for tin to 6.2×10^{-12} g. This effect was not observed with phosphates such as sodium hydrogenphosphate. Phosphoric acid has similar effects in the atomic absorption of other elements which form gaseous covalent hydrides. The favourable effect of phosphoric acid on atomization of tin in a graphite atomizer has been described by Czobik and Matousek [17].

The interferences of 100-fold amounts of arsenic(III), bismuth, calcium, chromium(III), copper, iron(III), potassium, sodium, antimony(III) and zinc on 0.5 ng of tin were investigated. Calcium, chromium, copper, iron, potassium, sodium and antimony did not interfere. Arsenic depressed the tin absorption, while bismuth and zinc showed enhancing effects. Phosphoric acid served to depress these interferences. The interferences of arsenic and bismuth and their removal by phosphoric acid are illustrated in Fig. 5. Addition of phosphoric acid also eliminated interferences from organic acids as well as the variations of response from different forms of tin. However, although interferences from diverse elements were depressed in this manner, prior separation is advisable for determining traces of tin in complex matrices.

Determination of tin in canned juice and drinks

Foods stored in cans, and particularly fruit juices which retain some acidity, tend to dissolve traces of tin from the container. The determination of this

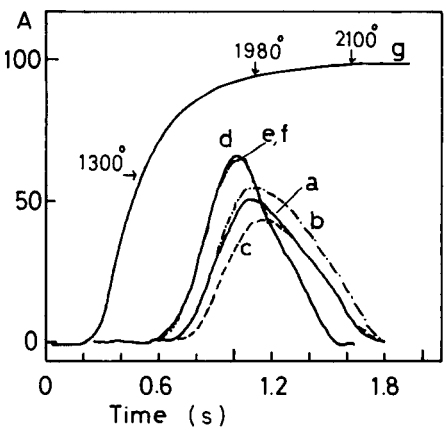

Fig. 5. Interferences of diverse elements on tin atomization. (a) 0.5 ng Sn(II); (b) 0.5 ng Sn(II) + 50 ng Bi; (c) 0.5 ng Sn(II) + 50 ng As; (d) 0.5 ng Sn(II) in 0.05 M H_3PO_4; (e) 0.5 ng Sn(II) + 50 ng Bi in 0.05 M H_3PO_4; (f) 0.5 ng Sn(II) + 50 ng As in 0.05 M H_3PO_4; (g) temperature increase. Gas flow rates, 480 ml Ar min^{-1} and 20 ml H_2 min^{-1}.

tin is important in food analysis. Tin in canned fruit juices and drinks can be determined simply after dilution with phosphoric acid. The micro-tube atomizer permits high dilution of samples because of its great sensitivity. Phosphoric acid eliminates interferences from organic matter and the effect of different forms of tin. All that it is necessary to do is to dilute the sample 50—100-fold with phosphoric acid (0.05 M), and then analyze 1-μl aliquots of this solution under the conditions recommended in the Experimental part. The calibration curve is prepared by treating standard tin(II) chloride solutions in the same way.

The results obtained for some fruit juices and drinks are listed in Table 1; the recovery study, with addition of known quantities of tin to the sample, was satisfactory. Inorganic tin(II) solutions were used for calibration because the tin in these canned liquids seemed to be present in inorganic forms. Organotin compounds may appear in plastic food packaging, and inorganic tin standard solutions might then be unsatisfactory; this requires further study.

Determination of tin in geological materials

Prior separation was necessary for the determination of tin in geological samples because of the complex matrix. Chloride extraction [6] was adequate: more than 90% of the tin could be extracted by a single extraction, which was sufficiently reproducible for the present work. Decompose 0.1—0.3 g of sample with 2 ml of nitric acid (14 M) and 2 ml of hydrofluoric acid (40%) in a Uni-Seal decomposition vessel by heating at 120°C for 2 h. After decomposition, transfer the solution to a Teflon beaker and evaporate by heating on a water bath. Take up the residue in 11 M hydrochloric acid and repeat the evaporation. Dissolve the residue in hydrochloric acid to give a solution of acidity 9.6 M in a volume of 10 ml.

The results obtained for tin in rock samples by the procedure given in the Experimental are listed in Table 2. The agreement with the certified values is good.

Micro-tube atomizers need only brief heating to provide an environment with a uniform temperature throughout the atomizer. The maximum atom

TABLE 1

Determination of tin in some canned drinks

Sample	Tin (ppm)		Sample	Tin (ppm)	
	Added	Found		Added	Found
Orange drink	—	0.6	Peach juice	—	48
	1.3	1.9		53	105
	2.5	3.2		105	160
Pineapple drink	—	1.6	Orange juice	—	52
	1.3	2.9		50	103
	2.5	4.3		80	133

TABLE 2

Determination of tin in rock samples

Rocks	Tin found (ppm)[a]	Certified value (ppm)
JB-1	2.3 ± 0.7	2.3
JG-1	2.8 ± 0.4	3.0
AGV-1	5.5 ± 1.4	4.2

[a]Three determinations.

cloud concentration is formed in an extremely short period of time. Accordingly, effective measurements are possible only if a fast-response detection system is available. The determination of tin is very sensitive and only small samples are needed if the tin is distributed homogeneously.

Appreciation is expressed to Dr. A. Ando, Geological Survey of Japan, for the rock samples.

REFERENCES

1 J. C. Meranger, J. Assoc. Off. Anal. Chem., 58 (1975) 1143.
2 H. L. Trachman, A. J. Tyberg and P. D. Branigan, Anal. Chem., 49 (1977) 1090.
3 K. Ohta and M. Suzuki, Anal. Chim. Acta, 96 (1978) 77.
4 K. Ohta and M. Suzuki, Anal. Chim. Acta, 77 (1975) 288.
5 K. Ohta and M. Suzuki, Anal. Chim. Acta, 83 (1976) 381.
6 H. Goto, Y. Kakita and T. Furukawa, Nippon Kagaku Zasshi, 79 (1958) 1513.
7 Y. Ishihara and H. Komuro, Bunseki Kagaku, 12 (1963) 380.
8 N. Jordanov, St. Mareva and M. Koeva, Anal. Chim. Acta, 59 (1972) 75.
9 H. Hashitani, K. Katsuyama and K. Motojima, Bunseki Kagaku, 16 (1967) 478.
10 R. A. Chalmers and D. M. Dick, Anal. Chim. Acta, 31 (1964) 520.
11 R. E. Sturgeon, C. L. Chakrabarti, I. S. Maines and P. C. Bertels, Anal. Chem., 47 (1975) 1240.
12 G. L. Everett, T. S. West and R. W. Williams, Anal. Chim. Acta, 70 (1974) 291.
13 I. Rubeška, Spectrochim. Acta, Part B, 29 (1974) 263.
14 J. Aggett and A. J. Sprott, Anal. Chim. Acta, 72 (1974) 49.
15 R. E. Sturgeon, C. L. Chakrabarti and C. H. Langford, Anal. Chem., 48 (1976) 1792.
16 M. L. Parsons, B. W. Smith and P. M. McElfresh, Appl. Spectrosc., 27 (1973) 471.
17 E. J. Czobik and J. P. Matousek, Talanta, 24 (1977) 573.

Analytica Chimica Acta, 107 (1979) 253—259

DETERMINATION OF GERMANIUM IN DIFFERENT MEDIA BY ATOMIC ABSORPTION SPECTROMETRY WITH ELECTROTHERMAL ATOMIZATION

YOSHIKI MINO* and SHIGERU SHIMOMURA

Faculty of Pharmaceutical Sciences, University of Tokushima, 1-78 Shomachi, Tokushima 770 (Japan)

NAGAYO OTA

Osaka College of Pharmacy, 2-10-65 Kawai, Matsubara City, Osaka 580 (Japan)

(Received 25th October 1978)

SUMMARY

Effects of acids, alkalis or salts on the atomic absorption spectrometry (electrothermal atomization) of germanium are described. Most of the species tested interfere with the absorption. The mechanisms of the interferences were investigated by using tantalum-coated and standard graphite tubes. The results showed that positive interferences are due to inhibition of the reaction of germanium dioxide with carbon to form volatile GeO, and that suppressive interferences are due to physical occlusion effects. The addition of sodium hydroxide to the sample solution provides a very sensitive analysis (0.004 ppm for 1% absorption) for germanium without matrix interferences. This is probably due to the formation of stable Na_2GeO_3 during the ashing step in the presence of sodium hydroxide.

Flameless atomic absorption spectrometry (a.a.s.) is most frequently used for trace analysis, so that the analyte is usually accompanied by an excess of other sample components (matrix) which may produce serious errors in the determination. These matrix effects are an important problem in flameless a.a.s. and have been widely investigated [1—10] for familiar metals such as Cu, Zn, Cd, Pb, in analytical work concerned with geochemistry or environmental pollution. The suppressive effects of the matrix on the sensitivity observed in flameless a.a.s. of such metals have been discussed in detail and their mechanisms have been elucidated considerably. It is generally agreed that interferences result from complex combinations of several factors such as gas-phase interaction [1], metal and compound volatility [2, 4] and physical occlusion [5, 8]. In contrast, little information is available about enhancing effects of matrices on the sensitivity.

The present paper deals with the determination of germanium by a.a.s. with a graphite tube atomizer. Very high positive interferences were found from some acids, alkalis and salts. The mechanisms of the enhancing effects is discussed, and a method of overcoming various interferences is described.

---

*Present address: Osaka College of Pharmacy, 2-10-65 Kawai, Matsubara City, Osaka 580 (Japan).

EXPERIMENTAL

Apparatus and materials

A two-channel, dual-phase atomic absorption spectrometer (Nippon Jarrell-Ash model AA-8500) was used in combination with a graphite tube atomizer (model FLA-10), and two-pen recorder (Hitachi model 056), a germanium hollow-cathode lamp (Hamamatsu TV:L-233) and a deuterium lamp background corrector, respectively. Argon was used to provide the inert atmosphere in the graphite tube. Samples (10 μl) were introduced by an Eppendorf micropipette with disposable plastic tips. Unless otherwise mentioned, each graphite tube had already been used for about 30 injections. The optimal instrument parameters were as follows: analytical line, 265.12, 265.16 nm (doublet); background correction, 265.5 nm; germanium lamp current, 10 mA; deuterium lamp current, 200 mA; argon flow, 2.0 l min^{-1}; ramp mode, 0. The atomization program was: drying at 18 A (150°C) for 30 s, ashing at 50 A (700°C) for 30 s, and atomization at 280 A (3000°C) for 8 s; the temperatures in parentheses are those given in the instrument manual.

An x-ray diffractometer (Rigakudenki Rotaflex RU-200) equipped with both graphite bent-monochromator and scintillation counter was employed. The working conditions have been given previously [11].

Stock solutions of (500 ppm) were prepared as reported previously [11]. All chemicals used were of reagent-grade or the highest quality available.

Procedure for tantalum coating

Weigh about 100 mg of tantalum powder into a 10-ml test tube and add 2 ml of deionized water. Transfer 100 μl of this suspension to a graphite tube with a micropipette. Dry slowly at about 100°C, increase the temperature to about 1500°C, and heat at 3200°C for 10 s.

X-ray diffractometric measurements

Transfer 40 ml of solution containing 0.250 g of germanium dioxide into a crucible, evaporate to dryness, and heat at 150°C or 700°C for 3 h in a muffle furnace. After cooling to about 100°C, grind the contents in an agate mortar. Pack the powdered sample into the cavity of the specimen glass holder for diffractometric analysis. Each sample was identified by the Hanawalt method [12, 13] from the x-ray diffraction pattern obtained.

RESULTS AND DISCUSSION

Effect of acids or alkalis

The variation of the absorbance was studied as a function of the concentration of acids or alkalis, for aqueous germanium solutions of constant concentration. The addition of acids or alkalis markedly affected the atomization signal of germanium (Fig. 1). When 0.1 M HNO_3 was added to a pure germanium solution, the enhancement of sensitivity observed was about five-fold,

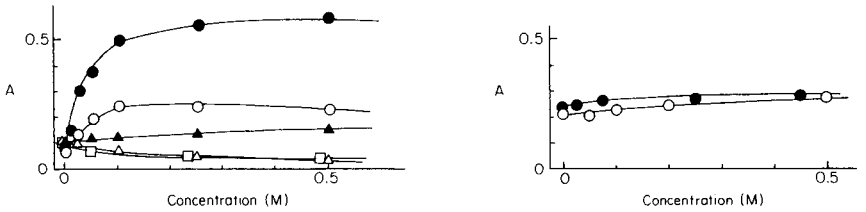

Fig. 1. Effects of acids or alkalis on absorption of germanium with a graphite tube atomizer. (—●—) NaOH; (—▲—) NH_3; (—△—) HCl; (—□—) H_2SO_4; (—○—) HNO_3. Ge concentration: 0.5 ppm for HNO_3 and NaOH; 1.0 ppm for H_2SO_4, HCl and NH_3.

Fig. 2. Effects of sodium hydroxide and nitric acid on absorption of germanium (0.5 ppm) with a tantalum-coated atomizer. (—●—) NaOH; (—○—) HNO_3.

but 0.1—0.3 M NaOH caused an extremely high enhancement. Little variation of signal was observed over the range 0.2—0.6 M NaOH; the signal at 0.5 M NaOH; corresponds to about ten-fold enhancement compared to pure germanium solution. Clearly, the behavior of the germanium atomization signal is not related to the acidic or alkaline conditions, but to the form of germanium injected. The suppressive interferences of HCl and H_2SO_4 can be explained as follows: the HCl interference can be attributed to the formation of volatile chlorides such as $GeCl_4$ in the drying stage; with H_2SO_4, the atomization signal is suppressed by physical occlusion in the sulfuric acid mist during its rapid vaporization.

The extremely positive interferences of nitric acid and sodium hydroxide do not seem to have been discussed in the literature, and appear to be characteristic of the flameless a.a.s. of germanium. It has been reported [14—16] that the reaction $GeO_2 + C \rightarrow GeO + CO$ predominates when germanium dioxide is heated in the presence of carbon. Germanium monoxide is volatile at the reaction temperature, and sublimes without undergoing further reduction. Johnson et al. [17], who first studied the determination of germanium by flameless a.a.s., suggested that difficulties in the determination of germanium are due to GeO formation, and recommended rapid increase in temperature to prevent loss of sample as germanium monoxide.

To investigate the behavior of the germanium signal in the absence of carbon, tantalum-coated graphite tubes were used. Figure 2 shows that considerable enhancement of the germanium signal was achieved simply by inhibiting contact of germanium dioxide with carbon and that the addition of HNO_3 or NaOH did not then affect the germanium signal significantly. Figures 1 and 2 support the view of Johnson et al. [17] and suggest that the positive interferences of HNO_3 and NaOH are related to the reaction with carbon (see below).

Calibration curves

Figure 1 indicates that analytical sensitivity can be increased by measurement of sodium hydroxide solutions; a suitable concentration was 0.5 M; changes in sensitivity were small for lower or higher concentrations. Calibration curves were obtained under six different sets of conditions because the signals obtained varied considerably depending on the age of the graphite tube. All calibration graphs were linear (Fig. 3), and used graphite tubes provided increased sensitivity compared with new tubes. However, with the 0.5 M NaOH solution, the difference in sensitivity between the used and new tubes was small. The enhancing effect of used tubes is probably due to the increase in temperature being faster with old tubes than with new tubes.

Effect of salts

Table 1 shows the effects of the addition of salts to pure germanium solutions and to 0.5 M NaOH solutions with untreated and tantalum-coated tubes. Whereas many serious interferences were found for pure aqueous germanium solutions, there was little variation in the signals when chloride or nitrate ions were added to 0.5 M NaOH solutions. The chloride interference with tantalum coated tubes was similar to that in untreated tubes, whereas the nitrate interference was very different. These results indicate that the nitrate, but not the chloride, interference is related to reaction with the graphite tube. Further, as the enhancing effect of NH_4NO_3 is small, and as NaOH and KOH have effects similar to those of $NaNO_3$ and KNO_3, respectively, it appears that the alkali metal cation plays a role.

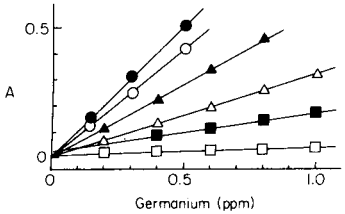

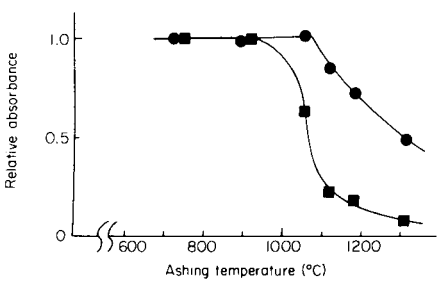

Fig. 3. Calibration graphs for germanium under various conditions. (—□—) Pure solution, new graphite tube; (—■—) pure solution, used graphite tube; (—△—) pure solution, new Ta-coated tube; (—▲—) pure solution, used Ta-coated tube; (—○—) 0.5 M NaOH solution, new graphite tube; (—●—) 0.5 M NaOH solution, used graphite tube.

Fig. 4. Loss of germanium (0.5 ppm) at various ashing temperatures with and without addition of sodium hydroxide. Only ashing temperature was varied in the recommended instrumental parameters. (—●—) With NaOH; (—■—) without NaOH. The absorbance obtained for ashing at 700°C is regarded as the standard in each case.

TABLE 1

Interferences observed in the determination of germanium (expressed in %)

on	Salt	Untreated tube				Ta-coated tube	
		Pure solution[a]		0.5 M NaOH[b]		Pure solution[b]	
		100 ppm ion	1000 ppm ion	100 ppm ion	1000 ppm ion	100 ppm ion	1000 ppm ion
Na	NaCl	−30	−60	0	0	−40	−60
	$NaNO_3$	230	>1000	0	0	0	80
K	KCl	−20	−40	0	0	−30	−50
	KNO_3	400	>1000	0	0	−40	30
NH_4	NH_4Cl	0	0	0	0	0	0
	NH_4NO_3	10	50	0	0	0	0

[a]2.5 ppm Ge. [b]0.5 ppm Ge.

Germanium species in the ashing step

The germanium species formed on heating various solutions were studied by x-ray diffractometry. When the solutions tested were heated at the temperature (700°C) corresponding to the ashing step, some solutions which gave strong enhancing effects produced Na_2GeO_3 (m.p. 1060°C without decomposition [18]) or an unknown substance, whereas the others formed only germanium dioxide (Table 2). Therefore, the extreme enhancing effect of NaOH, $NaNO_3$, KOH or KNO_3 on the atomization signal can be explained by the low reactivity of carbon with the germanium species, e.g. Na_2GeO_3, formed in the ashing step.

The reactivity of Na_2GeO_3 with carbon was studied as follows. Figure 4 shows the variation of relative absorbance, as a function of the temperature at the ashing step, for pure and 0.5 M NaOH solutions containing germanium. In the absence of NaOH, loss of germanium during the ashing step starts at about 900°C, and increases very sharply; in the presence of NaOH, losses

TABLE 2

Effect of matrices on germanium species formed in the drying and ashing steps

Matrix	Ge species formed at		Matrix	Ge species formed at	
	150°C	700°C		150°C	700°C
Pure	GeO_2	GeO_2	KNO_3	GeO_2	X[a]
NaCl	GeO_2	GeO_2	NH_4Cl	GeO_2	GeO_2
NaOH	X[a]	Na_2GeO_3[b]	NH_4NO_3	GeO_2	GeO_2
$NaNO_3$	GeO_2	Na_2GeO_3[b]	NH_3	GeO_2	GeO_2
KCl	GeO_2	GeO_2	HNO_3	GeO_2	GeO_2
KOH	X[a]	X[a]	H_2SO_4	GeO_2[c]	GeO_2[c]

[a]Unidentified because of an amorphous product.
[b]Corresponding to American Society for Testing and Materials Card 18-1217.
[c]Containing a small amount of insoluble form [11].

start only at 1050°C, and increase more gradually. These results prove that higher ashing temperatures can be tolerated when NaOH is present and that the Na_2GeO_3 formed is much less reactive than GeO_2 with carbon.

Essentially, the enhancing effect of NaOH or $NaNO_3$ on the atomization signal of germanium can be ascribed to the stability of Na_2GeO_3 in the presence of carbon at high temperature. The effects of KOH and KNO_3 can be explained analogously. The effect of NaOH in minimizing nitrate or chloride interferences can be attributed to the properties of the Na_2GeO_3 formed, regardless of the salts added, in the ashing step. When NaOH is present, the germanium signal is only slightly affected by faster rates of heating in the graphite tube; this would account for the fact that variations of signal with age of the graphite tube are less in the presence of NaOH (Fig. 3).

Thus, although the determination of germanium by flameless a.a.s. can be difficult because of losses of germanium monoxide before atomization, a highly sensitive analysis for germanium becomes possible if NaOH is added to the sample solution.

The proposed method in which the measurement was carried out after preparing sample solutions in 0.5 M NaOH, gave a significant increase in sensitivity compared with the method of Johnson et al. (Table 3). The standard deviation for a 0.5-ppm solution was 2.9% in 10 consecutive measurements.

TABLE 3

Comparison of this method with earlier methods [17, 19]

Method	Graphite tube	Solution	Characteristic concentration (ppm for 1% absorption)
This method	Untreated	0.5 M NaOH	0.004
Johnson et al. [17]	Designed	Pure	0.017
Hocquellet and Labeyrie [19]	Ta-treated	Pure	0.005[a]

[a]The value obtained by using gas-stop during atomization.

REFERENCES

1 D. Ager, R. G. Anderson, I. S. Maines and T. S. West, Anal. Chim. Acta, 57 (1971) 271.
2 D. A. Segar and J. G. Gonzalez, Anal. Chim. Acta, 58 (1972) 7.
3 C. W. Fuller, Anal. Chim. Acta, 62 (1972) 442.
4 J. Aggett and A. J. Sprott, Anal. Chim. Acta, 73 (1974) 49.
5 R. B. Cruz and J. C. Van Loon, Anal. Chim. Acta, 73 (1974) 231.
6 W. C. Campbell and J. M. Ottaway, Talanta, 21 (1974) 837.
7 C. W. Fuller, Analyst, 99 (1974) 739.
8 J. Smeyers-Verbeke, Y. Michotte, P. Van den Winkel and D. L. Massart, Anal. Chem., 48(1) (1976) 125.
9 J. Smeyers-Verbeke, Y. Michotte and D. L. Massart, Anal. Chem., 50(1) (1978) 10.
10 D. J. Churella and T. R. Copeland, Anal. Chem., 50(2) (1978) 309.
11 S. Shimomura, H. Sakurai, H. Morita, Y. Mino and M. Inoue, Anal. Chim. Acta, 91 (1977) 4

12 L. E. Alexander and H. P. Klug, X-Ray Diffraction Procedures, 2nd edn., J. Wiley, New York, 1974, p. 505.
13 L. G. Berry, Powder Diffraction File, Search Manual (Hanawalt Method), Inorganic Compounds, Joint Committee on Powder Diffraction Standards, Pennsylvania, 1973.
14 N. F. Turkalov, R. L. Magunov and A. V. Zagorodnyuk, Ukr. Khim. Zh., 38 (1972) 215.
15 V. I. Davydov, B. V. Teplyakov and G. K. Romanov, Zh. Prikl. Khim., 35 (1962) 1625.
16 L. Barton and C. A. Heil, J. Less-Common Met., 22 (1970) 11.
17 D. J. Johnson, T. S. West and R. M. Dagnall, Anal. Chim. Acta, 67 (1973) 79.
18 S. G. Tresvyatskii, Dopovidi Akad. Nauk Ukr. R. S. R., (1958) 295.
19 P. Hocquellet and N. Labeyrie, Analusis, 3(9) (1975) 505.

Analytica Chimica Acta, 107 (1979) 261—271

THE APPLICABILITY OF THE SECOND-DERIVATIVE METHOD TO ROOM-TEMPERATURE PHOSPHORESCENCE ANALYSIS

T. VO-DINH* and R. B. GAMMAGE

Health and Safety Research Division, Oak Ridge National Laboratory, Oak Ridge, Tennessee 37830 (U.S.A.)

(Received 10th October 1978)

SUMMARY

The use of the second-derivative (d^2) technique to overcome some of the problems encountered in room-temperature phosphorescence analysis is investigated. Despite some reduction in the signal-to-noise values, the d^2-technique was shown to be particularly suited to improving the selectivity of the assay. The utility of this method for applications in multicomponent mixture analysis is discussed. The two most significant figures of merit for room-temperature phosphorescence are the reduction of spectral overlap and the decrease of background interference.

Increasing attention has recently been devoted to a novel and simple analytical technique based on phosphorescence at room temperature from organic molecules adsorbed in various substrates such as silica gel, asbestos [1], filter paper [2—8], and sodium acetate powder [9]. Progress in this method of analysis, which offers good sensitivity and is a powerful tool in analysis for organic pollutants collected on filter surfaces, has been reviewed [7]. Not only has the possibility of using repetitive room-temperature phosphorescence analysis (r.t.p.a.) been demonstrated [6], but progress has also been reported in the use of heavy atom perturbers to increase the sensitivity of the method [4, 5, 8]. Its qualitative potential, however, has not yet been fully realized. One of the main problems associated with the method is the frequent occurrence of broad emission bands in r.t.p. spectra. Therefore, extracting the spectral data of a simple compound from the composite emission of mixtures is not straightforward. A second major limitation is the presence of a broad background emission from the substrate. The present study exploits the advantages offered by the second-derivative (d^2) method to reduce such limitations.

Many authors have described various derivative techniques related to molecular absorption spectrometry [10], atomic flame emission and absorption spectrometry [11—13], infrared spectrometry [14, 15], and luminescence spectrometry [16]. Second-derivative signals can be obtained by several methods: numerical differentiation [17], dual-wavelength spectrometry [18], modulation techniques [10, 19, 20], and direct electronic differentiation [16]. For absorption spectrometry or flame emission spectrometry, the modulation

technique is preferred because analog differentiation of the detector output may significantly degrade the signal-to-noise ($S:N$)) values of the d^2 signal as compared to the original values [19, 21]. For luminescence spectrometry no significant difference was found between the $S:N$ values of the d^2 spectra obtained by differentiation or by the modulation technique. It was concluded that because of the different nature of the noise in luminescence spectrometry compared to that in absorption spectrometry (multiplicative noise instead of additive noise), the wavelength-modulation derivative technique would have no $S:N$ advantage over the much simpler electronic differentiation method [16]. Accordingly, d^2 signals were obtained by the electronic differentiation technique in this investigation, which is concerned with figures of merit as well as limitations of the technique specific to r.t.p. assay in practical applications. Procedures for improved $S:N$ values and for the use of heavy atom effects on the d^2 signals are reported. The analysis of mixtures of several polynuclear aromatic (PNA) compounds of environmental interest is discussed. The results indicate that the combined d^2—r.t.p. technique is capable of the selectivity required for direct analysis of simple mixtures and of the sensitivity necessary for monitoring organic compounds at trace levels.

EXPERIMENTAL

Apparatus

A commercial electronic differentiator (Perkin-Elmer Model 200-0507) was used to convert the output from the spectrophotometer to signals that were proportional to the first (d^1) and second (d^2) derivative with respect to time. These signals were converted to wavelength derivative spectra by scanning the monochromator wavelength at a uniform rate. Although the d^1 output was available, analysis of this signal showed it to be less satisfactory than the d^2 signal.

A Perkin-Elmer spectrofluorimeter (Model 43A) was used with a 150-W xenon arc lamp as the excitation light source. When comparison was needed, direct spectra and second-derivative measurements were made under identical conditions of scan speed, slit width, and time constants of the spectrofluorimeter. For evaluation of the instrument, various scan speeds (0.5 nm s^{-1}, 1 nm s^{-1}, 2 nm s^{-1}, and 4 nm s^{-1}), band widths (0—15 nm), and time constants (0.3 s, 1.5 s, and 3 s) were selected to be compatible with the band width of the spectral structure under study. A 5-nm band width in the emission and a 15-nm band width in the excitation were used to determine the limits of detection. The detector was a Hamamatsu R777 photomultiplier, which has a photocathode spectral response from 185 to 850 nm. The good sensitivity of this photodetector in the long-wavelength region was essential to allow the detection of the phosphorescence emission from some compounds such as naphthalene and acridine.

Procedure

The main steps to prepare the samples for r.t.p. measurements have already been described [2—5]. In this work, the procedures used to add heavy atom solutions differ from the previous method [4], in which the heavy atom solutions were mixed with the sample solutions prior to measurement. Solvent incompatibility and differences in solubility between the heavy atoms and the analytes have, in the past, been among the main problems. Addition of heavy atom solutions was performed here by delivering 3 μl of heavy atom solution followed immediately by the spotting of 3 μl of sample solution on the same substrate area. This procedure, which is simpler and would be more easily automated, gave results with good reproducibility (a standard deviation of about 5% in the observed phosphorescence intensities from sample to sample measured under identical conditions).

Reagents

All the PNA compounds tested were commercially available. The filter paper was Schleicher and Schuell (591-c type). A mixture of ethanol and water (1 + 1, v/v) was used as solvent. The concentrations of heavy atoms were 2 M for sodium iodide and 0.5 M for silver nitrate.

RESULTS AND DISCUSSION

Reduction of background phosphorescence from the substrate

The paper background phosphorescence is one source of interference in r.t.p. analysis. For strongly phosphorescent compounds, such as pyrene and phenanthrene, the effect of this background emission can be neglected, but for weakly phosphorescent compounds, such as naphthalene and acridine, the intensity of the background is often similar to that emitted by the analyte. The phosphorescence emission spectrum of the background also covers a wide spectral region from 450 to 700 nm with a maximum near 500 nm. This emission thus interferes in the determination of a large number of organic substances.

However, there are several possible methods of reducing this background emission. First, an appropriate chemical treatment of the substrate with specific quenchers may decrease (suppress) selectively the background emission without affecting the emission from the compounds investigated; this approach requires a detailed knowledge of the nature and chemical composition of the substrate and needs further investigation. Secondly, the derivative method can be employed to minimize the effect. Figure 1 shows the r.t.p. spectrum of 62 ng of pyrene (left-hand curve) adsorbed on filter paper. Under the experimental condition used (excitation at 346 nm), the ratio of the phosphorescence background intensity from the paper, I_B, to the sample intensity, I_s, is about 0.75. Because the second-derivative mode enhances narrow emission peaks more than broader bands, the d^2 signal of the broad background should be significantly decreased; Fig. 1 also shows the second-derivative signal of the

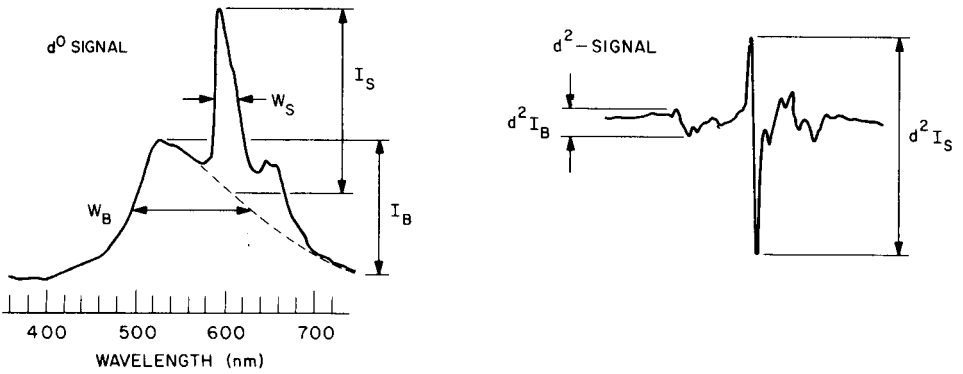

Fig. 1. Decrease of background interference by differentiation of the r.t.p. spectrum of pyrene.

same r.t.p. spectrum. In this Figure, as in the following ones, the r.t.p. spectru and the corresponding d^2 signal are shown in relative intensity scales. The decrease in the ratio of the background signal to the analyte signal in the derivative mode, $d^2I_B/d^2I_s = 0.12$, is noteworthy. This decrease allows the r.t.p spectrum of a compound to be analyzed more accurately. Weak shoulders of the pyrene spectrum are also converted to distinct and resolved peaks in the derivative signal. The more structured pattern of the d^2 signal can better serve as a fingerprint for qualitative analysis, whereas the enhancement of a few sharp peaks (for pyrene, peak 1) leads to less spectral interference for multi-component analysis.

Signal-to-noise enhancement with the scan rate

The electronic differentiation technique optimizes the *S:N* ratio. Two important experimental parameters should be considered: the wavelength scar rate R_s and the response time t_r of the instrument. Because a narrower peak is more enhanced, a faster scan for a given spectral band will generate a larger d^2 signal. To illustrate this process in a general case, a simple spectral band was chosen: the Raman band of water at 397 nm (λ_{ex} = 350 nm) and its d^2 signal at various scan rates are shown in Fig. 2. The time constant was kept constant at the lowest value available (0.3 s). The lower curves (Fig. 2) show that the d^0 signal intensity of the Raman emission band (d^0) is independent of scan rate. The corresponding d^2 signals show that the second-derivative intensities increase with higher scan speed. The calculated data showed that the *S:N* values obtained with the d^2 signals are enhanced almost four-fold whe the scan speed is doubled, whereas the *S:N* values of the conventional spectru remain nearly constant. The instrument output, d^2I/dt^2, is therefore proportional to the square of the scan rate, R_s, for a limited range.

Experimentally, it is not possible to increase the scan speed over a critical value, R_{max}. The optimal conditions must be determined by the structure of

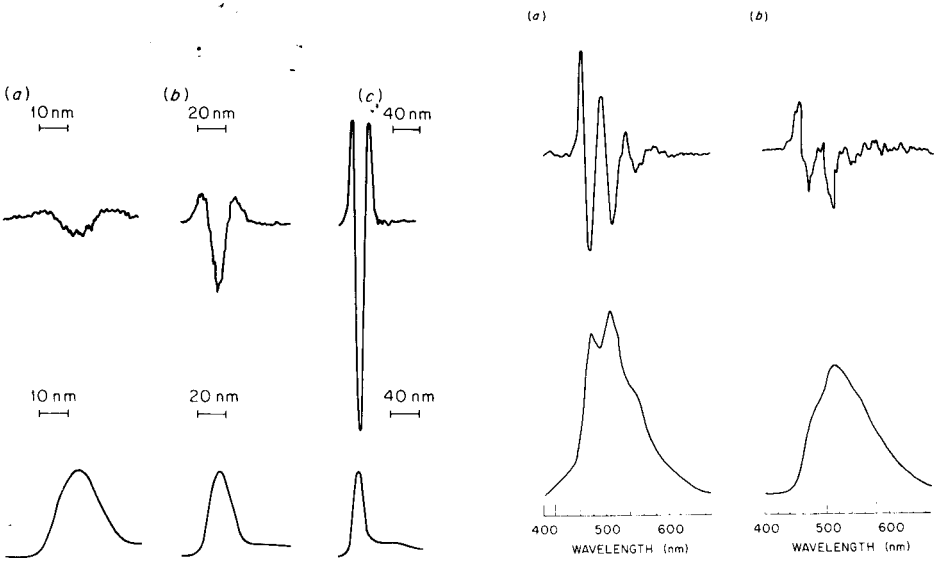

Fig. 2. Effect of the scan rate on the *S:N* ratio of the d^0 and d^2 signals. Scan rates: (a) 0.5 nm s^{-1}; (b) 1.0 nm s^{-1}; (c) 2.0 nm s^{-1}.

Fig. 3 R.t.p. spectra (bottom) and d^2 signals (top) for phenanthrene with (a) sodium iodide, (b) silver nitrate.

the spectra. For a spectrum showing emission bands having a half-width equal to or larger than $\delta\lambda_b$, where $\delta\lambda_b$ is the half-width (in nm) of the narrowest spectral feature, the scan speed and the response time t_r must satisfy the condition [22] $R_s \leqslant R_{max} = \delta\lambda_b/t_r$, where $t_r = 4.6\ t_c$, and t_c = the time constant of the instrumental system. For r.t.p. spectra that have emission bands equal to or larger than 15 nm and for time constants of 1 s, the maximum scanning rate that can be used is 3.26 nm s^{-1}. A faster scan rate would, in this case, produce a distorted d^2 signal. All subsequent measurements in the present study were made at 2 nm s^{-1} with $t_c = 1$ s.

Choice of heavy atom for derivative measurements

The criteria for selection of the appropriate heavy atom perturber are different for the d^0 and d^2 modes of spectral recording. It has been shown that the addition of various heavy atoms from salts such as sodium iodide [4], silver nitrate [5], and thallium acetate and lead acetate [8] can significantly increase the intensity of the phosphorescence emission. In the conventional mode, the choice of the most effective heavy atom is determined by the intensity of the r.t.p. emission, but in the d^2 mode the sharpness of the emission band is also of major importance. Although silver nitrate is quite effective in enhancing the phosphorescence emission of polyaromatic hydrocarbons, a general blurring and broadening of the spectral structure also occurs. Figure 3

shows the r.t.p. spectra of 165 ng of phenanthrene and the corresponding d^2 signals measured with filter paper previously impregnated with sodium iodide and silver nitrate.

For comparison purposes, the experimental conditions were selected such that the conventional spectra show intensities of a similar order of magnitude. Whereas the intensity of the 507-nm band observed with sodium iodide is only 1.5-fold stronger than the same band observed with silver nitrate, the corresponding d^2 signal with sodium iodide is 2.5-fold larger than that measured with silver nitrate. Another example of reversal in the optimal choice of heavy atom is given in Fig. 4. Under the present experimental conditions and with 270 ng of pyrene, the *S:N* ratios at 600 nm are equivalent in the d^0 mode, whereas the *S:N* ratio measured in the d^2 mode with sodium iodide is 3.5-fold larger than that measured with silver nitrate. This larger ratio is due to the sharper spectral structures obtained with sodium iodide.

Analysis of mixtures

The results for combinations of various PNA compounds showed that the use of the d^2 technique allows an easier and more accurate analysis of mixtures than does the conventional d^0 mode. There is, however, a trade-off between sensitivity and accuracy. Whereas the conventional signals of some compounds can have, in some cases, higher *S:N* ratios when measured individually, the severe overlap between their spectra can render the analysis complex and

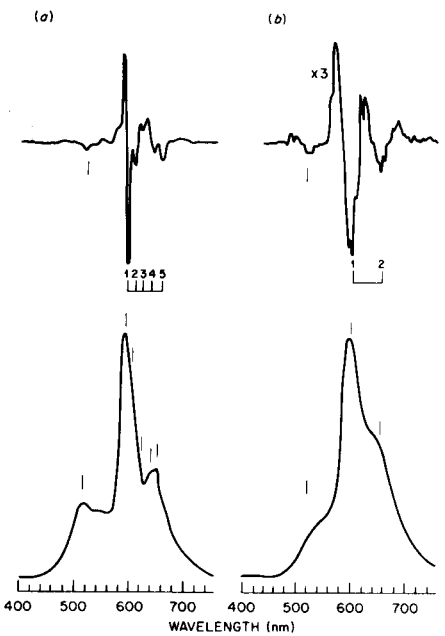

Fig. 4. Effect of heavy atoms on the r.t.p. spectra (bottom) and d^2 signal (top) of pyrene with (a) sodium iodide, (b) silver nitrate.

often impractical. It was therefore important to establish if the d^2 method sufficiently improves the structure of the r.t.p. spectrum of a mixture to give data unattainable by the d^0 method.

To illustrate the usefulness of the d^2 method, a sample was selected which contained compounds that showed such closely spaced absorption bands that selective excitation could not successfully single out the emission of a particular compound. The analysis of a sample containing 34 ng of naphthalene, 8 ng of fluorene, 0.2 ng of pyrene, and 8 ng of acridine is shown in Fig. 5. Selective excitation cannot produce spectra of individual compounds: excitation of a 15-nm band width at 280 nm gives rise to emissions from fluorene and naphthalene (Fig. 5a), whereas excitation at 350 nm is needed to induce emission from pyrene and acridine (Fig. 5b). The lower curve in Fig. 5(a) shows a broad emission from 410 to 620 nm with a series of weak peaks and shoulders. This spectrum should be compared to the lower curves in Fig. 6, which are the conventional r.t.p. spectra of the individual compounds. In the r.t.p. spectrum of the individual compounds, the vibrational bands quite often show up as indistinct shoulders on the side of a prominent but structureless emission. This feature causes r.t.p. spectra in their normal representation (d^0 spectrum) to be relatively poor compared to, say, low-temperature spectroscopy in special solvents such as Shpolskii matrices [23]. The r.t.p. spectrum of the mixture (Fig. 5a) might reveal the presence of fluorene but does not give an immediate visual indication of naphthalene.

In contrast, if the d^2 signals are measured, simple inspection indicates the presence of fluorene and naphthalene: the typical peak patterns of fluorene

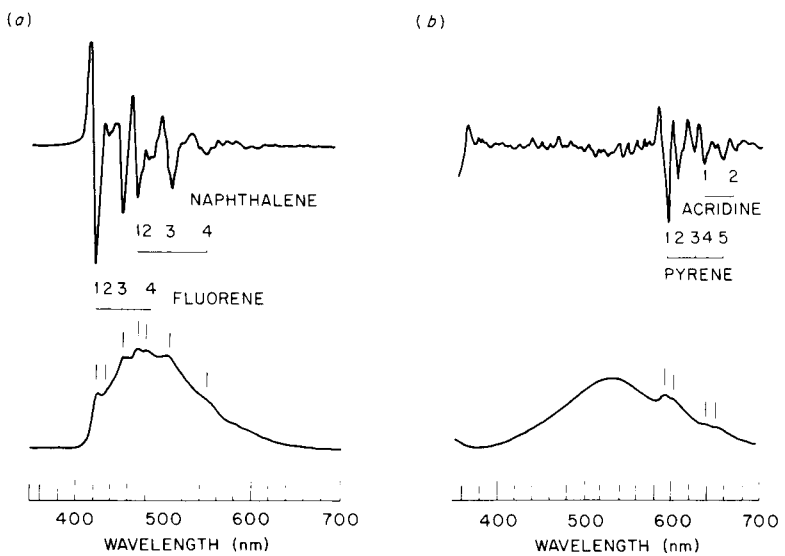

Fig. 5. Comparison of the d^0 (bottom) and d^2 (top) r.t.p. spectra for a mixture of fluorene, naphthalene, pyrene, and acridine: (a) λ_{ex} = 280 nm; (b) λ_{ex} = 350 nm.

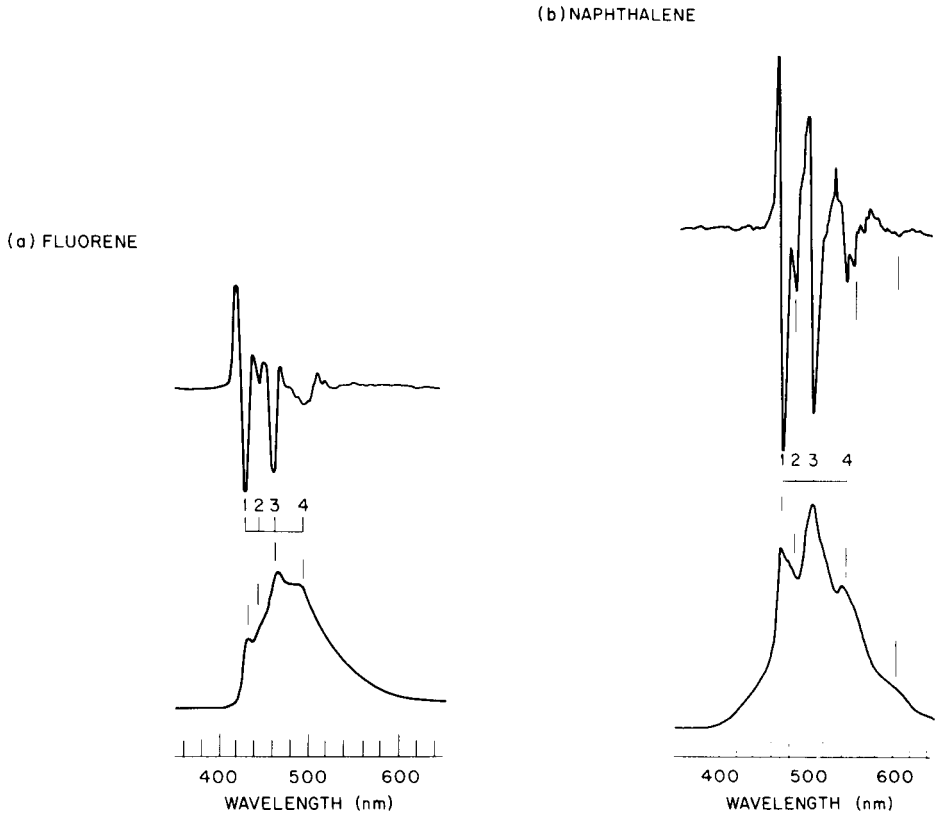

Fig. 6. Comparison of the d^0 and d^2 signals of (a) fluorene and (b) naphthalene.

and naphthalene (Fig. 6) are clearly evident in the d^2 signals of the mixture. Figure 5(a) demonstrates the ability of the d^2 technique to provide unequivocal spectral signatures — suitable for identification — of two compounds that have strongly overlapping r.t.p. spectra. Similarly, detailed analysis of the spectra in Fig. 5(b) reveals the superior capability of the d^2 mode in providing characteristic spectra for pyrene and acridine. The spectra shown in the lower curve correspond to a situation with highly overlapping components in the presence of a strong background; the sloping of the paper emission makes baseline estimation difficult in most cases. In contrast, the broad background phosphorescence from the paper in the d^2 signal is eliminated almost entirely (Fig. 5b). These figures show clearly the advantage of the d^2 technique for r.t.p. assay of mixtures.

Analytical curve and limit of detection

The usefulness of the d^2 method in fluorescence analysis has been investigated by O'Haver and Green [24]. In a general treatment with simulated

computational algorithm, these authors compared the basic features of the analytical curves in various modes (zero-, first-, and second-derivative). The d^2 signal of a given substance is generally the most appropriate measure in multicomponent analysis because it is least affected by variations in the concentration of the other compounds, i.e. by spectral overlap. Various measurements were done to demonstrate the possibility of using the d^2 signals in quantitative r.t.p. analysis. The analytical curve given in Fig. 7 pertains to pyrene in samples containing 105 ng of acridine. The curve is linear for more than two orders of magnitude and has a slope close to unity. The deviation from linearity at high concentrations, that is also observed for the d^0 signal, could be due, in part, to the low solubility of pyrene in the aqueous ethanol solution. It is also of interest to compare the limit of detection obtained for various PNA compounds in the d^0 and d^2 modes. Even with the individual compounds there is no obvious rule of thumb. The present data (Table 1) show that the decrease of *S:N* ratios can vary from a factor of 2.8 to as much as 14. This variation is understandable because the noise (background noise, detector noise, etc.) remains basically the same at similar intensity level conditions, but the spectral features (bandwidth of peaks, curvature) vary substantially between various compounds. The compounds that have the sharpest structure in the conventional spectrum, e.g. pyrene and naphthalene, would have the least *S:N* deterioration in the d^2 mode.

Absolute comparison of *S:N* values and limits of detection between the direct (d^0) spectra and their corresponding d^2 signals is not straightforward because of the different nature of the two signals. Although evaluation is done at the most intense spectral band in the d^0 spectrum, it is done at the position of the band with highest curvature in the d^2 mode. For a given spectrum, it is frequently found that the *S:N* ratio of the d^0 signal to the d^2 signal varies significantly with the emission bands; some typical data are given in Table 2. It is therefore difficult to draw general conclusions or to extrapolate limits of detection based on simple *S:N* consideration obtained under particular

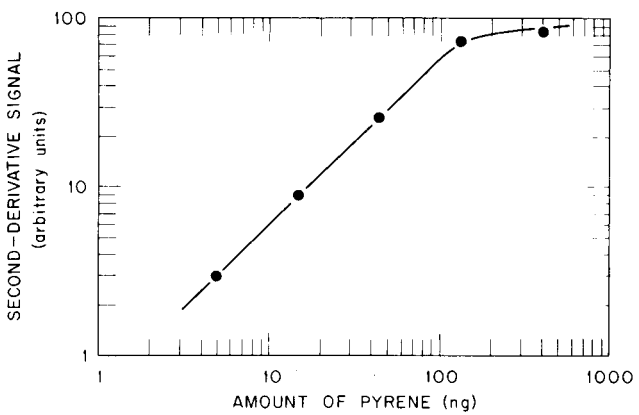

Fig. 7. Analytical curve for pyrene with measurement of the d^2 signal at 600 nm.

TABLE 1

Limits of detection (LOD) of some polyaromatic hydrocarbons with sodium iodide as the heavy atom matrix

Compounds		d^0 spectrum		d^2 signal	
	λ_{ex} (nm)	λ_{em} (nm)	LOD (ng)	λ_{em} (nm)	LOD (ng)
Pyrene	346	597	0.2	597	0.67
Naphthalene	289	510	1.2	480	34
Phenanthrene	300	507	0.33	460	4.7

TABLE 2

Signal-to-noise (*S:N*) values of the d^0 and d^2 signals at various emission bands with sodium iodide as heavy atom perturber at a scan rate of 2 nm s^{-1}

Compounds	λ_{em} (nm)	Maximum value of *S:N*	
		d^0 spectrum	d^2 signal
Pyrene	598	188	55
Naphthalene	472	100	45
	508	125	34
Phenanthrene	460	260	21
	507	300	13

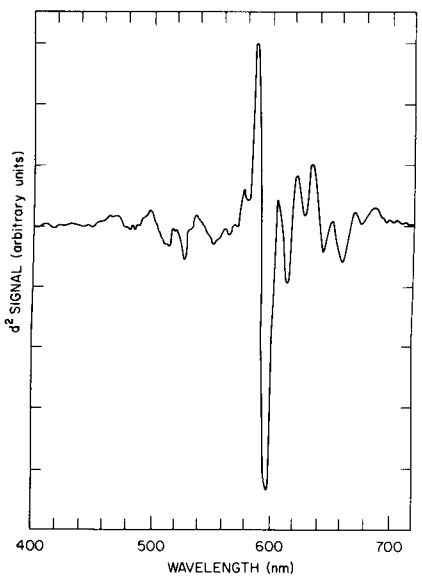

Fig. 8. The identificaton of pyrene in Synthoil by the d^2—r.t.p. technique.

experimental conditions. Table 2 shows the *S:N* values for pyrene, naphthalene, and phenanthrene determined at various emission bands. With pyrene, the highest *S:N* value obtained in the d^0 spectrum occurs at the same wavelength in the d^2 signal (597 nm). With naphthalene, however, the largest *S:N* value in the d^0 spectrum (510 nm) does not correspond to that obtained in the d^2 signal (480 nm). The results obtained with phenanthrene also indicate that different emission bands should be considered for quantitative analysis.

Figure 8 illustrates the potential application of the d^2—r.t.p. technique in monitoring organic pollutants from synthetic fuel production. This d^2—r.t.p. signal of an ether extract from Synthoil reveals unambiguously the presence of pyrene (cf. Fig. 1). A detailed account of the analysis of various environmental samples by r.t.p. will be given elsewhere [25]. In conclusion, the d^2 technique has two significant advantages: reduction of overlapping bands and decrease of interfering background, and these advantages allow easier identification of mixtures.

This research was sponsored by the Division of Biomedical and Environmental Research, U.S. Department of Energy, under contract W-7405-eng-26 with the Union Carbide Corporation.

REFERENCES

1 E. M. Schulman and C. Walling, Science, 178 (1972) 53.
2 S. L. Wellons, R. A. Paynter and J. D. Winefordner, Spectrochim. Acta, Part A, 30 (1974) 2133.
3 R. A. Paynter, S. L. Wellons and J. D. Winefordner, Anal. Chem., 46 (1974) 736.
4 T. Vo-Dinh, E. LueYen and J. D. Winefordner, Anal. Chem., 48 (1976) 1186.
5 T. Vo-Dinh, E. LueYen and J. D. Winefordner, Talanta, 24 (1976) 146.
6 T. Vo-Dinh, G. Walden and J. D. Winefordner, Anal. Chem., 49 (1977) 1126.
7 T. Vo-Dinh and J. D. Winefordner, Appl. Spectrosc. Rev., 13 (2) (1977) 261.
8 I. M. Jakovljevic, Anal. Chem., 49 (1977) 2048.
9 R. M. A. von Wandruska and R. J. Hurtubise, Anal. Chem., 48 (1976) 1784.
10 R. N. Hagar, Anal. Chem., 45 (1973) 1131A.
11 R. E. Elser and J. D. Winefordner, Anal. Chem., 44 (1972) 698.
12 W. K. Fowler, D. O. Knapp and J. D. Winefordner, Anal. Chem., 46 (1974) 601.
13 W. Snelleman, Spectrochim. Acta, Part B, 23 (1968) 403.
14 I. G. McWilliam, J. Sci. Instrum., 36 (1959) 51.
15 G. L. Collier and F. Singleton, J. Appl. Chem., 6 (1956) 495.
16 G. L. Green and T. C. O'Haver, Anal. Chem., 46 (1974) 2191.
17 A. Savitzky and M. Golay, Anal. Chem., 36 (1967) 1627.
18 S. Shibata, M. Furukawa and K. Goto, Anal. Chim. Acta, 65 (1973) 49.
19 A. Perregaux and G. Ascarelli, Appl. Opt., 8 (1969) 2031.
20 D. T. Williams and R. N. Hagar, Appl. Opt., 9 (1970) 1597.
21 G. Bonfiglioli and P. Brovetts, Appl. Opt., 3 (1964) 1417.
22 J. D. Winefordner (Ed.), Trace Analysis, Spectroscopic Methods for Elements, J. Wiley, N. Y., 1970, p. 23.
23 E. V. Shpolskii, Sov. Phys.-Usp., 5 (1962) 522.
24 T. C. O'Haver and G. L. Green, Anal. Chem., 48 (1976) 312.
25 T. Vo-Dinh and J. R. Hooyman, to be published (1978).

Analytica Chimica Acta, 107 (1979) 273—278

SYSTEMATIC ATOMIC NUMBER EFFECTS IN COMPLEXES EXHIBITING LIGAND LUMINESCENCE
Part 2. Salicylidene-*o*-Aminophenolates

T. L. CRAVEN and F. E. LYTLE*

Department of Chemistry, Purdue University, West Lafayette, Indiana 47907 (U.S.A.)

(Received 18th December 1978)

SUMMARY

The room-temperature fluorescence properties of Group IIIA metal complexes with salicylidene-*o*-aminophenol (SoAP) in aqueous 20% methanol are reported. The data include absorption, emission and excitation maxima, quantum yields and luminescence lifetimes. A systematic heavy atom effect influences the fluorescence decay to an extent sufficient for simultaneous kinetic analysis of ternary metal ion mixtures, based on decay-rate measurements.

The determination of metals by use of luminescent chelates has attracted much attention over the years [1—3]. Most of the reported methods have involved a single emitting species since multicomponent approaches are usually hindered by a wavelength distribution determined primarily by the ligand. Consequently, methodology designed for mixtures usually involves physical separations or chemical masking prior to the instrumental step. To circumvent the problem of spectral overlap, Lytle et al. [4] suggested that the chelate fluorescence decay could be utilized in a manner similar to simultaneous kinetic schemes based on reaction rates. In addition it was suggested that lifetime changes within a given group of metals could generally be expected because the heavy atom effect would produce a systematic variation in the rate constants for the excited states.

To date, two chemical systems have been reported which indicate the merit of the basic idea. The 8-quinolinolates of Ca(II), Sc(III), Zn(II), Ga(III) and Ge(IV) in dimethylformamide (DMF) had characteristic lifetimes of 23, 18, 9, 5 and 3 ns, respectively [4]. The 5-sulfo-8-quinolinolates of Al(III) and Ga(III) at pH 4.5 and Mg(II) and Cd(II) at pH 10 had characteristic lifetimes of 11 and 4 ns, and 11 and 5 ns, respectively [5]. In Part 1 of this series [4] analytical procedures were suggested but not demonstrated, whereas in the latter investigation [5], determinations were done on both synthetic and real samples.

The basic problem in generalizing the methodology for any arbitrary set of metals is the difficulty in generating a unidirectional trend in lifetimes for a particular periodic group; that is, the ligand must be ultrasensitive to a

given change in atomic number in order to offset the increased ionic radius within a group. An example of this difficulty is shown by the 8-quinolinolates of Al(III), Ga(III) and In(III) where the lifetimes are 11, 5 and 7 ns, respectively [4]. As a result, much effort has been devoted since the publication of Part 1, to an examination of various luminescent chelates with the object of obtaining chemical patterns of the extent to which the ligand senses the heavy atom [6, 7]. Unfortunately, any existing patterns are difficult to identify.

One empirically discovered class of ligand which has shown promise in a simultaneous kinetic scheme is the aromatic Schiff base. The definitive work with these compounds is that of Morisige [8] who has recently examined many metal chelates in aqueous 8% DMF and reported their spectral and temporal behavior. In the present studies, an examination has been made of the room-temperature emission properties of Group IIIA metal complexes with the Schiff base salicylidene-*o*-aminophenol (SoAP) in aqueous 20% methanol. The reported data include absorption, emission and excitation maxima, quantum yields and luminescence lifetimes. From these results it is concluded that a systematic heavy atom effect is present to an extent suitable for a simultaneous kinetic analysis of Group IIIA metal ion mixtures.

EXPERIMENTAL

Reagents

All common organic and inorganic chemicals were of reagent grade or better and were not further purified. Quinine hydrogensulfate (Eastman) was twice recrystallized from ethanol. Salicylidene-*o*-aminophenol (Manganon; J. T. Baker) was twice recrystallized from methanol.

Apparatus

Absorption spectra were measured on a Cary Model 15 spectrophotometer with 10-cm path length cells. Excitation and emission fluorescence measurements were done on a Spex Fluorolog fluorimeter equipped with an RCA C31024 photomultiplier and photon counting circuitry. Excited-state decay measurements were made on one of two instruments. A modified TRW Nanosecond Spectral Source (pulse-width 7.5 ns) [9] was utilized for the mor routine studies, while a nitrogen laser-based system (pulse-width 4.5 ns) was utilized to obtain the best time resolution [10]. The fluorimeters were calibrated with respect to wavelength accuracy, bandpass, and emission and excitation efficiencies [11].

Procedures

Preparations. Al(III), Ga(III) and In(III) chelates were prepared by refluxin the anhydrous metal chlorides with the pure ligand in ether. The product was collected and dried at 110°C for 24 h. The thallium chelate could not be successfully dried. Measurements were made on both the dissolved solid preparations and mixtures of ligand and metal ion.

Quantum yields. All samples had absorbances of less than 0.05 to minimize inner filter effects. Each solution was bubbled with solvent-saturated prepurified nitrogen for 10 min prior to obtaining an emission spectrum. Emission curve areas were corrected for background emission and excitation efficiencies. Quantum yields are relative to quinine hydrogensulfate in 0.5 M sulfuric acid excited at 365 nm, whose quantum yield is taken to be 0.546 [12].

Lifetimes. Solutions were prepared as described above. With the TRW instrument, complementary glass filters were used in the excitation and emission branches to minimize scattered light interference. With the laser system a 1/4-m monochromator was used in the emission branch to minimize scattered light interference. Lifetimes were determined by a graphical convolution—comparison method [9].

RESULTS

Stability

There are two trends with regard to stability. One is the acid or base hydrolysis of the ligand as reported by Tumanov and Efimychev [13] and the other is increased decomposition rates with larger metal ions, attributed to weaker complexation. Of the solvents examined (ethanol, methanol and water of various pH values), an aqueous 20% methanol solution gave the best stability for the entire group. The aluminum and gallium chelates were stable for $\geqslant$2 h, while the indium chelate solutions were usable for $\geqslant$15 min.

Every effort was made to obtain data for the thallium chelate in the above solvents, but measurements were severely hindered by stability problems. When ether was used as a solvent, it was possible to record absorption and emission spectra. The instability and weak intensity made accurate lifetime measurements difficult; the value is estimated to be $\leqslant$400 ps. This limit is predicated on long-term experience, indicating that the shortest distinguishable lifetime is one twentieth of the instrumental pulse width, i.e. $\sim$400 ps for the TRW. The excited-state rate parameters for the compound were computed on this basis.

Spectra

Typical spectra for the aluminum chelate are shown in Fig. 1, while band maxima for all four compounds are given in Table 1. The absorption spectra were reproducible, with only small differences in the location of peak maxima. Uncomplexed ligand, which peaked at 330 nm, overlapped the chelate absorption band. Excitation spectra were featureless except for the single maximum. Given the 9-nm bandwidth of the fluorimeter, the excitation data agree very well with the absorption values for every metal but thallium. The emission spectra were also simple, but broader than the corresponding excitation spectra. Again, other than for thallium, the Stokes shift increased as heavier metals were attached to the ligand.

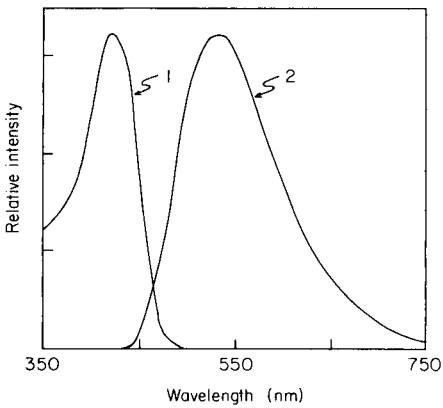

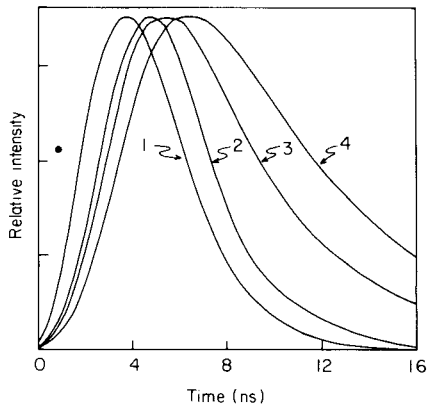

Fig. 1. Al(III)—SoAP fluorescence spectra. (1) Corrected excitation spectrum; (2) corrected emission spectrum.

Fig. 2. Decay curves for Group IIIA—SoAP chelates. (1) Instrumental response to scattered light; (2) In(III) chelate; (3) Ga(III) chelate; (4) Al(III) chelate.

TABLE 1

Spectral data for SoAP chelates[a]

	Al	Ga	In	Tl
λ_{abs} (nm)	406	410	408	398
$\log \epsilon$	3.95	3.75	3.81	4.99
λ_{ex} (nm)	405	410	407	420
λ_{em} (nm)	530	545	550	535
ϕ_f	0.340	0.204	0.038	0.00
τ_f (ns)	5.39	2.50	0.82	($\leqslant$0.4)
$\log k_f$	7.80	7.91	7.67	(7.2)
$\log k_x$	8.09 (±5%)	8.50 (±12%)	9.07 (±14%)	(9.4)
$\log k_x = 6 \log n$	10.95	12.11	13.26	(14.1)

[a]For definition of terms, see text.

Lifetimes and excited-state rate parameters

The fluorescence decays exhibited single exponential behavior only. Exampl of data obtained with the nitrogen laser system are shown in Fig. 2.

When fluorescence data are analyzed, it is usually assumed that there are only two pathways out of the lowest excited singlet state. These are fluorescence and intersystem crossing, and are characterized by the two rate constan k_f and k_x, respectively. When the kinetic definitions of the quantum yield, ϕ_f, and lifetime, τ_f, are utilized, it is possible to compute k_f from the quantit ϕ_f/τ_f. In a similar manner, k_x is computed from the quantity $(1 - \phi_f)/\tau_f$. The values of these parameters are given in Table 1, along with the uncertaint in k_x caused by the propagated precision in $(1 - \phi_f)$ and τ_f.

DISCUSSION

The chief impetus for this work was the belief that the lifetimes of the chelates would vary sufficiently from one metal to another to allow the design of a simultaneous kinetic analytical procedure. It was considered that such a variation would occur naturally by the quenching of fluorescence via an increase in the intersystem crossing rate caused by spin—orbit coupling, i.e. the heavy atom effect. This phenomenon was first formalized for molecules by McClure [14] and applied to metal chelates by Lytle et al. [4].

For the case of the single-electron central potential field, the spin—orbit coupling constant is reflected in a Z^4 dependence (Z = atomic number), modified by the screening of the nucleus, n^3, and the orbital penetration into the nucleus, $(l + 1)(l + 1/2)l$. The rate constant for intersystem crossing is proportional to the square of the coupling constant and thus the square of the above atomic parameters. In a chelate system it would be improbable that an exact Z^8 dependence would be observed; however, an experimentally determined exponent would reflect the extent to which the metal nucleus influences the ligand.

To ascertain if the heavy atom effect is operative, and to determine the extent of spin—orbit coupling, a plot is made of $\log k_x + 6 \log n$ versus $\log Z$. Such an approach is based on the premise that l remains constant for a given group of the periodic table and that the n^6 dependence is exact. The results for the compounds in this study are shown in Fig. 3. A least-squares fit to the data yields a slope of 3.74. This Z dependence is very close to the required value of 4 and is significantly larger than any observed for the 8-quinolinolates [4].

The practical conditions necessary to achieve a multicomponent analysis are concerned with both that instrumentation and the mathematical processing of the resultant data. Long-term experience in time-resolved fluorimetry has

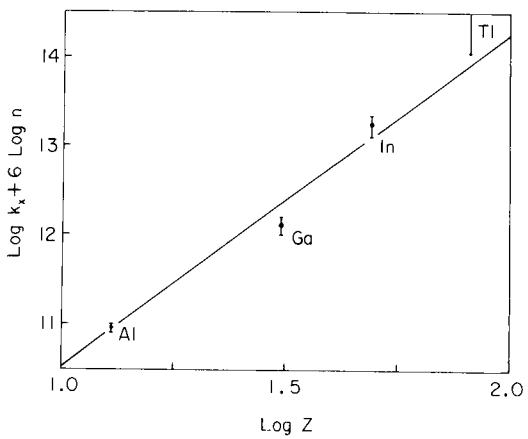

Fig. 3. Plot to evaluate the heavy atom effect for Group IIIA—SoAP chelates.

established that a lifetime value greater than the width of the scattered light response will produce a pure exponential curve over a major portion of the decay. Thus, a sampled photon-counting instrument described previously [15] could obtain usable data for lifetimes $\gg 0.77$ ns, and is well suited for the SoAP compounds. In addition, the sensitivity of this device with 457-nm excitation is sufficient to permit the determination of the chelates at nanomol levels. The restrictions on the relative values of the decay rates can be obtainec from the work of Ridder and Margerum [16]. These authors demonstrated a three-component simultaneous kinetic scheme with the two closest reaction rates having a ratio of 1:2.3 and the overall range having a ratio of 1:20.3. The fluorescence lifetimes shown in Table 1 have ratios of 1:3.1:6.6 which are well within the capabilities of the published algorithm. Work is currently in progress to develop a kinetic method which will permit the simultaneous determination of Al, Ga and In at trace levels.

The authors would like to thank T. G. Matthews for help with lifetime measurements utilizing the nitrogen laser. This research was supported in part through funds provided by the National Science Foundation under Grant No. MPS75-05907.

REFERENCES

1 C. E. White and R. J. Argauer, Fluorescence Analysis, M. Dekker, New York, 1970.
2 G. G. Guilbault, Practical Fluorescence, M. Dekker, New York, 1973.
3 F. E. Lytle, Appl. Spectrosc., 24 (1970) 319.
4 F. E. Lytle, D. R. Storey and M. E. Juricich, Spectrochim. Acta, Part A, 29 (1973) 1357.
5 K. Hiraki, K. Morisige and Y. Nishikawa, Anal. Chim. Acta, 97 (1978) 121.
6 M. D. Kerner, M. S. Thesis, Purdue University, West Lafayette, Indiana, 1975.
7 F. C. DeZutter, M. S. Thesis, Purdue University, West Lafayette, Indiana, 1977.
8 K. Morisige, J. Inorg. Nucl. Chem., 40 (1978) 843.
9 F. E. Lytle, Photochem. Photobiol., 17 (1973) 75.
10 T. G. Matthews and F. E. Lytle, Anal. Chem., submitted.
11 F. E. Lytle, Ph.D. Thesis, Mass. Inst. of Tech., Cambridge, Mass., 1968.
12 J. N. Demas and G. A. Crosby, J. Phys. Chem., 75 (1971) 991.
13 A. A. Tumanov and V. S. Efimychev, Zh. Anal. Khim., 20 (1965) 889.
14 D. S. McClure, J. Chem. Phys., 17 (1949) 665.
15 J. M. Harris and F. E. Lytle, Rev. Sci. Instrum., 48 (1977) 1469.
16 G. M. Ridder and D. W. Margerum, Anal. Chem., 49 (1977) 2090.

Analytica Chimica Acta, 107 (1979) 279—289

A COMPUTER-BASED SPECTROPHOTOMETRIC STUDY OF THE KINETICS OF THE AQUATION OF HALOGENOPENTAMMINE-CHROMIUM(III) PERCHLORATE

TREVOR R. GRIFFITHS* and D. C. PUGH**

Department of Inorganic and Structural Chemistry, The University, Leeds LS2 9JT (Gt. Britain)

(Received 25th September 1978)

SUMMARY

Conventional determinations of rate constants k from absorption spectra employ a few selected wavelengths: by digitizing the complete spectrum computer calculations of k can be made at most wavelengths, and hence with better precision. This has here been satisfactorily tested for the aquation of halogenopentamminechromium(III) perchlorate. Two independent procedures are described, which are approximately equally onerous on computer time. Additionally, these procedures are shown to yield identical computer-generated spectra for the halogeno-complex before aquation commences, and accurate time infinity spectra, of the aquo-complex, for long half-life reactions. They also efficiently eliminate the effects of spectrophotometer instability over long periods of time.

In an earlier paper [1], a computer-based study of the effect of pH and temperature on the electronic absorption spectra of acid—base indicator solutions was presented. This study is the first that extends the concepts described therein to spectrophotometric studies of first-order reaction kinetics. The current common practice is to monitor a few suitable wavelengths as a function of time, and then calculate or compute [2] the rate constant. Because spectra are digitized over the complete wavelength range, a rate constant is obtained at every digitized wavelength (except near isosbestic points). The advantages are that a proper statistically determined rate constant is obtained (after it has been shown that it is wavelength-independent); more accurate rate constants are obtained for slow reactions where the time interval required to reach no further reaction (generally considered ten times the half-life of the reaction) is greater than the time during which the spectrophotometer remains stable and does not drift; and the spectrum at zero time can be generated, which gives for the first time the profiles of species before they begin to react.

General acquaintance with the earlier article [1] is assumed and only the

---

**Present address: Smith and Nephew Research, Gilston Park, Harlow CM20 2RT, Essex, England.

additional computing aspects necessary for reaction-rate studies are discussed below.

GENERATION OF SPECTRA

Because in first-order rate reactions the total concentration of reactant (A) and product (B) remains constant, the spectra obtained as a function of time contain one or more isosbestic points, assuming that the profiles of A and B overlap. A stylized example has already been given (Fig. 1 [1]). It has since been shown [3—5] that for those situations where it is impossible, for experimental reasons, to measure the spectrum of A free from contributions of B, and vice versa, these discrete spectra can be generated by an appropriate choice of the internal linearity constant β [1]. A unique feature concerning reaction-rate studies is that it is not now necessary to choose appropriate β values to generate the spectra of A and B, the initial and final spectra of the reaction.

Internal linearity

Sound conclusions may not be drawn from sets of spectra containing isosbestic points unless these spectra have first been examined for internal linearity. Provided that the spectra of component species are invariant with respect to the external parameter (in this case, time), the concentrations of absorbing species in an internally linear system are linearly related to a single reaction parameter. Usually this dependence indicates the presence of a two-species equilibrium in the system. In other cases, changes in spectra can frequently be interpreted in terms of a pseudo-two-species equilibrium. However, additional chemical evidence is required before a definitive interpretation can be proposed.

Two procedures have been put forward for establishing internal linearity relationships in a set of spectra. The first, formalized mathematically by Chylewski [6], involves plotting the absorbances at any two wavelengths against each other for a set of spectra. Internally linear spectra exhibit a linear relationship in such plots. The second, more rigorous procedure, described by Brynestad and Smith [7], determines the relationships in a set of spectra over an extensive range of wavelengths. Any one spectrum in an internally linear set can be obtained by a linear combination of any two other spectra from that set. This may be expressed mathematically as: $\epsilon_3 = (1 - \beta)\,\epsilon_1 + \beta\epsilon_2$, where ϵ_1, ϵ_2, and ϵ_3 are the formal absorbances of three spectra at any wavelength; β is the constant of internal linearity relative to the spectra ϵ_1 and ϵ_2, and is an abbreviation of $\beta(3, 1, 2)$, which specifies the order in which the spectra appear; ϵ_1 and ϵ_2 are termed the reference spectra. If β_n is computed at each digitized wavelength, a meaningful average value ($\bar{\beta}$) can be calculated, and the deviation (δ_n) from ideal linearity can then be computed at each wavelength. The equations and procedure to obtain a meaningful average $\bar{\beta}$ value have been described in detail [1]. Until now it has been necessary to select two spectra from a set as reference spectra. This presents problems, which are discussed below.

hoice of reference spectra

The decision as to which two spectra are to be reference spectra, and hence ssumed "absolute", is somewhat arbitrary, and has usually been based on xperience. Ideally, from a set of N spectra there are $N(N-1)/2$ possible ombinations; the factor 2 reflects the fact that $\beta_{3,2,1} = -\beta_{3,1,2}$. This number f effective pairs of reference spectra is reduced by eliminating adjacent pectra and spectra separated by only one other spectrum. The number of ffective combinations (C) is then $C = (N^2 - 5N + 6)/2$. Thus in a set of 10 pectra there are 28 effective pairs of reference spectra, whereas in a set of 0 spectra there are 378 pairs. These numbers might appear large, but other pectra may be discounted on the observational grounds that they are too oisy. The use of a noisy spectrum as one of the reference spectra will lead o high values for the δ_n functions [1], and may lead to doubts on the alidity of the analysis. The number of choices open to the operator is thus mited, and he is also usually aware of spectra during the recording of which inor errors or instrumental malfunctions have occurred. These, too, will not e considered.

The utilization of the reference spectra to yield appropriate β values, via uitable threshold values and gates, has been discussed [1]. By an appropriate hoice of β(A) and β(B) for the spectra of species A and B, respectively, the olar absorbance at each recorded wavelength for A and B may be generated; hen these are amalgamated, the spectra of A and B are obtained. This pre-umes a correct choice for β(A) and β(B). The problem arises as to how to ecognize the terminal spectra, and what constitutes the "correct" β values.

ecognition of terminal spectra

The severity of the problem depends, to some extent, on the nature of the xternal parameter which alters the equilibrium; but each spectrum should be eated initially as a special case. This was concluded [3—5] after attempts ad been made to implement the procedure of Brynestad et al. [8]. It was ound necessary to exercise judgement, e.g. concluding that the spectrum was at of, say, species A free from any contribution by B, when all shoulders ttributable to B had disappeared and the average absorbance in regions where was not (but B was) expected to absorb, appeared by eye to be zero. In prin-iple, the second and fourth and derivative spectra would show, ultimately, the bsence of peaks from B as β approached βA [5]. The difficulties of this are at the generated spectra show enhanced noise, hence derivative spectra are lso noisy and harder to interpret. The present system has in-built character-tics which avoid these difficulties.

n-built advantages for kinetic determinations

Since the external parameter that is varied to produce the set of internally near spectra containing isosbestic points is time, and since the time of mixing r dissolving the reactants is known, all spectra are associated with a time dif-erence from zero time. Certain handling difficulties may make this start time

a little imprecise, but, as shown below, it is possible to extrapolate the data back to obtain a precise time, and hence a precise value of $\beta_{t=0}$, which will yield the spectrum of species A before it reacts. Also, since first-order rate kinetics involve a logarithmic relationship and so an infinite time before the reaction is completed, this time can, in principle, be measured with sufficie accuracy after a time interval of ten half-lives of the reaction. In practice, errors arise from spectrophotometer instability over long time periods, but again this can be corrected.

The specific system investigated to test these procedures must be discuss before the relationship between β and k, the rate constant for the reaction, derived.

EXPERIMENTAL

The time dependences of the aquation of halogenopentamminechromiur complexes were monitored spectrophotometrically. The reaction

$$[Cr(NH_3)_5X]^{2+} + H_2O \rightarrow [Cr(NH_3)_5H_2O]^{3+} + X^-$$

is well characterized [9—11] and follows first order reaction kinetics. It ha been shown [10] that the rate constant is independent of the initial chrom concentration and pH (below pH 10), and thus the reaction is eminently su for rigorous internal linearity analysis. The chromium(III) salts were kindly prepared by Dr. T. R. Ramasami, who used modifications [12] of standard techniques [13]. In all cases, the counter-anion used was perchlorate, and t reactions were performed in 0.1 M perchloric acid. As the molar absorptivit of these salts are all approximately 40 l mol^{-1} cm^{-1} [10], the concentration used were in the range 0.01—0.02 M.

Spectra were recorded on an Applied Physics Cary 14H spectrophotome in 1-cm cells thermostatted at 25°C, and digitized at 1-nm intervals. Details of the digitizing apparatus and its interfacing have been given [3—5]. The r erence solution used was 0.1 M perchloric acid. Initially spectra were recor every 15 min, and then at increasing time intervals over a period of 45 h fo the bromide and 316 h for the chloride. As the peak maxima of the haloge complexes are quite near to those of the aquo-complex, the resultant spect of the aquation reactions lie close together. Figure 1 shows a representative sample of the spectra of the aquation of bromopentamminechromium(III) perchlorate.

Internal linearity analysis

A preliminary analysis by the method of Chylewski [6] is shown in Fig. The absorbance at 522 nm, the peak maximum with the greatest molar abs tivity of the bromo complex, is plotted against that at 482 nm, the most intense peak of the aquo complex. Over most of the time scale the relation is linear, and with a negative slope. This indicates that there is an internal linearity relationship within the set of spectra. The deviations from linearit

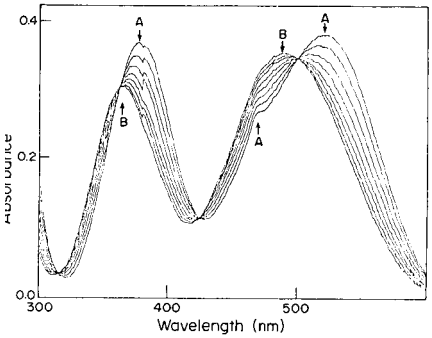

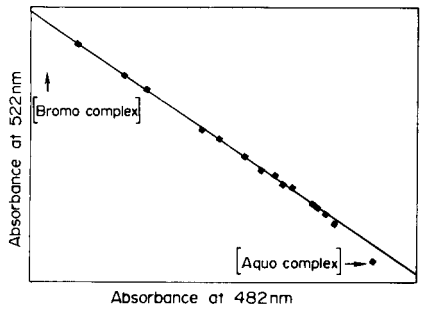

Fig. 1. Variation with time over a period of 45 h of the spectrum of bromopentammine-chromium(III) perchlorate in aqueous perchloric acid (0.1 M) at 25°C as aquation proceeds. A indicate main bands of bromo complex, and *B* those of the aquo complex.

Fig. 2. Time-dependent variation of the absorbance at 522 nm (bromo complex) with that at 482 nm (aquo complex) for bromopentamminechromium(III) perchlorate in aqueous perchloric acid (0.1 M) at 25°C.

at the high end of the time scale could be due to further reaction of the aquopentamminechromium(III) complex, and thus a breakdown of the two-species equilibrium. More likely they result from a loss in stability and a slight drift in the electronics of the spectrophotometer, not unreasonable after 45 h. These deviations will be discussed later.

After the reference spectra had been chosen, mean values of β_n were calculated; from these, δ_n functions [1] were calculated at all wavelengths, and not just at those for which the β value was considered acceptable because it had passed the threshold and gate criteria. The δ_n functions for the bromo and chloro complexes (the aquation rate of the iodo complex was too fast to be monitored by this method) do not exhibit any large deviations from zero, and it is therefore concluded that a representative mean $\bar{\beta}_n$ was calculated by the averaging process. Examples of the δ_n function are shown in Fig. 3. These were calculated from the values of β_n relative to spectra 2 and 26 of the set recorded for the bromo complex.

The deviations from linearity are less obvious from the r.m.s. deviations of β_n than from the Chylewski-type plot (Fig. 2), being less than 2% for all except the last in the set for the bromo complex (1 in 32). The r.m.s. deviations are greater in the set from the chloro complex, but this is due to the much larger time scale involved. It can be concluded that the analyses of the sets of spectra of the halogeno complexes show these sets to be internally linear over the entire time scale involved.

CALCULATION OF TERMINAL SPECTRA

A familiar way of expressing a first-order reaction is: $\ln (a - X) = kt + c$,

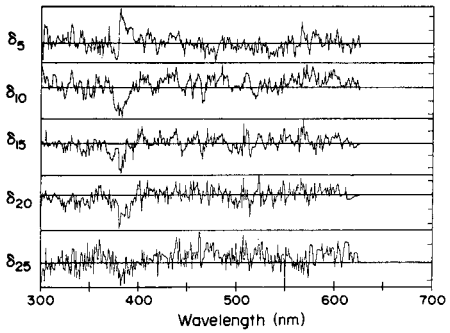

Fig. 3. Wavelength dependence of the deviation (δ) from internal linearity for five of the spectra in the set obtained for the aquation of bromopentamminechromium(III) perchlorrate. δ_n is the deviation of the n th spectrum in the set, relative to the reference spectra. The scale marks on the right-hand side indicate absorbance intervals of 0.002 absorbance units from the mean for each plot.

where a is the initial concentration of species A, X the concentration of species B at time t, k is the first-order rate constant, and c is a constant. The molar absorbance (ϵ_t) at time t is directly proportional to the concentration of the two species, thus

$$\ln (\epsilon_\infty - \epsilon_t) = kt + c \tag{1}$$

and

$$\epsilon_t = \epsilon_\infty + ce^{-kt} \tag{2}$$

where ϵ_∞ is the molar absorbance when no further change in absorbance can be detected with change in time. Thus for the reaction $A \xrightarrow{k} B$, the absorbance (ϵ_B) of species B is equivalent to the absorbance at time infinity. From the definition of β [1],

$$\beta_t = (\epsilon_t - \epsilon_1)/(\epsilon_2 - \epsilon_1) \text{ and } \beta_\infty = (\epsilon_\infty - \epsilon_1)/(\epsilon_2 - \epsilon_1)$$

therefore

$$\beta_t = \beta_\infty + c'e^{-kt} \tag{3}$$

Equation (3) is analogous to eqn. (2), and thus first-order rate constants may be calculated by using the internal linearity procedure.

Effect of scanning period

For any one spectrum, β_t is constant, whereas there is a finite time difference between the beginning and end of the recording of that spectrum. This difference is constant if all the spectra in the set are recorded at the same spectral scan rate, which is the usual procedure. Thus β_t may be associated with the time at which a certain wavelength in the spectrum is attained. This point must remain constant throughout the set of spectra for the rate constant

) have any significance. If the recording of a spectrum is commenced immedi-ely reactants are mixed, then a value of β_0 would be associated with that ero-time spectrum. In the present work, there was commonly a manipulative me delay between bringing the reactants together and recording the first ectrum. Thus, except for very slow reactions, β_0 is not obtainable experi-entally; but at time zero eqn. (3) reduces to

$$_0 = \beta_\infty + c' \tag{4}$$

A plot of β_t against time for the bromo complex is shown in Fig. 4. As this an exponential plot, manual determination of accurate values for the par-meters is difficult. Accordingly, the program INTERLIN (available on request om the authors), which incorporates NAG routine [14] E04GAA, was used o obtain the "best" values for these β values by least-squares minimization echniques. Also plotted in Fig. 4 is the curve obtained on substituting the best" values of the parameters into eqn. (2), and the difference between the xperimental and calculated values. The difference plot shows an excellent fit o the experimental data.

Values for β_t at the high end of the time scale were not included in the alculations as they were considered not sufficiently accurate because of nstrumental drift. The consequences of this inaccuracy are discussed below.

Difficulties in obtaining β_∞

Removing the exponential factor from eqn. (3) by the use of natural log-arithms yields

$$\ln (\beta_\infty - \beta_t) = \ln c' + kt \tag{5}$$

Thus a plot of $\ln (\beta_\infty - \beta_t)$ against t should be linear with a gradient equal to he rate constant. If, however, a "poor" value is used for β_∞, then the plot

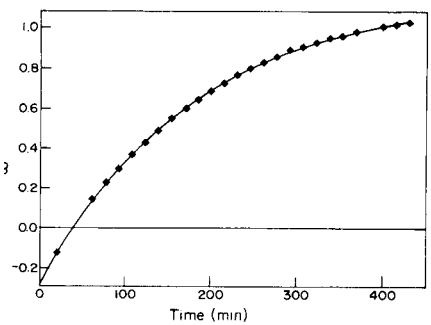

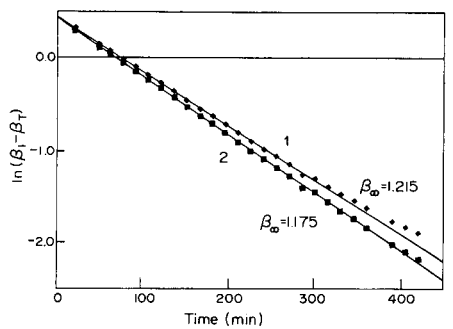

Fig. 4. Plot of β_t against time for the internally linear set of spectra arising from the aquation of bromopentamminechromium(III) perchlorate. The curve is the calculated best fit to the experimental data. The difference plot between experimental and calculated data is also shown.

Fig. 5. Plot of $\ln (\beta_\infty - \beta_t)$ against time, showing the effect of (1) "bad" values for β_∞ (1.215) and (2) "good" values (1.175).

will show deviations from linearity. Figure 5 shows the effects of "good" and "bad" values for β_∞ as applied to eqn. (5). The data correspond to the β_t values plotted in Fig. 4. The points in line (1) were obtained by using a valu of 1.215 for β_∞. This was the value of β_t corresponding to the spectrum at t = 2700 min (45 h), when the reaction was considered finished. At $t > 300$ mir the data show systematic deviations from linearity, thus implying that this value for β_∞ was inaccurate.

Incomplete reaction can be discounted, since a reaction is usually considere complete after ten half-lives, and the half-life is approximately 2 h. Further reaction of the aquopentamminechromium(III) ion is also unlikely, because this ion is extremely inert in the low pH solution used.

The inaccuracy is therefore due to instrumental drift, which can be correct Figure 4 shows the values of β_t obtained during the first 7 h of reaction, over which instrumental drift would not be expected. Substitution of these data into eqn. (3) yields, by least-squares minimization, a value of 1.175 for β_∞. Substitution of this value in eqn. (5) gives the points on line (2) (Fig. 5) whicl shows no deviations from linearity.

Precise terminal spectra

The above method is thus, by compensating for instrumental drift, capable of producing a more accurate terminal spectrum than can be measured experimentally. (It should be remembered that the spectrophotometer used is one of the best currently available.) Use of the value of 1.175 for β_∞ in eqn. (4) gives a value of −0.278 for β_0. The spectra calculated corresponding to these two terminal β_t values are plotted in Fig. 6. Also plotted for comparison purposes, are the first spectrum recorded (commenced 3 min after the onset of reaction) and the last "accurate" spectrum recorded (420 min).

CALCULATION OF RATE CONSTANTS

Rearrangement of eqn. (5) gives

$$k = (1/t) \ln [(\beta_\infty - \beta_t)/c'] \qquad (6)$$

For an ideal set of internally linear spectra, k is independent of the two spectı used as reference spectra. In a real set, however, the reference spectra are not noise-free and the deviations from internal linearity are a function of the two reference spectra. The deviations are reflected in the values for β_∞ and β_t, whic in turn influence k; thus in practice k depends on the choice of reference spectra. To obtain a meaningful value for k, the internal linearity analysis should be repeated with different reference spectra, if suitable spectra are available, and the resulting values of k averaged. This method, however, can be very time-consuming, even in a computer, especially if plots similar to those in Figs. 3, 4 and 6 are obtained in each analysis.

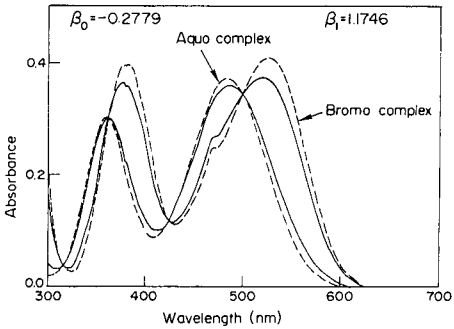

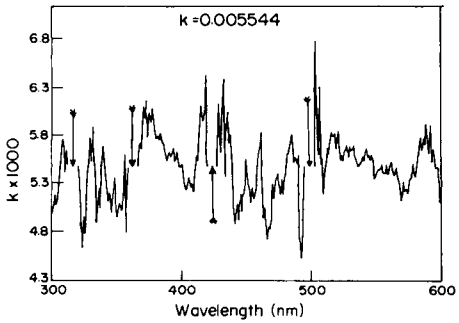

Fig. 6. Calculated terminal spectra (dashed lines) for the aquation of bromopentammine-chromium(III) perchlorate, together with the first spectrum recorded, and the last spectrum (after 7 h) before the spectrophotometer electronics began to drift (solid lines). β_0 used was −0.2779 and β_∞ was 1.1746.

Fig. 7. Variation of k, the first-order rate constant for the aquation of bromopentammine-chromium(III) perchlorate at 25°C, with wavelength. The arrows indicate the positions of the isosbestic points, and the gaps the wavelength ranges around the isosbestic points where absorbance differences were too small for the calculation of meaningful k values. The average value of k was 5.544×10^{-3} s^{-1}.

Comparison with the conventional method

Normally the change in absorbance at several pre-selected wavelengths is plotted as a function of time, the rate constant being proportional to the gradient for first-order reactions (eqn. 1). It is impractical, as well as expensive on computer time, to plot the absorbance changes as a function of time at every (digitized) wavelength. However, rearrangement of eqn. (1) gives an equation which is analogous to eqn. (3), and can be used in internal linearity analysis. If the time of commencement of each spectrum relative to the onset of reaction and the (constant) recording rate of the spectra are known, then each recorded datum point may be defined uniquely on a time scale. A program was therefore written, again incorporating NAG [14] routine E04GAA, to fit, at every wavelength, the values of absorbance against time to eqn. (2). As with program INTERLIN, the "best" values for the three parameters (ϵ_∞, k, and c) are obtained by least-squares minimization techniques.

This program also employs a rejection "gate" to eliminate spurious values of k. Spurious values of k will be obtained if, at any wavelength, the difference in absorbance between initial and final spectra is small and not much greater than the inherent noise in the spectra. Obviously no k value can be determined at isosbestic points, and calculations were not attempted in their vicinity. The minimum absorbance difference considered suitable was obtained by inspection, and this value entered into the program. In this study, each spectrum recorded consisted of 301 data points, and the absorbance data recorded at five wavelengths on either side of each of the four isosbestic points were not employed. Thus k values were calculated at some 257 wavelengths. Figure 7 shows the

variation of k with wavelength, and the wavelength regions where it was not appropriate to calculate k.

Advantages

One advantage of this method over the conventional method is that the absorbance at time infinity (i.e., the terminal spectrum) is not required. Thus errors caused by instrumental drift are eliminated. It also allows rate constants to be evaluated directly at lower temperatures, because for slow reactions high temperatures are normally required to complete the reaction and yield the terminal spectrum. Rate constants at lower temperatures are then calculated via the Eyring equation. These problems do not arise with the present method.

An additional feature of this kinetic program is that it allows the calculation of essentially the same terminal spectra as those obtained via internal linearity. At time zero, eqn. (2) reduces to $\epsilon_0 = \epsilon_\infty + c$. As the program obtains the "best" values for ϵ_∞ and c at most wavelengths, it is thus possible to calculate the "best' value of ϵ_0 at these wavelengths. In the vicinity of the isosbestic points, ϵ_∞ and c are not calculated for the reasons given above. Thus ϵ_∞ and c in these regions have to be approximated, and at present no satisfactory method has been found for this purpose. The terminal spectra calculated from the kinetic program for the aquation of the bromo complex were essentially identical to those shown in Fig. 6 from the internal linearity procedure, both visually and by detailed examination of the computed data.

RESULTS AND COMPARISON OF THE METHODS

Rate constants calculated by both methods are shown in Table 1. Also included for comparison are the values obtained by three independent groups, each of whom used the conventional method of calculation. The present rate constants agree well with those of other workers.

TABLE 1

First-order rate constants for aquation of halogenopentamminechromium(III) perchlorate at 25°C and 0.1 M ionic strength

Chloride k ($min^{-1} \times 10^{-4}$)	Bromide k ($min^{-1} \times 10^{-3}$)	Iodide k ($min^{-1} \times 10^{-2}$)	Reference
2.8	5.1	—	a
4.0	5.5	—	b
4.8	3.0	1.0	9
5.6	6.2	6.0	10
9.2[d]	4.5[d]	5.9[d]	c

[a]This work, via internal linearity program. [b]This work, via kinetic program. [c]T. Ramasami and A. G. Sykes, Inorg. Chem., 15 (1976) 2885. [d]Ionic strength 1.0 M, rate constants measured at 50°C and extrapolated to 25°C via Eyring equation.

For a comparable set of data, the internal linearity program is about five times faster than the kinetic program, as the latter has many more time-consuming least-squares minimization calculations to perform. However, a minimum of five internal linearity analyses is considered necessary to obtain a meaningful value for the rate constant. Thus the two programs are of approximately equal duration. Therefore, if the rate constant alone is required, then either program is suitable, but if terminal spectra are also required, then better results are obtained from the internal linearity program.

Finally, it might be suggested that the difficulties of obtaining an accurate spectrum giving ϵ_∞ values could be overcome by preparing a solution several days in advance of the kinetic measurements, and recording its spectrum during the kinetic run, when the spectrophotometer does not drift. This is possible, but only if (a) the solutions made up on different days have exactly the same precision, (b) no side-reactions take place during the waiting period, and (c) the compound remains stable (the halogenopentamminechromium(III) perchlorates do decompose and are best used and analyzed immediately after preparation). The method described above is also the only route to the spectra of species before aquation.

We thank the S.R.C. for a grant for the Cary 14 H spectrophotometer. The digitizing equipment was purchased out of Harwell Contract EMR 1913. D. C. P. thanks the University of Leeds for a research grant, and T. R. G. the Royal Society for a travel grant and the Chemistry Department, Michigan State University, East Lansing, for hospitality and facilities during the preparation of this paper.

REFERENCES

1 T. R. Griffiths and P. J. Potts, Anal. Chim. Acta, 71 (1974) 1.
2 J. S. Mattson, H. B. Mark and H. C. MacDonald (Eds.), Computers in Chemistry and Instrumentation, Vol. 3, Spectroscopy and Kinetics, M. Dekker, New York, 1973.
3 T. R. Griffiths and P. J. Potts, Inorg. Chem., 14 (1975) 1039.
4 T. R. Griffiths and P. J. Potts, J. Chem. Soc. Dalton Trans., (1975) 344.
5 J. R. Dickerson, T. R. Griffiths and P. J. Potts, J. Inorg. Nucl. Chem., 37(1975) 511, 520.
6 C. Chylewski, Angew. Chem. Int. Ed. Engl., 10 (1971) 195.
7 J. Brynestad and G. P. Smith, J. Phys. Chem., 72 (1968) 296.
8 J. Brynestad, C. R. Boston and G. P. Smith, J. Chem. Phys., 47 (1967) 3179.
9 H. Freundlich and R. Bartels, Z. Phys. Chem.. 101 (1922) 177.
10 M. A. Levine, T. P. Jones, W. E. Harris and W. J. Wallace, J. Am. Chem. Soc., 83 (1961) 2453.
11 N. V. Duffy and J. E. Earley, J. Am. Chem. Soc., 89 (1967) 272.
12 T. Ramasami, Ph. D. thesis, University of Leeds, 1976.
13 T. Moeller, in T. Moeller (Ed.), Inorganic Syntheses, Vol. 5, McGraw-Hill, New York, 1951, p. 132.
14 Numerical Algorithms Group, University of Oxford.

Analytica Chimica Acta, 107 (1979) 291—299

COMPARATIVE STUDIES ON THE FLUORESCENCE BEHAVIOUR OF SOME MONO- AND DIAMINOPYRIDINES

W. BAEYENS* and P. DE MOERLOOSE

State University of Ghent, Faculty of Pharmaceutical Sciences, Department of Pharmaceutical Chemistry and Drug Quality Control, Akademisch Ziekenhuis, De Pintelaan 135, B-9000 Gent (Belgium)

(Received 31st October 1978)

SUMMARY

The fluorescence characteristics of 2-, 3- and 4-aminopyridine, 2,3-, 3,4- and 2,6-diaminopyridine, and 2-amino-6-picoline were investigated in various solvents and at different pH values. 4-Aminopyridine exhibits negligible fluorescence probably because of (n, π^*) transitions. All other compounds are strong fluorophores, which is mainly due to the (π, π^*) nature of the lowest excited state. Practical data for the fluorimetric determination of small amounts of these molecules are reported, i.e. excitation and emission maxima, relative fluorescence intensities, optimum pH, limits of linearity, detection limits, and ultraviolet absorption maxima; 0—0 bands, and variation of excitation and emission wavelengths and of fluorescence intensities with pH are also reported. Even nanogram amounts can be identified and determined.

Pyridine, the simplest nitrogen heteroaromatic, unexpectedly possesses no luminescence characteristics [1, 2]; azines with the lowest excited singlet state (S1) of an (n, π^*) type often emit intense phosphorescence [3]. Most azines including pyridazine, pyrimidine and pyrazine are weakly fluorescent [4] ($\pi^* \rightarrow$ n fluorescence). Recently, fluorescence of pyridine in the vapor phase was observed [5]; photochemical reactions can however be responsible for some deactivation processes of photo-excited nitrogen heterocyclic compounds, e.g. pyridine isomerizes to a transient Dewar structure on ultraviolet irradiation [6]. Symmetry-allowed n $\rightarrow \pi^*$ transitions in pyridine and related *N*-heterocycles can be ascribed to the asymmetry of the *n*-orbital of the nitrogen atom [7]. Strange absorption and emission shifts arising from pH and medium effects in pyridine derivatives were noticed by Chamma et al. [8]. Although pyridine exhibits practically no luminescence, Weisstuch and Testa [9] and Hotchandani and Testa [10] observed fluorescence and phosphorescence emission in aminopyridines. Kimura et al. [11] recently reported quantum yields and lifetimes of fluorescence and phosphorescence of some monoaminopyridines and related molecules. Hotchandani and Testa [2, 12] also described phosphorescence emission and polarization studies of hydroxypyridine isomers.

As n, π^* transitions are associated with very weak or negligible fluorescence emission properties, the fluorescent behaviour of aminopyridines might offer information concerning the nature of excited states. Also, as the aminopyridine nucleus often occurs in drugs, a knowledge of the luminescent characteristics of these components is useful analytically in the determination of these compounds and derivatives in pharmaceutical combinations. Such theoretical studies are often useful in analytical and biological chemistry, e.g. 2-aminopyridine proved to be a metabolic transformation product of difenpiramide, a new anti-inflammatory drug [13]. Some aminopyridines have powerful effects on neuromuscular transmission and can also enhance muscle contraction [14]; neuromuscular blockade produced by some aminoglycoside antibiotics is reversed by 4-amino- and 3,4-diaminopyridine [15]. 3,4-Diaminopyridine reverses muscle paralysis induced by some antibiotics [16], and 2,3-, 2,6- and 3,4-diaminopyridine increase both stimulated and spontaneous acetylcholine release in the chick biventer cervicis muscle [17]. The effects of 4-aminopyridine on isolated chick oesophagus was studied recently [18]. 2-Aminopyridine has been used as a fluorescence emission standard [19]. 2,6-Diaminopyridine serves as a reagent for the sensitive fluorimetric determination of primary aromatic amines on the nanogram scale [20].

In this paper, more practical analytical information on the fluorescence characteristics of some mono- and diaminopyridines is reported.

EXPERIMENTAL

Chemicals

All aminopyridines (AP) and diaminopyridines (DAP) (Aldrich Chemical Co. Ltd.) were recrystallized several times in the presence of activated charcoal from the following solvents: 2-aminopyridine (benzene), 3-aminopyridine (benzene), 4-aminopyridine (benzene—methanol, 95 + 5), 2,3-diaminopyridine (benzene), 3,4-diaminopyridine (benzene—methanol, 85 + 15), 2,6-diaminopyridine (benzene), 2-amino-6-picoline (2-A-6-P) (petroleum ether, b.p. 25—70°). They were then dried over silica gel at room temperature in vacuo. Melting points were determined and purity control tests were carried out by thin-layer chromatography on silica gel 60F 254 plates (200 × 200 × 0.2 mm), in several eluents i.e., chloroform, chloroform—methanol (90 + 10), and propane-2-ol—25% (w/w) ammonia (90 + 10).

Pyridine and aniline were dried over potassium hydroxide followed by distillation before use. All compounds were stored in the dark below 10°C under a nitrogen atmosphere.

De-ionized water was used throughout; the quality was controlled by fluorimetric scanning at the highest instrumental sensitivity settings. Thallium(I) acetate and lead tetraacetate of "purum" quality (Fluka AG) were found satisfactory. All other reagents were of analytical grade (E. Merck and J. T. Baker Chemical Co.) and were checked before use for absence of

fluorescent background signal. A series of buffer solutions (pH 1—13) of the composition described previously [21] was prepared.

Apparatus

Fluorescence spectra and measurements were taken on an Aminco-Bowman spectrophotofluorimeter (American Instrument Co., Silver Spring, Md.) fitted with a Hanovia 150-W xenon arc lamp, grating excitation and emission monochromators, 1 × 1 cm quartz cells, a photomultiplier (R 446 S) operated at 700—800 V, and an X-Y recorder; the slits varied between 1 and 4 mm (spectral band pass of 5.5 nm per mm slit width). Lamp stabilization was achieved by means of a magnetic arc stabilizer (Aminco); checks to ascertain that no fluctuations in lamp intensity occurred were carried out with polymer fluorescence standard samples (anthracene, naphthalene and *p*-terphenyl; ISA Belgium Groupe Instruments S.A., no. 16.156.139). No corrections were made for variations in source radiance, monochromator transmission or photomultiplier sensitivity with wavelength. The wavelengths reported for maxima are averages of at least five experimental values. The detection limit is defined as the concentration of solute yielding a signal that exceeds the background signal for pure solvent by 5% of the full scale deflection at maximum "sensitivity" and "percent full scale" settings on the instrument.

Ultraviolet absorption spectra were recorded on a Zeiss spectrophotometer, Model DMR 21, equipped with a hydrogen lamp, 1-cm quartz cuvettes and a photomultiplier. Melting-points were taken on a Mettler FP 1 apparatus. A Camag TL 900 Universal u.v. lamp was used at 254 and 350 nm for viewing the thin-layer chromatograms.

Procedures

Preliminary experiments showed that the oxygen concentration had no significant effect on the fluorescence properties of the aminopyridines under the experimental conditions used. Hence precautions were not taken to exclude oxygen.

The dependence of the excitation and emission maxima of the aminopyridines on pH was established by mixing 8.0 ml of aqueous solution of the compound of interest at concentrations of 0.01—0.50 $\mu g\ ml^{-1}$ with 2.0 ml of buffer solution (pH 1—13) followed directly by scanning the excitation and emission spectra. Blank solutions were subsequently scanned at the wavelength maxima of the fluorophore under investigation to compensate for any fluorescing contaminants. From the curves obtained, suitable excitation and emission maxima were chosen for determining the pH dependence of the fluorescence emission intensities; the same dilution ratio (8 + 2) was maintained. From the shape of these curves, uncorrected Stokes shifts were calculated; these involve solvent environments and vibrational structures of the ground and lowest excited singlet states and the sequence of events in the absorption and emission processes [22, 23]. Analytical calibration curves were then plotted, for analogous mixing conditions (8 + 2),

at the appropriate maxima and pH values taking optimum emission intensity and fluorophore stability into account. From these curves, the ranges of linear response were established and detection limits were calculated.

RESULTS AND DISCUSSION

The effect of ionization on the fluorescent behaviour of the aminopyridines investigated was studied. Figure 1 shows the changes in the excitation and emission wavelengths of these compounds as a function of pH. Figure 2 illustrates the fluorescence intensity corrected for blank signals as a function of buffer pH, measured for the appropriate excitation and emission wavelengths given in Fig. 1.

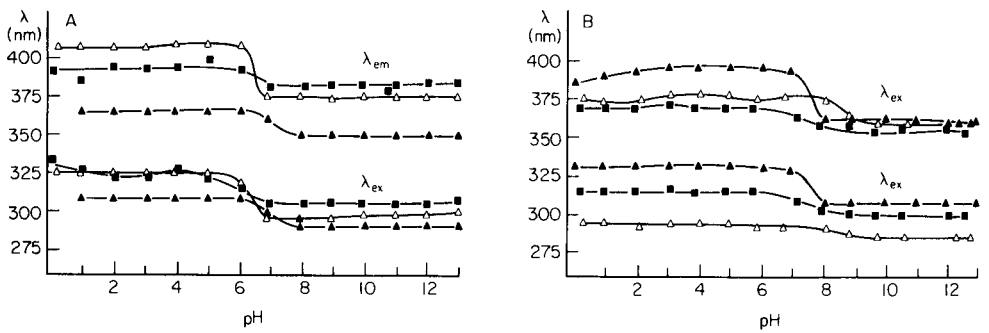

Fig. 1. Excitation and emission wavelengths in relation to pH (8.0 ml aqueous solution + 2.0 ml buffer solution). A: (▲) 2-aminopyridine; (△) 3-aminopyridine; (■) 2,3-diaminopyridine. B: (▲) 2,6-diaminopyridine; (△) 3,4-diaminopyridine; (■) 2-amino-6-picoline. Each point is the average of at least three independent determinations.

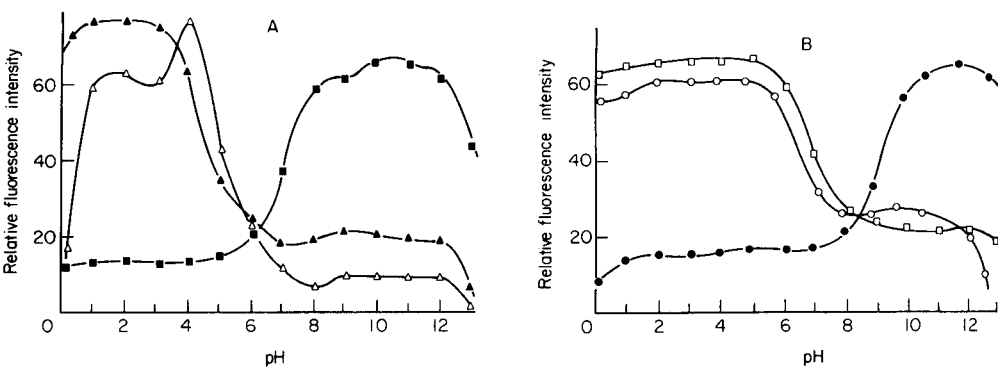

Fig. 2. Fluorescence intensity in relation to pH (8.0 ml aqueous solution + 2.0 ml buffer solution). A: (▲) 2-aminopyridine; (△) 3-aminopyridine; (■) 2,3-diaminopyridine. B: (□) 2,6-diaminopyridine; (●) 3,4-diaminopyridine; (○) 2-amino-6-picoline. Each point is the average of at least three independent determinations.

Pyridine and aniline, purified as described above, did not fluoresce under any of the conditions described, even at the highest instrumental sensitivity settings. The ultraviolet absorption maxima in water, 0.1 M hydrochloric acid, and 0.1 M sodium hydroxide were measured as a basis for discussion of the absorption and excitation spectra of the aminopyridines under investigation.

Table 1 presents a summary of the absorption and fluorescence characteristics of the aminopyridines. 0—0 Band positions for the lowest singlet were taken as the wavenumber (cm^{-1}) of intersection [24] of the two curves representing plots of relative absorption and emission intensities vs. wavelength as they exhibited good mirror-image symmetry; when 0—0 band positions were determined as the mean of absorption and emission maxima (used when mirror-image symmetry is not satisfactory), significant differences were not noticed. In Table 1, the most remarkable phenomenon is the absence of a significant fluorescence signal for 4-AP when measured under nearly identical instrumental conditions to those for the other compounds. In fact, 4-AP does fluoresce extremely weakly (quantum efficiency < 0.003); in aqueous solution, fluorescence emission was noted at 339 nm (λ_{ex} = (235), 277 nm): addition of the buffer solutions described for the other substances yielded only weak fluorescence (average λ_{ex} = 340 nm; average λ_{em} = 395 nm). The other aminopyridines fluoresce more efficiently as shown in Table 2. The relatively low fluorescence intensity of 2-AP and 3-AP in diethyl ether may be caused by an important n, π^* character in the first excited singlet state.

The fluorescence intensity of 2-AP is much stronger in water and in 0.1 M HCl than that of the 3-AP isomer. Surprisingly, both 2-AP and 3-AP fluoresce more strongly in water than in 0.1 M HCl. As the salt formation primarily appears at the pyridine nitrogen, an increased fluorescence yield could be expected as the n, π^* nature of the lowest excited state is removed. Weisstuch and Testa [9] attributed this phenomenon to the external heavy-atom effect of the halogen ion. This supposition was tested by measuring the effect of some heavy atoms on the native fluorescence properties of 2-AP and 3-AP in aqueous solutions. The results are shown in Table 3. The heavy-atom effect causes a decrease in the fluorescence efficiencies, although the direction of this phenomenon was not expected for 3-AP. Thallium(I) acetate produces a significant fluorescence shift from about 405 nm to 358 nm for 3-AP but not for 2-AP. This blue shift, indicating an energetically higher emitting level for 3-AP in ionic solutions, may arise from a dipole moment reversal in the excited state [9]. The enhanced quenching by heavy atoms, generally a result of high spin—orbital coupling favouring intersystem crossing, can be caused by the nonplanar nature of complexes formed with very heavy elements such as thallium and lead [23].

Optimum fluorescence in acidic medium is obtained for 2-AP, 3-AP, 2,6-DAP and 2-A-6-P; 2,3-DAP and 3,4-DAP exhibit their most intense emission in alkaline medium. The results from Table 2 should be interpreted in terms of the curves illustrated in Figs. 1 and 2, taking into account the

TABLE 1

Absorption, excitation and emission spectra of the mono- and diaminopyridines, pyridine and aniline

Compound	Excitation and emission spectra[a, b]								
	pH 1		pH 7		pH 13		0—0 band (cm^{-1})		
	λ_{ex} (nm)	λ_{em} (nm)	λ_{ex} (nm)	λ_{em} (nm)	λ_{ex} (nm)	λ_{em} (nm)	pH 1	pH 7	pH 13
2-Aminopyridine	(235)*, 308	365	(235)*, 300	360	(233)*, 290	350	30200	30400	31300
3-Aminopyridine	(253)*, 325	407	(240)*, 296	375	(240)*, 299	375	27500	29600	29500
4-Aminopyridine	v.w.		v.w.		v.w.		—	—	—
2,3-Diaminopyridine	(250)*, 327	386	(245)*, 306	382	(245)*, 309	385	28200	29000	29000
3,4-Diaminopyridine	(227)*, 312	358	(234)*, 306	354	(250)*, 282	359	30000	30200	31100
2,6-Diaminopyridine	(247)*, 331	390	(248)*, 329	393	(248)*, 308	362	28000	28400	30000
2-Amino-6-picoline	(240)*, 315	370	(244)*, 310	365	(240)*, 300	356	30000	30200	31000
Pyridine	—	—	—	—	—	—	—	—	—
Aniline	—	—	—	—	—	—	—	—	—

Compound	Absorption spectra[c] (nm)		
	0.1 M HCl	Water	0.1 M NaOH
2-Aminopyridine	300, 229, 199	295, 228, 193	284, 226, (215 sh)
3-Aminopyridine	316, 248, 212	311, 247, 212	287, 230, (214 sh)
4-Aminopyridine	262, 206	262, 206, 191	242, 214
2,3-Diaminopyridine	316, 249, 215, 193	317, 248, 214, 200	299, 236, 215
3,4-Diaminopyridine	(284 sh), 268, 224, 206	286, 224, 206	283, 245, 216
2,6-Diaminopyridine	331, 242	326, 241, 192	304, 239, 214
2-Amino-6-picoline	306, 230, 198	299, 230, 192	289, 228, (214 sh)
Pyridine	(260 sh), 254, (250 sh), 200	252, 245, 239, (235 sh)	262, 256, 249, 243
Aniline	(205 sh), 203	280, 229, 196	280, 230, (214 sh)

[a]8.0 ml of aqueous 0.25 $\mu g\ ml^{-1}$ solution + 2.0 ml of buffer solution; for 4-AP, concentrations up to 2.0 $\mu g\ ml^{-1}$ were tested; for 2,3-DAP 0.01 $\mu g\ ml^{-1}$; for pyridine and aniline, 20 $\mu g\ ml^{-1}$. [b]Weaker, secondary excitation maxima are asterisked; v.w. mea.. very weak. [c]5.0 $\mu g\ ml^{-1}$ solutions; pyridine and aniline, 10.0 $\mu g\ ml^{-1}$; sh indicates shoulder.

TABLE 2

Fluorescence intensities[a] of the mono- and diaminopyridines in various solvents (2 $\mu g\ ml^{-1}$)

Compound	Water	0.1 M HCl	0.1 M NaOH	Methanol	Diethyl ether
2-Aminopyridine	100	160	3	19	8
3-Aminopyridine	18	6	2	19	5
4-Aminopyridine	0.5	0.1	0	0	0.1
2,3-Diaminopyridine	29	9	22	70	52
3,4-Diaminopyridine	0.6	0.5	0.1	3	—[b]
2,6-Diaminopyridine	74	62	51	14	38
2-Amino-6-picoline	69	92	5	15	10

[a]Emission monochromator set on 372 nm and excitation monochromator 309 nm; maxima were taken as a compromise from Table 1. Instrumental sensitivity was set at 100; the per cent full scale setting was varied from 30 to 0.1. Fluorescence intensities, after deduction of blank signals, are given in arbitrary units, calculated relative to the anthracene polymer fluorescence standard sample (no. 1) taken as 10. [b]Insoluble.

TABLE 3

Effect of heavy atoms on excitation and emission maxima and on the fluorescence intensity (F.I.) of 2- and 3-aminopyridine[a]

Solvent	2-Aminopyridine (2 μg ml^{-1})			3-Aminopyridine (2 μg ml^{-1})		
	λ_{ex} (nm)	λ_{em} (nm)	F.I.	λ_{ex} (nm)	λ_{em} (nm)	F.I.
Water	(238)[b], 308	364	52	(255)[b], 323	404	9
0.1 M HCl	(238)[b], 310	365	44	(257)[b], 325	403	4
0.05 M H_2SO_4	(238)[b], 310	365	49	(258)[b], 325	406	19
0.01 M NaI	308	366	20	(268)[b], 323	405	2.5
0.01 M Tl(I) acetate	308	362	17	310	358	3
0.01 M Pb tetraacetate[c]	307	360	10	(258)[b], 320	404	4

[a]Measurements were carried out with the monochromators set at the average maxima (λ_{ex} = 315 nm, λ_{em} = 380 nm). Blanks were subtracted and the arbitrary units are calculated relative to the anthracene polymer fluorescence standard sample (no. 1) = 10. Instrumental sensitivity was set at 100; the percent full scale setting was varied from 0.3 to 3.0. The values given are the averages of at least 3 determinations. [b]Weaker, secondary excitation maximum. [c]Lead tetraacetate is hydrolyzed with the formation of brown lead dioxide and acetic acid. To prepare the solvent, 2.22 g of lead tetraacetate was treated with methanol to give 1 l of solution. The mixture was stirred continuously in a glass-stoppered flask until the original brown suspension became colorless (3—4 h). This solution was stable for several months at room temperature [25].

average wavelength maxima used for the intensity measurements. All of these compounds show a distinct blue shift in excitation and emission wavelengths when the pH is increased above 6.

The significant bathochromic shift of the excitation spectra of 2-AP, 3-AP, 2,3-DAP, 3,4-DAP, 2,6-DAP and 2-A-6-P with increasing polarity when going from alkaline to acidic solutions is typical of π—π^* transitions. Accordingly, the lowest excited singlet states (S1) of these compounds at room temperature are assigned to (π—π^*). Table 1 and Fig. 1 show that when the pH of the solutions is decreased so that these basic molecules occur in polar salt forms, a general increase in excitation and emission wavelength maxima is observed. In contrast, 4-AP, for which distinct fluorescence emission could not be observed, shows practically no differences in absorption spectrum in neutral and acidic media. In alkaline medium, however, the strongest absorption peak at 262 nm shifted towards 242 nm (free base). Weisstuch and Testa [9] suggested that the low fluorescence efficiency of this particular molecule should be attributed to an (n—π^*) transition and gave a possible explanation for the fluorescence quenching of 2-AP and 3-AP in the presence of hydroxide ion shown in Fig. 2: a proton transfer occurs in the hydrogen-bonded species formed between the excited aminopyridine and the hydroxide ion followed by radiationless decay of the imine anion. These processes can be represented as:

$Py\text{-}NH_2 + h\nu_1 \rightarrow Py\text{-}NH_2^*$ (absorption)

$Py\text{-}NH_2^* \rightarrow Py\text{-}NH_2 + h\nu_2$ (normal fluorescence; $\nu_2 < \nu_1$)
$Py\text{-}NH_2^* + OH^- \rightarrow Py\text{-}NH_2^*\ldots OH^-$ (hydrogen-bonded complex in the excited state)
$Py\text{-}NH_2 + OH^- \rightarrow Py\text{-}NH_2\ldots OH^-$ ($\sim$ in the ground state)
$Py\text{-}NH_2^*\ldots OH^- \rightarrow Py\text{-}NH^{*-} + H_2O$ (fast proton transfer)
$Py\text{-}NH^{*-} \rightsquigarrow Py\text{-}NH^-$ (radiationless decay)
$Py\text{-}NH^- + H_2O \rightarrow Py\text{-}NH_2 + OH^-$

This hypothesis might explain the decreased intensities of fluorescence of 2-AP, 3-AP, 2,6-DAP and 2-A-6-P in alkaline medium; the 2,3- and 3,4-diamino isomers behave in the opposite way. For 3,4-DAP, this can be concluded from Fig. 2; Table 2 does not represent its true behaviour because the intensities are too low as a result of the average excitation and emission wavelength maxima used.

Important analytical data for the detection and determination of the aminopyridine compounds are shown in Table 4. Even nanogram amounts can be detected. All of these measurements were carried out directly after the solutions were prepared as the stability (to light and oxygen) at different pH values was unknown. 3-AP, 2,3-DAP and 2,6-DAP exhibit visual strong fluorescence emission on silica gel layers when irradiated with u.v. light. Nanogram quantities of these molecules can be detected visually on thin layers.

2,6-DAP is an excellent reagent for the fluorimetric determination of primary aromatic amines [20]; after diazotization of the amino group, coupling occurs with 2,6-DAP followed by treatment of the resulting azo dye with ammoniacal copper(II) sulfate. An investigation has been carried out [26] to isolate and elucidate the structure of the intensely fluorescent derivative which allows determinations of primary aromatic amines on the nanogram scale.

TABLE 4

Analytical data of the fluorescence characteristics of the mono- and diaminopyridines[a]

Compound	Stokes shift [22] (cm^{-1})[b]		Optimum pH[c]	Optimum maxima for determination		Limit of linearity ($\mu g\ ml^{-1}$)	Dete limit (ng r
	H^+	OH^-		λ_{ex} (nm)[d]	λ_{em} (nm)		
2-Aminopyridine	5100	5900	2.0	308	366	0.8	0.5
3-Aminopyridine[e]	6200	7000	4.0	325	410	2.0	3.0
2,3-Diaminopyridine[f]	5300	6600	10.0	306	383	0.2	0.5
3,4-Diaminopyridine	4500	7400	11.0	282	356	1.0	10.0
2,6-Diaminopyridine	5000	4900	4.0	332	396	0.2	0.5
2-Amino-6-picoline	4900	5700	4.0	310	365	1.0	0.5

[a]8.0 ml of 0.01—2.0 $\mu g\ ml^{-1}$ in H_2O + 2.0 ml buffer solution, pH 1—13. [b]H^+ before pH transition region; OH^- after pH transition region. Wavelengths from Fig. 1. [c]pH values from Fig. 2 [d]Second order (shoulder) excitation maxima are not mentioned. [e]Negligible signals were obtained for 4-aminopyridine, even in water; results obtained from various experiments are of doubtful value and are not listed. [f]Aqueous solutions quickly turn yellow-brown; fresh preparation is therefore recommended for all these compounds.

REFERENCES

1 M. Zander, Phosphorimetry, Academic Press, London, 1968, p. 89.
2 S. Hotchandani and A. C. Testa, Spectrochim. Acta, Part A, 32 (1976) 1659.
3 S. P. McGlynn, T. Azumi and M. Kinoshita, Molecular Spectroscopy of the Triplet State, Prentice-Hall, New Jersey, 1969, Chaps. 3 and 6.
4 G. G. Guilbault, Practical Fluorescence, M. Dekker, New York, 1973, p. 95.
5 I. Yamazaki and H. Baba, J. Chem. Phys., 66 (12) (1977) 5826.
6 K. E. Wilzbach and D. J. Rausch, J. Am. Chem. Soc., 92 (1970) 2178.
7 J. Griffiths, Colour and Constitution of Organic Molecules, Academic Press, London, 1976, p. 63.
8 A. Chamma, M. Deumie, B. Saperas, P. Viallet, P. Jacquignon and F. Perrin, in Excited States of Biological Molecules, J. B. Birks (Ed.), Wiley, London, 1975, p. 23.
9 A. Weisstuch and A. C. Testa, J. Phys. Chem., 72 (1968) 1982.
10 S. Hotchandani and A. C. Testa, J. Chem. Phys., 59 (1973) 596.
11 K. Kimura, H. Takaoka and R. Nagai, Bull. Chem. Soc. Jpn., 50, 5 (1977) 1343.
12 S. Hotchandani and A. C. Testa, J. Chem. Phys., 67 (11) (1977) 5201.
13 E. Grassi, G. L. Passetti, A. Trebbi and A. Frigerio, in A. Frigerio and E. L. Ghisalberti (Eds.), Mass Spectrometry in Drug Metabolism, Plenum, London, 1977, p. 99.
14 A. L. Harvey and I. G. Marshall, Comp. Physiol. Biochem., 58c (1977) 161.
15 Y. N. Singh, I. G. Marshall and A. L. Harvey, Br. J. Anaesth., 50 (1978 b) 109.
16 Y. N. Singh, I. G. Marshall and A. L. Harvey, J. Pharm. Pharmacol., 30 (1978) 249.
17 A. L. Harvey and I. G. Marshall, Eur. J. Pharmacol., 44 (1977) 303.
18 H. A. Al-Haboubi, W. C. Bowman, J. Houston and A. O. Savage, J. Pharm. Pharmacol., 30 (1978) 517.
19 C. E. White and R. J. Argauer, Fluorescence Analysis, M. Dekker, New York, 1970, p. 50.
20 L. J. Dombrowski and E. L. Pratt, Anal. Chem., 43, 8 (1971) 1042.
21 W. Baeyens and P. De Moerloose, Analyst, 103 (1978) 359.
22 S. Udenfriend, Fluorescence Assay in Biology and Medicine, Vol. II, Academic Press, London, 1969, p. 7.
23 J. D. Winefordner, S. G. Schulman and T. C. O'Haver, Luminescence Spectrometry in Analytical Chemistry, Wiley-Interscience, London, 1972, pp. 58—65.
24 E. J. Bowen, in W. A. Noyes, Jr., G. S. Hammond and J. N. Pitts, Jr. (Eds.), Advances in Photochemistry, Vol. I, J. Wiley, New York, 1963, pp. 26—29.
25 I. M. Jakovljevic, Anal. Chem., 49 (1977) 2048.
26 W. Baeyens, G. Bens, P. De Moerloose and L. De Taeye, Pharmazie, in press.

Analytica Chimica Acta, 107 (1979) 301—307

DOUBLE INDICATION IN CATALYTIC-KINETIC ANALYSIS: SIMULTANEOUS PHOTOMETRIC AND THERMOMETRIC INDICATION OF THE IODINE—AZIDE REACTION IN CLOSED AND FLOW SYSTEMS

HERBERT WEISZ*, WOLFGANG MEINERS and GUENTER FRITZ

Lehrstuhl für Analytische Chemie, Chemisches Laboratorium der Universität Freiburg i.Br. (Federal Republic of Germany)

(Received 20th December 1978)

SUMMARY

The iodine—azide reaction catalyzed by sulphur-containing compounds is followed simultaneously by optical and thermometric measurements in closed and flowing systems. In the closed system, thiosulphate can be determined in the range 32.4—324 $\mu g\ ml^{-1}$, by observing the turbidity caused by the nitrogen formed during the reaction and the temperature changes. With the flow apparatus, thiosulphate can be determined in the range 112—1120 $\mu g\ ml^{-1}$ by continuously mixing the sample and reagent solutions. H_2S in nitrogen (5—100 ppm) is measured by sweeping the gas into the reaction cuvette. In a third flow procedure, H_2S is liberated continuously from sodium sulphide solutions (0.1—10 $\mu g\ S^{2-}\ ml^{-1}$) by ascorbic acid, and swept to the measuring cuvette with nitrogen.

Double indication in catalytic-kinetic analysis makes it possible to follow the course of a catalyzed reaction simultaneously by two independent methods, so that the accuracy and precision of the determination can be improved. The application of the technique to some reaction systems has already been described [1].

The well-known iodine—azide reaction [2, 3] is catalyzed by substances which contain sulphur in the 2— oxidation state: $I_2 + 2N_3^- \rightarrow 3N_2 + 2I^- + \Delta H$. In this paper, two catalysts (Na_2S, $Na_2S_2O_3$) are used as models to illustrate methods suitable for double indication in this reaction system. The determinations are carried out in both open and closed systems. Optical (turbidimetric) and thermometric measurements are used simultaneously for indication.

DETERMINATIONS IN A CLOSED SYSTEM

Thermometric indication

The change of temperature is quick in the exothermic iodine—azide reaction catalyzed by thiosulphate. In a side-reaction, the catalyst itself is oxidized and made inactive by iodine, so that the iodine—azide reaction ceases. The temperature change caused by the exothermic oxidation of thiosulphate by iodine itself can be neglected.

If the reaction system contains a comparatively high concentration of catalyst, then its oxidation takes longer and a comparatively large amount of product is formed. In contrast, if the concentration of the catalyst is low, its complete oxidation will be rapid and the catalyst will be active for only a short time. The reaction turnover is represented by the height of the temperature maximum in the recorded graph, which therefore provides a measure of the concentration of the catalyst.

Figure 1 shows schematically a graph produced by the two-channel recorder. The temperature jump demonstrates the rapidity of the catalyzed reaction. The length of time of the chemical reaction is roughly indicated in Fig. 1 by two vertical strokes at R.

Optical indication

Optical indication is carried out in a novel way by measuring the turbidity. In the highly viscous solution (75% glycerol in water) the nitrogen formed in the reaction forms small gas bubbles which rise slowly. These bubbles decrease the transmittance of the solution because of light scattering, whereas the reduction of the iodine to iodide increases the transmittance of the solution by about 10%. This decrease in the transmittance is easily observed by using a focussed light beam as applied in the photometric arrangement already described [1].

Compared to the rapid chemical reaction itself, the physical phenomenon, i.e. the formation and rising of the nitrogen bubbles, is very slow. The optical recorder curve runs through a maximum (see Fig. 1), which represents the turbidity after completion of the catalyzed reaction. This maximum is higher and is reached more quickly, the more nitrogen is formed in the catalytic reaction. Thus the height of the maximum (H_m) as well as the time required

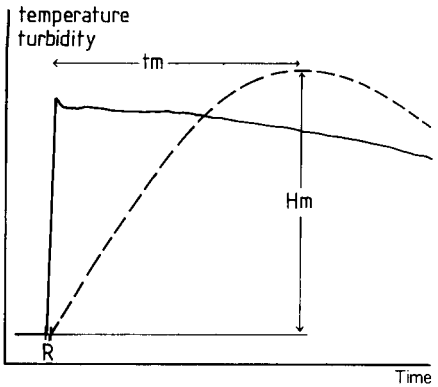

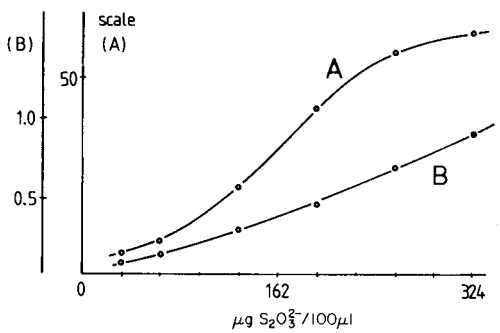

Fig. 1. Schematic representation of recorded curves for change of temperature (—) turbidity (---) with time.

Fig. 2. Standard graphs for the determination of thiosulphate. (A) Thermometric indication; (B) optical indication.

to reach the maximum (t_m) are both a measure of the concentration of the catalyst. The quotient of these two measured values, H_m/t_m, proved to give better results than either used separately. This method can be called gas turbidimetry, and might be useful in other applications where gaseous products are formed.

Experimental

Apparatus. The home-made photometer used has already been described [1] (cf. Fig. 3). The temperature in the cuvette is followed by a thermistor (ITT/SEL F15D). The changes in the temperature and absorbance are recorded simultaneously versus reaction time on a two-channel recorder (Metrawatt RE 571).

Procedure. The stock solution is prepared by dissolving 3.4 g of sodium azide in 100 ml of an aqueous 0.1 M solution of iodine (containing 2 g of potassium iodide), and mixing with 300 ml of glycerol.

For each measurement, 8 ml of this solution is pipetted into the cuvette. To start the reaction, 100 μl of the thiosulphate sample solution is added and the sudden rise of temperature and the slower decrease in the transmittance are recorded. (The curves are similar to those shown schematically in Fig. 1). The concentration of thiosulphate is evaluated from the height of the temperature jump and from the quotient H_m/t_m.

Results

The standard graphs shown in Fig. 2 were prepared with solutions of sodium thiosulphate in the range 32.4—324 μg $S_2O_3^{2-}$/100 μl; each point is the average of three separate measurements. Table 1 gives some results for thiosulphate determinations.

Several other catalysts for the iodine—azide reaction can be determined in the same way. The thermal and optical effects for the following catalysts were comparable to those for thiosulphate: H_2S (30.2—302 μg); S^{2-} from Na_2S (30—300 μg); thiourea (38—380 μg); cysteine (35—350 μg); cystine (150—1500 μg); thiocyanate from KSCN (120—1200 μg).

TABLE 1

Determination of thiosulphate in the closed system (All results are given as μg $S_2O_3^{2-}$/100 μl)

Taken	36	71	110	165	194	220	243	266	292	318
Found										
(thermometric)	42	68	97	181	188	240	249	259	301	324
(optical)	34	68	102	162	190	228	234	252	290	340

The same reactions can be used in flow-through systems. The solution of the reactants is pumped into the reaction cuvette continously, and the catalyst is also introduced continuously. If the sample itself is a solution or a gas it can be transferred directly to the reaction solution. Alternatively, hydrogen sulphide can be produced continuously from a sulphide-containing sample solution in a separate generating cell and transported to the reaction solution by an inert carrier gas. Figure 3 is a schematic diagram of the flow-through apparatus and shows the three possibilities of adding the catalyst. The measuring cuvette itself is the same as described above for the application of the closed system. The volume of the cuvette is limited by a simple overflow (see Fig. 3, j).

Determination of a solution of catalyst (thiosulphate)

The solution of azide and iodine in aqueous glycerol (see above) is continuously thermostated and added to the reaction cuvette (see Fig. 3, I) at a rate of 2.5 ml min^{-1}. The thiosulphate sample solution is pumped into the cuvette at a rate of 0.1 ml min^{-1} (112—1120 μg $S_2O_3^{2-}$ ml^{-1}). The time required to measure one sample until a plateau in the graph is reached is about 30 min, corresponding to 3 ml of sample solution.

Figure 4 shows the graphs produced during the determination of various thiosulphate samples. The height of the curve for the transmittance (steady concentration of gas bubbles resulting in a plateau) is a measure of the concentration of the catalyst. The temperature of the reaction solution should increase continuously because of the continuously produced heat of reaction; however, when the cuvette was deliberately poorly insulated, the temperature also reached a level (stationary state) depending on the concentration of catalyst. Figure 5 shows the standard curves, and Table 2 some results of determinations.

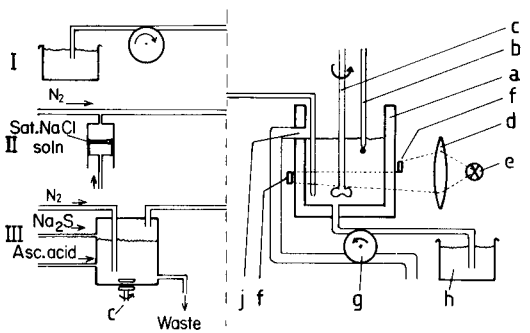

Fig. 3. Apparatus for flow methods. (a) Cuvette; (b) thermistor; (c) stirrer; (d) lens; (e) low-voltage lamp; (f) photoelements (Siemens BPY 11/II); (g) pump; (h) iodine—azide solution; (j) overflow. Methods of sample addition: (I) solution; (II) gas; (III) gas from generating cell.

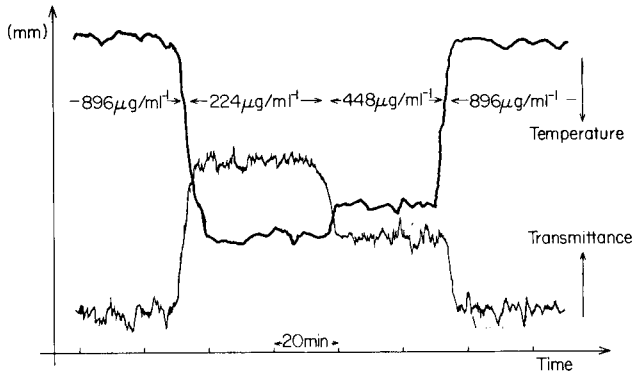

Fig. 4. Recorded curves for the determination of thiosulphate.

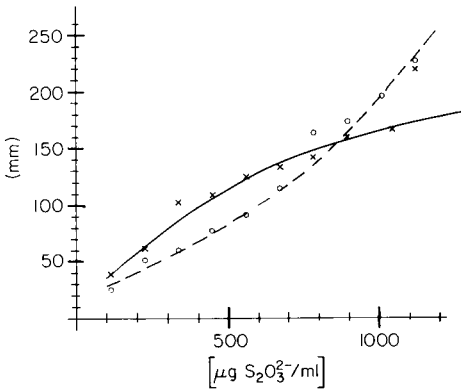

Fig. 5. Standard graphs for the determination of thiosulphate.

TABLE 2

Determination of thiosulphate in the flow system (all results are given as μg $S_2O_3^{2-}$ ml^{-1})

Taken	112	224	224	448	448	560	672	840	840	1064
Found										
(thermometric)	134	269	269	381	571	493	717	829	918	829
(optical)	112	213	280	426	470	493	739	795	952	1053

Determination of gaseous samples

A gaseous sample of a catalyst can be measured directly with the same measuring system. To simulate gaseous samples in various hydrogen sulphide concentrations, definite dilutions of hydrogen sulphide in nitrogen were introduced into a constant stream (the manometer used is not shown in Fig. 3) of nitrogen carrier gas (Fig. 3, II) with a motor-driven syringe burette

(with saturated sodium chloride solution as sealing liquid). The concentrations of hydrogen sulphide in the gas stream finally entering the cuvette were in the range 5—100 ppm. The bubbles caused by the nitrogen carrier gas were of large diameter and so did not affect the optical method of indication. Both recorded plots again reached plateaux which could be evaluated. The standard graphs for the range of 5—100 ppm H_2S in the carrier gas were similar to those shown in Fig. 5. Table 3 gives the results of some determinations.

As an interesting practical example, the growth of a culture of bacteria was observed with this measuring system. Under anaerobic conditions the bacterial strain *Escherichia coli* produces hydrogen sulphide from cysteine. When the hydrogen sulphide in the head space was transported to the cuvette by a constant stream of nitrogen for measurement, the amount of hydrogen sulphide produced per unit time gave a measure of the bacterial activity. The dependence of the H_2S production on the temperature has been followed. In principle, it should be possible to observe similarly the variation of the activity of *E. coli* with other parameters such as concentration of inhibitors.

Determination of hydrogen sulphide from sodium sulphide via a generating cell

Hydrogen sulphide can be liberated from a sample solution containing sodiur sulphide with ascorbic acid (15%); other acid-soluble sulphides would react similarly.

The hydrogen sulphide was liberated continuously from a flowing stream of the sodium sulphide solution in the apparatus shown in Fig. 3 (III), and then transported continuously to the measuring cuvette by a nitrogen carrier stream. It was shown that about 80% of the sulphide present in the sample solution left the cell as hydrogen sulphide.

The measuring system and the evaluation of the optical and thermometric traces were identical to those described above. The sample solution (2.25 ml min^{-1}) and the ascorbic acid solution (15%; 2.25 ml min^{-1}) were pumped continuously into the generating cell by a peristaltic pump; the level in the cell was kept constant by pumping off 4.5 ml of the solutions per minute. Nitrogen carrier gas (65 ml min^{-1}) was blown through the head space of the generating cell. For the calibration curves, the sodium sulphide solutions used contained 0.1—10 $\mu g\ S^{2-}\ ml^{-1}$.

The results of the determination of some unknown sulphide samples are given in Table 4.

TABLE 3

Determination of hydrogen sulphide in the flow system (All results are given as ppm; 1 ppm = 1 $\mu l\ H_2S\ l^{-1}$ of nitrogen)

Taken	14	16	28	30	40	40	40	50	60	85
Found										
(thermometric)	20	25	36	36	40	43	44	50	56	100
(optical)	16	17	30	31	36	32	38	45	55	100

TABLE 4

Determination of hydrogen sulphide from sodium sulphide with the generating cell (All results are given as $\mu g\ S^{-2}\ ml^{-1}$)

Taken	0.19	0.40	0.92	1.14	1.56	1.75	2.19	3.20	6.90	9.21
Found										
(thermometric)	0.27	0.23	0.89	0.92	1.30	1.83	3.28	3.62	7.30	9.60
(optical)	0.13	0.42	1.14	1.16	1.76	1.92	1.72	2.86	7.30	9.31

REFERENCES

1 H. Weisz and W. Meiners, Anal. Chim. Acta, 90 (1977) 71.
2 F. Feigl, Fresenius Z. Anal. Chem., 74 (1928) 369.
3 E. Friedmann, J. Prakt. Chem., 146 (1936) 179.
4 H. Weisz and H. Ludwig, Anal. Chim. Acta, 60 (1972) 385.

.nalytica Chimica Acta, 107 (1979) 309—317
' Elsevier Scientific Publishing Company, Amsterdam — Printed in The Netherlands

1ERGING ZONES IN FLOW INJECTION ANALYSIS
'art 3. Spectrophotometric Determination of Aluminium in Plant and Soil 1aterials with Sequential Addition of Pulsed Reagents

:. F. REIS, H. BERGAMIN F?*, E. A. G. ZAGATTO and F. J. KRUG

'entro de Energia Nuclear na Agricultura, CEP 13400 Piracicaba, Sao Paulo (Brazil)

Received 2nd January 1979)

UMMARY

A flow injection procedure is described for the spectrophotometric determination of luminium in plant and soil material with eriochrome cyanine R. This system utilizes ıerging zones and sequential addition of pulsed reagents. A high degree of sample dispersion nd pulsed neutralization reagent allow precise pH control; acid plant digests can therefore e analysed without pre-treatment. Iron(III) interference is avoided with ascorbic acid, and phosphate interference is negligible. The sampling rate is 120 samples per hour, reproducibility is better than 1% for a 5.0-ppm Al standard, and the calibration plot is linear in the range 0—20 ppm Al. Applied to soil and plant samples, the method gives recoveries of 98—101%.

Flow injection analysis, devised by Růžička and Hansen [1] has undergone fast development, as indicated in comprehensive reviews [2, 3]. Recently, the original idea of flow injection analysis was expanded with the concept of merging zones [4, 5], based on synchronized injection of sample and reagent into inert carrier streams, with further merging and reaction of the injected species. The reagent is, therefore, consumed only when the sample is present and is otherwise continuously recovered. Previous papers of this series have emphasized the low consumption of ascorbic acid in the spectrophotometric determination of phosphate [4], and of lanthanum in the atomic absorption spectrometry of calcium and magnesium [5].

A logical evolution of this concept is to utilize merging zones for the sequential addition of analytical reagents. This idea was adopted here in a flow injection procedure for the spectrophotometric determination of aluminium. The method should be valuable in agricultural laboratories where the number of plant and soil samples to be analysed for aluminium is high, because of the importance of this element in soil chemistry and plant nutrition.

Of the analytical reagents available for the colorimetric determination of aluminium, eriochrome cyanine R and aluminon are most frequently employed [6, 7]. The method based on eriochrome cyanine R, despite its rigid pH control requirement, is less affected by temperature changes, does not require a colloid stabilizer [8] and was therefore adapted by Reis [9] to a flow injection procedure.

The aim of the work described here was to investigate the possibility of sequential addition of pulsed reagents via merging zones, and to improve the flow injection procedure for the spectrophotometric determination of aluminium in plant digests and soil extracts. The merging zones allow reduced reagent consumption, and provide an initial neutralization of the injected digests, avoiding the pH adjustment of the samples prior to analysis.

Preliminary considerations

Eriochrome cyanine R reacts with aluminium ions under acidic conditions (pH ca. 3) producing a red complex which is measured at 535 nm [10]. The unreacted cyanine, however, absorbs strongly, the absorbance being highly dependent on pH [6, 8]. At pH 6.0, the molar absorptivity of the cyanine is less affected by pH changes [6]; this pH value is therefore usually recommende for the development of the aluminium complex [6, 8, 11].

For the analysis of plant digests, adjustment to pH 3 is normally done before analysis [6]. This makes the final pH control easier, and can be achieved in a flow injection system by introducing the sample into an inert acid carrier stream and merging later with a sodium hydroxide stream [9]. Similar procedures have been used in earlier systems [12, 13].

In the present method, sodium hydroxide solution and sample are injected simultaneously and interact after merging of the injected zones. Ascorbic acid, used to mask iron(III), is also injected together with the sample but merging occurs downstream. The effects of changes in refractive index, which could be caused by interaction of the injected zones, are negligible because the system is characterized by a high degree of dispersion. The addition of buffer and eriochrome cyanine R via merging zones is not feasible because of refractive ("schlieren pattern") and colour effects [14, 15]. The consumption of both sodium hydroxide and perchloric acid is low, and the total ionic strength is reduced by using merging zones; decreasing the ionic strength increases the signal intensity [9].

EXPERIMENTAL

Apparatus

The manifold (Fig. 1) was made from polyethylene tubing (i.d. 0.86 mm) supported by suitable Lego blocks. All connectors were made from perspex. Details of the system construction have been given elsewhere [14, 16]. Coil lengths and pumping rates were chosen in order to achieve a high degree of sample dispersion, associated with a reasonable sampling rate. The streams were pumped at similar rates because, if the hydrodynamic pressures are similar in all confluent streams, the mixing conditions are better and the precision is improved. Synchronization of the injected zones is also easier if the linear speeds of the merging zones are similar.

A Technicon AAII peristaltic pump furnished with suitable tygon pumping tubes was employed.

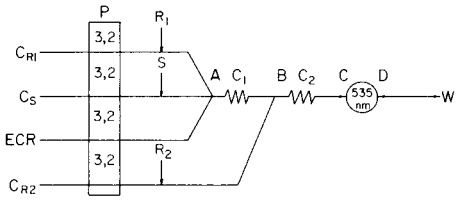

Fig. 1. Flow diagram of the proposed system. ECR is the colour reagent, P is the peristaltic pump; pumping rates are given in ml min^{-1}. The injected volumes are 20 μl for S (sample) and R_1 (0.25 M NaOH) and 50 μl for R_2 (masking agent). C_1 and C_2 are 40 cm and 200 cm long, respectively. The optical cell is between points C and D. For further explanations, see text.

Samples and reagents were introduced into the system by a multiple proportional injector made of perspex (Fig. 2) which is a development of the proportional injectors described earlier [4, 17]. In the loading position (Fig. 2A), the sample (S) is aspirated to fill the sample loop (L_S), which defines exactly the injected sample volume, the excess of sample going to waste (W). Simultaneously, the reagents R_1 and R_2 are pumped to fill the reagent loops (L_{R1} and L_{R2}) and their excesses, slightly diluted by the corresponding reagent carrier streams, are accumulated in the reagent recovery vessels (V_1 and V_2). In this position, the sample and reagent carrier streams (C_S, C_{R1} and C_{R2}) are pumped continuously to keep the system running. In the injection position (Fig. 2B), the selected volumes of sample and reagents are pushed by the corresponding carrier streams and the pumped reagents are directed back to the reagent reservoirs.

The Beckman model 25 spectrophotometer used was connected to a Beckman model 25 ACC recorder and furnished with a Hellma type 178 flow-cell (light path 10 mm, volume 80 μl). The dual-beam mode was used, and an aliquot of the stream going to waste (Fig. 1) was collected before running analysis, to serve as a blank. The coloured complex was measured at 535 nm.

The model 63 pH meter was connected to a Servograph REC 61 with a

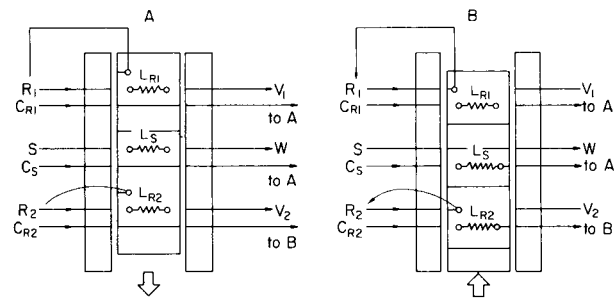

Fig. 2. Schematic representation of the proportional injector in the loading (A) and injection (B) positions. The symbols are explained in the text. Points A and B refer to Fig. 1.

REA 112 high-sensitivity unit (Radiometer, Copenhagen). For continuous potentiometric measurements, the assembly described earlier [18] was used. Dispersion factors were measured with a nitrate-selective electrode [19] and pH values with a flat glass electrode (Radiometer). A K401 saturated calomel reference electrode (Radiometer) was employed.

Samples and standards

Plant materials were mineralized by wet digestion with nitric and perchloric acids on a Technicon BD 40 digestion block [14]. Soil extracts were obtained with 1 M KCl solution, by a standard procedure [11].

Working standards in the range 0—20 ppm Al were prepared weekly by appropriate dilution of a 500-ppm aluminium stock solution, which was made by dissolving 8.752 g of $KAl(SO_4)_2 \cdot 12H_2O$ in 1 l of a 10^{-3} M HCl solution. For plant analysis, the working standards were made 0.25 M in perchloric acid.

Reagents

All reagents were of analytical grade and distilled water was employed throughout. Both sodium hydroxide and perchloric acid were standardized before use.

The eriochrome cyanine R stock solution, which was stable for several months, was prepared by dissolving 3.0 g of the dye in about 800 ml of water, adjusting to pH 3.0 with hydrochloric acid and diluting to 1 l with water. Before use, an appropriate volume of this reagent was diluted (1 + 9) with water.

The acetate carrier solution was prepared by dissolving 308 g of ammonium acetate in 1 l of water and adding enough 6 M acetic acid or ammonia solution to attain pH 6.0 at point D (Fig. 1).

For the masking solution, 5 g of ascorbic acid was dissolved in 100 ml of the above ammonium acetate solution [9]. The acetate is necessary to avoid pH gradients after injection, which would create a blank signal.

Analytical procedure

The flow diagram for the determination of aluminium in plant digests and soil extracts is shown in Fig. 1. The sample (S) is injected simultaneously with both reagent R_1 (0.25 M sodium hydroxide for plant analysis, or water for soil analysis) and reagent R_2 (masking solution). The corresponding carrier streams are water (C_{R_1} and C_S) and ammonium acetate solution (C_{R_2}). At point A, the sample zone neutralized by the sodium hydroxide, if necessary, meets the eriochrome cyanine R stream. The reaction develops in the reaction coil (C_1) under the recommended acidic conditions [6], determined by the acidity of the colour reagent. At point B, the zone of ascorbic acid meets the sample zone in a synchronized manner as indicated in Fig. 3. In the following coil (C_2, Fig. 1), iron(III) is reduced and the sample zone is buffered to pH 6.0. As the sample zone reaches the flow-cell, the absorbance of the complex is measured at 535 nm and recorded.

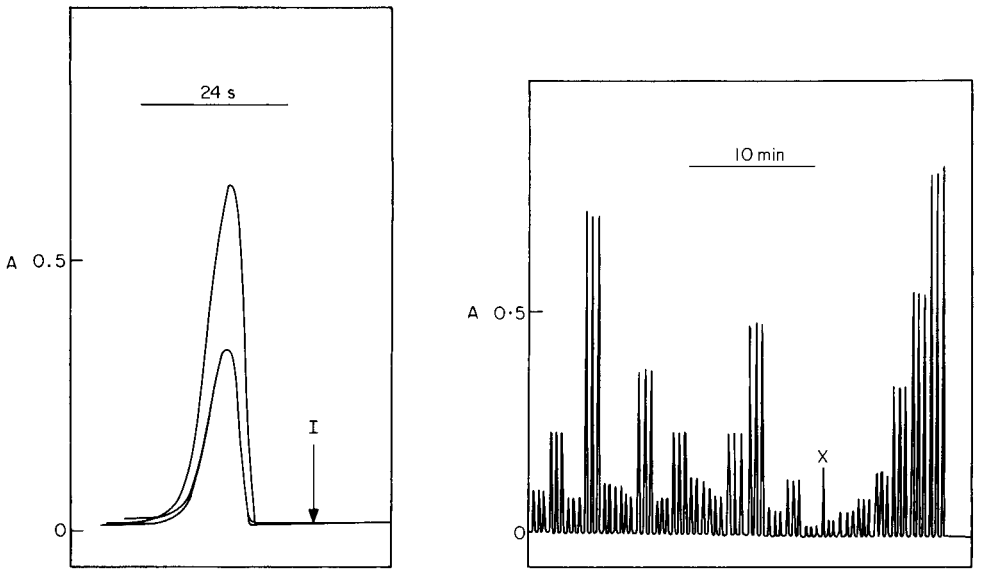

Fig. 3. Recorded peak profiles obtained with a 1% eriochrome cyanine R solution simulating the three merging zones, injected at I. The higher peak corresponds to the masking solution and the others to the sample and neutralization reagent (0.25 M NaOH).

Fig. 4. Routine analysis of digested plant samples, at an average sampling rate of 120 injections per hour. From left to right, 15 samples injected in triplicate and a calibration graph with Al standards (15—10—5—3—2—1—0.5—0 ppm Al). The peak marked X was caused by an air bubble in the flow system, easily distinguished by a very abrupt increase in absorbance.

Measurement of dispersion

Dispersion of the sample was evaluated by replacing all carrier solutions of the system (Fig. 1) by 0.01 M sodium tetraborate in 0.01 M sodium hydroxide solution [20]. The potentiometric assembly for nitrate [18] was set at point C and later, at point D. For each point, a series of sodium nitrate standards in the range 0.0001—0.05 M (also containing 0.01 M sodium tetraborate) was used for calibration. The dispersion factors were evaluated from the results obtained with the 0.0001 M nitrate standard, which was measured in two ways by the methodology described earlier [2, 12].

RESULTS AND DISCUSSION

Sample acidity and dispersion

The acidity of the sample is an especially important factor when the absorbance of the reagent is high and strongly dependent on pH. The acidity of 27 plant digests (*Coffea arabica* L., *Citrus* spp., *Sorghum* spp., *Saccharum officinarum* L. and *Phaseolus vulgaris* L.) was measured by titration with

sodium hydroxide to pH 7, showing an average value of 0.236 M ± 0.39 M related to perchloric acid. Therefore, 0.25 M sodium hydroxide was chosen as the neutralization reagent; this value is slightly higher than the mean sample acidity because, with the buffering system utilized, alkaline deviations are more readily minimized than acidic errors in the final stream.

Because of the very variable acidity of the samples, and the unfavourable characteristics of the colour reagent with respect to pH, a high degree of sample dispersion is necessary. The dispersion factors measured at points C and D (Fig. 1) were 0.013 and 0.012, respectively. The small difference in the degree of sample dispersion between points C and D indicates that the flow-cell dead volume has little influence when the degree of dispersion is high.

This high degree of sample dispersion was chosen after consideration of several points. Firstly, pH control is easier at high dispersions, because the variability of the sample acidity diminishes with increasing degree of dispersion. Secondly, the method is sensitive enough for soil and plant analysis, even with the sample dispersion used. Thirdly, the refractive index effect [14, 15] decreases with increasing degree of dispersion. Finally, the high dispersion of the sample zone permits easier control of interfering chemical species.

Colour reagent

The addition of the colour reagent to the sample via merging zones was not feasible because the blank value would be too high and dependent on pH. The peak profiles of Fig. 3 obtained with pulsed colour reagent give an idea of the magnitude of this blank. In cases where the colour reagent is strongly coloured, its addition to the sample zone must be through a confluence configuration [15].

The concentration of the eriochrome cyanine R solution was selected to provide good linearity of the calibration plot up to 20 ppm Al. Under the recommend conditions, the range of absorbance was 0.026—1.013 for 0—20 ppm Al, and the average error (related to 3 measurements at each of 9 points on the scale) was 0.002 absorbance units. Higher reagent concentrations were not employed because of the blank problem. As baseline drifts (caused by irregular pumping, commutation of the injector and pH-gradients in the sample zone) are proportiona to the blank absorbance, the use of a less concentrated reagent results in a more stable system.

Blank value

The blank value (Table 1, Fig. 4) is caused mainly by the injector. During its commutation, the carrier streams are suddenly blocked. At this moment, the relative contribution of the colour reagent at point A (Fig. 1) increases, giving a transient signal in the detector and thus causing the blank value. As this signal reflects an instantaneous increase in the reagent concentration, the blank is pH dependent (Table 1). This signal would probably be suppressed if a 4-stage injector were available. In this case, the colour reagent could pass

through the injector and, during commutation, all four streams would be equally blocked. Alternatively, an injector furnished with bypass could be employed [2].

Interferences

The major interferences in this method are pH, iron(III) and phosphate. Table 1 indicates the influence of the sample acidity on the recorded signal. Although the acidity range is large, and the reagent absorption is pH dependent, the pH effect seems to have been largely overcome; the standard deviation of the data corresponding to 5 ppm aluminium is only 1.21%. In preliminary tests, pH variations from 5.90 to 6.08 caused changes in the readings from 0.472 to 0.488 absorbance units in the final stream. The influence of sample acidity is reflected in the blank signal and not in the signal proportional to the aluminium content [10]; thus suppression of the blank signal (see above) minimizes this variation. Methods for aluminium analysis usually have a precision in the order of 0.5 ppm Al [6].

Table 2 indicates the influence of iron(III) and phosphate. Even when the iron(III) concentration is 40 ppm, its interference is not significant. It should be stressed that plant digests and soil KCl extracts do not generally contain

TABLE 1

Influence of acidity on the absorbances related to a 5-ppm Al standard and to the blank value (data obtained from 5 repeated runs)

Acidity[a]	5 ppm Al	Blank
0.15	0.246 ± 0.001	0.027 ± 0.001
0.20	0.247 ± 0.001	0.026 ± 0.002
0.25	0.250 ± 0.002	0.027 ± 0.002
0.30	0.251 ± 0.001	0.035 ± 0.002
0.35	0.254 ± 0.003	0.037 ± 0.001
0.40	0.252 ± 0.002	0.042 ± 0.002

[a]Expressed as molarity of $HClO_4$.

TABLE 2

Influence of iron(III) and phosphate on the determination of a 5-ppm Al standard in 0.25 M perchloric acid (data obtained from 5 runs at each level)

Iron(III) (ppm)	Absorbance	Phosphate (ppm)	Absorbance
0	0.252 ± 0.003	0	0.254 ± 0.002
5	0.245 ± 0.001	50	0.247 ± 0.001
10	0.252 ± 0.003	75	0.245 ± 0.002
20	0.253 ± 0.004	100	0.242 ± 0.003
30	0.266 ± 0.005	150	0.238 ± 0.002
40	0.261 ± 0.003	200	0.234 ± 0.001

TABLE 3

Recovery data related to soil extracts and plant digests. One standard addition was made and the measurement was performed in triplicate

Plant digests[a]			Soil extracts[a]		
Al measured (ppm)	Recovery (%)		Al measured (ppm)	Recovery (%)	
	A	B		C	D
1.40	95.0	97.8	12.07	97.0	98.0
1.45	95.8	99.8	7.65	99.2	98.5
2.20	105.9	104.6	2.80	104.6	98.2
1.35	94.5	98.3	5.75	103.5	99.0
1.40	97.0	102.8	2.90	98.5	97.2
1.65	100.3	97.5	7.80	103.0	97.0
2.40	94.3	97.8	4.70	102.2	98.8
2.85	95.8	98.6	2.80	99.8	95.5
1.92	95.4	107.9	2.95	96.3	98.5
1.72	100.0	100.7	8.57	101.5	96.8
5.60	101.4	99.0	12.12	100.7	98.9
2.10	100.0	105.2	12.50	104.0	101.5
Mean	97.95	100.83		100.86	98.16
R.s.d.	3.56	3.47		2.74	1.48

[a]A, after addition of 96 μg Al/20 ml digest. B, after addition of 175 μg Al/20 ml digest. C, after addition of 125 μg Al/20 ml extract. D, after addition of 275 μg Al/20 ml extract.

so much iron(III). The method is little affected by phosphate, probably because of the high degree of sample dispersion. For samples with high phosphate contents, the addition of phosphate to the standards is recommended.

Analytical results

The proposed method can be used for the determination of aluminium in plant digests and soil extracts in the range 0—20 ppm Al, at a typical sampling rate of 120 samples per hour (see Fig. 4). The precision of the method is better than 1% for a sample containing about 5 ppm Al. Table 3 shows that the recoveries are good for soil and plant samples.

Partial support of this project by DANIDA (Project 104DAN 8/241) and by FINEP (Financiadora de Estudos e Projetos Brasil) is greatly appreciated. The authors thank P. B. Vose, J. X. Medeiros and M. Fernanda Giné for assistance in preparing the manuscript.

REFERENCES

1 J. Růžička and E. H. Hansen, Anal. Chim. Acta, 78 (1975) 145.
2 J. Růžička and E. H. Hansen, Anal. Chim. Acta, 99 (1978) 37.
3 D. Betteridge, Anal. Chem., 50 (1978) 832A.
4 H. Bergamini Fº, E. A. G. Zagatto, B. F. Reis and F. J. Krug, Anal. Chim. Acta, 101 (1978) 17.

5 E. A. G. Zagatto, F. J. Krug, H. Bergamin Fº, S. S. Jørgensen and B. F. Reis, Anal. Chim. Acta, 104 (1979) 279 (Part 2).
6 L. H. Jones and D. A. Thurman, Plant and Soil, 9 (1957) 131.
7 American Public Health Association, American Water Works Association and Water Pollution Control Federation, Standard Methods for the Examination of Water and Wastewater, 14th Edn., American Public Health Association, New York, 1975, p. 171.
8 W. K. Dougan and A. L. Wilson, Analyst, 99 (1974) 413.
9 B. F. Reis, Thesis, ESALQ-USP, Piracicaba, Sao Paulo, Brazil, 1978.
10 H. Thaler and F. H. Mühlberger, Fresenius Z. Anal. Chem., 144 (1954) 16.
11 E. D. McLean, in C. A. Black (Ed.), Methods of Soil Analysis, American Society of Agronomy, Madison, 1965, p. 978.
12 M. F. Giné, E. A. G. Zagatto and H. Bergamin Fº, Analyst, in press.
13 J. W. B. Stewart and J. Růžička, Anal. Chim. Acta, 82 (1976) 137.
14 F. J. Krug, H. Bergamin Fº, E. A. G. Zagatto and S. S. Jørgensen, Analyst, 102 (1977) 503.
15 H. Bergamin Fº, B. F. Reis and E. A. G. Zagatto, Anal. Chim. Acta, 97 (1978) 427.
16 J. Růžička and J. W. B. Stewart, Anal. Chim. Acta, 79 (1975) 79.
17 H. Bergamin Fº, J. X. Medeiros, B. F. Reis and E. A. G. Zagatto, Anal. Chim. Acta, 101 (1978) 9.
18 J. Růžička, E. H. Hansen and E. A. G. Zagatto, Anal. Chim. Acta, 88 (1977) 1.
19 H. J. Nielsen and E. H. Hansen, Anal. Chim. Acta, 85 (1976) 1.
20 E. H. Hansen, F. J. Krug, A. K. Ghose and J. Růžička, Analyst, 102 (1977) 714.

Analytica Chimica Acta, 107 (1979) 319—326

THE DETERMINATION OF SOME SELECTED PENICILLINS BY ENZYMATIC ENTHALPIMETRY

J. KEITH GRIME*

Department of Chemistry, University of Denver, University Park, Denver, CO 80208 (U.S.A.)

BARRIE TAN

Department of Chemistry, University of Otago, P.O. Box 56, Dunedin (New Zealand)

(Received 31st October 1978)

SUMMARY

An enzymatic, enthalpimetric procedure is described for the determination of penicillin G, ampicillin sodium or phenoxymethylpenicillin in pure and dosage forms. The technique employed allows up to 20 assays with the same reagent solution. Enthalpy assignments are presented along with error (range) and precision data. The lower limit of determination is about 10^{-3} mol dm^{-3}.

The most commonly quoted chemical methods of penicillin assay are those based on the procedure described by Alicino [1] in which unconsumed iodine is back-titrated after incubation with the hydrolyzed penicillin. Hydrolysis can be done either with alkali or with a β-lactamase enzyme, penicillinase (E. C. No. 3.5.2.6) [2]. This technique, although selective for the intact penicillin molecule, has limitations in that the stoichiometry may vary with experimental conditions [3] including time, pH and iodine reagent concentration [4]. Furthermore, the presence of unsaturated side-chains in the penicillin molecule interferes with iodine uptake, which makes careful blank titrations essential. Recently a direct titration procedure with potassium iodate has been reported for the determination of both penicillins [5] and cephalosporins [6]. This method is however not sensitive to hydrolysis. All redox procedures are also subject to the restriction that oxidizable excipients will cause interferences.

Enzymatic analysis provides a more selective assay. Completely enzymatic procedures, in which a physical property related to the progress of the penicillinase—catalyzed hydrolysis of penicillin is monitored, have been reported. To date, the instrumental approaches used to determine penicillin in this manner have included colorimetric [7], potentiometric pH-stat [8—11] and flow calorimetric techniques [12]. Comprehensive reviews of all chemical methods of penicillin assay have been reported elsewhere [13, 14].

The calorimetric/enthalpimetric approach to pharmaceutical analysis has the distinct advantage that a high level of non-reacting excipients can be

present without significantly affecting the precision or accuracy of the results [15]. The combination of enzymatic hydrolysis with enthalpimetric instrumentation therefore provides the basis for a realistic alternative method of assay. In the only calorimetric method so far reported with penicillinase [12], the thermistor was incorporated into a thermostatted microcolumn filled with the enzyme immobilized on alkylamino glass, and the temperature change was monitored as a penicillin solution was pumped through the system. Analytical results were obtained from calibration graphs constructed for penicillin standards. The obvious advantage of this technique is the repeated use of the enzyme.

In the present paper, a static enzymatic procedure is described for the enthalpimetric assay of some selected penicillins in pure and dosage forms. The method involves a sequential injection technique similar to that described for the enthalpimetric determination of glucose [16]. Enthalpy assignments are presented in addition to the sequential analysis of three penicillins—penicillin G, ampicillin sodium and penicillin VK—in tablet and powder form.

EXPERIMENTAL

Reagents

Pure salts of penicillin VK (phenoxymethylpenicillin potassium; Sigma Chemical Co.), and penicillin G (benzylpenicillin sodium; Sigma Chemical Co.) and standard ampicillin trihydrate (6[D(—) α-amino-phenylacetamido]-penicillanic acid; D.S.I.R., N.Z.) were used. The following pharmaceutical-grade compounds obtained in vials were used without further purification: cloxacillin (3-[2-chlorophenyl]-5-methylisoxazol-4-yl penicillin sodium monohydrate), carbenicillin sodium (α-carboxybenzyl penicillin disodium salt), methicillin sodium (sodium 6-[2, 6-dimethoxybenzamido] penicillinate monohydrate), ampicillin sodium, penicillin G, cephaloridine (7-[(2-thienyl) acetamido]-3-(1-pyridylmethyl)-3-cephem-4-carboxylic acid betaine, δ form) and cephalothin sodium (7-[2-thienylacetamido] cephalosporanic acid). Tablets of penicillin VK and cephalexin capsules (7-[D-α-aminophenylacetamido]-3-methyl-3-cephem-4-carboxylic acid, monohydrate) were obtained from Dunedin Hospital.

The buffer solution used in all enthalpimetric investigations consisted of 0.2 mol dm^{-3} Tris (tris(hydroxymethylamino)methane) and Tris hydrochloride adjusted to pH 7.5. Penicillinase from *Bacillus cereus* (β-lactamase 1, penicillin amido-β-lactamhydrolase, E.C. No. 3.5.2.6; nominal activity 2200 IU mg^{-1} protein) was obtained from Sigma. Stock enzyme solutions were prepared by quantitative dissolution of ca. 2.0—3.0 mg of penicillinase in 200 cm^3 of Tris buffer solution. The penicillinase reagent and dry enzyme were stored at 2°C. No detectable loss in penicillinase activity was observed over a period of at least 9 weeks. In the analysis of carbenicillin sodium, a three-fold more concentrated enzyme solution was employed.

Penicillin sample solutions were prepared by quantitative dissolution of

ca. 300 mg of the sample in 10.00 cm^3 of distilled water. Fresh solutions were prepared prior to each series of experiments. Penicillin VK (tablet form, nominal content 250 mg/tablet) solutions were prepared by dissolution of three crushed tablets in 25.00 cm^3 of distilled water.

Apparatus

The apparatus has already been described [17]. Temperature changes were monitored by measurement of the unbalance potential produced in a d.c. Wheatstone bridge circuit incorporating a 10,000 Ω thermistor as one arm of the bridge. A bridge current of 7.8×10^{-5} A was normally employed and the signal was recorded on a strip-chart potentiometric recorder. Accurate reagent injection was obtained by means of gravimetrically calibrated, precision syringes (0.500 cm^3) equipped with Chaney adaptors. Temperature mismatch between substrate and enzyme solutions was minimized by immersion of the quasi-adiabatic reaction cell and syringe in a water bath thermostatted at 25.0°C (short term stability ± 0.002°C). Calibration of enthalpograms in terms of heat output (J) can be achieved by the Joule heating of a carbon resistor in situ, immediately after the recording of the enzymatic reaction enthalpogram. To reduce analysis time, however, a heat capacity calibration curve was prepared by sequential injection of reagent blanks. These predetermined heat-capacity data (ca. 0.27% r.s.d.) were used in all subsequent measurements without any significant decrease in precision or accuracy.

Preliminary experiments

The optimum experimental conditions for enthalpimetric assay were established as follows.

Assignment of reaction enthalpies and selection of buffer. The temperature change observed in the enthalpimetric assay is that engendered by the combined enthalpies of (enzymatic) hydrolysis and protonation of penicillin and buffer, respectively. Accordingly, the choice of buffer is important: its function is not only to maintain an invariant pH, but also to increase the sensitivity of the technique by amplification of the heat effect. Tris buffer, with an enthalpy of protonation of 47.7 ± 0.4 kJ mol^{-1} [17], provides a more sensitive assay than other "biological" buffers [18]. In experiments to establish the total enthalpy change, it was observed that penicillin solutions in Tris buffer at pH 7.5 underwent non-enzymatic hydrolysis during storage and thermal equilibration periods; this hydrolysis was not significant, however, during the actual measurement period. A stability study in the pH range 5.9—9.0 showed that solution stability increased with decreasing pH, but non-enzymatic hydrolysis was minimal (within experimental time limits) in aqueous penicillin solutions at their natural pH of ca. 6.6. Accordingly, unbuffered penicillin solutions, prepared immediately before use, were used.

On the basis of these results, the following sequential injection procedure was adopted for ΔH determinations; an aliquot of aqueous penicillin standard (ca. 0.5 cm^3) was injected into 10.00 cm^3 of buffered (Tris, pH 7.5) penicilli-

nase solution containing ca. 200 IU of enzyme, both solutions having been equilibrated at 25.00 ± 0.01°C. The reaction enthalpy was then calculated from the resultant calibrated enthalpogram in the usual manner. The results are presented in Table 1. Because of the limited solubility of the ampicillin trihydrate standards, sequential injection was not possible with this compound In this case, the standard was weighed directly into the reaction cell and dissolved in 10.00 cm^3 of distilled water. A concentrated penicillinase solution was then injected into the ampicillin solution and the enthalpogram recorded as before. This technique precludes the addition of buffer, because the concentration necessary in a 0.5-cm^3 injection results in error propagation from the resultant heat of dilution. The sequential addition procedure in buffered solution was, however, used for the assay of the more soluble ampicillin sodium compound. Consequently, the overall reaction enthalpy for the buffered hydrolysis of ampicillin is shown in Table 1.

pH—activity profile. A pH profile of penicillinase activity, with penicillin G as substrate, was constructed, based on enthalpimetric measurements of initial rates in a series of sulphonic acid buffers with known enthalpies of protonation [18] (Fig. 1). The profile reveals an activity maximum at ca. pH 7.0, i.e. outside the effective buffer capacity of Tris. In view of the amplification effect of Tris protonation, however, all measurements were made at pH 7.5 where penicillinase activity is still relatively large.

The above experiments produced a set of experimental conditions that allowed the enthalpimetric assay of penicillin G, ampicillin, phenoxymethylpenicillin and carbenicillin.

Recommended procedure

Buffered penicillinase solution (10.00 cm^3) containing ca. 200 IU of enzyme is introduced into the quasi-adiabatic reaction cell. The syringe is loaded with sample solution and the tip of the delivery tube is inserted just below the surface of the enzyme solution. The syringe and cell assembly are then lowered into a water-bath thermostatted at 25.0°C, the stirring mechanism is activated and the system is allowed to come to thermal equilibrium. This operation is facilitated by intermittent activation of the heating circuitry On the attainment of equilibrium, as evidenced by an isothermal baseline, the

TABLE 1

Assignment of overall reaction enthalpy for the concurrent reactions: penicillin + H_2O $\xrightarrow{\text{penicillinase}}$ penicilloic acid, and Tris NH_2 + H_3O^+ → Tris NH_3^+ + H_2O

Compound	ΔH/kJ mol^{-1}	No. of expts.
Penicillin G	114.7 ± 0.6	10
Ampicillin sodium	125.8 ± 1.2	8
Phenoxymethylpenicillin (Penicillin VK)	120.5 ± 1.3	10

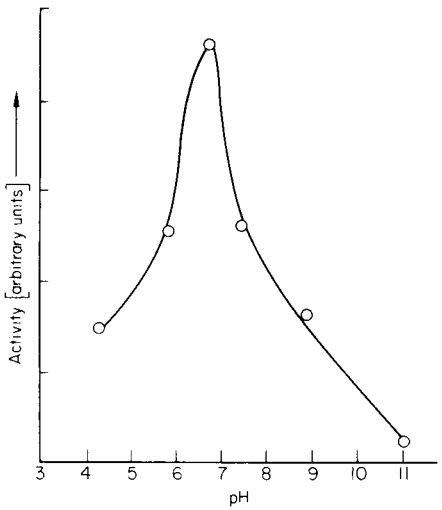

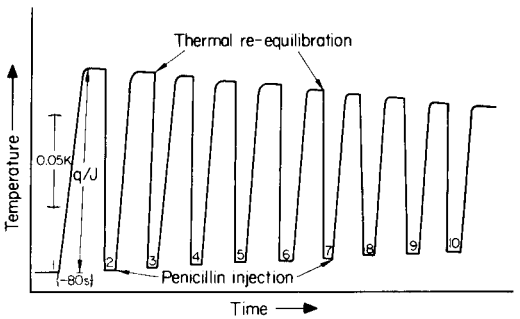

Fig. 1. pH profile for the penicillinase-catalyzed hydrolysis of penicillin G.

Fig. 2. Typical series of sequential enthalpograms.

sample is injected into the enzyme solution and the resultant temperature change is monitored. Under the conditions described, the duration of the enzymatic reaction is typically 80 s. After the reaction has ceased, as indicated by a post-reaction baseline, the cell and its contents are raised from the water-bath and allowed to cool. The syringe is reloaded and the entire assembly returned to the water-bath. This sequential injection procedure can be repeated 10 times with the same enzyme solution during a period of ca. 2 h (see below).

The same procedure, involving the injection of a slurry of active ingredient and tablet excipients, was adopted for the assay of phenoxymethylpenicillin tablets (see below).

RESULTS AND DISCUSSION

A typical series of 10 sequential enthalpograms for penicillin G is represented in Fig. 2. The low value of K_M ($50—100 \times 10^{-6}$ mol dm^{-3} [19]) for the penicillinase/penicillin system results in well-defined enthalpograms and correspondingly precise data. The absence of inhibition by the products [20] is apparent from the lack of curvature in the enthalpograms even after 10 experiments. The limits of enzyme re-use are defined, at least in part, by the sensitivity required, because heat capacity considerations mean that the initial signal is progressively attenuated by sequential additions of sample. At low penicillin concentrations, the number of sequential additions will be reduced. However, because of the relatively large heat effects involved, up to 20 determinations were possible in the same enzyme solution with reasonable precision and accuracy, under the experimental conditions used here.

Analytical data, representing 60 assays each of penicillin G and ampicillin sodium from vials and phenoxymethylpenicillin in tablet form, are presented in Table 2. The average recovery figures of 100.7%, 89.3% and 104.7%, respectively, compare favourably with the recommended ranges [21].

The day-to-day precision of the technique is illustrated in Fig. 3, which shows the reproducibility of the signal (ΔT) for penicillin aliquots assayed at intervals of one day from freshly prepared solutions. The signals shown in curve 2 are necessarily attenuated by the concomitant increase in heat capacity.

To investigate the scope of the technique, the relative rates of hydrolysis (with respect to penicillin G) of a series of antibiotics which are "resistant" and "non-resistant" to penicillinase hydrolysis were studied. The compounds examined were ampicillin, phenoxymethylpenicillin, carbenicillin, cloxacillin, methicillin, cephaloridine, cephalexin and cephalothin. Initial rate measure-

TABLE 2

Error (range) and precision (r.s.d.) data
(Each series number represents the results of 10 sequential analyses on aliquots of a penicillin sample solution.)

Series No.	1	2	3	4	5	6
Penicillin G (vial)						
Mass taken (mg)	18.58	15.07	15.54	15.44	15.14	15.00
Av. mass found (mg)	18.36	15.22	15.58	15.62	15.40	15.22
Range found (mg)	17.81—18.69	14.82—15.54	15.38—15.80	15.50—16.01	15.55—15.84	15.07—15.71
R.s.d. (%)	1.50	1.33	0.79	1.14	0.59	1.30
Ampicillin sodium (vial)						
Mass taken (mg)	15.02	15.08	15.06	15.13	15.07	15.03
Av. mass found (mg)	13.30	13.23	13.10	13.75	13.68	13.54
Range found (mg)	13.03—13.62	13.00—13.61	13.00—13.27	13.61—13.88	13.43—13.86	13.23—13.72
R.s.d. (%)	1.49	1.52	0.65	0.69	1.13	1.39
Phenoxymethyl penicillin (tablets)						
Nominal mass taken (mg)	15.00	15.00	15.00	15.00	15.00	15.00
Av. mass found (mg)	15.67	15.74	15.19	16.31	15.60	15.90
Range found (mg)	15.05—16.33	14.98—16.60	14.73—16.36	15.23—16.65	14.92—16.59	14.69—16.55
R.s.d. (%)	3.42	3.81	3.99	2.63	4.25	4.00

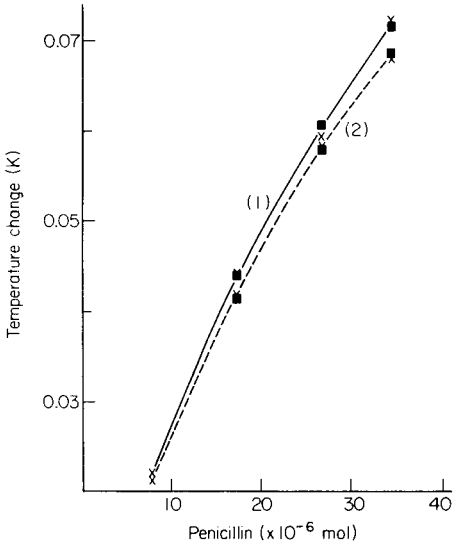

Fig. 3. Reproducibility of sequential assays on different days. Curves 1 and 2 show the results for two series of sequential injections on each day. Results obtained on different days are indicated by X and ■.

ments [22] showed that, of the "resistant" penicillins, only carbenicillin hydrolyses at a rate large enough to be of analytical potential (Table 3). It is possible therefore to determine carbenicillin, although an increased penicillinase concentration is required. In the absence of a carbenicillin standard, detailed analytical results are not presented for this compound. However, a series of 20 assays showed a relative standard deviation of 1.5%.

The injection of a slurry in the assay of phenoxymethylpenicillin tablets, with the resultant decrease in precision (Table 2), is necessary to maintain a sequential technique. More precise, although more time-consuming, assays were achieved by dissolving crushed tablets in the reaction cell and then injecting penicillinase solution (1.8% r.s.d., 9 experiments).

TABLE 3

Relative rates of penicillinase-catalysed hydrolysis with respect to the rate for penicillin G

Substrate	Relative rate of hydrolysis (%)
Penicillin G	100
Phenoxymethylpenicillin	120
Ampicillin	107
Carbenicillin	24
Cloxacillin, methicillin, cephaloridine, cephalexin, cephalothin	<3.0

Sequential assays of ampicillin trihydrate capsules, syrup and procaine penicillin were not successful because of the limited solubility of these preparations.

Conclusion

The enthalpimetric technique described represents a realistic alternative method of penicillin assay. The utilization of an enzymatic reaction introduces a degree of selectivity, whilst allowing an efficient sequential procedure. The sequential technique, although slightly less sensitive than the flow method [12] (lower limit 1×10^{-3} mol dm^{-3}; cf. 0.25×10^{-3} mol dm^{-3}), possesses the main advantage of a flow technique, i.e. a re-usable reagent, without entering into immobilization technology. Indeed, some of the rigid experimental constraints inherent in flow techniques such as precise control of flow rates and thermistor placement, are avoided. Moreover, once an enthalpy assignment has been made by using a pure sample, calibration standards are not required. However, if a calibration procedure is required for automation of "on-line" batch assay, the instrumentation will adapt easily to this mode of operation.

One of us (B.T.) thanks the University of Otago for the provision of a Senior Demonstratorship during this period of research.

REFERENCES

1 J. F. Alicino, Ind. Chem. Eng., Anal. Ed., 18 (1946) 619.
2 M. R. Pollock, J. Gen. Microbiol., 1 (1961) 239.
3 J. M. T. Hamilton-Miller, J. T. Smith and R. Knox, J. Pharm. Pharmacol., 15 (1963) 81.
4 K. Ilver, O. I. Johansen and F. Reimers, Acta Pharm. Int., 1 (1950) 225.
5 J. K. Grime and B. Tan, Anal. Chim. Acta, 105 (1979) 361.
6 J. K. Grime and B. Tan, Anal. Chim. Acta, 105 (1979) 369.
7 W. E. Hornby, J. Campbell, D. J. Inman and D. L. Morris, in E. K. Pye and L. B. Wingard (Eds.), Enzyme Engineering, Plenum, New York, 2 (1974) 401.
8 H. Nilsson, A. C. Akerlund and K. Mosbach, Biochim. Biophys. Acta, 320 (1973) 529.
9 G. J. Papariello, A. K. Mukherji and C. M. Shearer, Anal. Chem., 45 (1973) 790.
10 L. F. Cullen, J. F. Rusling, A. Schleifer and G. J. Papariello, Anal. Chem., 46 (1974) 1955.
11 R. E. Adams, S. R. Betso and P. W. Carr, Anal. Chem., 48 (1976) 1989.
12 K. Mosbach, B. Danielsson, A. Borgerud and M. Scott, Biochim. Biophys. Acta, 403 (1975) 256.
13 D. W. Hughes, A. Vilim and W. L. Wilson, Can. J. Pharm. Sci., 11 (1976) 97.
14 J. E. Fairbrother, Pharm. J., 218 (1977) 509.
15 L. S. Bark and J. K. Grime, Anal. Chim. Acta, 64 (1973) 276.
16 C. D. McGlothlin and J. Jordan, Clin. Chem., 21 (1975) 741.
17 J. K. Grime, K. Lockhart and B. Tan, Anal. Chim. Acta, 91 (1977) 243.
18 C. D. McGlothlin and J. Jordan, Anal. Lett., 9 (1976) 245.
19 D. R. Thatcher, in J. H. Hush (Ed.), Methods in Enzymology, Academic Press, New York 1974, Vol. 43, pp. 640—687.
20 M. R. Pollock, in P. D. Boyer (Ed.), The Enzymes, Vol. 4A, 2nd end., Academic Press, New York, 1960, p. 272.
21 British Pharmacopoeia, H.M.S.O., 1973.
22 J. K. Grime and K. R. Lockhart, Anal. Chim. Acta, in press.

Analytica Chimica Acta, 107 (1979) 327—334

THE CHARACTERIZATION OF CLOSELY RELATED POLYMERIC MATERIALS BY THERMOGRAVIMETRY—MASS SPECTROMETRY

K. W. SMALLDON, R. E. ARDREY* and L. R. MULLINGS**

Home Office Central Research Establishment, Aldermaston, Reading, Berks. RG7 4PN (Gt. Britain)

(Received 15th November 1978)

SUMMARY

The potential of a new technique in forensic science, thermogravimetry—mass spectrometry, is illustrated by its application to the examination of acrylic fibres and white alkyd gloss paints, small samples of which are difficult to differentiate even by a combination of current techniques. A simple interface allowing the coupling of a magnetic sector mass spectrometer to a thermobalance is described. This combination allows up to five experimental parameters to be determined simultaneously either for classification of the material under investigation or for the detailed direct comparison of samples. The thermobalance allows the temperatures at which weight losses occur and their relative proportions to be determined; the basic parameter obtained from the mass spectrometer is the total ion current trace. From this, single qualitative mass spectra may be chosen for examination and ions, whose presence or absence may be diagnostic or which vary characteristically throughout the analysis, can be selected. The variations of these ions may then be examined by computer-generated mass thermograms (analagous to mass chromatograms in g.c.—m.s.) or, if computer facilities are not available, by multiple ion detection. The residue from the analysis can be used for trace element analysis, e.g. by energy-dispersive x-ray fluorescence spectrometry.

The polymeric materials used in the production of synthetic textile fibres and household paints are usually modified with minor components to improve properties such as dye uptake [1], mechanical strength [2], and deterioration on ageing [2]. The characterization of such materials is therefore of interest in diverse fields such as industrial trouble-shooting [3—7] and forensic science. In crime investigations, a significant limiting factor is frequently the quantity of the material available for analysis (often of the order of micrograms, or even less).

The identification and differentiation of commercial acrylic fibres and chips from glossy household paints of various brands has been of interest recently. The generic term acrylic fibre is restricted by the U.S. Federal Trade Commission to materials which contain at least 85% by weight of acrylonitrile units. Some commercial fibres are spun from 100% polyacrylonitrile; others are

**Permanent address: Western Australian Institute of Technology, Hayman Road, Bentley South, Western Australia 6102.

modified with 3—10% of other vinyl monomers [8]. Household full gloss paints encountered in forensic science are often linear and crosslinked condensation polymers of polybasic acids (e.g. phthalic anhydride) and polyhydric alcohols (e.g. pentaerythritol). Such *o*-phthalate alkyd resins are usually modified with drying oils and regularly with small amounts of other materials such as styrene, vinyltoluene, melamine, formaldehyde, etc., depending on the application [2, 6]. In this paper, the use of thermogravimetry—mass spectrometry (t.g—m.s), a new technique in forensic sciences, is described for the detailed microanalysis of acrylic fibres and dried gloss paint flakes.

In contrast to earlier reports [9—12] a simple capillary interface has been fitted to a magnetic sector mass spectrometer so that the equipment remains available for other routine analyses, e.g. gas chromatography—mass spectrometry and solids-probe insertion.

EXPERIMENTAL

The standard glass flange which provides a seal at the top of the thermobalance furnace (TG750 with DTG750 time derivative unit, Stanton Redcroft Ltd., Copper Mill Lane, London SW17 0BN) was replaced with an electrically heated stainless steel flange. A glass-lined capillary (90 cm long, 1/16-in. o.d., 0.5 mm i.d.; SGE Ltd., 657 North Circular Road, London NW2 7AY) passed through the steel flange with its end positioned ca. 3 mm above the sample in the furnace. The other end of the capillary was connected to the mass spectrometer (VG Micromas 16F, VG Organic Ltd., Altrincham, Cheshire) via a standard glass capillary inlet, 50 mm long, 0.1 mm i.d. (VG Organic Ltd.). The furnace lid and capillary tubing were heated (230°C) electrically (5.5 A, 8.5 V) and the glass inlet was maintained at 190°C with external heating tape. The thermobalance was flushed with helium (15 ml min^{-1}) with a flow of 10 ml min^{-1} into the source of the mass spectrometer. Although the resulting source pressure (ca. 10^{-4} torr) yields less than optimum sensitivity and resolution, this provided no significant limitations in the current work. However, this relatively high pressure did cause a slight reduction in the lifetime of filaments and source heaters.

The samples (10—500 μg) were loaded into the pan of the thermobalance. To ensure that the larger fibre samples remained in position, they were compressed tightly into a ball. After loading, a period of ca. 3 min was allowed for air to be eliminated from the system and for the indicated source pressure to return to its original value (ca. 10^{-4} torr) before the heating programme was started. The samples were heated from ambient temperature to 700°C at 50°C min^{-1}.

The mass spectrometer was operated with 100-μA trap current, 70-eV electron energy, and a source temperature of 200°C. Mass spectrometric data were obtained by continuous magnet scanning downwards from *m/e* 450 to *m/e* 45 in an exponential mode at 1 s $decade^{-1}$ and acquired on magnetic tape

with a Carrick Interface (Instem Ltd., Mount Industrial Estate, Stone, Staffs). The data were processed off-line on a Hewlett-Packard 2100A computer, for which appropriate software was developed within this Establishment.

The smaller samples (ca. 10 μg) were examined with the mass spectrometer scanning in the multiple ion detection (m.i.d.) mode. Each sample was analysed at least twice.

RESULTS AND DISCUSSION

Fibre analysis

Twenty-seven commercial acrylic fibres can be classified into about 17 groups by t.g. alone [13]. The more detailed information that can be obtained by t.g—m.s., even on samples two orders of magnitude smaller (10 μg), will now be illustrated.

The acrylic fibres Courtelle and Tacryl, produced from acrylonitrile—methyl acrylate copolymers [8], are difficult to distinguish as small samples by pyrolysis gas chromatography (unpublished results) and infrared spectrometry [14]. The time derivative of the weight losses (d.t.g.) for Courtelle and Tacryl (500-μg samples) are compared in Fig. 1 with the total ion current (t.i.c.) traces obtained simultaneously with the mass spectrometer. Whether all of the evolved species are being transported through the capillary cannot be determined but the t.i.c. follows the d.t.g. trace closely with no appreciable delay.

Mass spectra produced during the thermal degradation cycle may be examined for ions whose presence or absence may be diagnostic or which may vary characteristically during the analysis.

The spectrum (Fig. 2a) obtained at the position of the first t.i.c. maximum for Tacryl (310°C) may be characterized as typical of a paraffin (a high boiling kerosene is used as solvent during the manufacture of this fibre [8]) and thus the ion of *m/e* 57 is diagnostic. The spectrum at the first position of maximum t.i.c. for Courtelle (360°C) is shown in Fig. 2b.

The intensity of the ion of *m/e* 106 closely follows the t.i.c. for the polymer degradation of both fibres and this ion is therefore useful for sensitive determinations involving multiple ion detection (m.i.d.). Figure 2 (c and d) shows the m.i.d. traces (*m/e* 57 and 106) for 10-μg samples of the two fibres thus illustrating how a sensitive and highly discriminating approach can be developed.

Paint analysis

Small samples of dried chips from white alkyd gloss paints are not easily distinguished; even a combination of seven analytical techniques failed [15] to distinguish between the samples obtained from eleven manufacturers. During more recent work, in which ten of the same samples were subjected to trace element analysis by energy-dispersive x-ray fluorescence spectrometry (x.r.f.), this situation has been improved to the point where only one

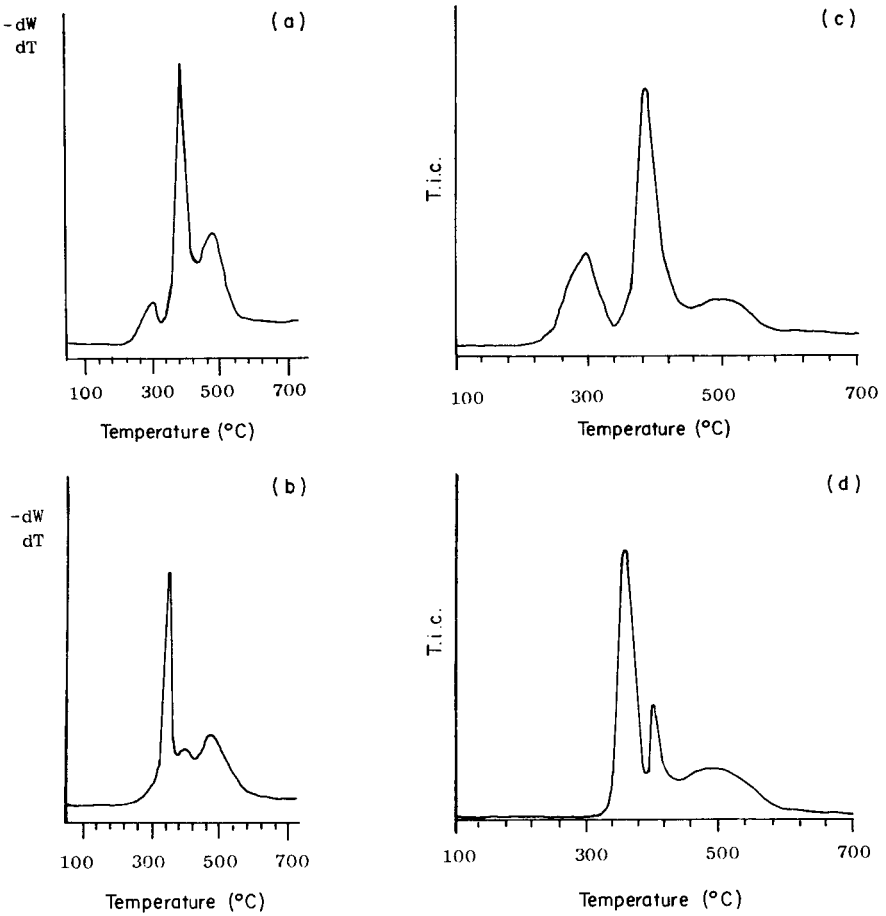

Fig. 1. Traces obtained by time-derivative thermogravimetry (d.t.g.) for 500-μg samples of the acrylic fibres Tacryl (a) and Courtelle (b). The linear temperature programme used was from ambient to 700°C at 50°C min^{-1} in an atmosphere of helium. The total ion currents (t.i.c.) for Tacryl (c) and Courtelle (d) were obtained simultaneously from *m/e* 450 to *m/e* 50 at 1 s $decade^{-1}$ with 100-μA trap current, 70-eV electron energy, and a source temperature of 200°C.

pair of samples could not be distinguished [16]. Current work has shown that t.g.—m.s. is similarly effective for the examination of the polymeric material in the paint film so that these two unrelated techniques (x.r.f. and t.g.—m.s.) can easily differentiate between all the samples.

The weight losses during examination of the white paints by t.g. occur much more slowly than for the acrylic fibres and the t.i.c. traces obtained for 500-μg samples (Fig. 3) are therefore much more definitive than the d.t.g. traces. The ten paints can readily be classified into seven groups. The t.i.c. traces from replicate analyses on any of these paints show only minor quantitative variations. The t.i.c. traces from paints 4, 13, 19, 22 and 28 are unique; those from

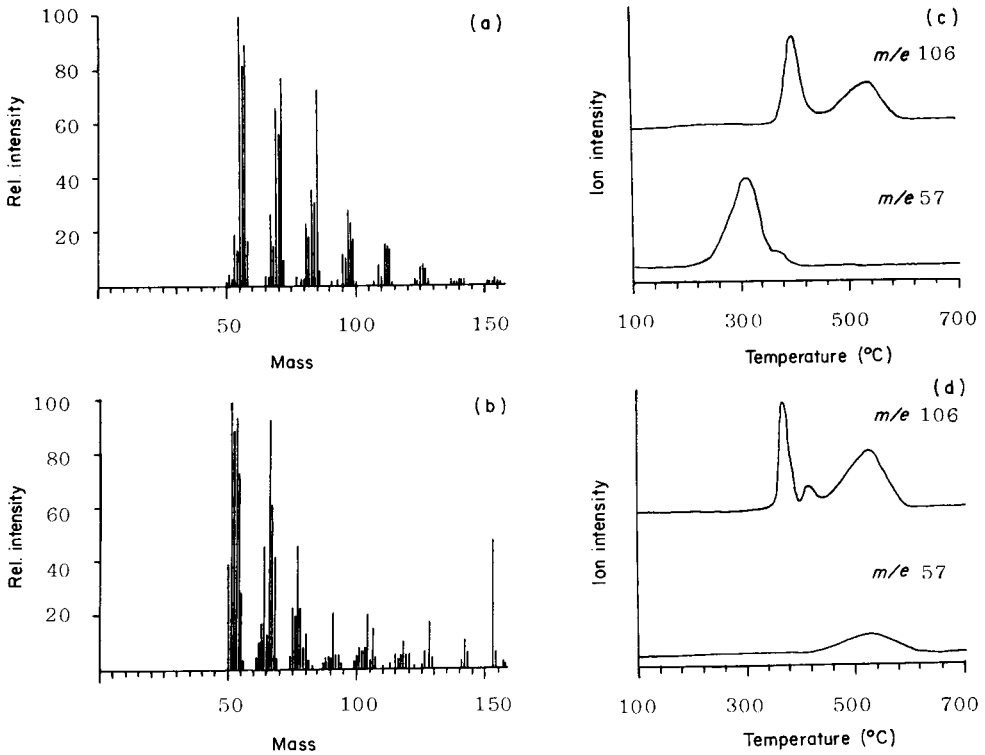

Fig. 2. Mass spectra obtained at the first maximum in the total ion current (310°C and 362°C, respectively) during the degradation of 500-μg samples of the acrylic fibres Tacryl (a) and Courtelle (b). The corresponding single ion traces (*m/e* 106 and 57) for 10-μg samples of Tacryl (c) and Courtelle (d) are also shown. The experimental conditions are as shown in Fig. 1.

paints 1, 10 and 25 and from paints 7 and 16 may be qualitatively grouped together.

The development of an analytical scheme for microgram samples is once again based on a selective m.i.d. procedure and is illustrated with reference to the results obtained for Valspar (paint 4) and Beaver (paint 7) paints, which are indistinguishable on the earlier basis of applying seven analytical techniques [15]. The d.t.g. responses for 500-μg samples of these paints are shown in Fig. 4 and compared with the t.i.c. traces obtained from the mass spectrometer.

The weight of the residue obtained after the thermal analysis (mainly filler) is also of particular interest. Valspar and Beaver paints gave significantly different residual weights at 700°C of 43.3% and 46.5%, respectively (four-fold replication, $P < 0.01$).

Once again, detailed examination of the mass spectra obtained from 500-μg samples allows the selection of ions which follow the overall polymer degra-

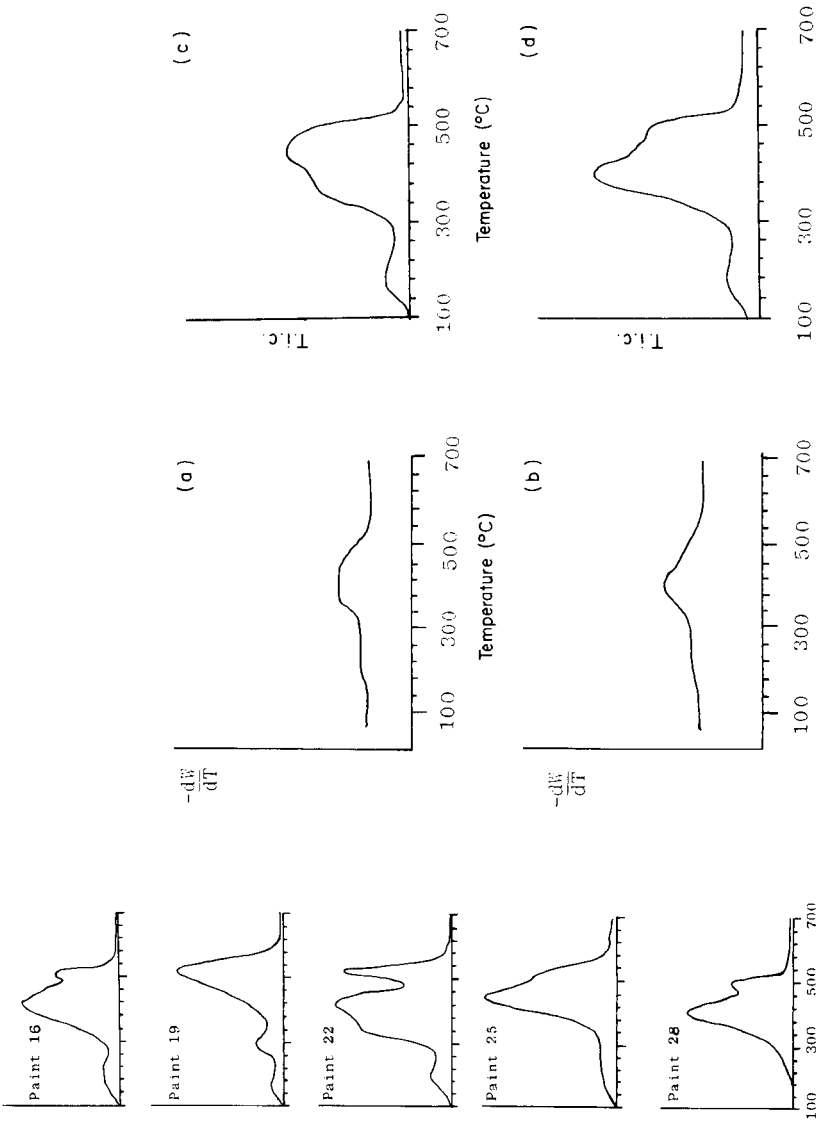

Fig. 3. T.i.c. traces obtained during thermogravimetry of 500-μg samples of ten white gloss paints. The experimental conditions are as shown in Fig. 1.

Fig. 4. Traces obtained by time-derivative thermogravimetry (d.t.g) for 500-μg samples of the white gloss paints Valspar (a) and Beaver (b). The corresponding t.i.c. plots are also shown for Valspar (c) and Beaver (d). The experimental conditions are as shown in Fig. 1.

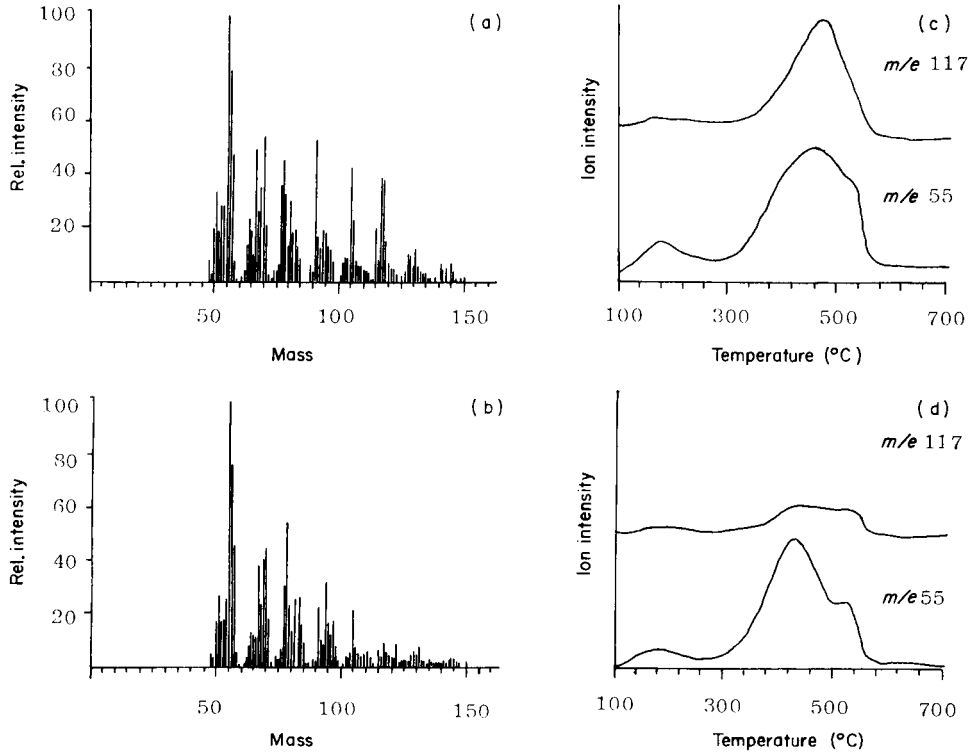

Fig. 5. Mass spectra obtained at the position of maximum total ion current (460°C and 400°C, respectively) during the degradation of 500-μg samples of the paints Valspar (a) and Beaver (b). The corresponding single ion traces (*m/e* 117 and 55) for 10-μg samples of Valspar (c) and Beaver (d) are also shown. The experimental conditions are as shown in Fig. 1.

dation and of others which vary greatly between the samples. The mass spectra shown in Fig. 5 (a and b) were obtained at the maximum of the t.i.c: obvious differences occur at *m/e* 117 and 118 (probably indicating the presence of vinyltoluene in the Beaver paint). The base peak at *m/e* 55 follows the t.i.c. closely and therefore this ion is useful for sensitive analysis by m.i.d. The m.i.d. traces (*m/e* 117 and 55) obtained from 10-μg samples of the two paints are also shown in Fig. 5 (c and d); ready discrimination is again obtained.

Conclusion

T.g—m.s. shows considerable potential for detailed polymer analysis, particularly in forensic science where the samples available for analysis are so limited. Although the short-term reproducibility of the t.g.—m.s. system described is satisfactory, significant differences occur when new interfaces are constructed. It is hoped that instruments designed specifically for thermal analysis will give fewer problems with sample transport and long-term reproducibility. The costs of such equipment would, however, be much greater than those of the modifications described here.

REFERENCES

1 R. H. Peters, Physical Chemistry of Dyeing, Vol. III, Elsevier, Amsterdam, 1975, p. 549.
2 P. Nylen and E. Sunderland, Modern Surface Coatings, Interscience, London, 1965, p. 153.
3 D. Grime, The British Ink Maker, (August 1967), 222.
4 D. Grime, The British Ink Maker, (November 1967), 36.
5 J. D. Frazee, J. Oil. Col. Chem. Assoc., 57 (1974) 300.
6 J. G. Frazer, N. M. Peacock and A. W. Pross, in C. P. A. Kappelmeier (Ed.), Chemical Analysis of Resin Based Coating Materials, Interscience, London and New York, 1959, p. 407.
7 Chicago Society for Paint Technology Official Digest, 33 (1961) 72.
8 R. E. Sanders, Chem. Proc. Eng., (Sept. 1968), 100.
9 F. Zitomer, Anal. Chem., 40 (1968) 1091.
10 G. J. Mol, Thermochim. Acta, 10 (1974) 250.
11 E. Baumgartner and E. Nachbaur, Thermochim. Acta, 19 (1977) 3.
12 R. L. Hassell, Dupont Application Brief TA45 (1974).
13 R. E. Ardrey, K. W. Smalldon and L. R. Mullings, Thermochim. Acta, in press.
14 K. W. Smalldon, J. Forens. Sci., 18 (1973) 69.
15 R. W. May and J. Porter, J. Forens. Sci. Soc., 15 (1975) 137.
16 C. R. Howden, R. J. Dudley and K. W. Smalldon, J. Forens. Sci. Soc., 17 (1977) 161.

Analytica Chimica Acta, 107 (1979) 335—338

NEGATIVE-ION COUNTING TECHNIQUES FOR GAS CHROMATOGRAPHY—MASS SPECTROMETRY

TOSHIHIRO FUJII* and KEIICHIRO FUWA

Division of Chemistry and Physics, National Institute for Environmental Studies, Yatabe, Tsukuba, Ibaraki 300-21 (Japan)

(Received 23rd October 1978)

SUMMARY

Negative-ion counting techniques for gas chromatography—electron-impact ionization quadrupole mass spectrometry (g.c.—m.s.) are described. Signal-to-noise performance is good and data acquisition is fast. Digital processing of the negative ion signals is done with an ion-counting device and data acquisition with a multi-channel analyzer. The negative-ion mass spectra from g.c.—m.s. measurements are shown for a mixture of tetrachloromethane, 1,2,2-trichloroethane and 1,1,2,2-tetrachloroethane.

Chemical ionization and related techniques [1, 2] have led to a renewal of interest in the analytical applications of the negative ions formed on electron-impact ionization. Under electron-impact conditions, molecular anion and structurally significant negative fragment ions [3, 4] are generated from the interaction of samples with a small population of low energy electrons produced in the ion source. However, abundance is very low and detection is difficult. Consequently, the analytical use of these negative ions has been limited to metallo-organics [3], aromatic hydrocarbons [4], and organophosphorus compounds [5]; these negative ions have not been employed in the field of gas chromatography—mass spectrometry (g.c.—m.s.).

An ion-counting technique [6, 7] used in mass spectrometry gives better detection capability for relatively low signal levels than the conventional electrometer technique [8], and this methodology [9, 10] therefore gives an interesting approach for the detection of negative ions of relatively low abundance. The present paper describes a new combination [11] of an ion-counting device with a multichannel analyzer for negative-ion g.c.—m.s. and negative-ion mass spectra obtained from g.c.—m.s. runs illustrate its potential.

EXPERIMENTAL

Equipment and chemicals

Negative-ion counting techniques. The ion-counting device—multichannel analyzer combination has been described [11]. The output of the ion-counting device was passed to an OMEGA-1 1024-channel analyzer (Canberra, Meriden, Conn.) operated in the multiscaling mode [11] via an interface unit [11]

made in this laboratory; the quadrupole mass spectrometer scan signal (0—10 V, ramp voltage) was converted to supply logic pulses to the analyzer for channel advance and start/stop of channel advance. Data in the channel memory (negative-ion mass spectrum) were displayed as described previously [11]; the analyzer has both data acquisition and display modes. The stored data were not displayed until data acquisition was complete and the analyzer was in the display mode. When the repetitive mass spectrometer scan was synchronized alternately to data acquisition and display mode during the g.c.—m.s. runs, the time variation data (parameters of integrated negative-ion counts) on the cathode-ray tube during the display duration gave the gas chromatographic elution information. At least 1 s was required to read out these data visually, and this determined the minimum mass spectrometer scan rate (1 s/scan). In the data acquisition mode, the channel advance and stop signals were generated as described previously [11].

Mass spectrometer. A Finnigan 3300F gas chromatograph—quadrupole mass spectrometer was operated in the electron-impact mode (ion chamber potential, —2.4 V; extractor potential, 1.1 V; focusing lens potential, 96 V). The electron trap electrode and ion source power supply have been described [11]. An electron energy of 4 eV gave the most abundant peak (m/z 35) for all the compounds in the present study. Other instrumental conditions were held constant (pressure in the mass spectrometer, 6×10^{-6} torr; repetitive scan time, 5 s; emission current 12 μA).

Gas chromatograph. The metal column (300 cm × 0.2 cm i.d.) used contained 5% SE-30 on 60/80 Chromosorb W.AW.DMCS; temperature was programmed from 50°C to 80°C at 4°C min^{-1} and the helium flow rate was 30 ml min^{-1}. The retention times of CCl_4, $CHCl{=}CCl_2$, and $CCl_2{=}CCl_2$ were 4.0, 6.2, and 7.1 min, respectively.

Chemicals. Tetrachloromethane, 1,2,2-trichloroethane and 1,1,2,2-tetrachloro ethane were of reagent grade (Wako Chemicals, Osaka, Japan).

Operation

The sample was injected with a syringe at the gas chromatographic inlet and repetitive scanning by the mass spectrometer was started after a preset time interval. The resulting negative ions were counted, processed, and stored in the acquisition memory of the analyzer. Background contributions to measured negative ions were negligible (usually less than 3 counts min^{-1}) so that background subtraction was unnecessary. The stored mass spectrum data were recorded on a T-Y recorder by manual operation of the analyzer during the display duration.

RESULTS AND DISCUSSION

Figure 1 shows the negative ion mass spectrum of $CCl_2{=}CCl_2$ obtained by g.c.—m.s. for a scan time of 5 s with a 10-μl injection of $CCl_2{=}CCl_2$ (0.02% in pentane). To demonstrate the detection capability for low-level signals,

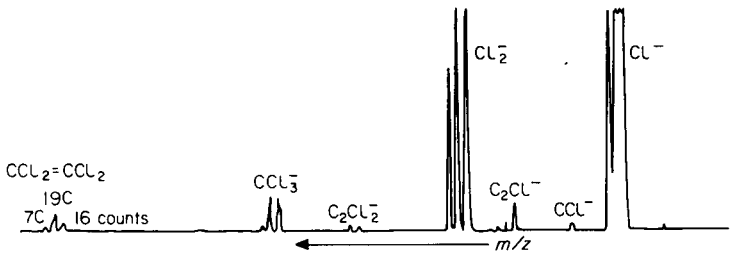

Fig. 1. Negative-ion mass spectrum of CCl_2=CCl_2 by g.c.—m.s.

the molecular negative-ion peak intensity is indicated by ion count numbers in Fig. 1.

Table 1 gives the negative-ion mass spectra from g.c.—m.s. of an injection (10 μl) of a mixture of CCl_4, CHCl=CCl_2 and CCl_2=CCl_2 in pentane (0.3% v/v of each compound). These spectra exhibit simple, easily interpretable patterns in contrast to the many fragment ions shown in positive-ion mass spectra [12]. The CCl_2=CCl_2 spectrum is particularly informative [13]; assignment of 164 as the molecular weight is easily confirmed. The CCl_4 and CHCl=CCl_2 spectra exhibited only the fragment ions.

For 10-μl injections, the response—concentration relationship for CCl_2=CCl_2 was linear over the 50—1000 ppm range for the molecular anion. This indicates that negative ion g.c.—m.s. with the present system can be used quantitatively.

The combination of the ion-counting device with the multichannel analyzer should be valuable for gas chromatography—quadrupole mass spectrometry; the improved detection capability and rapid data acquisition of the negative ions makes g.c.—m.s. measurements particularly applicable to the determination of organic compounds with efficient electron-capture groups. Mixtures of mercaptans [14] can be determined by this approach.

TABLE 1

Negative-ion mass spectra of organohalides by g.c.—m.s.

Compound	Nominal mass (relative intensity[a]) identification
CCl_4	*m/z* 35 (1000) Cl^-; *m/z* 47 (6) CCl^-; *m/z* 70 (82) Cl_2^-; *m/z* 82 (5) CCl_2^-; *m/z* 117 (11) CCl_3^-.
CHCl=CCl_2	*m/z* 35 (1000) Cl^-; *m/z* 47 (1) CCl^-; *m/z* 59 (2) C_2Cl^-; *m/z* 70 (77) Cl_2^-; *m/z* 94 (5) $C_2Cl_2^-$; *m/z* 95 (8) $C_2HCl_2^-$; *m/z* 127 (2) $C_2Cl_3^-$.
CCl_2=CCl_2	*m/z* 35 (1000) Cl^-; *m/z* 47 (1) CCl^-; *m/z* (5) C_2Cl^-; *m/z* 70 (48) Cl_2^-; *m/z* 94 (1) $C_2Cl_2^-$; *m/z* 117 (6) CCl_3^-; *m/z* 164 (2) $C_2Cl_4^-$.

[a]Sum of all intensities in a given isotopic cluster.

REFERENCES

1 H. P. Tannenbaum, J. D. Roberts and R. C. Dougherty, Anal. Chem., 47 (1975) 49.
2 D. F. Hunt, G. C. Stafford, Jr., F. W. Crow and J. W. Russell, Anal. Chem., 48 (1976) 2098.
3 J. H. Bowie and A. C. Ho, Aust. J. Chem., 24 (1971) 1093.
4 I. W. Fraser, J. L. Garnett, I. K. Gregor and K. J. Jessop, Org. Mass Spectrom., 10 (1975) 69.
5 P. C. Rankin, J. Assoc. Off. Anal. Chem., 54 (1971) 1340.
6 G. Goby and L.-D. Nguyer, Int. J. Mass Spectrom. Ion Phys., 20 (1976) 305.
7 E. Yellin, L. I. Yin and I. Adler, Rev. Sci. Instrum., 41 (1970) 18.
8 T. Fujii, Anal. Chim. Acta, 92 (1977) 117.
9 H. Miyake and M. Michijima, Mass Spectrochem. (Japanese), 19 (1971) 110.
10 J. Freudenthal and L. G. Gramberg, Anal. Chem., 49 (1977) 2205.
11 T. Fujii, Anal. Chim. Acta, 104 (1978) 167.
12 E. Stenhagen, S. Abrahamson and F. W. McLafferty, Registry of Mass Spectral Data, J. Wiley, New York, 1974.
13 K. A. G. MacNeil and J. C. J. Thynne, Trans. Faraday Soc., 64 (1968) 2112.
14 H. Knof, R. Large and G. Albers, Anal. Chem., 48 (1976) 2120.

Analytica Chimica Acta, 107 (1979) 339—347

DETERMINATION OF THE TYPES OF NITROGEN IN STEELS CONTAINING ALUMINIUM OR TITANIUM BY AN EXTRACTION METHOD WITH HYDROGEN

A. A. BAKER, J. B. HEADRIDGE*, S. R. KEOWN, G. D. LONG, P. A. VERGNANO and M. I. WILSON

Departments of Chemistry and Metallurgy, The University, Sheffield S3 7HF (Gt. Britain)

(Received 6th November 1978)

SUMMARY

The extraction method with hydrogen, hitherto used to determine mobile nitrogen in steels over the temperature range 350—450°C, has been employed at higher temperatures to determine nitrogen bound as aluminium nitride, or as titanium nitride or carbonitride. In steels containing only silicon and titanium as deoxidizers, the nitrogen remaining after passage of hydrogen at 600 or 750°C is present as titanium nitride or carbonitride and can be determined by difference. In steels containing only silicon and aluminium as deoxidizers, the nitrogen remaining after passage of hydrogen at 600°C is present as aluminium nitride and can also be determined by difference. This was verified by determining the aluminium nitride indirectly. The nitrogen released from both the aluminium and titanium steels in hydrogen at 600°C probably results from dissociation of submicroscopic particles of manganese silicon nitride.

The presence of nitrogen can have profound effects on the mechanical properties of steels and the determination of total nitrogen in steel has been a requirement for many years. Essentially nitrogen increases the strength and decreases the ductility and toughness of steels. To explain these effects there are many mechanisms which are related to the type of steels and to whether the nitrogen is present as combined nitrogen in nitride precipitates or is in interstitial solid solution in the matrix austenite or ferrite phases. For example, widely dispersed precipitate particles are able to restrict grain coarsening such that fine-grain mild steels or structural steels are produced by controlling, through heat treatment, the precipitation of aluminium nitride, niobium carbonitride, titanium carbonitride and vanadium carbonitride.

The metallurgically soluble nitrogen is referred to as mobile or free nitrogen and can be present interstitially in the iron lattice, in association with substitutional solutes in the iron lattice such as manganese, or in association with dislocations or at grain boundaries. Mobile nitrogen also includes any nitrogen present in discrete nitride phases of the rather unstable iron and manganese nitrides which may possibly be present in some steels [1]. The sum of mobile plus combined nitrogen is the total nitrogen in the steel.

The well known yield phenomena and strain ageing in low carbon steels are

due to the segregation of nitrogen in dislocations. At higher temperatures substitutional—interstitial reactions also produce strengthening by a dislocation locking mechanism. Recently, an important correlation between the impact transition temperature and soluble nitrogen has been discovered in reinforcing steels. The addition of titanium to mild steels in the correct stoichiometric ratio with respect to total nitrogen content to give titanium nitride precipitates, results in a tenfold decrease in mobile nitrogen content associated with a 60°C decrease in the impact transition temperature [2].

These are only a few of the effects of combined nitrogen and mobile nitrogen in steels. By suitable heat treatment or by the addition of certain elements to steels, the ratio of mobile to combined nitrogen can be altered to produce the properties sought by the metallurgist. A knowledge of the concentrations of the various types of nitrogen in steels would be particularly helpful, especially when coupled with information on the distribution of the phase or phases that make up combined nitrogen.

The determination of mobile nitrogen in steels is most conveniently undertaken by passing hydrogen over fine particles of steel at 450°C. At this temperature the mobile nitrogen is removed from the steel as ammonia, which can be determined continuously by using a cell incorporating an ion-selective electrode [3], coulometrically [4] or conductometrically [5]. It has been appreciated for some time that high results for mobile nitrogen could arise if any of the precipitated nitrides dissolved during the passage of hydrogen, and low results would be produced if any further precipitation was to occur in the steel through reaction of a nitride-forming element with mobile nitrogen not yet removed from the steel.

The method has been shown to be reliable for steels containing aluminium, silicon and titanium at 350—450°C [5—7] and vanadium at 350—440°C [8], and to be useful for steels containing niobium at 350°C [9]. Generally, the highest temperature within a recommended range is used to remove all the mobile nitrogen within the shortest time.

In the course of this work, it became clear that the extraction method with hydrogen might be extended to higher temperatures in order to determine the concentrations of the types of nitrogen left in a steel after removal of mobile nitrogen. Many carbon steels contain manganese and silicon along with a stronger deoxidizer such as aluminium or titanium. In such steels, combined nitrogen may exist as aluminium nitride or titantium nitride or carbonitride, and as manganese silicon nitride [7, 10]. The thermodynamic stability of these nitrides lies in the order $TiN > AlN > MnSiN_2$. Titanium nitride is stable at the temperature of molten iron [11]. Manganese silicon nitride is slightly dissociated at 600°C and the atomic nitrogen from it is completely removed from a steel as ammonia in a stream of hydrogen [7]. Therefore it should be possible to determine mobile nitrogen, manganese silicon nitride and titanium nitride in a steel containing only these types of nitrogen by collecting ammonia produced on the surface of millings of the steel in a stream of hydrogen first at 450°C and then at 600°C. The nitrogen left in the steel at 600°C should be in the form of titanium nitride or carbonitride and

is determined by difference when the total nitrogen content is known. Results will be presented to show that this is so.

It seemed possible that mobile nitrogen, manganese silicon nitride and aluminium nitride in a steel containing only these types of nitrogen could be determined in a similar way. However, aluminium nitride is less stable than titanium nitride and it was important to know that aluminium nitride is not dissociated in steels at 600°C if the method is to be reliable. Therefore an independent method for determining aluminium nitride in a series of steels containing aluminium and silicon was devised. Results will be presented to show that a hydrogen extraction method can be used to determine aluminium nitride by difference in such steels, when the total nitrogen content is known. The independent method for determining aluminium nitride was based on the relationship:

$$\text{Al as nitride} = \text{total Al} - \text{elemental Al} - \text{Al as oxide} \qquad (1)$$

The elemental aluminium was determined by dissolving the steel in a mixture of bromine and acetonitrile, filtering off undissolved precipitates, distilling off most of the bromine from the filtrate and determining the aluminium in the acetronitrile solution by atomic absorption spectrometry. This method was preferred to the Beeghly method for aluminium nitride, because of uncertainty about the complete solubility of manganese silicon nitride in bromine—methyl acetate mixtures [7].

A considerable amount of nitrogen was removed from some of the steels tested at 600°C in a stream of hydrogen, after prior removal of mobile nitrogen. In this study, it was not possible to identify the phase from which this nitrogen was dissociating at 600°C as manganese silicon nitride; therefore, this nitrogen will be referred to as nitrogen released at 600°C.

EXPERIMENTAL

Titanium steels

Preparation of the steels. The series of steels used was prepared in the Metallurgy Department from pure materials. The compositions of these steels are shown in Table 1; it can be seen that they fall into three groups. The final treatment of these steels involved hot rolling at 950°C and cooling in air.

Nitrogen determinations. Mobile nitrogen was determined by the extraction method with hydrogen at 440°C on fine millings [3]. The milling operations were undertaken very slowly to minimize any localized heating of the steel bars. When all the mobile nitrogen had been released and collected as ammonia after about 2 h, the temperature of the furnace was raised to 600°C and any further release of nitrogen as ammonia was recorded. Collection times of about 2 h were required. When the release of nitrogen at 600°C had ceased, the furnace temperature was further increased to 750°C to see if any more nitrogen would be released over a period of 2 h.

Microscopic examination of precipitates. In an attempt to identify the nitride phases present in the series of manganese—silicon—titanium steels,

TABLE 1

Compositions of the manganese—silicon—titanium steels

Steel	C (%)	Mn (%)	Si (%)	Ti (%)	Total N (%)
1	0.041	3.64	0.42	—	0.010
2	0.028	3.42	0.38	0.019	0.011
3[a]	0.035	3.50	0.28	0.036	0.007
6	0.21	1.33	0.28	0.005	0.0034
7	0.21	1.35	0.30	0.015	0.0036
9	0.24	1.13	0.29	0.020	0.0045
12	0.20	1.58	0.29	0.016	0.010
11	0.21	1.74	0.33	0.027	0.010

[a]Also contained 0.12% chromium.

steels 1, 2 and 3 were examined, where appropriate, by optical microscopy in conjunction with electron microprobe analysis with lithium fluoride, pentaerythritol and stearate crystals, and by electron microscopy and electron diffractio These latter techniques were applied to inclusions isolated from the steels after bromine—methyl acetate dissolution and examination of the particles on carbon films, and to carbon extraction replicas.

Aluminium steels

Preparation of the steels. The steels tested (Table 2) were specially prepared in a vacuum induction furnace from pure materials. The high-purity iron and graphite were melted and vacuum-degassed to remove carbon monoxide, before silicon, aluminium and manganese nitride were added. After preparation these steels were held at 1150°C for 1 h and cooled in the furnace.

Nitrogen determinations by extraction with hydrogen. Mobile nitrogen was determined at 450°C on fine millings [3]. Further release of nitrogen at 600°C and 750°C was examined as described for titanium steels.

TABLE 2

Compositions of the manganese—silicon—aluminium steels

Steel	C (%)	Si (%)	Mn (%)	Al (ppm)	O (ppm)	Total N (ppm)
A	0.13	0.32	0.93	<50	32	140
B	0.20	0.32	0.90	100	21	110
C	0.19	0.40	1.10	200	18	130
D	0.17	0.34	0.88	300	21	100
E	0.18	0.35	0.93	700	23	140
F	0.17	0.36	1.00	120	12	100
G	0.18	0.37	1.02	200	13	100
H	0.19	0.31	1.48	300	5	110

Determination of elemental aluminium. The steel sample (0.5 g) was dissolved in 15 ml of dry acetonitrile and 2 ml of dry bromine in a stoppered flask cooled in ice. Excess of bromine was removed by distillation, and the flask was cooled, stoppered and transferred to a dry glove-box. The solution was then filtered through Whatman GF/C glass fibre discs to remove any precipitate and made up to 50 ml in a graduated flask. It was necessary to work in the glove-box because aluminium bromide is readily hydrolysed by water vapour from the atmosphere.

The concentration of aluminium in the acetonitrile solution was determined with a Unicam SP90A atomic absorption spectrometer and nitrous oxide—acetylene flame at the aluminium 309.3-nm resonance line. The calibration graph was prepared from acetonitrile solutions that contained 1% (w/v) iron and aluminium in the range 2—10 μg ml^{-1}. These solutions were prepared by appropriate dilution of standard solutions of iron and aluminium in acetonitrile containing a stoichiometric excess of bromine.

RESULTS AND DISCUSSION

Titanium steels

For all 8 steels no further nitrogen was released at 750°C after collection of nitrogen as ammonia from steels heated first at 440°C and then at 600°C. The nitrogen remaining in the steels at 600°C and 750°C must therefore be in the form of the very stable titanium nitride or titanium carbonitride. The concentrations of the various types of nitrogen in these steels are shown in Table 3.

It should be noted that all of the nitrogen was removed from steel 1 by

TABLE 3

The concentrations of the various types of nitrogen in the manganese—silicon—titanium steels

Steel	Ti (ppm)	Total N (ppm) *A*	Mobile N released at 440°C (ppm) *B*[a]	Further N released at 600°C (ppm) *C*[a]	N as TiN or Ti (C, N) (ppm) $A-(B+C)$
1	—[b]	100	40	60	0
2	190	110	37	42	31
3	360	70	12	9	49
6	50	34	29	4	1
7	150	36	26	6	4
9	200	45	23	8	14
12	160	100	54	32	14
11	270	100	39	17	44

[a]Averages of two results agreeing within 5 ppm. [b]Not detected.

treatment with hydrogen at 440°C and 600°C; this steel contained no added titanium. Almost all the nitrogen was also released from steel 6, which contained a low concentration of titanium, after similar treatment. As expected, however, the concentration of titanium nitride or carbonitride in these steels increased as the concentration of titanium increased within any of the three groups.

When optical microscopy was used, titanium nitride particles were found in steels 2 and 3, occurring more frequently in steel 3 with the higher titanium concentration. The particles were very yellow in colour, indicating that they contained very little or no carbon [12]. Two such particles were shown by electron microprobe analysis to contain titanium and nitrogen, but no manganese or sulphur.

Inclusions isolated from steels 1, 2 and 3 after bromine—methyl acetate dissolution of the iron were examined by electron microscopy and diffraction but clear diffraction patterns were not found with steels 1 and 2. With steel 3 a good diffraction pattern was observed from one large particle; this pattern corresponded to a f.c.c. crystal with a unit cell length of 4.24 Å. The literature value for f.c.c. TiN is 4.235 Å [13], and undoubtedly the particle was a small secondary titanium nitride crystal.

Electron diffraction patterns could not be found from carbon replicas from steels 1, 2 and 3 that would correspond to a manganese silicon nitride phase. In the steels investigated, any precipitated phase containing silicon and nitrogen should be $MnSiN_2$ [10]. However, the heat treatment received by these samples was not such as to encourage the growth of even moderately sized crystals of this phase; the phase is probably present but only as submicroscopic particles. Certainly the release of nitrogen at 600°C from a steel, from which mobile nitrogen has already been removed, would be expected if the $MnSiN_2$ phase is present [7].

Aluminium steels

The concentrations of the various types of nitrogen in these steels obtained by the extraction method with hydrogen are shown in Table 4. The calculated standard deviation for all results in the last column was 7 ppm. The biggest contribution to the standard deviation of the results for nitrogen as aluminium nitride came from the results for total nitrogen, which were determined chemically by a Kjeldahl method.

It can be seen that as the Al:total N ratio increases, the mobile N:total N ratio decreases, as expected. The further nitrogen released at 600°C is probably produced by the breakdown of manganese silicon nitride as found by Kretschm [7] for manganese—silicon—aluminium steels. Comparison of the results for further nitrogen released at 600°C for steels A, B and C shows that the concentration of this type of nitrogen increases as the concentration of aluminium nitride increases, provided that the atomic ratio of Al:total N<1. It appears that precipitation of aluminium nitride induces further precipitation of manganese silicon nitride, as noted by Okada et al. [14].

TABLE 4

The concentrations of the various types of nitrogen in the manganese—silicon—aluminium steels

Steel	Al (ppm)	Total N (ppm) K	Mobile N released at 450°C (ppm) L[a]	Further N released at 600°C (ppm) M[a]	Further N released at 750°C (ppm) N[a]	N as AlN (ppm) $K-(L+M)$
A	<50	140	105	23	<5	12
B	100	110	32	37	11	41
C	200	130	19	55	16	56
D	300	100	6	<5	<5	~94
E	700	140	<5	<5	<5	~140
F	120	100	29	44	16	27
G	200	100	13	41	11	46
H	300	110	3	4	3	103

[a]Averages of two results agreeing within 5 ppm.

Unlike the situation with the titanium steels, a little further nitrogen was released from the aluminium steels at 750°C. This nitrogen probably originated from slight breakdown of very fine particles of aluminium nitride [4]. Hence the nitrogen as aluminium nitride in these steels was calculated by using the equation: nitrogen as AlN = $K - (L + M)$. It seems most unlikely that any manganese silicon nitride remains undissociated after hydrogen is passed over steel millings for 2 h at 600°C because no nitrogen remained to be released at 750°C from the simple manganese—silicon steel 1 (see Table 3).

Verification of the above equation for nitrogen as AlN was obtained by determining the concentrations of aluminium nitride in these steels through an aluminium mass balance by making use of relation (1) and comparing these results with those in the last column of Table 4. These results are calculated and compared in Tables 5 and 6, respectively. The agreement between the results for nitrogen as aluminium nitride determined by these two independent methods is quite good, when the standard deviations are taken into consideration. This agreement verifies that the difference method after extraction with hydrogen is reliable for determining the concentration of nitrogen bound as aluminium nitride in carbon steels containing no other strong nitride-forming elements. It is much more convenient to use than the method based on an aluminium mass balance.

The Beeghly method for determining aluminium nitride as described by Swinburn [1] was applied to steels B and F with atomic ratios of total Al: total N $<< 1$ to see if it would give a reliable result for aluminium nitride in the presence of manganese silicon nitride. However, the results were 53 ppm and 51 ppm of nitrogen as aluminium nitride in B and F, respectively, which are appreciably in excess of the results reported by the recommended methods in Tables 4 and 5. This indicates that manganese silicon nitride is not dissolved

TABLE 5

Determination of nitrogen as aluminium nitride in manganese—silicon—aluminium steels based on aluminium mass balance

Steel	O (ppm)	Total Al (ppm) X	Elemental Al (ppm) Y	Al bound as oxide (ppm) Z	Al for AlN (ppm) $X-(Y+Z)$	Nitrogen as AlN (ppm) $[X-(Y+Z)]\times$
A	32	<50	<10	—	<50	<26
B	21	100	20	24	56	29 (12)[a]
C	18	200	70	20	110	57 (12)
D	21	300	105	24	171	89 (12)
E	23	700	335	26	339	176 (16)
F	12	120	40	14	66	34 (11)
G	13	200	80	15	105	54 (11)
H	5	300	140	6	154	80 (11)

[a]Calculated standard deviations in parenthesis. The biggest contribution to the standard deviation of the results for N as AlN comes from the results for total aluminium, which were determined by direct-reading arc—spark emission spectrometry.

TABLE 6

Comparison of the results for nitrogen as aluminium nitride determined by nitrogen mass balance and by aluminium mass balance

Steel		A	B	C	D	E	F	G	H
N as AlN (ppm)	N mass balance	12	41	56	≈94	≈140	27	46	103
	Al mass balance	<26	29	51	89	176	34	54	80

completely on treatment with bromine—methyl acetate solution and that undissolved manganese silicon nitride is broken down to produce ammonia in the Beeghly procedure. Similar results were reported by Kretschmer [7] and the Beeghly method should not be used for steels that may contain manganese silicon nitride.

The authors thank the Science Research Council for a studentship (to A.A and a postdoctoral research assistantship (to P.A.V.), and Steel Castings Research and Trade Association for studentships (to G.D.L. and M.I.W.).

REFERENCES

1 D. G. Swinburn, Proceedings of the 27th Chem. Conf., British Steel Corporation, 1974 p. 86.
2 J. S. Smaill, L. A. Erasmus and S. R. Keown, Met. Technol., N.Y., 3 (1976) 194.
3 J. B. Headridge and G. D. Long, Analyst, 101 (1976) 103.
4 K. Kawamura, T. Otsubo and T. Mori, Trans. Iron Steel Inst. Jpn., 14 (1974) 347.
5 M. Kretschmer, J. de Boer, K. H. Sauer, G. Schmolke and K. Zimmermann, Arch. Eisenhütten., 46 (1975) 649.

6 R. Fisher and G. White, British Steel Corporation Open Report, CAPL/SM/G/51/73 (October 1973).
7 M. Kretschmer, Arch. Eisenhütten., 47 (1976) 15.
8 J. B. Headridge, S. R. Keown and P. A. Vergnano, Anal. Chim. Acta, 98 (1978) 157.
9 J. B. Headridge, S. R. Keown and P. A. Vergnano, unpublished work.
10 W. Roberts, P. Grieveson and K. H. Jack, J. Iron Steel Inst., 210 (1972) 931.
11 L. M. Melnick, L. L. Lewis and B. D. Holt (Eds.), Determination of Gaseous Elements in Metals, Wiley, New York, 1974, p. 507.
12 T. R. Allmand, Microscopic Identification of Inclusions in Steel, British Iron and Steel Research Association, MG/A/25/62 (May 1962).
13 R. W. G. Wyckoff, Crystal Structures, 2nd edn., Vol. 1, Interscience, New York, 1963, p. 90.
14 T. Okada, T. Nakayama, Y. Sakamoto and E. Miyoshi, Trans. Iron Steel Inst. Jpn., 11 (1971), Suppl. II, 1144.

Analytica Chimica Acta, 107 (1979) 349—358

CONSTANTES DE FORMATION DES COMPLEXES DE L'ARGENT(I) AVEC DIFFERENTS LIGANDS

M. MACHTINGER*, M. SLOIM-BOMBARD et B. TREMILLON

Laboratoire d'Electrochimie Analytique et Appliquée, associé au C.N.R.S., 11 rue Pierre et Marie Curie, 75231-Paris, Cedex 05 (France)

(Reçu le 17 Octobre 1978)

SUMMARY

Formation constants of silver(I) complexes with various ligands

The various complexes AgL, AgL_2 and Ag_2L and the associated protonated or hydroxo complexes, formed between silver(I) ions and aminopolycarboxylic acids (DTPA, DCTA, EGTA, HEDTA, NTA), glutamic acid, α-alanine, diethylenetriamine and triethylenetetramine are described. Formation constants were calculated from potentiometric measurements with glass and silver electrodes at ionic strength 0.1 and 25°C.

RESUME

Les divers complexes AgL, AgL_2, Ag_2L et les complexes acido—basiques associés, formés entre l'argent(I) et un des neuf ligands L suivants: DTPA, DCTA, EGTA, HEDTA, NTA, acide glutamique, α-alanine, diéthylènetriamine et triéthylènetétramine, ont été mis en évidence, par des mesures de pAg et de pH. Les constantes de formation correspondantes ont été déterminées.

Ringbom et Harju [1] ont proposé une méthode simple de détermination des constantes de formation des complexes M_mL_n, $M_mL_nH_i$ et $M_mL_n(OH)_j$. Cette méthode ne nécessite, du point de vue expérimental, que des mesures de potentiel grâce à une électrode métallique sélective de M, et de pH, dans une solution ne contenant que le cation métallique M et le ligand L; ces deux espèces sont introduites, dans un rapport de concentrations qui dépend de la stoechiométrie du complexe étudié, dans la solution qui est progressivement neutralisée. Une exploitation mathématique des résultats expérimentaux obtenus permet de calculer rapidement, avec précision, les valeurs cherchées. Ringbom et Harju [2] ont appliqué leur méthode à l'étude de quelques complexes du cuivre(II) et de l'argent(I). Par la suite Harju [3], puis van der Linden et Beers [4] ont adapté la même méthode à la mise en évidence de complexes mixtes.

Si les complexes du type M_mL_n ont déjà fait l'objet de nombreuses déterminations par diverses méthodes, telles que les titrages potentiométriques, la polarographie ou la spectrophotométrie, il n'en est pas de même des complexes acido—basiques associés qui sont en général peu connus. Notre but a

donc été la détermination systématique, par la méthode de Ringbom et Harju [1], de tous les complexes formés entre les ions Ag(I), les ions H^+ ou OH^- et un des neuf ligands suivants: diéthylènetriamine pentaacétate (DTPA), diamino-1,2-cyclohexanetétraacétate (DCTA), éthylèneglycol-bis(amino-2)éthyl-ethertétraacétate (EGTA), hydroxy-2-éthylènediaminetriacétate (HEDTA), nitrilotriacétate (NTA), glutamate, α-alanine, diéthylènetriamine (dien) et triéthylènetétramine (trien) et le calcul des constantes de formation correspondantes.

PARTIE THEORIQUE

Terminologie

A la réaction de formation de complexe $mM + nL \leftrightharpoons M_mL_n$;
est associée la constante d'équilibre intrinsèque de formation

$$K^{mM,nL}_{M_mL_n} = [M_mL_n]/[M]^m\,[L]^n$$

Lorsque M, L et M_mL_n existent sous des formes protonées ou hydroxylées, l'introduction des concentrations totales de ces espèces en solution

$$[M'] = [M] + \sum_y [M(OH)_y]\,;\ [L'] = [L] + \sum_x [LH'_x];$$

$$[M_mL'_n] = [M_mL_n] + \sum_i [M_mL_nH_i] + \sum_j [M_mL_n(OH)_j]$$

permet de définir la constante conditionnelle de formation,
$K^{mM',nL'}_{M_mL_n} = [M_mL'_n]/[M']^m[L']^n$. En posant, selon la notation de Ringbom [5],

$$\alpha_{M(OH)} = [M']/[M] = 1 + \sum_y K^{M,yOH}_{M(OH)_y}\,[OH]^y \text{ ou } \alpha_{M(OH)} = 1 + \sum_y K^{M,-yH}_{M(OH)_y}\,[H]^{-y}$$

$$\alpha_{L(H)} = [L']/[L] = 1 + \sum_x K^{L,xH}_{LH_x}\,[H]^x$$

$$\alpha_{M_mL_n(H,OH)} = [M_mL'_n]/[M_mL_n] = 1 + \sum_i K^{M_mL_n,iH}_{M_mL_nH_i}[H]^i + \sum_j K^{M_mL_n,-jH}_{M_mL_n(OH)_j}\,[H]^{-j}$$

il vient $K^{mM',nL'}_{M_mL'_n} = K^{mM,nL}_{M_mL_n} \cdot \alpha_{M_mL_n(H,OH)}/\alpha^m_{M(OH)}\,\alpha^n_{L(H)}$

Les constantes ainsi définies,

$$K^{M_mL_n,iH}_{M_mL_nH_i} = [M_mL_nH_i]/[M_mL_n]\,[H]^i \text{ et } K^{M_mL_n,-jH}_{M_mL_n(OH)_j} = [M_mL_n(OH)_j]\,[H]^j/[M_mL$$

sont les constantes de formation globale des complexes protonés et hydroxylé
On définit les constantes de formation partielle

$$K^{M_mL_nH_i-1,H}_{M_mL_nH_i} = [M_mL_nH_i]/[M_mL_nH_{i-1}]\,[H] \text{ et}$$

$$K^{M_mL_n(OH)_j-1,-H}_{M_mL_n(OH)_j} = [M_mL_n(OH)_j]\,[H]/[M_mL_n(OH)_{j-1}]$$

Rappel du principe de la méthode

Les cas développés ici sont ceux des dérivés des complexes 1:1 ($m = n = 1$), 1:2 ($m = 1; n = 2$) et 2:1 ($m = 2; n = 1$), en insistant particulièrement sur les aspects non développés par Ringbom et Harju [1], à savoir l'influence des phénomènes de dilution et d'instabilité relative des complexes formés sur la détermination des constantes.

Complexes 1:1. La solution initiale doit contenir l'ion métallique M et le ligand L dans le rapport molaire $C_M/C_L = 0{,}5$. Si la réaction de formation du complexe est pratiquement quantitative, on peut écrire, à l'équilibre,

$$[ML'] \approx 0{,}5; [L'] \approx 0{,}5; [M] = \epsilon.$$

Il n'est pas nécessaire de considérer [M'] dans la mesure où [M] est directement accessible par mesure du potentiel de l'électrode métallique correspondante. On peut exprimer la constante conditionnelle

$$K_{ML'}^{M,L'} = [ML']/[M]\,[L'] \approx 1/[M]$$

soit encore $\log K_{ML'}^{M,L'} = pM_{0,5}$, l'indice 0,5 traduisant le rapport molaire des concentrations initiales du cation et du ligand en solution.

On a, d'autre part,

$$\log K_{ML'}^{M,L'} = \log K_{ML}^{M,L} + \log (\alpha_{ML(H,OH)}/\alpha_{L(H)})$$

soit $\log K_{ML'}^{M,L'} = pM_{0,5} = \log K_{ML}^{M,L} + \log \alpha_{ML(H,OH)} - \log \alpha_{L(H)}$

D'où: $pM_{0,5} + \log \alpha_{L(H)} = \log K_{ML}^{M,L} + \log \alpha_{ML(H,OH)}$.

La représentation graphique de la somme $pM_{0,5} + \log \alpha_{L(H)} = f(pH)$, qui peut être calculée à toute valeur de pH, à partir des mesures expérimentales de $pM_{0,5}$ et des valeurs connues des constantes $K_{LH_x}^{L\,xH}$ donne un type de courbe déjà décrite et interprétée [1]. Il est possible de déterminer, à partir de cette courbe, les constantes de formation de ML, MLH_i et $ML(OH)_j$ par une méthode purement graphique, si ces constantes correspondent à des complexes stables [1]. Des corrections graphiques peuvent être effectuées dans le cas où les stabilités des différents complexes sont voisines.

Mais dans le cas où le complexe ML lui-même n'est pas très stable, des corrections mathématiques doivent être envisagées pour tenir compte du fait que lorsque M et L sont introduits dans le rapport molaire 0,5, le quotient [ML']/[L'] est différent de 1.

Soient V_i le volume initial de solution étudiée et V_t le volume total, après addition de réactif titrant. Le principe de conservation des quantités initiales de cation métallique et de ligand se traduit par les deux relations suivantes: $V_i C_M = V_t\{[M'] + [ML']\}$ et $V_i C_L = V_t\{[L'] + [ML']\}$. De ces deux relations on tire

$$[ML']/[L'] = \{(V_i/V_t)\,C_M - [M']\}/\{(V_i/V_t)\,(C_L - C_M) + [M']\}$$

ou, comme $C_L = 2\,C_M$, avec $[M'] = \alpha_{M(OH)}\,[M]$:

$$[ML']/[L'] = \{(C_L/2) - (V_t/V_i)\,[M']\}/\{(C_L/2) + (V_t/V_i)\,[M']\}$$

Pour déterminer les constantes de formation des complexes ML, il suffit donc de représenter graphiquement la fonction

$$pM_{0,5} + \log \alpha_{L(H)} + \log ([ML']/[L']) = f(pH)$$

de tracer les tangentes à la courbe dont les pentes ont des valeurs entières et de chercher l'abscisse de leurs points d'intersection deux à deux.

Complexes 1:2. La solution initiale doit contenir l'ion métallique M et le ligand L dans le rapport molaire $C_M/C_L = 1/100$. Si la réaction de formation du complexe ML_2 est suffisamment quantitative, on peut écrire en considérant l'équilibre de formation du complexe, $M + 2L' \rightleftharpoons ML'_2$, $[L'] \approx 1$; $[ML'_2] \approx 10^{-2}$. D'où $K^{M,2L'}_{ML'_2} = [ML'_2]/[M]\,[L']^2 \approx 1/[M]$, soit encore $\log K^{M,2L'}_{ML'_2} = pM_{0,01}$.

On a, d'autre part,

$$\log K^{M,2L'}_{ML'_2} = \log K^{M,2L}_{ML_2} + \log \alpha_{ML_2(H,OH)}/\alpha^2_{L(H)}$$

$$\log K^{M,2L'}_{ML'_2} = pM_{0,01} = \log K^{M,2L}_{ML_2} + \log \alpha_{ML_2(H,OH)} - 2 \log \alpha_{L(H)}$$

d'où: $$pM_{0,01} + 2 \log \alpha_{L(H)} = \log K^{M,2L}_{ML_2} + \log \alpha_{ML_2(H,OH)}$$

La courbe $pM_{0,01} + 2 \log \alpha_{L(H)}$ peut être exploitée de manière analogue à celle décrite pour les complexes 1:1.

Dans le cas où le complexe ML_2 n'est pas très stable, dans la mesure où le rapport molaire des concentrations n'est pas égal à 10^{-2}, il est indispensable d'évaluer le quotient $[ML'_2]/[L']^2$.

La conservation des quantités de cation métallique M et de ligand L conduit aux deux relations suivantes.

$$V_i C_M = V_t\{[M'] + [ML'] + [ML'_2]\} \text{ et } V_i C_L = V_t\{[L'] + [ML'] + 2[ML'_2]\}$$

En associant à ces deux relations, celle donnant la constante de formation du complexe 1:1, $K^{M,L'}_{ML'} = [ML']/[M]\,[L']$, il est possible de calculer le rapport

$$\frac{[ML'_2]}{[L']^2} = \frac{V_t\{1 - K^{M,L'}_{ML'}\,[M]\}\{(C_M - [M']\,V_t/V_i)(1 + K^{M,L'}_{ML'}\,[M]) - K^{M,L'}_{ML'}\,[M]\,C_L\}}{V_i\{C_L - 2(C_M - [M']\,V_t/V_i)\}^2}$$

Dans cette expression, tous les éléments peuvent être déterminés soit expérimentalement, soit par calcul préalable. La détermination des constantes de formation des complexes 1:2 se fait donc à partir de l'exploitation de la courbe,

$$pM_{0,01} + 2 \log \alpha_{L(H)} + \log [ML'_2]/[L']^2 = f(pH)$$

courbe obtenue grâce aux résultats expérimentaux du titrage d'une solution contenant le cation métallique M et le ligand L dans des concentrations telles que $C_L \gg C_M$.

Complexes 2:1. La solution idéale doit contenir l'ion métallique M et le ligand L dans le rapport molaire $C_M/C_L = 1{,}5$. Si on suppose un processus de formation de M_2L en 2 étapes et des réactions quantitatives: $M + L' \rightleftharpoons ML'$, et

$ML' + M \rightleftharpoons M_2L'$, on a donc, à l'équilibre, une solution-tampon de M, pour laquelle $[ML'] \approx [M_2L']$. D'où $K_{M_2L'}^{M,ML'} = [M_2L']/[M]\,[ML'] \approx 1/[M]$, soit $\log K_{M_2L'}^{M,ML'} = pM_{1,5}$. On a, par ailleurs,

$$\log K_{M_2L'}^{M,ML'} = \log K_{M_2L}^{M,ML} + \log \alpha_{M_2L(H,OH)} - \log \alpha_{ML(H,OH)}$$

D'où: $$pM_{1,5} + \log \alpha_{ML(H,OH)} = \log K_{M_2L}^{M,ML} + \log \alpha_{M_2L(H,OH)}$$

Le tracé de la courbe $pM_{1,5} + \log \alpha_{ML(H,OH)} = f(pH)$ nécessite la connaissance préalable des complexes acides et hydroxyde de ML. Son exploitation est ensuite analogue à celle décrite précédemment pour les complexes 1:1 et 1:2.

Des corrections mathématiques doivent être faites dans le cas où les complexes ML et M_2L ne se forment pas quantitativement; il faut alors évaluer le rapport $[M_2L']/[ML']$ en fonction de données connues.

La conservation des quantités initiales de M et de L permet d'écrire les deux relations.

$$V_iC_M = V_t\{[M'] + [ML'] + 2[M_2L']\} \text{ et } V_iC_L = V_t\{[L'] + [ML'] + [M_2L']\}$$

On peut en tirer l'expression suivante.

$$[M_2L']/[ML'] = \{(V_i/V_t)(C_M - C_L) - [M'] + [L']\}/\{(V_i/V_t)(2C_L - C_M) - 2[L'] + [M']\}$$

Et, en tenant compte du fait que $C_M = 1{,}5\ C_L$.

$$[M_2L']/[ML'] = \{(V_i/V_t)\ C_L/2 - [M'] + [L']\}/\{(V_i/V_t)\ C_L/2 + [M'] - [2L']\} \quad (1)$$

$[L']$ n'est pas connue; on peut obtenir sa valeur en combinant les deux relations exprimant la conservation de M et de L avec la constante $K_{ML'}^{M,L'} = [ML']/[M]\,[L']$. Il vient.

$$[L'] = (V_i/V_t)\ C_L/2 + [M']/\{2 + K_{ML'}^{M,L'}\,[M]\}$$
$$= (V_i/V_t)\ C_L/2 + [M']/\{2 + K_{ML}^{M,L}\,[M]\ \alpha_{ML(H,OH)}/\alpha_{L(H)}\}$$

Il suffit de reporter cette expression de $[L']$ dans l'égalité (1) pour avoir le rapport $[M_2L']/[ML']$, en fonction d'éléments déterminés soit expérimentalement, soit par le calcul.

La détermination des constantes de formation des complexes 2:1 se fait donc à partir du titrage d'une solution contenant le cation M et le complexant L dans le rapport molaire $C_M/C_L = 1{,}5$ et de l'exploitation graphique de la courbe

$$pM_{1,5} + \log \alpha_{ML(H,OH)} + \log [M_2L']/[ML'] = f(pH)$$

PARTIE EXPERIMENTALE

Toutes les manipulations ont été réalisées à force ionique 0,10 M; pour cela, les solutions à titrer ont été préparées dans du nitrate de potassium 0,10 M

et les réactifs titrants: potasse ou acide nitrique étaient à la concentration 0,10 M. Cependant, au cours des titrages, la force ionique a pu varier dans certains cas de 0,10 à 0,12 M. Les solutions ont été initialement dégazées, puis conservées sous atmosphère d'azote pendant les titrages, elles ont été maintenues à 25°C en utilisant une cellule de mesure RMO4 (Solea Tacussel) reliée à un thermostat Lauda K2.

Les valeurs de pH ont été mesurées à l'aide d'un pH-mètre ISIS 4000 (Solea Tacussel) préalablement étalonné avec des solutions tampons; les valeurs de potentiel, à l'aide d'un millivoltmètre Aries 10000 (Solea Tacussel).

Les trois électrodes utilisées étaient les suivantes: (a) une électrode de référence au calomel saturée (jonction double, KNO_3 0,10 M); (b) une électrode de verre indicatrice de pH (Solea Tacussel haute alcalinité) répondant correctement sur la gamme de pH 1—13; (c) une électrode d'argent indicatrice des ions Ag^+. Un étalonnage préalable de cette dernière électrode a été nécessaire. Par mesure du potentiel de solutions de nitrate d'argent (10^{-1}—5×10^{-5} M) dont la force ionique était ajustée à 0,10 M, les paramètres de l'équation de Nernst ont pu être déterminées.

$$E = E_0 + 2{,}3\, RTF^{-1} \log [Ag^+] = E_0 - 2{,}3\, RTF^{-1}\, pAg$$

$E_0 = (546{,}1 \pm 0{,}4)$ mV; $2{,}3\, RTF^{-1} = (58{,}7 \pm 0{,}1)$ mV; d'où la relation: $pAg = (546 - E)/58{,}7$.

Les calculs ont été effectués sur un calculateur Hewlett-Packard 9820 A modèle 20.

RESULTATS ET DISCUSSION

Dans tout le domaine de pH étudié (2—12) le coefficient $\alpha_{Ag(OH)}$ est voisin de 1, car les complexes hydroxyde du cation Ag(I) sont peu stables; [Ag'] et [Ag] sont donc confondus dans les calculs. Pour chacun des neuf ligands associés au cation Ag(I), les trois types de complexes ont été envisagés successivement en modifiant le rapport molaire du cation métallique et du complexant. Chaque fois qu'un type de complexes a été mis en évidence, les points expérimentaux de coordonnées pH et $S_{1:1}$ ou $S_{1:2}$ ou $S_{2:1}$ (l'indice affecté à S traduisant le type de complexes dont il s'agit) ont été représentés sur une figure. S a été calculé d'après les expressions

$$S_{1:1} = pAg + \log \alpha_{L(H)} + \log [AgL']/[L']$$

$$S_{1:2} = pAg + 2 \log \alpha_{L(H)} + \log [AgL'_2]/[L']^2$$

$$S_{2:1} = pAg + \log \alpha_{AgL(H,OH)} + \log [Ag_2L']/[AgL']$$

A l'aide de ces représentations graphiques, la nature des complexes formés et les constantes de formation correspondantes ont été déterminées, en faisant si nécessaire des corrections graphiques.

Les courbes $S = f(pH)$ ont alors été recalculées à partir des expressions suivantes

$$S_{1:1} = \log K_{AgL}^{Ag,L} + \log \alpha_{AgL(H,OH)}$$

$$S_{1:2} = \log K_{AgL_2}^{Ag,2L} + \log \alpha_{AgL_2(H,OH)}$$

$$S_{2:1} = \log K_{Ag_2L}^{AgL,Ag} + \log \alpha_{Ag_2L(H,OH)}$$

Quelques exemples de courbes $S = f(\text{pH})$ sont donnés (Figs. 1—5) où sont représentés les points expérimentaux et les courbes recalculées. Dans chaque

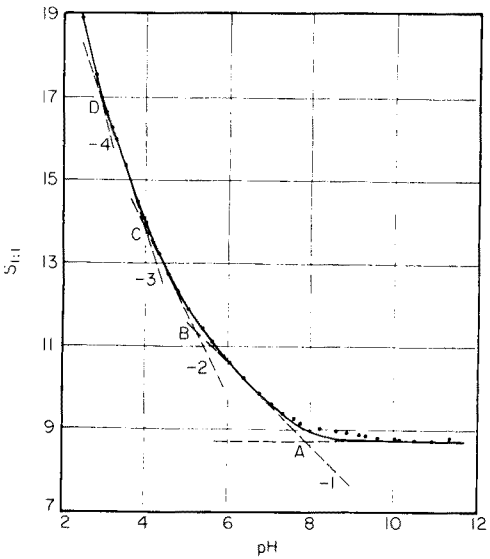

Fig. 1. Complexes Ag(I)—DTPA: courbe $S_{1:1} = f(\text{pH})$. (—) Courbe calculée; (···) points expérimentaux; (---) tangentes à la courbe définie par les points expérimentaux permettant la détermination des constantes.

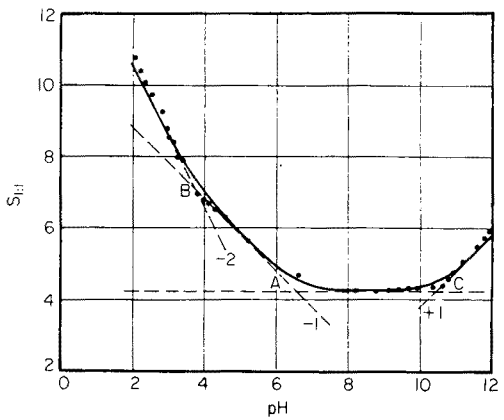

Fig. 2. Complexes Ag(I)—acide glutamique: courbe $S_{2:1} = f(\text{pH})$.

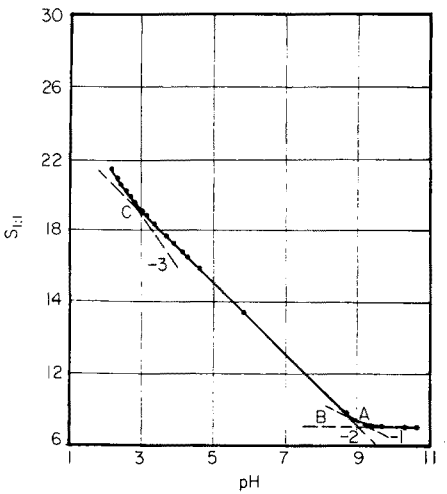

Fig. 3. Complexes Ag(I)—Trien: courbe $S_{1:1} = f(\text{pH})$.

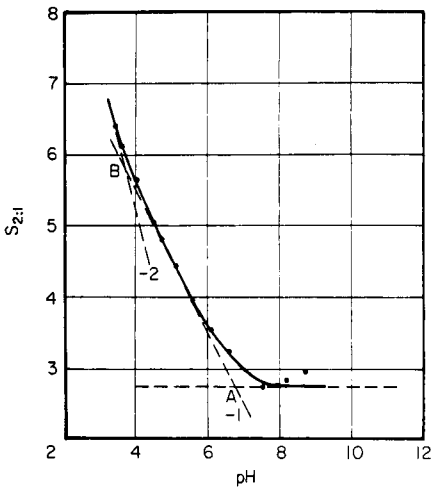

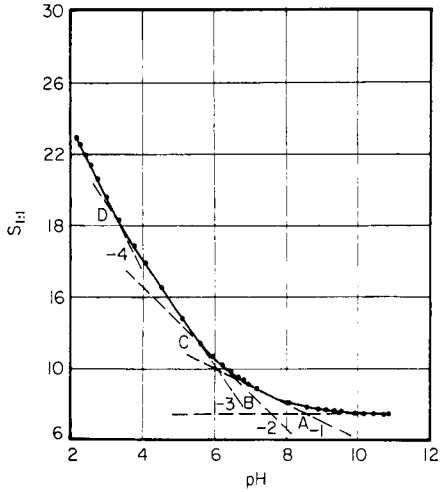

Fig. 4. Complexes Ag(I)—α-alanine: courbe $S_{1:1} = f(\text{pH})$.

Fig. 5. Complexes Ag(I)—α-alanine: courbe $S_{1:2} = f(\text{pH})$.

cas, la plupart des points expérimentaux sont situés sur la courbe correspondante, ce qui permet de conclure que l'ajustement des valeurs des logarithmes de constantes est satisfaisant.

Pour chacun des ligands étudiés, sont données les valeurs de pK_A des couples acides—bases dans les conditions opératoires, ainsi que la liste des différents complexes mis en évidence. Les valeurs des logarithmes des constantes de formation des complexes sont regroupées dans les Tableaux 1—3, sur lesquels figurent aussi les valeurs des mêmes constantes déjà publiées, mais obtenues par d'autres méthodes.

L = DTPA. pK_A [6]: 10,56; 8,69, 4,37, 2,87; 1,94.
Complexes mis en évidence: AgL, AgLH, $AgLH_2$, $AgLH_3$, $AgLH_4$.

L = DCTA. pK_A [6]: 11,78; 6,20; 3,60; 2,51.
Complexes mis en évidence: AgL, AgLH, $AgLH_2$, $AgLH_3$.

L = EGTA. pK_A [6]: 9,54; 8,93; 2,73; 2,08.
Complexes mis en évidence: AgL, AgLH, $AgLH_2$.

L = HEDTA. pK_A [6]: 9,81; 5,41; 2,72.
Complexes mis en évidence: AgL, AgLH, $AgLH_2$.

L = NTA. pK_A [5]: 9,81; 2,57; 1,97.
Complexes mis en évidence: AgL, AgLH.

L = glutamate. pK_A [7]: 9,20; 3.95; 2,20.
Complexes mis en évidence: AgL, AgLH, $AgLH_2$, $AgLH_3$, Ag_2L, Ag_2LH, Ag_2LH_2.

L = Base de l'α-alanine. pK_A [8]: 9,87; 2,36.
Complexes mis en évidence: AgL, AgLH, $AgLH_2$, AgLOH, AgL_2, AgL_2H, AgL_2H_2, AgL_2H_3.

L = diéthylènetriamine. pK_A [5]: 10,02; 9,21; 4,42.

TABLEAU 1

Logarithmes des constantes de formation des complexes 1:1

L	log K					
	Ag, L AgL	AgL, H AgLH	AgLH, H $AgLH_2$	$AgLH_2$, H $AgLH_3$	$AgLH_3$, H $AgLH_4$	AgL, —H AgLOH
DTPA	8,72 8,70 [6]	7,86	5,07	3,92	3,1	
DCTA	8,39 8,41 [6] 8,15 [9]	6,90	5,13	3,64		
EGTA	7,04 7,06 [6] 6,88 [10]	7,64 7,59 [10]	6,18			
HEDTA	6,63 6,71 [6]	5,82	4,96			
NTA	5,35 5,16 (9)	6,80				
Acide glutamique	3,79	7,03	3,15	2,92		
α-Alanine	4,23 3,64 [8] 3,60 [11] 4,86 [12]	6,52	3,74			—10,39
Dien	6,10 6,1 [13]	7,96 7,12 [13]	7,27	4,46		
Trien	7,50 7,7 [14]	8,40 8,1 [14]	6,45 6,28 [14]	5,74	3,52	

TABLEAU 2

Logarithmes des constantes de formation des complexes 1:2

L	log K			
	Ag, 2L AgL_2	AgL_2, H AgL_2H	AgL_2H, H AgL_2H_2	AgL_2H_2, H AgL_2H_3
α-Alanine	7,02 7,18 [8] 7,06 [11]	9,07	8,95	2,85

Complexes mis en évidence: AgL, AgLH, $AgLH_2$, $AgLH_3$.

L = triéthylènetétramine. pK_A [5]: 10,00; 9,28; 6,75; 3,40.

Complexes mis en évidence: AgL, AgLH, $AgLH_2$, $AgLH_3$, $AgLH_4$, Ag_2L.

TABLEAU 3

Logarithmes des constantes de formation des complexes 2:1

L	log K		
	AgL, Ag Ag_2L	Ag_2L, H Ag_2LH	Ag_2LH, H Ag_2LH_2
Acide glutamique	2,76	6,76	3,72
Dien	1,4 [13]		
Trien	<3		
	2,4 [14]		

Compte tenu de la précision des mesures expérimentales et de la détermination graphique, l'incertitude sur la valeur des logarithmes des constantes peut varier entre 0,05 et 0,1 unité de logarithme; que la deuxième décimale n'est donc pas significative. En examinant les Tableaux 1—3, on constate une concordance relativement bonne entre les valeurs des constantes que nous avons déterminées et celles qui étaient déjà publiées; on observe, de plus, que très peu de complexes acido—basiques étaient déjà connus.

La méthode utilisée n'a pas permis la détermination de constantes faibles, par exemple celle de Ag_2—dien. Par ailleurs, son caractère systématiquement trop mathématique a conduit à mettre en évidence la formation de certains complexes protonés, alors que la structure du complexant ne permet pas d'en justifier l'existence: sont au nombre de ceux-ci les complexes protonés supérieurs de l'argent(I) avec l'acide glutamique, l'α-alanine, la den et la trien. Cependant, la simplicité de sa mise en oeuvre et la possibilité de déterminer rapidement et avec précision les constantes de formation des complexes acido—basiques sont les avantages incontestables de cette méthode.

BIBLIOGRAPHIE

1 A. Ringbom et L. Harju, Anal. Chim. Acta, 59 (1972) 33.
2 A. Ringbom et L. Harju, Anal. Chim. Acta, 59 (1972) 49.
3 L. Harju, Anal. Chim. Acta, 63 (1973) 95.
4 W. E. Van der Linden et C. Beers, Talanta, 22 (1975) 89.
5 A. Ringbom, Complexation in Analytical Chemistry, Interscience, New York, 1963.
6 H. Wikberg et A. Ringbom, Suom. Kemistil. B, 41 (1968) 177.
7 G. Kortüm, W. Vogel et K. Andrussow, Dissociation Constants of Organic Acids in Aqueous Solutions, Butterworths, London, 1961.
8 C. B. Monk, Trans. Faraday Soc., 47 (1951) 292.
9 J. Stary, Anal. Chim. Acta, 28 (1963) 132.
10 J. J. R. F. da Silva et J. G. Calado, Rev. Port. Quim., 5 (1963) 121.
11 Yu. M. Azizov, A. Kh. Miftakhova et V. F. Toropova, Russ. J. Inorg. Chem., 12 (1967) 341
12 R. M. Keefer et H. G. Reiber, J. Am. Chem. Soc., 63 (1941) 689.
13 J. E. Pru et G. Schwarzenbach, Helv. Chim. Acta, 33 (1950) 985.
14 G. Schwarzenbach, Helv. Chim. Acta, 33 (1950) 974.

Analytica Chimica Acta, 107 (1979) 359—363

MULTICOMPONENT TWO-PHASE BUFFER SYSTEMS†

T. J. JANJIC*, E. B. MILOSAVLJEVIĆ and M. K. SRDANOVIĆ

Chemical Institute, Faculty of Sciences, University of Belgrade, P.O. Box 550, 11001 Belgrade (Yugoslavia)

(Received 20th November 1978)

SUMMARY

Two-phase buffer systems containing two or more acid—base pairs and having a considerable buffer capacity over a wide pH range are described. When acid—base pairs of the same type are combined, the rule of additivity of buffer capacity is valid, but when the two-phase buffers contain an organic acid and an organic base, the rule of additivity does not apply if ion-pair extraction occurs to a significant extent. Equations for calculation of buffer capacity curves in the latter case are reported. The differentiating effect of the organic solvent allows multicomponent two-phase buffers to be prepared from acids whose strength in water is practically equal.

In an earlier paper [1] two-phase buffer systems were described, and it was shown that they have two important advantages over classical single-phase buffers: (1) the pH value of the maximum buffer capacity of a particular acid—base pair may be varied by changing the experimental conditions; and (2) acids or bases which are almost water-insoluble can be used for the preparation of two-phase buffers with an aqueous working phase.. The effects of dilution of such buffers were also studied [1, 2]. The two-phase buffers studied in these papers contained only one acid—base pair. In the present paper, two-phase buffer systems containing two or three acid—base pairs are discussed.

EXPERIMENTAL

All experiments were done at constant ionic strength, $I = 0.15$, sodium chloride being added to solutions when necessary. In order to maintain constant ionic strength during titrations, sodium salts of the organic acids tested were titrated with a hydrochloric acid solution, while hydrochlorides of the organic bases were titrated with a sodium hydroxide solution.

In all cases, 1-octanol was the organic solvent, and the organic and aqueous phases were equal in volume.

---

†This work was presented in part at the 21st Annual Meeting of the Serbian Chemical Society, Belgrade, January 20, 1978.

The partition coefficients of hexanoic acid and 1-hexylamine were calculated from the pH values of maximum buffer capacity found experimentally for the corresponding two-phase buffers containing only the one component. By means of eqn. (10) of ref. [1], the partition coefficients (K_p) of hexanoic acid and 1-hexylamine were calculated as 114 ± 5 and 111 ± 5, respectively, at 25°C.

The equilibrium constant (K_d) of extraction of the ion pair (A^-, HB^+, where HA is hexanoic acid, and B is 1-hexylamine) was determined as follows: 20 ml of a 0.050 M solution of BHA was mixed with 20 ml of 1-octanol; after equilibration, the analytical concentration of the base in each layer was determined by potentiometric titration with hydrochloric acid solution. From the data obtained, K_d was calculated to be 120 ± 15 at 25°C.

All titrations were carried out in a nitrogen atmosphere to exclude the effect of carbon dioxide. For calculations, a Texas Instruments TI-58 programmable calculator was used. Other experimental arrangements were the same as described earlier [1, 2].

RESULTS AND DISCUSSION

Two-phase buffers containing single acid—base pairs

The six acid—base pairs which were later to be studied in combinations were first investigated separately. In each case, the apparent total concentration of the acid—base pair in the aqueous phase (C_{tot}^{app}) was 0.050 M. The apparent concentration of a component in the aqueous phase is the concentration that would exist if the total amount of that component in the entire system were dissolved in the aqueous phase alone.

The experimental data for the buffer capacity, β, of the selected two-phase buffers are presented in Fig. 1, along with the theoretical buffer curves calculated by the equations derived previously [1]. In alkaline solutions (above

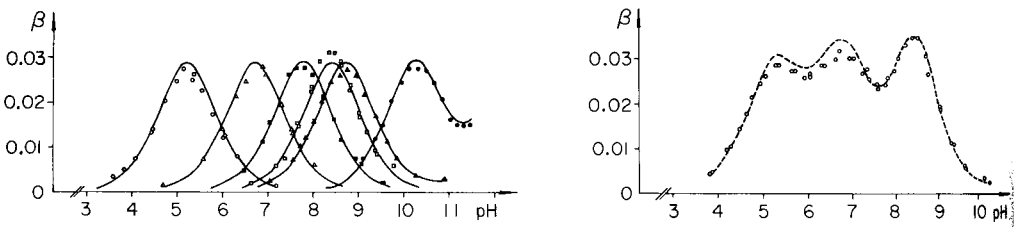

Fig. 1. Experimental data points and calculated curves (see text) for the buffer capacities of two-phase buffers containing propanoic acid (○), hexanoic acid (△), decanoic acid (□), 1-propylamine (●), 1-hexylamine (▲) and 1-decylamine (■). Solvent pair, 1-octanol—water (1 + 1). C_{tot}^{app} = 0.050 M.

Fig. 2. Buffer capacity as a function of pH for a two-phase buffer containing propanoic acid, hexanoic acid and decanoic acid: (○) experimental values; (---) calculated sum of buffer capacities of the corresponding single-component two-phase buffers. Solvent pair, 1-octanol—water (1 + 1). C_{tot}^{app} = 0.050 M for each acid—base pair.

pH 10), it was necessary to increase the calculated values by an amount β_{OH^-}, where $\beta_{OH^-} = 2.3\ C_{OH^-}$. It can be seen that the experimental and theoretical buffer capacities are in fairly good agreement.

Multicomponent two-phase buffers

Three systems were studied. The first buffer contained three organic acids: propanoic acid, hexanoic acid and decanoic acid. The last two acids are only very slightly soluble in water. The thermodynamic acid dissociation constants of the first two acids at 25°C have been reported to be pK (propanoic acid) = 4.874 [3] and pK(hexanoic acid) = 4.879 [4]. Although the pK value of decanoic acid has not been determined because of its extremely low solubility in water, it may be assumed that it does not differ appreciably from the values determined for the other two acids. (The difference in the pK values of acetic acid and nonanoic acid is only about 0.2 pK-units [5].)

Owing to the differentiating effect of the organic solvent, this buffer has a considerable buffer capacity ($\beta > 0.19\ C_{tot}^{app}$) in th pH range 4.3—9.4 (Fig. 2). The good agreement between the experimental values of the buffer capacity for this multicomponent system and the sum of the buffer capacities of the separate single-component buffers is noteworthy. It can be concluded that the rule of additivity of buffer capacities is valid for this system.

The second buffer tested contained three organic bases: 1-propylamine, 1-hexylamine and 1-decylamine. The last two amines are very slightly soluble in water. The corresponding thermodynamic acid dissociation constants at 25°C are 10.69 [6], 10.64 [7] and 10.64 [7], respectively. Because of the differentiating effect of the organic solvent, this system has a considerable buffer capacity at pH values higher than 6.8 (Fig. 3). Again, there is good agreement between the experimental values of the buffer capacity for this multicomponent system and the sum of the buffer capacities of the corresponding single-component buffers, so that the rule of additivity of buffer capacities is valid in this case also.

The third buffer tested contained one organic acid (hexanoic acid) and one organic base (1-hexylamine). This buffer exhibits a considerable buffer capacity in the pH ranges 5.1—7.2 and 8.1—10.3 (Fig. 4). However, Fig. 4 also shows a large difference between the experimental values for β and those calculated from the buffer curves of the corresponding single-component systems. The assumption is that this difference is due to a considerable extraction of the ion-pair

$$[CH_3(CH_2)_4COO^-]_{aq} + [CH_3(CH_2)_5NH_3^+]_{aq} \rightleftharpoons [CH_3(CH_2)_4COO^-, CH_3(CH_2)_5NH_3^+]_{org}$$ (Equilibrium constant K_d)

Direct calculation of buffer capacity in this case is very complicated. It is much simpler to calculate first the apparent total concentration of the base (C_B^{app}) as a function of the pH and then to calculate the buffer capacity from the equation

$$\beta = \lim_{\Delta pH \to 0} (\Delta C_b^{app}/\Delta pH) \qquad (1)$$

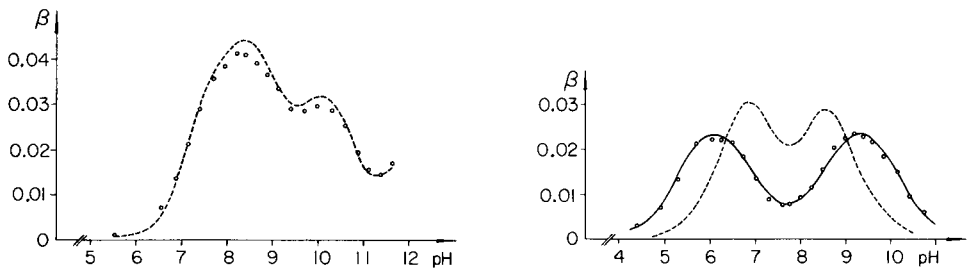

Fig. 3. Buffer capacity as a function of pH for a two-phase buffer containing 1-propylamine, 1-hexylamine and 1-decylamine: (○) experimental values; (---) calculated sum of buffer capacities of the corresponding single-component two-phase buffers. Solvent pair, 1-octanol—water (1 + 1). C_{tot}^{app} = 0.050 M for each acid—base pair.

Fig. 4. Buffer capacity as a function of pH for a two-phase buffer containing hexanoic acid and 1-hexylamine: (○) experimental values; (---) calculated sum of buffer capacities of the corresponding single-component two-phase buffers; (——) values calculated by equations derived in this work. Solvent pair, 1-octanol—water (1 + 1). C_{tot}^{app} = 0.050 M for each acid—base pair.

The values of C_b^{app} are calculated from the equation

$$C_b^{app} = c_A \left[(K_p)_B \frac{R}{S} + \frac{R}{S} + 1 \right] + c_A^2 K_d \frac{R}{T} \quad (2)$$

where $c_A = -(T/2K_d) + [(T^2/4K_d^2) + (C_{tot}^{app}\, T/K_d R)]^{\frac{1}{2}}$ (3)

$$R = 1 + [a_H/K_A] + [(K_p)_A\, a_H/K_A] \quad (4)$$

$$S = 1 + [a_H/K_B] + (K_p)_B \quad (5)$$

$$T = 1 + [K_B/a_H] + [(K_p)_B\, K_B/a_H] \quad (6)$$

and $K_A = a_H\, c_A/c_{HA}$, $K_B = a_H\, c_B/c_{HB}$, $(K_p)_A = (c_{HA})_{org}/c_{HA}$, $(K_p)_B = (c_B)_{org}/c_B$, $K_d = (c_{A,HB})_{org}/c_{A,HB}$, $a_H = 1 \times 10^{-pH}$. In these equations HA stands for hexanoic acid, B for 1-hexylamine and A,HB for the corresponding ion pair. For simplicity, the charges of individual ions and "aq" for concentrations in the aqueous phase are omitted.

Equations (2)—(6) are valid only in the case of equal phase volumes and equal apparent total concentrations of the two acid—base pairs. They are derived from the following mass-balance equations: $c_A\, R = c_{HB}\, T = c_B\, S$; $C_{tot}^{app} = c_A\, R + K_d\, c_A\, c_{HB}$, $C_b^{app} = c_A + c_B + (K_p)_B\, c_B + K_d\, c_A\, c_{HB}$.

The solution of eqns. (1)—(6) for C_{tot}^{app} = 0.050 M, pK_A = 4.75, pK_B = 10.64, log $(K_p)_A$ = 2.06, log $(K_p)_B$ = 2.05 and log K_d = 2.08, gives values of β which are in very good agreement with the experimental values over the entire pH range investigated (Fig. 4). The constants K_A and K_B were taken from the literature [4, 7] and recalculated for I = 0.15; the constants $(K_p)_A$, $(K_p)_B$ and K_d were determined experimentally in this work. Thus the general rule of additivity of buffer capacities is not valid in this case, because of the considerable extraction of the ion pair (A^-, HB^+).

It can be concluded that single-component two-phase buffers may be combined to give multicomponent two-phase buffers which possess considerable buffer capacity over a wide pH range. The capacity curves of these buffers may be calculated or determined experimentally.

The authors are grateful to the Serbian Republic Research Fund for financial support.

REFERENCES

1 T. J. Janjić and E. B. Milosavljević, Anal. Chem., 50 (1978) 597.
2 T. J. Janjić and E. B. Milosavljević, Bull. Soc. Chim. Beograd, 43 (1978) 553.
3 H. S. Harned and R. W. Ehlers, J. Am. Chem. Soc., 55 (1933) 2379.
4 J. F. Dippy, J. Chem. Soc., (1938) 1222.
5 G. Kortüm, W. Vogel and K. Andrussow, Dissociation Constants of Organic Acids in Aqueous Solution, Butterworths, London, 1961, pp. 241, 249.
6 L. H. Sommer and J. Rockett, J. Am. Chem. Soc., 73 (1951) 5130.
7 C. W. Hoerr, M. R. McCorkle and A. W. Ralston, J. Am. Chem. Soc., 65 (1943) 328.

Analytica Chimica Acta, 107 (1979) 365—371

DETERMINATION OF OXYGEN IN TERNARY URANIUM OXIDES BY A GRAVIMETRIC ALKALINE EARTH ADDITION METHOD

TAKEO FUJINO* and HIROAKI TAGAWA

Chemistry Division, Japan Atomic Energy Research Institute, Tokai-mura, Ibaraki-ken (Japan)

(Received 9th October 1978)

SUMMARY

The applicability of a gravimetric method based on alkaline earth metal addition for the determination of oxygen in ternary uranium oxides of the type M—U—O (M=La, Ce and Th) is described. The oxide sample is mixed with MgO or $Ba_{2.8}UO_{5.8}$ and heated in air under suitable conditions. Because uranium is completely oxidized to the hexavalent state during the reaction, oxygen can be determined from the weight change. Oxygen in $La_yU_{1-y}O_{2+x}$ is determined up to $y = 0.8$ with a standard deviation for x of ±0.006 with MgO. For $Th_yU_{1-y}O_{2+x}$, the value of x is determined with $Ba_{2.8}UO_{5.8}$ with a standard deviation of ±0.01 at $y = 0.8$. For $Ce_yU_{1-y}O_{2+x}$, the method can be applied only for low cerium concentrations where $y = 0$—0.2; the value for x with $Ba_{2.8}UO_{5.8}$ at $y = 0.2$ showed a standard deviation of ±0.002.

Non-stoichiometry occurs frequently in ternary uranium oxides, i.e., mixed oxides with uranium and another metal. The determination of oxygen in these oxides is of importance because their physical, chemical and/or thermodynamic properties often vary considerably with the extent of the oxygen non-stoichiometry.

Wet chemical methods, which involve the determination of U(IV) and U(VI) ratios by titrimetry [1], coulometry [2] or polarography [3] after dissolution of the samples in a non-oxidizing acid, are currently used. The precision of the redox titration methods, which seem to be the most widely applied, is ±0.003 for the O:U ratios in samples of $UO_{2.02}$ to U_3O_8 in an excellent case [1], but in routine use it is of the order of ±0.01—0.02 [4]. Methods which involve measurements of gas volume [5] or weight change during oxidation or reduction to a well established composition e.g. U_3O_8 or UO_2 cannot be applied to ternary uranium oxides (although the methods give better accuracies [6]) because of lack of knowledge of O/(M+U) ratios for ternary oxides where M indicates the foreign metals. Difficulties arise because the uranium in mixed oxides is not always oxidized to the hexavalent state by heating in air or an oxygen atmosphere, and is not reduced to the tetravalent state by heating in hydrogen [7, 8].

A previous paper [9] presented a simple gravimetric method in which the

exact hexavalency of uranium in alkaline earth uranates over certain continuous ranges of alkaline earth metal to uranium ratios was used to determine oxygen in oxide samples. The method can be used for uranium oxides, and for ternary uranium oxides having an alkaline earth element as the foreign metal, with a precision of ±0.0008 in the values for x in UO_{2+x} and $Mg_yU_{1-y}O_{2+x}$ (with $y = 0.2$ and 0.25) test samples. This method is now extended to the determination of oxygen in ternary uranium oxides with tri- or tetravalent metals which bear a close resemblance in nature to solid solutions [10]. Analytical conditions were examined for compounds in the La—U—O, Ce—U—O and Th—U—O systems.

Method of analysis

The present method is based on the fact [9] that uranium is hexavalent in alkali and/or alkaline earth uranates formed in air at 700—900°C; the hexavalency is conserved in continuous ranges of the M/U ratios (M = alkali or alkaline earth metals) between certain discrete M/U values. Thermodynamic considerations lead to the conclusion that two phase mixtures of the hexavalent uranates should exist in these continuous ranges [9]; the stability of the hexavalent uranium in the solid oxides increases in the presence of alkali or alkaline earth metal ions. If the hexavalency is retained for ternary uranium oxides with trivalent or tetravalent metals when these oxides are mixed with magnesium oxide and heated in air, the following reactions will take place:

$$M_y^{3+}U_{1-y}O_{2+x} + p\cdot MgO + 0.5\,(1-x-1.5y)\,O_2 = [Mg_pM_y^{3+}U_{1-y}O_{3+p-1.5y}] \quad (1)$$

$$M_y^{4+}U_{1-y}O_{2+x} + p\cdot MgO + 0.5\,(1-x-y)\,O_2 = [Mg_pM_y^{4+}U_{1-y}O_{3+p-y}] \quad (2)$$

where p is the mixing ratio, and M^{3+} and M^{4+} represent trivalent and tetravalent metal ions, respectively; the square brackets indicate that the chemical formulae are merely bulk compositions. Equations (1) and (2) show that the weights of the products are increased by $(1-x-1.5y)/2$ and $(1-x-y)/2$ mol of oxygen per mol of $M_y^{3+}U_{1-y}O_{2+x}$ and $M_y^{4+}U_{1-y}O_{2+x}$, respectively. Thus, from the weight difference, the value of x can be obtained for a known concentration of the foreign metal; of course, samples are not confined to compounds of the form $M_y^{3+}U_{1-y}O_{2+x}$ and $M_y^{4+}U_{1-y}O_{2+x}$ and alkaline earth compounds can be used instead of MgO. In alkaline earth metal—lanthanide element—uranium—oxygen systems [11—14], uranium is in the hexavalent state in compounds formed by heating in air at reaction temperatures of 500—1280°C.

EXPERIMENTAL

Apparatus and chemicals

Samples were prepared in vacuum and in hydrogen in a vacuum furnace with tantalum heating elements and in a SiC tube furnace, respectively. The muffle furnace and x-ray diffraction apparatus have been described [9].

U_3O_8 and UO_2 were prepared as described earlier [9]. The x values in UO_{2+x} were calculated from the relation $a_0 = 5.4704 - 0.094x$, where a_0 is the lattice constant [15]. Reagent-grade magnesium oxide and thorium dioxide, and 99.99% purity lanthanum sesquioxide and cerium dioxide (Shinetsu Chemical Co. Ltd.) were heated in air at 1000°C before use.

Barium uranate, $Ba_{2.8}UO_{5.8}$, was prepared by heating a mixture of calculated amounts of U_3O_8 and $BaCO_3$ in air at 1200°C for 24 h. The product was re-ground (agate mortar) and re-heated at 1200°C to complete the reaction. The solid solution, $Th_yU_{1-y}O_2$, with a stoichiometric oxygen content, was prepared by hydrogen reduction at 1000°C of the urania—thoria solid solution formed by heating pellets of UO_2 and ThO_2 mixtures at 1300°C at 5×10^{-6} mm Hg.

General procedure

Weigh the uranium oxide (0.5—2 g) and a calculated amount of the alkaline earth compound on a microbalance so that the alkaline earth metal to uranium atom ratio is between 1 and 3. Mix the components as described earlier [9].

Weigh 0.5—2 g of the UO_{2+x} standard sample, and mix with a weighed amount of the alkaline earth compound; transfer the mixture into crucibles and correct for moisture content as before [9]. The subsequent heating and weighing procedure has been described [9].

RESULTS AND DISCUSSION

To examine the applicability of this method, it is necessary that standard samples, $M_yU_{1-y}O_{2+x}$, be available or that the values of x and y can be determined by another method. Standard samples could not be prepared except for the Th—U—O system, and the precise determination of the composition by an alternative method was practically impossible. The gross compositions of the La_2O_3—UO_{2+x}, ThO_2—UO_{2+x} and CeO_2—UO_{2+x} mixtures were therefore examined because the value of x in UO_{2+x} could be obtained by the x-ray method. For these compounds, the reactions are

$$\frac{y}{2} \cdot La_2O_3 + (1-y) \cdot UO_{2+x} + p \cdot MgO + 0.5\,(1 - x - y + xy)\,O_2 = [Mg_pLa_yU_{1-y}O_{3+p-1.5y}] \quad (3)$$

$$y \cdot MO_2 + (1-y) \cdot UO_{2+x} + p \cdot MgO + 0.5\,(1 - x - y + xy)\,O_2 = [Mg_pM_yU_{1-y}O_{3+p-y}] \quad (4)$$

where M represents Th and Ce.

The results for lanthanum uranium oxides, which are expected to show the behavior typical of the ternary uranium oxides containing trivalent ions, are shown in Table 1. The transfer of all of the mixtures prepared (3.186400 and 3.975930 g, respectively) to the crucibles is not required. Correction for the water absorbed during the mixing process is, however, essential because it causes significant systematic errors. The correction was made as described

TABLE 1

Determination of the x value[a] of UO_{2+x} in mixtures of La_2O_3 and UO_{2+x} with MgO as the compound added

Value of y in $y/2 \cdot La_2O_3 + (1-y) \cdot UO_{2+x}$	Mixture added to each crucible[b] (g)	Weight corrected for moisture (g)	Weight after heating (g)	Value of x (from eqn. 5)
0.2086	0.648130	0.646660	0.671340	0.0062
	0.694860	0.693284	0.719630	0.0102
	0.955125	0.952959	0.989170	0.0103
	0.828885	0.827005	0.858560	0.0064
				Av. = 0.008 ±0.002
0.8000	0.568045	0.565427	0.572315	−0.0045
	1.299465	1.293477	1.308985	0.0105
	1.012585	1.007919	1.020010	0.0100
	1.001210	0.996596	1.008590	0.0070
				Av. = 0.006 ±0.006

[a]The x value of UO_{2+x} is 0.007 (±0.002) by the x-ray method. Molar mixing ratios, MgO: La_2O_3:$UO_{2.007}$, were 2.0452:0.1043:0.7915 and 2.0017:0.4000:0.2000 for y = 0.2086 and 0.8000, respectively. Heating conditions were 900°C (50 h) then 800°C (50 h).
[b]After grinding.

previously [9]. The correction for UO_{2+x} was carried out by comparing the values of x for standard UO_{2+x} samples from this method with those from the x-ray method. Because the weight of UO_{2+x}, W, in the test sample is known and the weight increase, ΔW, due to eqn. (3) has been obtained as the difference between the corrected weight and the weight after heating, the value of x in the mixtures of La_2O_3 and UO_{2+x} is given by

$$15.9994\,(1-x)\,W = (270.0278 + 15.9994x)\Delta W \qquad (5)$$

The average values obtained for x, 0.008 and 0.006 respectively are in good agreement with the x-ray value (0.007).

The above results are for mixtures of La_2O_3 and UO_{2+x}. However, from phase rule considerations, different compounds are not formed, regardless of the nature of the starting materials if their bulk La/U ratio is the same and the reaction is made in air (open system) at the same temperature. The results in Table 1 therefore show that the oxygen in lanthanum uranium oxides can be determined with magnesium oxide as an addition compound. The standard deviation for the samples of higher y value is three times that for the other samples because of the smaller amount of UO_{2+x} in the former mixture.

Results for thorium uranium oxides are shown in Tables 2 and 3. Table 2 shows the values of x in UO_{2+x} in mixtures of ThO_2 and UO_{2+x} with mixing ratios ranging from 0.1009 to 0.8015: the x value increases with increasing y

TABLE 2

Determination of the x value of UO_{2+x} in mixtures of ThO_2 and UO_{2+x} with MgO as the compound added

Value of y in $y \cdot ThO_2 + (1-y) \cdot UO_{2+x}$	MgO molar ratio[a]	x value[b]	Standard deviation
0.1009	2.0082	0.007	±0.001
0.2004	2.0008	0.007	±0.001
0.4005	2.0065	0.010	±0.003
0.8015	1.9883	0.039	±0.003

[a]Per mole of normalized sample mixture.
[b]Average of 3 determinations. The x value from the x-ray method is 0.007±0.002. Heating conditions: 900°C (50 h) then 800°C (50 h) in air. Correction for moisture was made for MgO, ThO_2 and a UO_{2+x} standard sample.

TABLE 3

Determination of oxygen in standard samples of $Th_yU_{1-y}O_{2.000}$ solid solutions

y value	Compound added	Molar ratio added[a]	x value[b]	Standard deviation
0.2012	MgO	2.0111	0.054	±0.008
0.4847	MgO	2.0019	0.05	±0.01
0.8001	MgO	2.0000	0.13	±0.03
0.2012	$Ba_{2.8}UO_{5.8}$	0.6663	0.001	±0.003
0.4847	$Ba_{2.8}UO_{5.8}$	0.6648	−0.001	±0.006
0.8001	$Ba_{2.8}UO_{5.8}$	0.6626	0.01	±0.01

[a]Per mol of solid solution.
[b]Average of 3 determinations. The x value in $Th_yU_{1-y}O_{2+x}$ will be very nearly zero. Heating conditions: 900°C (50 h) then 800°C (50 h) in air. Correction for moisture was made for MgO (or $Ba_{2.8}UO_{5.8}$), ThO_2 and a UO_{2+x} standard sample (x = 0.007 ± 0.002).

value, which may be due to insufficient oxidation power of the magnesium ions. With magnesium oxide as addition compound, uranium is not completely oxidized to U(VI) under the present heating conditions in systems containing thorium(IV) ions.

Table 3 shows the results of a series of experiments with $Th_yU_{1-y}O_2$ solid solutions and magnesium oxide. Although, as described above, there should be no difference in the compounds formed by the reaction (heating in air) of magnesium oxide with $Th_yU_{1-y}O_2$ or with a mixture of ThO_2 and UO_{2+x} provided that the metal atom ratio is the same in both mixtures, it seemed worthwhile to verify this thermodynamic prediction practically. The urania–thoria solid solutions used were prepared by heating pellets prepared from mixtures of ThO_2 and UO_{2+x} in vacuum (5×10^{-6} mm Hg) at 1300°C for 15 h followed by reduction of the products in hydrogen at 1000°C for 10 h. The compositions are therefore reasonably estimated to be $Th_yU_{1-y}O_{2.000}$.

However, the x values with magnesium oxide are not zero; the value increases with y, as in Table 2, and uranium in the thorium uranium oxides is not oxidized completely to uranium(VI) by magnesium oxide. In this situation, $Ba_{2.8}UO_{5.8}$ was used as the addition compound; barium is more ionic than magnesium and was expected to lead to more complete oxidation to uranium(VI) in the reactions. The use of $Ba_{2.8}UO_{5.8}$ (a mixture of Ba_2UO_5 and Ba_3UO_6) stems from the fact that hygroscopic barium oxide tends to co-exist in Ba_3UO_6 which is the highest Ba/U compound in the Ba—U—O system. Table 3 shows that the x values obtained with $Ba_{2.8}UO_{5.8}$ are zero within the standard deviations, so that the oxygen in thorium uranium oxides can be determined if $Ba_{2.8}UO_{5.8}$ is used. Magnesium oxide is not applicable for this system. The larger standard deviations in Table 3 may result from a smaller reactivity of the sintered $Th_yU_{1-y}O_2$.

Table 4 presents the results for cerium uranium oxides. In this system, since preparation of the solid solutions of composition $Ce_yU_{1-y}O_{2.000}$ was very difficult, the determination was also carried out for the x value of UO_{2+x} in mixtures of CeO_2 and UO_{2+x}. The value of x obtained increases with y value for the determinations involving magnesium oxide; this may be characteristic of the determination of oxygen in tetravalent metal containing uranium oxides when magnesium oxide is used. The x value diminishes with increasing y value when $Ba_{2.8}UO_{5.8}$ is used. This effect can be explained if oxygen non-stoichiometry occurs in cerium dioxide; if the cerium dioxide has the composition $CeO_{1.990}$, x values of 0.008 and 0.004, which agree with the x-ray value 0.007±0.002 within standard deviations, are obtained in contrast to the values shown in Table 4. The lattice constant of cerium dioxide used was 5.4111 ± 0.0002 Å, in accord with the values of Bevan and Kordis [16] (5.4110 Å) and Mulford and Ellinger [17] (5.4112 Å), but Bevan and Kordis assumed the composition to be $CeO_{2.000}$. Therefore, the discrepancy may result from a systematic error in the present method; this error does not appear at $y = 0.2$ and the method can be used for cerium uranium oxides at cerium concentrations between $y = 0$ and 0.2.

TABLE 4

Determination of the value of x in UO_{2+x} for mixtures of CeO_2 and UO_{2+x}

y value[a]	Compound added	Molar ratio[b] added	x value	Standard deviation
0.2002	MgO	2.0101	0.005[c]	±0.001
0.5013	MgO	2.0121	0.011[c]	±0.002
0.7997	MgO	1.9972	0.017[c]	±0.007
0.7999	MgO	0.4027	0.020[c]	±0.006
0.1998	$Ba_{2.8}UO_{5.8}$	0.6537	0.005[d]	±0.002
0.8004	$Ba_{2.8}UO_{5.8}$	0.6586	−0.027[d]	±0.007

[a]For normalized mixture, $y \cdot CeO_2 + (1-y) \cdot UO_2$. [b]Per mole of the normalized sample mixture. [c]Average of 3 determinations. [d]Average of 4 determinations.

In conclusion, the applicability of the present method may be summarized as follows. For the La—U—O system, magnesium oxide gives good results as shown for the ternary uranium oxides of alkaline earth elements [9]. The standard deviation at $y = 0.8$ is ca. ±0.006. For the Th—U—O system, magnesium oxide is incapable of oxidizing uranium completely to the hexavalent state, and $Ba_{2.8}UO_{5.8}$ should be used; the standard deviation at $y = 0.8$ is ca. ±0.01. The Ce—U—O system shows a systematic error which increases at higher cerium concentrations, but can be applied at lower cerium concentrations, $y = 0$—0.2; the standard deviation at $y = 0.2$ is ±0.002.

REFERENCES

1 D. R. Dharwadkar and M. S. Chandrasekharaiah, Anal. Chim. Acta, 45 (1969) 545.
2 R. W. Stromatt and R. E. Connally, Anal. Chem., 33 (1961) 345.
3 R. M. Burd and G. W. Goward, AEC-Reports WAPD-205 (1959).
4 See, e.g., U. Berndt, R. Tanamas and C. Keller, J. Solid State Chem., 17 (1976) 113.
5 T. L. Marken, A. J. Walter and R. J. Bones, AEC-Reports AERE-R 4608 (1964).
6 E. A. Schaefer and J. O. Hibbits, Anal. Chem., 41 (1969) 254.
7 R. Braun, S. Kemmler-Sack, H. Roller, I. Seemann and I. Wall, Z. Anorg. Allg. Chem., 415 (1975) 133.
8 S. Kemmler-Sack and I. Seemann, Z. Anorg. Allg. Chem., 409 (1974) 23.
9 T. Fujino, H. Tagawa, T. Adachi and H. Hashitani, Anal. Chim. Acta, 98 (1978) 373.
10 C. Keller, Gmelins Handbuch der anorganischen Chemie, Uran (Ergänzungsband, Teil c-3), Springer, Berlin, 1975, p. 213.
11 A. W. Sleight and R. Ward, Inorg. Chem., 1 (1962) 790.
12 G. Blasse, J. Inorg. Nucl. Chem., 38 (1976) 2126.
13 S. Kemmler-Sack and I. Hofelich, Z. Anorg. Allg. Chem., 388 (1972) 4.
14 S. Kemmler-Sack, Z. Anorg. Allg. Chem., 402 (1973) 232.
15 H. Nickel, Nukleonik, 8 (1966) 366.
16 D. J. M. Bevan and J. Kordis, J. Inorg. Nucl. Chem., 26 (1964) 1509.
17 R. N. R. Mulford and F. H. Ellinger, J. Phys. Chem., 62 (1958) 1466.

Analytica Chimica Acta, 107 (1979) 373—376

Short Communication

NEW UNIT FOR TRACE CONTENTS: Second Communication

O. G. KOCH

Chemisches Laboratorium, Neunkircher Eisenwerk AG, D-6680 Neunkirchen/Saar (West Germany)

(Received 12th September 1978)

In general, trace contents are stated in the units "per cent (%)" and "part per million (ppm)" [1—4], but with increasing demands for determinations of lower trace contents, certain difficulties arise in applying these units. On the one hand, the units % and ppm become increasingly impractical with decreasing contents at concentrations below ppm; on the other hand, differences of language oppose the logical derivation of even smaller units from the well-established ppm unit. These circumstances have led to several proposals [5—8] for the definition and statement of trace contents and ranges. These units proposed for trace contents, however, do not seem to be either expedient or practicable, as their lack of general acceptance indicates.

For this reason, the author proposed new units for trace contents in a previous paper [9]. With regard to the general interest of the theme, it was noted [9] that in the event of sufficient response the correspondence would be published in a summarized form. The interest shown by scientists was unexpectedly great, as was apparent from the many requests for reprints and the numerous comments. The results of this correspondence are summarized below, but first, for better understanding, the definition of the proposed new units for trace contents [9] is briefly recapitulated.

Definition of the proposed units

There is no doubt that the term ppm is used most frequently for the designation of trace contents. This must be attributed primarily to the fact that ppm has proved very serviceable and clear; the commonest trace contents can be stated with the ppm unit in simple numbers in contrast to the awkwardness of the per cent usage.

Because of the proven expediency of the ppm unit, there is an increasing tendency in the American literature for contents below 1 ppm to be given in the units ppb (part per billion; 10^{-7}%) and ppt (part per trillion; 10^{-10}%), which are derived logically and consistently from ppm (part per million; 10^{-4}%). However, the ppb and ppt units have not found universal application in the literature, although they seem just as expedient as the ppm unit, largely

because of the differences between the numbering systems in the U.S.A. and in Europe: 1 US-billion = 10^9 = 1 European milliard; 1 US-trillion = 10^{12} = 1 European billion; 1 European trillion = 10^{18}. These linguistic differences unavoidably lead to confusions and difficulties of understanding. Another source of confusion arises from the old, but still sporadically used, ppt unit meaning part per thousand (10^{-1}% or 1‰).

These difficulties can be easily avoided by the units proposed earlier [9]. The numerical concept needed for the definition of these units is derived from the connection between the internationally used "per cent" unit and the ppm unit. In percentage units, for example, 1% = 1 per cent = 1 part per 100 parts. Application to smaller units in logical sequence gives 1 part per thousand .... 1 ppm = 1 part per million = 1 part per 1000000 parts. If the million, billion, etc. in the ppm, ppb, etc. are replaced by the appropriate numbers 10^6, 10^9, etc., which stands for the amount of ballast (matrix), then at least the linguistic difficulties are eliminated.

The *quantity ratio of trace element to matrix* is thus the basis of the units for trace contents defined in the following paragraphs.

(a) *Fully written form.* The amount of ballast (matrix), which determines the level of the trace element content, is designated as the power of ten. For example, 1 ppm = 1 part per 1000000 parts = 1 pp10^6, or in the general form

Trace content = a parts per 10^x parts = a pp10^x

(b) *Partial logarithmic form.* Here the power of ten level of the trace element content, determined by the amount of ballast (matrix), is given in logarithmic form. For example, 1 ppm = 1 part per 1000000 parts = 1×10^{-6}. Substituting the negative logarithm for the factor 10^{-6} and applying a symbol analogous to the pH unit, namely pT (where T represents the word "trace") gives the form: 1 ppm = 1 pT 6. The general form is:

Trace content = a parts per 10^x parts = a $1/10^x$ = a 10^{-x} = a $(-\log 10^{-x})$ = a pT x

where a = quantity of trace element at a defined power of ten level; T = power of ten level of trace element; pT = negative logarithm of T; and x = numerical quantity for pT.

It must be emphasized that here only the power of ten is converted to the logarithm and that the first number a is never involved in the logarithmic conversion.

(c) *Full logarithmic form.* The trace element content is stated completely in logarithmic form, analogous to pH. From the preceding section, this gives the general form

Trace content = a 10^{-x} = $-\log$ (a 10^{-x}) = pX

where p = negative logarithm of the trace element content, and X = symbol of trace element.

This form of statement, however, has the disadvantage that the trace

contents measured must always be converted to their logarithms, in contrast to the simple measurement of pH by means of a pH meter without additional calculations.

Discussion

Numerical concepts appear to be the most expedient and significant for the designation of trace contents and trace ranges. Concepts in words e.g. mesotrace, millitrace, microtrace, ultratrace etc., should be avoided. Therefore, in the earlier communication [9], the use of the proposed unit, preferably in form (a) [a $pp10^x$] or form (b) [a $pT\,x$] as derived above, was recommended for its simplicity, adaptability and ready intelligibility.

Considerable interest was shown in these proposals, as indicated by the numerous letters received. In their comments, correspondents agreed with the author that: (a) the present situation should be improved; (b) there is a need for new units; (c) the proposed units are a practical solution to the problem. The results of the correspondence are summarized in Table 1. Most correspondents preferred the a $pp10^x$ notation because of its easy intelligibility and simple transition from the hitherto familiar ppm [10—16]; others preferred the a $pT\,x$ notation because of its simpler spelling and because it seemed desirable to have a clearer distinction from the ppm used at present [17—21]. The unit a $pp10^x$ found most favour (Table 1). This unit has already been applied sporadically in the literature in the fully written form, i.e. part per 10^9 [20] and in the proposed form a $pp10^x$ [21].

The comments received are a valuable contribution to the evaluation, choice and introduction of the proposed unit for general usage. They represent a realistic basis for proposing

a $pp10^x$

as the new unit for trace contents to the international organizations for acknowledgement and adoption.

TABLE 1

Result of the choice of the new unit

Proposed unit general form	a $pp10^x$	a $pT\,x$	pX
0.005 ppm Cu, stated in the new unit	5 $pp10^9$ Cu	5 pT 9 Cu	pCu 8.30
Share of votes (%)	68	32	0

The author thanks all correspondents for their interest and valuable comments. Particular thanks are due to Dr. A. Koch (Graz, Austria) for linguistic revision of the manuscript.

REFERENCES

1 O. G. Koch and G. A. Koch-Dedic, Handbuch der Spurenanalyse, Springer, Berlin, 2. Aufl. 1974.
2 G. H. Morrison, Trace Analysis: Physical Methods, Interscience, New York, 1965.
3 M. Pinta, Recherche et Dosage des Éléments Traces, Dunod, Paris, 1962.
4 E. B. Sandell, Colorimetric Determination of Traces of Metals, Interscience, New York, 3rd edn., 1959.
5 IUPAC, Anal. Chem. Division, Comm. Anal. Nomenclature, Recommendations on nomenclature of scales of working in analysis, IUPAC Inform. Bull. No. 18, February 1972; IUPAC Compendium of Analytical Nomenclature, Pergamon Press, Oxford, 1978.
6 G. Gottschalk, R. Kaiser, H. Malissa, J. Rendl, E. Schwarz v. Bergkampf, W. Simon, H. Spitzy, R. D. Werder and H. Zettler, Fresenius Z. Anal. Chem., 261 (1972) 1.
7 H. Kaiser, Pure Appl. Chem., 34 (1973) 35.
8 G. Tölg, Talanta, 19 (1972) 1489.
9 O. G. Koch, Anal. Chim. Acta, 82 (1976) 19.
10 H. Duetinger-Skrube, personal communication, May 1976.
11 H. Hecht, personal communication, June 1977.
12 P. Kramer II, personal communication, June 1976.
13 H. Meier, personal communication, June 1976.
14 F. Oehme, personal communication, June 1976.
15 E. Uhlemann, personal communication, June 1976.
16 J. Veselsky, personal communication, March 1977.
17 G. Jecko, personal communication, April 1976.
18 V. Jokl, personal communication, May 1976.
19 K. Schwabe, personal communication, May 1976.
20 P. Schiller, G. B. Cook, A. Kitzinger and E. Wölfl, Analyst, 97 (1972) 601.
21 M. L. Verheijke, Philips Tech. Rev., 34 (1974) 330.

Analytica Chimica Acta, 107 (1979) 377—381

Short Communication

DETERMINATION OF THE EQUIVALENCE POINT IN POTENTIOMETRIC TITRATIONS WITH GRAN'S FIRST METHOD USED TO TEST THE ELECTRODE RESPONSE

EBBE STILL*

Laboratory of Inorganic and Analytical Chemistry, Helsinki University of Technology, Otaniemi (Finland)

(Received 30th October 1978)

Summary. Gran's first method is compared to the standard addition (subtraction) method. It is shown that Gran's first method can be used to test the electrode response of, for example, a copper-selective electrode.

During recent years, the use of Gran plots [1] to evaluate the end-point in potentiometric titrations has attracted considerable interest. In principle, the method uses functions which transform the sigmoidal potentiometric titration curve to a linear form. The method makes it possible to calculate the value of the equivalence volume from several points of the titration curve by standard linear regression techniques. The functional transformations given by Gran require that the electrode system has a Nernstian response, and that the activity coefficients are constant during the titration.

The simple expressions given by Gran are approximations and an extension to weak acids has been derived without approximations [2]. The following additional requirements must then be fulfilled: (a) the electrode must be properly calibrated, i.e., the correct value of the standard potential of the electrode system has to be known; (b) the stability constant of the titration reaction must be known; (c) the correct concentration (titre) of the titrant must be known; and (d) the value of the autoprotolysis constant must be known.

The linear functions commonly called Gran functions were described by Gran in 1952 in his second article on the "Determination of the Equivalence Point in Potentiometric Titrations" [1]. In the first article in the series [3] published in 1950 he described a differential method in which $\Delta V/\Delta E$ was plotted as a function of V, where V denotes the added volume of titrant and E the measured potential.

In the present communication, Gran's first method is compared to the standard addition (subtraction) method, and the assumptions behind these

*Present address: Department of Chemistry, Åbo Akademi, SF-20500 Åbo 50, Finland.

techniques are discussed. It will be shown that Gran's first method in a more exact form can be used to test the electrode response of, for example, an ion-selective electrode.

A complexation reaction M + L = ML with the stability constant K_{ML} is considered. The initial concentration of the metal ion is denoted by C_M and the initial volume by V_0. The concentration of the titrant is denoted by C_L and the volume added by V. The consumption of titrant at the equivalence point is denoted by V_{eq}. The derivation is based on the conditions $C_M V_0/(V_0 + V) = [M] + [ML]$, $C_L V/(V_0 + V) = [L] + [ML]$, and $V_{eq} C_L = V_0 C_M$, which combine to give

$$C_L (V_{eq} - V)/(V_0 + V) = [M] - [L] \tag{1}$$

A complete titration reaction is assumed, so that the concentration of free ligand ions before the equivalence point and the concentration of metal ions after the equivalence point are negligible. *Before the equivalence point*, $[L] \ll [M]$, and the following expressions will determine the shape of the titration curve:

$$C_L (V_{eq} - V)/(V_0 + V) = [M] \tag{2}$$

$$E = Q \log [M] + E_0 \tag{3}$$

where $Q = RT \ln 10/zF$. Equation (2) is valid for two consecutive titration points, (V_i, E_i) and (V_{i+1}, E_{i+1}), so that

$$\frac{(V_0 + V_i)}{(V_0 + V_{i+1})} \frac{(V_{eq} - V_{i+1})}{(V_{eq} - V_i)} = \frac{[M]_{i+1}}{[M]_i} \tag{4}$$

Rearrangement of this equation, making use of the identity $V_{eq} - V_i = V_{eq} - V_{i+1} + V_{i+1} - V_i$, gives

$$V_{eq} - V_{i+1} = (V_{i+1} - V_i) \Big/ \left\{ \frac{(V_0 + V_i)[M]_i}{(V_0 + V_{i+1})[M]_{i+1}} - 1 \right\} \tag{5}$$

where $\log [M]_i/[M]_{i+1} = (E_i - E_{i+1})/Q$.

The formulae given in Gran's first paper can be derived from eqn. (5) by assuming that the dilution effect is negligible, and that the numerical value of ΔE is small so that the approximation $e^{\Delta E} = 1 + \Delta E$ is valid. Equation (5) will then be reduced to

$$V_{i+1} - V_{eq} = \{RT/zF\}\{(V_{i+1} - V_i)/(E_{i+1} - E_i)\} = RT\, \Delta V/zF\, \Delta E \tag{6}$$

or

$$\Delta V/\Delta pM = 2.30\, (V_{eq} - V_{i+1}) \tag{7}$$

Corresponding equations were given by Gran [3]. It will also be noted that the formulae for the standard subtraction (addition) method and eqn. (5) are equivalent [4].

After the equivalence point, L is present in excess, so that [M] ≪ [L]. Hence

$$C_L\,(V_{eq} - V)/(V_0 + V) = -[L] \tag{8}$$

The following expression is derived in an analogous way to eqn. (5)

$$V_{eq} - V_i = (V_i - V_{i+1}) \Big/ \left\{ \frac{(V_0 + V_{i+1})\,[L]_{i+1}}{(V_0 + V_i)\,[L]_i} - 1 \right\} \tag{9}$$

The law of mass action states that $[L] = [ML]/[M]\,K_{ML}$ where $[ML] = V_0\,C_M/(V_0 + V)$. Accordingly

$$V_{eq} - V_i = (V_i - V_{i+1})/\{([M]_i/[M]_{i+1}) - 1\} \tag{10}$$

The corresponding approximate formulae valid after the equivalence point are

$$V_{eq} - V_i = RT\,\Delta V/zF\,\Delta E \tag{11}$$

and

$$\Delta V/\Delta pM = 2.30\,(V_i - V_{eq}) \tag{12}$$

The stability constant K_{ML} denotes a conditional constant, consequently eqn. (10) is valid only if the numerical value of K_{ML} is unaltered during the titration; eqn. (10) does not contain the constant explicitly, but the equation is derived assuming a constant value of K_{ML}.

At this point it must be stressed that the derivation of these equations requires a stoichiometric titration reaction, constant activity coefficients during the titration, and Nernstian response of the electrode system. It should be noted that the slope of $RT\,\Delta V/zF\,\Delta E$ vs. V_i is affected neither by the concentration of the titrant solution nor by the standard potential. Before the equivalence point, the metal ion may take part in various side-reactions; the requirement is that α_M will remain constant during the titration. Analogously, after the equivalence point, α_L and α_{ML} must remain constant.

The expressions derived can be used for the location of the equivalence point in potentiometric titrations of the strong acid—strong base type. In the ideal case, the plot consists of one straight line with a slope of −1 (or of two straight lines with slopes of −1 and +1), intersecting the volume axis at the equivalence point. A drawback of the linear functions derived is that the expressions contain differences between consecutive readings and therefore the plot can be seriously affected by random errors in the readings.

The differential method described above is presented in its simplest form. The smoothing effect of averaging can be taken into account by rewriting eqns. (5) and (10). These expressions are valid for consecutive data pairs and the corresponding equations can be added. For example, the addition of n eqns. (10) yields

$$V_{eq} - \frac{1}{n}\sum_{r=i}^{i+n} V_r = \frac{1}{n}\sum_{r=i}^{i+n} (V_r - V_{r+1}) \Big/ \left\{ \frac{[M]_r}{[M]_{r+1}} - 1 \right\} \tag{13}$$

Another possibility is to combine data pairs farther away from each other.

The problem of testing ion-selective electrodes for Nernstian behaviour is a common one. Calibration is essential in analytical applications, and is very significant in solution chemistry for determination of the stability of metal chelates. An electrode system can be calibrated by a dilution technique starting with the strongest solution and finishing with the weakest one, or by the reversal technique [4]. These methods are suitable for solutions of low pM values; testing electrodes for higher pM values requires the use of metal buffers. The validity of the Nernst equation, which gives a linear plot with a slope of Q, can also be tested by a potentiometric titration. Another possibility is to use the expressions derived above to test the response of the electrode system.

The result of plotting the expressions (5) and (10) as a function of V will be a straight line with a slope of −1. A slight deviation from Nernstian response, which is common with many ion-selective electrodes, will result in a linear plot with a slope deviating from the correct value of −1, as can be seen from eqns. (6), (7), (11) and (12).

Behaviour of the copper-selective Selectrode

The theory outlined was used in testing a copper-selective Selectrode. The Cu—NTA system was chosen as the metal buffer system, as an anomalous behaviour for the electrode response has been reported for the system [5, 6]; it should be noted, however, that these results were obtained with different types of electrode. The surface of the electrode was prepared as described by Hansen et al. [7]. A high-purity Ag_2S—CuS mixture was used as the electroactiv material. A Metrohm piston buret was used to deliver the titrant, and the potentials were recorded with a Radiometer PHM 4 meter ($\mu(KNO_3)$ = 0.1 mol l temperature = 25°C). The pH value of the solution titrated was kept constant during the titration.

Figure 1 shows the linear plot obtained in a titration of 50 ml of a solution containing 0.00500 mol l^{-1} $CuSO_4$ solution at pH 5 (acetate buffer) with a 0.085 mol l^{-1} NTA solution. Before the equivalence point, eqn. (5) is plotted as a function of the volume added. In the buffer region, eqn. (10) is plotted as a function of V. This part of the curve is also reflected in the volume axis in order to obtain a plot similar to the Gran plot. The data pairs exhibit a slight scatter around the straight line because of random errors in the readings as discussed above. The result of the test was an almost ideal Nernstian response of the electrode pair with a slope of 29.6 mV/decade.

EDTA and NTA have been proposed as ligands in metal buffers for the calibration of copper-selective electrodes. These buffer systems are not optimal, as the species L and ML show side-reactions with hydrogen ion and hydroxide, respectively. Metal buffers with low pH sensitivity can be obtained by using ligands with pyridyl residues [8]. In this study, the Cu—NTA buffer system was chosen because it was intended to investigate the stability of Cu—NTA and ternary Cu—NTA—amino acid complexes with the Selectrode as pM sensor. The latter results are reported separately [9].

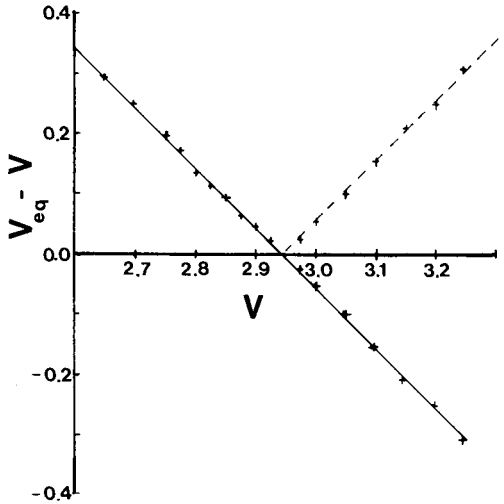

Fig. 1. Straight line(s) obtained when data from a titration of 50 ml of a solution containing 5.00×10^{-3} mol l^{-1} copper(II) ion at pH 5 with a 8.5×10^{-2} mol l^{-1} NTA solution are used to compute $V_{eq} - V$ from eqn. (5) (before the equivalence point) and eqn. (10) (after the equivalence point).

Thanks are due to Prof. Folke Ingman, The Royal Institute of Technology, Stockholm, for valuable discussions.

REFERENCES

1 G. Gran, Analyst, 77 (1952) 661.
2 F. Ingman and E. Still, Talanta, 13 (1966) 1431.
3 G. Gran, Acta Chem. Scand., 4 (1950) 559.
4 P. L. Bailey, Analysis with Ion-Selective Electrodes, Heyden, London, 1976.
5 G. Nakagawa, H. Wada and T. Hayakawa, Bull. Chem. Soc. Jpn., 48 (1975) 424.
6 G. J. M. Heijne and W. E. van der Linden, Anal. Chim. Acta, 96 (1978) 13.
7 E. H. Hansen, C. G. Lamm and J. Růžička, Anal. Chim. Acta, 59 (1972) 403.
8 G. Anderegg, in E. Wänninen (Ed.), Analytical Chemistry — Essays in Memory of Anders Ringbom, Pergamon Press, Oxford, 1977, p. 51.
9 E. Still, Anal. Chim. Acta, 107 (1979) 105.

Analytica Chimica Acta, 107 (1979) 383—386

Short Communication

DETERMINATION OF CHLORITE ION IN DILUTE SOLUTION BY PULSE POLAROGRAPHY

W. J. MASSCHELEIN*, M. DENIS and R. LEDENT

Laboratories of the Brussels' Intercommunal Waterboard, 764, Chaussée de Waterloo, 1180 Brussels (Belgium)

(Received 23rd August 1978)

Summary. Chlorite is determined in the range 0—1.3 mg l^{-1} by pulse polarography at pH 4.25—4.65. The detection limit is 0.05 mg l^{-1}.

The determination of low concentrations of chlorite, e.g. sodium chlorite, is of primary importance in the preservation of foodstuffs by chlorine dioxide. In drinking water particularly, the possibility of chlorite formation by the reduction $ClO_2 + 1e = ClO_2^-$ must be considered. There are strong indications that with most organic products, the oxidation stops at this stage [1]. The question is of fundamental importance because chlorite is toxic and can cause methemoglobinaemia, the LD 50 for rats being 140 mg kg^{-1} body weight [2]. Although the use of chlorine dioxide at the usual concentrations is not likely to cause any harmful concentration of chlorite in foodstuffs [3], there is still a need for reliable and selective analytical methods for trace concentrations.

A study of the literature [1, 4] shows that the available colorimetric and titrimetric methods usually lack selectivity as well as sensitivity. Therefore, electrochemical methods were considered. The chemistry of chlorite being related to that of the oxychlorine compounds in general, the selectivity of the method is essential.

Electrochemical methods for the determination of chlorites

The d.c. polarographic characteristics of the chlorite ion have been studied by Hartley and Adams [5]. In slightly acidic medium (pH 4.2—4.5), a well-defined diffusion-controlled but irreversible wave is found at a half-wave potential of —0.33 V versus SCE. The reaction at the electrode is globally expressed as $HClO_2 + 4e + 3H^+ = Cl^- + 2\ H_2O$. The diffusion current is proportional to the concentration in the range 0.2—2 × 10^{-3} M, or 13.5—135 mg ClO_2^- l^{-1}. At lower concentrations the signal is affected by capacitive currents but semi-quantitative estimates remain possible at concentrations down to 1 mg l^{-1}. With increasing pH, the wave gradually stretches out and the half-wave moves to more negative values [5].

In a phosphate buffer of pH 6.9—7.0, the polarographic determination of

chlorite is possible if chlorine and chlorine dioxide are absent. The detection limit is in the neighbourhood of 2 mg l^{-1}, the precision [6] is about 0.5 mg l^{-1}. The half-wave potential is about 0.9 V and KCl is a good supporting electrolyte; better defined characteristics are claimed in presence of lanthanum trichloride [4, 6, 7].

In alkaline medium of pH 11—14.5, the primary irreversible wave observed in neutral medium disappears gradually and a secondary chlorite wave then develops [8]. Appearing at pH 10—11, it increases suddenly when the pH attains 13.8—14. This complex wave appears to be only partially related to chlorite. It seems that other compounds such as traces of iron play a determining role, according to the mechanism $Fe^{2+} \xrightarrow{ClO_2^-} Fe^{3+} \xrightarrow{\text{(electroreduction)}} Fe^{2+}$. According to Gierst et al. [10], the mechanism is a catalysed reduction of chlorite in 0.1 M NaOH. Similarly, vanadium(V) is reduced to $V(OH)_3$ at a mercury electrode [11], and the process also develops a secondary wave of chlorite. The analytical possibilities of using these catalytic techniques for determination of traces of chlorite have not been examined Anodic oxidation at a platinized-platinum microelectrode has been proposed [12, 13]; the sensitivity of these voltammetric techniques is about 2 mg l^{-1}.

On the basis of previous techniques, it appeared that the chlorite could be determined by advanced polarographic methods with elimination of residual currents.

Experimental

A Bruker E 100 d.c./pulse polarograph was used in the pulse mode under the following conditions: time constant, 0.1 s; capillary diameter, 70—80 μm; 0—1.6 V scanning at a rate of 20 mV s^{-1}; pulse sequence and mercury drop life-time, 0.5 s; current scale, 20 μA.

In the final method, the chlorite-containing sample (at least 100 ml) is made 0.04 M in sodium acetate, 0.06 M in acetic acid and 0.01 M in ammonium sulphate. The final pH of the medium is 4.4—4.5. The Bruker (Metrohm) cell is filled with a 25-ml aliquot through which nitrogen is bubbled during 10 min at a rate of 5 ml s^{-1}.

Any chlorine and chlorine dioxide present are stripped by the nitrogen bubbling before the scan. The interference of trace amounts of chlorine would only be minor, as the addition of ammonium sulphate forms chloramines. If necessary, the interferences by other oxidants and by heavy metals could probably be eliminated by passing the solution through a cationic resin such as Chelex 100 in its calcium form.

Results and discussion

The polarograms obtained are illustrated in Fig. 1(a). Although they are not very well shaped, the direct curves allow as little as 0.05 mg ClO_2^- l^{-1} to be detected. Subtraction of the blank polarogram obtained for zero chlorite concentration from the sample polarogram gives the curves illustrated in Fig. 1(b). At pH 4.5, if the total concentration of chlorite is about 10^{-5} M, only about 10^{-8} M can be present as $HClO_2$, which is highly hydrated and not

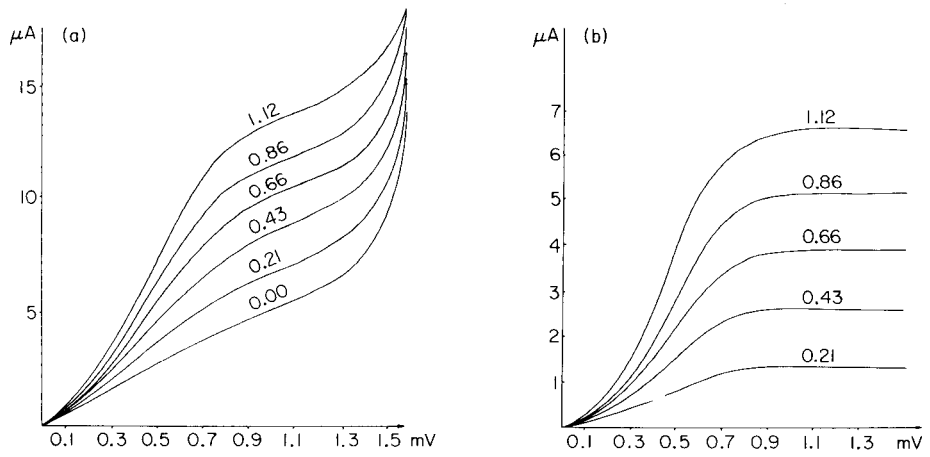

Fig. 1. (a) Polarograms of chlorite obtained in the pulse mode; (b) curves obtained after subtraction of the blank polarogram.

significantly volatile. At the 1-mg l^{-1} level of chlorite, the loss by volatilization is less than 5% even on prolonged stripping for 3 h. If chlorous acid or chlorine dioxide is formed significantly, a secondary wave develops as shown in Fig. 2 at pH 4.00. The error caused by change in pH is below 3% if the pH is maintained between 4.25 and 4.65 and the analysis is based on the apparent diffusion current as described.

The apparent diffusion current measured after the differential construction,

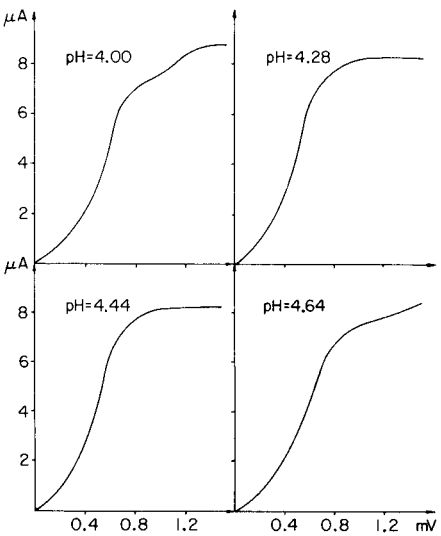

Fig. 2. Polarograms for chlorite (1.45 mg l^{-1}) in the pH range 4—4.65.

plotted against the concentration of the chlorite ion in solution, gives a straight-line correlation over the range 00—35 mg l^{-1} with a slope of 5.8 μA mg^{-1} of chlorite. With the equipment used, the detection limit is 0.05 mg l^{-1} (S/N = 2). The regression line for the linear relationship is ClO_2^- (mg l^{-1}) = $(I - 0.1)/5.8$, where I is the apparent diffusion current (μA).

The method avoids most likely interferences, and in normal use the errors are less than 5%.

REFERENCES

1 W. J. Masschelein, Chlorine Dioxide, Ann Arbor Press, Michigan, 1978.
2 J. Musil, Sb. Vys. Sk. Chem. Technol. Praze Technol. Vody, 8 (1965) 327, Chem. Abstr., 65 (1966) 1960.
3 W. J. Masschelein, Communication at the Symposium on the Use of Oxidants in Water Disinfection, University of Karlsruhe, September 1978.
4 W. Masschelein, Le Bioxyde de Chlore et le Chlorite de Sodium, Dunod, Paris, 1969.
5 A. M. Hartley and A. C. Adams, J. Electroanal. Chem., 6, (1963) 460.
6 A. Ruis and A. M. Gorriz, An. R. Soc. Esp. Fis. Quim., Ser. B, 46 (1950) 683.
7 E. Werner and N. Konopik, Fresenius Z. Anal. Chem., 152 (1956) 203.
8 N. Konopik and E. Werner, Monatsh. Chem., 86 (1955) 937.
9 R. Delevi, J. C. Kreuzer and H. Moreira, Anal. Chem., 43 (1971) 784.
10 L. Gierst, L. Vandenberghen and E. Nicholas, J. Electroanal. Chem., 12 (1966) 462.
11 R. L. Birke and Th. D. Santa Cruz, J. Electrochem. Soc., 120 (1973) 366.
12 G. Raspi and F. Pergola, J. Electroanal. Chem., 20 (1969) 419.
13 O. Schwarzer and R. Landsberg, J. Electroanal. Chem., 14 (1967) 339.

Analytica Chimica Acta, 107 (1979) 387—390

Short Communication

DETERMINATION OF CARBON DISULFIDE IN WATER AT THE 1 $\mu g\ l^{-1}$ LEVEL BY DIFFERENTIAL PULSE POLAROGRAPHY

HUA-CHING HU

FMC Corporation, P.O. Box 8, Princeton, New Jersey 08540 (U.S.A.)

(Received 7th November 1978)

Studies of the contamination of waters by carbon disulfide require simple, sensitive and accurate methods of analysis. The classical colorimetric method [1, 2] based on formation of copper diethyldithiocarbamate appears to be widely used. The gas chromatographic method [3, 4] is primarily used for determining carbon disulfide in gas streams or atmospheres; the gas sample can be analyzed directly or carbon disulfide can be collected on charcoal and then extracted with toluene or benzene to improve sensitivity. The polarographic method [5—7] is based on formation and measurement of diethyldithiocarbamate. The sensitivity of these methods is usually in the low mg l^{-1} range.

The method described below is significantly more sensitive than those reported, being viable down to 1 $\mu g\ CS_2\ l^{-1}$. This improved sensitivity results primarily from the use of a gas purging step to pre-concentrate the carbon disulfide in ethanol and diethylamine, and from the application of differential pulse polarographic measurements.

Experimental

Apparatus. The PAR (Princeton Applied Research Corporation) Model 174A Polarographic Analyzer used was equipped with a M174/170 drop timer, a PAR polarographic cell and a Hewlett-Packard 7040A x-y recorder. A platinum foil counter electrode and a saturated calomel reference electrode were employed. The bottom of the polarographic cell was modified by attaching a two-way Teflon capillary stopcock for washing.

The absorption system (Fig. 1) is a modification of the design of Bellar and Lichtenberg [8]. The capacity of the sample vessel is 350 ml when filled to the level just below the first bulb; this is suitable for samples containing 1—20 $\mu g\ CS_2\ l^{-1}$. A 50-ml sample vessel can be used for samples of higher concentrations. The standard inlet port is made from a Kontes socket (5 mm o.d.) with a Teflon septum. The absorbing tube (6—8-ml capacity) is connected to the sample vessel by a Teflon sleeve. The tubes and frits must be cleaned daily to ensure efficient contact between gas and solution.

Standard solutions. Initially, stock solutions containing 300—400 μl of

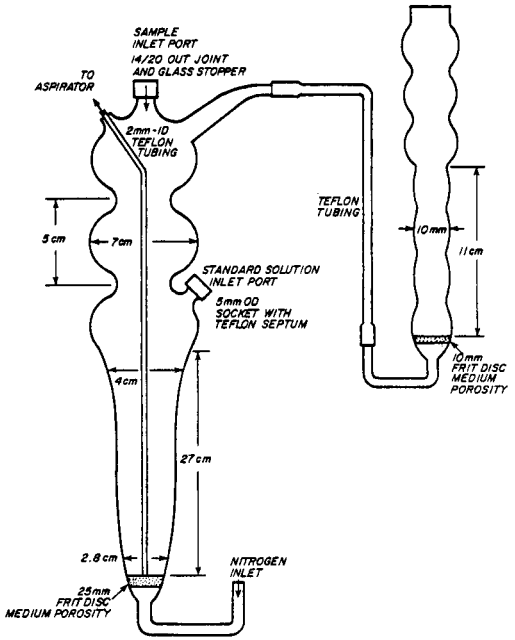

Fig. 1. Diagram of sample vessel and absorbing tube.

carbon disulfide in 25 ml of ethanol were used to prepare appropriate working solutions; inconsistent results were obtained, probably because of volatilization of CS_2 during the manipulation. These difficulties were overcome by weighing carbon disulfide in a capped vial, cooling it in an ice bath and diluting it with ice-cold hexane. Kept in an ice bath, this solution was stable for 3—4 h; after 25 h, the concentration decreased by about 30%.

Reagents. A 2% (w/v) solution of diethylamine (Baker Analyzed Reagent) was prepared in 100% pure ethanol (U.S. Industrial Chemical Company). Lithium chloride solution (1 M) was prepared from Fisher certified-grade reagent in organic-free water (prepared by passing deionized-distilled water through an activated carbon column). The reagent solution was prepared by mixing equal volumes of the diethylamine solution and the lithium chloride solution; this was stable for several days.

Procedure. Place 350 ml of water sample in sample vessel and 4 ml of reagent solution in the absorption tube. Purge the sample with nitrogen at a flow rate of 35—40 ml min^{-1} for about 15 min. Transfer the solution in the absorbing tube to the polarographic cell together with 2 ml of organic-free water. Deaerate this solution by bubbling nitrogen through it for 10 min. It is necessary to minimize contact between the mercury and the diethyldithiocarbamate solution, especially at very low concentrations (1—2 μg CS_2 l^{-1}); the electrode is therefore removed from the solution during deaeration. Record the differential pulse polarogram from −0.35 to −1.0 V vs. SCE at a scan rate of 5 mV s^{-1} (pulse height, 25 mV; drop time, 1 s; mercury flow

rate, 2.4 mg s^{-1}). Measure the diethyldithiocarbamate peak which appears at about —0.85 V vs. SCE. Prepare a calibration graph by injecting aliquots of the standard carbon disulfide solution from a microsyringe into 350-ml portions of purified water, mixing thoroughly, and following the above procedure.

Results and discussion

Purging and trapping. Pre-concentration is important in the proposed method. The sample vessel used for purging in this work has two main differences from the earlier design [8]. First, the three bulbs added between the reservoir and the exit port are more effective than a Kjeldahl connecting bulb in controlling foam and are easier to clean. Secondly, the standard inlet port permits injection of standard solution directly into the sample vessel; this modification avoids loss of carbon disulfide during manipulation caused by its immiscibility with water.

The flow rate and the total volume of the purging gas are critical. All the carbon disulfide must be removed from the sample solution and must react instantaneously with the diethylamine reagent. Because of the large volume ratio between the sample vessel and the absorbing tube, the flow rate is controlled so that the purging gas produces enough tiny bubbles in the solution without blowing the solution out of the absorbing tube; a flow rate of 35—40 ml min^{-1} for a period of 15 min is adequate. The recovery of the pre-concentration step under these conditions is about 65%. Prolonging the purging time at the same flow rate did not improve the recovery efficiency.

The temperature and the concentration of the reagent solution were investigated in attempts to improve the recovery. Below room temperatures, the vapor becomes less volatile so that it has a longer residence time in the reagent solution. However, the efficiency dropped considerably at 0°C, presumably because of slow reaction with diethylamine. Temperatures above 25°C generally accelerated the reaction rate between carbon disulfide and diethylamine, but although the efficiency improved at 40°C, the results were not reproducible. Increasing the concentration of the reagent from 2% to 4% (w/v) caused distorted polarograms.

Polarography. Typical polarograms are shown in Fig. 2. The calibration graph shown in Fig. 3 was prepared by combining results obtained over four days for concentrations in the range 0.8—3.2 $\mu g\ l^{-1}$. The results obtained for 9 different concentrations within this range fitted the linear equation $Y = 0.4 + 5.7X$ with a correlation coefficient of 96.8%; the line does not pass the origin because some diethyldithiocarbamate reacts with mercury.

Interferences. No interferences were observed in the analysis of various water samples. Copper, iron and other involatile impurities remain in the water during pre-concentration. Hydrogen sulfide, which is oxidized at a more negative potential, does not interfere in amounts up to 5—10-fold [5]. At larger concentrations, it can be removed by passing the purging gas through a lead acetate solution before it enters the absorbing tube.

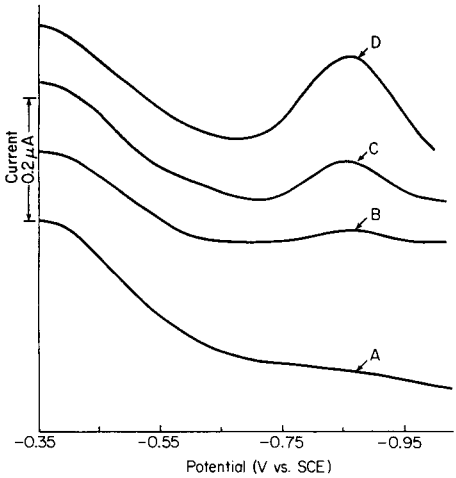

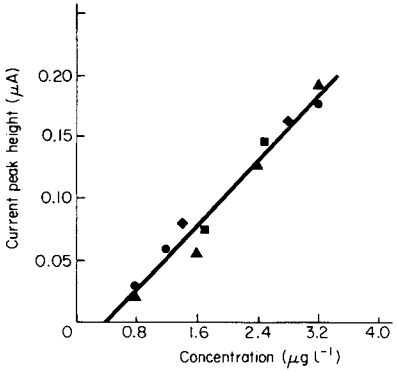

Fig. 2. Differential pulse polarograms of diethyldithiocarbamate in 0.33 M LiCl—33% ethanol solution: (A) residual current; (B) 0.8 $\mu g\ l^{-1}$; (C) 1.7 $\mu g\ l^{-1}$; (D) 2.5 $\mu g\ l^{-1}$ CS_2.

Fig. 3. Calibration graph for carbon disulfide; the different symbols represent standards prepared on different days.

The author thanks the FMC Corporation for permission to publish this paper, Dr. C. F. Ferraro for encouragement, and Mr. J. S. Migliacci and Mr. R. H. Schipmann for experimental help.

REFERENCES

1 E. C. Hunt, W. A. McNally and A. F. Smith, Analyst, 98 (1973) 585.
2 F. J. Viles, J. Ind. Hyg. Toxicol., 22 (1940) 188.
3 W. L. Thornsberry, Jr., Anal. Chem., 43 (1971) 453.
4 L. Kremer and L. D. Spicer, Anal. Chem., 45 (1973) 1963.
5 P. Zuman, R. Zumanova and B. Souček, Collect. Czech. Chem. Commun., 18 (1953) 632.
6 T. Kambara, S. Tanaka and K. Hasebe, J. Chem. Soc. Jpn. Pure Chem. Sec., 88 (1967) 644.
7 V. Jedlicka and A. Pasěk, Chem. Zvest, 14 (1960) 757.
8 T. A. Bellar and J. J. Lichtenberg, J. Am. Water Works Assoc., 66 (1974) 739.

Analytica Chimica Acta, 107 (1979) 391—393

Short Communication

DIFFERENTIAL PULSE POLAROGRAPHIC DETERMINATION OF ZINC DIALKYLDITHIOPHOSPHATE IN NON-AQUEOUS MEDIUM AND ITS APPLICATION TO COMMERCIAL LUBRICANT ADDITIVES

A. M. SHAFIQUL ALAM, J. M. MARTIN* and Ph. KAPSA

Ecole Centrale de Lyon, Laboratoire de Technologie des Surfaces 36, route de Dardilly, 69130 Ecully (France)

(Received 19th September 1978)

Zinc dialkyldithiophosphate (DTPZn) is a common additive (multi-functional antioxidant and anti-wear) in most motor oils, being used at a concentration of about 1% (w/w) [1]. DTPZn in non-aqueous media has been determined by several analytical methods [2]: e.g. complexometry with EDTA, atomic absorption, x-ray fluorescence [3], thin-layer chromatography [4] and electrochemical methods such as potentiometric titration of DTPZn in DMF with potassium hydroxide [5] or classical polarography [6].

The work described here shows that the detection limit for zinc (and thus DTPZn) in a paraffinic solution can be greatly reduced when differential pulse polarography is used with a suitable non-aqueous medium. Determination of DTPZn in commercial lubricant additives is also possible with a few microliters of the solution. The advantages of this procedure for DTPZn make it suitable for studies of anti-wear mechanisms as well as in routine analyses for the additive in commercial lubricants.

Experimental

Instrumentation and reagents. A Solea-Tacussel PRG5 polarograph with a three-electrode circuit was used. All potentials were measured with respect to the Ag/AgCl (saturated KCl) electrode. A platinum wire was used as auxiliary electrode. The characteristics of the dropping mercury electrode (DME) were as follows: 8 s drop time for a mercury height of 50 cm (open circuit); flow rate, 0.3—0.4 mg s^{-1}. An MPO 3 hammer drop timer, and an E 410 Metrohm hanging mercury drop electrode (HMDE) were used.

Tetraethylammonium perchlorate (0.1 M) served as the supporting electrolyte and the solvent was dimethylformamide (DMF). Solutions (10^{-2} M) of zinc diisopropyldithiophosphate were prepared by dissolving a measured quantity in n-dodecane. A 50-μl Hamilton syringe was used for all additions.

Procedure. The supporting electrolyte (20 ml) was transferred to the thermostated cell, and oxygen was removed by passing nitrogen for 30 min. Then the blank polarographic curve was measured. Calibration curves were

obtained by successive additions of 20-μl aliquots of 10^{-2} M zinc diisopropyldithiophosphate. When the HMDE (radius, 0.57 mm; area, 4.11 mm^2) was used, a new drop was formed for each voltammogram; an intermediate drop was removed each time to avoid memory effects. Magnetic stirring was continuous during the pre-electrolysis at 2.2 V vs. Ag/AgCl; 30 s were allowed to elapse before the voltammograms were recorded. All the precautions usual in polarography were taken.

Results and discussion

The potential range in DMF containing 0.1 M tetraethylammonium perchlorate is sufficiently large for the detection of zinc in lubricant additives, and the base current is not very high. The peak potential for zinc is 0.900 V vs. Ag/AgCl (saturated KCl) (Fig. 1). The detection limits obtained for zinc are shown in Table 1. The detection limit was taken as the concentration for which the peak had a measurable width and the peak potential could be determined accurately. Results show that detection limit is improved tenfold by anodic stripping with the HMDE.

Commercial additives are usually available in a paraffinic base and their concentrations are very high (about 40% w/w). For analysis, suitable aliquots of the sample were dissolved in pure n-dodecane. An aliquot (50 μl) of this solution was introduced from a microliter syringe into the measuring cell containing the supporting electrolyte, and the differential pulse polarogram was recorded; then successive known increments of standard solution were added and the polarograms recorded to establish the unknown concentration. For example, commercial additives containing about 0.1 mol DTPZn/100 g could be analyzed with a relative standard deviation of about 20% (n = 10).

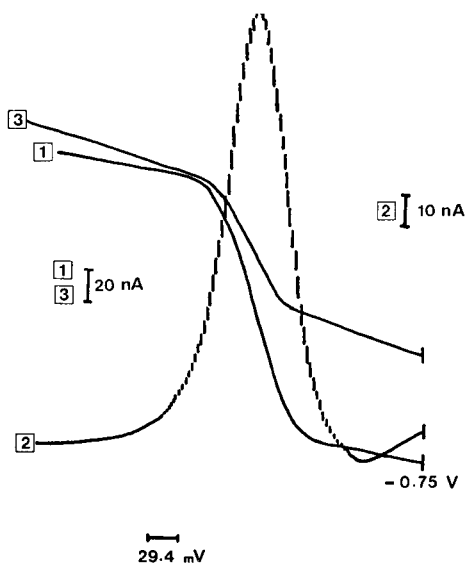

Fig. 1. Polarograms for zinc diisopropyldithiophosphate in 0.1 M tetraethylammonium perchlorate in DMF: (1) and (3), 1 x 10^{-4} M DTPZn; (2) 8 x 10^{-5} M DTPZn.

TABLE 1

Determination of zinc(II) in zinc isopropyldithiophosphate in 0.1 M tetraethylammonium perchlorate in DMF

Method	Detection limit	Linear range
Differential pulse polarography, DME	5×10^{-5} M (0.0032% w/w)	5×10^{-5}—2×10^{-4} M
Pulse polarography, HMDE[a]	2×10^{-6} M (0.000131% w/w)	2×10^{-6}—10^{-5} M

[a]Preelectrolysis for 10 min.

The results show that 0.1 M tetraethylammonium perchlorate in DMF is a good supporting electrolyte for determining zinc in synthetic DTPZn additives by differential pulse polarography.

REFERENCES

1 J. M. Martin, H. Montes and M. Marichy, Revue de l'I.F.P., in preparation.
2 J. M. Martin and J. M. Georges, Revue de l'I.F.P., Vol. XXX, n°2 (1975) 333—350.
3 J. M. Martin, Thèse Docteur d'Etat n° 7827, 1978, Lyon, France.
4 A. Lamotte and J. Auvray, J. Chromatogr., 97 (1974) 213.
5 D. Morel and M. Marichy, Talanta, 24 (1977) 582.
6 V. A. Kuznetson and L. G. Fedorenko, Khim Teckhnol. Topl. Masel., 10 (1974) 56.

Analytica Chimica Acta, 107 (1979) 395—398

Short Communication

DETERMINATION OF ARSENIC IN SEDIMENTS BY CHLORIDE FORMATION AND D.C. PLASMA ARC EMISSION SPECTROMETRY

AKIRA MIYAZAKI*, AKIRA KIMURA and YOSHIMI UMEZAKI

National Research Institute for Pollution and Resources, Ukima, Kita-ku, Tokyo (Japan)

(Received 18th October, 1978)

Summary. The sediment sample is heated in an induction furnace in hydrogen chloride—argon; arsenic trichloride evolved is trapped and then swept into a d.c. plasma arc. Calcium sulfate addition enhances the signals and suppresses interference from organic matter. The limit of detection is 15 ng As; the relative standard deviation is 3.4% (n = 10) for 1.5 μg As_2O_3.

Arsenic in sediments is usually determined after dissolution of the samples. This procedure is time-consuming and arsenic may be lost in the pretreatment. A more direct method of analysis would therefore be advantageous. Conventional arc or spark emission spectrometry is not satisfactory for the determination of arsenic in sediments because of its poor sensitivity and reproducibility. Morrison and Talmi [1, 2] reported that heating solids in an induction furnace is useful for microanalysis of solids, and several authors have since used this technique [3—9]. However, arsenic has not been determined with this device. This communication describes a method in which sediments are heated in an induction furnace in an atmosphere of hydrogen chloride [10]. Arsenic is converted to the volatile trichloride which is collected in a dry ice—ethanol trap. The trap is then heated, the chloride is swept into a d.c. plasma arc, and the arsenic is determined by emission spectrometry.

Experimental

Apparatus. A Spectraspan Model 101 d.c. plasma arc emission spectrometer was used with a cross-type plasma jet (Spectrajet II), a Nippon-Denshi Kagaku Model U-125M recorder and a Hamamatsu R166 photomultiplier. The induction (r.f.) furnace (3 kW) was made by the Abe Trading Company. An RFS Model 2002 freeze drier and a Spex Model 8000 mixer/mill were used for the preparation of samples. The furnace and the associated gas flow system are shown in Fig. 1.

The operating conditions for the d.c. plasma arc emission spectrometer were as follows: plasma current, 7.5 A; electrode gas and carrier gas flow rates, 3.5 and 7.0 units, respectively (1 unit = 0.47 l min^{-1}); entrance and exit slit areas, 400 × 600 μm and 200 × 400 μm, respectively; maximum voltage, 800 V; amplification, ×10.

Reagents. National spectrometric graphite powder L4100 (Union Carbide,

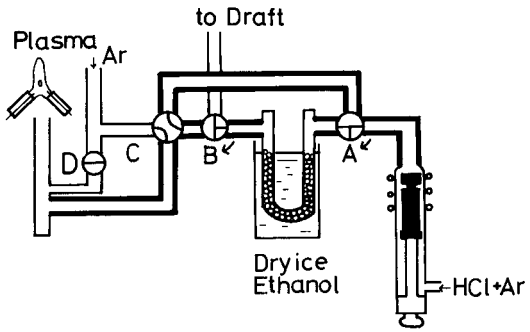

Fig. 1. Apparatus for production, trapping and determination of arsenic trichloride. The U-tube is connected to taps A and B with Teflon tubing. The parts indicated by thick lines are heated with tapes to about 150°C to prevent condensation of $AsCl_3$. Silica tubing is used where the tubes are heated inductively; other parts are of borosilicate glass.

U.S.A.) was used. All other chemicals were of analytical-reagent grade. Standards (10—200 μg As_2O_3 g^{-1}) were prepared by mixing homogeneously As_2O_3, 20% graphite powder and 15% $CaSO_4 \cdot \frac{1}{2}H_2O$, made up with silica [11]; the As_2O_3 was first mixed with silica powder to give standards containing 100 or 1000 μg g^{-1}, which were then diluted further as described.

Procedure for determination of arsenic in sediments. Set up the plasma spectrometer for the conditions given above. Freeze-dry the sample or standard and pulverize to <200 mesh. Add 20% of graphite powder and 15% of $CaSO_4 \cdot \frac{1}{2}H_2O$ and mix well (15 min) with a Spex mixer. Transfer 30 mg of the mixture to a graphite electrode and place the electrode in the induction furnace. With the stopcocks in the positions shown in Fig. 1, heat the graphite electrode to 600°C in a hydrogen chloride—argon atmosphere and collect the arsenic trichloride in the cold trap for 90 s. Turn stopcocks A and B clockwise through 90°. Remove the Dewar from around the U-tube and heat with an electric furnace at 200°C for 60 s to volatilize the arsenic trichloride. Open tap C fully to sweep the evolved arsenic trichloride into the arc. Measure the 235.0-nm As emission line intensity. Open the by-pass tap D slowly and return taps A, B and C to the positions shown in Fig. 1. Record the maximum emission intensity.

Results and discussion

Changes in the power of the furnace from 1.4 to 2.6 kW (300—1100°C) had little effect on the emission intensity of arsenic; a power of 1.8 kW (600°C) was used routinely. The effect of heating time on the signal from 1.5 μg of arsenic trioxide (1.1 μg As) was examined. The emission intensity increased linearly with time up to 70 s and became constant thereafter. Consequently, a heating time of 90 s was chosen for later work.

The trap was heated by a furnace at 200°C after removal from the cold bath, to vaporize the collected arsenic trichloride. The maximum emission intensity became constant after a heating period of 45 s. A heating time of

60 s was used routinely. Under these conditions the emission—time response from the plasma was a sharp peak.

Interferences. Addition of 5% (w/w) $CaSO_4 \cdot \frac{1}{2}H_2O$ to standards containing As_2O_3 (0.005%), graphite (20%) and silica (74.995%) enhanced the intensity of the arsenic emission by about 20%. A constant enhancement by 40% was obtained when the mixtures contained 10—30% $CaSO_4 \cdot \frac{1}{2}H_2O$, so that 15% was selected for routine use. In the presence of $CaSO_4 \cdot \frac{1}{2}H_2O$, no interference was caused by 1.5 mg of Na_2CO_3, K_2CO_3, CaO, MgO, Al_2O_3, NaCl, $KMnO_4$ or $Fe_2(SO_4)_3(NH_4)_2SO_4 \cdot 24H_2O$, in the determination of 1.5 μg of As_2O_3; these compounds also did not interfere in the absence of calcium sulfate.

The effect of organic compounds which may be present in sediments was examined. Results are shown in Fig. 2. In the presence of calcium sulfate, no interference was observed for humic acid and tannic acid up to 3%; in its absence, these compounds seriously depressed the emission. Addition of sodium sulfate, in place of the calcium salt, was also successful in avoiding interference from these organic compounds.

Recovery of other forms of arsenic. Recovery of arsenic(V) added as KH_2AsO_4 was 97%, calculated on the basis of calibration against As_2O_3. Thus almost all the arsenic in sediments is likely to be converted to arsenic trichloride (b.p. 130°C) in the proposed method. A preliminary result showed that recovery of cacodylic acid, $(CH_3)_2AsO_2H$, which was not detected after conventional wet digestion, was 70%.

Analytical results. The calibration graphs obtained under the recommended operating conditions were linear for 0.3—4.5 μg As_2O_3. The relative standard deviation was 3.4% for ten determinations of 1.5 μg As_2O_3. The limit of detection, defined as the concentration giving a signal-to-noise ratio of 2, was 15 ng As or 5 μg As g^{-1}.

Table 1 compares the results obtained for the determination of arsenic in various sediments and sludges by the proposed method and by a conventional

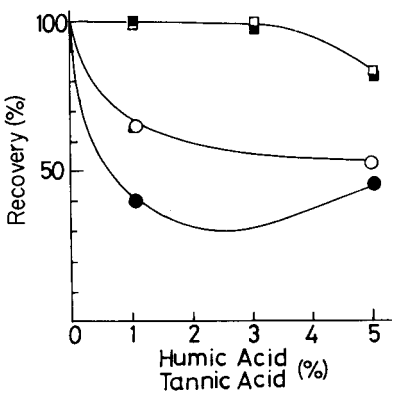

Fig. 2. Effects of humic acid (open symbols) and tannic acid (filled symbols) on the emission from 1.1 μg of arsenic without calcium sulfate (○●) and with 15% calcium sulfate (□■).

TABLE 1

Results for arsenic ($\mu g\ g^{-1}$) in sediments

Sample	Proposed method	Wet method [12]
River sediments near arsenic mines		
A	79±2[a]	80
B	194±5	189
C	760±31	790
Sea sediments		
D	15±1	13
Sludges from industrial waste water		
E	47±3	46
F	72±3	77

[a]Average deviation from the mean of 3 determinations.

wet method [12] in which samples were decomposed with nitric and sulfuric acids in the presence of permanganate. For the plasma method, the samples which contained large concentrations of arsenic, such as B and C, were diluted by mixing with silica powder before analysis. Satisfactory results were obtained for all the samples.

The proposed method is rapid, because the time-consuming wet decomposition of samples is unnecessary, and is precise and accurate. It is readily applied to sediments but should also be applicable to the determination of submicrogram amounts of arsenic in soils and related samples.

REFERENCES

1 G. H. Morrison and Y. Talmi, Anal. Chem., 42 (1970) 809.
2 Y. Talmi and G. H. Morrison, Anal. Chem., 44 (1972) 1455.
3 F. J. Langmyhr and Y. Thomassen, Fresenius Z. Anal. Chem., 264 (1973) 122.
4 F. J. Langmyhr and S. Rasmussen, Anal. Chim. Acta, 72 (1974) 79.
5 F. J. Langmyhr, Y. Thomassen and A. Massoumi, Anal. Chim. Acta, 67 (1973) 460.
6 F. J. Langmyhr, J. R. Stubergh, Y. Thomassen, J. E. Hanssen and J. Doležal, Anal. Chim. Acta, 71 (1974) 35.
7 D. G. Andrews and J. B. Headridge, Analyst, 102 (1977) 436.
8 R. Nakashima and S. Sasaki, Bunseki Kagaku, 102 (1977) 145.
9 R. Nakashima, Bunseki Kagaku, 27 (1978) 199.
10 R. K. Skogerboe, D. L. Dick, D. A. Pavloca and F. E. Lichte, Anal. Chem., 47 (1975) 568.
11 A. Yauchi, M. Tominaga and Y. Umezaki, Report of the Annual Meeting of the Mining and Metallurgical Institute of Japan, 1976, p. 283.
12 S. Terashima, Bunseki Kagaku, 23 (1974) 1331.

Analytica Chimica Acta, 107 (1979) 399—400

Short Communication

GLASS COLUMN CONNECTOR FOR A GAS CHROMATOGRAPH

A. GOLAN (GOLDHIRSH) and F. H. WOLFE*

Department of Food Science, University of Alberta, Edmonton, Alberta T6G 2N2 (Canada)

(Received 5th September 1978)

Summary. A cheap glass—metal connector is described for use with glass columns, to avoid the problems of O-rings or special ferrules. The device is valuable in gas chromatography of amino acid derivatives.

The common method of connecting glass columns to a gas chromatograph (g.c.) relies on the standard Swagelok brass fittings plus O-rings or special ferrules [1]. Teflon ferrules can be used but since Teflon tends to creep and has a practical operating limit of 225°C, the use of silicone rubber O-rings is preferred. Ordinary rubber O-rings will not endure high oven temperatures; their deterioration usually results in leakage problems, the columns may slip out of the fittings and break, and degradation products of the rubber may produce ghost peaks or background noise and drift. Graphite or Vespel ferrules, although more heat-resistant, are much more expensive.

During a study of the g.c. separation of amino acid derivatives, these limitations were encountered and as a result the device reported below was developed.

Description and construction of the connector

The column connector (Fig. 1) is constructed of a glass tube (a) sealed to a metal (Kovar) tube (b) ca. 3 cm long and 0.25-in. i.d.; this was made at the University of Alberta, Department of Chemistry, but is available from Cajon Company, 32550 Old South Miles Road, Cleveland, Ohio 44139, and others. A narrow glass tube c (see Fig. 2) is sealed to the internal side of the glass-to-metal transition, inside the Kovar tube, so that a continuous glass tube is

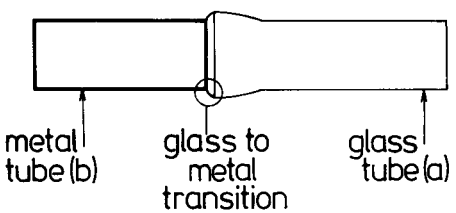

Fig. 1. Glass—metal transition tube.

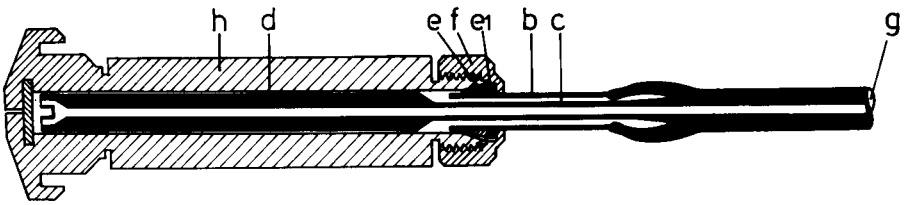

Fig. 2. Overall view of the glass column connector connected to injection port.

formed. To the top of the internal glass tube, another glass tube (d) is connected, with a funnel-shaped end with a slot for the carrier gas, which fits up against the septum on the injector side; on the detector side only a straight tube is needed. The length and diameter of this piece is chosen according to the specifications of the design of the injector and detector ports. The rest of the chromatographic column is sealed to the bottom of this tube at g (Fig. 2). The column is connected to the gas chromatograph by Swagelok-type fittings which fit over the metal tube (b), as is done with a metal column, by using front ferrule (e), back ferrule (el) and nut (f). The overall view of the connector, connected to injection port (h) is shown in Fig. 2.

Conclusion

This device has at least four advantages over other existing methods. First, the all-glass column avoids possible reactions of the injected sample with metals, thus preventing degradation of certain amino acid derivatives [2, 3]. Secondly, it is easy to handle and easy to assemble in the gas chromatograph without leaks. Thirdly, it solves the problems of slippage and breakage which can occur in high-temperature programming, especially with heavy glass columns in g.c. ovens such as the Varian Aerograph 2100 or Bendix 2500 and others. Finally, it is inexpensive; the glass—Kovar seal piece can be purchased ready-made, and the rest can be easily constructed. Several of these connectors have been built and used in the Varian Aerograph 2100 series, and have proved very useful in amino acid analysis [4]. This simple device should aid chromatographers in a wide variety of situations.

We thank Mr. Peter Lea for his help in making the device. This research was supported in part by the National Research Council of Canada (FHW-A5751).

REFERENCES

1 F. W. Rowland, The Practice of Gas Chromatography, Hewlett-Packard Co., Leaflet 173, p. 319—320.
2 W. M. Lamkin and C. W. Gehrke, Anal. Chem., 37 (1965) 383.
3 D. L. Stalling and C. W. Gehrke, Biochem. Biophys. Res. Commun., 22 (1966) 329.
4 A. Golan (Goldhirsh) and F. H. Wolfe, Can. Inst. Food Sci. Technol. J., (1979) in press.

Analytica Chimica Acta, 107 (1979) 401—404

Short Communication

SPECTROPHOTOMETRIC DETERMINATION OF NITROFURAZONE WITH PHLOROGLUCINOL

J. L. FABREGAS** and E. CASASSAS*

Department of Analytical Chemistry, University of Barcelona, Barcelona (Spain)

(Received 20th September 1978)

The extended use of nitrofurazone (5-nitro-2-furaldehyde semicarbazone) in the prophylaxis of poultry coccidiosis has entailed the development of methods for its determination in feeds. Several non-selective photometric procedures have been described [1—6] which can be used in conjunction with chromatographic or electrocataphoretic techniques [7—11]. Accurate results have also been obtained by superimposed a.c. polarography [12] and by fluorimetry with 2-aminobenzenethiol [13].

The present communication describes a new spectrophotometric procedure for the determination of nitrofurazone. A phloroglucinol solution containing hydrochloric acid is used; its acidity is high enough to produce hydrolysis of the sample with subsequent condensation of the liberated 5-nitro-2-furaldehyde with phloroglucinol to yield a deeply coloured diarylmethane derivative [14, 15]. The new procedure is highly sensitive and operationally simple, and its higher selectivity allows the determination to be carried out without any of the pre-treatments that made former methods tedious and more susceptible to error.

Experimental

Apparatus. A Beckman (Acta III) double-beam spectrophotometer, with 1.0-cm fused-silica cells, and an electrically-heated water bath thermostated to ±0.1°C, were used.

Reagents. The reagents (analytical grade) and solvents (spectroscopic grade) were all from E. Merck (Darmstadt). The nitrofurazone samples, of the highest quality available, were tested without further purification after drying to constant weight over phosphorus pentoxide.

The reagent solution (0.30% phloroglucinol—0.92 M hydrochloric acid) was prepared by mixing 110.0 ml of glacial acetic acid, 10.0 ml of concentrated hydrochloric acid and 10.0 ml of a methanolic 5% solution of phloroglucinol dihydrate; the solution was prepared freshly before use.

**Present address: Laboratorios Almirall, S.A., Barcelona, Spain.

Procedure

A 2.0-ml sample of a nitrofurazone solution in *N*,*N*-dimethylformamide—water (1:4 v/v), containing 30—200 μg of nitrofurazone per ml, is transferred to a 10.0-ml volumetric flask; 5.0 ml of reagent solution is added, and the contents are homogenized. The flask, well-stoppered, is placed in a bath of boiling water for exactly 30 min, and then immersed for 1 min in an ice-water bath to stop the reaction and bring the contents to room temperature; the mixture is then diluted to volume with unheated reagent solution and homogenized. The absorbance of this solution at 450 nm is measured against a reference obtained by processing 2.0 ml of a *N*,*N*-dimethylformamide—water (1:4) mixture identically. The absorbance is stable for at least 60 min under white light.

Results and discussion

Agreement with Beer's Law. Agreement with Beer's Law was checked for series of ten standard nitrofurazone-containing solutions, covering the range from 1.70×10^{-5} M to 2.30×10^{-4} M. The absorbance was a linear function of concentration, fitting a straight line of slope 5100 (absorbance units per mole), which gives log $\epsilon = 3.708$, and intercept 0.0006 absorbance units, with a correlation coefficient of 0.999 (significant to a $P = 0.001$ level [16]). The concentration range for maximum precision, obtained from the steepest portion of a Ringbom plot [17], extends from 3.66×10^{-5} M to 11.7×10^{-5} M (nitrofurazone final concentrations in the final solutions, which correspond to 36.0—120.2 μg ml^{-1} in the sample solution).

The coefficient of variation of the results is 1.06%, as determined on ten sample solutions containing 100 μg of nitrofurazone per ml.

Effect of reaction time and temperature. Nitrofurazone solutions treated with the acidic reagent solution at 100°C in a water bath develop a deep brown colour. The spectrum of the coloured solution is strongly dependent on the length of the incubation period (Table 1). The spectrum of the solution heated at 100°C for only 5 min shows two distinct maxima, one of higher absorbance at 414 nm and the other of lower absorbance at 450 nm. When the solution is heated for longer periods, the relative importance of the maximum at 450 nm successively increases and the other eventually becomes

TABLE 1

Effect of reaction time at 100°C on absorbance for 1.21×10^{-4} M nitrofurazone solution

Time (min)	*A* (414 nm)	*A* (450 nm)	Time (min)	*A* (414 nm)	*A* (450 nm)
5	0.448	0.432	30	0.537	0.618
10	0.484	0.485	40	0.548	0.632
15	0.502	0.522	50	0.560	0.640
20	0.516	0.567	60	0.568	0.647

a mere shoulder on the main band. The increase in absorbance at 450 nm becomes slower for incubation periods at 100°C longer than 30 min; this can be adopted as the working time for a practical analysis; to obtain accurate results with the previously given coefficient of variation, the time must be exactly measured.

Absorbance readings on a single nitrofurazone solution at 450 nm at different times after stopping the reaction with phloroglucinol showed that the reaction product was stable for at least 60 min.

The analytical method does not give maximum intensity of colour development when the mixtures are incubated at 25, 45 or 75°C.

Raw-material colour. Nitrofurazone gives an absorption band at 376 nm [18] which shifts to 358 nm in the acidic medium where the reaction is carried out. However, after heating at 100°C in acidic medium (phloroglucinol absent) there was no absorption in the visible part of the spectrum.

Selectivity and sensitivity. The brown colour developed in the procedure is due to phloroglucinol condensation with the 5-nitro-2-furaldehyde formed in the acid hydrolysis of nitrofurazone; a polycyclic diarylmethane chromophore is formed [14]. This mechanism would also operate on related molecules, e.g. nitrofurantoin and furazolidone to which the present procedure would be presumably applicable. Interference is not caused by compounds which do not give substituted furan derivatives on acid hydrolysis. The *N*,*N*-dimethylformamide used as a solvent does not participate in the reaction.

The literature contains no information about degradation products from nitrofurazone in its pharmaceutical formulations; the compound was shown to be stable for at least 11 days at 80°C. No interference is therefore expected from the presence of degradation products in nitrofurazone-containing formulations which usually contain compounds such as trypsin, chymotrypsins, L-carbamoylglutamic acid, methionine, and 8-hydroxyquinoline sulphate that do not interfere with the proposed method.

The present procedure is twenty times more sensitive than existing methods, which, furthermore, are not selective for the determination of nitrofurazone. Operational simplicity, high sensitivity (lowest limit ca. 1.2×10^{-5} M), selectivity and precision combine to make the new method suitable for accurate determinations of nitrofurazone in complex pharmaceutical mixtures.

REFERENCES

1 W. R. Ellis, E. S. McKay and E. H. Paul, J. Assoc. Off. Agric. Chem., 36 (1953) 417.
2 J. A. Buzard, W. R. Ellis and M. F. Paul, J. Assoc. Off. Anal. Chem., 39 (1956) 512.
3 J. A. Buzard, O. M. Vrablic and M. F. Paul, Antibiot. Chemother. (Washington, D.C.), 6 (1956) 702.
4 A. H. J. Cross, R. A. Hendey and S. G. E. Stevens, Analyst, 85 (1960) 355.
5 S. S. Thompson, Analyst, 81 (1956) 443.
6 A. B. Narbutt-Mering, Farmac. Pol., 29 (1973) 55.
7 S. C. Lee, Chem. Taipei, 1 (1969) 1; 4 (1969) 94.
8 R. T. Wang, S. S. Chon and C. H. Lin, Chem. Taipei, 1 (1969) 27.

9 R. C. d'A. DeCarnevale-Bonino, J. Dobrecky, C. Garber, N. M. Lombardi and E. M. Assem de Juarez, Rev. Asoc. Bioquim. Argent., 34 (1969) 95.
10 E. M. Rutczynska-Skonieczna, Rocz. Panstw. Zakl. Hig., 24 (1973) 579.
11 F. Fontani, E. Massarani, D. Narci and A. Tajana, J. Pharm. Sci., 61 (1972) 1502.
12 P. Hocquellet and A. Pevendrat, Analusis, 1 (1972) 192.
13 H. Taniguchi, K. Mikoshiba, K. Tsuge and S. Nakamo, Yakugaku Zasshi, 94 (1974) 717.
14 E. Casassas, J. L. Fabregas and A. Margalet, Anal. Biochem., in press.
15 J. L. Fabregas, E. Casassas and A. Margalet, Anal. Biochem., in press.
16 R. A. Fischer and F. Yates, Statistical Tables, Longmans, Edinburgh, 1974, p. 63.
17 A. Ringbom, Fresenius Z. Anal. Chem., 115 (1939) 232.
18 E. G. C. Clarke, Isolation and Identification of Drugs, Pharmaceutical Press, London, 1969, p. 445.

Analytica Chimica Acta, 107 (1979) 405—409

Short Communication

SPECTROPHOTOMETRIC DETERMINATION OF SODIUM BOROHYDRIDE WITH 2,4,6-TRINITROBENZENESULFONIC ACID

BABIKER ELAMIN and GARY E. MEANS*

Department of Biochemistry, The Ohio State University, 484 W. 12th Avenue, Columbus, Ohio 43210 (U.S.A.)

(Received 23rd October 1978)

Sodium borohydride is usually determined by measuring the amount of hydrogen released by acids [1, 2], by iodimetric titration [3—7], potentiometrically after reaction with silver nitrate—ethylenediamine [8] or by indirect u.v. spectrophotometric determination [9]. Trinitrobenzenesulfonate anion was used for the semiquantitative determination of sodium borohydride [10]; this report describes a sensitive, accurate and rapid determination of sodium borohydride.

Experimental

Reagents and solutions. Sodium borohydride (98 + %) and 2, 4, 6-trinitrobenzenesulfonic acid (Sigma Chemical Co.), sodium cyanoborohydride (Alfa Products) and sodium dithionite (J. T. Baker Co.) were used. Twice-distilled, deionized water was used; all other chemicals were reagent grade. Standard solutions (ca. 0.01 M) of sodium borohydride were prepared by dissolving carefully weighed samples (75—150 mg) in 25 or 50 ml of 0.02 M NaOH in glass-stoppered flasks. The titer of these solutions decreased by ca. 1% after 24 h in the refrigerator at about 3°C. Fresh solutions (kept on ice) were prepared prior to each set of experiments.

Instrumentation. Absorbances were measured with a Coleman 124 spectrophotometer and spectra were obtained with a Cary 118C recording spectrophotometer. pH was measured with a Corning pH-Meter with Leeds and Northrup miniature glass electrodes.

Procedure. Solutions containing from zero to ca. 0.3 μmol of sodium borohydride in 0.1 ml or less are added to 1.0 ml of 2×10^{-3} M trinitrobenzenesulfonic acid in 0.06 M triethanolamine—HCl buffer (pH 8.0) at room temperature and gently mixed until homogeneous. After standing for 15 min, the absorbance at 460 nm is measured and referred to a standard curve obtained in the same way with known concentrations of sodium borohydride. These conditions can be varied slightly as indicated under "Results". Other buffers may be used but should be near pH 8 and free of ammonia and sterically unhindered primary amines (See Discussion). Larger amounts of

sodium borohydride are easily accommodated by taking larger volumes of reagent solution.

Results

Sodium borohydride reacts with trinitrobenzenesulfonate ion in alkaline aqueous solutions to give a red-orange product(s) with an absorption maximum at 460 nm (Fig. 1). The reaction is complete in ca.10 min with 0.002 M trinitrobenzenesulfonate ion in 0.06 M triethanolamine buffer at pH 8.0 and room temperature (23°C). Variation in the reaction time from 10 to 90 min does not affect the results. The absorbance at 460 nm is stable for at least 3 h, is highly reproducible and is directly proportional to amounts of added borohydride up to ca. 0.25 μmol under the stated conditions. Based on the amount of borohydride, the product has an apparent molar absorptivity of 2.8×10^3 l mol^{-1} at 460 nm.

The suggested assay conditions are based on the results of assays run under a variety of conditions. As shown in Table 1, concentrations of trinitrobenzenesulfonate ion of 10^{-4} M or less give noticeably lower absorbances. With 10^{-2} M trinitrobenzenesulfonate, assay solutions are yellow, give slightly higher blank readings, and the absorbance is not proportional to added borohydride (Table 1). Maximum sensitivity to sodium borohydride with low blank readings is obtained with ca. 2×10^{-3} M trinitrobenzenesulfonate.

Formation of the red-orange product is strongly dependent on the pH of the assay solution. At low pH values, the evolution of hydrogen gas increases in rate [7] and competes with color formation; as shown in Table 2 the absorbance at 460 nm is sharply reduced. At higher pH values less breakdown

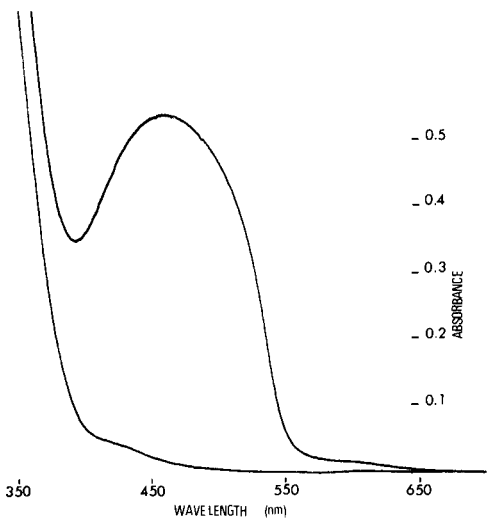

Fig. 1. Absorption spectrum of the reaction product of 0.2 μmol $NaBH_4$ with 1.0 ml of 2×10^{-3} M TNBS in 0.06 M triethanolamine/HCl buffer at pH 8.0 after 15 min incubation at room temperature (upper curve) and a corresponding blank without addition of $NaBH_4$ (lower curve).

TABLE 1

Absorbances at 460 nm after reaction of sodium borohydride with increasing concentrations of TNBS[a]

$NaBH_4$ (μmol) \ TNBS (M)	2×10^{-5}	2×10^{-4}	2×10^{-3}	1×10^{-2}
0.05	0.05	0.119	0.13	—
0.10	0.051	0.263	0.272	0.440
0.15	0.071	0.389	0.425	0.800
0.20	0.100	0.580	0.595	0.880
0.30	0.129	0.670	0.760	0.900
0.40	0.170	0.800	0.830	0.900

[a]Blanks obtained without $NaBH_4$ have been subtracted.

TABLE 2

Absorbances at 460 nm for solutions of different pH values after reaction of 2×10^{-3} M TNBS with sodium borohydride

pH	2.7[a]	6.0[b]	7.0[b]	8.0[b]	10.2[b]	12.0[b]
Background	0.18	0.18	0.18	0.18	0.21	0.34
0.2 μmol $NaBH_4$	0.06	0.06	0.52	0.61	0.66	0.71

[a]0.06 M Sodium formate. [b]0.06 M Triethanolamine adjusted with HCl or NaOH; pH determined prior to reaction.

of sodium borohydride occurs but hydrolysis of trinitrobenzenesulfonate becomes more of a problem (11). The increase in blank readings above pH 8 (Table 2) presumably results from increased formation of the yellow picrate anion.

The described procedure is not generally applicable to other reducing agents without modification. With sodium dithionite no color change is observed under the indicated conditions nor is there a detectable change in absorbance at 460 nm, With sodium cyanoborohydride, a similar color develops but the intensity is reduced to ca. 33%. The absorption spectrum has a similar maximum at about 460 nm but there is an additional shoulder around 510 nm.

Discussion

In comparison with other procedures [1—9], the reaction with 2,4,6-trinitrobenzenesulfonate affords an extremely sensitive method for the detection and determination of sodium borohydride. Only a simple colorimeter is required. For qualitative or semiquantitative analyses the characteristic color produced is easily seen. Under the suggested conditions, ca. 0.01—0.25 μmol of sodium borohydride can be easily determined with standard deviations of ± 3% of the observed values or better.

The specified conditions may be varied considerably to satisfy different analytical situations or to accommodate the presence of other substances. Larger amounts of sodium borohydride can be handled by increasing the volume of the reagent solution. The pH and the buffer species can be varied considerably; as shown in Table 2, the optimum pH chosen appears only slightly preferable to other values between 7 and 10. The use of pH 8.5 hydrogencarbonate buffer gives virtually identical results to those shown.

Of the most likely sources of interference, ammonia, primary amines, and other reducing agents may lead to spuriously high results. The reactions of trinitrobenzenesulfonate with ammonia and many primary amines, for example, are relatively rapid and give similarly colored sulfite complexes of the corresponding picramides [11]. Tris(hydroxymethyl)aminomethane reacts very slowly, however, and small amounts of Tris buffer should not interfere. In very alkaline solutions, hydrolysis to give the intensely yellow picrate anion may also be a problem. Sodium cyanoborohydride and sodium borohydride give similarly colored products and so may some other hydride donors. Sodium dithionite, the only other reductant examined, did not interfere. Many strong reducing agents are not stable in aqueous solutions; presumably they would not be determined by this method but might still interfere in some cases.

The product(s) of the reaction between sodium borohydride and trinitrobenzene sulfonate under the conditions indicated have not been identified. The reaction of tetramethylammonium borohydride with trinitrobenzene, however, appears to give a similar product, reported to be 1,1-dihydro-2,4,6-trinitrohexadienate anion [12, 13]. An apparently similar reduction of trinitrobenzenesulfonate ion by the coenzyme, nicotinamide adenine dinucleotide (NAD)and other 1-substituted-4, 4-dihydropyridines appears to involve the transfer of hydride primarily to the 1-position, as the initial colored product gives rise to 1,3,5-trinitrobenzene and hydrogen sulfite ion on slight acidification [14—17]. In contrast, the stability of the present colored product to such conditions suggests that hydride addition occurs primarily at the 1-position to give the 1,1-dihydro-2,4,6-trinitrohexadien-3-sulfonate dianion.

Acknowledgement is made to the donors of the Petroleum Research Fund, administered by the American Chemical Society, for support of this research. We also thank Andrew Britton and Michael J. Moffitt for technical assistance and Drs. E. J. Behrman and G. P. Royer for helpful discussion.

REFERENCES

1 S. W. Chaikin and W. G. Brown, J. Am. Chem. Soc., 71 (1949) 122.
2 H. C. Brown, Hydroboration, W. C. Benjamin, New York, 1962, p. 227.
3 C. Harzdorf, Fresenius Z. Anal. Chem., 210 (1965) 12.
4 M. B. Mathews, J. Biol. Chem., 176 (1948) 229.
5 D. A. Lyttle, E. H. Jensen and W. A. Struck, Anal. Chem., 24 (1952) 1843.
5 H. C. Brown, O. H. Wheeler and K. Ichikawa, Tetrahedron, 1 (1957) 214.
7 M. M. Kreevoy and J. E. C. Hutchins, J. Am. Chem. Soc., 94 (1972) 6371.

8 B. Rickborn and M. T. Wuesthoff, J. Am. Chem. Soc., 92 (1970) 6894.
9 I. E. Lichtinstein and J. S. Mars, J. Franklin Inst., 281 (1966) 481.
10 G. E. Means and R. E. Feeney, Biochemistry, 7 (1968) 2191.
11 G. E. Means, W. I. Congdon and M. L. Bender, Biochemistry, 11 (1972) 3564.
12 R. P. Taylor, Chem. Commun., (1970) 1463.
13 R. P. Taylor and J. B. Vatz, J. Am. Chem. Soc., 95 (1973) 5819.
14 D. J. Bates, B. R. Goldin and C. Frieden, Biochem. Biophys. Res. Commun., 39 (1970) 502.
15 L. C. Kurz and C. Frieden, J. Am. Chem. Soc., 97 (1975) 677.
16 A. Brown and H. F. Fisher, J. Am. Chem. Soc., 98 (1976) 5682.
17 L. C. Kurz and C. Frieden, Biochemistry, 16 (1977) 5207.

Analytica Chimica Acta, 107 (1979) 411—414

Short Communication

pH-DEPENDENCE OF THE FLUORESCENCE OF ACRIDONE IN AQUEOUS MINERAL ACID SOLUTIONS

STEPHEN G. SCHULMAN* and WILLY J. M. UNDERBERG**
College of Pharmacy, University of Florida, Gainesville, Florida 32610 (U.S.A.)
(Received 12th October 1978)

In a recent paper [1] it was stated that the pH-dependence of the fluorescence of acridone (9-(10H)-acridanone), in aqueous perchloric acid solutions, was identical to the pH-dependence of its absorption spectrum. This observation suggested that, in aqueous perchloric acid solutions, acridone was incapable of becoming protonated, during the lifetime of its lowest excited singlet state, notwithstanding that, in mixed water—ethanol—mineral acid solutions, protonation of acridone in the excited state had been observed [2]. The fact that acridone has a fairly long-lived lowest excited singlet state in water [1] made it difficult to rationalize its failure to exhibit excited-state protonation, especially because the structurally similar compound xanthone (9-xanthenone) becomes protonated in its lowest excited singlet state at pH > pK_a [3].

Re-examination of the fluorescence spectra of acridone and its conjugate acid in dilute aqueous perchloric acid solutions, employing excitation at the isosbestic point at 350 nm, in the absorption spectrum, yielded the reproducible fluorimetric pH titration curve shown in Fig. 1, which clearly indicates that excited-state protonation of acridone occurs at ca. 1.3 pH units more basic than the ground-state pK_a. Obviously, the earlier report [1] of the failure of acridone to become protonated in the excited state is in error.

In the previous study [1] the fluorescence spectra of the cation in the more concentrated perchloric acid solutions were much more intense than the spectra taken in dilute perchloric acid. In the present spectra the fluorescence of the cation is slightly weaker than that of the neutral molecule; the error in the previous study may therefore have been due to inadvertent excitation at a wavelength where the cation absorbs much more intensely than the neutral molecule. Since the ground- and excited-state ionization are so close in this compound, it would be easy for the excited-state process to be completely obscured by the intense fluorescence arising from the directly excited cation formed in the ground-state reaction.

For acridone, the data represented in Fig. 1 and the excited-state dis-

**Permanent address: Farmaceutisch Laboratorium, Rijksuniversiteit, Utrecht, The Netherlands.

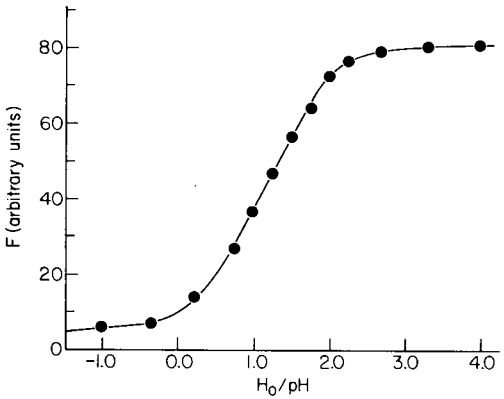

Fig. 1. Fluorescence intensity of acridone at 416 nm, as a function of pH. Excitation was effected at 350 nm.

sociation constant $K^*_{CN} = 2.5 \times 10^{-2}$ [1] calculated from a Förster cycle [4] were employed to estimate the rate constants for excited-state protonation of the neutral molecule ($\vec{k}_B$) and dissociation of the cation ($\overleftarrow{k}_B$) from

$$\phi_B/\phi^0_B/(1 - \phi_B/\phi^0_B)\,[H_3O^+] = (1 + \overleftarrow{k}_B\tau'_0)/\vec{k}_B\tau_0 \qquad (1)$$

where ϕ_B/ϕ^0_B is the relative fluorescence efficiency of the neutral molecule at any value of $[H_3O^+]$; $\tau_0 = 14.8 \pm 0.5$ ns and $\tau'_0 = 26.0 \pm 0.4$ ns (measured on a TRW nanosecond decay time fluorimeter with an 18 W deuterium lamp, Corning CS7-60 excitation filter, and a Corning CS-72 emission filter) are, respectively, the fluorescence decay times of the neutral molecule and cation; and $K^*_{CN} = \overleftarrow{k}_B/\vec{k}_B$.

From the fluorescence intensity F at 416 nm, where fluorescence of the neutral molecule is maximal and that of the cation minimal, ϕ_B/ϕ^0_B was calculated at each value of $[H_3O^+]$ as follows:

$$F = 2.3\,\phi_B I_0 \epsilon [B] l + 2.3\,\phi_{BH^+} I_0 \epsilon [B] l + 2.3\,\phi^0_{BH^+} I_0 \epsilon [BH^+] l \qquad (2)$$

where I_0 and ϵ are the intensity of the exciting light and the molar absorptivity at the isosbestic exciting wavelength, respectively; l is the optical depth of the sample; $\phi^0_{BH^+}$ is the quantum yield of fluorescence of directly excited cation; ϕ_{BH^+} is the quantum yield of fluorescence of the cation formed from the photoprotonation of the neutral molecule; and ϕ_B is the quantum yield of fluorescence of the neutral molecule (at pH $\geqslant$ 3, $\phi_B = \phi^0_B$). At very low solution acidity (pH $\geqslant$ 3) under identical conditions of excitation, the fluorescence intensity F becomes that of the isolated, directly excited neutral molecule, F^0_B, i.e. $F^0_B = 2.3\,\phi^0_B I_0 \epsilon C_B l$, where C_B is the formal concentration of acridone. At very high solution acidity ($H_0 \leqslant -2$), F becomes that of the isolated, directly excited cation, $F^0_{BH^+}$, i.e. $F^0_{BH^+} = 2.3\,\phi^0_{BH^+} I_0 \epsilon C_B l$. Combination of these two equations with eqn. (2) yields

$$F = F^0_B(\phi_B/\phi^0_B)[B]/C_B + F^0_{BH^+}(\phi_{BH^+}/\phi^0_{BH^+})[B]/C_B + F^0_{BH^+}[BH^+]/C_B \qquad (3)$$

If proton exchange is the only bimolecular process occurring in the lowest excited states of B and BH^+ [5], then $(\phi_B/\phi_B^0) + (\phi_{BH^+}/\phi_{BH^+}^0) = 1$. Since $[B]/C_B = K_a/([H_3O^+] + K_a)$, and $[BH^+]/C_B = [H_3O^+]/([H_3O^+] + K_a)$, combination of these last three equalities with eqn. (3) and subsequent rearrangement yields

$$\frac{(\phi_B/\phi_B^0)}{(1-\phi_B/\phi_B^0)} = \frac{(F - F_{BH^+}^0)(1 + [H^+]/K_a)}{(F_B^0 - F) - (F - F_{BH^+}^0)\dfrac{[H^+]}{K_a}} \tag{4}$$

For the value $K_a = 2.1$ ($pK_a = -0.32$ [6]), combination of eqns. (1) and (4) permits the calculation of $(1 + \overleftarrow{k}_B\tau_0')/\vec{k}\tau_0$. Eight points from the fluorimetric titration represented in Fig. 1 were used to calculate $(1 + k_B\tau_0')/\vec{k}_B\tau_0 = 0.078 \pm 0.007$. The expression for K_{CN}^* was then used to estimate $\vec{k}_B = 2 \times 10^9$ $mol^{-1}\ s^{-1}$ and $\overleftarrow{k}_B = 5 \times 10^7\ s^{-1}$. The uncertainty in the estimation of pK_a^* is about 0.3 log unit (about 1 nm in each spectroscopic measurement) so that the uncertainty in K_a^* is about a factor of 2. If we define $(1 + \overleftarrow{k}_B\tau_0')/\vec{k}_B\tau_0 = m$, $\vec{k}_B$ can be expressed, explicitly, from the expression for K_{CN}^*, as

$$\vec{k}_B = 1/(m\tau_0 - k_a^*\tau_0') \tag{5}$$

Unless $K_a^*\tau_0'$ is much smaller than $m\tau_0$, i.e. the system is far removed from equilibrium in the excited state, the substantial uncertainty in K_a^* can result in very great uncertainty in the estimation of $\vec{k}_B$ and even more so in the estimation of $\overleftarrow{k}_B$ which is given by

$$\overleftarrow{k}_B = K_a^*/(m\tau_0 - K_a^*\tau_0') \tag{6}$$

For example, if as a lower limit $K_a^* = 1.3 \times 10^{-2}$, $\vec{k}_B = 1 \times 10^9\ mol^{-1}\ s^{-1}$ and $\overleftarrow{k}_B = 2 \times 10^7 s^{-1}$ while if in the upper limit of uncertainty $K_a^* = 5 \times 10^{-2}$, $\vec{k}_B$ and $\overleftarrow{k}_B$ are negative: a physically impossible situation. More reasonably, an upper value to $\vec{k}_B$ can be taken as a diffusion-limited value of $2 \times 10^{10}\ mol^{-1}\ s^{-1}$ [7] which upon substitution into eqn. (5) gives an upper limit of K_a^* as 4×10^{-2} and an upper limit to the value of $\overleftarrow{k}_B$ as $8 \times 10^8\ s^{-1}$. Consequently, in the case of excited-state protonation of acridone and deprotonation of its conjugate acid, the estimated rate constants of $\vec{k}_B = 2 \times 10^9\ mol^{-1}\ s^{-1}$ and $\overleftarrow{k}_B = 5 \times 10^8\ s^{-1}$ are probably no better than order-of-magnitude estimates. It appears then that estimation of rate constants of excited-state proton transfer in very weak bases (requiring H_3O^+ rather than H_2O for protonation) and in very weak acids (requiring OH^- rather than H_2O for dissociation), with an excited-state equilibrium constant calculated from a Förster cycle, offers no great advantage over the complex quenching method advanced by Watkins [8, 9] in which the rate constants of the second-order reactions must sometimes be estimated from the theory of diffusion-controlled reactions [9].

REFERENCES

1 S. G. Schulman and R. J. Sturgeon, Anal. Chim. Acta, 93 (1977) 239.
2 H. Kokobun, Z. Elektrochem., 62 (1958) 599.
3 J. F. Ireland and P. A. H. Wyatt, J. Chem. Soc. Faraday Trans. 1, 68 (1972) 1053.
4 T. Förster, Z. Phys. Chem. N. F., 54 (1950) 42.
5 A. Weller, Z. Elektrochem., 56 (1952) 662.
6 A. Albert and J. N. Phillips, J. Chem. Soc., (1956) 1294.
7 D. F. Othmer and M. S. Thakar, Ind. Eng. Chem., 45 (1953) 589.
8 A. R. Watkins, Z. Phys. Chem. N.F., 75 (1971) 327; J. Chem. Soc. Faraday Trans. 1, 68 (1972) 28.
9 A. R. Watkins, Z. Phys. Chem. N.F., 78 (1972) 103.

Analytica Chimica Acta, 107 (1979) 415—418

Short Communication

A DISCREPANCY IN THE ANALYTICAL CHEMISTRY OF TELLURIUM
Separation of Selenium and Tellurium with Application to Anode Slimes

M. M. ALI, H. B. DESAI and Ch. VENKATESWARLU

Analytical Chemistry Division, Bhabha Atomic Research Centre, Bombay — 400 085 (India)

(Received 23rd October 1978)

Bondin [1] synthesized tellurates of copper and nickel by heating tellurides of these metals with sodium hydroxide solution at elevated temperatures (100—200°C) under oxygen pressure (10—15 atm.). These were reported to be insoluble in water as well as in alkaline solutions. Nevertheless, standard books [2—5] recommend the extraction of tellurium and selenium into water, after fusing a sample with sodium peroxide in a nickel or iron crucible. In this communication, it is shown that the recommended procedure, though valid for selenium, needs reassessment for tellurium. An analytical separation of tellurium from selenium is developed and applied to the analysis of anode slimes.

Experimental

Reagents. Standard 0.05 M solutions of nickel and iron were prepared from the pure metals; the final acidity was 2% (v/v) hydrochloric acid. Selenium and tellurium were freshly precipitated as the elements from hydrochloric acid solutions and dried. All other reagents were of analytical grade.

Effect of nickel and iron on selenium and tellurium in alkaline peroxide solution. Tellurium (0.2 mmol in hydrochloric acid solution) was mixed with varying amounts of the nickel or iron solution; this was diluted to 100 ml and boiled with 5—6 g of sodium peroxide. The precipitate formed was filtered, washed with 2% (w/v) sodium hydroxide solution, and dissolved in hydrochloric acid. Tellurium was then reduced with tin(II) chloride (20% in 6 M HCl); the precipitate was filtered off and redissolved. Finally, the solution was analysed for tellurium by the dichromate oxidation method [6].

The amount of tellurium precipitated increases with the amount of nickel or iron added and is quantitative when 1.5 mol of nickel or 4—5 mol of iron is present for each mole of tellurium (Fig. 1). This behaviour was verified by fusing 10—100 mg of tellurium with 5—6 g of sodium peroxide in a nickel crucible at red heat for 5 min, boiling the melt with water and analysing the insoluble residue for tellurium as described above. Six tests with 10—100 mg of tellurium showed that tellurium remained quantitatively in the residue. When 5 g of sodium peroxide was fused in a clean 15-ml nickel crucible at red heat for 5 min, about 0.5 g of nickel was lost from the crucible. This nickel is sufficient to precipitate nearly 0.7 g of tellurium.

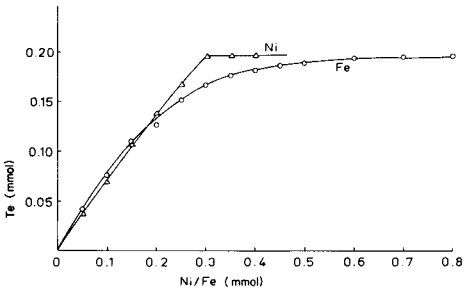

Fig. 1. Precipitation of tellurium as a function of nickel or iron added in alkaline peroxide solution.

When selenium (10 mg) was subjected to similar treatments, it appeared entirely in the water leach, as expected from the literature. No selenium was detected in the residue.

Separation of tellurium from selenium

Mixtures of solutions of the two elements and nickel (in excess) were boiled with 5—6 g of sodium peroxide in a total volume of about 100 ml. The insoluble residues were filtered and washed 6—7 times with hot 2% sodium hydroxide solution. Selenium in the filtrate was determined gravimetrically by reduction to the metal; tellurium was determined in the residue as described above. Quantitative separation was obtained (Table 1). Some experiments were done with selenium tagged with ^{75}Se tracer. All the activity added was found in the filtrate. The separation was further confirmed (Table 1) by analysing mixtures of powdered selenium and tellurium as described below.

Procedure. Weigh a mixture of selenium and tellurium powders (containing not more than 100 mg of tellurium) into a clean nickel crucible and mix with about 3 g of sodium peroxide. Cover with another 3-g portion of the flux and melt slowly over a low flame. Then fuse at red heat for 5 min, gently swirling the crucible. Cool and digest the melt with about 70 ml of water. Remove the crucible, wash and set aside.

TABLE 1

Separation of tellurium from selenium by precipitation with sodium peroxide in the presence of excess of nickel

Te (mg)		Se (mg)		Te (mg)		Se (mg)	
Taken	Found	Taken	Found	Taken	Found	Taken	Found
Mixtures of standard solutions				*Mixtures of metals*			
11.7	11.6	9.9	9.8	20.0	19.6	20.0	19.8
9.4	9.5	49.8	49.8	30.0	29.8	30.0	29.7
10.4	10.1	101.9	101.3	40.0	39.7	40.0	39.6
50.0	49.8	20.1	19.9				
99.8	99.2	20.6	20.2				
100.2	99.6	10.2	10.0				

Filter the suspension through a Whatman No. 540 filter paper, and wash thoroughly with hot 2.0% sodium hydroxide solution. Combine the filtrate and washings and analyse for selenium as described below. Dissolve the residue in a hot mixture of 15 ml of 4.5 M sulphuric acid and 3 ml of 11 M hydrochloric acid. If the suspension is centrifuged, the supernatant liquid should be filtered through a No. 540 filter paper; the precipitate in the tube is then dissolved in the acid mixture and the solution passed through the same filter paper. Dissolve any precipitate adhering to the nickel crucible in 5 ml of 4.5 M sulphuric acid and add to the solution. Digest on a water bath to expel chlorine (and to coagulate any silver chloride which may appear when anode slimes are analysed). Filter off the precipitate, add 25 ml of 11 M hydrochloric acid to the filtrate and dilute to 150 ml. Add 3 g of tartaric acid followed by 20 ml of tin(II) chloride solution. Boil for 2—3 min, digest on a water bath for about 1 h, and allow to cool. Filter the solution under gentle suction through a sintered glass crucible. A cylindrical suction flask with a lid is used for this purpose, as solutions can be sucked directly into beakers placed inside the flask. Wash the precipitate with 5% (v/v) hydrochloric acid. Reject the filtrate. Dissolve the precipitate in hot dilute nitric acid and evaporate to dryness. Heat the residue with 2 ml of 18 M sulphuric acid to fumes. Destroy any organic matter by heating to fumes with 2 ml of concentrated nitric acid. Dilute with 25 ml of water and boil to expel nitrogen oxides. Add 10 ml of 11 M hydrochloric acid and warm to obtain a clear solution. Determine tellurium by the dichromate oxidation method. In some experiments, the standard gravimetric procedure, involving reduction with sulphurous acid, was also followed.

Determination of selenium. Evaporate the filtrate containing selenium by boiling to 75—100 ml, and neutralize slowly with hydrochloric acid, cooling in ice-water. Acidify with 15 ml of 11 M hydrochloric acid and heat to 60—70°C with constant stirring to expel chlorine. Add 3 g of tartaric acid, followed by 20 ml of tin(II) chloride solution. Leave the solution in a warm place until the precipitate coagulates (ca. 4 h). Then filter under gentle suction through a sintered glass crucible and wash with cold 5% (v/v) hydrochloric acid. Reject the filtrate. Treat the precipitate in the crucible with cold 11 M hydrochloric acid saturated with bromine and collect the solution in the original beaker. After complete dissolution, wash the crucible thoroughly with cold 11 M hydrochloric acid, collecting the washings in the same beaker. Cool in ice, add 25 ml of saturated sulphurous acid solution with constant stirring, and allow the precipitate to settle overnight in a refrigerator. Filter through a tared sintered glass crucible, and wash first with cold dilute hydrochloric acid containing a little sulphurous acid, and then successively with cold water, hot water, alcohol and ether. Dry the precipitate first at 40°C and then at 120°C for 1 h, and weigh as the element.

Application to anode slimes. Anode slime samples (0.5—1.0 g) were analysed as described above, and by a standard method [3]. The results (Table 2) prove that the proposed method is quite satisfactory for quantitative separations of tellurium from selenium.

TABLE 2

Analysis of anode slimes for tellurium and selenium

Sample	Standard method		Proposed method	
	Se(%)	Te(%)	Se(%)	Te(%)
1	6.0	6.4	6.0, 6.1	6.4, 6.4
2	6.2	6.5	6.1, 6.2	6.5, 6.5
3	6.1	6.3	6.0, 6.0	6.3, 6.2

Discussion

Standard text books recommend that samples containing selenium and tellurium should be fused with sodium peroxide in a nickel or iron crucible, the melt being leached with water to obtain the elements in solution. The present studies prove that under ordinary fusion conditions only selenium is extracted into water, tellurium remaining in the residue. Retention is quantitative in the presence of sufficient nickel (1.5 mol Ni/mol Te). In the presence of iron, retention of tellurium in the residue is quantitative only when a 4—5-fold excess of iron is present. It is immaterial whether nickel or iron is already present in the sample or is introduced from the crucible during fusion.

Bondin [1] reported that copper and nickel tellurates are insoluble in water and in alkaline solutions. The present study shows that the compound separating from alkaline peroxide solution is not a normal nickel tellurate, but contains nickel and tellurium in the mole ratio 3:2; this is also insoluble in alkaline solutions.

The insolubility of tellurium in alkaline peroxide solution in the presence of nickel was successfully used as a basis for the analytical separation of tellurium from selenium.

The authors express their sincere thanks to Dr. M. Sankar Das for his keen interest, and to Shri M. C. Dutta, Deputy General Manager, Hindustan Copper Limited, for providing the anode slimes.

REFERENCES

1 S. M. Bondin, Inst. Khim. Tekhnol. Redkikh Elem. i Min. Syr'ya, 1964, 10 (C. A. 1965, 62 1354 g).
2 W. F. Hillebrand, G. E. F. Lundell, H. A.. Bright and J. I. Hoffman, Applied Inorganic Analysis, 2nd edn., Wiley, New York, 1955, p. 329.
3 W. R. Schoeller and A. R. Powell, The Analysis of Minerals and Ores of Rarer Elements, Griffin, London, 1955, p. 246.
4 I. M. Kolthoff and P. J. Elving, Treatise of Analytical Chemistry, Part II, Vol. 7, Wiley-Interscience, New York, 1961, pp. 150—151.
5 F. D. Snell and L. S. Ettre, Encyclopedia of Industrial Chemical Analysis, Vol. 17, Wiley-Interscience, 1973, p. 589.
6 V. Lehner and H. E. Wakefield, J. Am. Chem. Soc., 45 (1923) 1423.

Analytica Chimica Acta, 107 (1979) 419—424

Book Reviews

E. P. Bertin, *Introduction to X-ray Spectrochemical Analysis*, Plenum, New York, 1978, xiv + 485 pp, price U.S. $34.20.

The book is a condensed and slightly adapted version of the second edition of *Principles and Practice of X-ray Spectrometric Analysis* by the same author which was published in 1971. It is intended as an instruction text for workshops and courses in the rapidly expanding field of x-ray spectrometric analysis, because the earlier 1079-page book is considered too exhaustive, voluminous and comprehensive for beginning students.

The new book with its emphasis on pedagogical treatment of the field is a welcome addition to the texts available and certainly fulfils a need. The treatment is methodical, starting from the right level and progressing smoothly towards the basic problems inherent in the exploitation of the method. The text is clearly written, well organized and commendably free of typographical errors, although there are occasional repetitions in different chapters. The illustrations are mostly extremely clear and well-made.

The shortcomings of the text can mostly be traced back to two individual chapters. The chapter on detection and readout and x-ray intensity measurement is too detailed, and tends to distract the attentive reader from the essentials; there is no point in wasting time on the long outdated vacuum-tube equipment. What is worse is that some basic principles in this chapter are presented wrongly and may confuse the student. It is untrue that in the scintillation detector 3 eV is lost per light photon created, as most of the energy is dissipated thermally and does not yield fluorescence at all. It is mysterious how after a thorough and exact explanation of energy loss of x-rays in the sample in previous chapters, Dr. Bertin later repeatedly assumes that the photoelectric process occurs primarily in the outer electron orbitals, which is in direct contradiction to earlier data. The energy resolution capability of the semiconductor detector, which forms the basis of the energy-dispersive method is systematically and grossly underestimated. The chapter on energy-dispersive x-ray spectrometry is oversimplified; for example, the multichannel analyser is treated as a device consisting of a series of fixed energy windows each with its own accumulator, something which it stopped being around 1955.

Despite the caution necessary for these two chapters, the new book can be recommended as a practical text for teaching and laboratory courses and as a primer on x-ray fluorescence analysis. The price is certainly very reasonable by present standards.

F. Adams

G. Charlot, *Dosages Absorptiométriques des Éléments Minéraux*, 3° éd., Masson SA, Paris, 1978, x + 444 pp., price on application.

Les méthodes absorptiométriques de dosage continuent de connaître un développement important, à la fois parce qu'elles constituent une méthode de dosage des traces et parce que les perfectionnements récents de la technique permettent d'atteindre une précision égale ou parfois supérieure à celle des autres méthodes. L'ouvrage est constitué de deux parties. La première est consacrée aux généralités et caractéristiques de la méthode absorptiométrique. Après un rappel de la loi de Beer et des conditions de sa validité, sont donnés les principes des méthodes de mesure absorptiométrique (visuelle ou instrumentale). Le chapitre suivant est consacré aux caractéristiques analytiques de la méthode (fidélité, sensibilité, précision). Puis sont fournies les conditions de réalisation d'un dosage. Après deux brefs chapitres sur des aspects particuliers de l'absorptiométrie (fluorimétrie, turbidimétrie et néphélométrie), les titrages absorptiométriques sont traités (caractéristiques et exemples). Les dosages devant être bien souvent précédés d'une séparation du constituant à doser des autres ions interférants, l'auteur consacre ensuite quatre chapitres aux différents modes de séparations analytiques (par extraction, par échange d'ions, etc.). La première partie de l'ouvrage s'achève par une revue des principaux réactifs organiques utilisés en absorptiométrie.

La seconde partie de l'ouvrage est consacrée au dosage, par des méthodes sélectionnées, des principaux éléments (environ 65). Pour chacun d'eux sont fournis des modes de séparation et des exemples de dosage absorptiométrique (avec le mode opératoire, les ions interférants, la sensibilité etc.). Des références bibliographiques abondantes complètent chacun de ces chapitres.

Au total il s'agit d'un ouvrage extrêmement intéressant, surtout par ses aspects pratiques, et qui veut être un guide non seulement pour l'analyste, mais également pour tout chimiste qui a à résoudre un problème de dosage d'éléments minéraux. C'est un livre que le seul nom de l'auteur suffit à recommander.

G. Durand

M. L. Gross (Ed.), *High-Performance Mass Spectrometry*, American Chemical Society, ACS Symposium Series, 1978, ix + 358 pp., price U.S. $28.00.

This handy volume in the ACS Symposium Series reports a meeting held at the University of Nebraska, Lincoln in November 1976. It contains 18 original contributions of highly competent authors dealing with subjects which presently carry much of the impetus of organic mass spectrometry in scientific research and practical application. They include metastable ion investigations and its various exciting consequences in fundamental ion chemistry studies, advanced applications of high-resolution, chemical-ionization, field- and thermal-desorption ionization, collisional-activation and negative-ion mass spectrometry. The question as to whether or not such a symposium

report is a desirable publication must here be answered positively. If of appropriate standard it constitutes a very convenient learning aid, providing the necessary current awareness of the most advanced developments in the field to everybody with only moderate delay. It would have been better though if this volume had appeared in 1977 rather than together with *Advances in Mass Spectrometry, Vol. 7*, which reports on a larger conference organized only a few months earlier and covering a wider range of subjects including those presented here. Even so, the advantage of a more selective choice of subjects makes this volume recommendable to interested non-specialists as well as experts.

J. Seibl

J. E. Cross, *The Spectrum in Chemistry*, Academic Press, New York, 1978, pp. x + 313, price £12.60.

Many books devoted to spectroscopy appear to fall into one of three classes: those which are written for spectroscopists, who are usually not analytical chemists, and who apparently will never need to apply their erudition to real-life situations; those books written for workers who apparently do not need to know sufficient theoretical background to understand how the results arise; lastly there is the class which deals only with one particular wavelength range and apparently does not recognize the value of any other range.

The author has chosen to present a hybrid of all classes, since he aims his book at "the graduate and undergraduate reader . . . also . . . the practising chemist who wishes to be brought up-to-date on modern spectroscopic techniques". There are eleven chapters, each dealing with a particular wavelength region of the electromagnetic spectrum and arranged in order of increasing frequency, from a chapter dealing with the microwave region and concerned with molecular rotations and perturbations, to one dealing with Mössbauer spectroscopy and concerned with nuclear transitions. Additionally, there are chapters dealing with n.m.r. and e.s.r. The author states that he gives a "detailed treatment of many spectroscopic techniques that are often omitted or only briefly mentioned in texts at this level", and instances Fourier transform spectroscopy, atomic absorption spectrometry, ESCA, and others. When atomic emission, atomic absorption and atomic fluorescence spectrometries occupy less than four pages in total, then one must pose the question: "How superficial would be a non-detailed treatment?".

It may be that the book may benefit chemistry students, but it lacks realistic applications, so much so that after reading some of the chapters it is difficult to account for the widespread use of the particular technique being discussed.

The author has attempted an exceedingly difficult task; he has tried to give a condensed version of what could have required several monographs. He has not succeeded in making it apparent that spectroscopy does have a

large number of industrial, commonplace and useful applications other than for the determination of structures and physical parameters of single substances. The book might be useful for answering esoteric examination questions, but very few practising chemists will find much use for it.

L. S. Bark

E. Sawicki and C. R. Sawicki, *Aldehydes — Photometric Analysis, Vol. 5, Formaldehyde Precursors*, Academic Press, London, 1978, xii + 408 pp., price U.S. $45.00, £22.00.

This book is the fifth volume in this series on the photometric analysis of aldehydes. The book is entirely concerned with the great variety of formaldehyde precursors in the environment and in biological tissues and fluids. Formation of formaldehyde and formaldehyde reactions may play a role in a large number of biological processes including mutagenicity, carcinogenicity, and teratogenicity. The subject should therefore be of interest to many different groups of scientists. The formation of formaldehyde is discussed from the aspect of possible analytical utility of the reaction; the structure and physiological and environmental prevalence of the precursors; the reactions involved in the formation of formaldehyde; the type of environment or biological tissue wherein these reactions take place; the physiologically useful or toxic phenomena resulting directly or indirectly from the formation of formaldehyde; and the types of structures or bonds formed in the reaction of the metabolically derived formaldehyde with the chemicals and biopolymers in the living tissue.

The book has a total of 78 chapters, most of which describe the different classes of formaldehyde precursors; the chapters vary from a few lines to 16 pages. Although it might seem unnecessary to include some of the smaller chapters, it does add to the logical and systematic construction of the book. For the larger chapters, tables summarize the reagents used and the type of reaction, and give extensive references. Three chapters discuss the application of formaldehyde and formaldehyde precursors in analytical chemistry, including reactions useful in the direct formation of formaldehyde and reactions between chromogen-forming or fluorogen-forming reagents.

The book is well written and contains an ocean of information on formaldehyde precursors. The tables and figures allow the reader to go directly to the point of interest. In addition, a detailed subject index enables the reader to locate quickly the appropriate data. The extensive bibliography also makes this volume very valuable as a reference book. The book is recommended to all scientists working in the field of formaldehyde and formaldehyde precursors. As a reference book it belongs in the library of all scientists engaged in the study of organic compounds in internal or external environments. The only drawback is that the production time of the book was so long that, of the total of 1537 references, very few are more recent than 1975. A more up-to-date reference list would have made the book even more valuable.

A. Bjørseth

M. F. C. Ladd and R. A. Palmer, *Structure Determination by X-Ray Crystallography*, Plenum Press, New York, xv + 393, price $17.70.

This clearly-written paperback has many illustrations and provides as simple an introduction to the subject as is possible. It will be chiefly of value to chemistry students who wish to enter the subject practically, but its thoughtful approach will be of use to all interested in crystals. The only statement that might be considered at all doubtful is in the first paragraph, where the authors state that crystallography is a new discipline "dating from 1912". They then devote two long chapters to the classical work of the previous century!

The rest of the text seems to be beyond criticism. It carries enough mathematics to give a real understanding of the subject, and has many practical examples in the text; for example, it gives a very helpful numerical exercise on Fourier synthesis. There is no doubt that the authors are experienced teachers. At the end of each chapter is a set of examples, with the answers at the end of the book. The final chapter is a work-through of a complete structure determination of two monoclinic crystals. An appendix covers some extra points, including how to make your own stereo-viewer, and a model of a crystal with symmetry $\bar{4}$. It is not clear why the remainder of the Appendix is not in the text itself. The balance in the coverage is excellent. Space group theory is fully covered. The book shows very nicely how to find the positions of the variety of mirror and glide planes in the space groups. Another useful section is on the use of the polarizing microscope, a subject apt to be left to mineralogists, but one most useful to the practical chemist as well as the x-ray analyst.

Chapter 7 covers Direct Methods and Anomalous Scattering and so brings the coverage right up to the present day; this difficult subject is presented in as straightforward a manner as possible. This is altogether an excellent book.

C. A. Beevers

A. Zlatkis and R. E. Kaiser (Eds.), *High-performance Thin-layer Chromatography* Elsevier, Amsterdam, 1977, 240 pp., price Dfl. 100.

This book, Volume 9 in the Journal of Chromatography Library, maintains the high standard achieved by earlier volumes in this series; the fact that it was printed in Germany, presumably from a translation of original German manuscripts, is sufficient to explain the occurrence of rather more frequent printers' errors than usual. The team of German authors successfully present convincing arguments for the acceptance of high-performance thin-layer chromatography as an elegant, rapid, sensitive, precise and inexpensive analytical technique which has distinct advantages, for many applications, over high-performance liquid chromatography. The overall performance of the h.p.t.l.c. techniques described is the result of step-wise improvements over the past 20 years — the formation of a second generation of thin-layer chromatography. This is the result of successive improvements in the theoretical

understanding of the techniques and the coatings used for the plates, in the method of application of test substances to the plates, and in the elution and development systems.

For those who either do not use thin-layer chromatography extensively or are not aware of the limits of performance attainable, there is a great deal to be learned from reading this book. A series of colored plates shows clearly what can be achieved, but on pp. 173—178 it would have been helpful if the appropriate diagrams could have been presented on the same page as the experimental details. Page 51 unfortunately tries to tell us that "Over two centuries passed before Tswett's column chromatography was re-discovered by Kuhn and Lederer and again twice that time before its further introduction into modern h.p.l.c. A similar period of time elapsed between the first successful experiments in thin-layer chromatography by Izmailov and Shraiber in 1938 and the real breakthrough by Egon Stahl. Paper chromatography had to wait even longer for full recognition"! Let us hope that this does not mislead future generations of students into believing that the rate of progress since Tswett was ten times slower than it actually was.

D. M. W. Anderson

Analytica Chimica Acta, 107 (1979) 425—426

Announcements

J. Heyrovský Memorial Congress on Polarography

This Congress will take place in Prague, Czechoslovakia, from August 25th till 29th 1980 (not from 18th till 22nd, as was announced originally). The Congress will be organized on the occasions of the 90th anniversary of the birth of Professor Jaroslav Heyrovský, Nobel prize laureate in Chemistry 1959, and of the 30th anniversary of the foundation of the Polarographic Institute which now forms part of the J. Heyrovský Institute of Physical Chemistry and Electrochemistry of the Czechoslovak Academy of Sciences. The aim of the Congress is to survey the present state of polarography and related methods in the fields of basic research, contemporary instrumental techniques, analytical chemistry and applications in industry, biology, medicine and environmental science.

The Congress will proceed in two parallel sections. The main topics will be outlined in five plenary and twelve section lectures. Thematically related groups of problems of current interest will be discussed in five microsymposia and four panel discussions. Original contributions will be accepted in a practically unlimited number for poster presentation. Besides the scientific program, a social program will be available. English is recommended as the working language. Final applications for participation at the Congress must be sent in before 30.11. 1979. For detailed information, write to the Secretariat of the J. Heyrovský Memorial Congress on Polarography, Vlašská 9, 118 40 Praha 1 — Malá Strana, Czechoslovakia.

ISEC'80—International Solvent Extraction Conference 1980

The next International Solvent Extraction Conference will be held during September 6—12, 1980, at the University of Liège, Belgium. Previous conferences took place at the Hague (1971), Lyon (1974) and Toronto (1977). The continuation of this series of conferences is a logical consequence of the increasing interest in solvent extraction.

As in the past, the program will deal with all aspects of solvent extraction: chemistry and physical chemistry of extraction, extraction equipment, industrial processes and economics, nuclear chemistry, application to petrochemical and pharmaceutical industries. The conference will consist of a series of invited plenary lectures and submitted research papers.

Further details are available from the Conference Secretary, ISEC'80, Department of Chemistry, University of Liège, Sart Tilman, B-4000 Liège, Belgium.

Sixth Annual Meeting — Federation of Analytical Chemistry and Spectroscopy Societies

The Sixth Annual Meeting will be held during September 16—21, 1979, at the Philadelphia Sheraton Hotel, Philadelphia, Pennsylvania. A cordial invitation from the sponsoring organizations and the city of Philadephia is extended to all chemists and spectroscopists to attend and participate in the sixth annual FACSS meeting. In addition to the technical sessions, the meeting will feature an instrument exposition, workshops, an employment bureau, and social and cultural events.

Further information is available from: Douglas W. Robinson, Pennwalt Corporation, Box C, King of Prussia, PA 19406 (215) 265-3200 X309, U.S.A.

ANALYTICA CHIMICA ACTA, Vol. 107 (1979)

AUTHOR INDEX

75 Years of Chromatography

A Historical Dialogue

.. S. ETTRE *and* A. ZLATKIS (Editors).

ournal of Chromatography Library - Volume 17

)n the occasion of the 75th anniversary of the invention of chromatography, this book compiles ıe personal stories of 59 pioneers of the various chromatographic techniques (including five Nobel Prize laureates). In their contributions to this volume, these pioneers review the events which influenced them to enter the field; explain the background of their inventions; summarize their activities and results during their professional lives; and discuss their interactions with other scientists and other disciplines.

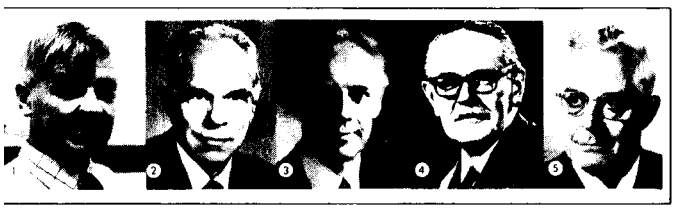

his book is more than a nostalgic recollection of the past for those who have been in chro- ıatography for some time. It also provides, for the younger generation of chromatographers, unique record of how present-day knowledge was accumulated.
he final chapter is devoted to "Those who are no longer with us".

:ontributors:

. R. Adlard
I. Boer
. Cremer
). H. Desty
. Dijkstra
. S. Ettre
. Flodin
. W. Gehrke
C. Giddings
. Glueckauf
1. J. E. Golay
). W. Grant
. Heftmann
. Hesse
. H. Higgins
E. C. Horning
M. G. Horning
C. Horváth
J. F. K. Huber
A. T. James
J. Janák
R. E. Kaiser
A. Karmen
J. G. Kirchner
J. J. Kirkland
A. V. Kiselev
E. sz. Kováts
E. Lederer
M. Lederer
A. Liberti
S. R. Lipsky
J. E. Lovelock
* A. J. P. Martin ④
* S. Moore ③
H. W. Patton
C. S. G. Phillips
J. Porath
V. Pretorius
G. R. Primavesi
N. H. Ray
L. Rohrschneider
K. I. Sakodynskii
G. Schomburg
G.-M. Schwab
R. D. Schwartz
C. D. Scott
R. P. W. Scott
* G. T. Seaborg ②
M. S. Shraiber
L. R. Snyder
E. Stahl
* W. H. Stein ⑤
H. H. Strain
F. H. Stross
* R. L. M. Synge ①
R. Teranishi
J. J. van Deemter
A. A. Zhukhovitskii
A. Zlatkis

'Nobel Prize laureates)

eb. 1979 *530 pages* *US $49.75/Dfl. 112.00* *ISBN 0-444-41754-0*

ELSEVIER

P.O. Box 211,
1000 AE Amsterdam
The Netherlands

52 Vanderbilt Ave
New York, N.Y. 10017

ıe Dutch guilder price is definitive. US $ prices are subject to exchange rate fluctuations

(continued from page opposite)

(continued from outside of cover)

(continued on page opposite)

CONTENTS

(continued on inside page of the cover)

Printed in The Netherlands